

AD-A013 880

EXPLORATORY DEVELOPMENT ON OXIDATION
BEHAVIOR OF TITANIUM ALLOYS UNDER HIGH
HEATING RATES

James S. Wolf

Clemson University

Prepared for:

Air Force Materials Laboratory
Advanced Research Projects Agency

April 1975

DISTRIBUTED BY:

NTIS

National Technical Information Service
U. S. DEPARTMENT OF COMMERCE

245052

AFML-TR-74-265

**EXPLORATORY DEVELOPMENT ON OXIDATION
BEHAVIOR OF TITANIUM ALLOYS
UNDER HIGH HEATING RATES**

*CLEMSON UNIVERSITY
CLEMSON, SOUTH CAROLINA*

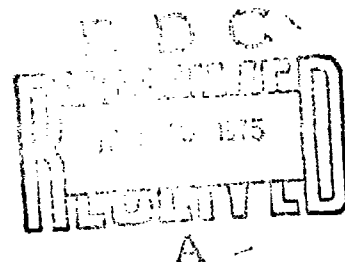
AD A 013880

TECHNICAL REPORT AFML-TR-74-265

FINAL REPORT FOR PERIOD 1 MAY 1973 - 31 OCTOBER 1974

APRIL 1975

Approved for public release; distribution unlimited.



prepared for
ADVANCED RESEARCH PROJECTS AGENCY
1400 WILSON BOULEVARD
ARLINGTON, VIRGINIA 22209

AIR FORCE MATERIALS LABORATORY
AIR FORCE SYSTEMS COMMAND
WRIGHT-PATTERSON AIR FORCE BASE, OHIO 45433

NOTICE

When Government drawings, specifications, or other data are used for any purpose other than in connection with a definitely related Government procurement operation, the United States Government thereby incurs no responsibility nor any obligation whatsoever; and the fact that the government may have formulated, furnished, or in any way supplied the said drawings, specifications, or other data, is not to be regarded by implication or otherwise as in any manner licensing the holder or any other person or corporation, or conveying any rights or permission to manufacture, use, or sell any patented invention that may in any way be related thereto.

Approved for public release; distribution unlimited.

This technical report has been reviewed and is approved.

Stephen R. Lyon

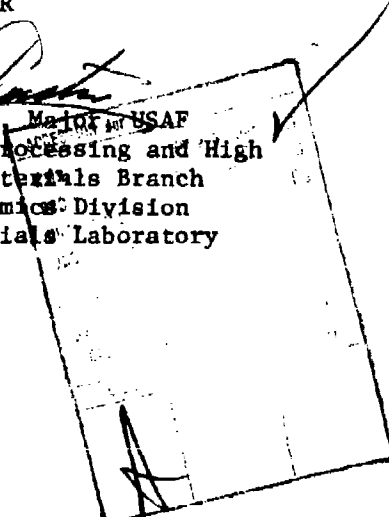
STEPHEN R. LYON
Project Engineer
Processing and High Temperature
Materials Branch

Norman M. Geyer

NORMAN M. GEYER
Technical Manager for High Temperature
Materials Development
Processing and High Temperature Materials Branch

FOR THE DIRECTOR

Roger J. Austin
ROGER J. AUSTIN, Major, USAF
Acting Chief, Processing and High
Temperature Materials Branch
Metals and Ceramics Division
Air Force Materials Laboratory



Copies of this report should not be returned unless return is required by security considerations, contractual obligations, or notice on a specific document.

UNCLASSIFIED

SECURITY CLASSIFICATION OF THIS PAGE (When Data Entered)

REPORT DOCUMENTATION PAGE		READ INSTRUCTIONS BEFORE COMPLETING FORM									
1. REPORT NUMBER AFML-TR-74-265	2. GOVT ACCESSION NO.	3. REC. PIEN'T'S CATALOG NUMBER									
4. TITLE (and Subtitle) Oxidation Behavior of Titanium Alloys Under High Heating Rates		5. TYPE OF REPORT & PERIOD COVERED Final, 01May1973-31Oct1974									
		6. PERFORMING ORG. REPORT NUMBER									
7. AUTHOR(s) James S. Wolf		8. CONTRACT OR GRANT NUMBER(s) F33615-73-C-5151									
9. PERFORMING ORGANIZATION NAME AND ADDRESS Division of Interdisciplinary Studies College of Engineering, Clemson University Clemson, South Carolina 29631		10. PROGRAM ELEMENT, PROJECT, TASK AREA & WORK UNIT NUMBERS 23870004									
11. CONTROLLING OFFICE NAME AND ADDRESS DARPA 1400 Wilson Blvd. Arlington, VA 22209		12. REPORT DATE April 1975									
		13. NUMBER OF PAGES 356									
14. MONITORING AGENCY NAME & ADDRESS (if different from Controlling Office) AFML/LLM W-PAFB, Ohio 45433		15. SECURITY CLASS. (of this report) Unclassified									
		15a. DECLASSIFICATION/DOWNGRADING SCHEDULE N/A									
16. DISTRIBUTION STATEMENT (of this Report) Approved for public release; distribution unlimited											
17. DISTRIBUTION STATEMENT (of the abstract entered in Block 20, if different from Report)											
18. SUPPLEMENTARY NOTES											
19. KEY WORDS (Continue on reverse side if necessary and identify by block number) <table border="0"> <tr> <td>Titanium alloy</td> <td>Activation energy</td> <td>Ignition</td> </tr> <tr> <td>Oxidation</td> <td>Oxygen</td> <td>Combustion</td> </tr> <tr> <td>Heating rate</td> <td>Nitrogen</td> <td></td> </tr> </table>			Titanium alloy	Activation energy	Ignition	Oxidation	Oxygen	Combustion	Heating rate	Nitrogen	
Titanium alloy	Activation energy	Ignition									
Oxidation	Oxygen	Combustion									
Heating rate	Nitrogen										
20. ABSTRACT (Continue on reverse side if necessary and identify by block number) <p>The initial stages of reaction of unalloyed titanium, Ti-4V, Ti8Mn, and β-III titanium alloy specimens with oxygen, nitrogen and atmospheres bearing these gases has been studied over the temperature range from 800° to 1300°C. The kinetics of these reactions were analyzed for specimens subjected to linear heating rates in the range from 0.5° to 100° C/s. Mathematical techniques were devised for modeling: 1) the oxygen uptake by unalloyed titanium during heating, and 2) the deposition of the chemical heat of reaction into oxidizing substrates. (see reverse side)</p>											

DD FORM 1473 1 JAN 73 EDITION OF 1 NOV 65 IS OBSOLETE

UNCLASSIFIED

SECURITY CLASSIFICATION OF THIS PAGE (When Data Entered)

UNCLASSIFIED

SECURITY CLASSIFICATION OF THIS PAGE(When Data Entered)

Analyses of the data indicate that the specific linear reaction rate maximizes during heating, that its magnitude increases with increasing heating rate, and that at higher heating rates (30° to 100°C/s) it is causal to the ignition of thin titanium specimens in 200 torr stagnant oxygen at temperatures as low as 400°C. The latter effect was inferred to arise from strain-enhanced reactivity of titanium-base materials coupled with localized deposition of the heat of reaction. Thin substrates, the presence of stored energy of cold work, and the presence of alloying elements were found to produce enhanced reactivity during oxidation and to increase the susceptibility to ignition and sustained burning.

UNCLASSIFIED

SECURITY CLASSIFICATION OF THIS PAGE(When Data Entered)

FOREWORD

This final technical report covers all work performed under U.S. Air Force Contract No. F33615-73-C-5151, supported by the Advanced Research Project Agency under Project Order- 2387. Inclusive dates of research performance were 1 May 1973 through 31 October 1974. The manuscript of this report was submitted by the author on 1 Dec. 1974 for publication.

This project was performed by Clemson University, Clemson, South Carolina under Materials Laboratory Project 7312, "Metal Surface Deterioration for Advanced Air Force Weapon System Components". It was accomplished under the technical direction of Stephen R. Lyon of the High Temperature Materials and Processing Branch (AFML/LLM), Metals and Ceramics Division, Air Force Materials Laboratory, Wright-Patterson Air Force Base, Ohio.

Dr. James S. Wolf, Division of Interdisciplinary Studies, College of Engineering was the principal investigator. Dr. A. B. Pruitt, Postdoctoral Research Associate, J. M. Grochowski, Graduate Research Assistant, and J. C. Carter, Laboratory Technologist were involved in the technical effort.

Table of Contents

<u>Section</u>	<u>Page</u>
I INTRODUCTION	1
II EXPERIMENTAL PROCEDURE	7
1. Materials and Specimen Preparation	7
2. Heating and Recording Equipment	13
2a. Air Furnace	13
2b. Volumetric Apparatus	20
3. Methods of Data Analysis	28
4. Tests Performed	30
4a. Air Furnace	30
4b. Volumetric Apparatus	32
III RESULTS AND DISCUSSION	43
1. Appearance and Dimensional Change	43
1a. Air Furnace	43
1b. Volumetric Apparatus	46
2. Weight Changes of Exposed Specimens	63
2a. Air Furnace	64
2b. Volumetric Apparatus	67
3. Microscopic Analyses of Exposed Specimens	87
3a. Microscopic Features	88
3b. Dimensional Analyses	110
3c. Microhardness Determinations	119
4. Reaction of Titanium and Titanium-Base Alloys in the Volumetric Apparatus	137
4a. General Behavior	137
4b. Reaction of Unalloyed Titanium with Oxygen-(RHC) Tests	139

Table of Contents - continued

<u>Section</u>	<u>Page</u>
4c. Reaction of Unalloyed Titanium with Nitrogen and Mixed Gases-(RHC) Tests	199
4d. Reaction of Titanium-Base Alloys with Oxygen - (RHC) Tests	228
4e. Summary of Reaction Parameters for (RHC)- Type Tests of Titanium-Base Materials	276
4f. Special Tests	290
5. Reaction of Titanium-Base Materials in Oxygen Leading to Ignition	314
IV CONCLUSIONS	335
REFERENCES	339
APPENDICES	341

List of Illustrations

<u>Figure</u>		<u>Page</u>
1	Flat specimen design used for titanium specimens. All dimensions are in cm. Specimen thickness is determined by available sheet thicknesses.	19
2	Schematic diagram of the equipment complement to be used in oxidation research. Numbered items correspond to those called out in this section of the text.	22
3	Volumetric equipment used in oxidation testing.	23
4	Photograph of the 12-KW quartz-tube furnace illustrating the Vycor reaction tube, thermocouple and specimen positioning.	25
5	Overall view of thermocouple assembly and mounted specimen.	26
6	Specific weight change of unalloyed titanium (type 1) specimen oxidized in air at 1000 °C for various times. Note deviation from initial parabolic behavior at longer times.	66
7	Temperature dependence of the parabolic reaction rate constant for unalloyed titanium (Type 1) specimens oxidized in air.	68
8	Temperature dependence of the parabolic reaction rate constant for unalloyed titanium (Type 1) specimens oxidized in 200 torr oxygen. Heating rate 8 °C/s.	82
9	Temperature dependence of the parabolic reaction rate constant for 5 titanium-base material specimens oxidized in 200 torr oxygen.	84

List of Illustrations - continued

<u>Figure</u>		<u>Page</u>
10	Photomicrographs illustrating the structure of the 5 types of unalloyed titanium used in this investigation. All materials in the as-received condition. Magnification 400X; Kroll's Etch, (a) - Type 1, (b) - Type 2, (c) - Type 3, (d) - Type 4 and (e) - Type 5.	89
11	Photomicrographs illustrating the structures of the 3 types of Ti-6Al-4V alloys used in this investigation. All materials in the as-received condition. Magnification 400X; Kroll's Etch, (a) - Type 2, (b) - Type 1 and (c) - Type 3.	92
12	Photomicrographs illustrating the structure of the Ti-8Mn (a) and β -III (b) alloys used in this investigation. Both materials in the as-received condition. Magnification 400X; Kroll's Etch, (a) and (b).	93
13	Photomicrographs of an unalloyed titanium (Type 1) specimen heated at the rate of 0.5 °C/s to 1000 °C in 200 torr oxygen to 1000 °C and cooled at 0.5 °C/s. (a) oxide scale, magnification 400X, unetched; (b) substrate, magnification 200X, anodized, (a) - Spec. No. 06141 and (b) - Spec. No. 06141.	94
14	Photomicrographs of unalloyed titanium specimens heated at the rate of 8 °C/s to 1000 °C in 200 torr oxygen. Magnification 200X; Kroll's Etch, (a) Type 1: Spec. No. 06132 and (b) Type 2: Spec. No. 09191.	96
15	Photomicrographs of titanium-base specimens heated at the rate of 8 °C/s to 1000 °C in 200 torr oxygen. Magnification 80X; Kroll's Etch. Part (d) only; dark field, (a) Ti (Type 3); Spec. No. 09194, (b)	

List of Illustrations - continued

<u>Figure</u>		<u>Page</u>
	Ti-6Al-4V (Type 1); Spec. No. 407161, (c) Ti-8Mn; Spec. No. 406032 and (d) β -III; Spec. No. 406191.	97
16	Photomicrographs of titanium-based specimens heated at the rate of 8 C/s to 1100 C in 200 torr oxygen. Magnification 80X; Kroll's Etch, (a) Ti (Type 3); Spec. No. 405021, (b) Ti-6Al-4V (Type 1); Spec. No. 405072, (c) Ti-8Mn; Spec. No. 405073 and (d) β -III; Spec. No. 406173.	98
17	Photomicrographs of titanium-base specimens heated at the rate of 5.9 C/s to 1200 C in 200 torr oxygen. Magnification 80X; Kroll's Etch. Part (d) only: dark field, (a) Ti (Type 3); Spec. No. 405023, (b) Ti-6Al-4V (Type 1) Spec. No. 408081, (c) Ti-8Mn; Spec. No. 407242 and (d) β -III; Spec. No. 407241.	99
18	Photomicrograph of unalloyed titanium (Type 1) specimen no. 05011 oxidized for 4 hours in air at 1000 C. Note attack of columnar diffusion zone. Magnification 200X; Kroll's Etch.	101
19	Photomicrographs of unalloyed titanium (Type 1) heated at various rate to 1100 C in 200 torr oxygen. Magnification 200X; Kroll's Etch, (a) 0.5 C/s; Spec. No. 06131, (b) 8 C/s; Spec. No. 06071, (c) 22 C/s; Spec. No. 06142.	103
20	Photomicrographs of titanium-base alloy specimens heated at the rate of 0.5 C/s to 1100 C in 200 torr oxygen. Magnification 80X; Kroll's Etch. Part (d) only: dark field, (a) Ti-6Al-4V (Type 1) Spec. No. 401091, (b) Ti-6Al-4V (Type 2) Spec. No. 402042, (c) Ti-8Mn Spec. No. 405074 and (d) β -III Spec. No. 406174.	104

List of Illustrations - continued

<u>Figure</u>		<u>Page</u>
21	Photomicrographs of titanium-base alloy specimens heated at the rate of 0.5 C/s to 1100 C in 200 torr oxygen. Magnification 80X; Kroll's Etch. Part (d) only: dark field, (a) Ti-6Al-4V (Type 1) Spec. No. 401091, (b) Ti-6Al-4V (Type 2) Spec. No. 402042, (c) Ti-8Mn Spec. No. 405074 and (d) B-III Spec. No. 406175.	105
22	Photomicrographs of thin unalloyed titanium specimens heated in 200 torr oxygen. (a) 8 C/s to 1000 C, Magnification 400X, Kroll's Etch; (b) 8 C/s to 1100 C, Magnification 200X, Unetched; (c) 8 C/s to 1100 C, Magnification 200X, Kroll's Etch; (a) Type 3; Spec. No. 09194, (b) Type 4; Spec. No. 407162 and (c) Type 5; Spec. No. 408282.	107
23	Photomicrographs of thin titanium-base alloy specimens heated to 1100 C in 200 torr oxygen. Magnification 200X; Kroll's Etch. (a) Heated at 8 C/s; (b) heated at 22 C/s, (a) Ti-6Al-4V (Type 3); Spec. No. 406171 and (b) B-III; Spec. No. 409231.	109
24	Photomicrographs of unalloyed titanium heated at the rate of 8 C/s to 1100 C in 200 torr oxygen. Various degrees of prior cold work. (a and b) Magnification 80X; (c and d) Magnification 200X. Kroll's Etch, (a) 39% C.W.; Spec. No. 11201, (b) 61% C.W.; Spec. No. 408141, (c) 76% C.W.; Spec. No. 408191, and (d) 87% C.W.; Spec. No. 405151.	111
25	Photomicrographs of unalloyed titanium specimens heated at the rate of 8 C/s in 200 torr nitrogen. a) Type 2 material oxidized at 1000 C; b) Type 1 material oxidized at 1100 C. Magnification 400X; Kroll's Etch, (a) Spec. No. 09193 and (b) Spec. No. 07312.	112
26	Hardness of as-received unalloyed titanium (Type 2) as a function of traverse depth from the surface.	120

List of Illustrations - continued

<u>Figure</u>		<u>Page</u>
27	Photomicrograph of unalloyed titanium (Type 1) specimen no. 05011 illustrating a portion of one typical hardness traverse. Oxidized in air for 4 hours at 1000° C. Magnification 400X; Kroll's Etch.	121
28	Hardness of unalloyed titanium (Type 1) specimen no. 05011 exposed for 4 hours in air at 1000° C.	122
29	Hardness of unalloyed titanium (Type 1) specimen no. 05072 exposed for 16 hours in air at 1000° C.	123
30	Hardness of unalloyed titanium (Type 1) specimen no. 06132 heated in 200 torr O ₂ at the rate of 8 C/s to 1000° C. Isothermal time 60 min.	124
31	Hardness of unalloyed titanium (Type 1) specimen no. 06131 heated in 200 torr O ₂ at the rate of 0.5 C/s to 1100° C. Isothermal time 60 min.	125
32	Hardness of unalloyed titanium (Type 1) specimen no. 06071 heated in 200 torr O ₂ at the rate of 8 C/s to 1100° C. Isothermal time 60 min.	126
33	Hardness of unalloyed titanium (Type 1) specimen no. 06142 heated in 200 torr O ₂ at the rate of 22 C/s to 1100° C. Isothermal time 60 min.	127
34	Hardness of unalloyed titanium (Type 1) specimen no. 08013 heated in 200 torr O ₂ at the rate of 7.5 C/s to 1200° C. Isothermal time 27 min.	128
35	Hardness of unalloyed titanium (Type 1) specimen no. 07091 heated in 200 torr O ₂ at the rate of approximately 4.5 C/s to 1300° C. Isothermal time approximately 4.5 min. Hardness of unoxidized titanium approximately 200 KHN.	129

List of Illustrations - continued

<u>Figure</u>		<u>Page</u>
36	Hardness of unalloyed titanium (Type 1) specimen no. 07311 heated in 200 torr N ₂ at the rate of 8 °C/s to 1000 °C. Isothermal time 60 min.	130
37	Hardness of unalloyed titanium (Type 1) specimen no. 07312 heated in 200 torr N ₂ at the rate of 8 °C/s to 1100 °C. Isothermal time 60 min.	131
38	Hardness of Ti-6Al-4V alloy (Type 1) specimen no. 11202 heated in 200 torr O ₂ at the rate of 8 °C/s to 1100 °C. Isothermal time 60 min.	132
39	Hardness of Ti-8Mn alloy specimen no. 405073 heated in 200 torr O ₂ at the rate of 8 °C/s to 1100 °C. Isothermal time 41 min.	133
40	Hardness of the β-III alloy specimen no. 406173 heated in 200 torr O ₂ at the rate of 8 °C/s to 1100 °C. Isothermal time 22 min.	134
41	Schematic illustration of the primary and secondary data derived from the volumetric apparatus. (a) Temperature vs. time; (b) power index vs. time; (c) pressure vs. time; (d) specific gas consumption vs. time; (e) specific reaction rate vs. time; (f) square of specific gas consumption vs. isothermal time.	138
42	Initial time-temperature profile for unalloyed titanium (Type 1) specimen no. 06051 heated in 200 torr O ₂ at the rate of 0.5 °C/s to 1000 °C.	141
43	Initial behavior of the specific gas consumption (N) for unalloyed titanium (Type 1) specimen no. 06051 heated in 200 torr O ₂ at the rate of 0.5 °C/s to 1000 °C.	142

List of Illustrations - continued

<u>Figure</u>		<u>Page</u>
44	Initial behavior of the specific linear reaction rate (\dot{N}) for unalloyed titanium (Type 1) specimen no. 06051 heated in 200 torr O_2 at the rate of 0.5 $^{\circ}C/s$ to 1000 $^{\circ}C$.	143
45	Overall behavior of the specific gas consumption (N) for unalloyed titanium (Type 1) specimen no. 06051 heated in 200 torr O_2 at the rate of 0.5 $^{\circ}C/s$ to 1000 $^{\circ}C$.	144
46	Overall behavior of the square of specific gas consumption (N^2) for unalloyed titanium (Type 1) specimen no. 06051 heated in 200 torr O_2 at the rate of 0.5 $^{\circ}C/s$ to 1000 $^{\circ}C$.	145
47	Initial behavior of the power index (W) for unalloyed titanium (Type 1) specimen no. 06051 heated in 200 torr O_2 at the rate of 0.5 $^{\circ}C/s$ to 1000 $^{\circ}C$.	146
48	Initial behavior of the specific gas consumption (N) for unalloyed titanium (Type 1) specimen no. 06141 heated in 200 torr O_2 at the rate of 0.5 $^{\circ}C/s$ to 1000 $^{\circ}C$.	147
49	Initial behavior of the specific linear reaction rate (\dot{N}) for unalloyed titanium (Type 1) specimen no. 06141 heated in 200 torr O_2 at the rate of 0.5 $^{\circ}C/s$ to 1000 $^{\circ}C$.	148
50	Initial behavior of the specific gas consumption (N) for unalloyed titanium (Type 1) specimen no. 06132 heated in 200 torr O_2 at the rate of 8 $^{\circ}C/s$ to 1000 $^{\circ}C$.	149
51	Initial behavior of the specific linear reaction rate (\dot{N}) for unalloyed titanium (Type 1) specimen no. 06132 heated in 200 torr O_2 at the rate of 8 $^{\circ}C/s$ to 1000 $^{\circ}C$.	150

List of Illustrations - continued

<u>Figure</u>		<u>Page</u>
52	Initial behavior of the specific gas consumption (N) for unalloyed titanium (Type 1) specimen no. 06133 heated in 200 torr O ₂ at the rate of 25 °C/s to 1000 °C.	151
53	Initial behavior of the specific linear reaction rate (N) for unalloyed titanium (Type 1) specimen no. 06133 heated in 200 torr O ₂ at the rate of 25 °C/s to 1000 °C.	152
54	Initial behavior of the specific gas consumption (N) for unalloyed titanium (Type 1) specimen no. 06131 heated in 200 torr O ₂ at the rate of 0.5 °C/s to 1100 °C.	153
55	Initial behavior of the specific linear reaction rate (N) for unalloyed titanium (Type 1) specimen no. 06131 heated in 200 torr O ₂ at the rate of 0.5 °C/s to 1100 °C.	154
56	Initial behavior of the specific gas consumption (N) for unalloyed titanium (Type 1) specimen no. 06071 heated in 200 torr O ₂ at the rate of 8 °C/s to 1100 °C.	155
57	Initial behavior of the specific linear reaction rate (N) for unalloyed titanium (Type 1) specimen no. 06071 heated in 200 torr O ₂ at the rate of 8 °C/s to 1100 °C.	156
58	Initial behavior of the specific gas consumption (N) for unalloyed titanium (Type 1) specimen no. 06142 heated in 200 torr O ₂ at the rate of 22 °C/s to 1100 °C.	157
59	Initial behavior of the specific linear reaction rate (N) for unalloyed titanium (Type 1) specimen no. 06142 heated in 200 torr O ₂ at the rate of 22 °C/s to 1100 °C.	158
60	Initial behavior of the specific gas consumption (N) for unalloyed titanium (Type 1) specimen no. 08012 heated in 200 torr O ₂ at the rate of 0.5 °C/s to 1200 °C.	159

List of Illustrations - continued

<u>Figure</u>		<u>Page</u>
61	Initial behavior of the specific linear reaction rate (\dot{N}) for unalloyed titanium (Type 1) specimen no. 08012 heated in 200 torr O_2 at the rate of $0.5^\circ C/s$ to $1200^\circ C$.	160
62	Initial behavior of the specific gas consumption (N) for unalloyed titanium (Type 1) specimen no. 08013 heated in 200 torr O_2 at the rate of $7.5^\circ C/s$ to $1200^\circ C$.	161
63	Initial behavior of the specific linear reaction rate (\dot{N}) for unalloyed titanium (Type 1) specimen no. 08013 heated in 200 torr O_2 at the rate of $7.5^\circ C/s$ to $1200^\circ C$.	162
64	Initial behavior of the specific gas consumption (N) for unalloyed titanium (Type 2) specimen no. 09191 heated in 200 torr O_2 at the rate of $8^\circ C/s$ to $1000^\circ C$.	163
65	Initial behavior of the specific linear reaction rate (\dot{N}) for unalloyed titanium (Type 2) specimen no. 09191 heated in 200 torr O_2 at the rate of $8^\circ C/s$ to $1000^\circ C$.	164
66	Initial behavior of the specific gas consumption (N) for unalloyed titanium (Type 2) specimen no. 09192 heated in 400 torr O_2 at the rate of $8^\circ C/s$ to $1000^\circ C$.	165
67	Initial behavior of the specific linear reaction rate (\dot{N}) for unalloyed titanium (Type 2) specimen no. 09192 heated in 400 torr O_2 at the rate of $8^\circ C/s$ to $1000^\circ C$.	166
68	Initial behavior of the specific gas consumption (N) for unalloyed titanium (Type 2) specimen no.	

List of Illustrations - continued

<u>Figure</u>		<u>Page</u>
	401151 heated in 200 torr O ₂ at the rate of 8 °C/s to 1100 °C.	167
69	Initial behavior of the specific linear reaction rate (N) for unalloyed titanium (Type 2) specimen no. 401151 heated in 200 torr O ₂ at the rate of 8 °C/s to 1100 °C.	168
70	Initial time-temperature profile for unalloyed titanium (Type 2) specimen no. 405151 heated in 200 torr O ₂ at the rate of 8 °C/s to 1100 °C. Note temperature instability for material cold worked 87 percent.	169
71	Initial behavior of the power index (W) for unalloyed titanium (Type 2) specimen no. 405151 heated in 200 torr O ₂ at the rate of 8 °C/s to 1100 °C. Note power instability for material cold worked 87 percent.	170
72	Initial behavior of the specific gas consumption (N) for unalloyed titanium (Type 2) specimen no. 405151 heated in 200 torr O ₂ at the rate of 8 °C/s to 1100 °C. Material cold worked 87 percent.	171
73	Initial behavior of the specific linear reaction rate (N) for unalloyed titanium (Type 2) specimen no. 405151 heated in 200 torr O ₂ at the rate of 8 °C/s to 1100 °C. Material cold worked 87 percent.	172
74	Initial time-temperature profile for unalloyed titanium (Type 2) specimen no. 405221 heated in 200 torr O ₂ at the rate of approximately 10 °C/s to 1100 °C. Material cold worked 87 percent.	173

List of Illustrations - continued

<u>Figure</u>		<u>Page</u>
75	Initial behavior of the specific gas consumption (N) for unalloyed titanium (Type 2) specimen no. 405221 heated in 200 torr O_2 at the rate of approximately 10 C/s to 1100 C. Material cold worked 87 percent.	174
76	Initial behavior of the specific linear reaction rate (N) for unalloyed titanium (Type 2) specimen no. 405221 heated in 200 torr O_2 at the rate of approximately 10 C/s to 1100 C. Material cold worked 87 percent.	175
77	Initial behavior of the specific gas consumption (N) for unalloyed titanium (Type 2) specimen no. 408191 heated in 200 torr O_2 at the rate of 22 C/s to 1100 C. Material cold worked 76 percent.	176
78	Initial behavior of the specific linear reaction rate (N) for unalloyed titanium (Type 2) specimen no. 408191 heated in 200 torr O_2 at the rate of 22 C/s to 1100 C. Material cold worked 76 percent.	177
79	Initial behavior of the specific gas consumption (N) for unalloyed titanium (Type 2) specimen no. 408141 heated in 200 torr O_2 at the rate of 22 C/s to 1100 C. Material cold worked 61 percent.	178
80	Initial behavior of the specific linear reaction rate (N) for unalloyed titanium (Type 2) specimen no. 408141 heated in 200 torr O_2 at the rate of 22 C/s to 1100 C. Material cold worked 61 percent.	179
81	Initial behavior of the specific linear reaction rate (N) for unalloyed titanium (Type 2) specimen no. 401021 heated in 200 torr O_2 at the rate of 8 C/s to 1100 C. Specimen descaled and reoxidized.	180

List of Illustrations - continued

<u>Figure</u>		<u>Page</u>
82	Initial behavior of the specific linear reaction rate (\dot{N}) for unalloyed titanium (Type 2) specimen no. 401021 heated in 200 torr O_2 at the rate of 8 C/s to 1100 C. Specimen descaled and reoxidized.	181
83	Initial behavior of the specific gas consumption (\dot{N}) for unalloyed titanium (Type 3) specimen no. 09194 heated in 200 torr O_2 at the rate of 8 C/s to 1000 C.	
84	Initial behavior of the specific linear reaction rate (\dot{N}) for unalloyed titanium (Type 3) specimen no. 09194 heated in 200 torr O_2 at the rate of 8 C/s to 1000 C.	183
85	Initial behavior of the specific gas consumption (\dot{N}) for unalloyed titanium (Type 3) specimen no. 11201 heated in 200 torr O_2 at the rate of 8 C/s to 1100 C. Material cold worked 39 percent.	184
86	Initial behavior of the specific linear reaction rate (\dot{N}) for unalloyed titanium (Type 3) specimen no. 11201 heated in 200 torr O_2 at the rate of 8 C/s to 1100 C. Material cold worked 39 percent.	185
87	Initial behavior of the specific gas consumption (\dot{N}) for unalloyed titanium (Type 3) specimen no. 405021 heated in 200 torr O_2 at the rate of 8 C/s to 1100 C.	186
88	Initial behavior of the specific linear reaction rate (\dot{N}) for unalloyed titanium (Type 3) specimen no. 405021 heated in 200 torr O_2 at the rate of 8 C/s to 1100 C.	18

List of Illustrations - continued

<u>Figure</u>		<u>Page</u>
89	Initial behavior of specific gas consumption (N) for unalloyed titanium (Type 3) specimen no. 405023 heated in 200 torr O ₂ at the rate of 5.9° C/s to 1200° C.	188
90	Initial behavior of the specific linear reaction rate (Ṅ) for unalloyed titanium (Type 3) specimen no. 405023 heated in 200 torr O ₂ at the rate of 5.9° C/s to 1200° C.	189
91	Initial behavior of the specific gas consumption (N) for unalloyed titanium (Type 4) specimen no. 407162 heated in 200 torr O ₂ at the rate of 8° C/s to 1100° C.	190
92	Initial behavior of the specific linear reaction rate (Ṅ) for unalloyed titanium (Type 4) specimen no. 407162 heated in 200 torr O ₂ at the rate of 8° C/s to 1100° C.	191
93	Initial behavior of the specific gas consumption (N) for unalloyed titanium (Type 5) specimen no. 408143 heated in 200 torr O ₂ at the rate of 8° C/s to 1100° C.	192
94	Initial behavior of the specific linear reaction rate (Ṅ) for unalloyed titanium (Type 5) specimen no. 408143 heated in 200 torr O ₂ at the rate of 8° C/s to 1100° C.	193
95	Initial behavior of the specific gas consumption (N) for unalloyed titanium (Type 5) specimen no. 408282 heated in 200 torr O ₂ at the rate of approximately 19° C/s to 1100° C.	194
96	Initial behavior of the specific linear reaction rate (Ṅ) for unalloyed titanium (Type 5) specimen	

List of Illustrations - continued

<u>Figure</u>		<u>Page</u>
	no. 408282 heated in 200 torr O_2 at the rate of approximately $18^\circ C/s$ to $1100^\circ C$.	195
97	Initial response of unalloyed titanium (Type 1 and 2) specimens in 200 torr oxygen for the temperature range 1000° to $1300^\circ C$.	197
98	Initial behavior of the specific gas consumption (N) for unalloyed titanium (Type 1) specimen no. 07311 heated in 200 torr N_2 at the rate of $8^\circ C/s$ to $1000^\circ C$.	200
99	Initial behavior of the specific linear reaction rate (N) for unalloyed titanium (Type 1) specimen no. 07311 heated in 200 torr N_2 at the rate of $8^\circ C/s$ to $1000^\circ C$.	201
100	Initial behavior of the specific gas consumption (N) for unalloyed titanium (Type 1) specimen no. 07312 heated in 200 torr N_2 at the rate of $8^\circ C/s$ to $1100^\circ C$.	202
101	Initial behavior of the specific linear reaction rate (N) for unalloyed titanium (Type 1) specimen no. 07312 heated in 200 torr N_2 at the rate of $8^\circ C/s$ to $1100^\circ C$.	203
102	Initial behavior of the specific gas consumption (N) for unalloyed titanium (Type 2) specimen no. 09193 heated in 200 torr N_2 at the rate of $8^\circ C/s$ to $1000^\circ C$. Data less certain; system leak noted.	204
103	Initial behavior of the specific gas consumption (N) for unalloyed titanium (Type 2) specimen no. 402192 heated in 200 torr N_2 at the rate of $8^\circ C/s$ to $1100^\circ C$.	205
104	Initial behavior of the specific gas consumption (N) for unalloyed titanium (Type 2) specimen no. 402192 heated in 200 torr N_2 at the rate of $8^\circ C/s$ to $1100^\circ C$.	206

List of Illustrations - continued

<u>Figure</u>		<u>Page</u>
105	Initial behavior of the specific gas consumption (N) for Ti-6Al-4V (Type 1) specimen no. 401162 heated in 200 torr N ₂ at the rate of 8 °C/s to 1100 °C.	207
106	Initial behavior of the specific linear reaction rate (N) for Ti-6Al-4V alloy (Type 1) specimen no. 401162 heated in 200 torr N ₂ at the rate of 8 °C/s to 1100 °C.	208
107	Initial behavior of the specific gas consumption (N) for unalloyed titanium (Type 1) specimen no. 07313 heated in 200 torr O ₂ plus 200 torr N ₂ at the rate of 8 °C/s to 1000 °C.	209
108	Initial behavior of the specific linear reaction rate (N) for unalloyed titanium (Type 1) specimen no. 07313 heated in 200 torr O ₂ plus 200 torr N ₂ at the rate of 8 °C/s to 1000 °C.	210
109	Initial behavior of the specific gas consumption (N) for unalloyed titanium (Type 1) specimen no. 08011 heated in 200 torr O ₂ plus 200 torr N ₂ at the rate of 8 °C/s to 1100 °C.	211
110	Initial behavior of the specific linear reaction rate (N) for unalloyed titanium (Type 1) specimen no. 08011 heated in 200 torr O ₂ plus 200 torr N ₂ at the rate of 8 °C/s to 1100 °C.	212
111	Initial behavior of the specific gas consumption (N) for unalloyed titanium (Type 2) specimen no. 402193 heated in 100 torr O ₂ plus 100 torr N ₂ at the rate of 8 °C/s to 1100 °C.	213
112	Initial behavior of the specific linear reaction rate (N) for unalloyed titanium (Type 2) specimen no. 402193 heated in 100 torr O ₂ plus 100 torr N ₂ at the rate of 8 °C/s to 1100 °C.	214

List of Illustrations - continued

<u>Figure</u>		<u>Page</u>
113	Initial behavior of the specific gas consumption (\dot{N}) for unalloyed titanium (Type 2) specimen no. 402194 heated in 50 torr O_2 plus 150 torr N_2 at the rate of 8 C/s to 1100 C.	215
114	Initial behavior of the specific linear reaction rate (\dot{N}) for unalloyed titanium (Type 2) specimen no. 402194 heated in 50 torr O_2 plus 150 torr N_2 at the rate of 8 C/s to 1100 C.	216
115	Initial behavior of the specific gas consumption (\dot{N}) for unalloyed titanium (Type 1) specimen no. 08021 heated in 200 torr O_2 plus 200 torr He at the rate of 8 C/s to 1000 C.	217
116	Initial behavior of the specific linear reaction rate (\dot{N}) for unalloyed titanium (Type 1) specimen no. 08021 heated in 200 torr O_2 plus 200 torr He at the rate of 8 C/s to 1000 C.	218
117	Initial behavior of the specific gas consumption (\dot{N}) for unalloyed titanium (Type 1) specimen no. 08171 heated in 200 torr O_2 plus 200 torr He at the rate of 8 C/s to 1100 C.	219
118	Initial behavior of the specific linear reaction rate (\dot{N}) for unalloyed titanium (Type 1) specimen no. 08171 heated in 200 torr O_2 plus 200 torr He at the rate of 8 C/s to 1100 C.	220
119	Initial behavior of the specific gas consumption (\dot{N}) for unalloyed titanium (Type 1) specimen no. 08023 heated in 200 torr N_2 plus 200 torr He at the rate of 8 C/s to 1000 C.	221
120	Initial behavior of the specific linear reaction rate (\dot{N}) for unalloyed titanium (Type 1) specimen no. 08023	

List of Illustrations - continued

<u>Figure</u>		<u>Page</u>
	heated in 200 torr N ₂ plus 200 torr He at the rate of 8 °C/s to 1000 °C.	222
121	Initial behavior of the specific gas consumption (N) for unalloyed titanium (Type 1) specimen no. 09051 heated in 200 torr N ₂ plus 200 torr He at the rate of 8 °C/s to 1100 °C.	223
122	Initial behavior of the specific linear reaction rate (N) for unalloyed titanium (Type 1) specimen no. 09051 heated in 200 torr N ₂ plus 200 torr He at the rate of 8 °C/s to 1100 °C.	224
123	Initial behavior of the specific gas consumption (N) for Ti-6Al-4V alloy (Type 1) specimen no. 407161 heated in 200 torr O ₂ at the rate of 8 °C/s to 1000 °C. Material milled from .152 cm to .119 cm.	229
124	Initial behavior of the specific linear reaction rate (N) for Ti-6Al-4V alloy (Type 1) specimen no. 407161 heated in 200 torr O ₂ at the rate of 8 °C/s to 1000 °C. Material milled from .152 cm to .119 cm.	230
125	Initial behavior of the specific gas consumption (N) for Ti-6Al-4V alloy (Type 1) specimen no. 401161 heated in 200 torr O ₂ at the rate of 0.5 °C/s to 1100 °C.	231
126	Initial behavior of the specific linear reaction rate (N) for Ti-6Al-4V alloy (Type 1) specimen no. 401161 heated in 200 torr O ₂ at the rate of 0.5 °C/s to 1100 °C.	232
127	Initial behavior of the specific gas consumption (N) for Ti-6Al-4V alloy (Type 1) specimen no. 11202 heated in 200 torr O ₂ at the rate of 8 °C/s to 1100 °C.	233

List of Illustrations - continued

<u>Figure</u>		<u>Page</u>
128	Initial behavior of the specific linear reaction rate (\dot{N}) for Ti-6Al-4V alloy (Type 1) specimen no. 11202 heated in 200 torr O_2 at the rate of $8^\circ C/s$ to $1100^\circ C$.	234
129	Initial behavior of the specific gas consumption (N) for Ti-6Al-4V alloy (Type 1) specimen no. 405071 heated in 200 torr O_2 at the rate of $8^\circ C/s$ to $1100^\circ C$. Material milled from .152 cm to .119 cm.	235
130	Initial behavior of the specific linear reaction rate (\dot{N}) for Ti-6Al-4V alloy (Type 1) specimen no. 405071 heated in 200 torr O_2 at the rate of $8^\circ C/s$ to $1100^\circ C$. Material milled from .152 cm to .119 cm.	236
131	Initial behavior of the specific gas consumption (N) for Ti-6Al-4V alloy (Type 1) specimen no. 405072 heated in 200 torr O_2 at the rate of $8^\circ C/s$ to $1100^\circ C$. Material milled from .152 cm to .119 cm.	237
132	Initial behavior of the specific linear reaction rate (\dot{N}) for Ti-6Al-4V alloy (Type 1) specimen no. 405072 heated in 200 torr O_2 at the rate of $8^\circ C/s$ to $1100^\circ C$. Material milled from .152 cm to .119 cm.	238
133	Initial behavior of the specific gas consumption (N) for Ti-6Al-4V alloy (Type 1) specimen no. 401092 heated in 200 torr O_2 at the rate of $22^\circ C/s$ to $1100^\circ C$.	239
134	Initial behavior of the specific linear reaction rate (\dot{N}) for Ti-6Al-4V alloy (Type 1) specimen no. 401092 heated in 200 torr O_2 at the rate of $22^\circ C/s$ to $1100^\circ C$.	240
135	Initial behavior of the specific gas consumption (N) for Ti-6Al-4V alloy (Type 1) specimen no. 407243 heated in 200 torr O_2 at the rate of $5.9^\circ C/s$ to $1200^\circ C$. Material milled from .152 cm to .119 cm.	241

List of Illustrations - continued

<u>Figure</u>		<u>Page</u>
136	Initial behavior of the specific linear reaction rate (\dot{N}) for Ti-6Al-4V alloy (Type 1) specimen no. 407243 heated in 200 torr O_2 at the rate of $5.9^\circ C/s$ to $1200^\circ C$. Material milled from .152 cm to .119 cm.	242
137	Initial behavior of the specific gas consumption (N) for Ti-6Al-4V alloy (Type 1) specimen no. 408081 heated in 200 torr O_2 at the rate of $5.9^\circ C/s$ to $1200^\circ C$. Material milled from .152 cm to .119 cm.	243
138	Initial behavior of the specific linear reaction rate (\dot{N}) for Ti-6Al-4V alloy (Type 1) specimen no. 408081 heated in 200 torr O_2 at the rate of $5.9^\circ C/s$ to $1200^\circ C$. Material milled from .152 cm to .119 cm.	244
139	Initial behavior of the specific gas consumption (N) for Ti-6Al-4V alloy (Type 2) specimen no. 402042 heated in 200 torr O_2 at the rate of $0.5^\circ C/s$ to $1100^\circ C$.	245
140	Initial behavior of the specific linear reaction rate (\dot{N}) for Ti-6Al-4V alloy (Type 2) specimen no. 402042 heated in 200 torr O_2 at the rate of $0.5^\circ C/s$ to $1100^\circ C$.	246
141	Initial behavior of the specific gas consumption (N) for Ti-6Al-4V alloy (Type 2) specimen no. 401152 heated in 200 torr O_2 at the rate of $8^\circ C/s$ to $1100^\circ C$.	247
142	Initial behavior of the specific linear reaction rate (\dot{N}) for Ti-6Al-4V alloy (Type 2) specimen no. 401152 heated in 200 torr O_2 at the rate of $8^\circ C/s$ to $1100^\circ C$.	248
143	Initial behavior of the specific gas consumption (N) for Ti-6Al-4V alloy (Type 2) specimen no. 402043 heated in 200 torr O_2 at the rate of $22^\circ C/s$ to $1100^\circ C$.	249

List of Illustrations - continued

<u>Figure</u>		<u>Page</u>
144	Initial behavior of the specific linear reaction rate (\dot{N}) for Ti-6Al-4V alloy (Type 2) specimen no. 402043 heated in 200 torr O_2 at the rate of 22 °C/s to 1100 °C.	250
145	Initial behavior of the specific gas consumption (\dot{N}) for Ti-6Al-4V alloy (Type 3) specimen no. 406171 heated in 200 torr O_2 at the rate of 8 °C/s to 1100 °C.	251
146	Initial behavior of the specific linear reaction rate (\dot{N}) for Ti-6Al-4V alloy (Type 3) specimen no. 406171 heated in 200 torr O_2 at the rate of 8 °C/s to 1100 °C.	252
147	Initial behavior of the specific gas consumption (\dot{N}) for Ti-8Mn alloy specimen no. 406032 heated in 200 torr O_2 at the rate of 8 °C/s to 1000 °C.	253
148	Initial behavior of the specific linear reaction rate (\dot{N}) for Ti-8Mn alloy specimen no. 406032 heated in 200 torr O_2 at the rate of 8 °C/s to 1000 °C.	254
149	Initial behavior of the specific gas consumption (\dot{N}) for Ti-8Mn alloy specimen no. 405074 heated in 200 torr O_2 at the rate of 0.5 °C/s to 1100 °C.	255
150	Initial behavior of the specific linear reaction rate (\dot{N}) for Ti-8Mn alloy specimen no. 405074 heated in 200 torr O_2 at the rate of 0.5 °C/s to 1100 °C.	256
151	Initial behavior of the specific gas consumption (\dot{N}) for Ti-8Mn alloy specimen no. 405073 heated in 200 torr O_2 at the rate of 8 °C/s to 1100 °C.	257
152	Initial behavior of the specific linear reaction rate (\dot{N}) for Ti-8Mn alloy specimen no. 405073 heated in 200 torr O_2 at the rate of 8 °C/s to 1100 °C.	258

List of Illustrations - continued

<u>Figure</u>		<u>Page</u>
153	Initial behavior of the specific gas consumption (N) for Ti-8Mn alloy specimen no. 406031 heated in 200 torr O ₂ at the rate of 22 °C/s to 1100 °C.	259
154	Initial behavior of the specific linear reaction rate (N) for Ti-8Mn alloy specimen no. 406031 heated in 200 torr O ₂ at the rate of 22 °C/s to 1100 °C.	260
155	Initial behavior of the specific gas consumption (N) for Ti-8Mn alloy specimen no. 407242 heated in 200 torr O ₂ at the rate of 5.9 °C/s to 1200 °C.	261
156	Initial behavior of the specific linear reaction rate (N) for Ti-8Mn alloy specimen no. 407242 heated in 200 torr O ₂ at the rate of 5.9 °C/s to 1200 °C.	262
157	Initial behavior of the specific gas consumption (N) for Ti-β-III alloy specimen no. 406191 heated in 200 torr O ₂ at the rate of 8 °C/s to 1000 °C.	263
158	Initial behavior of the specific linear reaction rate (N) for Ti-β-III alloy specimen no. 406191 heated in 200 torr O ₂ at the rate of 8 °C/s to 1000 °C.	264
159	Initial behavior of the specific gas consumption (N) for Ti-β-III alloy specimen no. 406174 heated in 200 torr O ₂ at the rate of 0.5 °C/s to 1100 °C.	265
160	Initial behavior of the specific linear reaction rate for Ti-β-III alloy specimen no. 406174 heated in 200 torr O ₂ at the rate of 0.5 °C/s to 1100 °C.	266
161	Initial behavior of the specific gas consumption (N) for Ti-β-III alloy specimen no. 406173 heated in 200 torr O ₂ at the rate of 8 °C/s to 1100 °C.	267

List of Illustrations - continued

<u>Figure</u>		<u>Page</u>
162	Initial behavior of the specific linear reaction rate (\dot{N}) for Ti- β -III specimen no. 406173 heated in 200 torr O_2 at the rate of 8 $^{\circ}C/s$ to 1100 $^{\circ}C$.	268
163	Initial behavior of the specific gas consumption (N) for Ti- β -III alloy specimen no. 406175 heated in 200 torr O_2 at the rate of 22 $^{\circ}C/s$ to 1100 $^{\circ}C$.	269
164	Initial behavior of the specific linear reaction rate (\dot{N}) for Ti- β -III alloy specimen no. 406175 heated in 200 torr O_2 at the rate of 22 $^{\circ}C/s$ to 1100 $^{\circ}C$.	270
165	Initial behavior of the specific gas consumption (N) for Ti- β -III alloy specimen no. 409231 heated in 200 torr O_2 at the rate of 22 $^{\circ}C/s$ to 1100 $^{\circ}C$. Material milled and polished to .0330 cm.	271
166	Initial behavior of the specific linear reaction rate (\dot{N}) for Ti- β -III specimen no. 409231 heated in 200 torr O_2 at the rate of 22 $^{\circ}C/s$ to 1100 $^{\circ}C$. Material milled and polished to .0330 cm.	272
167	Initial behavior of the specific gas consumption (N) for Ti- β -III alloy specimen no. 407241 heated in 200 torr O_2 at the rate of 5.9 $^{\circ}C/s$ to 1200 $^{\circ}C$.	273
168	Initial behavior of the specific linear reaction rate (\dot{N}) for Ti- β -III alloy specimen no. 407241 heated in 200 torr O_2 at the rate of 5.9 $^{\circ}C/s$ to 1200 $^{\circ}C$.	274
169	Initial response to 0.102 cm thick titanium specimens in 200 torr oxygen for the temperature range 1000 $^{\circ}C$ to 1200 $^{\circ}C$. Nominal heating rate 8 $^{\circ}C/s$.	285

List of Illustrations - continued

<u>Figure</u>		<u>Page</u>
170	Time-temperature histories for specimens with "welded" and "near-surface" thermocouple configurations, heated in 200 torr O ₂ at 8 C/s to 1100 °C.	292
171	Transient thermal behavior for unalloyed titanium (Type 2) specimen no. 11151 heated successively three times in 200 torr O ₂ at the rate of 8 C/s nominally to 1100 °C; 600-grit finish.	294
172	Transient furnace power behavior for unalloyed titanium (Type 2) specimen no. 11151 heated successively three times in 200 torr O ₂ at the rate of 8 C/s nominally to 1100 °C; 600 grit finish.	295
173	Transient system pressure behavior for unalloyed titanium (Type 2) specimen no. 11151 heated successively three times in 200 torr O ₂ at the rate of 8 C/s nominally to 1100 °C; 600 grit finish.	296
174	Transient thermal behavior for unalloyed titanium (Type 2) specimen no. 11142 heated successively three times in 200 torr O ₂ at the rate of 8 C/s nominally to 1100 °C; 1µm finish.	297
175	Transient furnace power behavior for unalloyed titanium (Type 2) specimen no. 11142 heated successively three times in 200 torr O ₂ at the rate of 8 C/s nominally to 1100 °C; 1µm finish.	298
176	Transient system pressure behavior for unalloyed titanium (Type 2) specimen no. 11142 heated successively three times in 200 torr O ₂ at the rate of 8 C/s nominally to 1100 °C; 1µm finish.	299
177	Transient thermal behavior for unalloyed titanium (Type 2) specimen no. 401021 heated successively three times in 200 torr O ₂ at the rate of 8 C/s	

List of Illustrations - continued

<u>Figure</u>		<u>Page</u>
	nominally to 1100 °C; 600-grit finish after oxidation and descaling.	300
178	Transient furnace power behavior for unalloyed titanium (Type 2) specimen no. 401021 heated successively three times in 200 torr O ₂ at the rate of 8 C/s nominally to 1100 °C; 600-grit finish after oxidation and descaling.	301
179	Transient system pressure behavior for unalloyed titanium (Type 2) specimen no. 401021 heated successively three times in 200 torr oxygen at the rate of 8 C/s nominally to 1100 °C; 600-grit finish after preoxidation and descaling.	302
180	Schematic illustration of the effect of oxide plasticity arising as a result of differential thermal expansion during concurrent heating and oxidation. Dashed lines indicate diffusion flux paths available to the reaction.	319
181	Comparison of observed and predicted gas consumptions for unalloyed titanium (Type 1) specimen no. 06131 heated at the rate of 0.5 C/s to 1100 °C.	321
182	Comparison of observed and predicted gas consumptions for unalloyed titanium (Type 1) specimen no. 06142 heated at the rate of 22 C/s to 1100 °C.	322
183	Comparison of observed and predicted reactivities of unalloyed titanium (Type 1) specimens heated to 1100 °C and subsequently held isothermally. (a) Specimen no. 06142 heated at 22 C/s; (b) specimen no. 06071 heated at 8 C/s; (c) specimen no. 06131 heated at 0.5 C/s.	323

List of Illustrations - continued

<u>Figure</u>		<u>Page</u>
184	Ignition behavior of three unalloyed titanium (Type 5) specimens in stagnant 200 torr oxygen illustrating the inverse relation between heating rate and sensible ignition temperature.	328
185	Dependence of the heat delivery parameter upon heating rate and macroscopic surface-to-volume ratio for unalloyed titanium specimens which underwent oxidation and/or ignition.	329
186	Dependence of the heat delivering parameter upon heating rate and macroscopic surface-to-volume ratio for titanium-6% aluminum-4% vanadium specimens which underwent oxidation and/or ignition.	331
187	Dependence of the heat delivering parameter upon heating rate and macroscopic surface-to-volume ratio for titanium-8% manganese specimens which underwent oxidation and/or ignition.	332
188	Dependence of the heat delivering parameter upon heating rate and macroscopic surface-to-volume ratio for titanium-8-III specimens which underwent oxidation and/or ignition.	333
189	Schematic diagram of the system with its attached calibrated volume used in considerations for calculating system volume.	342
190	Graph based on equation (4) of Appendix used in determination of effective system volume (V_s).	345
191	Schematic representations of pressure-time and temperature-time traces for the volumetric system.	351

List of Tables

<u>Table</u>		<u>Page</u>
I	Chemical Analysis of Unalloyed Titanium (Type 1)	8
II	Chemical Analysis of Unalloyed Titanium (Type 2)	9
III	Chemical Analysis of Unalloyed Titanium (Type 3)	10
IV	Chemical Analysis of Unalloyed Titanium (Type 4)	11
V	Chemical Analysis of Unalloyed Titanium (Type 5)	12
VI	Chemical Analysis of Titanium - 6% Aluminum - 4% Vanadium Alloy (Type 1)	14
VII	Chemical Analysis of Titanium - 6% Aluminum - 4% Vanadium Alloy (Type 2)	15
VIII	Chemical Analysis of Titanium - 6% Aluminum - 4% Vanadium Alloy (Type 3)	16
IX	Chemical Analysis of Titanium - 8% Manganese Alloy	17
X	Chemical Analysis of Titanium β - III Alloy (Ti - 11.5% Mo - 6% Zr - 4.5% Sn)	18
XI	Oxidation Tests Performed in the Air Furnace Using Unalloyed Titanium (Type 1) Specimens	31
XII	Titanium Oxidation Tests Performed Using the Volumetric Heating Apparatus	33
XIII	Dimensional Changes and Appearance of Titanium (Type 1) Specimens Oxidized in Air Using the Air Furnace	44
XIV	Dimensional Changes and Appearance for Titanium-Base Specimens Oxidized in Various Atmospheres Using the Volumetric Apparatus	47

List of Tables - continued

<u>Table</u>		<u>Page</u>
XV	Weight Changes for Titanium (Type I) Specimens Oxidized in Air Using the Air Furnace	65
XVI	Total Weight Changes for Titanium-Base Specimens Oxidized for One Hour in Various Atmospheres Using the Volumetric Apparatus	69
XVII	Values of the Average Parabolic Reaction Rate Constant (K_p) for Unalloyed Titanium (Type I) Specimens Heated at 8°C. Per Second in Various Oxidizing Atmospheres	81
XVIII	Microscopic Dimensional Changes Induced in Unalloyed Titanium (Type I) Specimens During Exposure in 200 Torr Oxygen for One Hour	114
XIX	Microscopic Determination of Diffusion Zone Thick- nesses	116
XX	Values of the Maximum Linear Reaction Rate (N_{max}) and the Temperature at Which it Occurred for Titanium and Titanium-Base Alloy Specimens	278
XXI	Values of the Energy Coupling Parameter (W_5) as a Function of the Heating Rate, Maximum Temperature, and Gas Atmosphere for Unalloyed Titanium	286
XXII	Selected Values of the Energy Coupling Parameter (W_5) for Titanium and Titanium-Base Alloys Exposed in 200 Torr Oxygen at 1100°C	288
XXIII	X-Ray Diffraction Data for Unalloyed Titanium and its Compounds as Reported in the Powder Diffraction File (Ref. 15)	304

List of Tables - continued

<u>Table</u>		<u>Page</u>
XXIV	X-Ray Diffraction Data for Unalloyed Titanium (Type 2) Before and After Exposure to 200 Torr Oxygen at 1100 C. First Test Series: Specimen Blank and Specimen No. 401021	307
XXV	X-Ray Diffraction Data for Unalloyed Titanium (Type 2) After Exposure to 200 Torr Oxygen at 1100 C. Second Test Series: Specimen no. 401021	309
XXVI	X-Ray Diffraction Data for Unalloyed Titanium (Type 1) After Exposure in Air at 900 C for 4 Hours in the Conventional Heating Apparatus. Specimen No. 05151	312
XXVII	X-Ray Diffraction Data for Unalloyed Titanium and TI-6AL-4V alloy After Exposure in Nitrogen at 1100 C	313
XXVIII	Summary of Data for Tests of Titanium and Titanium-Base Alloys Leading to Ignition in 200 Torr Oxygen	326
XXIX	Pressure Data Used in Determination of Effective System Volume	344

SUMMARY

The initial stages of reaction of unalloyed titanium, Ti-6Al-4V, Ti-8Mn, and β -III titanium alloy specimens with oxygen, nitrogen, and atmospheres bearing these gases has been studied over the temperature range from 800° to 1300°C. The kinetics of these reactions were analyzed for specimens subjected to linear heating rates in the range from 0.5° to 100°C/s. Mathematical techniques were devised for modeling: 1) the oxygen uptake by unalloyed titanium during heating, and 2) the deposition of the chemical heat of reaction into oxidizing substrates.

Analyses of the data obtained indicated that the specific linear reaction rate maximizes during heating, that its magnitude increases with increasing heating rate, and that at higher heating rates (30° to 100°C/s) it is causal to the ignition of thin titanium specimens in 200 torr stagnant oxygen at temperatures as low as 400°C. The latter effect was inferred to arise from strain-enhanced reactivity of titanium-base materials coupled with localized deposition of the heat of reaction. Thin substrates, the presence of stored energy of cold work, and the presence of alloying elements were found to produce enhanced reactivity during oxidation and to increase the susceptibility to ignition and sustained burning.

Complementary data are included which describe: the macroscopic and microscopic nature of exposed specimens, the extent and hardness of diffusion zones, the reaction kinetics in single and mixed gases, the coupling of infrared energy to the specimens, and the results of special tests.

SECTION I

INTRODUCTION

Among the metallic materials used in the fabrication of modern aerospace vehicles are titanium and titanium-base alloys. Many newer systems utilize large quantities of these alloys, primarily because of their high strength-to-weight ratios relative to other candidate structural materials. As contemplated design speed and performance requirements increase, the projected skin and engine temperatures of these vehicles increase commensurately and one must take into account the interaction between the vehicle components and their gaseous environment. In addition, there are contemplated interactions of the vehicle components with other pulse-type thermal energy inputs such as those which may arise from transient aerodynamic effects. It therefore becomes necessary to obtain an understanding of the behavior of titanium alloys under the combined influences of steady temperatures and superimposed transient heating as might be associated with vehicle maneuvers or irradiation from external sources. Of special interest at this time is the definition of the regime in which titanium-base materials may undergo ignition and/or sustained burning given the environmental conditions cited above.

The types of problems associated with the system described above are manifold; however, some simplification can be achieved, or at least orderly thinking can be initiated, if one considers the events which occur as the temperature is continually increased. This thought process allows one to start at the point of low temperature oxidation, go through the various scaling regimes as temperature is increased during anisothermal oxidation and terminate at ignition or burning. The assumptions inherent in

this thought pattern are: 1) that oxidation is a precursor process leading to ignition and 2) that external impulse-type energy inputs other than those associated with heating, such as are discussed by White and Ward (ref.1), are excluded from the system.

According to Kofstad (ref. 2), at temperatures below about 400°C, titanium and its alloys undergo logarithmic oxidation and form rutile as a surface compound. As the temperature is increased to the range of 600° to 700°C, there is a transition from logarithmic to parabolic oxidation with rutile remaining as the major surface compound. In this same temperature range, Shambian and Redden (ref. 3) have pointed out that titanium and its alloys undergo an embrittling reaction due to contamination of the substrate material by oxygen and, further, that the degree of contamination increases with alloy content. This point becomes disconcerting because the chief purpose of the alloying elements is to provide the required mechanical strengths for these alloys. A further increase in temperature, to the range between 800° and 1000°C, produces what is commonly called parabolic oxidation as is noted by Kofstad (ref. 2) and is evident from the data of Layner, Bay and Tsypin (ref. 4). It is also in this temperature range that the n-type semiconductor rutile begins to exhibit a behavior indicative of a change in the predominant diffusing species from oxygen ions to titanium ions. Concurrently, there has been noted by Rosa (ref. 5) the formation of a superficial oxide layer which is oxygen deficient. In this temperature range also begins marked changes of the substrate. The inward diffusion of oxygen produces an intermediate layer of alpha grains in oxidized beta titanium (ref. 5) and, according to the data of Kellerer and Wingert (ref. 6), macroscopic dimensional changes are observable for specimens which have been oxidized. These observations strongly suggest the presence of large near-surface stresses.

As the temperature of oxidation is increased still further, the oxidation reaction becomes linear, a behavior which is usually indicative of a non-protective scaling process. However, the absolute value of the scaling rate constant diminishes as temperature is increased from approximately 1300° to 1500°C; a behavior which has been explained on the basis of the sintering of the oxide scale (ref. 2). Although the protective nature of the reaction is uncertain, in this temperature range, the lower oxides of titanium, such as TiO and Ti_2O_3 have been observed. From elementary considerations, this is an expected behavior based upon the $Ti-TiO_2$ phase diagram as presented by Wahlbeck and Gilles (ref. 7). However, it is equally obvious that we do not have a complete understanding of the behavior of the titanium-oxygen system in this temperature range because, according to the survey article by White and Ward (ref. 1) and Reynolds (ref. 8), ignition of titanium is to be associated with the upper portion of this temperature range; i.e., at temperatures between approximately 1400° and 1650°C.

Markstein (ref. 9) has pointed out that ignition temperatures seem well defined only for those metals that do not form a protective oxide layer and that induction periods for ignition are observed for those metals and alloys which do indeed form a protective oxide layer. As a result of this, widely divergent data concerning ignition has been presented for those metals which form protective oxide layers. We are thus faced with the decision of whether or not Kofstad's sintering process at elevated temperatures constitutes a protective layer for titanium and whether or not the linear kinetics for titanium at elevated temperatures are indicative of non-protective oxidation. As Markstein points out, further complications may arise due to the fact that the mutual solubility for the metal and oxide could interfere with normal transport

processes necessary to the burning reaction.

Rather early in the quantitative study of the ignition of metals, Reynolds (ref. 8) provided a simplified model based upon an energy balance which linked the oxidation and ignition processes. From this, followed a mathematical definition of ignition based upon the shape of a time-temperature curve for a model metal heated to ignition. Reynolds' model is essentially a mathematical expression of an effect in which the heat of reaction may be stored within a body and may be used to provide a temperature rise above ambient-as alluded to by Markstein. Reynolds' model, or a modification thereof, would allow us also to consider the case such as may occur when infrared radiation from an external source is incident upon the material of interest. In pursuing this line of thought, it immediately becomes apparent that a factor of major importance is the efficiency of coupling between the incident radiation and the subject body. This coupling, described by a coupling coefficient, must in turn be strongly dependent upon the physico-chemical properties (basically optical properties) of the surface oxide or phase.

In the case of titanium oxidizing at elevated temperature and simultaneously under the influence of infrared radiation, it becomes extremely important to know both what oxides or other compounds are present and whether or not they have normal structural configurations as these qualities will alter the coupling coefficients. That phases other than TiO_2 form at elevated temperature (TiO and Ti_2O_3) is already known; however, the infrared optical properties of these phases or of the oxygen-saturated metal, as formed during oxidation, has not been investigated in any detail. Further, the existence of non-equilibrium phases is also a distinct possibility, especially under the condition of rapid heating.

In the application of materials to aerospace vehicles we must face the certainty that heating will be of an uncontrolled and rapid nature. Conversely, most of the data which has been gathered concerning the oxidation of metals and alloys involved an attempt to define the phenomenology of gas-metal systems under conditions which are very nearly both isothermal and isobaric. It is the purpose of this research to simulate the more realistic condition wherein titanium-based materials would be subjected to high temperature oxidation under a variety of controlled heating rates. This technique provides to the specimen an energy impulse whose magnitude is dependent upon the controlled rate of heating. White and Ward (ref. 1) and also Markstein (ref. 9) have alluded to cases where external energy impulses reduce the effective ignition temperature of titanium or titanium alloys to levels below room temperature. That the thermal impulse of our technique will produce a similar effect in titanium-base materials is suggested by data generated at this laboratory indicating that the reaction kinetics of unalloyed magnesium (ref. 10) may be altered by high rates of infrared heating.

Although the rapid heating of an oxidizable metal or alloy in air appears to be a technically simple procedure, there are a multiplicity of processes which do or may occur concurrently. These processes may be artificially subdivided into three categories: chemical, mechanical, and physical; however, it is recognized that coupled processes, such as physico-mechanical, may also occur and be important. In order to gain insight into the behavior of rapidly-heated oxidizable metals, it is necessary to have at least a qualitative understanding of the processes which may be involved and their probable effects.

The experimental technique employed in this research involves an infrared radiation source as the sole supply of energy to the test metals and alloys. Specimens are heated at rates between approximately 0.5° and 100°C/sec., and various system and reaction parameters are plotted as a function of heating rate. Graphic extrapolation of these parameters may then be used to estimate probable occurrences at heating rates far in excess of the maximum rate attainable by our apparatus. The parameters in this case may include such quantities as: the initial oxidation rate, the subsequent "isothermal" behavior, the activation energy, and a qualitative description of the coupling efficiency. Should ignition or sustained burning occur, these qualities can be treated similarly. Because of the broad range of possible important processes which may occur during laser heating, and because experimental verification of most of these processes is necessary, this research effort was concentrated upon four substrate materials: unalloyed titanium, Ti-6Al-4V, Ti-8Mn, and the titanium-base alloy known as β -III.

SECTION II

EXPERIMENTAL PROCEDURE

The material which follows describes the specimens, equipment, and techniques used in pursuit of this research. During the course of the experimental program, the test materials used were unalloyed titanium and the Ti-8Mn, Ti-6Al-4V, and β -III alloys. The bulk of the oxidation testing and all of the ignition testing was conducted using a volumetric apparatus previously developed by the principal investigator at Clemson University (ref. 10).

1. MATERIALS AND SPECIMEN PREPARATION

The unalloyed CP (commercially pure) titanium used initially during this period of research was supplied to the principal investigator in the form of 0.062-inch (0.158 cm) thick sheet through the courtesy of the Titanium Metals Corporation of America. This specimen stock, commercially designated as type Ti-50A, possesses a purity of approximately 99.8% as indicated by the chemical analysis presented in Table I. In order to avoid confusion with materials of similar analysis used during this research period, this material has been here designated as: unalloyed titanium - (Type 1).

In accordance with the terms of the contract under which this research was performed, the AFML has supplied four other varieties of CP titanium for use as specimen stock. These materials, in various gauges, possess a purity of approximately 99.3% and have here been designated as: unalloyed titanium - (Type 2) through (Type 5). Detailed chemical analyses of these materials are presented in Tables II through V. The AFML has also supplied three lots of vacuum annealed Ti-6Al-4V alloy for use as specimen stock. These materials, supplied in three gauges, have been here designated Ti-6Al-4V alloy - (Type 1), (Type 2), and (Type 3).

TABLE I
CHEMICAL ANALYSIS OF UNALLOYED TITANIUM (TYPE 1)*

Element	Weight Percent
Non-metallic	
Carbon	0.010
Hydrogen	0.004(2)
Nitrogen	0.022
Oxygen	0.132
Metallic	
Aluminum	0.04
Copper	0.008
Iron	0.02
Molybdenum	0.09
Tin	<0.01
Tungsten	<0.01
Vanadium	<0.01
Zirconium	<0.01
Titanium	Balance (99.8 approx.)

* Analysis supplied by Air Force Materials Laboratory, Wright-Patterson Air Force Base, Ohio. Nominal thickness 0.062 inch. Commercial designation: Ti-50A.

TABLE II
CHEMICAL ANALYSIS OF UNALLOYED TITANIUM (TYPE 2)*

Element	Weight Percent
Non-metallic	
Carbon	0.014
Hydrogen	0.000(8)
Nitrogen	0.008
Oxygen	0.218
Metallic	
Aluminum	0.075**
Boron	<0.000(5)
Calcium	0.050**
Chromium	<0.001(5)
Copper	0.001(5)
Iron	0.300
Lead	0.001(5)
Magnesium	0.012
Manganese	0.007(5)
Molybdenum	0.001(5)
Nickel	0.000(8)
Silicon	0.015
Tantalum	<0.020
Tin	0.001(5)
Zirconium	0.001(5)
Titanium	Balance (99.3 approx.)

*Analysis and material supplied by Air Force Materials Laboratory,
Wright-Patterson Air Force Base, Ohio, Nominal thickness 0.057 inch.

**Values less certain

TABLE III
CHEMICAL ANALYSIS OF UNALLOYED TITANIUM (TYPE 3)*

Element	Weight Percent
Non-metallic	
Carbon	0.011
Hydrogen	0.000(6)
Nitrogen	0.008
Oxygen	0.197
Metallic	
Aluminum	0.030**
Boron	<0.000(5)
Calcium	0.050**
Chromium	<0.001(5)
Copper	0.001(5)
Iron	0.300
Lead	0.001(5)
Magnesium	0.012
Manganese	0.015
Molybdenum	0.001(5)
Nickel	0.000(5)
Silicon	0.015
Tantalum	<0.020
Tin	0.001(5)
Zirconium	0.001(5)
Titanium	Balance (99.3 approx.)

*Analysis and material supplied by Air Force Materials Laboratory,
Wright-Patterson Air Force Base. Nominal thickness 0.040 inch.

**Values less certain.

TABLE IV
CHEMICAL ANALYSIS OF UNALLOYED TITANIUM (TYPE 4)*

Element	Weight Percent
Non-metallic	
Carbon	ND
Hydrogen	ND
Nitrogen	0.014
Oxygen	0.255
Metallic	
Aluminum	0.080
Boron	0.006
Chromium	0.004
Copper	0.0015
Iron	0.150
Lead	0.002
Magnesium	0.005
Manganese	0.005
Molybdenum	0.002
Nickel	0.006
Silicon	0.030
Tin	0.010
Tungsten	0.004
Zirconium	0.001
Titanium	Balance (99.4 approx.)

*Analysis and material supplied by Air Force Materials Laboratory,
Wright-Patterson Air Force Base, Ohio. Nominal thickness 0.010 inch.

TABLE V
CHEMICAL ANALYSIS OF UNALLOYED TITANIUM (TYPE 5)*

Element	Weight Percent
Non-metallic	
Carbon	ND
Hydrogen	0.0090
Nitrogen	ND
Oxygen	0.269
Metallic	
Aluminum	0.080
Boron	0.010
Chromium	0.006
Copper	0.0015
Iron	0.200
Lead	0.002
Magnesium	0.005
Manganese	0.005
Molybdenum	0.004
Nickel	0.010
Silicon	0.030
Tin	0.010
Tungsten	0.004
Zirconium	0.004
Titanium	Balance (99.3 approx.)

*Analysis and material supplied by Air Force Materials Laboratory,
Wright-Patterson Air Force Base, Ohio. Nominal thickness 0.004 inch.
Commercial designation: Ti-75A.

The chemical analyses for these lots of Ti-6Al-4V alloy are presented in Tables VI, VII, and VIII. Finally, the AFML supplied one lot of each of the beta-stabilized alloys in sheet form: 0.040-inch (0.101 cm) thick Ti-8Mn and 0.048-inch (0.122 cm) thick β -III (Ti-11.5Mo-6Zr-4.5Sn) alloy. The chemical analyses of these materials are presented in Tables IX and X, respectively.

The specimen design used here was that adopted in previous studies (ref. 10) in which the specimen is essentially a flat strip 1 cm wide by 5 cm long. Specimen blanks of these dimensions were machined from the specimen stock and were subsequently provided with mounting holes as shown in Figure 1. Following the machine operations, each specimen was successively polished with 180-, 240-, 320-, 400-, and 600-grit silicon carbide metallographic papers using paraffin-saturated kerosene as a lubricant and with care being taken to "cross" the scratch directions between successive grits. After the specimens had been determined to be mechanically polished to a satisfactory degree, they were cleaned in acetone and absolute ethanol and were then stored in air-tight flasks for future use.

2. HEATING AND RECORDING EQUIPMENT

During the course of this research, two types of oxidation apparatus were employed: a conventional air furnace and a specially-constructed volumetric apparatus.

2a. AIR FURNACE

The furnace used in the early experiments was a wire-wound vertical tube-type having a Mullite Type MV-30 reaction tube. This unit was capable of continuous operation at approximately 1000°C and was controlled to within approximately $\pm 3^\circ\text{C}$ of the set-temperature by a Wheelco Model 401 "on-off" type controller. The atmosphere contained within the reaction

TABLE VI
CHEMICAL ANALYSIS OF TITANIUM - 6% ALUMINUM - 4% VANADIUM ALLOY (TYPE 1)*

Element	Weight Percent
Non-metallic	
Carbon	0.015
Hydrogen	0.000(3)
Nitrogen	0.009
Oxygen	0.135
Metallic	
Aluminum	6.1
Vanadium	3.9
Boron	0.000(3)
Calcium	0.030
Chromium	0.002
Copper	0.010
Iron	0.140
Lead	0.003
Magnesium	0.005
Manganese	0.005
Molybdenum	0.005
Nickel	0.002
Silicon	0.020
Tantalum	0.010
Tin	0.002
Tungsten	0.002
Zirconium	0.003
Titanium	Balance (89.5 approx.)

*Analysis and material supplied by Air Force Materials Laboratory,
Wright-Patterson Air Force Base, Ohio. Nominal thickness 0.064 inch.
AFML #1345, vacuum treated at 1725°F for one hour.

TABLE VII

CHEMICAL ANALYSIS OF TITANIUM - 6% ALUMINUM - 4% VANADIUM ALLOY (TYPE 2)*

Element	Weight Percent
Non-metallic	
Carbon	0.012
Hydrogen	0.000(3)
Nitrogen	0.013
Oxygen	0.103
Metallic	
Aluminum	6.1
Vanadium	3.8
Boron	0.000(3)
Calcium	0.030
Chromium	0.002
Copper	0.010
Iron	0.100
Lead	0.002
Magnesium	0.005
Manganese	0.010
Molybdenum	0.010
Nickel	0.002
Silicon	0.010
Tantalum	0.010
Tin	0.002
Tungsten	0.002
Zirconium	0.001
Titanium	Balance (89.8 approx.)

*Analysis and material supplied by Air Force Materials Laboratory, Wright-Patterson Air Force Base. Nominal thickness 0.086 inch. AFML #1346, vacuum treated at 1725°F for one hour.

TABLE VIII

CHEMICAL ANALYSIS OF TITANIUM - 6% ALUMINUM - 4% VANADIUM ALLOY (TYPE 3)*

Element	Weight Percent
Non-metallic	
Carbon	ND
Hydrogen	ND
Nitrogen	0.011
Oxygen	0.120
Metallic	
Aluminum	5.3
Vanadium	4.2
Boron	0.010
Chromium	0.002
Copper	0.0015
Iron	0.150
Lead	0.002
Magnesium	0.004
Manganese	0.005
Molybdenum	0.004
Nickel	0.002
Silicon	0.030
Tin	0.006
Tungsten	0.002
Zirconium	<0.001
Titanium	Balance (90.2 approx.)

*Analysis and material supplied by Air Force Materials Laboratory,
Wright-Patterson Air Force Base, Ohio. Nominal thickness 0.010 inch.

TABLE IX

CHEMICAL ANALYSIS OF TITANIUM - 8% MANGANESE ALLOY*

Element	Weight Percent
Non-metallic	
Carbon	0.029
Hydrogen	0.0083
Nitrogen	0.012
Oxygen	0.118
Metallic	
Manganese	7.5
Aluminum	0.006
Boron	0.006
Chromium	0.002
Copper	0.0015
Iron	0.230
Lead	0.002
Magnesium	0.003
Molybdenum	0.002
Nickel	0.010
Silicon	0.010
Tin	0.002
Tungsten	0.002
Zirconium	<0.001
Titanium	Balance (92.1 approx.)

* Analysis and material supplied by Air Force Materials Laboratory,
Wright-Patterson Air Force Base, Ohio. Nominal thickness 0.040 inch.

TABLE X
CHEMICAL ANALYSIS OF TITANIUM B - III ALLOY (Ti - 11.5% Mo - 6% Zr - 4.5% Sn)*

Element	Weight Percent
Non-metallic	
Carbon	0.013
Hydrogen	0.0122
Nitrogen	0.008
Oxygen	0.167
Metallic	
Iron	0.04
Molybdenum	11.52
Tin	5.08
Zirconium	5.56
Titanium	Balance (77.6 approx.)

*Analysis and material supplied by Air Force Materials Laboratory,
Wright-Patterson Air Force Base, Ohio. Nominal thickness 0.048 inch.
Solution heat treated 1325°F - 3 minutes, fast cool.

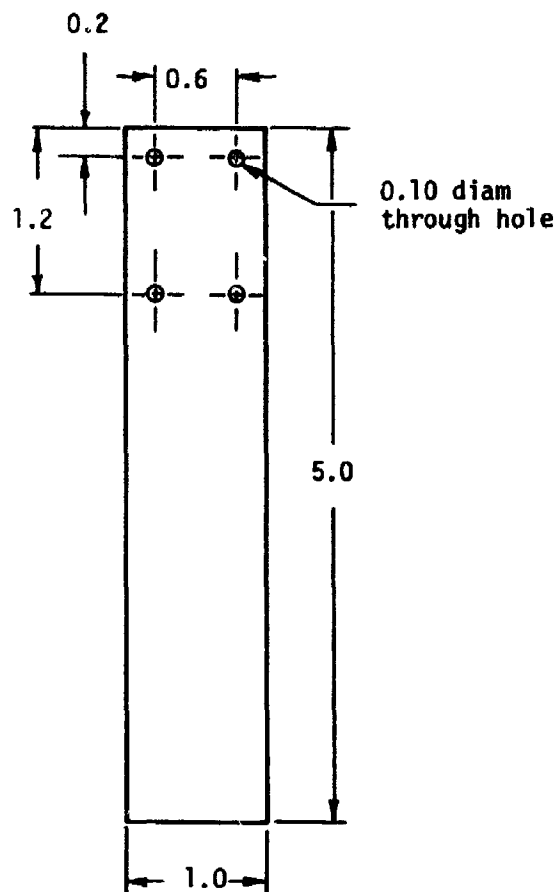


Figure 1. - Flat specimen design used for titanium specimens. All dimensions are in cm. Specimen thickness is determined by available sheet thicknesses.

tube was ambient air and was nearly stagnant as vertical convection was purposely limited by a shaped magnesia plug.

Through the magnesia plug at the top of the furnace tube passed an insulated chromel-alumel thermocouple which acted both as a temperature sensor and as a specimen support. During specimen exposures, the thermocouple signal was input to a recorder so that both the average heating rate (non-linear) and the maximum temperature was determinable.

Primary temperature measurement was made using a Leeds and Northrup Model 8662 portable precision potentiometer equipped with a cold junction compensation. This instrument was, in turn, used to calibrate a Honeywell Model Electronik-19 strip chart recorder with a time-based chart drive. Analyses of data so derived indicated that average heating rates ranged from 60 to 80°C per second for the range of maximum temperatures investigated: 800° to 1000°C.

2b. VOLUMETRIC APPARATUS

A major portion of the tests conducted during the course of this research involved an apparatus with a fixed internal volume. A portion of that volume consisted of a Vycor reaction tube approximately 600 mm in length and having an inside diameter of approximately 19 mm. Subsequent to the emplacement of the metallic specimen, the recording thermocouple, and the control thermocouple within this reaction tube, the system was evacuated and then back-filled with a reactive gas; usually oxygen at 0.262 atm (200 torr). Thermal energy was supplied to the specimen in a controlled manner by a six-element infrared furnace whose focused radiation passed through the transparent walls of the Vycor tube. Proper manipulation of the furnace controller subjected the specimen to a preselected time-temperature program. During the course of heating, the gas-metal

reaction proceeded and produced within the fixed volume of the system a pressure decrement which was sensed by a pressure transducer. Time-based graphic records of the specimen temperature, system pressure, and furnace voltage provided the records from which analyses of the gas-metal reaction were made.

The schematic diagram of Figure 2 and the photograph of Figure 3 illustrate the volumetric apparatus and its interconnection with auxiliary pieces of equipment. The numbered blocks on the schematic diagram of Figure 2 correspond to the major equipment and the accessory items listed below:

- 1) a custom-designed 12-KW Fostoria-Fannon quartz-tube furnace, used to heat the specimen within the reaction chamber,
- 2) a controller for item (1) with integral temperature programming capability.
- 3) a "Vycor" reaction tube, concentric with the centerline of the quartz-tube furnace and attached to the manifold system by "Swagelok" fittings with "Teflon" seals,
- 4) a Statham Model PM 180 TC pressure transducer (± 25 psig) complete with bridge amplifier, used to monitor pressure changes incurred by the gas-titanium reactions,
- 5) a Fisher "Roll-Around" portable vacuum pump, complete with "folded" mercury manometer for calibration of system pressures at levels between 10 and 760 torr,
- 6) a Honeywell type "Electronic 194" two-pen chart recorder used to monitor pressure and temperature simultaneously and on a common time base,
- 7) a stainless steel (Type 316) manifold fabricated using "Swagelok" fittings, "Nupro" high-vacuum valves, and a Helicoid Model 440 (SS-316) compound indicating gauge,

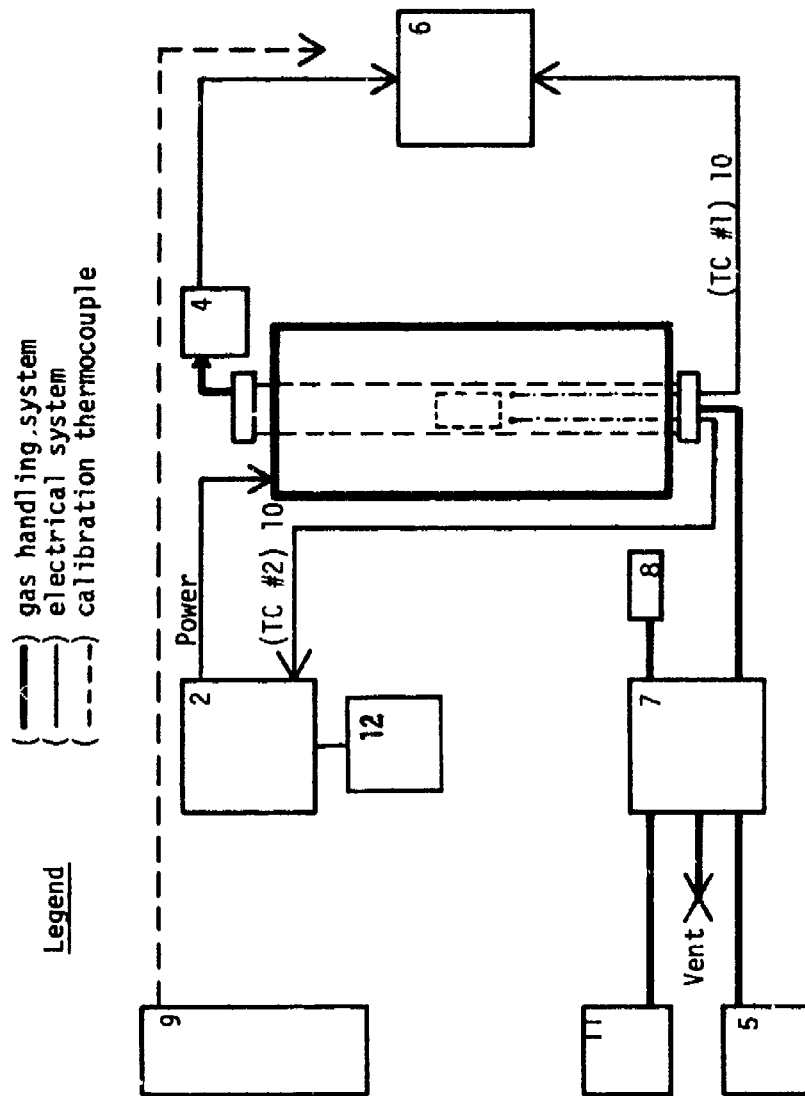


Figure 2. - Schematic diagram of the equipment complement to be used in oxidation research. Numbered items correspond to those called out in this section of the text.

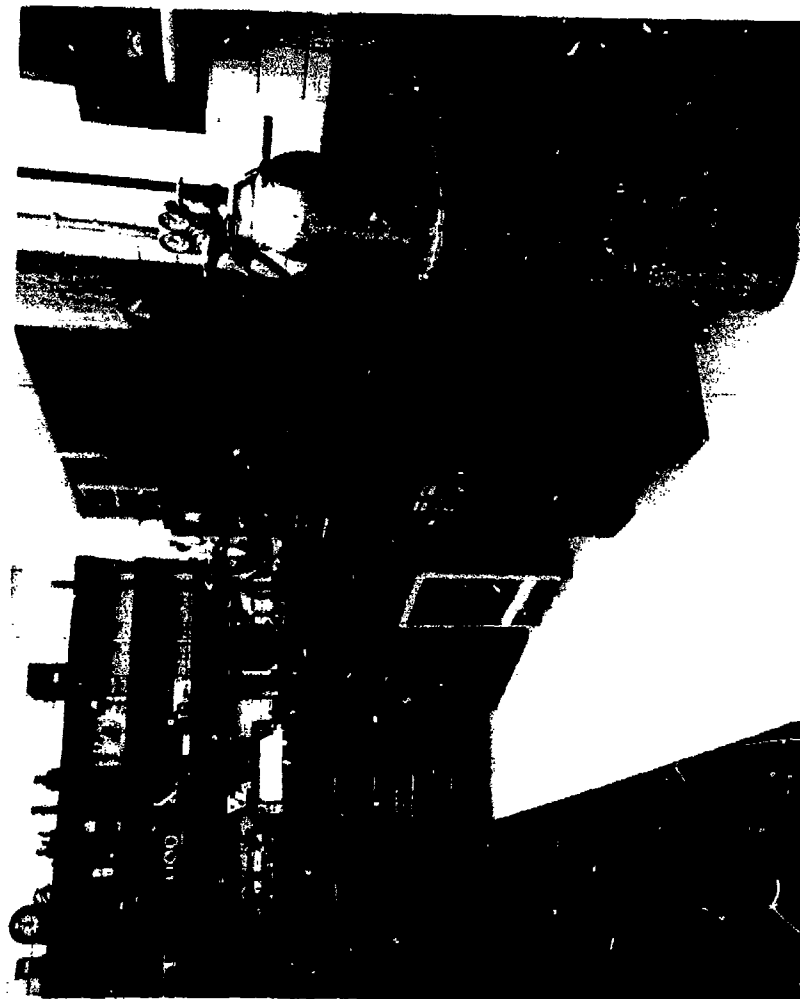


Figure 3. - Volumetric equipment used in oxidation testing.

8) a valved, fixed volume attachment to the manifold (64.5 ± 0.25 ml) for calibration of total system volume,

9) a Leeds and Northrup Model 8662 research potentiometer for use in thermal calibration procedures,

10) two platinum versus platinum-13% Rhodium (Pt vs. Pt-13%) thermocouples with high-purity alumina insulators for the purpose of supplying temperature analog signals to the recorder (item 6) and furnace controller (item 2),

11) tanks of dried gases (oxygen, nitrogen, and helium) complete with Matheson Model 19-540 metal diaphragm pressure regulators, and

12) a Honeywell type "Electronic 19" single-pen chart recorder used to monitor voltage to the heating elements of the infrared furnace.

Figure 4 illustrates the quartz-tube infrared furnace in the open position with the Vycor reaction tube, recording and control thermocouples, and specimen in place. The specimen is secured to the alumina insulators of the thermocouple assembly by relatively inert platinum wires. This assembly is illustrated in the photograph of Figure 5. In normal operation, the recording and control thermocouples are placed in the immediate vicinity of the specimen surface, as opposed to being spot-welded to it. Special tests were conducted using welded thermocouples for the purpose of validating this near-surface mode of thermocouple operation.

Because the volumetric apparatus is essentially a fixed-volume system, it is necessary to experimentally determine the effective volume of this system in order to translate observed pressure changes into quantities of gas consumed during reaction with titanium. The technique employed in this volume determination is described in Appendix I. Graphical analyses of pressure change data, induced by connecting the calibration volume to the system volume, indicated that the room temperature system volume (V_s)

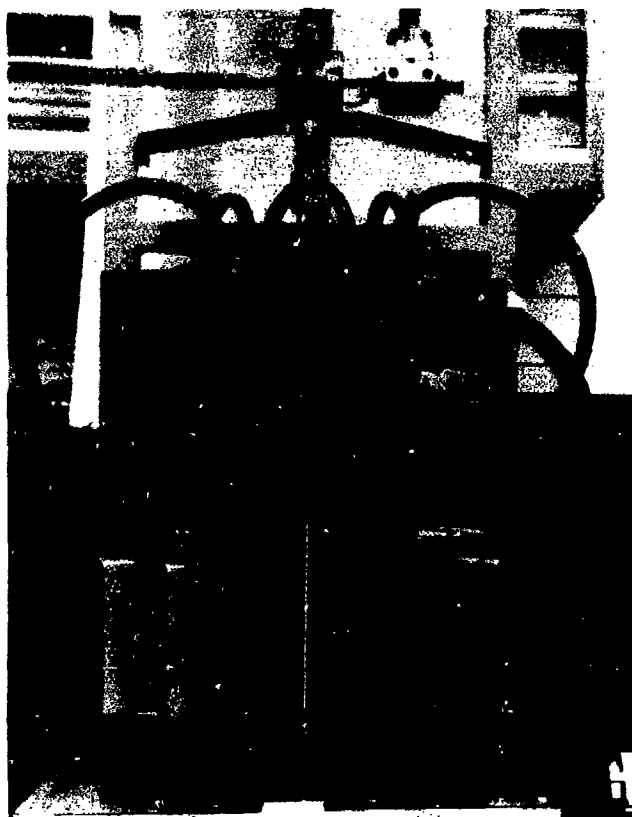


Figure 4. - Photograph of the 12-KW quartz-tube furnace illustrating the Vycor reaction tube, thermocouple and specimen positioning.

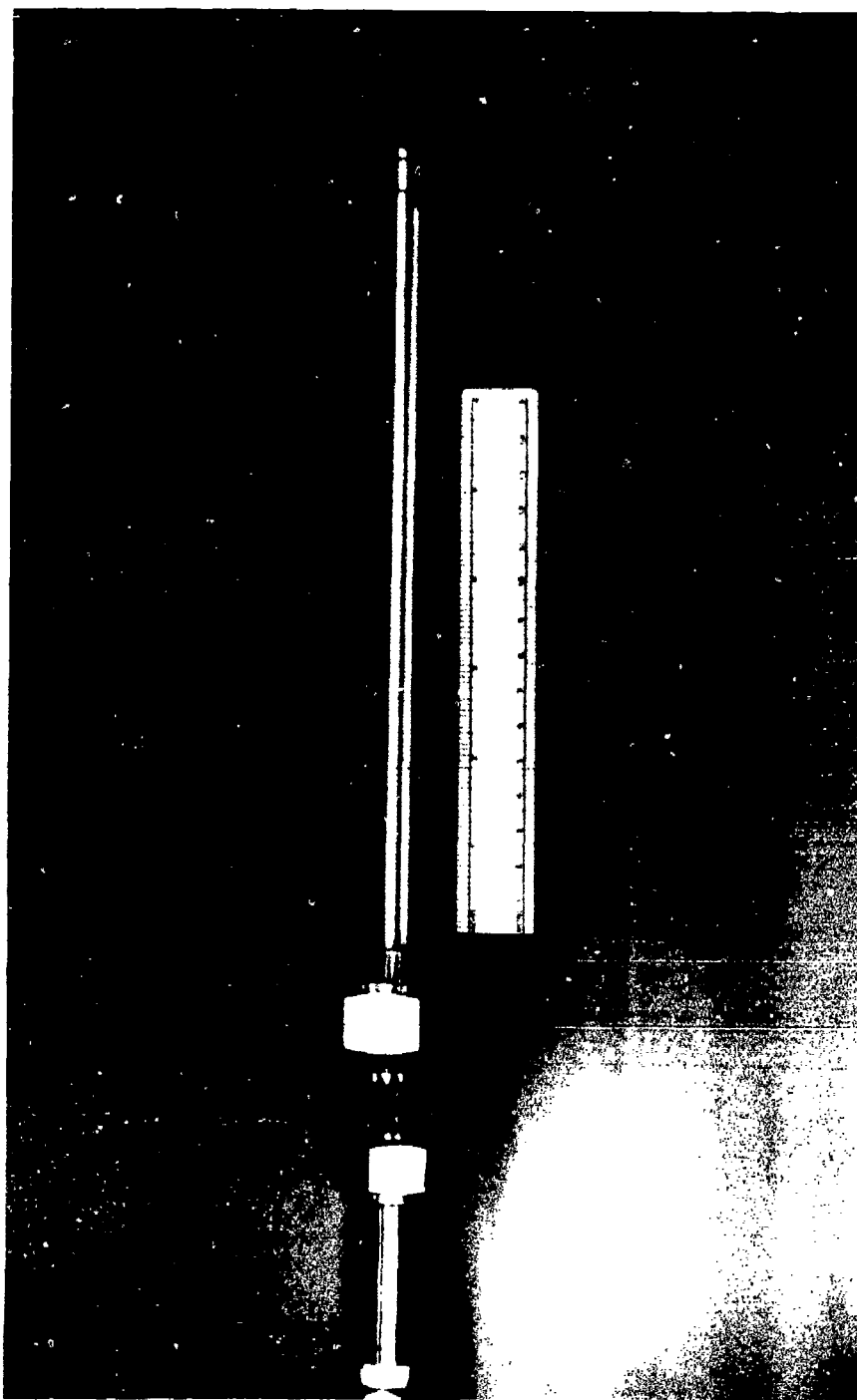


Figure 5. - Overall view of thermocouple assembly and mounted specimen.

was 559 ml. It is implicitly assumed in later calculations that this volume remains fixed during all heating cycles.

The quartz-tube furnace has been programmed and operated to provide closed-loop controlled heating rates from $1/2^{\circ}\text{C}$ per second to 8°C per second using flat titanium specimens. For this range of heating rates, truly linear heating has been closely approximated by programmer compensation for the non-linear electromotive force-temperature curve of the Pt vs. Pt-13% Rh thermocouples. Rates of heating greater than 8°C per second have been achieved by open-loop operation of the system wherein the voltage to the furnace is manually controlled. This mode of operation is necessary because, at faster heating rates, the thermal inertia of the specimen generated a lag time in excess of the programmed time associated with heating the specimen from ambient temperature to the maximum temperature.

Subsequent to reaching the maximum temperature, the specimen temperature was controllable to ± 0.05 mv or approximately $\pm 4^{\circ}\text{C}$. This magnitude of variation is within that normally encountered in high-temperature oxidation research. Most of the experimental problems associated with such heating and holding (ramp-hold) cycles involve the tendency for "temperature overshoot" just subsequent to the end of the heating (ramp) section of the desired temperature program. Because of the temperature sensitivity of oxidation reactions, no data is reported where an overshoot in excess of approximately 15°C was experienced.

The volumetric testing equipment was constructed so as to sense and record the pressure changes induced by the fixing of oxygen in its reaction with titanium. The system is normally operated at a pressure of 0.262 atm (200 torr gas) with the pressure transducer output continuously

available to the time-based two-pen recorder. The recorder scale may be expanded to provide a meaningful record over the pressure range from approximately 10 to 500 torr. The precision of this graphic pressure display is approximately 1 torr which corresponds to a change in system gas content of approximately 2.8×10^{-5} mole. For the flat specimens used in these experiments, the projected geometric area is approximately 10 cm^2 ; thus, the precision of detection is approximately $2.8 \text{ } \mu\text{-mole/cm}^2$. From the conversions given in Appendix II, this initial precision may be expressed either in terms of weight gain as $0.0898 \text{ mg O}_2/\text{cm}^2$, or in terms of uniform oxide thickness (TiO_2) as $0.52 \text{ } \mu\text{m}$ ($5200 \text{ } \text{\AA}$).

The voltage applied to the quartz-tube elements of the infrared furnace was monitored by a time-based strip chart recorder. The chart speed of the voltage recorder was kept in a 1-to-1 coincidence with the recorder measuring pressure and temperature changes. In this way, a direct comparison between temperature, pressure, and voltage could be made for any given test. Because of the electronic anticipation circuitry of the power controller, any rapid changes in the thermal behavior of the specimen are clearly discernible on the voltage-time record. It was noted that when specimen reactions involve vaporization and subsequent deposition of material on the reaction tube walls, then they give rise to characteristic slow increases in the voltage delivered to the furnace windings.

3. METHODS OF DATA ANALYSIS

During the course of this research, four basic types of analyses were conducted which involved specimen exposure under oxidizing conditions. These include: macroscopic analyses, microscopic analyses, gas uptake analyses, and energy coupling analyses.

The dimensions and mass of all test specimens were determined both prior to and subsequent to exposure in the air furnace or the volumetric apparatus. Machinist's micrometers were used to determine lengths to the nearest 0.0001 in (0.00025 cm) and a Mettler Type H-6 analytical balance was used to determine mass to the nearest 0.2 mg. The general character and color oxide films or scales formed during exposure of the test specimen were determined by visual inspection and noted.

Both the as-received materials and several selected test specimens were prepared for microscopic metallographic analyses using conventional techniques. Metallographic sections were inspected and photographed using a Bausch and Lomb "Dynazoom" metallurgical microscope and a limited number of photomicrographs were taken using this instrument. The details of modified metallographic specimen preparation technique are presented in Appendix III.

In operation of the volumetric apparatus to determine gas uptake, a continuous time-based recording of both specimen temperature and system pressure was made. The major classes of thermal programs which were explored were: 1) ramp-hold-cool (RHC) tests, 2) ramp-cool (RC) or cyclic tests, and 3) ramp-ignition (I) tests. Of these, only the first was treated quantitatively with regard to oxygen consumption during the course of the gas-metal reaction.

After loading and leak-checking the volumetric apparatus, both pressure and temperature calibrations were made prior to each test. The volumetric oxidation tests were normally initiated with the system at ambient temperature and with a gas pressure level at 200 torr*. Each test involved a

*Oxygen, nitrogen, helium, and their mixtures have been used as working gases in this apparatus.

"specimen pair" (two separate runs): first, the empty system which constituted a "calibration specimen", and then a reactive titanium specimen. The degree of gas consumption as a function of time $\{\delta n(t)\}$ was determined from the graphic pressure records by a technique outlined in Appendix IV.

The furnace voltage at the quartz-tube heating elements was continuously monitored and this information was used to estimate the amount of power delivered to the specimen and thereby to obtain a qualitative idea of the efficiency of coupling of the infrared energy to the specimen. The power delivered to the furnace, and therefore to the specimen is qualitatively proportional to the square of the applied voltage which is here defined as the power index (W). The use of this index implicitly assumes that the furnace was operating in near steady-state condition such that the temperature, and therefore the resistance, of the heater wires is approximately a constant value. The maximum values of (W) observed, (W_{max}), and the values of (W) observed 5 minutes after maximum temperature, (W_5), had been obtained, are used as parameters to describe the efficiency of coupling of infrared energy to the oxidizing specimens.

4. TESTS PERFORMED

4a. AIR FURNACE

The conventional air furnace was employed to conduct two types of oxidation tests in air using 9 flat titanium specimens. The conditions imposed upon the various specimens used in these tests are described and presented in Table XI. The following types of tests were conducted: 1) tests in which the specimen was intentionally cycled between predetermined temperature limits designated as RC (ramp-cool) tests, and 2) tests in which the specimen temperature was essentially constant after the heating period and during its fraction with air; designated as RHC (ramp-hold-cool) tests.

TABLE XI

OXIDATION TESTS PERFORMED IN THE
AIR FURNACE USING UNALLOYED TITANIUM (TYPE 1) SPECIMENS

Specimen Number	Test Type	Maximum Temperature ($^{\circ}\text{C}$)	Holding Time (hrs)
05162	RHC	1000	1
05011	RHC	1000	4
05072	RHC	1000	16
05081	RHC	1000	64
05171	RHC	800	4
05161	RHC	850	4
05151	RHC	900	4
05141	RHC	950	4
05021	RC	1000	*

* Cyclic heating for 4 hours; 20 minutes per cycle; 12 cycles.

Cyclic testing involved the heating of titanium specimens over the temperature range from 25° to 1000°C with a cycle period of approximately 20 minutes. In those tests which were nearly isothermal in character, specimens were heated to temperatures of 800°, 850°, 900°, 950°, and 1000°C for periods ranging from 1 to 64 hours. The nominal linear heating rates for these specimens was approximately 6° to 8°C per second.

In the analyses of the above specimens, emphasis was placed upon the determination of dimensional and weight changes and upon securing information regarding microstructural changes in the metallic substrate.

4b. VOLUMETRIC HEATING APPARATUS

The volumetric oxidation apparatus was employed to conduct basically the same two types of oxidation tests described in the section above; however, certain of those tests led to ignition. In all cases, flat titanium specimens were used for the test specimens and in most cases these specimens were heated in pure oxygen at a pressure of 200 torr; however, other gases, gas mixtures, and gas pressures were also employed. Specimens were heated at various preselected controlled rates ranging from 0.5°C/s to approximately 100°C/s. The course of the oxidation reaction for these specimens was followed from the commencement of the heating operation for times of up to approximately 60 minutes. Shorter test times were necessary in those cases where the subject reactions took place rapidly.

In Table XII are listed: the specimen number (our reference) the type of titanium specimens used (refer to Table I through X), and the experimental parameters investigated. The majority of the 87 tests conducted were of the (RHC) variety, only 7 being of cyclic (RC) nature. The oxidizing gases used included: oxygen, nitrogen, oxygen-nitrogen mixtures, oxygen-helium mixtures, and nitrogen-helium mixtures with all but one test being conducted at 200 torr

TABLE XII

TITANIUM OXIDATION TESTS PERFORMED USING THE VOLUMETRIC HEATING APPARATUS

Specimen Number	Test Atmosphere	Heating Rate (°C/S)	Maximum Temperature (°C)	Cooling Rate (°C/S)	Holding Time (min)	Remarks
A. UNALLOYED TITANIUM (TYPE 1); TEST TYPE (RHC)						
06051	200 torr O ₂	0.5	1000	8	60	
06141	200 torr O ₂	0.5	1000	0.5	60	
06132	200 torr O ₂	8	1000	8	60	
06133	200 torr O ₂	25	1000	8	60	
06131	200 torr O ₂	0.5	1100	8	60	
06071	200 torr O ₂	8	1100	8	60	
06142	200 torr O ₂	22	1100	8	60	
08012	200 torr O ₂	0.5	1200	8	60	
08013	200 torr O ₂	7.5	1200	8	27	Gas consumed
07091	200 torr O ₂	4	~ 1300	8	~ 4.5	Gas consumed not strictly isothermal
07311	200 torr N ₂	8	1000	8	60	

TABLE XII - continued

Specimen Number	Test Atmosphere	Heating Rate (°C/S)	Maximum Temperature (°C)	Cooling Rate (°C/S)	Holding Time (min)	Remarks
07312	200 torr N ₂	8	1100	8	60	
07313	200 torr O ₂ + 200 torr N ₂	8	1000	8	60	
08011	200 torr O ₂ + 200 torr N ₂	8	1100	8	60	
08021	200 torr O ₂ + 200 torr He	8	1000	0.5	60	
08171	200 torr O ₂ + 200 torr He	8	1100	0.5	60	
08023	200 torr N ₂ + 200 torr He	8	1000	0.5	60	
09051	200 torr N ₂ + 200 torr He	8	1100	0.5	60	
B. UNALLOYED TITANIUM (TYPE 1); TEST TYPE (RC)						
07101	200 torr O ₂	8	1000	8		Cycled from 800°C for 49 min
07261	200 torr O ₂	8	1100	8		Cycled from 900°C for 62 min
09052	200 torr O ₂	22	1100	8		Cycled from 25°C once; SEM specimen

TABLE XII - continued

Specimen Number	Test Atmosphere	Heating Rate (°C/S)	Maximum Temperature (°C)	Cooling Rate (°C/S)	Holding Time (min)	Remarks
C. UNALLOYED TITANIUM (TYPE 2); TEST TYPE (KHC)						
09191	200 torr O ₂	8	1000	0.5	60	
09192	400 torr O ₂	8	1000	0.5	60	
401151	200 torr O ₂	8	1100	0.5	60	
405151	200 torr O ₂	8	1100	0.5	60	87% cold worked
405221	200 torr O ₂	~10	1100	0.5	56	87% cold worked
408191	200 torr O ₂	22	1100	0.5	60	76% cold worked
408141	200 torr O ₂	22	1100	0.5	60	61% cold worked
09193	200 torr N ₂	8	1000	0.5	60	
402192	200 torr N ₂	8	1100	0.5	60	Synergism test
402281	200 torr N ₂	8	1100	0.5	60	Synergism test
402193	100 torr O ₂ + 100 torr N ₂	8	1100	0.5	60	Synergism test
402194	50 torr O ₂ + 150 torr N ₂	8	1100	0.5	60	Synergism test
121101	200 torr O ₂	8	1100	8	10	Welded Thermocouple

TABLE XII - continued

Specimen Number	Test Atmosphere	Heating Rate ($^{\circ}\text{C}/\text{S}$)	Maximum Temperature ($^{\circ}\text{C}$)	Cooling Rate ($^{\circ}\text{C}/\text{S}$)	Holding Time (min)	Remarks
121201	200 torr O_2	8	1100	8	60	X-Ray Examination
401021	200 torr O_2	8	1100	8	60	Reoxidized X-Ray Exam.
D. UNALLOYED TITANIUM (TYPE 2); TEST TYPE (RC)						
408151	200 torr O_2	0.5	1100	8		for SEM*
11141	200 torr O_2	8	1100	0.5 to 25°C	5	3 cycles: 600-grit
11151	200 torr O_2	8	1100	0.5 to 25°C	5	3 cycles: 600 grit
11142	200 torr O_2	8	1100	0.5 to 25°C	5	3 cycles: 1 μm
E. UNALLOYED TITANIUM (TYPE 2); TEST TYPE (I)						
405141	200 torr O_2	100	--	8	N/A	87% cold worked
405142	200 torr O_2	100	--	8	N/A	87% cold worked

*Cycled from 25°C once; SEM Specimen

TABLE XII - continued

Specimen Number	Test Atmosphere	Heating Rate (°C/S)	Maximum Temperature (°C)	Cooling Rate (°C/S)	Holding Time (min)	Remarks
F. UNALLOYED TITANIUM (TYPE 3); TEST TYPE (RHC)						
C9194	200 torr O ₂	8	1000	0.5	50	39% cold worked
11201	200 torr O ₂	8	1100	0.5	60	
405021	200 torr O ₂	8	1100	0.5	60	
405023	200 torr O ₂	5.9	1200	0.5	10	
G. UNALLOYED TITANIUM (TYPE 4); TEST TYPE (RHC)						
407162	200 torr O ₂	8	1100	0.5	53	
H. UNALLOYED TITANIUM (TYPE 4); TEST TYPE (I)						
406103	200 torr O ₂	100	--	8	N/A	
I. UNALLOYED TITANIUM (TYPE 5); TEST TYPE (RHC)						
408143	200 torr O ₂	8	1100	0.5	43	
408282	200 torr O ₂	~18	1100	0.5	23	
J. UNALLOYED TITANIUM (TYPE 5); TEST TYPE (I)						
408281	200 torr O ₂	28	--	8	N/A	

TABLE XII - continued

Specimen Number	Test Atmosphere	Heating Rate (°C/S)	Maximum Temperature (°C)	Cooling Rate (°C/S)	Holding Time (min)	Remarks
408271	200 torr O ₂	58	--	8	N/A	
408272	200 torr O ₂	58	--	8	N/A	
408273	200 torr O ₂	58	--	8	N/A	
406101	200 torr O ₂	100	--	8	N/A	
406102	200 torr O ₂	100	--	8	N/A	
K. TITANIUM - 6% ALUMINUM - 4% VANADIUM (TYPE 1); TEST TYPE (RHC)						
407161	200 torr O ₂	8	1000	0.5	60	milled from .152 cm to .119 cm
401161	200 torr O ₂	0.5	1100	0.5	60	
401091	200 torr O ₂	0.5	1100	0.5	60	
11202	200 torr O ₂	8	1100	0.5	60	
405071	200 torr O ₂	8	1100	0.5	25	milled from .152 cm to .119 cm
405072	200 torr O ₂	8	1100	0.5	60	milled from .152 cm to .119 cm
401092	200 torr O ₂	22	1100	0.5	60	

TABLE XII - continued

Specimen Number	Test Atmosphere	Heating Rate (°C/S)	Maximum Temperature (°C)	Cooling Rate (°C/S)	Holding Time (min)	Remarks
407243	200 torr O ₂	5.9	1200	0.5	15	milled from .152 cm to .119 cm
408081	200 torr O ₂	5.9	1200	0.5	15	milled from .152 cm to .119 cm
401162	200 torr N ₂	8	1100	0.5	60	
	L. TITANIUM - 6% ALUMINUM - 4% VANADIUM (TYPE 2); TEST TYPE (RHC)					
402042	200 torr O ₂	0.5	1100	0.5	60	
401152	200 torr O ₂	8	1100	0.5	50	
402043	200 torr O ₂	22	1100	0.5	60	
	M. TITANIUM - 6% ALUMINUM - 4% VANADIUM (TYPE 3); TEST TYPE (RHC)					
406171	200 torr O ₂	8	1100	0.5	60	
	N. TITANIUM - 6% ALUMINUM - 4% VANADIUM (TYPE 3); TEST TYPE (I)					
406104	200 torr O ₂	100	--	8	N/A	
	O. TITANIUM - 8% MANGANESE; TEST TYPE (RHC)					
406032	200 torr O ₂	8	1000	0.5	60	
405074	200 torr O ₂	0.5	1100	0.5	35	

TABLE XII - continued

Specimen Number	Test Atmosphere	Heating Rate (°C/S)	Maximum Temperature (°C)	Cooling Rate (°C/S)	Holding Time (min)	Remarks
405073	200 torr O ₂	8	1100	0.5	41	
406031	200 torr O ₂	22	1100	0.5	50	
407242	200 torr O ₂	5.9	1200	0.5	14	
P. TITANIUM - 8% MANGANESE ; TEST TYPE (I)						
409172	200 torr O ₂	75	--	8	N/A	milled and polished to .0251 cm
409192	200 torr O ₂	48	--	8	N/A	milled and polished to .0279 cm
409232	200 torr O ₂	53	--	8	N/A	milled and polished to .0343 cm
Q. TITANIUM β - III; TEST TYPE (RHC)						
406191	200 torr O ₂	8	1000	0.5	60	
406174	200 torr O ₂	0.5	1100	0.5	26	
406173	200 torr O ₂	8	1100	0.5	22	
406175	200 torr O ₂	22	1100	0.5	21	
409231	200 torr O ₂	22	1100	0.5	23	milled and polished to .0330 cm

TABLE XII - continued

Specimen Number	Test Atmosphere	Heating Rate (°C/S)	Maximum Temperature (°C)	Cooling Rate (°C/S)	Holding Time (min)	Remarks
407241	200 torr O ₂	5.9	1200	0.5	12	
		R. TITANIUM β - III; TEST TYPE (I)				
409171	200 torr O ₂	82	--	8	N/A	milled and polished to .0239 cm
409191	200 torr O ₂	72	--	8	N/A	milled and polished to .0287 cm

oxygen pressure. Most of these tests were conducted using holding temperatures of 1000° or 1100°C and holding times of 60 minutes. Tests at higher temperatures, 1100° to 1300°C were in some cases terminated prior to 60 minutes because the oxygen within the system had been consumed. In certain instances, the cooling rate was intentionally slowed from the natural condition (approximately 8°C per second) to a rate of 0.5°C per second in an attempt to provide oxide adherence subsequent to complete cooling; primarily for the purpose of metallographic examination. Other exploratory investigations involved post-reaction x-ray diffraction and microhardness examinations, calibration-type experiments, and the variation of specimen-associated parameters including: surface finish, thickness, and degree of cold work.

SECTION III

RESULTS AND DISCUSSION

1. APPEARANCE AND DIMENSIONAL CHANGE OF EXPOSED SPECIMENS

In this section are presented the macroscopic dimensional character of titanium-base specimens and the visual appearance of these specimens, primarily in terms of the oxide layers developed upon them. The identification numbers of the unalloyed titanium specimens used and the conditions to which they were exposed have previously been presented in Tables XI and XII for the conventional and volumetric apparatus, respectively.

In the high-temperature scaling range investigated (800° to 1300°C), interpretation of dimensional data is somewhat complex. The reaction between titanium and a reactive gas requires that some of the metal be consumed during the course of the reaction and further, that the metal compound be formed on or near the metal surface. As a direct result of this, total dimensional changes represent the summation of metal thickness decrements and compound thickness increments in addition to any "second order" effects such as those arising from solution of oxygen. Because the emphasis of this research program is centered upon only the earliest stages of gas-metal interaction, little effort has been placed on the analysis of longer-term dimensional data evolved during the course of these experiments.

1a. AIR FURNACE

The dimensional changes and appearance of unalloyed titanium (Type 1) specimens induced by oxidation in air and using the conventional heating apparatus are presented in Table XIII. The upper portion of this table indicates these qualities are affected by the duration of oxidation in stagnant air at 1000°C. Ideally the change (increase) in each of the

TABLE XIII
DIMENSIONAL CHANGES AND APPEARANCE OF TITANIUM (TYPE 1) SPECIMENS
OXIDIZED IN AIR USING THE AIR FURNACE

Specimen Number	Length (cm)		Width (cm)		Thickness (cm)		Specimen Appearance			
	Initial	Final	Initial	Final	Initial	Final				
05162	4.973	4.994	.021	.988	1.00	.012	.160	.175	.015	oxide brownish yellow & spalls in medium sized pieces
05011	4.989	5.042	.053	.992	1.03	.038	.165	.189	.024	as above
05072	4.989	5.049	.060	.996	1.04	.044	.162	.198	.036	oxide brownish yellow; very little spalling
05021	4.978	5.154	.176	.986	1.12	.134	.161	.296	.135	oxide black; no spalling
05171	4.986	4.989	.003	.988	.991	.003	.147	.147	.0	oxide bluish grey; no spalling; 800°C.
05161	4.983	4.989	.006	.991	.991	0	.159	.161	.002	oxide yellow; spalls in medium sized pieces; 850°C.
05151	4.983	5.011	.028	.993	1.00	.007	.161	.168	.007	oxide yellow; no spalling but oxide can be peeled off one piece per side; 900°C.
05141	4.989	5.019	.030	.993	1.01	.017	.162	.180	.018	as above; 950°C.
05021	4.990	5.009	.019	.992	.993	.001	.162	.152	-.010	oxide brownish yellow; spalling in small pieces during cooling cycle; 25° to 1000°C.

three macroscopic dimensions should be the same barring experimental difficulties associated with scale spalling and diffusion-related end effects. It is seen that the ideal case is met only semiquantitatively, in that the observed length and width changes are greater than thickness changes. The deviations from ideallity are probably due to the causes mentioned above. These same four specimens, if oxidizing under ideal parabolic conditions, should exhibit dimensional changes in the ratio 1:2:4:8; i.e., in proportion to the square root of the exposure time: $(1)^{\frac{1}{2}}:(4)^{\frac{1}{2}}:(16)^{\frac{1}{2}}:(64)^{\frac{1}{2}}$, as the tabular entries are read from top to bottom. Agreement with ideallity is again only semiquantitative but does exhibit a distinct trend for unusually large values of dimensional change after 64 hours of oxidation. The effect is believed to occur because the operational rate law is a paralinear one rather than a purely parabolic one; see (ref. 2).

The lower portion of Table XIII indicates the dimensional and appearance changes incurred by oxidation in air for 4 hours at temperatures of 800°, 850°, 900°, and 950°C, respectively. Ideally, the dimensional changes should increase exponentially for all macroscopic dimensions if the rate of reaction is governed by an Arrhenius relationship. This trend is indicated qualitatively; however, spalling of the oxide has influenced some of these data.

With regard to specimen appearance, there is a regular progression of color change as the degree of oxidation in air increases from the 4-hour test at 800°C to the 4-hour test at 950°C and through the 64-hour test at 1000°C. From the earliest stage of reaction investigated (800°C - 4 hours), the color sequence observed with increasing exposure is: blue-grey to yellow to brownish-yellow to black and represents, essentially, the appearance of the external surface of the oxide. These observations

appear to match very closely the color sequence observed under similar conditions by Morton and Baldwin (ref. 11). Spalling behavior appears to exhibit a retrograde behavior in the neighborhood of the titanium $\alpha - \beta$ transformation. At temperatures below and above this transformation, no spalling occurs; near the transformation (850°C), limited spalling is observed. The phenomenon may be associated with dilatations on the metal as it passes through the temperature (or temperature range) of transformation. As the degree of scaling becomes very large and the scale accrues mechanical strength, e.g., for longer times at 1000°C, the scale becomes more resistant to spalling. This effect is parallel to that observed for many other metal-metal oxide systems.

The final entry of Table XIII indicates the changes which occurred as a result of 12 cyclic thermal excursions between 25° and 1000°C. During this time, approximately 1.6 hours (of the 4-hour test time) of exposure at 1000°C were accumulated. Comparison with comparable isothermal tests indicates that the dimensional changes were less than those produced during either the 1 or 4 hour isothermal tests - due primarily to increased oxide spalling which occurred upon each cooling portion of the thermal cycle. In summary, it appears that very thin and very thick scales resist spalling and that thermal cycling encourages it.

1b. VOLUMETRIC APPARATUS

The dimensional changes and appearances of reacted titanium-base specimens as a result of exposure to various gases and gas mixtures and using the volumetric oxidation apparatus are presented in Table XIV and are there listed by alloy type. In these experiments, the investigation was concentrated upon initial behaviors only and, for that reason, tests were conducted under the condition that the exposure time after reaching

TABLE XIV

DIMENSIONAL CHANGES AND APPEARANCE FOR TITANIUM-BASE SPECIMENS OXIDIZED
IN VARIOUS ATMOSPHERES USING THE VOLUMETRIC APPARATUS

Specimen Number	Heating Rate (°C/S)	Thickness (cm)		Change	Oxide Appearance [1]		
		Initial	Final		Outside	Inside	Spall
A. UNALLOYED TITANIUM (TYPE 1)							
1) 200 torr O ₂ ; 1000°C							
06051	0.5	.154	.163	.004	brownish yellow	white	small pieces
06141	0.5	.157	.162	.005	brownish yellow	white	small pieces
06132	8	.156	.163	.007	light brownish yellow	white	small pieces
06133	25	.152	.155	.003	brownish yellow to light brown	white	small pieces
2) 200 torr O ₂ ; 1100°C							
06131	0.5	.151	.153	.002	brownish yellow	white	large pieces
06071	8	.157	.170	.013	brownish yellow	white	large pieces
06142	22	.157	.163	.006	brownish yellow	white	large sheets
3) 200 torr O ₂ ; 1200°C							
08012	0.5	.158	.165	.007	black	black	very little

TABLE XIV - continued

Specimen Number	Heating Rate ($^{\circ}\text{C}/\text{S}$)	Thickness (cm)		Change	Outside	Oxide Appearance [1]	
		Initial	Final			Inside	Spall
08013	7.5	.160	.175	.015	black	black	large sheets
07091	4	.157	4) 200 torr O_2 ; 1300 $^{\circ}\text{C}$				
			.163	.006	grey and brownish yellow	white or grey	large pieces
07311	8	.157	5) 200 torr N_2 ; 1000 $^{\circ}\text{C}$				
			.158	.001	gold	ND	none
07312	8	.157	6) 200 torr N_2 ; 1100 $^{\circ}\text{C}$				
			.158	.001	gold	ND	none
07313	8	.155	7) 200 torr O_2 ; 200 torr N_2 ; 1000 $^{\circ}\text{C}$				
			.156	.001	white and gold	purple	none
08011	8	.155	8) 200 torr O_2 ; 200 torr N_2 ; 1100 $^{\circ}\text{C}$				
			.163	.008	white	gold	none
08021	8	.158	9) 200 torr O_2 ; 200 torr He ; 1000 $^{\circ}\text{C}$				
			.164	.006	light brownish yellow	white	large pieces

TABLE XIV - continued

Specimen Number	Heating Rate (°C/S)	Thickness (cm)		Change	Oxide Appearance [1]		
		Initial	Final		Outside	Inside	Spall
08171	8	.156		10) 200 torr O ₂ ⁺ 200 torr He; 1100 °C			
				.168 .012	brownish yellow	white	very little
08023	8	.157		11) 200 torr N ₂ ⁺ 200 torr He; 1000 °C			
				.159 .002	purple	ND	none
09051	8	.159		12) 200 torr N ₂ ⁺ 200 torr He; 1100 °C			
				.159 0	gold	ND	none
07101	8	.156		13) 200 torr O ₂ ; cycled 800 °C to 1000 °C			
				.166 .010	brownish yellow	white	small pieces
07261	8	.156		14) 200 torr O ₂ ; cycled 900 °C to 1100 °C			
				.162 .006	light brownish yellow	white	small pieces

TABLE XIV - continued

Specimen Number	Heating Rate (°C/S)	Thickness (cm)		Change	Outside	Oxide Appearance [1]		
		Initial	Final			Inside	Spall	
B. UNALLOYED TITANIUM (TYPE 2)								
09191	8	.147	.158	.011	light brownish yellow	white	small pieces	
								1) 200 torr O ₂ ; 1000°C
09192	8	.148	.165	.017	brownish yellow	white	medium pieces	
								2) 400 torr O ₂ ; 1000°C
401151	8	.160	.175	.015	burned yellow	white	large pieces	
								3) 200 torr O ₂ ; 1100°C
401021	8	.157	.172	.015	burned yellow	white	large pieces	
405151 [2]	8	.0224	.0437	.0213	black	black	large pieces	
121201	8	.158	.187	.029	black	black	large pieces	
405221 [2]	10	.0224	.0439	.0215	black	black	small pieces	
408191 [3]	22	.0381	.0549	.0168	black	black	large pieces	
408141 [4]	22	.0625	.0742	.0117	burned yellow	white	large pieces	
405141 [2]	100	.0239	Ignition		burned yellow	white	small pieces	

TABLE XIV - continued

Specimen Number	Heating Rate (°C/S)	Thickness (cm)		Ignition	Change	Oxide Appearance [1]		
		Initial	Final			Outside	Inside	Spall
405142 [2]	100	.0224						
						burned yellow	white	small pieces
				4) 200 torr N ₂ ; 1000°C				
09193	8	.150	.157	.001	gold	gold	ND	none
				5) 200 torr N ₂ ; 1100°C				
402192	8	.158	.159	.001	black	black	gold	none
402281	8	.157	.158	.001	black	black	gold	none
				6) 100 torr O ₂ ⁺ 100 N ₂ ; 1100°C				
402193	8	.158	.162	.004	light yellow	white		small pieces
				7) 50 torr O ₂ ⁺ 100 torr N ₂ ; 1100°C				
402194	8	.163	.164	.001	white	white	white	small pieces
				C. UNALLOYED TITANIUM (TYPE 3)				
				1) 200 torr O ₂ 1000°C				
09194	8	.102	.116	.014	light brownish yellow	white		small pieces

TABLE XIV - continued

Specimen Number	Heating Rate (°C/S)	Thickness (cm)		Change	Oxide Appearance [1]		
		Initial	Final		Outside	Inside	Spall
11201 [5] 405021	8			2) 200 torr O ₂ ; 1100°C			
		.0584	.0674	.0090	black	light grey	large pieces
405023	8	.0876	.0940	.0064	burned yellow	white	large pieces
	5.9	.0892	.0950	.0058	black	black	very little
D. UNALLOYED TITANIUM (TYPE 4)							
407162 406103	8	.0249	.0373	.0124	black	black	small pieces
	100	.0251	Ignition		burned yellow	white	small pieces
E. UNALLOYED TITANIUM (TYPE 5)							
408143 408282	8	.00991	.0305	.0206	burned yellow	burned yellow	none
	18	.00991	.0249	.0168	burned yellow	yellow	none
408281	28.5	.00991	Ignition		burned yellow	white	none

TABLE XIV - continued

Specimen Number	Heating Rate ($^{\circ}\text{C}/\text{S}$)	Thickness (cm)		Outside	Oxide Appearance [1]	
		Initial	Final		Inside	Spall
408271	58	.00991	Ignition	burned yellow	white	none
408272	58	.00991	Ignition	burned yellow	white	none
408273	58	.00991	Ignition	burned yellow	white	none
406101	100	.0102	Ignition	burned yellow	white	none
406102	100	.0104	Ignition	burned yellow	white	none
F. TITANIUM - 6% ALUMINUM - 4% VANADIUM (TYPE 1)						
1) 200 torr O_2 ; 1000 $^{\circ}\text{C}$						
407161 [6]	8	.0922	.103	purple	white	small pieces
2) 200 torr O_2 ; 1100 $^{\circ}\text{C}$						
401161	0.5	.154	.166	black	brownish red	very little
401091	0.5	.157	.168	black	brownish red	very little
11202	8	.155	.164	black	brownish red	very little
405071 [6]	8	.0970	.111	black	gold	very little

TABLE XIV - continued

Specimen Number	Heating Rate (°C/S)	Thickness (cm)		Change	Oxide Appearance [1]		
		Initial	Final		Outside	Inside	Spall
405072 [6]	8	.0904	.101	.011	black	black	very little
401092	22	.148	.163	.015	black	brownish red	very little
				3) 200 torr O ₂ ; 1200°C			
407243 [6]	5.9	.0945	.118	.024	black	black	very little
408081 [6]	5.9	.0942	.114	.019	black	black	very little
				4) 200 torr N ₂ ; 1100°C			
401162	8	.155	.156	.001	gold	ND	none
				G. TITANIUM - 6% ALUMINUM - 4% VANADIUM (TYPE 2)			
				1) 200 torr O ₂ ; 1100°C			
402042	0.5	.213	.231	.018	black	grey	very little
401152	8	.226	.244	.018	black	black	very little
402043	22	.208	.223	.015	black	grey	very little
				H. TITANIUM - 6% ALUMINUM - 4% VANADIUM (TYPE 3)			
				1) 200 torr O ₂ ; 1100°C			
406171	8	.0262	.0528	.0266	black	black	very little

TABLE XIV - continued

Specimen Number	Heating Rate (°C/S)	Thickness (cm)		Change	Outside	Oxide Appearance [1]	
		Initial	Final			Inside	Spall
406104 [7]	100	Ignition			brownish red	ND	none
I. TITANIUM - 8% MANGANESE							
1) 200 torr O ₂ ; 1000°C							
406032	8	.101	.112	.011	purple	burned yellow	very little
2) 200 torr O ₂ ; 1100°C							
405074	0.5	.100	.113	.013	black	black	small pieces
405073	8	.102	.114	.012	black	black	very little
406031	22	.101	.110	.009	black	black	very little
409192 [8]	48	.0279	Ignition		brownish red	black	none
409232 [9]	53	.0343	Ignition		brownish red	black	none
409172 [10]	75	.0251	Ignition		brownish red	black	none
3) 200 torr O ₂ ; 1200°C							
407242	5.9	.0991	.113	.013	black	black	very little

TABLE XIV - continued

Specimen Number	Heating Rate (°C/S)	Thickness (cm)		Change	Oxide Appearance (1)		
		Initial	Final		Outside	Inside	Spall
J. TITANIUM - 8 - III							
1) 200 torr O ₂ ; 1000°C							
409161	8	.0980	.114	.016	white	grey	large pieces
2) 200 torr O ₂ ; 1100°C							
406174	0.5	.0968	.110	.0129	black	black	very little
406173	8	.0963	.116	.0195	black	black	very little
409231 [11]	22	.0356	.0610	.0254	black	black	large pieces
406175	22	.0953	.110	.0147	black	black	large pieces
409191 [12]	72	.0287	Ignition		black	black	none
409171 [13]	82	.0239	Ignition		black	black	none
3) 200 torr O ₂ ; 1200°C							
407241	5.9	.0980	.113	.015	black	black	very little

TABLE XIV - concluded

FOOTNOTES

- [1] See text for additional colorimetric information
- [2] Cold work 87% and polished to .023 cm
- [3] Cold work 76% and polished to .038 cm
- [4] Cold work 61% and polished to .063 cm
- [5] Cold work 39% and polished to .058 cm
- [6] Milled from .152 cm to .119 cm
- [7] Burned yellow deposit on vycor tube
- [8] Milled from .102 cm to .0508 cm and polished to .0279 cm
- [9] Milled from .102 cm to .0508 cm and polished to .0343 cm
- [10] Milled from .102 cm to .0508 cm and polished to .0251 cm
- [11] Milled from .119 cm to .0508 cm and polished to .0330 cm
- [12] Milled from .119 cm to .0508 cm and polished to .0287 cm
- [13] Milled from .119 cm to .0508 cm and polished to .0239 cm

maximum temperature be limited to 1 hour. It follows that oxidation time per se is not a variable in the presentation of data represented in Table XIV.

From Table XIV may be seen the indications of the effects several of the more important experimental parameters have upon the degree of reaction. These parameters include: material chemistry and purity, specimen thickness and degree of cold work, heating rate and maximum temperature, and gas quality among others. It is emphasized that the discussion which follows pertains to long-term (nominally 1 hour) post-test observations and does not necessarily reflect short-term behaviors which occur during heating or shortly thereafter.

For the case of unalloyed titanium exposed in 200 torr oxygen, it is clear that the thickness increments are less, by a factor of approximately 2, for the purer (Type 1) material. This observation conforms to the well-known trends indicating that purer materials are generally more corrosion-resistant. Comparison of results obtained using unalloyed and alloyed titaniums, and under conditions where other parameters are invariant, indicates similar trends in specimen thickening. The β -III alloy, especially, exhibited evidence for more rapid reaction. Further, and in support of the inferences drawn based on thickening, the alloys exhibited evidence of volatility as inferred from the appearance of the system components after reaction at elevated temperature. Unalloyed titanium left the apparatus in an apparently "clean" (colorless) state; whereas: 1) the Ti-6Al-4V alloy specimens produced a reddish deposit on the alumina thermocouple supports and a yellow deposit on the vycor tube, 2) the Ti-8Mn alloy specimens produced a brownish deposit on both the alumina and the vycor, and the β -III alloy specimens produced a black or grey deposit on

the alumina and the vycor. As the scales developed on these alloys take on similar colors, the coloration is attributed to the presence of volatilized (vapor phase) alloying elements which have subsequently entered into solid solution with the neighboring refractories to produce characteristic coloration as in the "borax bead" or similar tests (ref. 12). Finally, the alloys generally appear to be more resistant to spalling than does unalloyed titanium, with the possible exception of those β -III alloy specimens which were rapidly heated.

For two of the materials investigated, unalloyed titanium and the Ti-6Al-4V alloy, there is sufficient data available to indicate that there exists a specimen thickness at which the thickness change is a minimum.* For the unalloyed titaniums (Types 2 through 5) this gauge is approximately 0.040 in. (0.152 cm). For the alloy, this data is less certain as the thinnest (Type 3) material has higher vanadium and lower aluminum concentrations than the thicker stock; factors which also may produce enhanced reactivity. The gross similarities in behavior, however, suggest that the reactivities of thin specimens is increased by oxygen solution while that of the thick specimens is increased by the action of thermal stresses in the oxidizing substrate. As will be seen later, this gauge-sensitive effect is paralleled in the total weight change data. There is insufficient data available to make a strong statement regarding the effect of cold work per se; from the black scales developed upon the cold-worked specimens, they appear to have achieved a more advanced degree of reaction than less distorted materials of similar gauge.

For unalloyed titanium, the thickness increment usually increases as the exposure temperature is increased, as expected, if the test duration

*Based on specimens exposed in 200 torr oxygen which were not cold-worked.

is taken into account for the more rapid high-temperature tests. This temperature dependence is, however, not as strong as might be expected from considerations of the temperature dependence of the reaction as judged by usually accepted values of the activation energy and probably reflects the effects of interface retreat and solution at the higher temperatures. For the alloys, the effect of temperature upon specimen thickening appears to be even weaker than for the unalloyed material. Tests in 200 torr oxygen at temperatures between 1000°C and 1300°C indicated that the coloration of oxide over this temperature range was compatible with that noted previously for the conventional heating apparatus. The external surface of the oxide changed from brownish yellow (1000° and 1100°C) to black (1200°C) to grey (1300°C). The latter of these represents a very "immature" scale as the duration of oxidation was approximately only 4.5 minutes (vs. one hour). The darker appearance at higher temperatures (1200° and 1300°C) is similar to the darkening which occurred at long times (64 hours) at 1000°C in air (conventional heating apparatus). The inner scale layers are found to be consistently lighter (white to grey) that the corresponding external surface colors indicating that there exists some type of gradient through the scale; eg., stoichiometry or compositional (impurity) gradient are likely candidates. As expected, higher temperatures lead to increasing sizes of the spalled oxide pieces as the mechanical strength is enhanced by oxide thickening. The color of the scales produced on the alloys over the temperature range investigated followed a similar pattern in that the initial characteristic colors present at low temperatures evolved to a black coloration at the highest temperatures investigated.

The thickening of specimens during exposure also appeared to be

affected by heating rate per se. For the unalloyed titanium and the β -III alloy, the maximum specimen thickening tended to occur at the intermediate heating rate (8°C/s); whereas, the Ti-6Al-4V alloy specimens exhibited an inverse effect. For the case of the Ti-8Mn alloy, the specimen thickening appeared to be inversely related to heating rate. We can offer no ready explanations of these observed behaviors at this time.

Cooling rate does have a minor effect upon the long-term or overall behavior of exposed specimens in that slower rates of cooling produce more adherent scales on unalloyed titanium specimens. Careful inspection of specimens cooled at 0.5° and 8°C/s has indicated that additional reaction may have occurred during the more rapid cooling operation and while the temperature was yet elevated.

With the exception of a single test in nitrogen involving a Ti-6Al-4V specimen, the effect of gases other than 200 torr oxygen was explored using only unalloyed titanium specimens. A single test at higher oxygen pressure (400 torr) gave a strong indication of a greater degree of reaction and there was an attendant decrease in the tendency to spall which may be related to a thickness and mechanically stronger oxide. For those tests conducted in equal partial pressure of oxygen and helium, dimensional changes and appearances of specimens were similar to those exposed to oxygen alone.

In 200 torr nitrogen, the dimensional changes of both unalloyed titanium and Ti-6Al-4V alloy specimens are much smaller than those incurred under similar conditions in 200 torr oxygen. The appearance of specimens is strikingly different and reaction provides a spall-resistant scale of distinct gold color (1000° and 1100°C). Analyses of tests conducted

by others and under similar conditions (ref. 13) as well as the coloration (ref. 14) strongly indicate that the reaction product is titanium nitride, TiN . In 200 torr nitrogen diluted with an equal amount of helium, the dimensional change was smaller than for corresponding tests in nitrogen alone and a purple coloration was noted in one of the scales ($1000^{\circ}C$) formed on unalloyed material which may reflect either a change in scale stoichiometry or thickness. These scales were also spall-resistant.

For those tests conducted in equal partial pressures (200 torr) of oxygen and helium or of nitrogen and helium, the effect of the helium on dimensional changes and appearance was essentially nil. For tests conducted in mixtures of oxygen and nitrogen at equal partial pressures (200 torr), the dimensional changes and appearances of exposed specimens were intermediate to those specimens exposed in either pure gas. From the previous colorimetric data, it would appear that both gases had reacted with titanium and that the nitrogen reaction product was proximal to the metal-scale interface (oxide-like products distal). A series of unalloyed titanium specimens was used to investigate the possibility of oxygen-nitrogen synergism at a total gas pressure of 200 torr. The dimensional change data form a regular pattern indicating that as the oxygen content of the gas is increased, the degree of reaction is similarly increased. This behavior, for which the reactivity of titanium is approximately 10 times greater in oxygen than in nitrogen, provides a monotone specimen thickening for gas mixtures between the pure components. From the data available, there is no evidence for a synergistic reaction involving oxygen and nitrogen.

Changes in appearance for specimens thermally cycled between 800° and $1000^{\circ}C$ or between 900° and $1100^{\circ}C$ in oxygen were quite similar to those

specimens isothermally exposed at 1000° or 1100°C. Scales in these cases were typically yellowish-brown near the gas-oxide interface and white nearer the metal. Dimensional changes are difficult to interpret; however, it is apparent that there was no massive spalling during these tests as a thickness decrement was not observed as it was for the case of the specimen cycled between 25° and 1000°C in the air furnace.

In the majority of tests performed, and regardless of specimen chemistry, gas composition, or heating rate, specimens again exhibited evidence of an interaction with the recording and control thermocouple beads (Pt vs Pt - 13% Rh). The interaction is evidenced as a small (1-3 mm diameter) circular zone, usually darker than the surrounding material of the external scale. There is no evidence that this effect induces a "fast", localized reaction on titanium although such have been documented for magnesium (ref. 10).

Those specimens which experienced ignition exhibited the same general color character as did the specimens of similar alloys which survived oxidation at one hour. Changes in specimen dimensions were not recorded as all such specimens exhibited evidence of melting. In addition, in most instances the platinum-base thermocouple elements were melted, and in some cases the Al_2O_3 thermocouple insulators showed evidence of melting, indicating that sensible temperatures of the order of 2000°C had been achieved.

2. WEIGHT CHANGES OF EXPOSED SPECIMENS

In this section are presented the conventional weight gain data for exposed titanium-base specimens exposed in various gases and gas mixtures and over a range of maximum temperatures from 800° to 1300°C. In-depth analyses of these data have not been attempted as the emphasis of this

research program is centered more upon the initial stages of oxidation than upon the longer-term behavior which they represent.

2a. AIR FURNACE

Results of oxidizing unalloyed titanium (Type 1) specimens in air at 1000°C and for various relatively long times are presented in the upper portion of Table XV. In each of these tests, care was taken to collect the spalled reaction product so that the weight changes represent, to a good approximation, the total amount of combined oxygen (and nitrogen) either in the form of scale or dissolved gas. Because of the relatively low vapor pressure of titanium (ref. 15), it is not expected that metal vaporization per se would have any influence upon these data.

Analysis of the 1000°C weight gain data may be made on a graphical basis as illustrated in the conventional logarithmic plot of Figure 6. This graph indicates that the reaction proceeds under a rate law intermediate between pure parabolic and pure linear behavior; a regime commonly termed "paralinear." The initial data are more nearly parabolic than the longer-term data, in accord with the prior discussion concerning dimensional changes. This behavior and the magnitude of the specific weight gains are in general agreement with the data for air-oxidation as presented in the data summary of Morton and Baldwin (ref. 11).

If all of the specific weight gain data of Table XV are treated according to the parabolic relationship:

$$M^2 = K_p t \left(\frac{\text{mg}}{\text{cm}^2} \right)^2, \quad \text{Eq. (1)}$$

then values for the parabolic rate constant (K_p) may be obtained from these data; thus:

$$K_p = \frac{M^2}{t} \left(\frac{\text{cm}^2}{\text{mg}^2} \right). \quad \text{Eq. (2)}$$

TABLE XV
WEIGHT CHANGES FOR TITANIUM (TYPE 1) SPECIMENS OXIDIZED IN AIR USING
THE AIR FURNACE

Specimen Number	Oxidation Temp. (°C); Time (hr)	Initial Area (cm ²)	Weight (g)		Specific Weight Change (mg/cm ²)	Average Parabolic Reaction Rate Con- stant (mg ^{1/2} /cm ² /min)
			Initial	Final		
05162	1000; 1	11.74	3.4788	3.6014	0.1226	1.90
05011	1000; 4	11.88	3.5839	3.8340	0.2501	1.86
05072	1000; 16	11.88	3.5476	4.1402	0.5926	2.59
05081	1000; 64	11.74	2.4794	4.9726	1.4932	4.20
05171	800; 4	11.61	3.1050	3.1202	0.0152	0.00715
05161	850; 4	11.78	3.3851	3.4184	0.0333	0.0334
05151	900; 4	11.82	3.4533	3.5846	0.1313	0.513
05141	950; 4	11.85	3.4809	3.7585	0.2776	2.28 (?)
05021	cyclic; 4*	11.84	3.5589	3.7970**	0.2381**	20.1***

*Cycled 12 times between 25° and 1000°C with specimen at temperature for approximately 8 min of each 20 min cycle; effective time at temperature approximately 1.6 hour.

**Values uncertain because of severe spalling of oxide.

***Value is approximately 50.3 if calculation is based on 1.6 hours at temperature only.

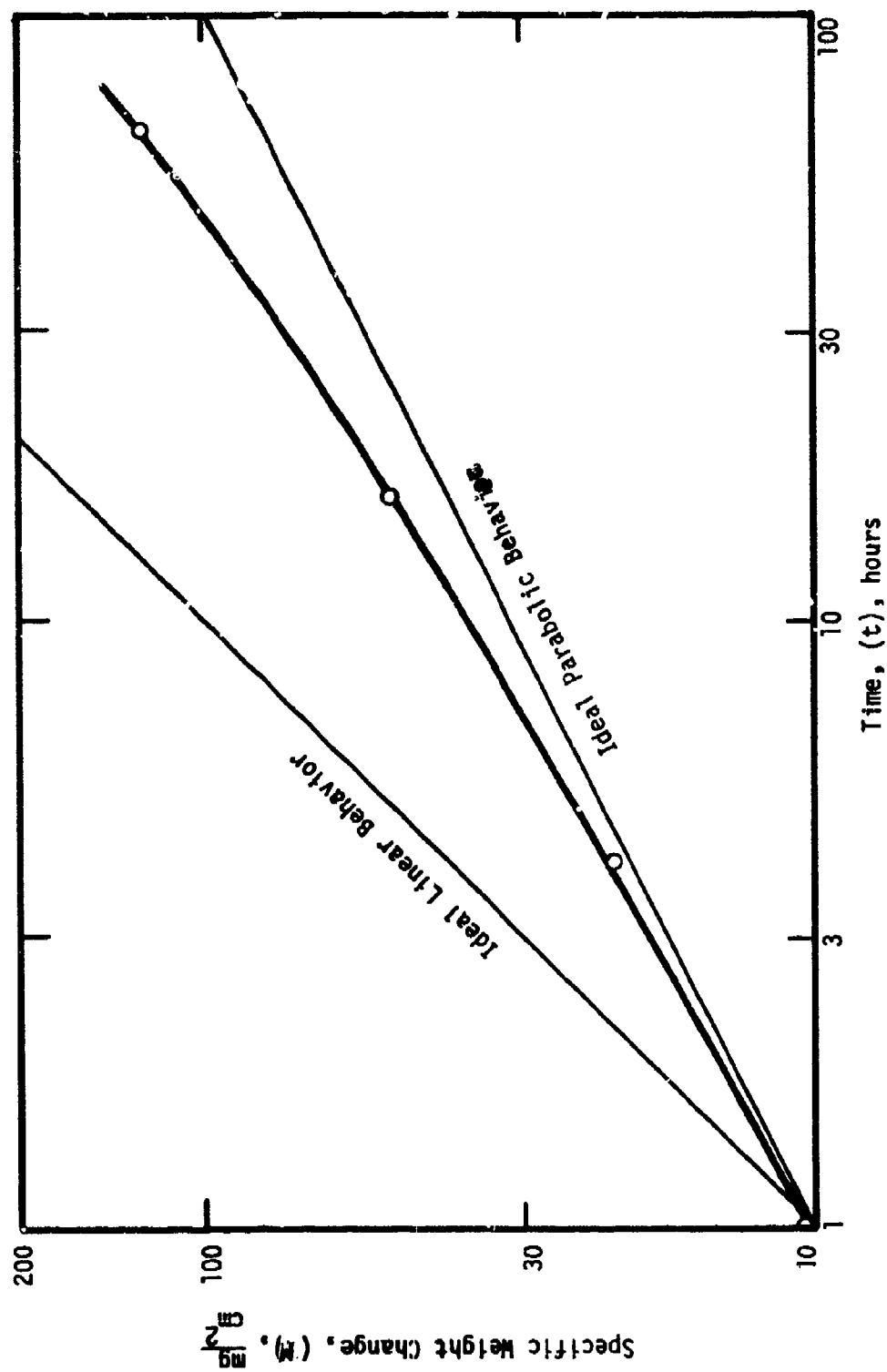


Figure 6. - Specific weight change of unalloyed titanium (Type 1) specimens oxidized in air at 1000°C for various times. Note deviation from initial parabolic behavior at longer times.

Further, utilizing relatively short time data (4-hour tests) where the reaction is very nearly parabolic in nature and assuming the Arrhenius relationship:

$$K_p = Ae^{-Q/RT}, \quad \text{Eq. (3)}$$

the activation energy (Q [$\frac{\text{K-cal}}{\text{mole}}$]) may be determined. This has been done graphically as is presented in Figure 7.

The line chosen to describe the data points of Figure 7 has been weighted heavily toward the point representing the 4-hour, 1000°C datum point in view of the behavior exhibited in Figure 6. This analysis gives a minimum possible value of (Q) of $75.4 \frac{\text{K-cal}}{\text{mole}}$. The data points for 900° and 950°C seem inordinately large (factor ~ 4) and may in some manner be associated with transformation ($\alpha \rightarrow \beta$) of the oxygen-enriched titanium solid solution. If persistent, this effect warrants further investigation and/or analysis.

2b. VOLUMETRIC APPARATUS

The weight change data resulting from exposure of unalloyed and alloyed titanium in oxygen, nitrogen, and mixed gases and at maximum temperatures between 1000° and 1300°C are presented in Table XVI. It is again emphasized that these data represent conditions after the full term of the test (usually one hour at maximum temperature) has been completed, and they therefore represent only terminal conditions resulting from reaction.

Throughout Table XVI are listed, for each specimen tested, both the weight gain as determined by conventional gravimetric means (from pre-test and post-test weights) and the weight gain as calculated from the number of moles of gas fixed during exposure (as determined from corresponding pressure changes)*. As is seen from the table, agreement of these two values was

*Note: for the case of mixed gases, weight gain calculations were based upon the average molecular weight of the reactive gases involved.

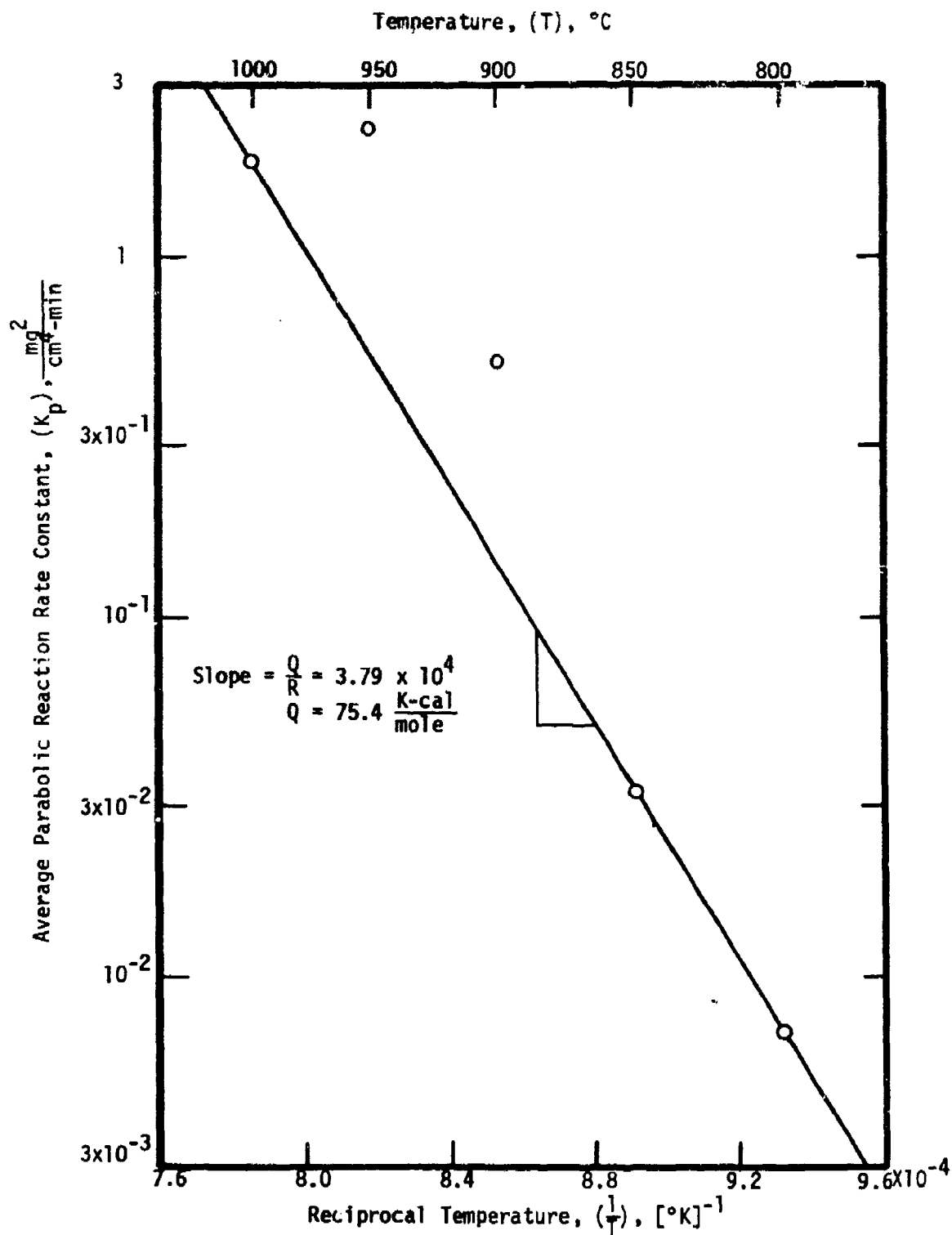


Figure 7- Temperature dependence of the parabolic reaction rate constant for unalloyed titanium (Type 1) specimens oxidized in air.

TABLE XVI

TOTAL WEIGHT CHANGES FOR TITANIUM-BASE SPECIMENS OXIDIZED FOR ONE HOUR
IN VARIOUS ATMOSPHERES USING THE VOLUMETRIC APPARATUS

Specimen Number	Heating Rate ($^{\circ}\text{C}/\text{S}$)	Gravimetric Wt. Change (mg)	Calculated Wt. Change (mg) [1]	Initial $\frac{2}{\text{Area (cm}^2\text{)}}$	Specific Wt. $\frac{2}{\text{Change (mg/cm}^2\text{)}}$ [2]
A. UNALLOYED TITANIUM (TYPE 1)					
1) 200 torr O_2 ; 1000 $^{\circ}\text{C}$					
06051	0.5	65.7	65.0	11.54	5.69
06141	0.5	57.5	54.4	11.85	4.85
06132	8	65.7	70.7	11.69	5.62
06133	25	37.6	40.7	11.64	3.23
2) 200 torr O_2 ; 1100 $^{\circ}\text{C}$					
06131	0.5	154.9	179	11.66	13.3
06071	8	143.8	143	11.70	12.5
06142	22	145.9	137	11.70	12.5
3) 200 torr O_2 ; 1200 $^{\circ}\text{C}$					
08012	0.5	184.0	157	11.73	15.7
08013	7.5	182.1	152	11.73	15.5

TABLE XVI - continued

Specimen Number	Heating Rate (°C/S)	Gravimetric Wt. Change (mg)	Calculated Wt. Change (mg)[1]	Initial Area (cm ²)	Specific Wt. Change (mg/cm ²)[2]
07091	4	4) 200 torr O ₂ ; 1300°C 168.0	173	11.68	14.4
07311	8	5) 200 torr N ₂ ; 1000°C 6.1	11.8	11.73	0.520
07312	8	6) 200 torr N ₂ ; 1100°C 20.7	16.6	11.72	1.77
07313	8	7) 200 torr O ₂ ⁺ 200 torr N ₂ ; 1000°C 16.3	11.8	11.67	1.40
08011	8	8) 200 torr O ₂ ⁺ 200 torr N ₂ ; 1100°C 59.6	61.8	11.69	5.10
03021	8	9) 200 torr O ₂ ⁺ 200 torr He; 1000°C 61.2	62.4	11.74	5.21

TABLE XVI - continued

Specimen Number	Heating Rate (°C/S)	Gravimetric Wt. Change (mg)	Calculated Wt. Change (mg)[1]	Initial Area (cm ²)	Specific Wt. Change (mg/cm ²)[2]	
08171	8	10) 200 torr O ₂ ⁺ 200 torr He; 1100°C			11.75	6.01
		70.6	65.9			
08023	8	11) 200 torr N ₂ ⁺ 200 torr He; 1000°C			11.71	0.862
		10.1	11.9			
09051	8	12) 200 torr N ₂ ⁺ 200 torr He; 1100°C			11.16	1.15
		12.8	22.8			
07101	8	13) 200 torr O ₂ ; cycled 800°C to 1000°C			11.69	4.67
		54.6	52.6			
07261	8	14) 200 torr O ₂ ; cycled 900°C to 1100°C			11.36	3.99
		45.3	45.1			
8. UNALLOYED TITANIUM (TYPE 2)						
09191	8	1) 200 torr O ₂ ; 1000°C			11.29	6.50
		73.4	64.6			

TABLE XVI - continued

Specimen Number	Heating Rate (°C/S)	Gravimetric Wt. Change (mg)	Calculated Wt. Change (mg) [1]	Initial Area (cm ²)	Specific Wt. Change (mg/cm ²) [2]
2) 400 torr O ₂ ; 1000°C					
09192	8	150.2	140	11.34	13.4
3) 200 torr O ₂ ; 1100°C					
401151	8	165.8	161	11.31	14.7
401021	8	152.6	150	11.33	13.5
405151 [3]	8	179.5	174	10.88	16.5
121201	8	180.5	181	11.63	15.5
405221 [3]	10	177.2	177	9.69	18.3
408191 [4]	22	160.2	157	13.53	11.8
408141 [5]	22	175.6	158	13.09	13.4
4) 200 torr N ₂ ; 1000°C					
09193	8	6.6	5.91	11.33	0.583
5) 200 torr N ₂ ; 1100°C					
402192 [6]	8	57.7	25.2	11.52	5.01
402281 [6]	8	58.5	24.6	11.74	4.98

TABLE XVI - continued

Specimen Number	Heating Rate ($^{\circ}\text{C}/\text{S}$)	Gravimetric Wt. Change (mg)	Calculated Wt. Change (mg) [1]	Initial Area (cm^2)	Specific Wt. Change (mg/cm^2) [2]
402193	8	44.9	6) 100 torr O_2^+ 100 torr N_2 ; 1100 $^{\circ}\text{C}$	11.58	3.88
			7) 50 torr O_2^+ 150 torr N_2 ; 1100 $^{\circ}\text{C}$		
402194	8	36.1	31.8	11.87	3.04
C. UNALLOYED TITANIUM (TYPE 3)					
09194	8	100.1	1) 200 torr O_2 ; 1000 $^{\circ}\text{C}$	10.80	9.27
			2) 200 torr O_2 ; 1100 $^{\circ}\text{C}$		
11201 [7]	8	147.9	118	10.59	14.0
405021	8	150.7	147	10.58	14.2
405023	5.9	179.2	3) 200 torr O_2 ; 1200 $^{\circ}\text{C}$ 181	10.78	16.6

TABLE XVI - continued

Specimen Number	Heating Rate ($^{\circ}\text{C}/\text{S}$)	Gravimetric Wt. Change (mg)	Calculated Wt. Change (mg) [1]	Initial A_2 Area (cm^2)	Specific Wt. Change (mg/cm^2) [2]
D. UNALLOYED TITANIUM (TYPE 4)					
1) 200 torr O_2 ; 1100 $^{\circ}\text{C}$					
407162	8	181.1	173	10.88	16.6
E. UNALLOYED TITANIUM (TYPE 5)					
1) 200 torr O_2 ; 1100 $^{\circ}\text{C}$					
408143	8	146.8	149	10.20	14.4
408282	18	135.3	135	9.71	13.9
F. TITANIUM - 6% ALUMINUM - 4% VANADIUM (TYPE 1)					
1) 200 torr O_2 ; 1000 $^{\circ}\text{C}$					
407161 [8]	8	81.5	73.1	11.05	7.38
2) 200 torr O_2 ; 1100 $^{\circ}\text{C}$					
401161	0.5	184.8	173	11.74	15.7
401091	0.5	173.7	167	11.73	14.8
11202	8	143.7	126	11.74	12.2

TABLE XVI - continued

Specimen Number	Heating Rate ($^{\circ}\text{C}/\text{S}$)	Gravimetric Wt. Change (mg)	Calculated Wt. Change (mg) [1]	Initial Area (cm^2)	Specific Wt. Change (mg/cm^2) [2]
405071 [8]	8	177.3	178	11.16	15.9
405072 [8]	8	180.5	165	11.05	16.3
401092	22	182.3	170	11.60	15.7
3) 200 torr O_2 ; 1200 $^{\circ}\text{C}$					
407243 [8]	5.9	179.4	176	11.11	16.1
408081 [8]	5.9	182.5	178	11.11	16.4
4) 200 torr N_2 ; 1100 $^{\circ}\text{C}$					
401162	8	9.9	10.6	11.73	0.844
G. TITANIUM - 6% ALUMINUM - 4% VANADIUM (TYPE 2)					
1) 200 torr O_2 ; 1100 $^{\circ}\text{C}$					
402042	0.5	184.8	175	12.42	14.8
401152	8	186.6	178	12.62	14.8
402043	22	177.1	168	12.38	14.3

TABLE XVI - continued

Specimen Number	Heating Rate (°C/S)	Gravimetric Wt. Change (mg)	Calculated Wt. Change (mg) [1]	Initial Area (cm ²)	Specific Wt. Change (mg/cm ²) [2]
H. TITANIUM - 6% ALUMINUM - 4% VANADIUM (TYPE 3)					
1) 200 torr O ₂ ; 1100°C					
406171	8	179.1	177	10.27	17.4
I. TITANIUM - 8% MANGANESE					
1) 200 torr O ₂ ; 1000°C					
406032	8	145.1	133	11.20	13.0
2) 200 torr O ₂ ; 1100°C					
405074	0.5	183.6	178	11.30	16.5
405073	8	180.9	176	11.16	16.2
406031	22	183.7	179	11.14	16.5
3) 200 torr O ₂ ; 1200°C					
407242	5.9	182.5	175	11.12	16.4
J. TITANIUM β - III					
1) 200 torr O ₂ ; 1000°C					
409161	8	139.0	156	11.20	12.4

TABLE XVI - continued

Specimen Number	Heating Rate ($^{\circ}\text{C}/\text{S}$)	Gravimetric Wt. Change (mg)	Calculated Wt. Change (mg) [1]	Initial Area (cm^2)	Specific Wt. Change (mg/cm^2) [2]
2) 200 torr O_2 ; 1100 $^{\circ}\text{C}$					
406174	0.5	179.0	174	11.14	16.1
406173	8	168.7	179	11.17	15.1
409231 [9]	22	174.1	174	10.47	16.6
406175	22	170.2	176	11.18	15.2
3) 200 torr O_2 ; 1200 $^{\circ}\text{C}$					
407241	5.9	179.7	178	11.18	16.1

TABLE XVI - concluded

FOOTNOTES

- [1] Calculation based on gas uptake determined from volumetric apparatus
- [2] Calculated using gravimetric weight change
- [3] Cold work 87%
- [4] Cold work 76%
- [5] Cold work 61%
- [6] Gravimetric weight change suspected of being incorrect
- [7] Cold work 39%
- [8] Milled from .152 cm to .119 cm
- [9] Milled from .119 cm to .0508 cm and polished to .0330 cm

within approximately 10% for 52 of the 66 tests analyzed; closer agreement being associated with the spall resistant alloy specimens. There was no apparent systematic relation governing the direction of these differences or those associated with the 14 tests where the agreement was less close. From a knowledge of the operational procedures employed and equipment characteristics, it is the opinion of the Principal Investigator that more confidence should be placed in the gravimetric than in the calculated weight changes. Although this choice infers that data gained from the volumetric apparatus may only be "semiquantitative" for full-term experiments, it in no way is meant to infer that the precision of this data is impaired for the earliest stages of oxidation; i.e., the volumetric apparatus is believed to be suitable for monitoring the reaction during the heating period and initial portions of the isothermal period; but less suitable at longer times when large pressure changes have occurred.

Comparison of the entries in Table XVI for unalloyed titanium (Type 1) and (Type 2) indicates that the less pure material oxidizes more rapidly. This conclusion is in agreement with that reached in the previous section which concerned dimensional changes. Other comparisons involving either unalloyed titanium or Ti-6Al-4V alloy specimens with regard to purity or alloying element concentration are less meaningful because gauge thickness effects also enter into any such analysis. The effect of alloying elements (alloy type) per se upon specific weight gain may also be deduced from the data of Table XVI. The general pattern evolved indicates that the relative rates of oxidation are as follows: β -III alloy > Ti-8Mn alloy > Ti-6Al-4V > unalloyed titanium. A more quantitative statement of this effect will be given below.

The effect of specimen gauge upon weight gain data is available for

unalloyed titanium and the Ti-6Al-4V alloy specimens. In both cases, the data indicate that there exists a specimen thickness at which the weight change is minimum; an observation in parallel with the specimen thickening data reported earlier. The gauge for minimum weight gain was approximately the same as that for minimum thickening. Again, these results indicate that the reactivity of thin specimens is enhanced, perhaps by oxygen solution or self-heating; while at the thickest gauges, reactivity may be enhanced by the action of thermal stresses.* The effect of cold work upon weight gain, exclusive of gauge effect, is somewhat uncertain; but, there appears to be a trend for first a slow decrease and subsequently (87% cold work) an increase in reactivity as the degree of cold work in unalloyed titanium (Type 2) is increased.

Table XVI also provides information regarding the effect of oxidation temperature (maximum temperature) upon the rate of reaction of titanium in 200 torr oxygen. In order to select a fair basis for determining this effect, a comparison has been made where all test parameters other than temperature were constant. From the specific weight changes given in Table XVI, the values of (K_p) for these selected tests was determined using Eq. (2) and are entered upon the first line of Table XVII. Following the usual Arrhenius analysis, Eq. (3), the logarithms of these values were plotted versus the reciprocal of the absolute temperature as illustrated in Figure 8. Analysis of these data indicate that the average activation energy for reaction is $60.8 \frac{\text{K-cal}}{\text{mole}}$ and that for the higher temperatures (dotted line of Figure 8) the activation energy is $71.6 \frac{\text{K-cal}}{\text{mole}}$. The latter of these values is in good agreement with the air oxidation data presented earlier (see Figure 7); however, the numerical value of the rate constant

*Note that limited data for β -III alloy are in agreement with the general trend of higher reactivities associated with thinner specimens.

TABLE XVII

VALUES OF THE AVERAGE PARABOLIC REACTION RATE CONSTANT (K_p)
FOR UNALLOYED TITANIUM (TYPE 1) SPECIMENS HEATED AT 8°C PER
SECOND IN VARIOUS OXIDIZING ATMOSPHERES*

Oxidizing Atmosphere	Maximum Temperature (°C)			
	1000	1100	1200	1300
200 Torr O ₂	0.526	2.61	8.90	46.1
200 Torr O ₂ + 200 Torr He	0.452	0.602	-	-
200 Torr O ₂ + 200 Torr N ₂	0.033**	0.434	-	-
200 Torr N ₂	0.005	0.052	-	-
200 Torr N ₂ + 200 Torr He	0.012	0.022	-	-

*Units of tabular entries are: (mg)²/(cm)⁴ min.

**May have had improper gas mixing in this test.

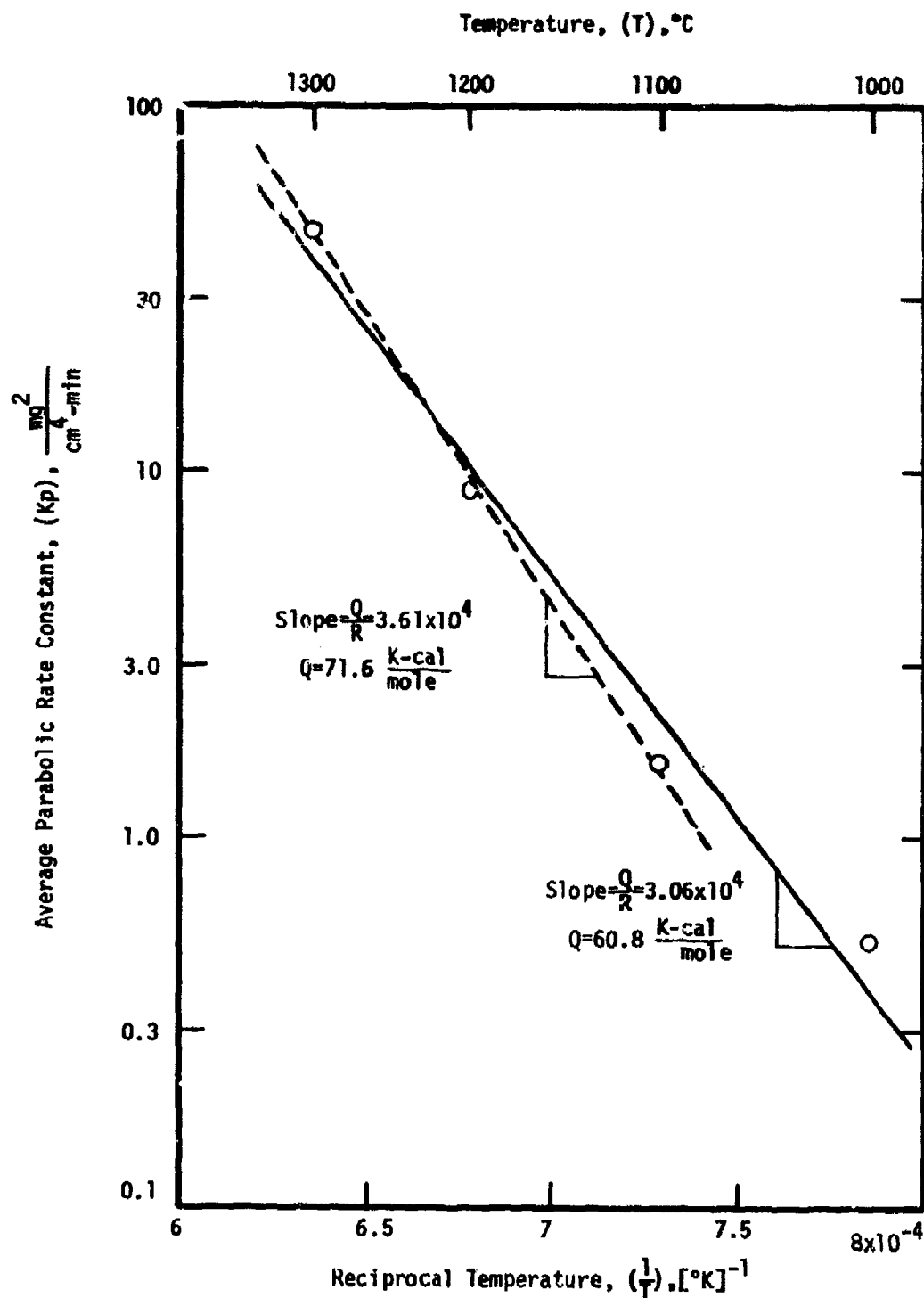


Figure 8 - Temperature dependence of the parabolic reaction rate constant for unalloyed titanium (Type 1) specimens oxidized in 200 torr oxygen. Heating rate 8°C/s.

appears to be approximately one order of magnitude larger in the tests performed in air (~ 150 torr O_2) than for those performed in 200 torr O_2 .^{*} This would require that the frequency factor (A) of Eq. (3) be approximately ten times larger for the case of air oxidation than for the case of oxidation in 200 torr oxygen and suggests either a synergistic effect of nitrogen or (furnace) impurity effect in the oxidation of titanium in air. That this is most probably an impurity effect will be demonstrated later.

The effect of holding temperature upon the oxidation of alloys in 200 torr oxygen and under conditions of constant heating rate (8°C/s) and gauge (0.040 inch) are illustrated in the Arrhenius plot of Figure 9. For exposure at maximum temperatures ranging from 1000° to 1200°C , it is seen that the rate of reaction is more rapid by factors of up to 5 for the alloys than for the unalloyed material. In general, the rates of reaction for specimens of these materials are in the order: β -III alloy > Ti-8Mn > Ti-6Al-4V > unalloyed titanium; however, there is a degree of "crossover" exhibited by these curves and a general tendency for smaller variations to occur at the highest temperature (1200°C). For purposes of comparison, the solid curve of Figure 8 is superimposed, which indicates that the thicker and purer unalloyed titanium oxidizes less rapidly than the thinner and less pure materials, regardless of composition. The data presented here is unsuitable for activation energy analysis other than to indicate that values of approximately 60 K-cal/mole may apply for the materials investigated.

The data of Table XVI also indicate that the specific weight changes in 200 torr oxygen are generally independent of heating rate with the exception of a trend for lower weight gains (smaller values of K_p) as the heating rate is increased to 22°C/s . This single long-term trend, as will

^{*}Comparison here is made on the basis of the single temperature (1000°C) common to both Figures 7 and 8.

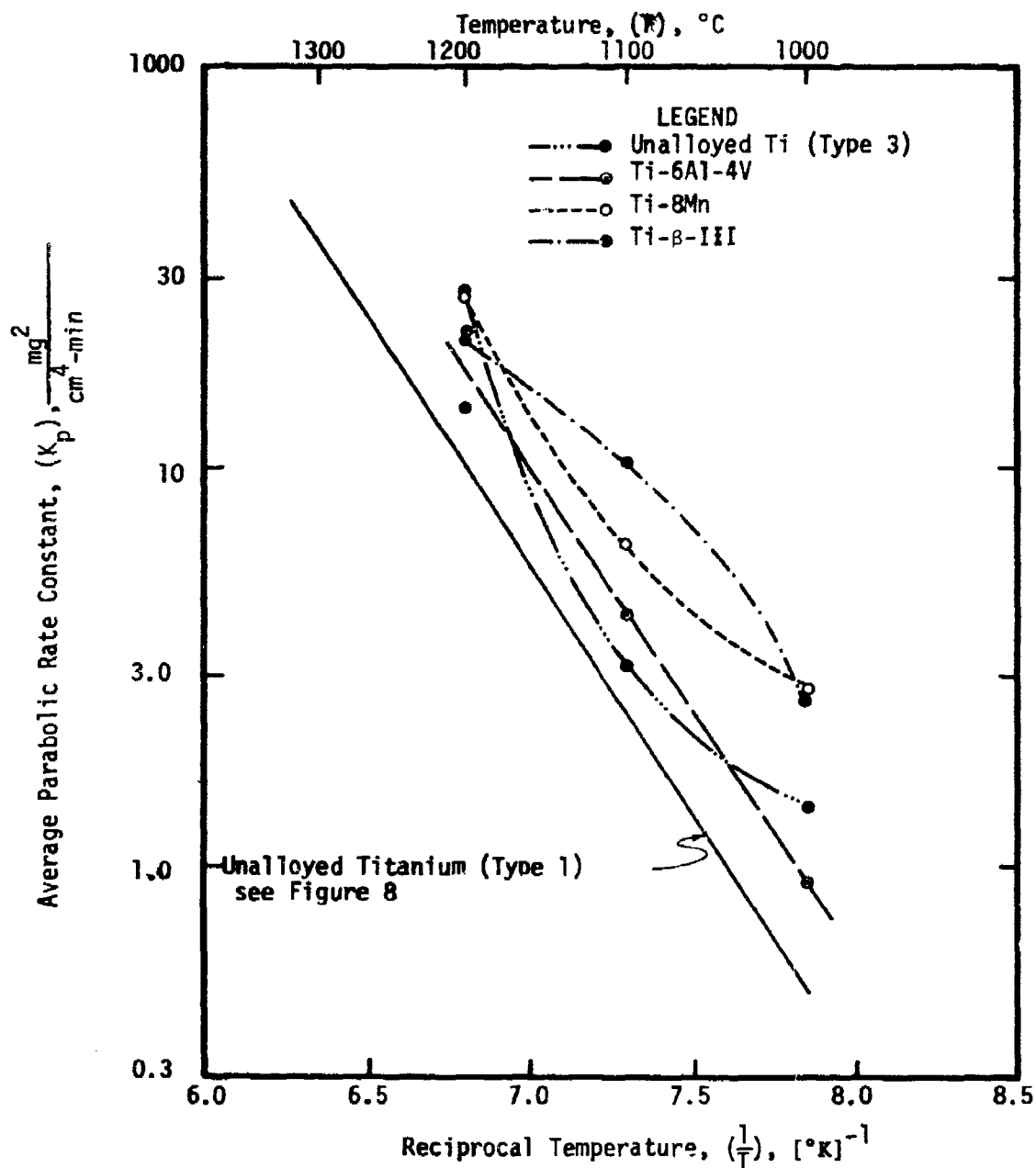


Figure 9.- Temperature dependence of the parabolic reaction rate constant for 5 titanium-base material specimens oxidized in 200 torr oxygen.

be seen later, is anomalous to the observation of more rapid initial reaction rate with higher heating rate for these same specimens.

With regard to the effect of total oxygen pressure, the data of Table XVI indicates that the degree of reaction is very nearly linearly related to oxygen pressure. This speaks strongly against any type of solid-state reaction control and reinforces the concept put forward by Stringer (ref. 16) that mechanical faults in the scale, such as pores, control the delivery of oxygen to the neighborhood of the metal-oxide interface.

Reaction of unalloyed titanium in 200 torr nitrogen is considerably slower than with oxygen alone as indicated by the data of Table XVI. The data presented indicates that the specific weight changes are approximately ten times smaller in nitrogen than in oxygen and, thus, the values of the average parabolic rate constant are of the order of 100 times smaller. These observations are in agreement with those of Richardson and Grant (ref. 13). No estimation of the activation energy for the titanium-nitrogen reaction has been made from these data; however, others have cited values ranging from 36 to 46 $\frac{\text{K-cal}}{\text{mole}}$ (see reference 12).

The only alloy tested in 200 torr nitrogen was Ti-6Al-4V and data from this test indicated that the reaction of this alloy in nitrogen was approximately 15 times less rapid than the same alloy exposed in 200 torr oxygen. Further, comparison with the data for unalloyed titanium specimens and the alloy indicate that the reactivity of the Ti-6Al-4V alloy is approximately 2 to 5 times less than the unalloyed material in 200 torr nitrogen at 1100°C. It is suspected that the formation of aluminum-bearing nitride(s) may be responsible for this behavior.

Titanium was also oxidized in three binary gas mixtures at both 1000° and 1100°C under conditions such that each component of these gases had

an ideal partial pressure of 200 torr. The mixtures so employed were: oxygen and helium, oxygen and nitrogen, and nitrogen and helium. The results of these tests, shown in Table XVII, indicate that for each of the six conditions investigated the observed rate of reaction was intermediate to the rates observed (or expected in the case of helium) for the individual components. That is, the less reactive gas essentially diluted the oxidizing effectiveness of the most reactive gas. These observations may be rationalized on the basis of localized depletion of the more reactive gas in the immediate neighborhood of the specimen. In the case of oxygen-nitrogen gas mixtures, the results infer that nitrogen provides no synergistic effect if the gases are present in a 1:1 ratio. Further tests, conducted at total pressures of 200 torr and with oxygen/nitrogen ratios of 1:1 and 1:3 also failed to uncover any evidence for a synergistic effect. From these tests and those performed in 200 torr undiluted gases, it was concluded that there exists a monotone relation between the weight change and the oxygen content of the working gas over the range 0 to 200 torr oxygen partial pressure.

The results of the cyclic tests conducted in 200 torr oxygen using unalloyed titanium specimens indicated abnormally large weight gains, especially considering their short residence at maximum temperature, when compared to (RHC) type tests of the same maximum temperature. This behavior strongly suggests that faults were mechanically induced in these scales by thermal stresses which, in turn, led to enhanced reactivity. It is noted that, in spite of the higher number of thermal cycles imposed on the higher temperature (900° to 1100°C) specimen, it exhibited a smaller weight gain than the lower temperature (800° to 1000°C) specimen. This observation suggests two possible rationale: 1) that higher temperatures tend to higher oxide plasticity or 2) as cited earlier, the α to β substrate

transformation may in some way accelerate the rate of reaction; i.e., for the lower temperature cyclicly exposed specimen only. That the oxide plasticity is limited is supported by the observation that faster cooling rates lead to larger specific weight changes. This observation supports the previously mentioned concept of reaction occurring during the cooling period, due to oxide spalling, and resulting in additional substrate oxidation.

3. MICROSCOPIC ANALYSES OF EXPOSED SPECIMENS

In this section are reported the microscopic features of selected unalloyed titanium and titanium-base alloy specimens as determined by microscopic examination and microhardness testing. Metallographic preparation procedures have been noted earlier, see Appendix III. Microhardness values have been determined using an A. I. Buehler "Micromet" microhardness tester equipped with a Knoop diamond and using an indentation load of 100 grams.

Microscopically, all exposed specimens may be subdivided into three major zones:

- 1) A zone of reaction product or scale which appears on the outermost portions of exposed specimens and which is essentially non-metallic in nature. This zone is nominally composed of oxides and/or nitrides of titanium.

- 2) An intermediate zone, between the reaction product and the "core" of the specimen which is here termed the "diffusion zone." This region is composed of base metal strongly enriched in selected components of the gaseous atmosphere which have reached the metal-reaction product interface and have subsequently entered into solution with the metallic phase(s) by the process of chemical diffusion.

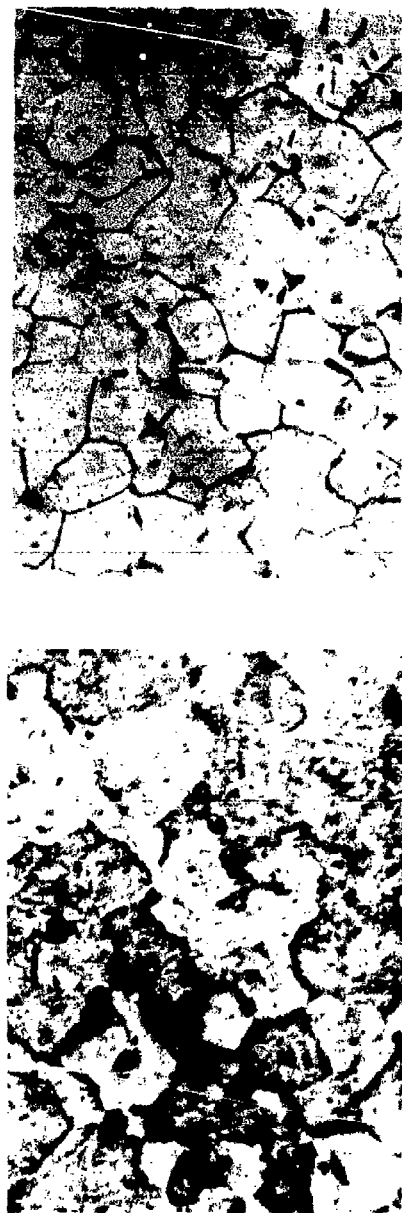
3) A zone deepest within the specimen and whose structure from the specimen centerline to the innermost edge of the diffusion zone is essentially constant. This region has here been termed the zone of unaffected metal or "core."

3a. MICROSTRUCTURAL FEATURES

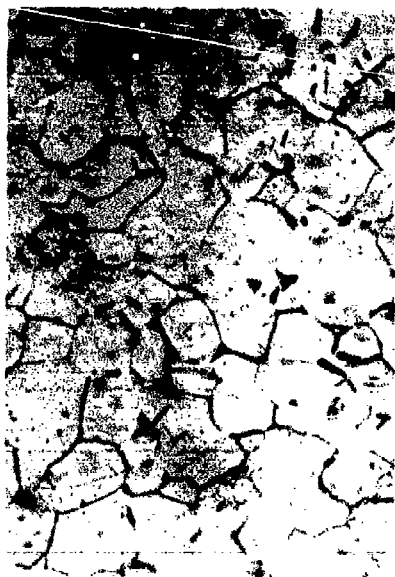
The microstructural character of selected unalloyed titanium and titanium-base specimens both prior to and subsequent to their exposure at elevated temperature is presented here. In a few instances, and then only when slow cooling was employed, was it possible to retain the scale layer in situ (or nearly so) upon the metal. In most instances, however, the scale spalled away prior to the time that the specimen was dip-coated with epoxy. For this reason, most of the metallographic evidence presented below centers primarily upon the diffusion zone and the unaffected metal immediately beneath it.

The oxidizing gases employed in this research contain oxygen and/or nitrogen which singly or in combination play a role as alpha-phase stabilizers (ref. 17). Thus, as will be seen, the untransformed diffusion zone differs in character from the core of the specimens which undergoes typical "basketweave" (ref. 17) or other transformation to greater or lesser degrees from specimen to specimen.

The photomicrographs of Figure 10 illustrate the microstructures of the 5 types of "as-received" unalloyed titanium investigated in this research. All photomicrographs are here (and elsewhere unless noted otherwise) of etched surface oriented with the rolling plane parallel to the horizontal (long) axis of the figure and with the rolling direction normal to the plane of the figure. The grains of the unalloyed titaniums appear equiaxial and of mean diameters which generally decrease with decreasing gauge thickness: 30 μm for types 1 through 3; 15 μm for Type 4; and 8 μm



(a) - Type 1



(b) - Type 2

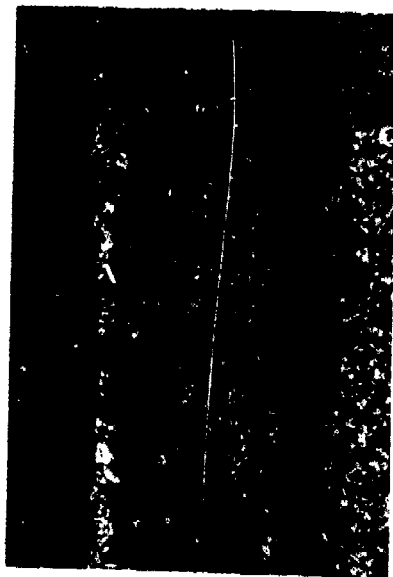


(c) - Type 3

Figure 10.- Photomicrographs illustrating the structures of the 5 types of unalloyed titanium used in this investigation. All materials in the as-received condition. Magnification 400X; Kroll's Etch.



(d) - Type 4



(e) - Type 5

Figure 10. - concluded.

for the Type 5 material.

The photomicrographs of Figure 11 illustrate the microstructures of the 3 types of "as-received" Ti-6Al-4V alloys investigated. Again, it is seen that the mean size of the microconstituents decreases with decreasing gage of the sheet. All alloy types exhibit an ($\alpha + \beta$) structure with the thickest (Type 2) material exhibiting a coarse Widmannstätten structure and the thinnest (Type 3) material exhibiting a fine, nearly equiaxial structure of 2 μm mean microconstituent dimension.

The "as-received" microstructures of the final two alloys investigated are illustrated in the photomicrographs of Figure 12. The structure of the Ti-8Mn alloy, Figure 12a, exhibits an ($\alpha + \beta$) structure, indicating that it had been worked and/or annealed in the ($\alpha + \beta$) field (ref. 17). Some orientation effects, evidently from the working operation, are seen in this fine ($\alpha + \beta$) dispersion. The structure of the β -III alloy, Figure 12b, exhibits an essentially all-(β) structure with evidence for what appears to be a minor amount of grain boundary (α) phase. There is some evidence for oriented segregation in this material which is composed of equiaxial grains of a 20 μm mean diameter.

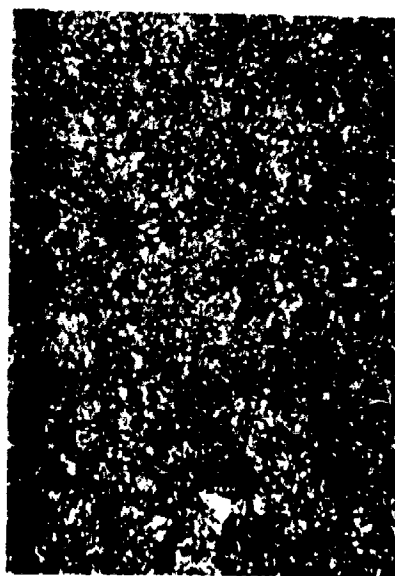
The photomicrographs of Figure 13 illustrate the gross structure of the oxide scale and the nature of the diffusion and unaffected metal zones of the unalloyed titanium (Type 1) substrate. The oxide is clearly lamellar in structure, exhibiting void alignment and densification at the outermost (gas-oxide) interface region. Although somewhat unclear, the diffusion zone appears to be composed of equiaxial (α) grains which overlay the coarse acicular "basketweave" structure. The coarseness is believed to be due primarily to the controlled slow cooling (0.5°C/s) which this specimen experienced. When specimens are processed identically, with the exception of more rapid cooling (8°C/s), then the acicular structure is developed



(a) - Type 2



(b) - Type 1



(c) - Type 3

Figure 11. - Photomicrographs illustrating the structures of the 3 types of Ti-6Al-4V alloys used in this investigation. All materials in the as-received condition. Magnification 400X; Kroll's Etch.



(a)



(b)

Figure 12.- Photomicrographs illustrating the structures of the Ti-8Mn (a) and B-III (b) alloys used in this investigation. Both materials in the as-received condition. Magnification 400X; Kroll's Etch.



(a) - Spec. No. 06141



(b) - Spec. No. 06141

Figure 13. - Photomicrographs of an unalloyed titanium (Type 1) specimen heated at the rate of 0.5°C/s to 1000°C in 200 torr oxygen to 1000°C and cooled at 0.5°C/s . (a) oxide scale, magnification 400X, unetched; (b) substrate, magnification 200X, anodized.

on a finer scale.

The 5 types of unalloyed titanium used in this investigation were somewhat different chemically, principally in the fact that Types 2 through 5 were less pure than was Type 1 by virtue especially of their higher iron concentrations. The photomicrographs of Figure 14 illustrate differences in structure after exposure at 1000°C in 200 torr oxygen which is believed to be due primarily to this difference in chemistry. This figure illustrates that the oxygen-stabilized diffusion zone is somewhat thinner for the Type 2 specimen and the grains in its unaffected core are less ragged, more strongly demarked, and highly acicular. It is suggested that these effects are due to the presence of the (β)-stabilizing iron impurity contained in the Type 2 material. In addition, it has been found that the scale formed on the unalloyed titanium (Type 2) specimens is much more compact (less lamellar) in character than that formed on the Type 1 material.

The independent effects of alloy additions and maximum exposure temperature are illustrated by the photomicrographs of Figures 15 through 17. For the specimens involved here, the heating rates, gages, test type (RHC), and exposure times in 200 torr oxygen are nominally constant so as to make intercomparison as valid as practicable. The materials involved include: unalloyed titanium (Type 3), Ti-6Al-4V (Type 1) alloy (mechanically milled to a nominal thickness of 0.110 cm), Ti-8Mn alloy, and β -III alloy; maximum exposure temperatures were 1000°, 1100°, and 1200°C.

In all cases, the "as-received" microstructure illustrated in Figures 10 through 12 have been coarsened by high-temperature exposure and there is a general tendency for the formation of typical "basketweave" structures to be formed upon cooling. Only the β -III alloy returns an equiaxial grain structure and that is outlined by transformation product on the grain



(a) Type 1: Spec. No. 06132



(b) Type 2: Spec. No. 09191

Figure 14.- Photomicrographs of unalloyed titanium specimens heated at the rate of 8°C/s to 1000°C in 200 torr oxygen. Magnification 200X; Kroll's Etch.



(a) Ti (Type 3); Spec. No. 09194



(b) Ti-6Al-4V (Type 1); Spec. No. 407161

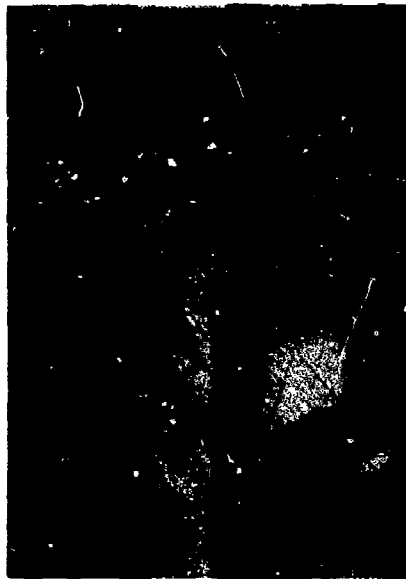


(c) Ti-8Mn; Spec. No. 406032



(d) β -III; Spec. No. 406191

Figure 15.- Photomicrographs of titanium-base specimens heated at the rate of 8°C/s to 1000°C in 200 torr oxygen. Magnification 80X; Kroll's Etch. Part (d) only; dark field.



(a) T1 (Type 3); Spec. No. 405021



(b) T1-6A1-4V (Type 1); Spec. No. 405072



(c) T1-8Mn; Spec. No. 405073



(d) β -III; Spec. No. 406173

Figure 16.- Photomicrographs of titanium-base specimens heated at the rate of 8°C/s to 1100°C in 200 torr oxygen. Magnification 80X; Kroil's Etch.



(a) T1 (Type 3); Spec. No. 405023



(b) Ti-6Al-4V (Type 1) Spec. No. 408081



(c) T1-8Mn; Spec. No. 407242



(d) α -III; Spec. No. 407241

Figure 17. - Photomicrographs of titanium-base specimens heated at the rate of 5.9°C/s to 1200°C in 200 torr oxygen. Magnification 80X; Kroll's Etch. Part (d) only: dark field.

boundary network after high-temperature exposure. The degree of coarsening of the microconstituents generally increases with increasing exposure temperature in the range of 1000° to 1200°C, as expected.

At 1000°C, the unalloyed titanium and Ti-6Al-4V alloy specimens exhibit well-defined (α) - stabilized diffusion zones while the Ti-8Mn and β -III alloy specimens do not, see Figure 15. In unalloyed titanium, this (α) - stabilized surface region is thermodynamically stable at temperatures of 1000° to 1200°C for dissolved oxygen concentrations in excess of approximately 2½% to 4%, respectively (refs. 7, 18). Figures 15a and 15b indicate some evidence for intergranular attack of this region during oxidation. A similar behavior has been noted for unalloyed titanium (Type 1) specimens subjected to long term exposure in air. This is illustrated clearly by the photomicrograph of Figure 18 for a specimen oxidized for 4 hours in air at 1000-C. It is noted that the cracks cease to propagate at the interface between the diffusion zone and the core material.* This indicates that the material of the diffusion zone may be more brittle than that of the core as would be expected if oxygen solution involved either hardening or ordering phenomena. The relative hardness of these zones will be discussed in a following section. The Ti-8Mn alloy specimen, Figure 15c does show some evidence for microconstituent coarsening at the metal/oxide interface and this is presumed to also occur as a result of oxygen solution. The β -III alloy specimen, Figure 15d, exhibits a fine acicular structure within those grains nearest the metal/oxide interface and this too is presumed to occur as a result of oxygen solution. In addition, this specimen exhibits a definite thinning near the edge.

*It is recognized that a portion of the void structures illustrated in Figure 15 through 18 could have arisen as a result either of cooling stress or metallographic artifacts induced; however, some faults were probably present at temperature.

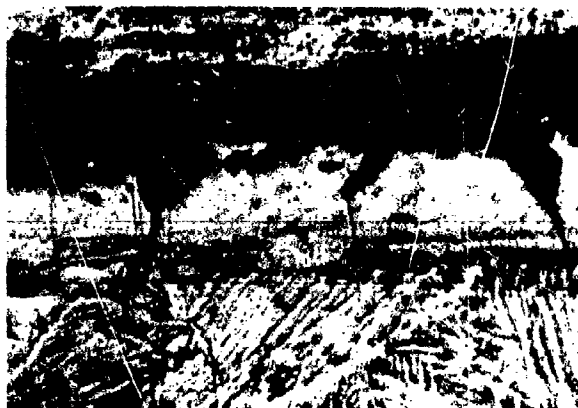


Figure 18. - Photomicrograph of unalloyed titanium (Type 1) specimen no. 05011 oxidized for 4 hours in air at 1000°C. Note attack of columnar diffusion zone. Magnification 200X; Kroll's Etch.

Those effects noted at 1000°C exposure are amplified at 1100°C, see Figure 16. Structures are generally coarser, diffusion-affected zones are deeper, and intergranular attack of these zones formed in the unalloyed titanium, Ti-6Al-4V alloy and Ti-8Mn alloy specimens is more pronounced. For the β -III alloy specimen, Figure 16d, rounding of the edges has occurred to a greater degree and a general "end effect" is noted, transformation product has been formed upon the grain boundaries throughout the specimen, and the acicular structure near the metal/oxide interface is better developed. At 1200°C, further amplification on the effects found at 1100°C are noted. Major changes involve; the apparent saturation of the entire Ti-6Al-4V alloy specimen with oxygen, Figure 17b, and a well defined rounding of previously square edges in combination with the formation of a cruciform scale layer, Figure 17d, typical of hard metal oxidation (ref. 19). It is presumed that local stress generation produces failure of the scale at temperature which, subsequently, allows the specimen edge to be more readily attacked. Throughout the sequence of specimens represented by Figures 15 through 18, it appears that grain and/or microconstituent boundaries in the metallic phases are sites for relatively more rapid transport of oxygen.

The photomicrographs of Figures 19 through 21 illustrate the effects of heating rate per se upon the structure of titanium-base materials oxidized in 200 torr oxygen at 1100°C. The microstructural data presented in Figures 20 and 21 represent the usual extremes of heating rate (0.5° and 22°C/s) used in our tests.*

The structures developed in unalloyed titanium (Type 1) specimens are shown in Figure 19. For these tests, the "basketweave" structure appears

*The effects illustrated in Figures 20 and 21 may be interpolated through the use of Figure 16.



(a) 0.5°C/s; Spec. No. 06131



(b) 8°C/s; Spec. No. 06071



(c) 22°C/s; Spec. No. 06142

Figure 19. - Photomicrographs of unalloyed titanium (Type 1) heated at various rates to 1100°C in 200 torr oxygen. Magnification 200X; Kroll's Etch.



(a) Ti-6Al-4V (Type 1) Spec. No. 401091



(b) Ti-6Al-4V (Type 2) Spec. No. 402042



(c) Ti-8Mn Spec. No. 405074

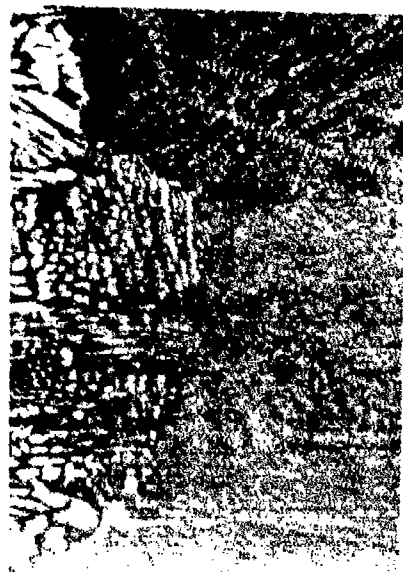


(d) β -III Spec. No. 406174

Figure 20. - Photomicrographs of titanium-base alloy specimens heated at the rate of 0.5°C/s to 1190°C in 200 torr oxygen. Magnification 80X; Kroll's Etch. Part (d) only: dark field.



(a) Ti-6Al-4V (Type 1) Spec. No. 40392



(b) Ti-6Al-4V (Type 2) Spec. No. 402043



(c) Ti-8Mn Spec. No. 406031



(d) β -Ti Spec. No. 406175

Figure 21. - Photomicrographs of titanium-base alloy specimens heated at the rate of 22°C/s to 1100°C in 200 torr oxygen. Magnification 80X; Kroll's Etch. Part (d) only: dark field.

to coarsen as the heating rate is increased and, for the specimen heated at the highest rate, the structure is so coarse as to apparently disappear. This effect may possibly be interpreted on the basis of recrystallization reactions occurring in the substrate as a result of thermal strains induced by the more rapid heating rates. The thicknesses of the diffusion zones in these specimens do not appear to be particularly sensitive to the heating rate and there is some evidence, especially for the specimens exposed to the lower maximum temperature (1000°C; not shown), that brittle fracture of the diffusion zone has occurred during the spalling operation.*

Comparison of Figures 20 and 21 indicates that heating at the slower rate (0.5°C/s) tends to accentuate the formation of oxygen-stabilized (α) - rich diffusion zones. This effect is most likely due to the fact that these specimens had a longer residence time (by 15 min) at temperatures in excess of 600°C where oxygen readily dissolves in titanium-base materials. Somewhat larger diffusion zones were formed in the thicker Ti-6Al-4V (Type 2) alloy specimen than in the chemically similar (Type 1) alloy at both heating rates. This observation suggests that larger thermal stresses, induced during heating, may have played a role in the development of the more well-defined diffusion zones. Qualitative evidence for such stress generation is also suggested from a comparison of the core structures for the Ti-8Mn alloy specimens; although corresponding effects were not noted for other alloy specimens.

The microstructural character of oxidized specimens changes drastically as the gage of the specimens is reduced. Figure 22 illustrates this effect for the case of annealed unalloyed titanium (Types 3, 4, and 5). The thickest

*This effect may be a polishing artifact if the diffusion zone is brittle and therefore friable.



(a) Type 3; Spec. No. 09194



(b) Type 4; Spec. No. 407162



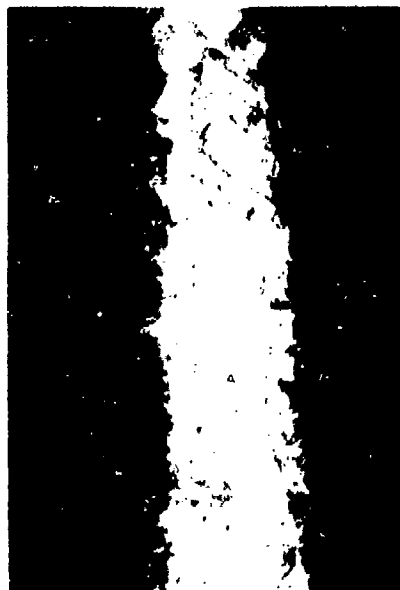
(c) Type 5; Spec. No. 408282

Figure 22. - Photomicrographs of thin unalloyed titanium specimens heated in 200 torr oxygen.
(a) 8°C/s to 1000°C, Magnification 400X, Kroll's Etch; (b) 8°C/s to 1100°C, Magnification 200X, unetched; (c) 8°C/s to 1100°C, Magnification 200X, Kroll's Etch.

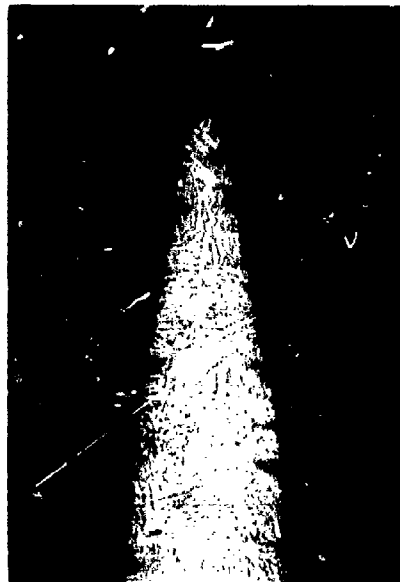
material when exposed at 1000°C develops a compact scale beneath which resides a relatively smooth-sided diffusion zone and a medium-to-fine acicular core structure. At higher temperatures (1100°C; Figure 16a) the diffusion zone is attacked and becomes roughened and the core structure coarsens and the demarcations of the microconstituents become diffuse. At this temperature, further reductions in the gage appear to produce an even more dense scale which overlays a large, α - grain core permeated by cracks, Figure 22b. Inspection of an etched section of this specimen (not shown) indicated that the cracks were basically transgranular in nature although this appeared to originate in the grain boundary network of the metal. The structure may be rationalized upon the basis of development of compressive oxide stresses at temperature (see refs. 6, 20) followed by grain boundary shearing in the metal and, finally, crack growth through the oxygen-saturated matrix. At yet thinner gages, the specimen is transformed totally to porous oxide in less than one hour after being heated at rates between 8° and 18°C/s to 1100°C in 200 torr oxygen, Figure 22c.

The photomicrographs of Figure 23 indicate that gross microstructural effects also occur in the thinner gages of annealed titanium-base alloy specimens when exposed to oxygen at 1100°C. The Ti-6Al-4V (Type 3) specimen exhibits a moderately dense scale (not shown) which overlies an unidentified diffusion zone of pearlitic nature and an essentially α - phase core compound of relatively fine acicular grains.* The thin β -III alloy specimens (mechanically thinned to 0.036 cm) evidently has been saturated with oxygen to the extent that an (α + β) basketweave structure was obtained. Such changes did not occur with thicker specimens even when exposed at higher temperatures, see Figure 17d.

*This structure has an appearance similar to coarse pearlite in carbon steel or a zone of internal oxidation (although this is not believed to be possible on the basis of thermodynamic considerations).



(a) Ti-6Al-4V (Type 3); Spec. No. 406171



(b) β -III; Spec. No. 409231

Figure 23. - Photomicrographs of thin titanium-base alloy specimens heated to 1100°C in 200 torr oxygen. Magnification 200X; Kroll's Etch. (a) Heated at 8°C/s; (b) heated at 22°C/s.

The microstructural character of oxidized specimens is also altered markedly by prior cold work. Figure 24 illustrates examples of this effect where it is seen that, especially for the lesser degrees of cold work, the oxygen stabilized (α) - phase diffusion zone is heavily attacked. This attack provides a much more irregular metal/oxide interface than that produced by oxidation of annealed materials of similar gage; compare for example Figures 22b and 24c. As was noted earlier, the site of attack appears to be located preferentially at the grain boundaries of the (α) - stabilized diffusion zone. Because cold-worked structures will recrystallize at the oxidizing temperatures, it is believed that the severity of attack in the diffusion zone may arise as a result of the recrystallization and oxidation processes occurring simultaneously, as such process would provide a larger number of highly reactive sites per unit area of exposed surface.

The structures developed in two types of unalloyed titanium upon exposure to 200 torr nitrogen at 1000° and 1100°C are presented in the photomicrographs of Figure 25. In both cases, the scales formed and the diffusion zones underlying them are thin relative to those formed during similar thermal programs in 200 torr oxygen. The (α) crystals of the diffusion zone are again believed to be stabilized by interstitial dissolved gas (here nitrogen) and exhibit a coarser structure than does the underlying metal. The acicular structures of the zones of unaffected metal again appear to be influenced by differences in material chemistry as cited just previously.

The structural features present in specimens subjected to gas mixtures (not shown) are intermediate in degree to those found in the individual unmixed gases. This experience parallels that determined by other measures of the gas-metal reaction cited earlier.

3b. DIMENSIONAL ANALYSES

The dimensions of each of the three zones discussed above (scale,



(a) 39% C.W.; Spec. No. 11201



(b) 61% C.W.; Spec. No. 408141



(c) 76% C.W.; Spec. No. 408191



(d) 87% C.W.; Spec. No. 405151

Figure 24.- Photomicrographs of unalloyed titanium heated at the rate of 8°C/s to 1100°C in 200 torr oxygen. Various degrees of prior cold work. (a and b) Magnification 80X; (c and d) Magnification 200X. Kroll's Etch.



(a) Spec. No. 09193



(b) Spec. No. 07312

Figure 25. - Photomicrographs of unalloyed titanium specimens heated at the rate of 8°C/s in 200 torr nitrogen. a) Type 2 material oxidized at 1000°C ; b) Type 1 material oxidized at 1100°C . Magnification 400X; Kroll's Etch.

diffusion zone, and core) were determined from polished metallographic sections of nine selected specimens subsequent to their exposure in the volumetric apparatus. The determined dimensions of these specimens, representing a variety of heating procedures in 200 torr oxygen, are presented in Table XVIII. It is seen from these data that the diffusion zone is usually larger than the zone of scale formation and that the thickness of each of these zones tends to increase with increasing temperature. These data appear somewhat irregular partly because the diffusion zone is both created and destroyed during the course of the reaction; its destruction occurring as a result of continued scale formation. The data describing the thickness of the zone of unaffected metal (core) exhibits a more regular pattern, there being a uniform decrease in this zone with increasing temperature of exposure.*

In order to test the precision of our dimensional measurements, contributions from each of the zones were summed and compared with the initial thickness as determined from micrometer measurements. The use of this comparison depends upon several assumptions as the dimensional observations must be recast into the initial dimensions from which they arose. As indicated in Table XVIII, twice the oxide thickness (x) divided by the Pilling-Bedworth Ratio (ref. 19) plus twice the diffusion zone thickness (y) plus the thickness of the zone of unaffected metal (z) should sum to an ideal initial thickness (Σ). The differences between the observed and ideal initial thickness ($\Sigma_0 - \Sigma$) is a measure of the error involved in this method (failure of dimensional closure). It is seen that these values range from (-28) to (+96) μm .

Other than observational error, negative values of ($\Sigma_0 - \Sigma$) may arise

*Assuming a reasonable thickness correction for short exposure times at the higher temperatures.

TABLE XVIII

MICROSCOPIC DIMENSIONAL CHANGES INDUCED IN UNALLOYED TITANIUM (TYPE 1)

SPECIMENS DURING EXPOSURE IN 200 TORR OXYGEN FOR ONE HOUR

Specimen Number	Heating Rate ($^{\circ}\text{C/s}$)	Thickness (μm)		Unaffected Metal [z]	Ideal Initial Thickness (μm)		Observed Initial Thickness (μm)	Difference (μm)
		Scale [x]	Diffusion Zone [y]		$\frac{2x}{1.73}$	$\frac{2x}{1.73} + 2y + z$		
1000 $^{\circ}\text{C}$ Maximum Temperature								
06051	0.5	25	71	1397		1568	1540 ± 10	-28
06041	0.5	46	89	1346		1577	1570 ± 10	-7
(Slow Cool)								
06132	3	46	80	1354		1567	1570 ± 10	+3
06133	25	15	48	1377		1490	1520 ± 10	+30
1100 $^{\circ}\text{C}$ Maximum Temperature								
06131	0.5	61	90	1237		1487	1510 ± 10	+23
06071	8	102	63	1270		1514	1570 ± 10	+56
06142	22	61	60	1283		1474	1570 ± 10	+96
1300 $^{\circ}\text{C}$ Maximum Temperature*								
07091	4	76	125	1295		1633	1570 ± 10	-63
Cycled 800 $^{\circ}\text{C}$ to 1000 $^{\circ}\text{C}$								
07101	8	33	36	1354		1464	1560 ± 10	+92

*Exposure time limited to ~ 4.5 minutes.

due to non-dense oxide or dilatation of the diffusion zone by oxygen solution, while positive values of this parameter may be indicative of material loss by such mechanisms as oxide spall or vaporization. Combined processes giving both positive and negative deviations, and with either net sign change dependent on the degree of each contribution, may also occur. Further investigation would be required for a more definitive analysis of these data.

An overall summary of diffusion zone thicknesses developed in selected titanium and titanium-base alloys and for various exposure conditions is presented in Table XIX. For the use of unalloyed titaniums, these data indicate that the diffusion depth is relatively unaffected by metal purity and that the depths developed during exposure in 200 torr oxygen were approximately four times greater than those developed in 200 torr nitrogen.

The apparent diffusion zone depths produced in the Ti-6Al-4V alloy specimens were abnormally large with respect to those formed in either unalloyed titanium or the other alloy specimens. It is postulated that the (α) - phase can be stabilized to some degree at 1100°C by the presence of oxygen and that (α - β) boundaries so formed may act as easy diffusion paths for oxygen. Materials which were either more or less (α) - stable would not necessarily produce either the same quality or quantity of (α - β) boundaries in their oxygen-rich diffusion zones. This concept is supported by the photomicrographs of Figures 16 and 17; however, further investigation is required to substantiate this hypothesis of "critical instability" and rapid oxygen movement.

As cited earlier, the trend for decreased diffusion depths with increasing heating rates, common to both the unalloyed and alloyed materials, is most probably due to decreased residence time at temperatures above 600°C associated with the higher heating rates. There is no evidence to indicate that thermal stress in the core material play any substantive role in

TABLE XIX
MICROSCOPIC DETERMINATION OF DIFFUSION ZONE THICKNESSES

Specimen Number	Heating Rate ($^{\circ}\text{C/s}$)	Diffusion Zone Thickness (μm)	Remarks
A. UNALLOYED TITANIUM (TYPE 1)			
05011	~8	100	4-hour exposure
		110	
05072	~8	71	16-hour exposure
		89	
		80	
		48	
06051	0.5	71	
		89	
		80	
		48	
06041	0.5	71	
		89	
06132	8	71	
		89	
06133	25	71	
		89	
07311	8	71	
		89	
06131	0.5	71	
		89	
06071	8	71	
		89	
06142	22	71	
		89	
07312	8	71	
		89	

TABLE XIX - continued

Specimen Number	Heating Rate ($^{\circ}\text{C/s}$)	Diffusion Zone Thickness (μm)	Remarks
08013	7.5	6) 200 torr O_2 ; 1200 $^{\circ}\text{C}$ 290	27 min. exposure
07091	4	7) 200 torr O_2 ; 1300 $^{\circ}\text{C}$ 125	4.5 min. exposure
07101	8	8) 200 torr O_2 ; Cycled 800 $^{\circ}\text{C}$ to 1000 $^{\circ}\text{C}$ 36	49 min. exposure
401151	8	B. UNALLOYED TITANIUM (TYPE 2) 1) 200 torr O_2 ; 1100 $^{\circ}\text{C}$ 63	
11201	8	C. UNALLOYED TITANIUM (TYPE 3) 1) 200 torr O_2 ; 1100 $^{\circ}\text{C}$ 188	Cold worked 39%
401161	0.5	D. TITANIUM - 6% ALUMINUM - 4% VANADIUM (TYPE 1) 1) 200 torr O_2 ; 1100 $^{\circ}\text{C}$ 188	
401091	0.5	113	
11202	8	150	
401092	22	88	

TABLE XIX - continued

Specimen Number	Heating Rate	Diffusion Zone Thickness (μm)	Remarks
E. TITANIUM - 6% ALUMINUM - 4% VANADIUM (TYPE 2)			
		1) 200 torr O_2 ; 1100°C	
402042	0.5	188	
401152	8	94	
402043	22	113	
F. TITANIUM - 8% MANGANESE			
		1) 200 torr O_2 ; 1100°C	
405073	8	60	41 min. exposure
G. TITANIUM - 8 - III			
		1) 200 torr O_2 ; 1100°C	
406173	8	45	22 min. exposure

increasing the diffusion zone thicknesses. Such effects are, however, present for the case of cold-worked substrates (via recrystallization) as indicated earlier.

3c. MICROHARDNESS DETERMINATIONS

Microhardness tests were made for selected unalloyed titanium and titanium-base alloy specimens which had been exposed in oxygen or nitrogen at elevated temperatures.* In each case, at least two and usually three hardness traverses were made from the outermost surface of the metal toward the centerline of the specimen for a distance (d) of approximately 800 μm . In addition, several hardness determinations were made at the specimen centerline in order to determine the core hardness range. The results of these tests were plotted for each specimen and compared with photomicrographs of the same transverse section upon which the hardness had been determined. Such comparisons were used to correlate changes in the hardness values as a function of (d) with the interface between the (α) - stabilized diffusion zones and the cores. The results of this effort are presented for 14 specimens in Figures 26 through 40.

Figure 26 illustrates that for unexposed, unalloyed titanium specimen stock there is essentially no dependence of hardness upon distance along the traverse from a point within approximately 25 μm from the specimen edge to the specimen centerline. This curve, then, serves as "baseline" data and certifies the quality of the testing technique. A photomicrograph of a portion of one typical traverse, shown in Figure 27, clearly illustrates the generally observed effect that the (α) - stabilized diffusion zone (top) is much harder than the core material immediately beneath it. A graph summarizing two traverses taken on this specimen, shown in Figure 28 illustrates:

*Hardnesses are reported as Knoop Hardness Number at 100 gram load (KHN_{100}); long axis of indenter parallel to metal-oxide interface.

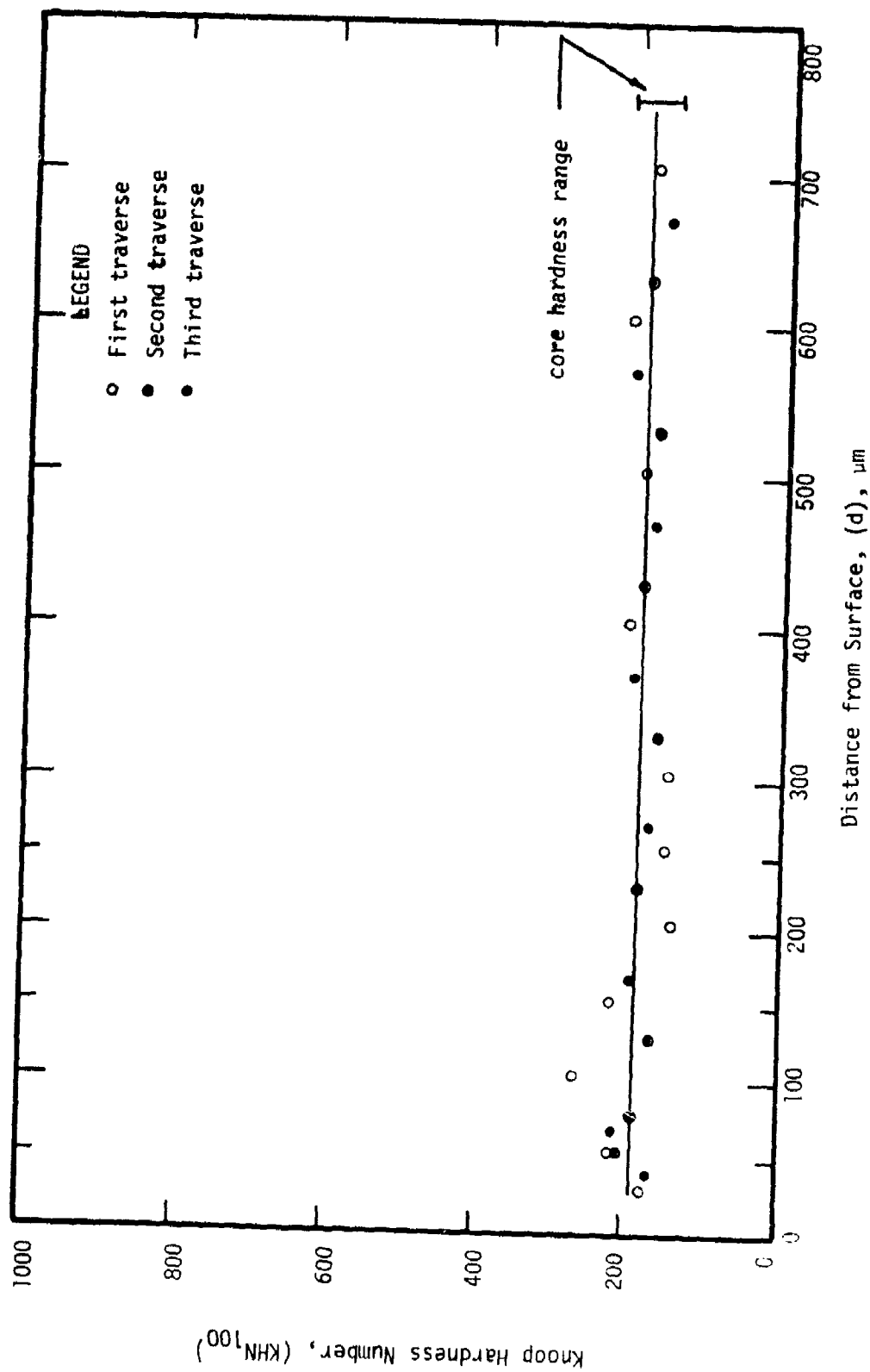


Figure 26. - Hardness of as-received unalloyed titanium (Type 2) as a function of traverse depth from the surface.



Figure 27. - Photomicrograph of unalloyed titanium (Type 1) specimen no. 05011 illustrating a portion of one typical hardness traverse. Oxidized in air for 4 hours at 1000°C. Magnification 400X; Kroll's Etch.

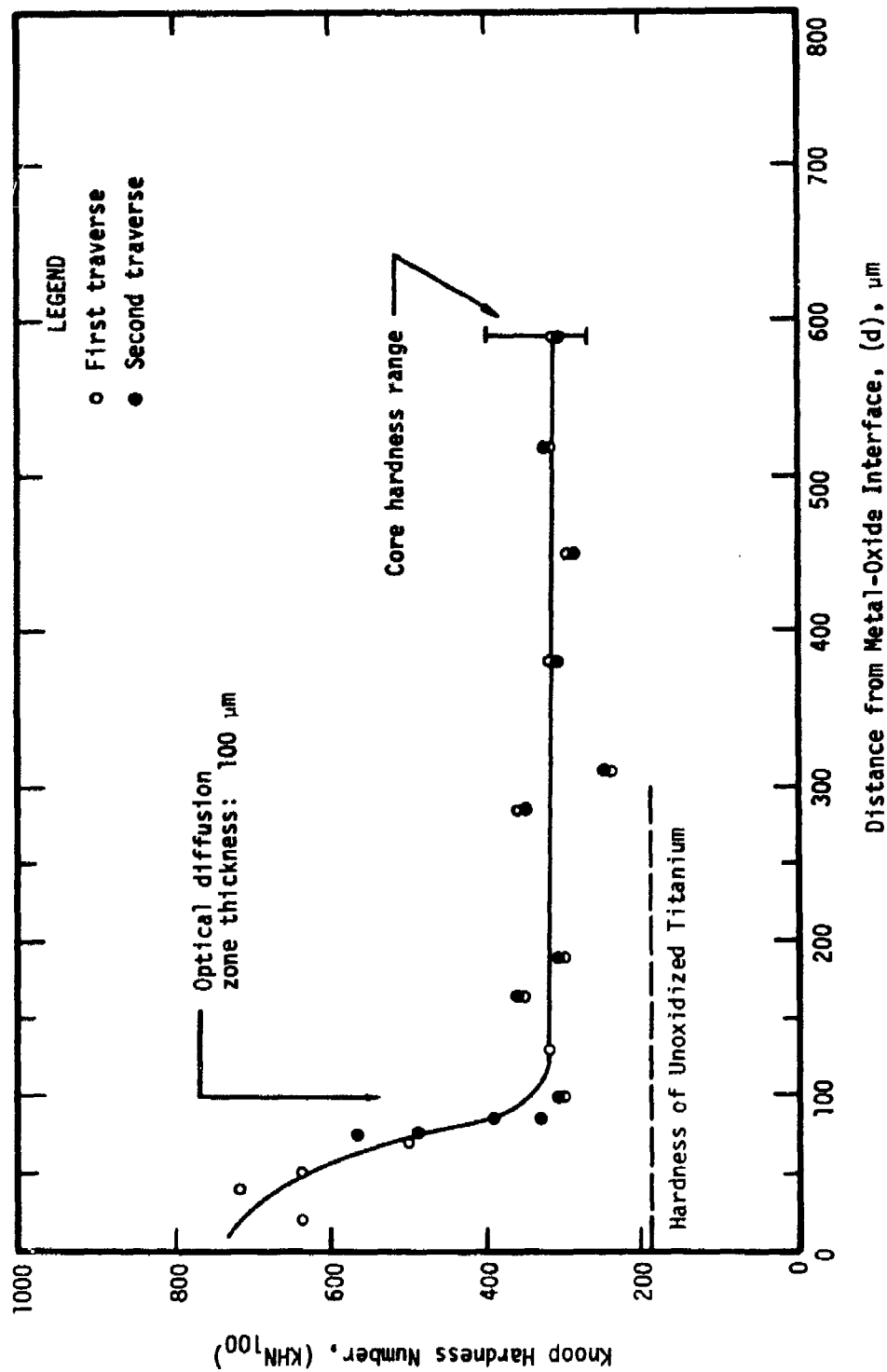


Figure 28. - Hardness of unalloyed titanium (Type 1) specimen no. 05011 exposed for 4 hours in air at 1000°C.

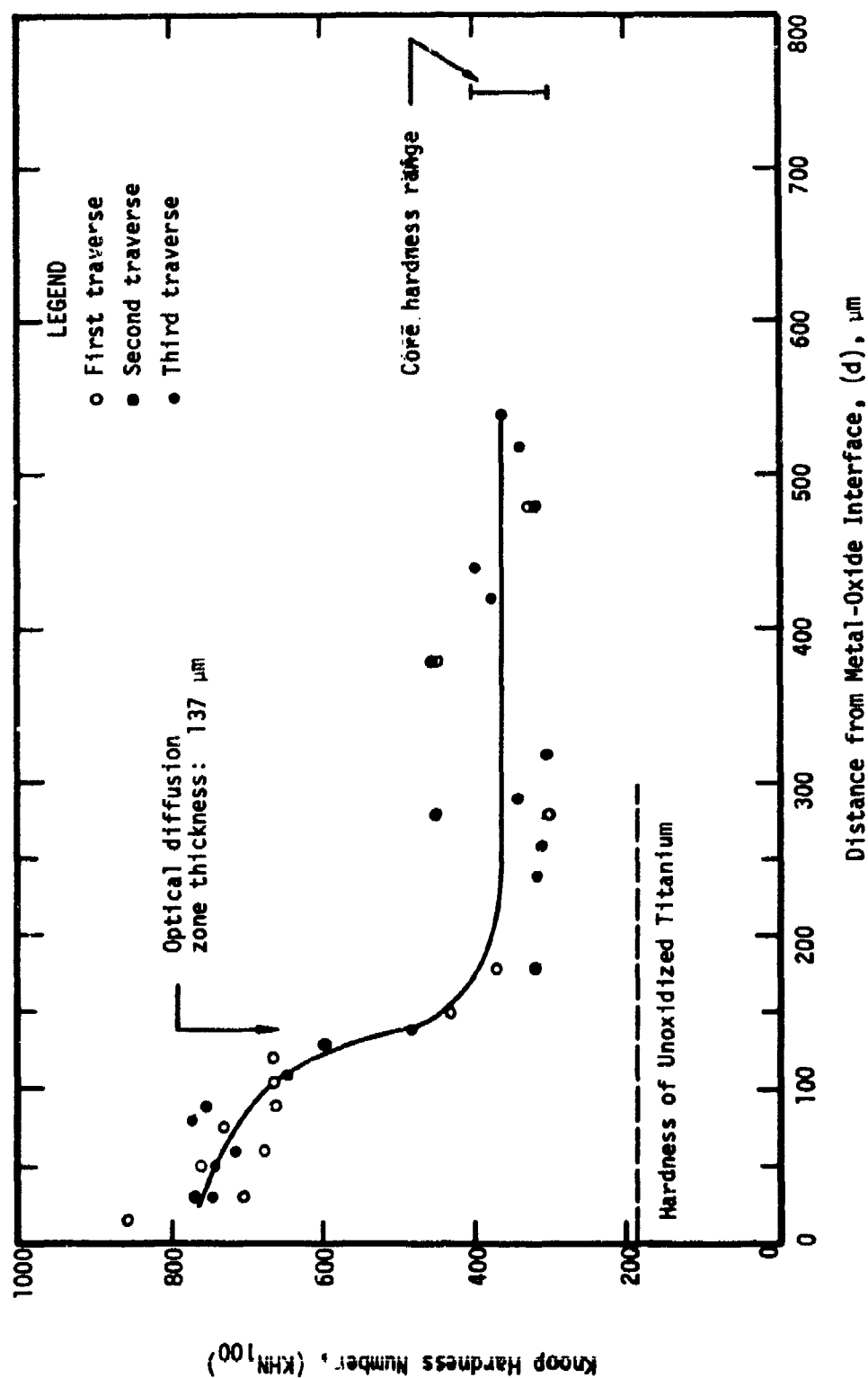


Figure 29. - Hardness of unalloyed titanium (Type 1) specimen no. 05072 exposed for 16 hours in air at 1000°C.

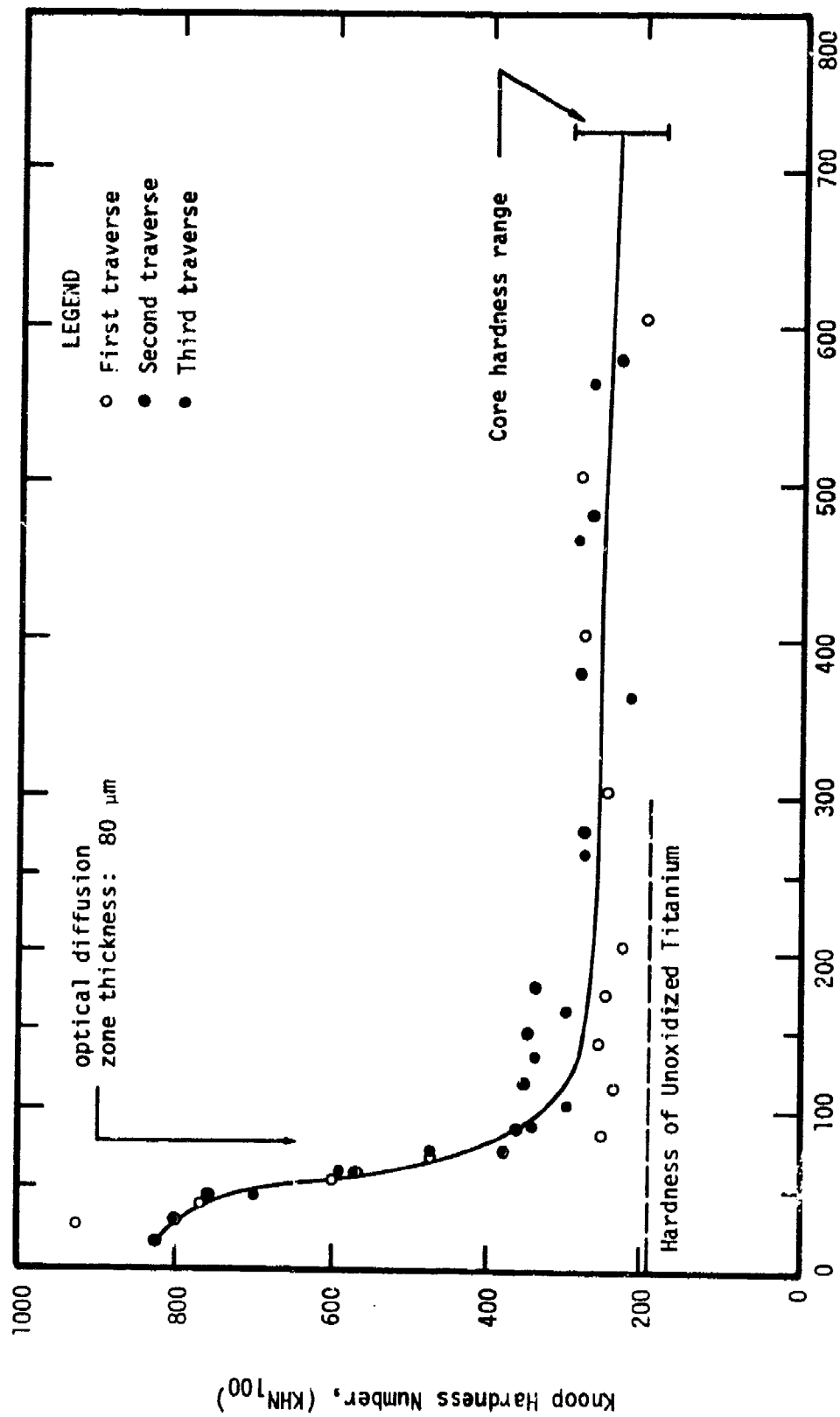


Figure 30. - Hardness of unalloyed titanium (Type 1) specimen no. 06132 heated in 200 torr O₂ at the rate of 8°C/s to 1000°C. Isothermal time 60 min.

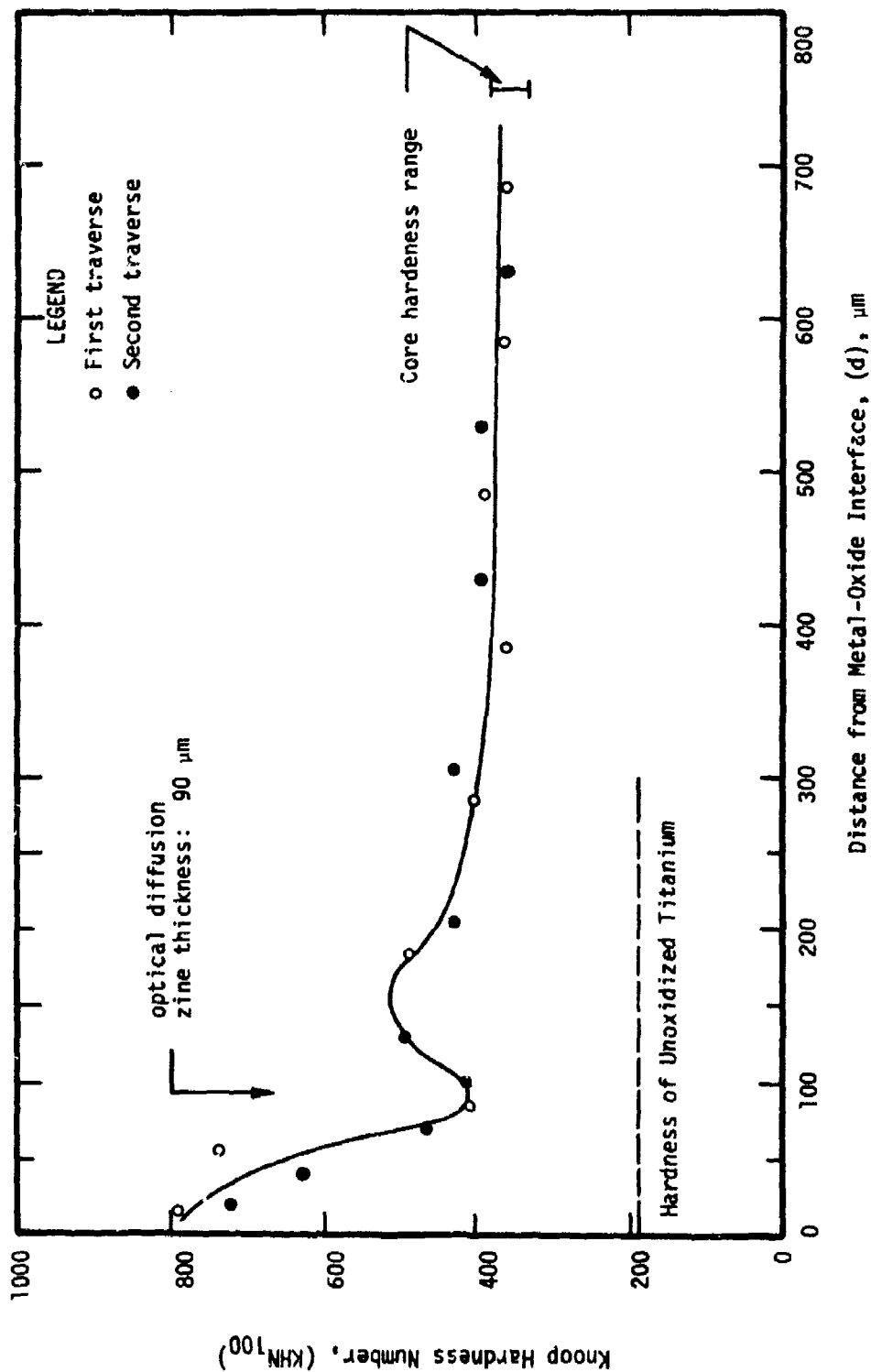


Figure 31. - Hardness of unalloyed titanium (Type 1) specimen no. 06131 heated in 200 torr O₂ at the rate of 0.5°C/s to 1100°C. Isothermal time 60 min.

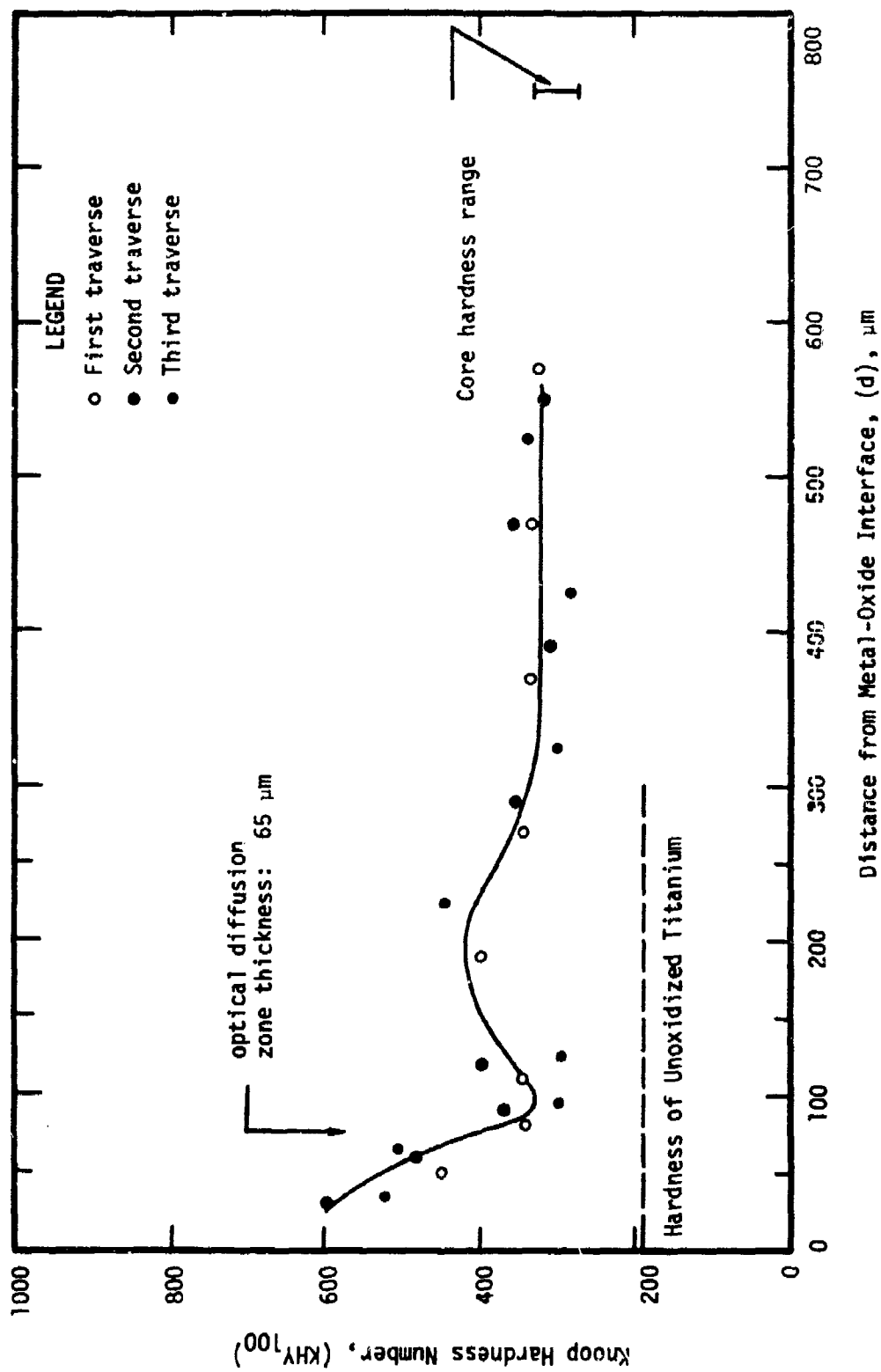


Figure 32. Hardness of unalloyed titanium (Type 1) specimen no. 06071 heated in 200 torr O₂ at the rate of 8°C/s to 1100°C. Isothermal time 60 min.

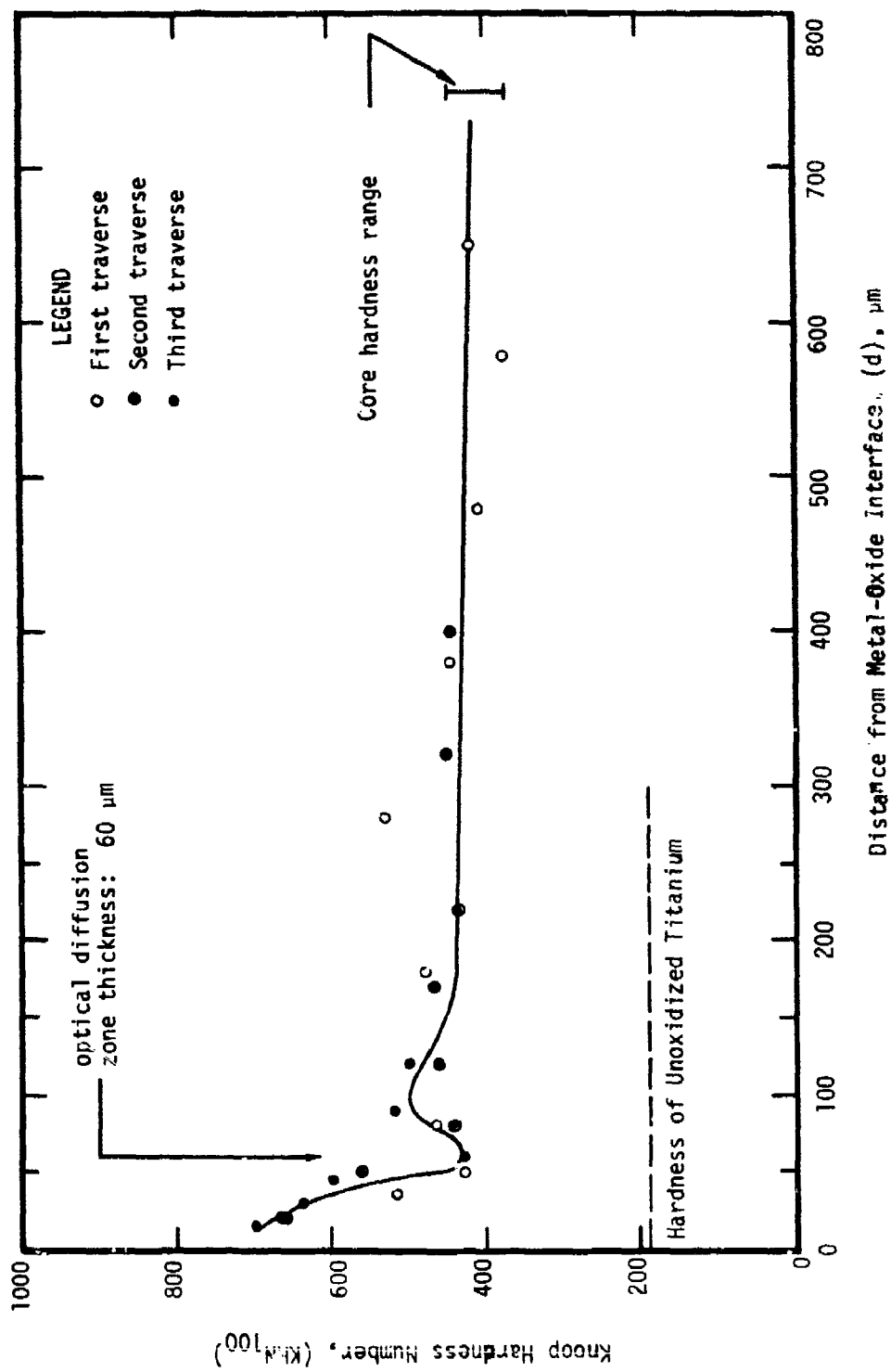


Figure 33. - Hardness of unalloyed titanium (Type 1) specimen no. 06142 heated in 200 torr O_2 at the rate of 22°C/s to 1100°C . Isothermal time 60 min.

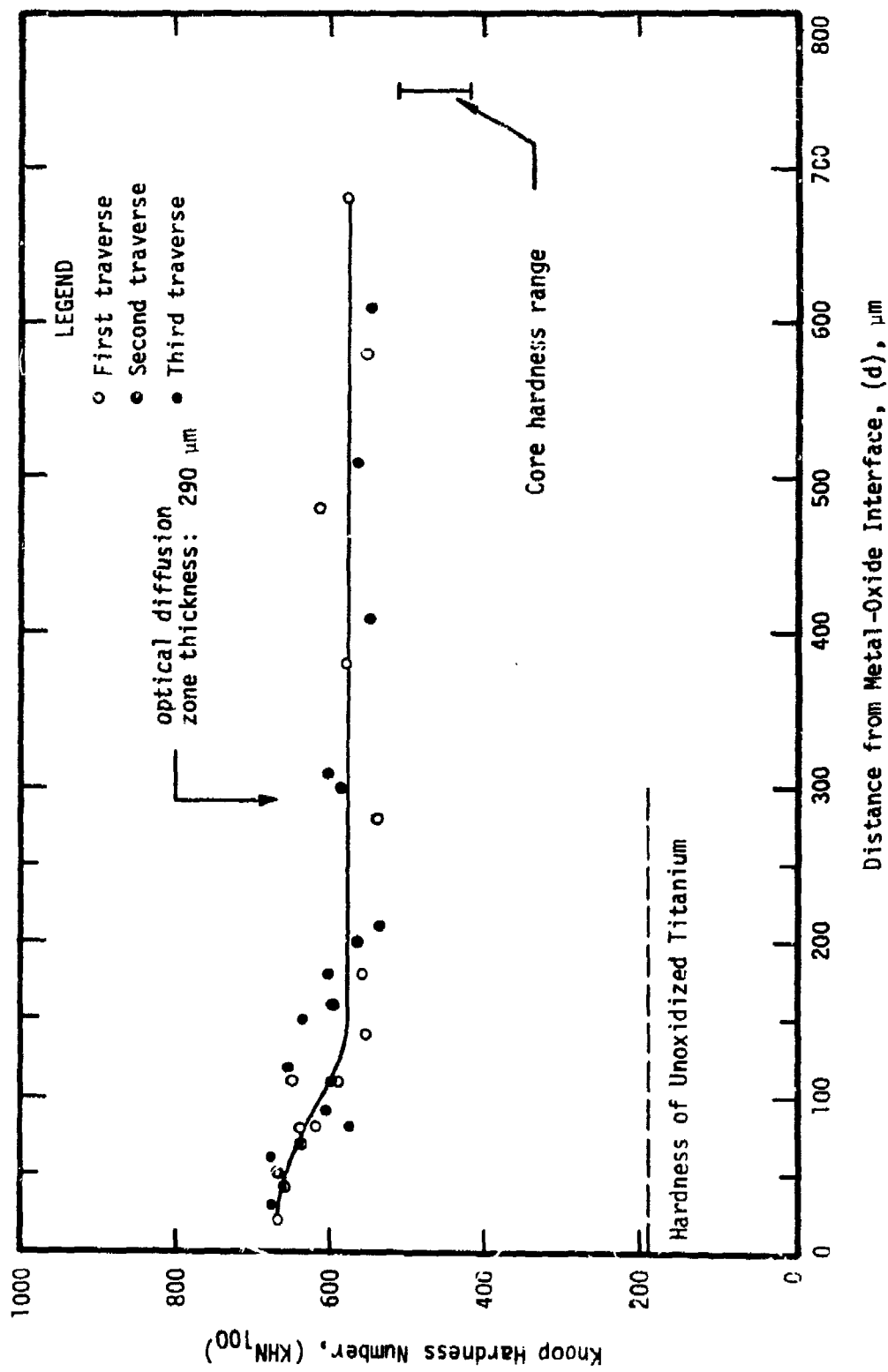


Figure 34. - Hardness of unalloyed titanium (Type 1) specimen no. 08013 heated in 200 torr O_2 at the rate of 7.5°C/s to 1200°C . Isothermal time 27 min.

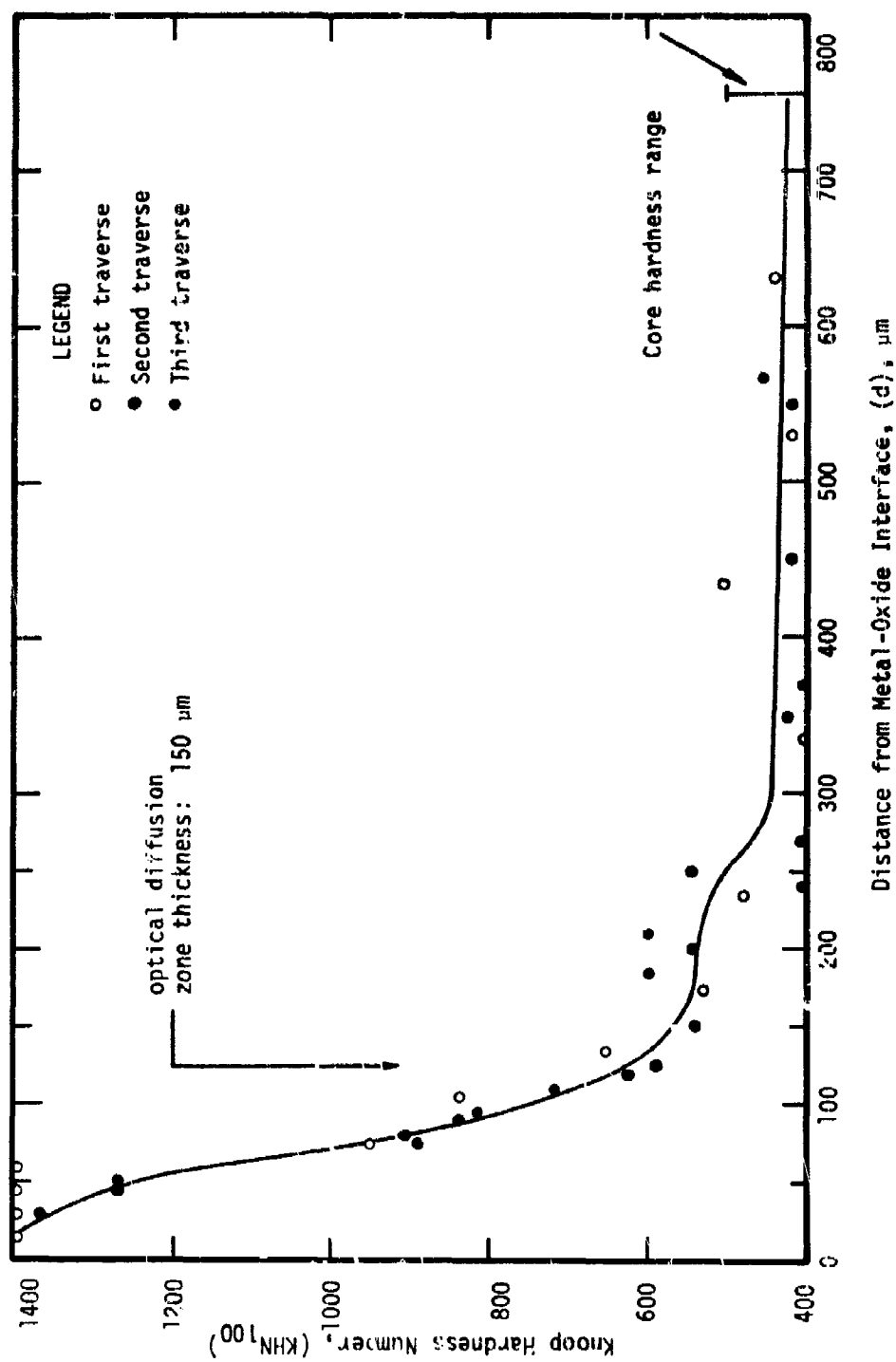


Figure 35. - Hardness of unalloyed titanium (Type 1) specimen no. 07091 heated in 200 torr O_2 at the rate of approximately 4.5°C/s to 1300°C . Isothermal time approximately 4.5 min. Hardness of unoxidized titanium approximately 200 KHN.

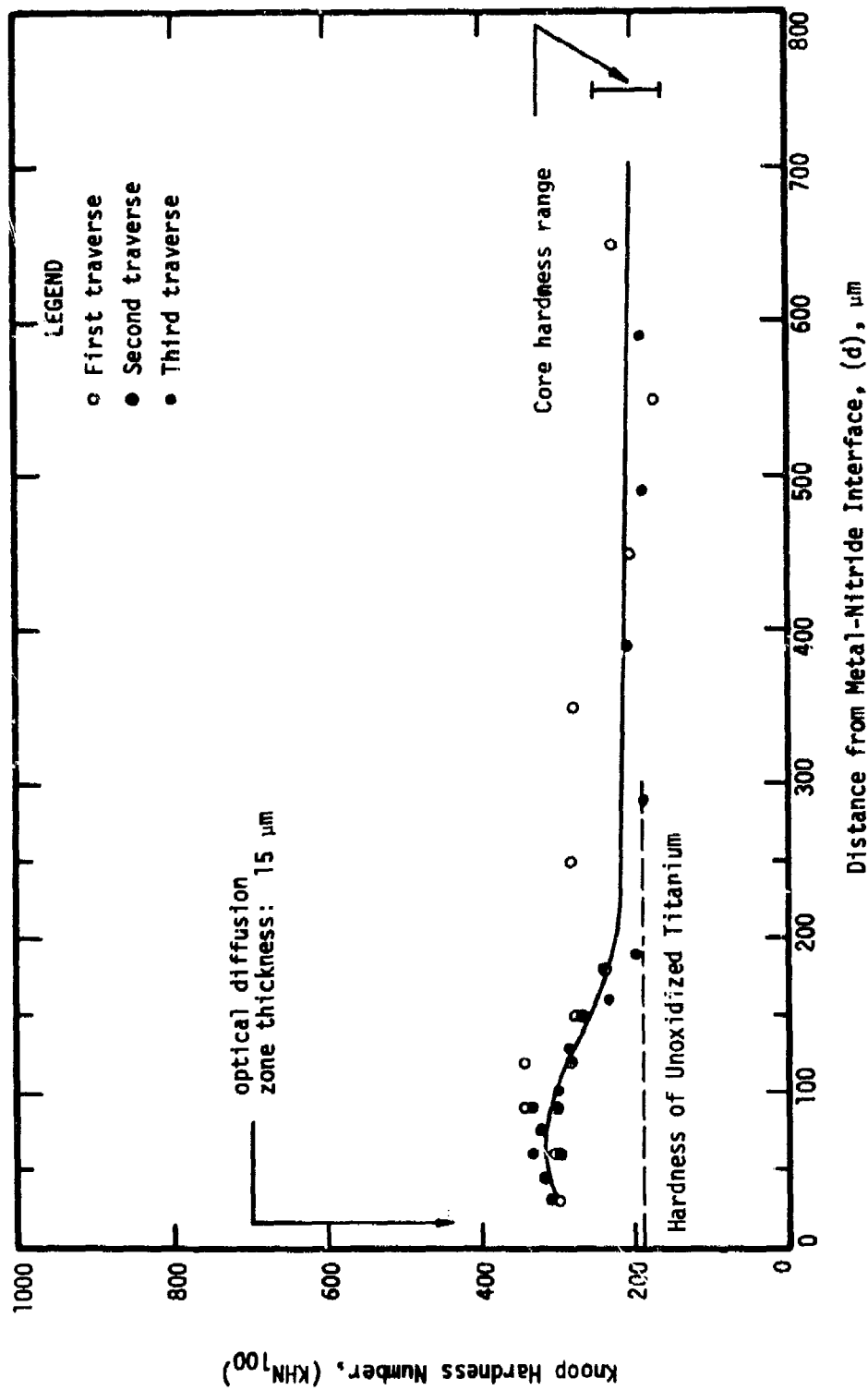


Figure 36. - Hardness of unalloyed titanium (Type 1) specimen no. 07311 heated in 200 torr N₂ at the rate of 8°C/s to 1000°C. Isothermal time 60 min.

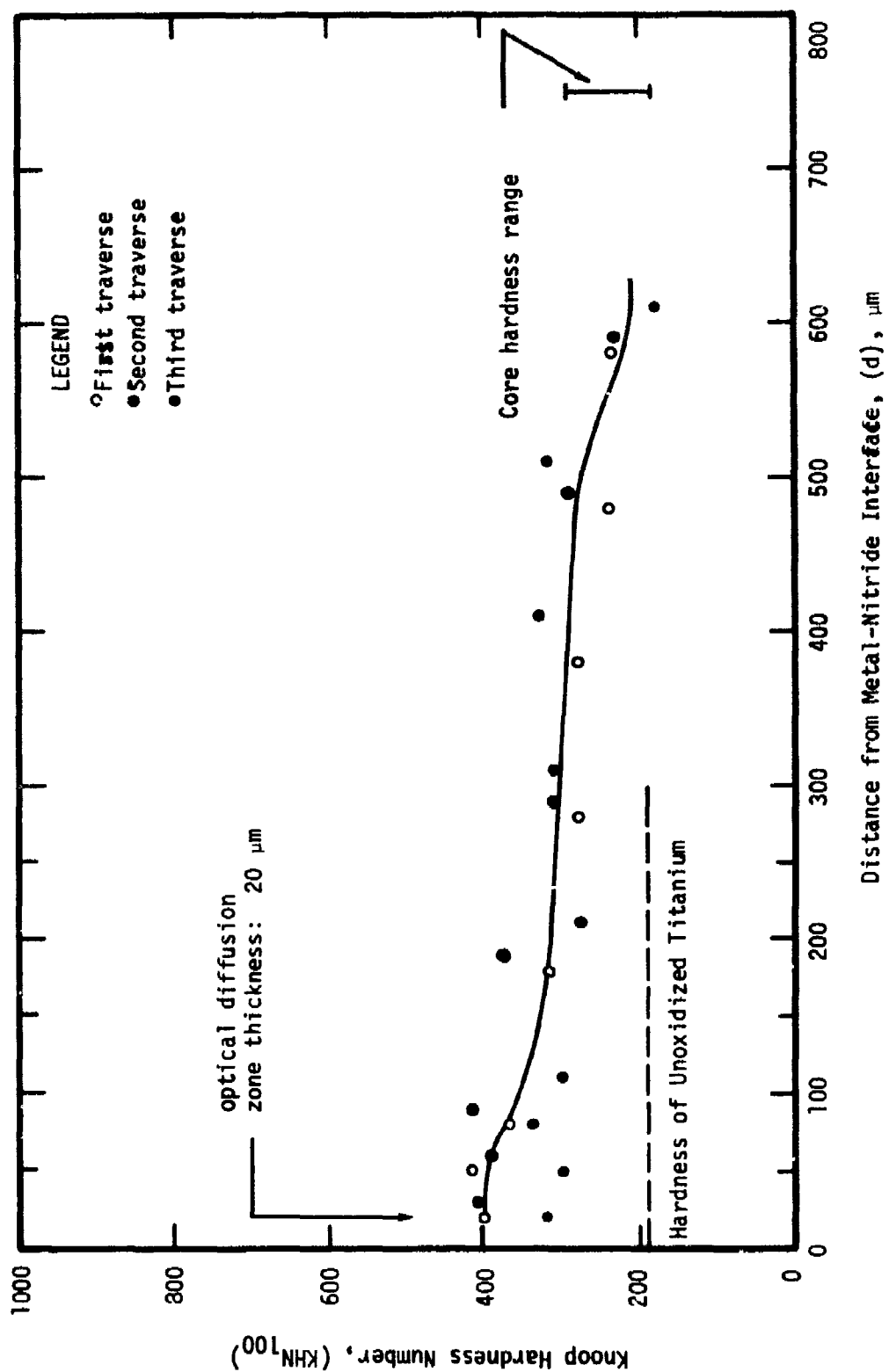


Figure 37. - Hardness of unalloyed titanium (Type 1) specimen no. 07312 heated in 200 torr N₂ at the rate of 8°C/s to 1100°C. Isothermal time 60 min.

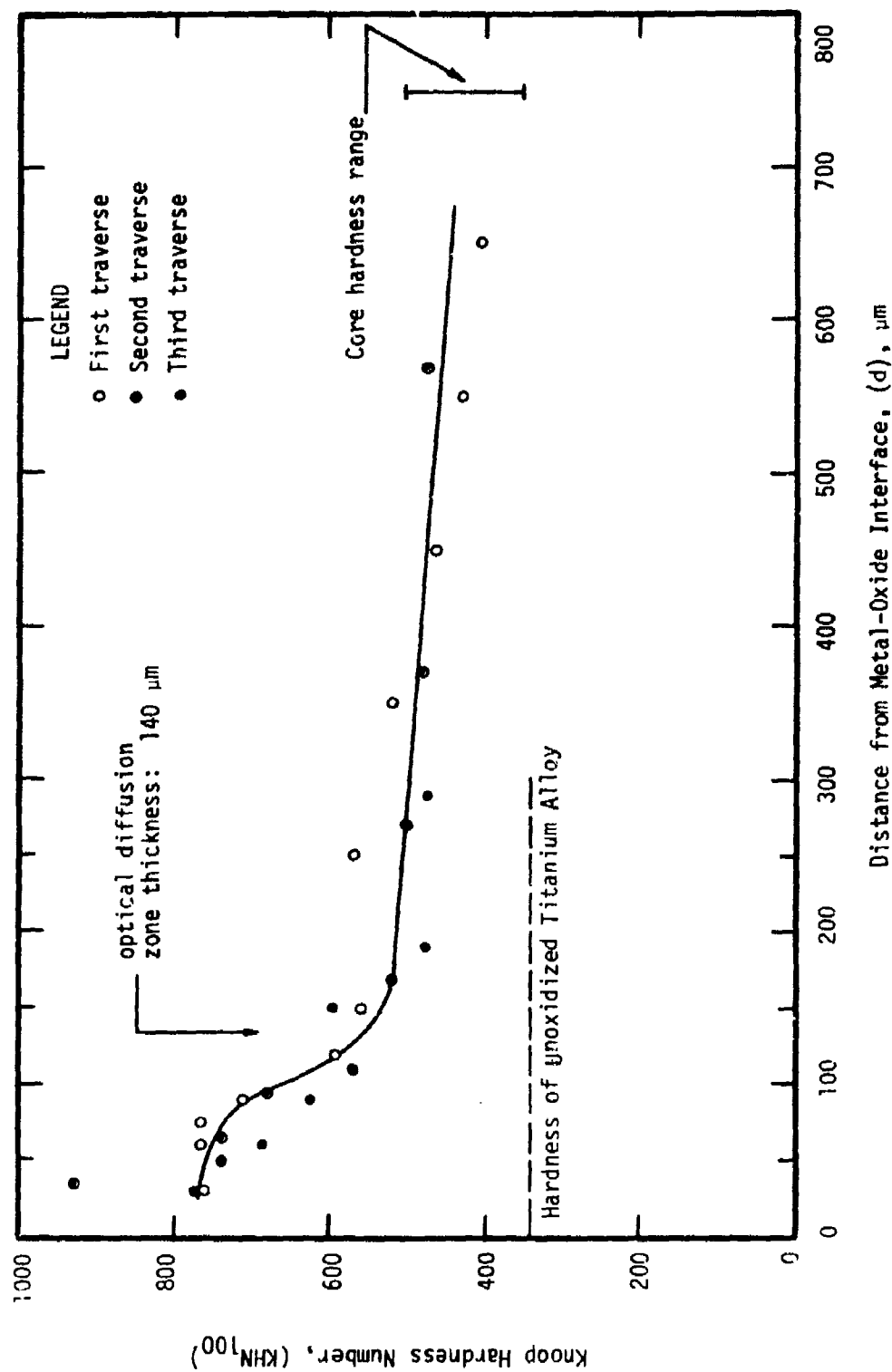


Figure 38. - Hardness of Ti-6Al-4V alloy (Type 1) specimen no. 11202 heated in 200 torr O₂ at the rate of 8°C/s to 1100°C. Isothermal time 60 min.

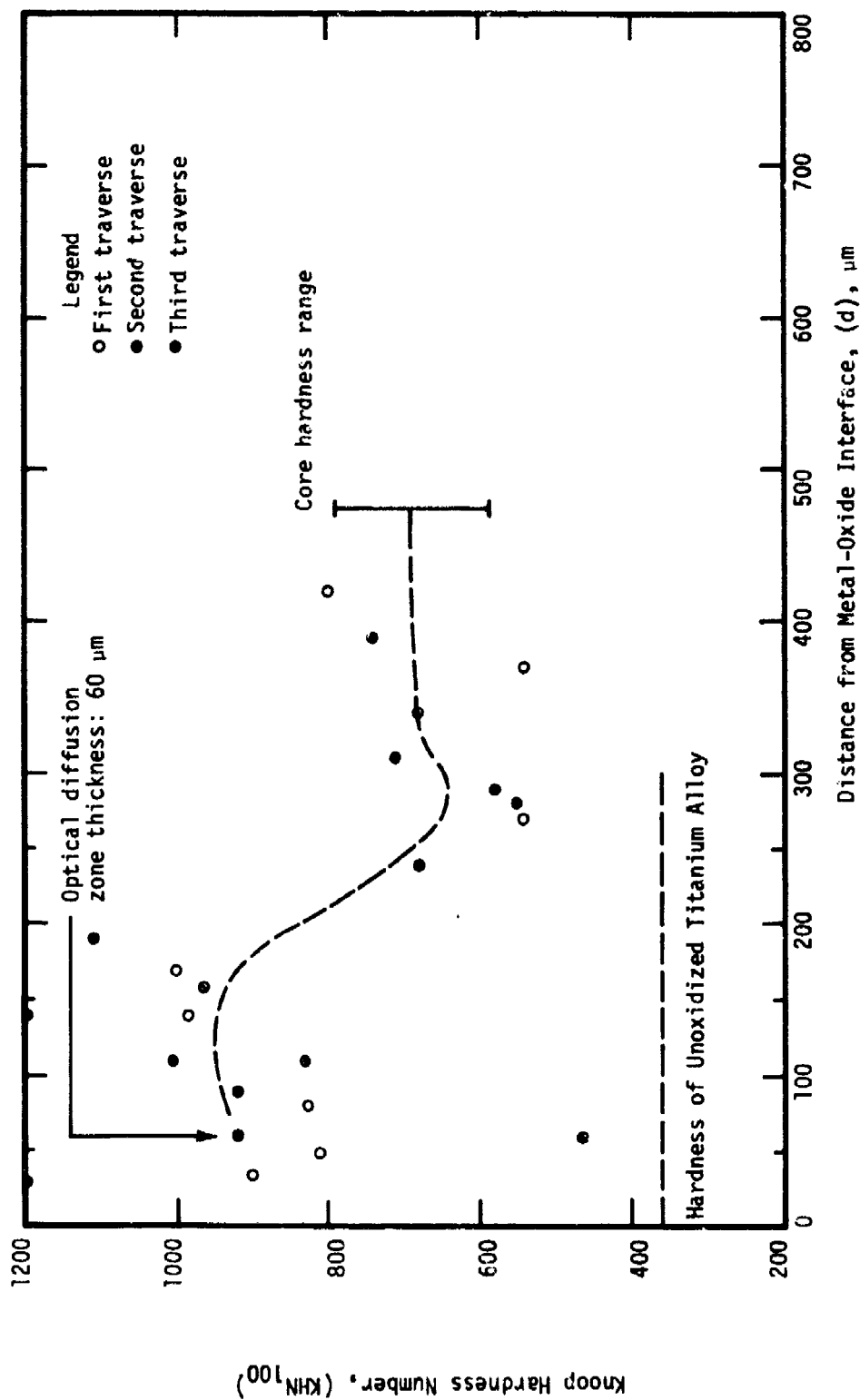


Figure 39. - Hardness of Ti-8Mn alloy specimen no. 405073 heated in 200 torr O_2 at the rate of 8°C/s to 1100°C . Isothermal time 41 min.

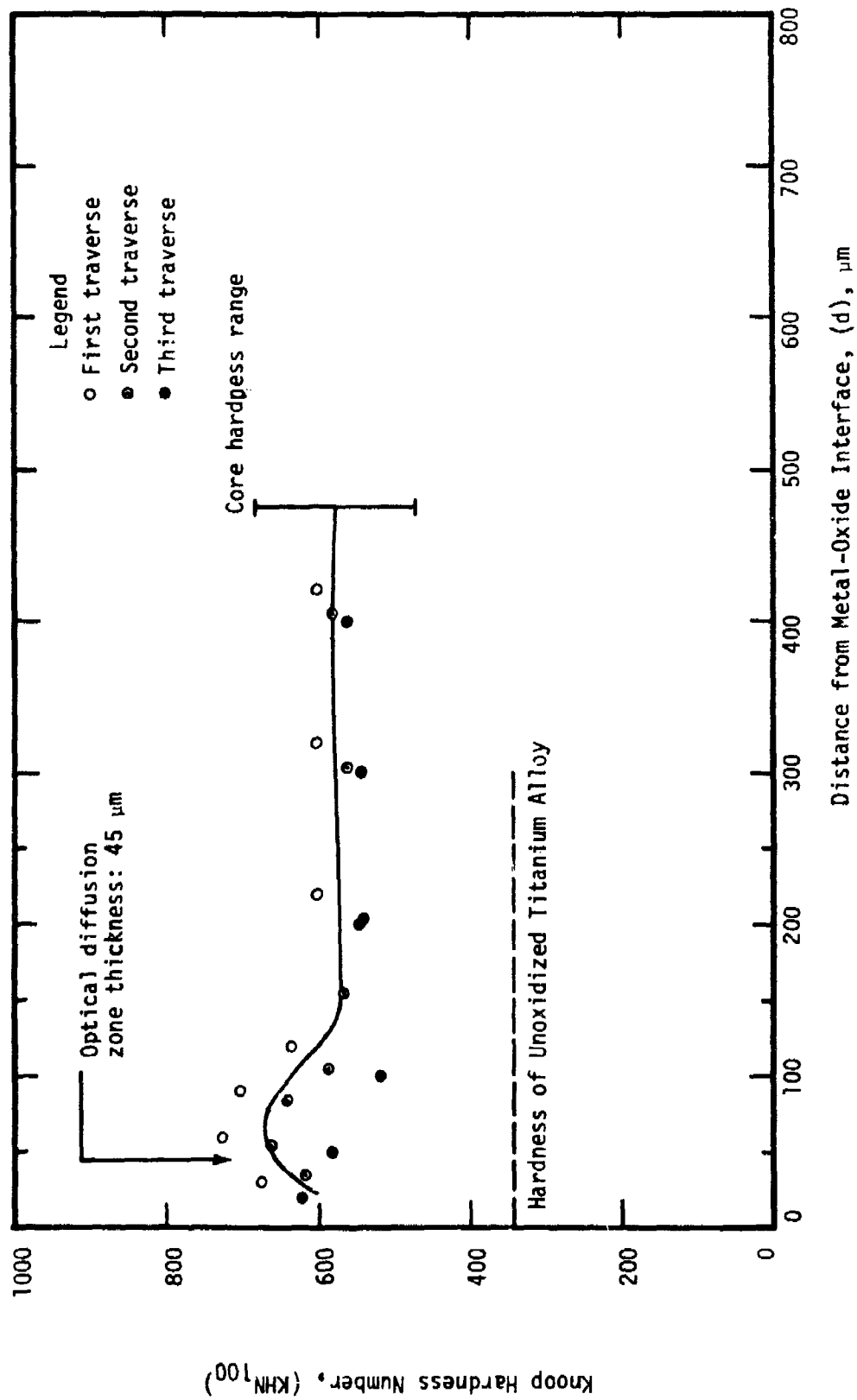


Figure 40. - Hardness of the β -III alloy specimen no. 406173 heated in 200 torr O_2 at the rate of 8°C/s to 1100°C . Isothermal time 22 min.

a) that the diffusion zone is considerably harder, and therefore probably more brittle, than the core, b) that the optically- and hardness-determined core diffusion zone interfaces correspond well, and c) that the basketweave structure formed upon cooling is slightly harder than the initial equiaxial (α) microstructure. As will be seen, these considerations generally prevail for all specimens tested.

As the exposure time is increased from 4 to 16 hours in air at 1000°C, the depth of the region exhibiting enhanced hardness increased, see Figure 29. Note that the core hardness and maximum (surface) hardness are essentially unaffected by this time extension. This behavior is to be expected if the width of the hardened diffusion zone is truly controlled by a diffusion process. Careful inspection of Figures 28 and 29 reveals that the midpoint hardness value for these specimens (550 KHN₁₀₀) occurs at a depth of 65 μ m for the 4-hour exposure and at a depth of 132 μ m for the 16-hour exposure. The ratio of these depths is precisely that which would be expected for a diffusion-controlled process and indicates that, at longer times, the external scaling process does not inordinately consume the diffusion zone material.*

Figures 30, 32, 34, and 35 illustrate the effect of temperature upon the character of the hardness-depth relations for unalloyed titanium specimens tested in 200 torr oxygen. As the temperature is increased: a) the core hardness increases from approximately 200 to 400 KHN₁₀₀, b) maximum (surface) hardness decreases from approximately 800 to 600 KHN₁₀₀ (with the exception of the short-term 1300°C test) and, c) the depth of the diffusion zone tends to increase. These results indicate that at temperatures in excess of 1000°C, the hardened diffusion zone is consumed by the external scaling reaction at a rate approximately equal to its formation rate. The 1300°C test specimen

*This discussion applies to regions of these specimens free of diffusion-zone grain boundary attack.

exhibited an extremely high value of surface hardness (1400 KHN_{100}) and it is assumed that this arises by excessive solution of oxygen in titanium at this highest test temperature. The same comment applies to the core material of the specimen exposed at 1200°C for a longer time.

Figures 31, 32, and 33 illustrate the effect of heating rate upon the character of the hardness-depth relations for unalloyed titanium specimens oxidized in 200 torr oxygen at 1100°C . As noted earlier, the depth of the hardened diffusion zone is slightly larger for the specimen heated at the slowest rate, indicating that diffusion has occurred during the heating period. Other than this effect, there appears to be no major influence of heating rate upon the hardness profiles. There is, for all heating rates, a region just within the core which exhibits "retrograde" hardening, the cause of which is uncertain. A similar behavior may be noted for the 1300°C test specimen, Figure 35.

Exposure of unalloyed titanium specimens to nitrogen at 1000° to 1100°C produces both a narrower optically-detectable diffusion and a lesser degree of hardening than does similar exposure in oxygen.* At depths greater than the optically-discernable diffusion zone, there is a degree of hardening similar to that formed for the case of these specimens similarly exposed in 200 torr oxygen; compare Figures 30 and 32 with Figures 36 and 37, respectively.

The single Ti-6Al-4V alloy specimens tested for hardness exhibited both a greater surface hardness and a deeper zone of hardening than did similarly exposed unalloyed titanium; compare Figures 32 and 38. In addition, there is a long-range ($500 \mu\text{m}$) near-linear decrease in hardness with distance into the core exhibited by the alloy but not by any of the unalloyed specimens

*It is possible that a very hard, very thin zone is present, but that its lack of extent prohibits detection by our microhardness testing technique.

tested. These observations taken together again suggest that oxygen may be mobile along the (α - β) interfaces than it is in the bulk (α)-phase.

The (β)-stabilized alloys, Figures 39 and 40, exhibited both higher and less-uniform hardnesses throughout the surface and core regions. Core hardening in these cases is certainly in part due to the (α - β) transformation induced by cooling from the (β) field; see Figure 16. Surface hardening for these materials probably results from the formation of stabilized acicular (α) crystals near the metal-oxide interface and in the region directly beneath it.

In all cases, the core hardnesses of the alloys were greater than those of the unalloyed material, reflecting directly the solid-solution and second-phase hardening capabilities of the alloyed materials.

4. REACTION OF TITANIUM AND TITANIUM-BASE ALLOY SPECIMENS IN THE VOLUMETRIC APPARATUS

In this section are presented data collected from the monitors of the volumetric apparatus and in a form suitable for quantifying the reactions. In most cases, these data are grouped in sets of two (2) time-based graphical presentations of short-term results for each test conducted and are based upon observed records of temperature and pressure. Where required for clarity or to illustrate special effects, auxiliary graphical presentations are introduced.

4a. GENERAL BEHAVIOR

Both the primary data collected directly from the sensors of the volumetric apparatus and the secondary qualities generated from them are schematically illustrated in Figure 41. Here, both primary short-term data and derived secondary qualities are plotted against similar time bases to facilitate intercomparison. In addition, parameters of special importance are denoted in each of the subsections of Figure 41. Part (a) of this figure

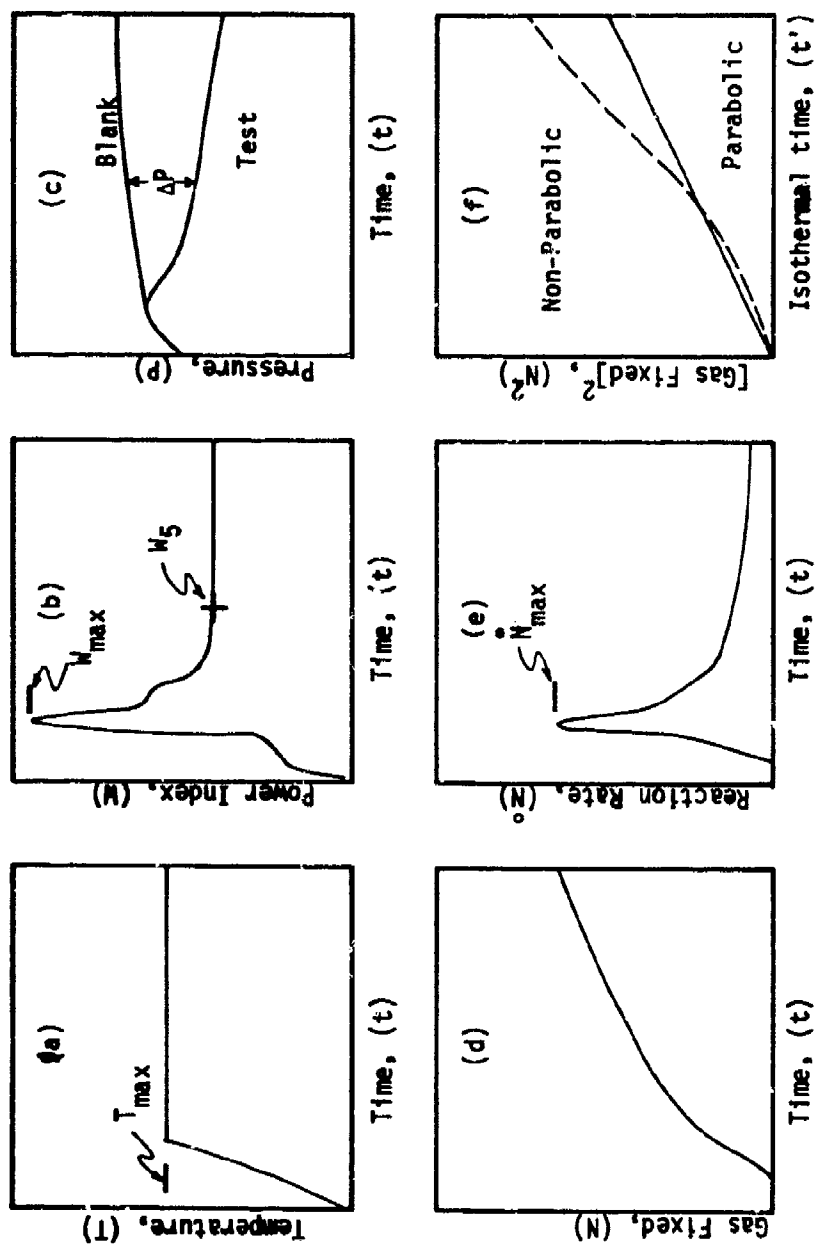


Figure 41. - Schematic illustration of the primary and secondary data derived from the volumetric apparatus. (a) Temperature vs. time; (b) power index vs. time; (c) pressure vs. time; (d) specific gas consumption vs. time; (e) specific reaction rate vs. time; (f) square of specific gas consumption vs. isothermal time.

illustrates the usual temperature (T)-time (t) profile experienced by test specimens exposed to (RHC) type programs with maximum (holding) temperature (T_{\max}). The furnace power index (volts squared) required to produce this thermal history is illustrated in part (b) of the figure with its maximum value, (W_{\max}), and its value after the fifth minute of operation, (W_5), denoted. Part (c) illustrates typical pressure (P) - time (t) behaviors for both the empty system and the system containing a test specimen. From the pressure difference, (ΔP), the specific gas consumption, (N) of each specimen is calculated by the methods of Appendix IV to give the gas fixation-time curve of part (d). This curve is generally sigmoidal in character so that its first true derivative, (\dot{N}), the specific linear reaction rate exhibits a maximum value, (\dot{N}_{\max}), as shown in part (e) of Figure 41. Finally, part (f) of the figure shows the variation in the square of the specific gas consumption, (N^2), with time. The values of (N^2) here must be corrected for any consumption of gas prior to the time of reaching the maximum temperature by a method similar to that employed by Zirin (ref. 21). This relation essentially tests the degree to which the reaction obeys the parabolic rate law.

With the exception of the (N^2) vs. (t') plots to be presented below, each graph has been provided with a time "marker" indicating the onset of isothermal conditions. The time scales are uniform where possible and indicate clock time from the instant of the heating program start; i.e., heating times are included in clock time.* The data will be discussed roughly in the sequence of specimens indicated in Table XII above.

4b. REACTION OF UNALLOYED TITANIUM WITH OXYGEN - (RHC) TESTS

Data derived from the volumetric apparatus for the various unalloyed

*There are in several instances a delay between the "clock time zero" and the start of heating due to programmer "backlash" which cause minor shifts in the time axes.

titaniums in 200 torr oxygen (RHC)-type tests are presented in Figures 42 through 96. A complete array of analytical curves is shown only for specimen 06051 which was oxidized at 1000°C, see Figures 42 through 47. In the case of other specimens, only the initial gas consumption (N) and linear reaction rate (\dot{N}) are illustrated unless unusual behaviors, deviating from those schematically described in Figure 41, were observed.

As titanium is heated in oxygen to the maximum temperature, and thereafter maintained at that temperature, the initial character of the specific oxygen consumption (N) is usually sigmoidal. The time derivatives of these curves, which represent a specific linear reaction rate (\dot{N}), therefore usually exhibit a single maximum and this maximum in many cases occurs prior to the time at which the "hold" portion of the test is in effect; i.e., (\dot{N}_{\max}) occurs prior to (T_{\max}).

Qualitatively, the sigmoidal behavior of (N) and the consequent maximization of (\dot{N}) may be explained on the basis of two concurrent processes which have opposing effects upon the rate of reaction: increasing temperature tends to accelerate the reaction during heating; whereas, the consumption of gas to form an oxide barrier film between the reactants tends to decrease the rate of reaction. Thus, a maximum in (\dot{N}) is to be expected sometime in the early portion of tests which follow the format used in this research. Whether or not this maximum should occur prior to the time of reaching maximum temperature in an RHC-type test is not decided by these considerations alone.*

There are several instances, especially pronounced in the lower-temperatures (1000°C and 1100°C)-intermediate heating rate (8°C/s) tests, where the initial portion of the specific gas consumption vs. time (N vs. t) curve is more complex; e.g., see Figures 50, 64, 66, 81, and 83. These curves may be

*This phenomenon will be discussed more fully below.

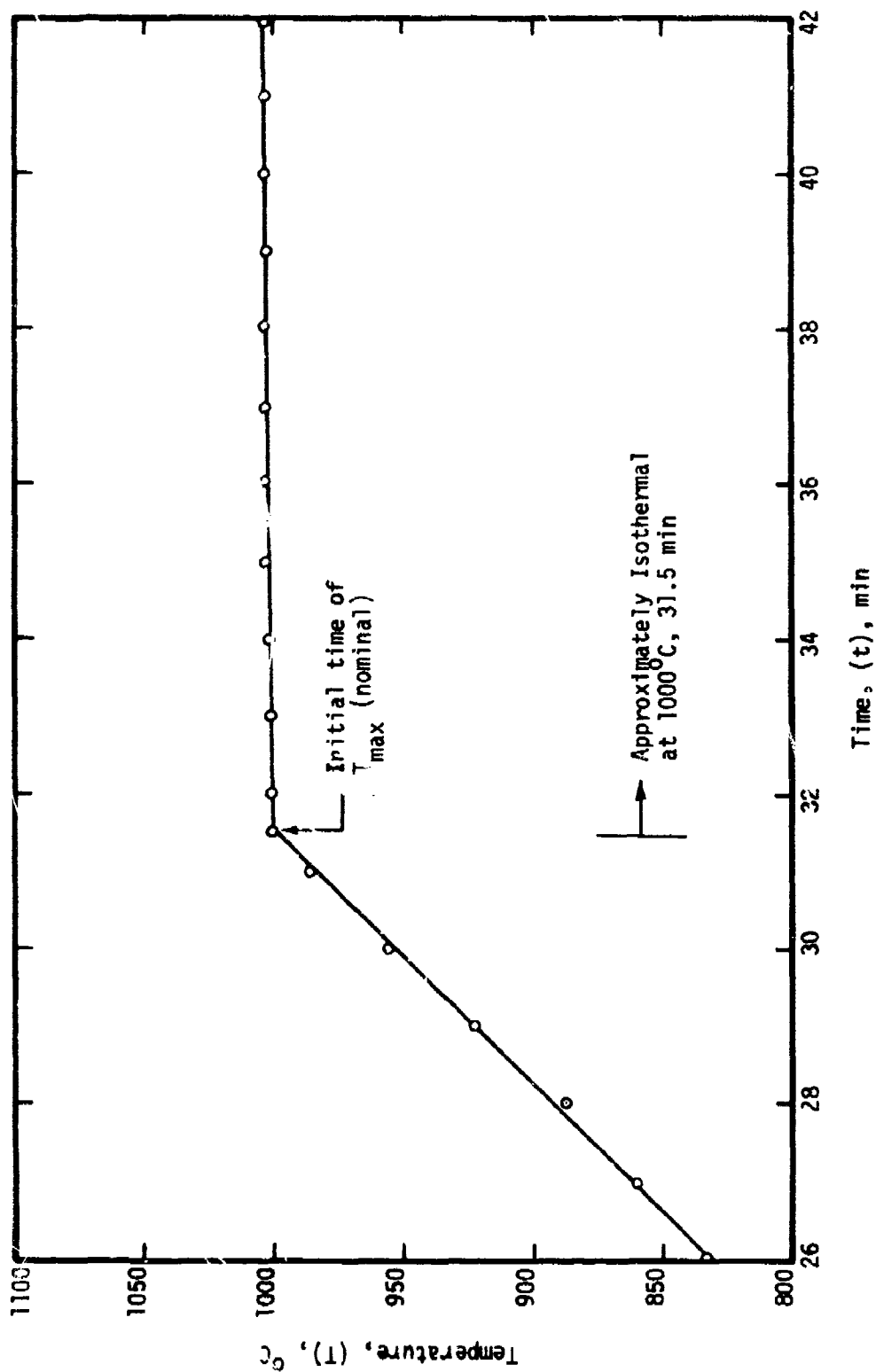


Figure 42. - Initial time-temperature profile for unalloyed titanium (Type 1) specimen no. 06051 heated in 200 torr O_2 at the rate of 0.5°C/s to 1000°C .

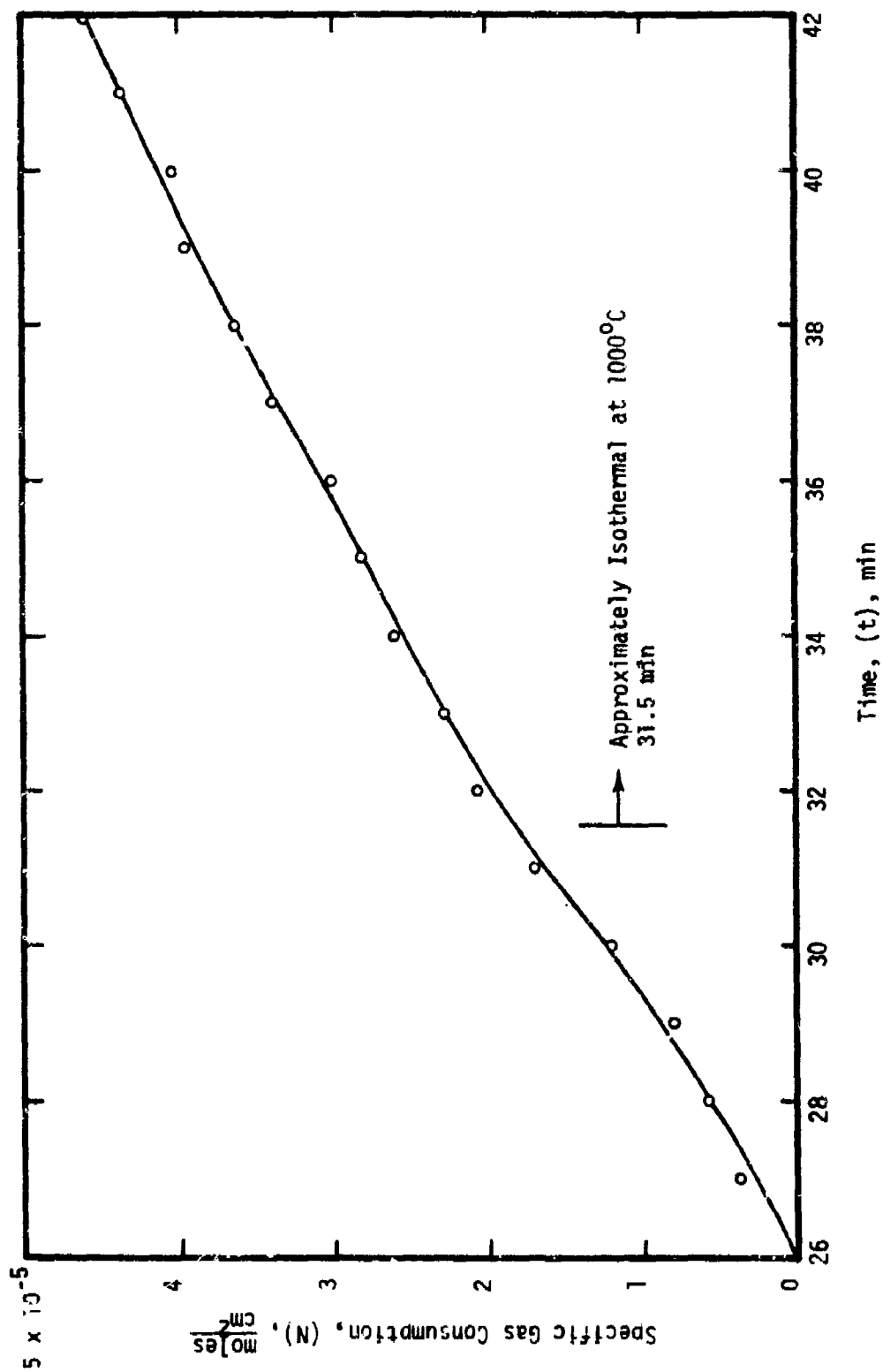


Figure 43. - Initial behavior of the specific gas consumption (N) for unalloyed titanium (Type 1) specimen no. 06051 heated in 200 torr O_2 at the rate of 0.5°C/s to 1000°C .

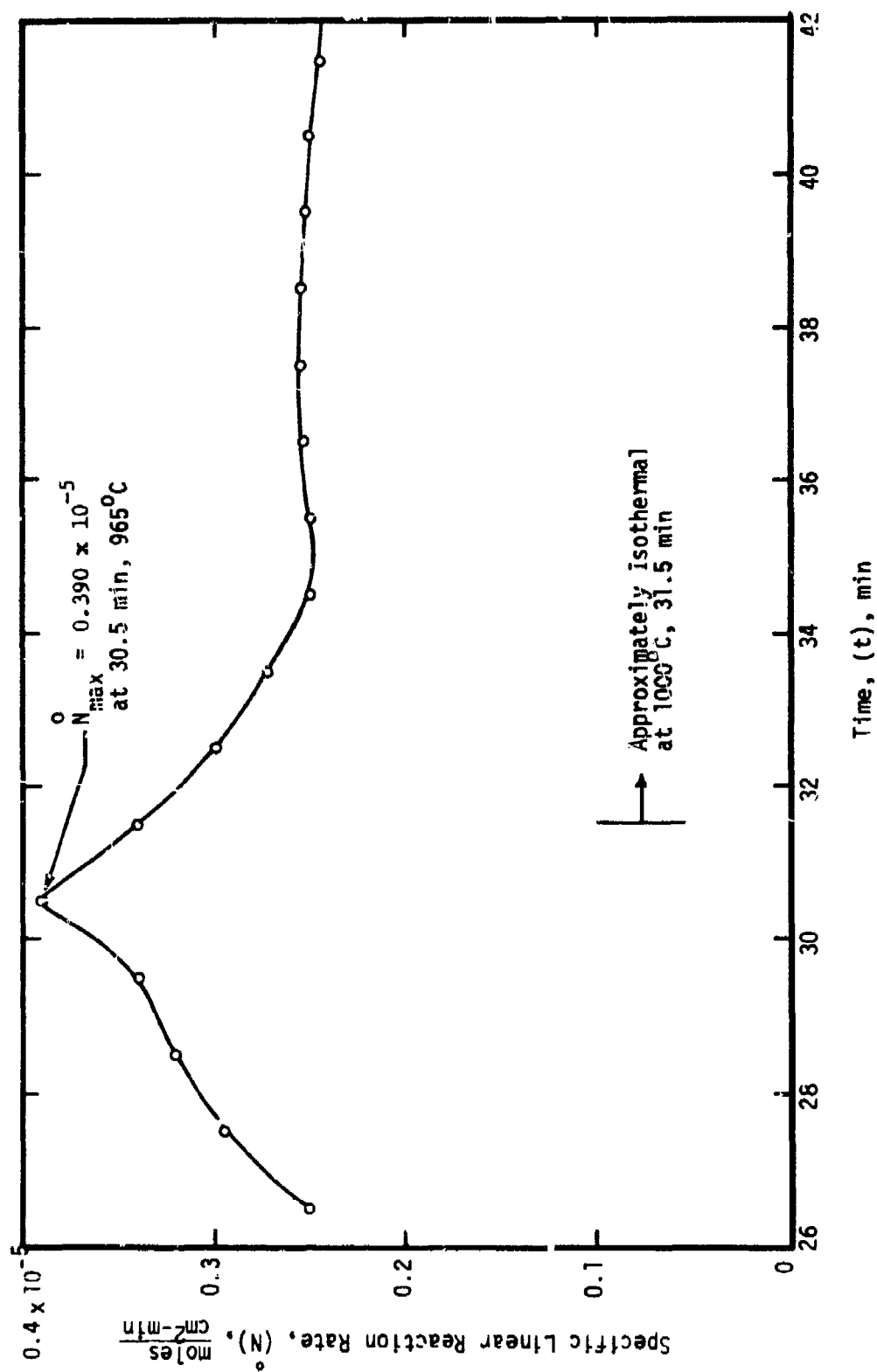


Figure 44. - Initial behavior of the specific linear reaction rate (N) for unalloyed titanium (Type I) specimen no. 06051 heated in 200 torr O_2 at the rate of 0.5°C/s to 1000°C .

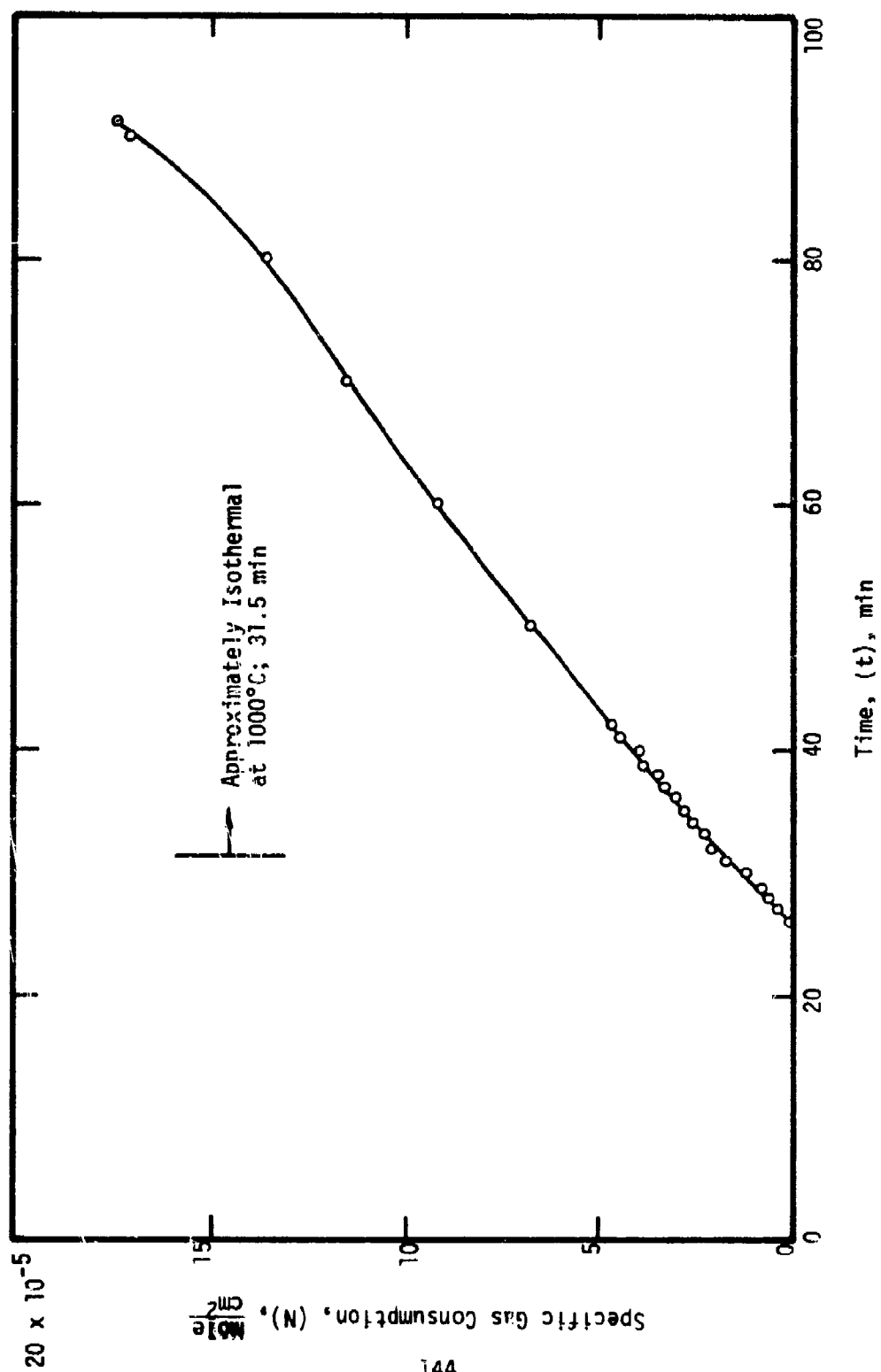


Figure 45. - Overall behavior of the specific gas consumption (N) for unalloyed titanium (Type 1) specimen no. 06051 heated in 200 torr O_2 at the rate of 0.5°C/s to 1000°C .

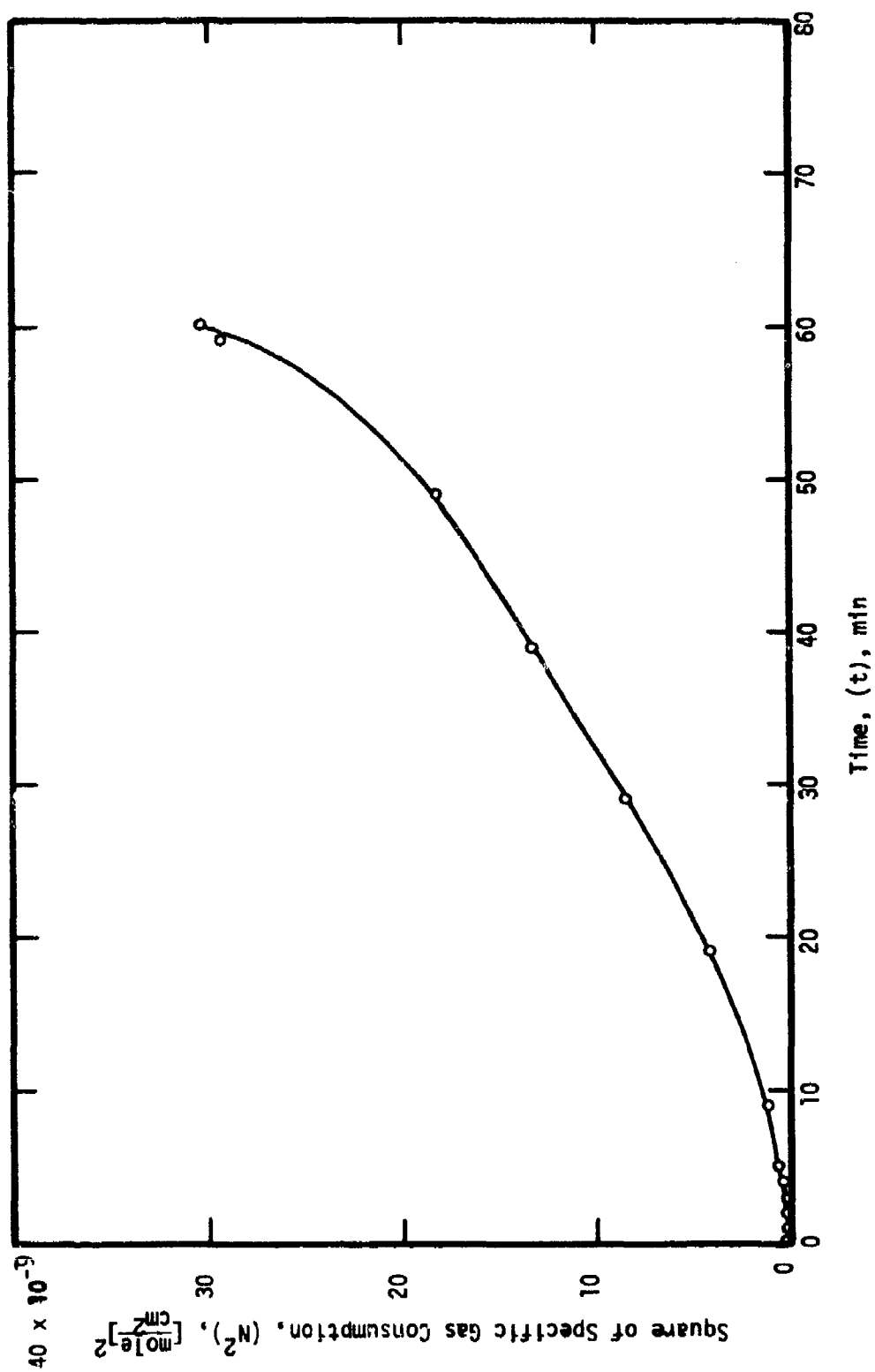


Figure 46. - Overall behavior of the square of specific gas consumption (N^2) for unalloyed titanium (Type 1) specimen no. 06051 heated in 200 torr O_2 at the rate of 0.5°C/s to 1000°C .

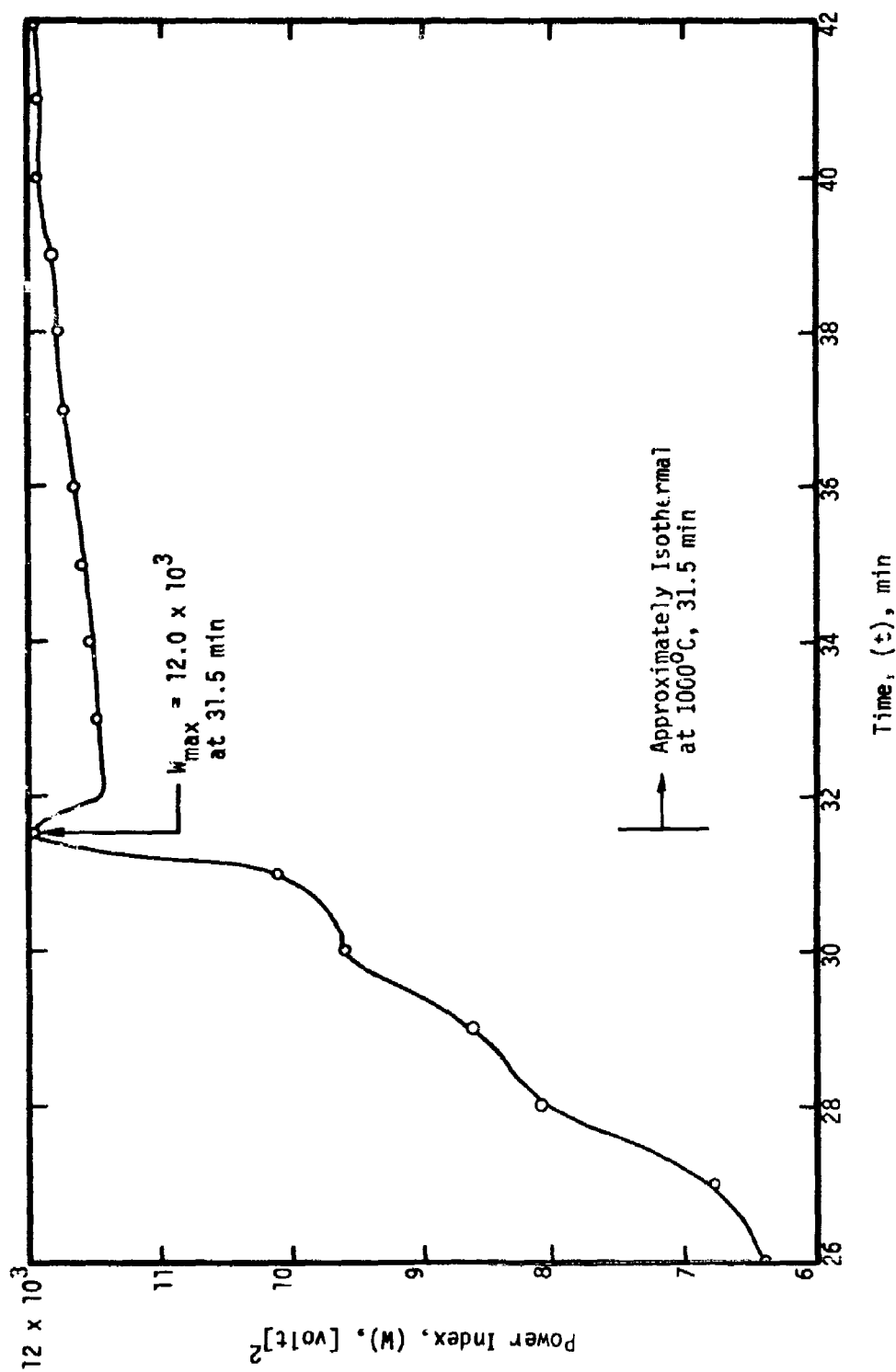


Figure 47. - Initial behavior of the power index (W) for unalloyed titanium (Type 1) specimen no. 06051 heated in 200 torr O₂ at the rate of 0.5°C/s to 1000°C.

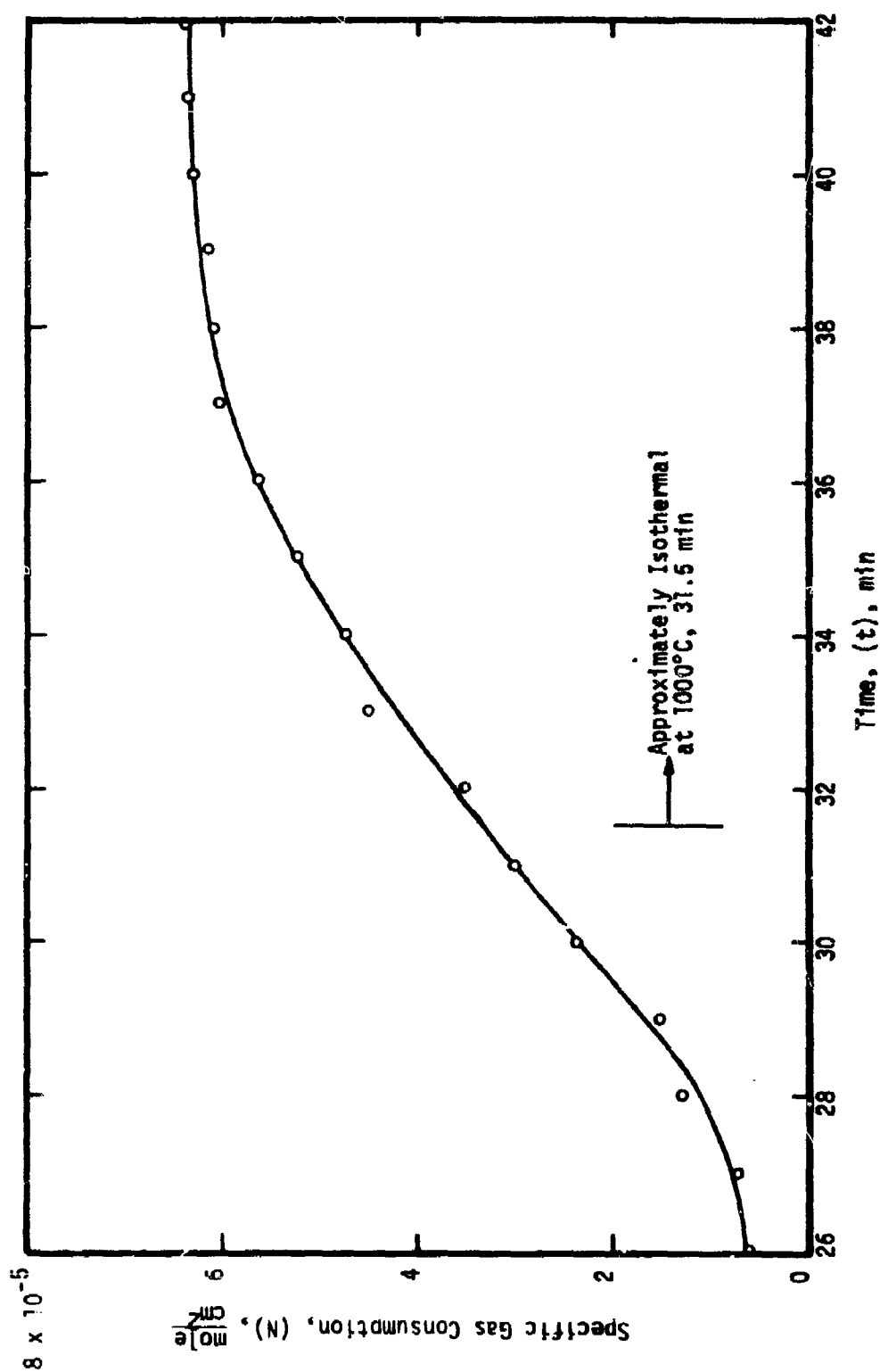


Figure 48. - Initial behavior of the specific gas consumption (N) for unalloyed titanium (Type 1) specimen no. 06141 heated in 200 torr O₂ at the rate of 0.5°C/s to 1000°C.

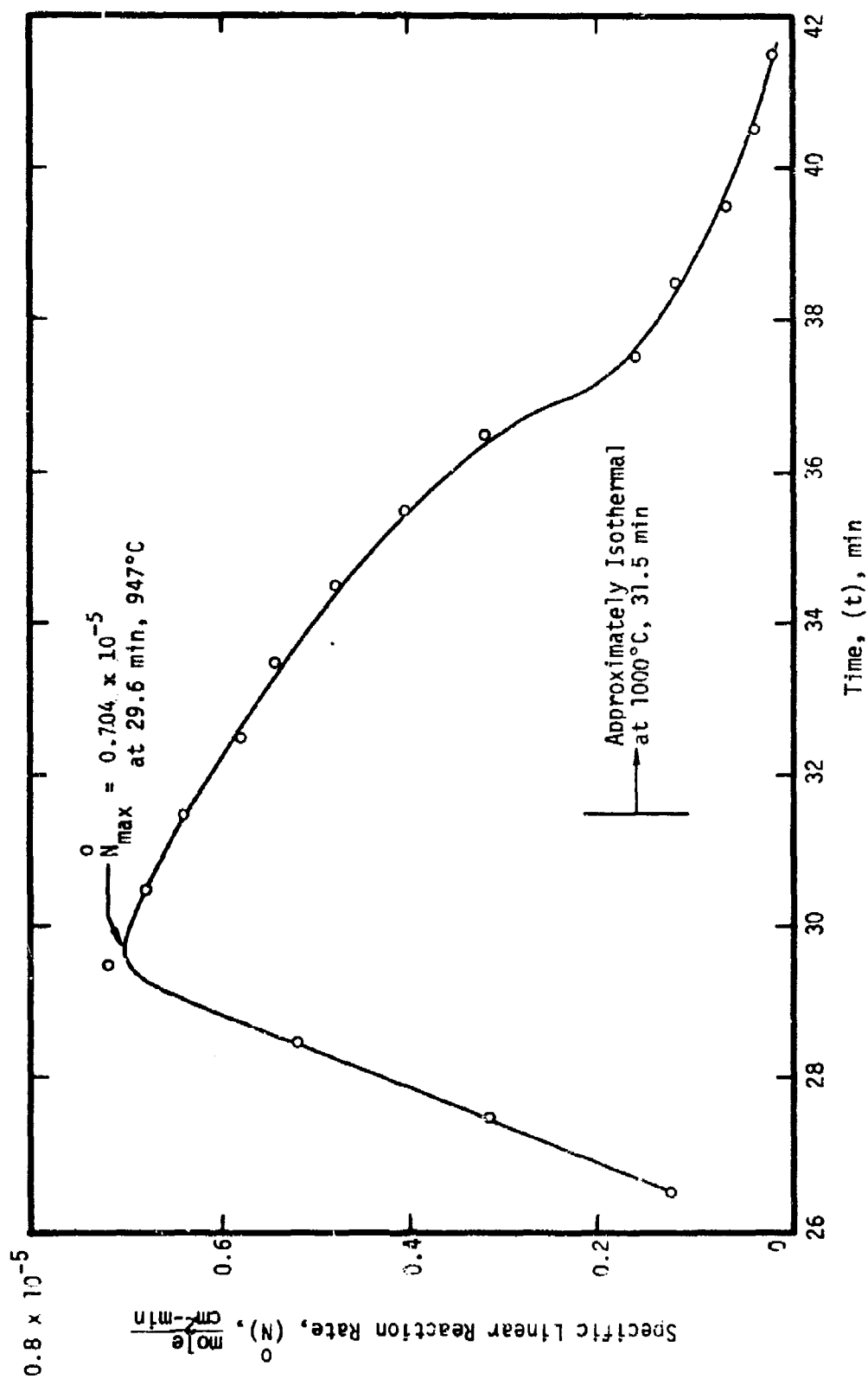


Figure 49. - Initial behavior of the specific linear reaction rate (N) for unalloyed titanium (Type 1) specimen no. 06141 heated in 200 torr O_2 at the rate of 0.5°C/s to 1000°C .

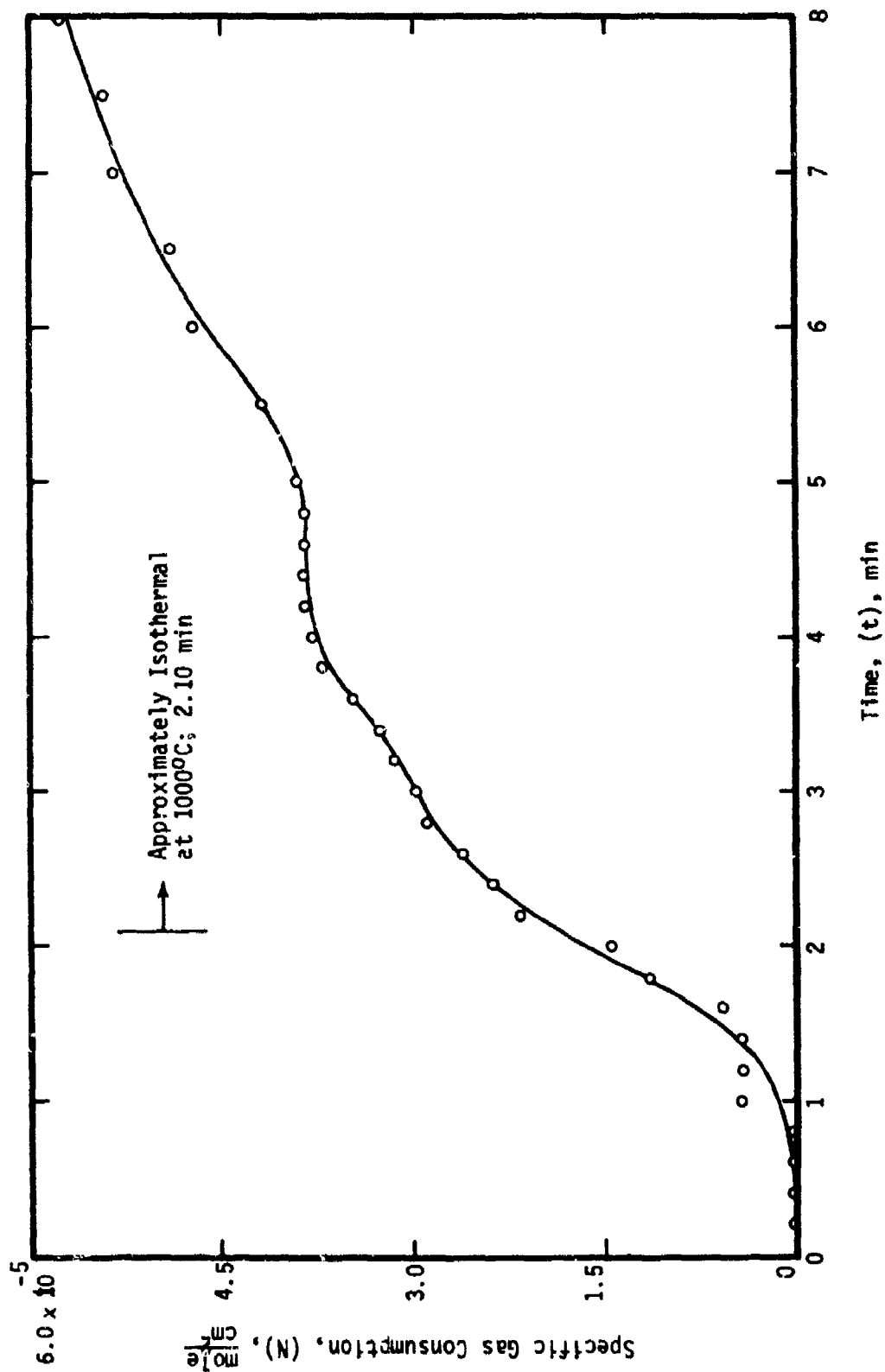


Figure 50. - Initial behavior of the specific gas consumption (N) for unalloyed titanium (Type 1) specimen no. 06132 heated in 200 torr O_2 at the rate of 8°C/s to 1000°C .

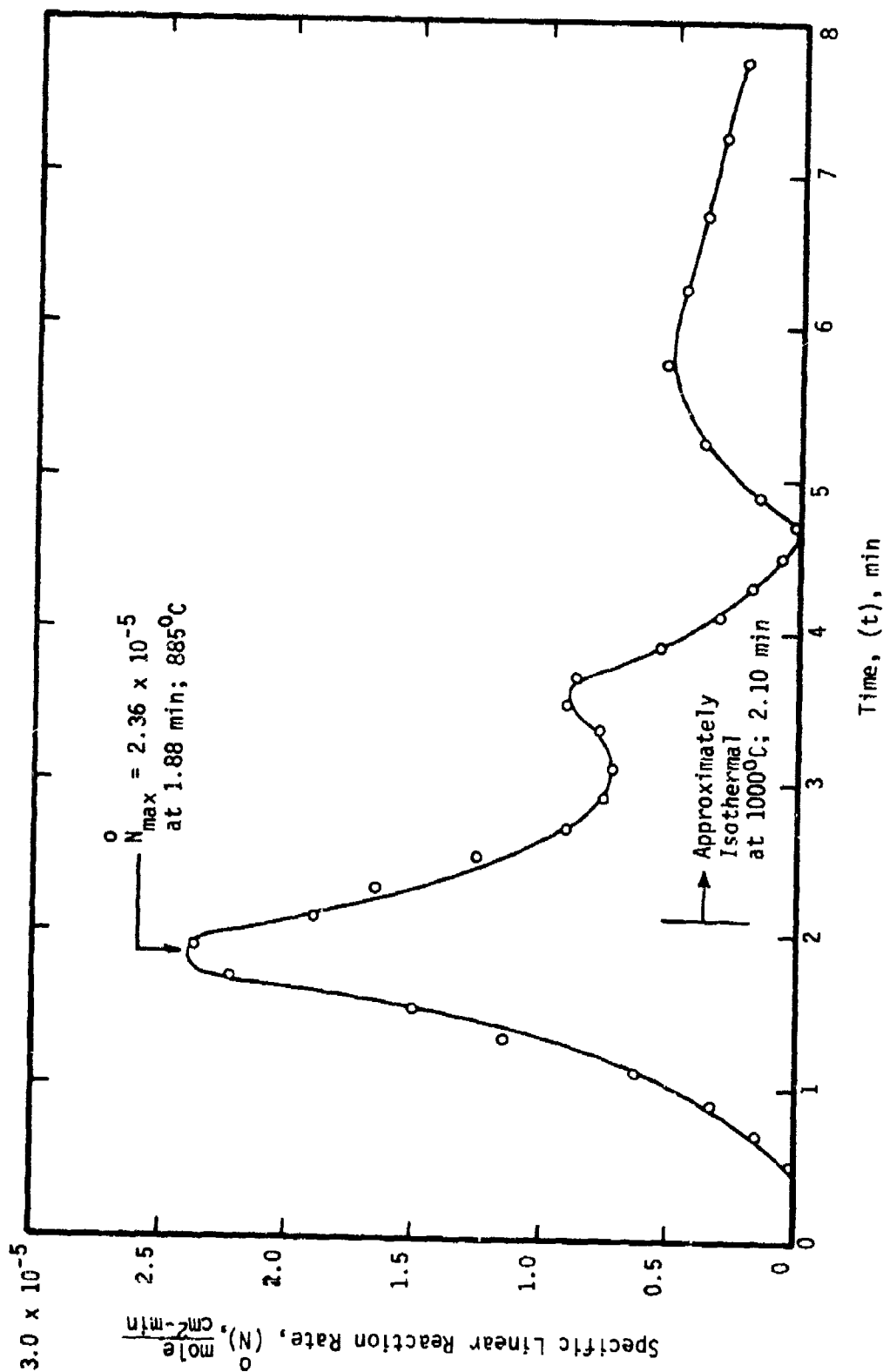


Figure 51. - Initial behavior of the specific linear reaction rate (\dot{N}) for unalloyed titanium (Type 1) specimen No. 06132 heated in 200 torr O_2 at the rate of 8°C/s to 1000°C.

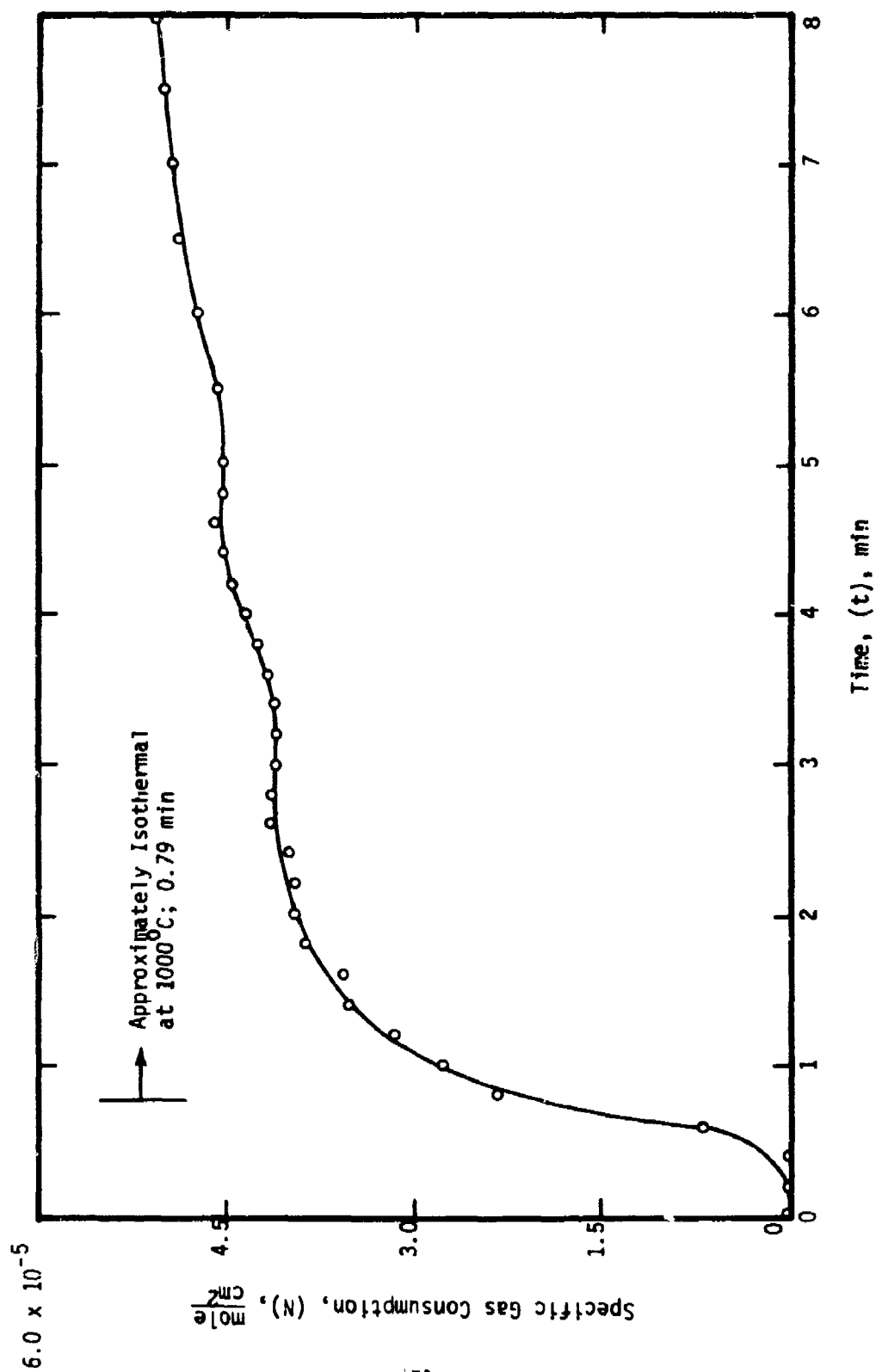


Figure 52. - Initial behavior of the specific gas consumption (N) for unalloyed titanium (Type 1) specimen no. 06133 heated in 200 torr O_2 at the rate of 25°C/s to 1000°C.

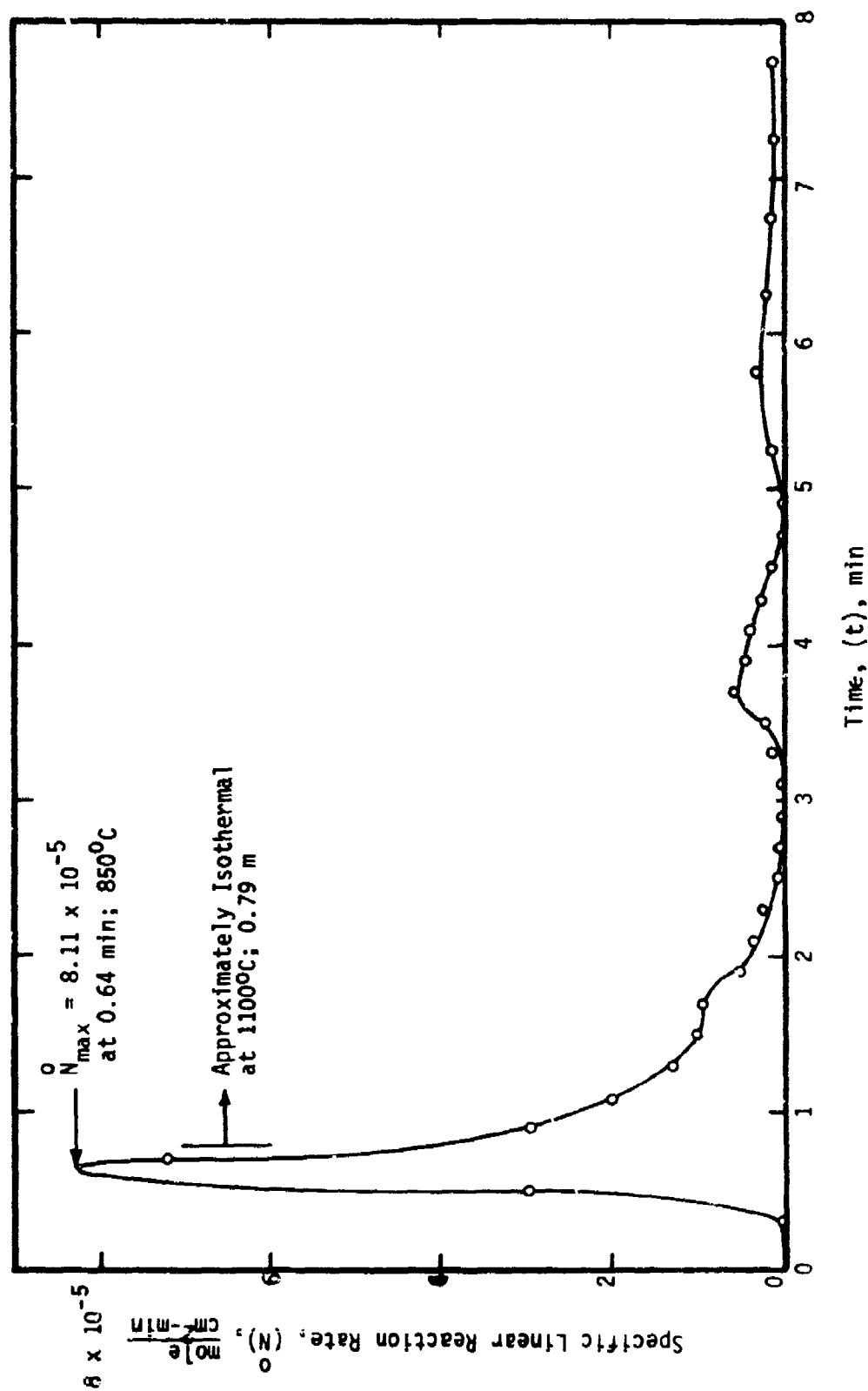


Figure 53. - Initial behavior of the specific linear reaction rate (\dot{N}) for unalloyed titanium (Type 1) specimen heated in 200 torr O_2 at the rate of 25°C/s to 1000°C.

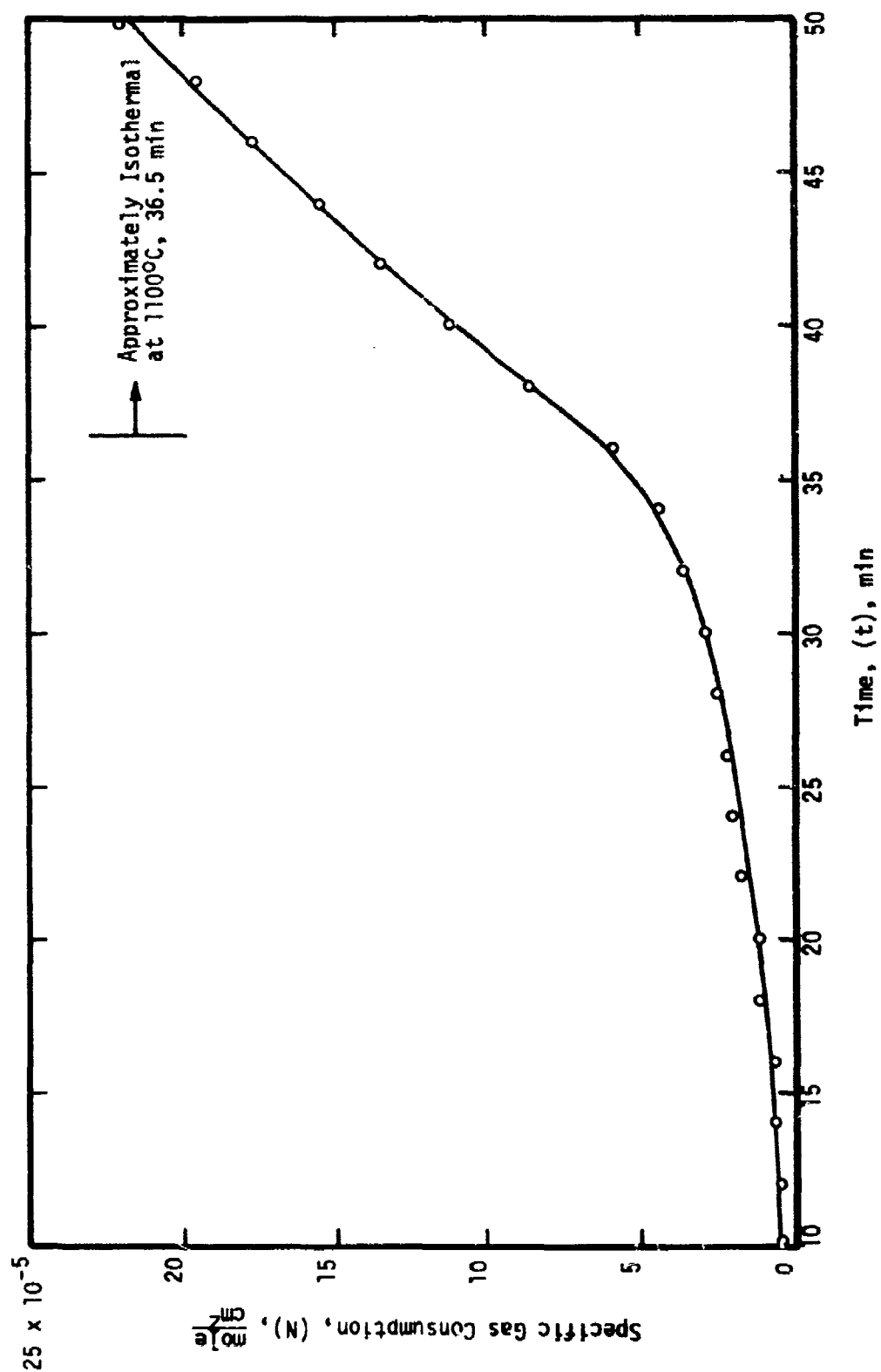


Figure 54. - Initial behavior of the specific gas consumption (N) for unalloyed titanium (Type 1) specimen no. 06131 heated in 200 torr O_2 at the rate of 0.5°C/s to 1100°C.

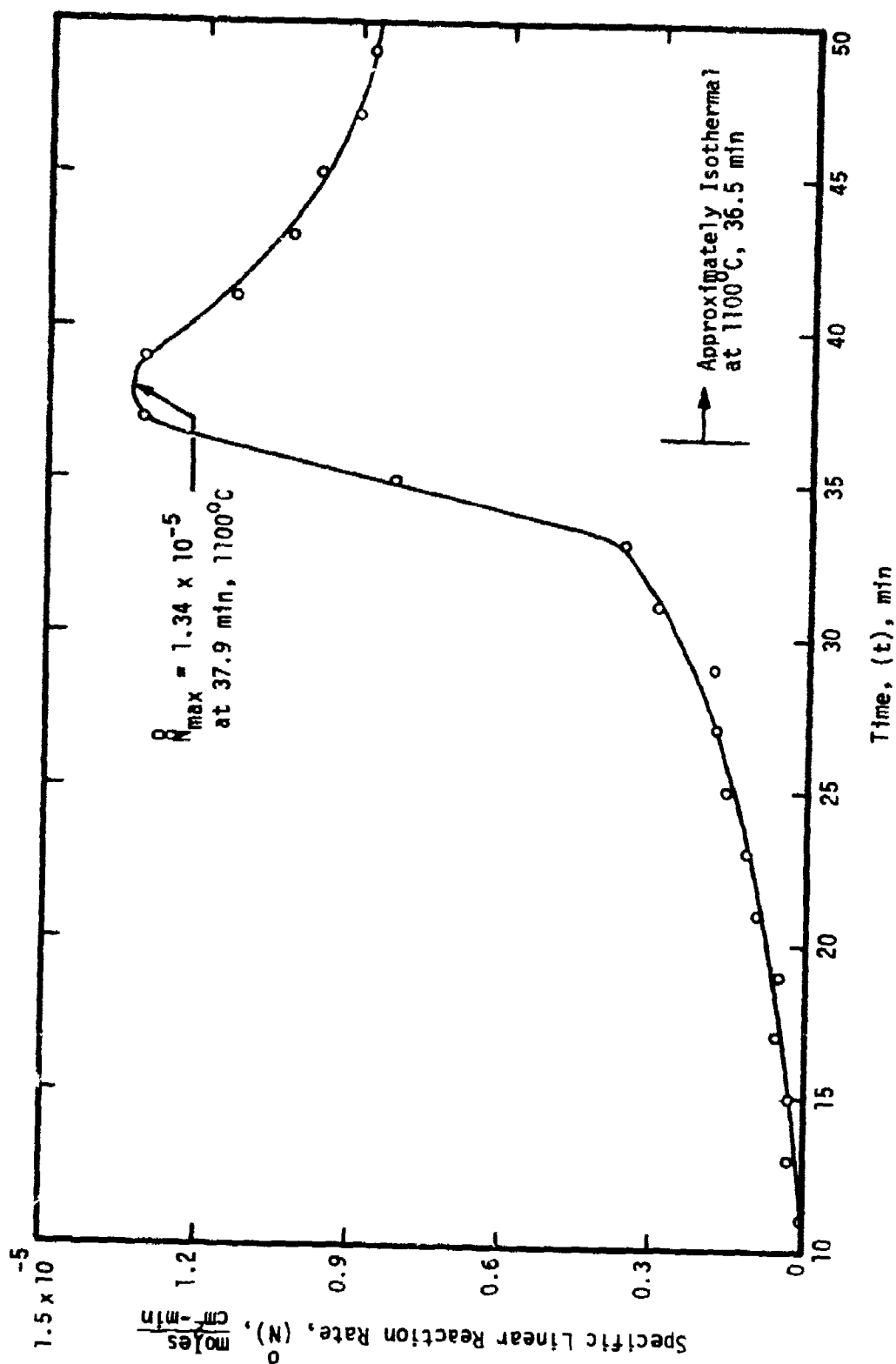


Figure 55. - Initial behavior of the specific linear reaction rate (\dot{N}) for unalloyed titanium (Type 1) specimen no. 06131 heated in 200 torr O_2 at the rate of 0.5°C/s to 1100°C .

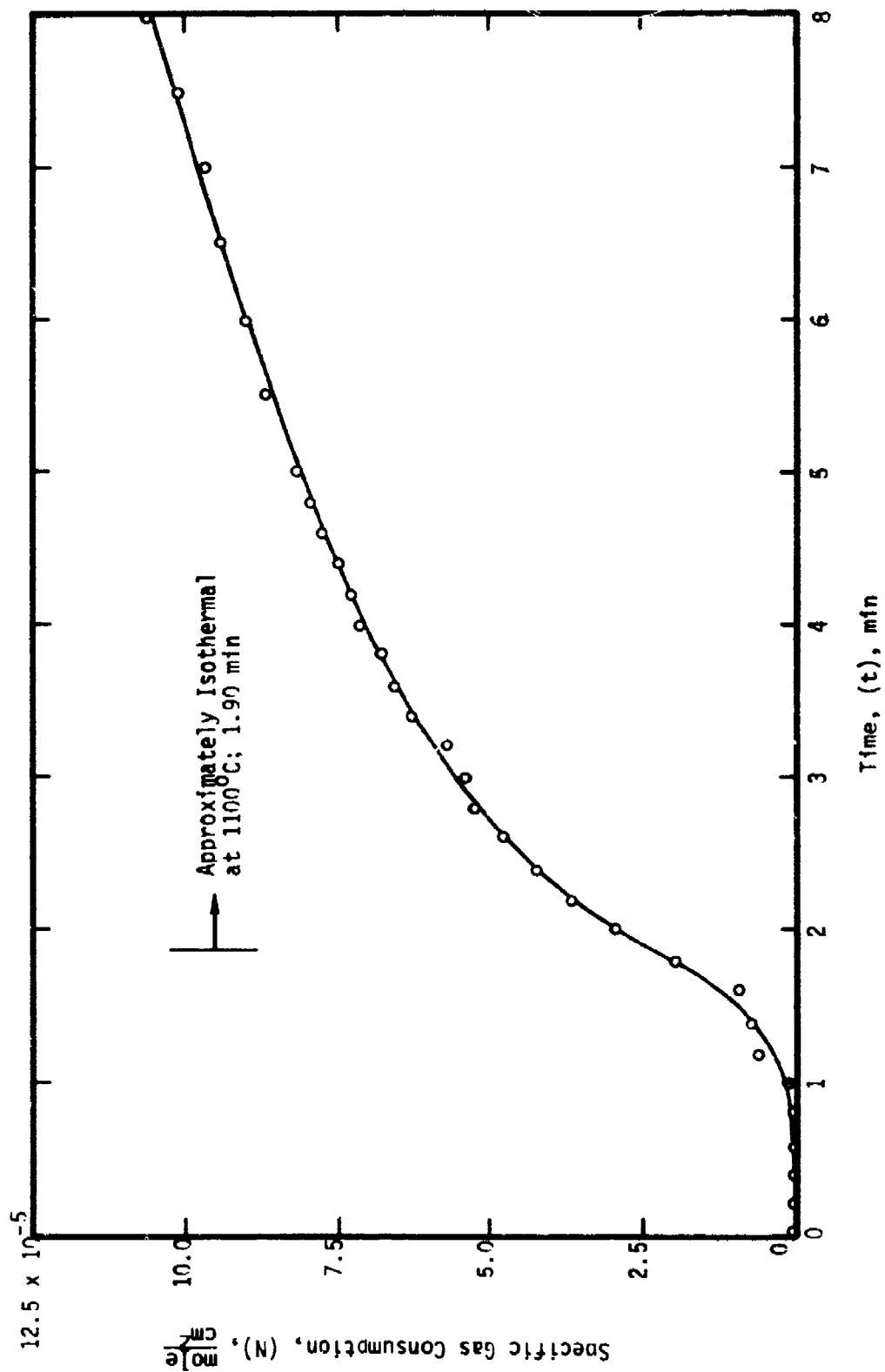


Figure 56. - Initial behavior of the specific gas consumption (N) for unalloyed titanium (Type 1) specimen no. 06071 heated in 200 torr O_2 at the rate of $8^\circ\text{C}/\text{s}$ to 1100°C .

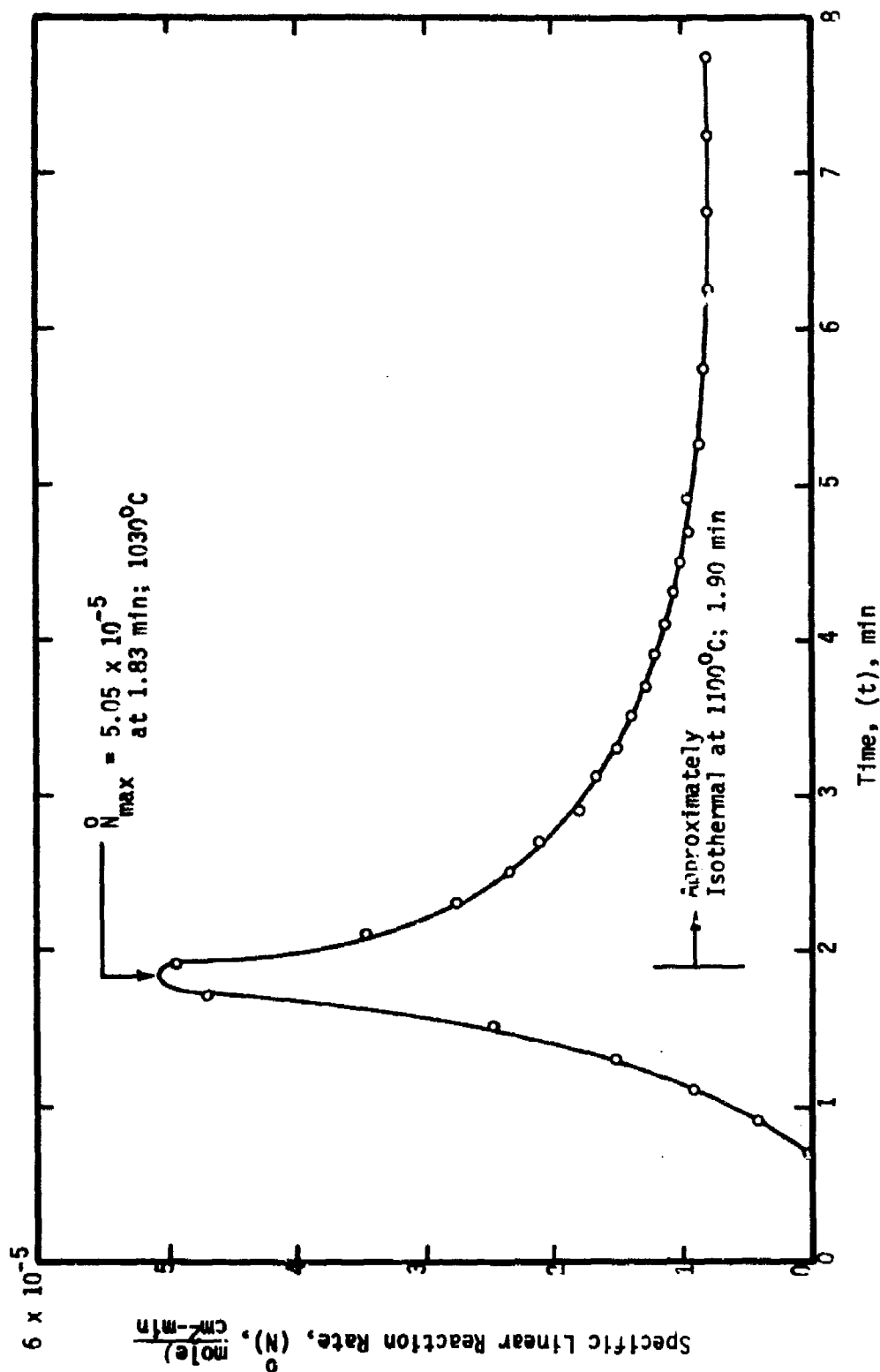


Figure 57. - Initial behavior of the specific linear reaction rate (\dot{N}) for unalloyed titanium (Type 1) specimen no. 06071 heated in 200 torr O_2 at the rate of 8°C/s to 1100°C.

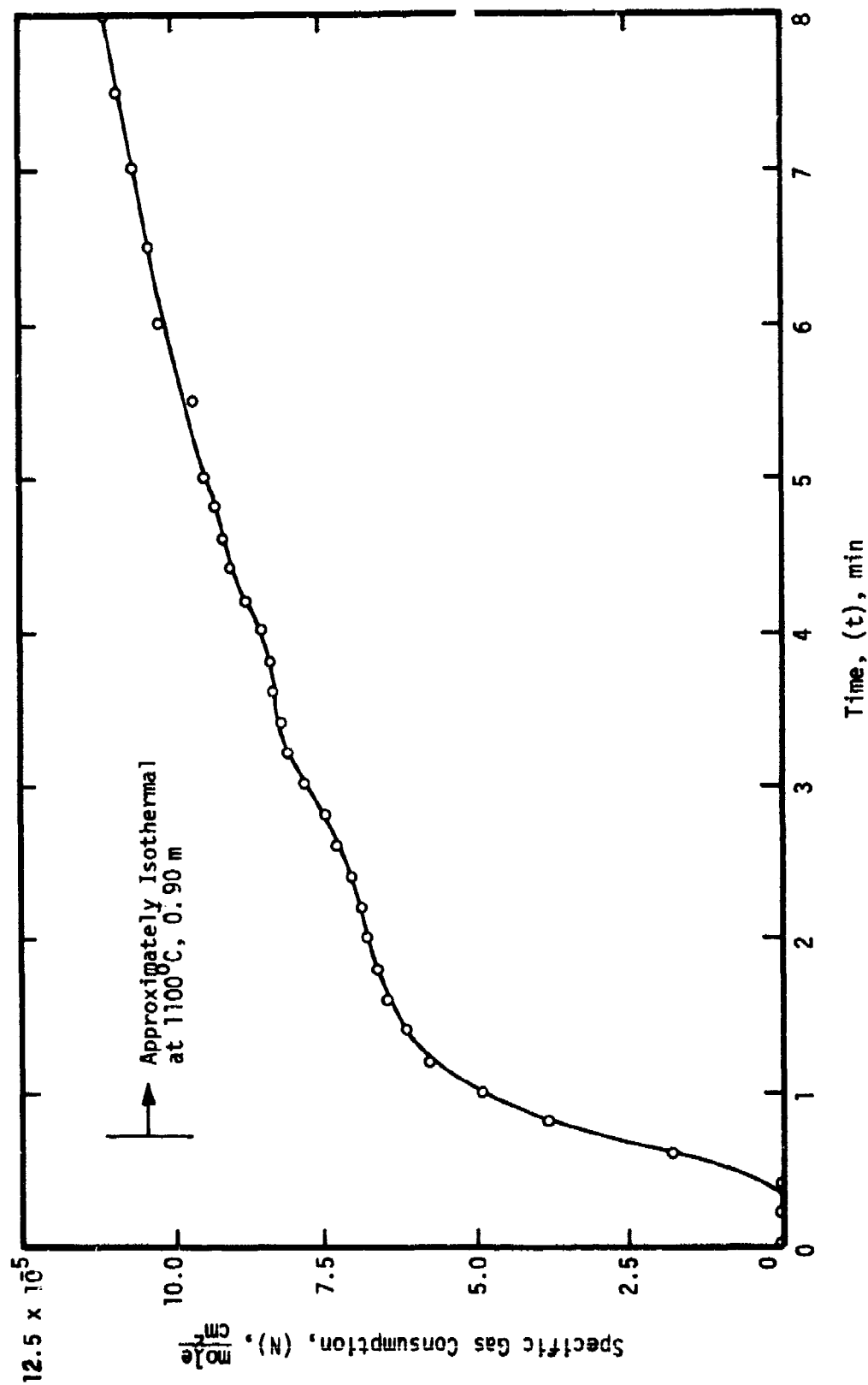


Figure 58. - Initial behavior of the specific gas consumption (N) for unalloyed titanium (Type 1) specimen no. 06142 heated in 200 torr O_2 at the rate of 22°C/s to 1100°C.

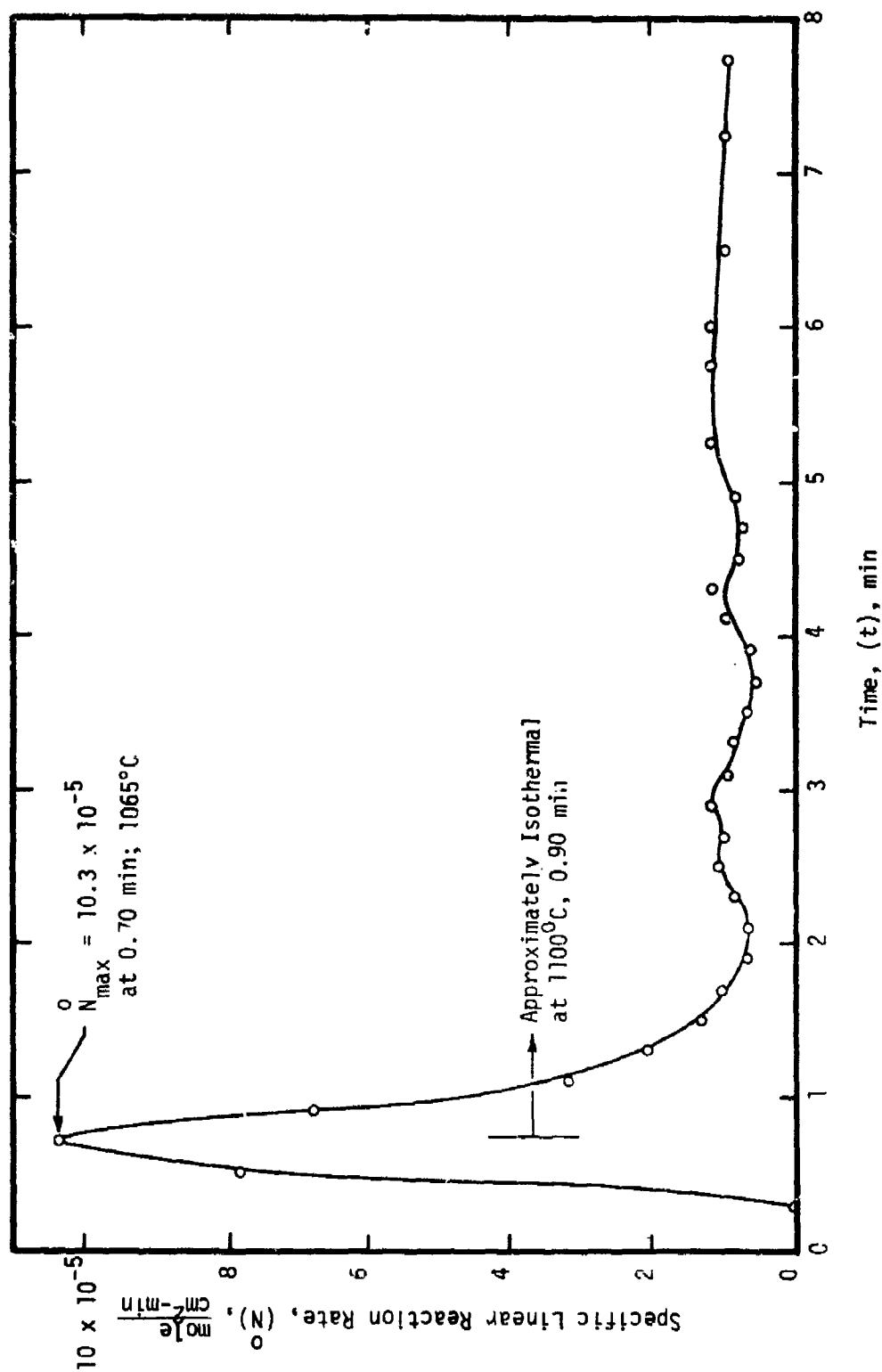


Figure 59. - Initial behavior of the specific linear reaction rate (N) for unalloyed titanium (Type 1) specimen no. 06142 heated in 200 torr O_2 at the rate of 22°C/s to 1100°C.

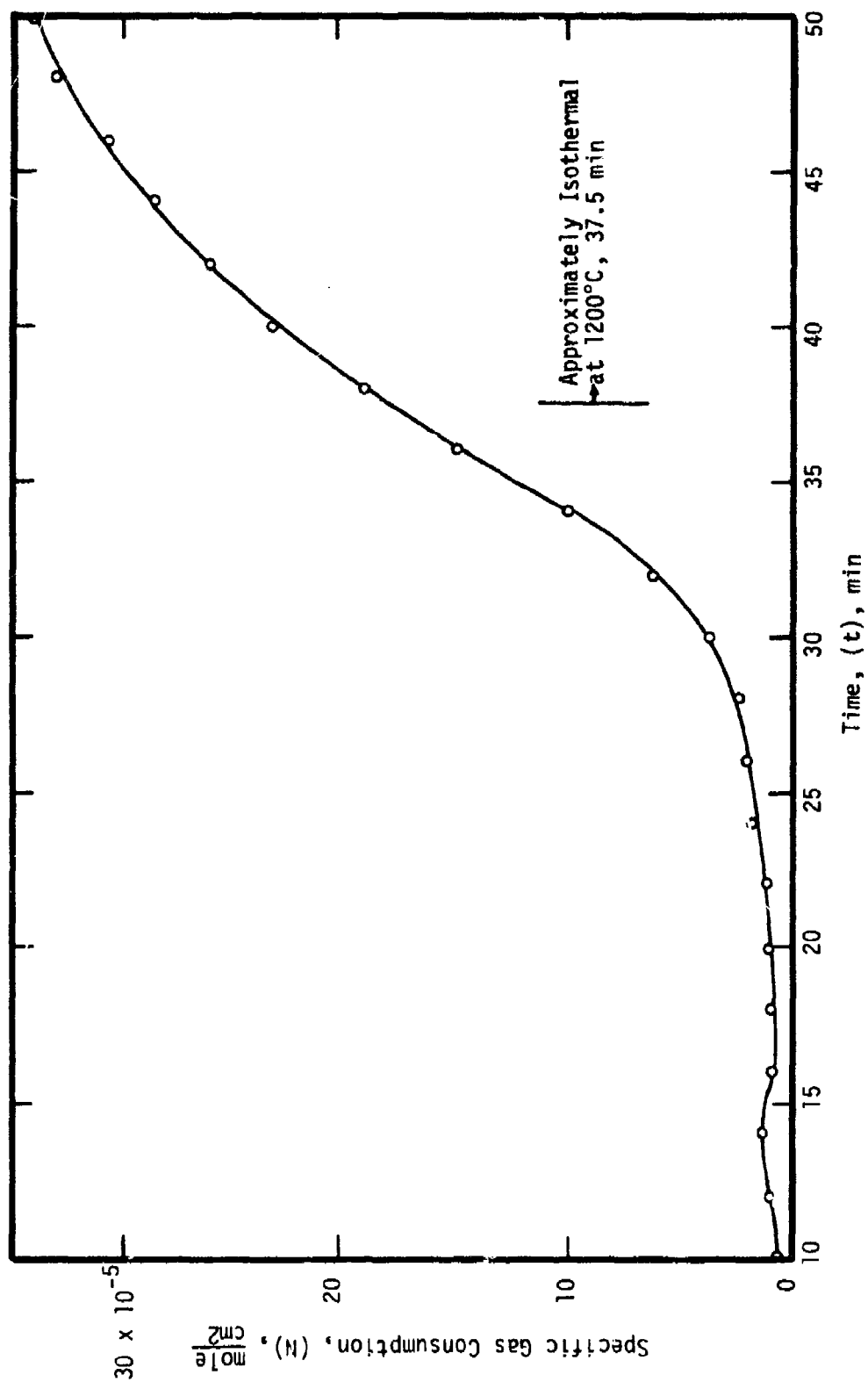


Figure 60. - Initial behavior of the specific gas consumption (N) for unalloyed titanium (Type 1) specimen no. 08012 heated in 200 torr O_2 at the rate of 0.5°C/s to 1200°C .

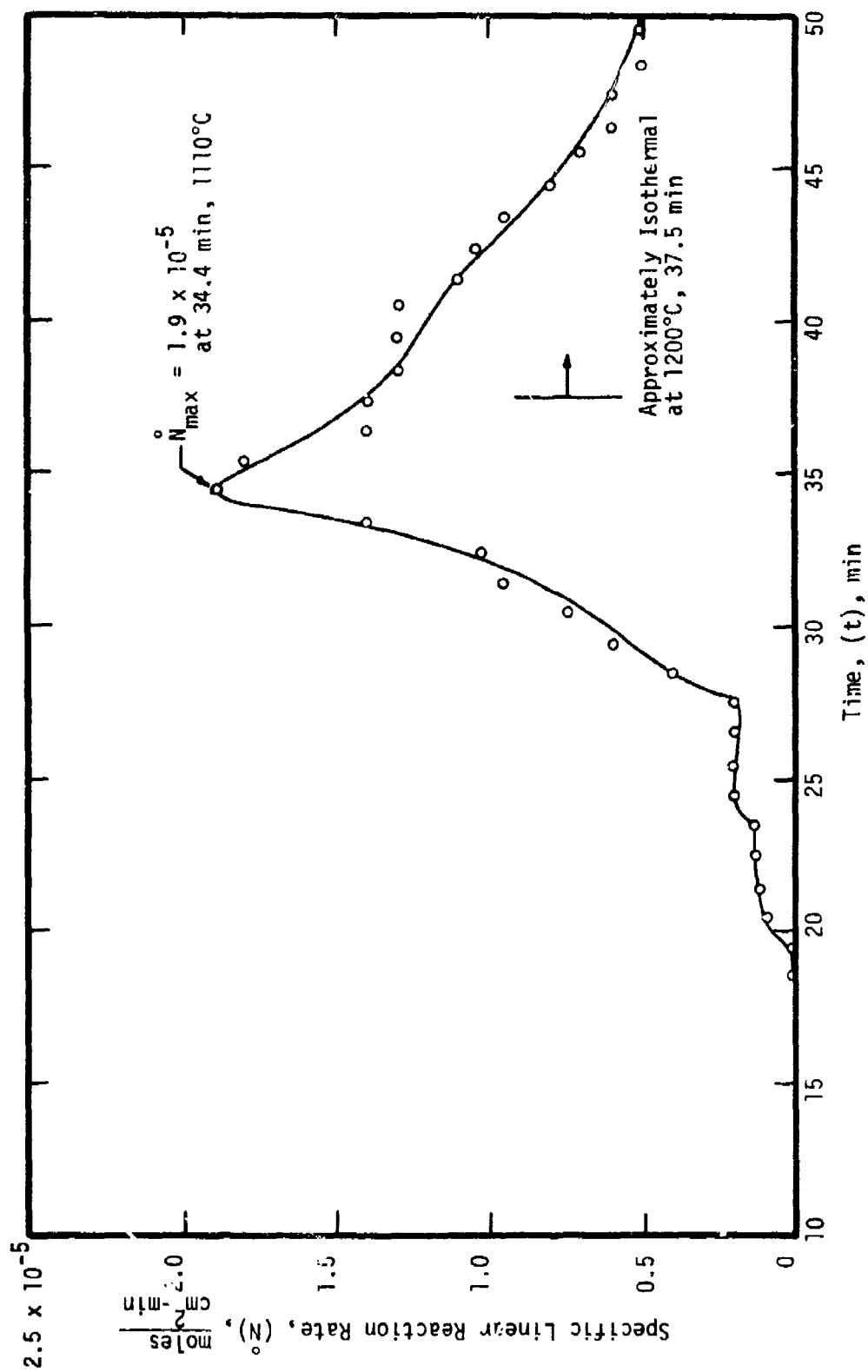


Figure 61. - Initial behavior of the specific linear reaction rate (\dot{N}) for unalloyed titanium (Type 1) specimen no. 08012 heated in 200 torr O_2 at the rate of 0.5°C/s to 1200°C .

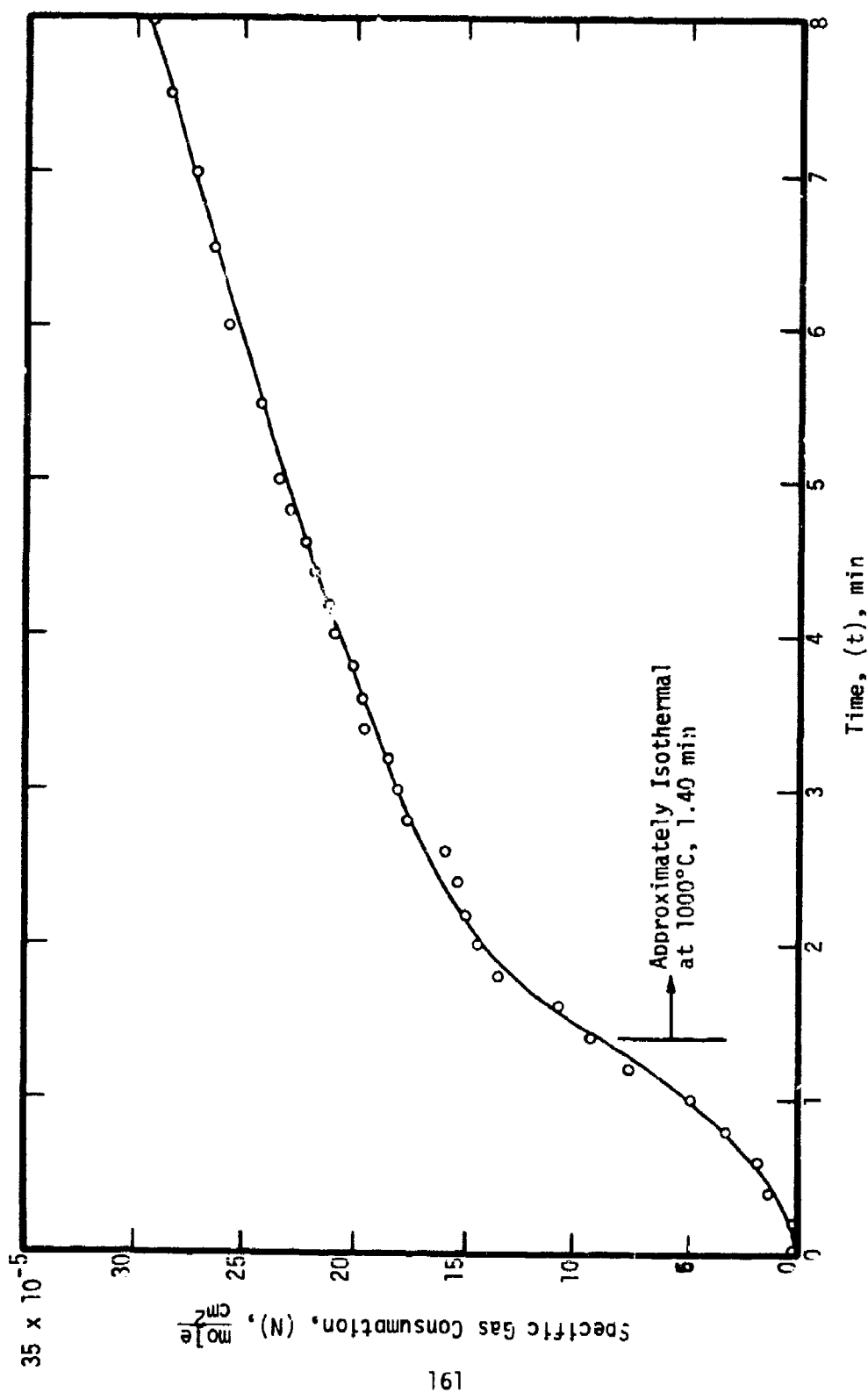


Figure 62. - Initial behavior of the specific gas consumption (N) for unalloyed titanium (Type 1) specimen no. 08013 heated in 200 torr O_2 at the rate of $7.5^\circ C/s$ to $1200^\circ C$.

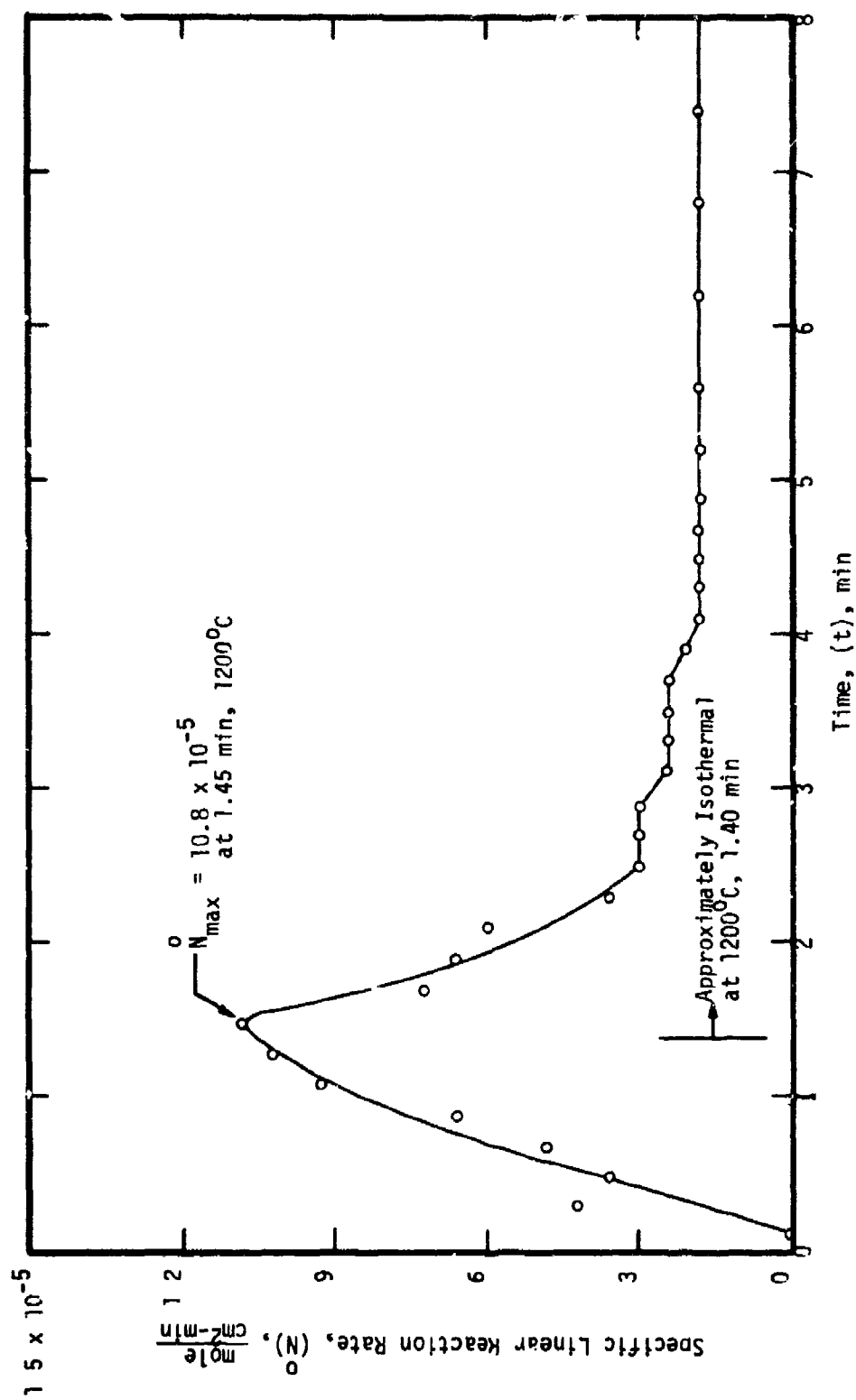


Figure 63. - Initial behavior of the specific linear reaction rate (\dot{N}) for unalloyed titanium (Type 1) specimen no. 08013 heated in 200 torr O_2 at the rate of 7.5°C/s to 1200°C.

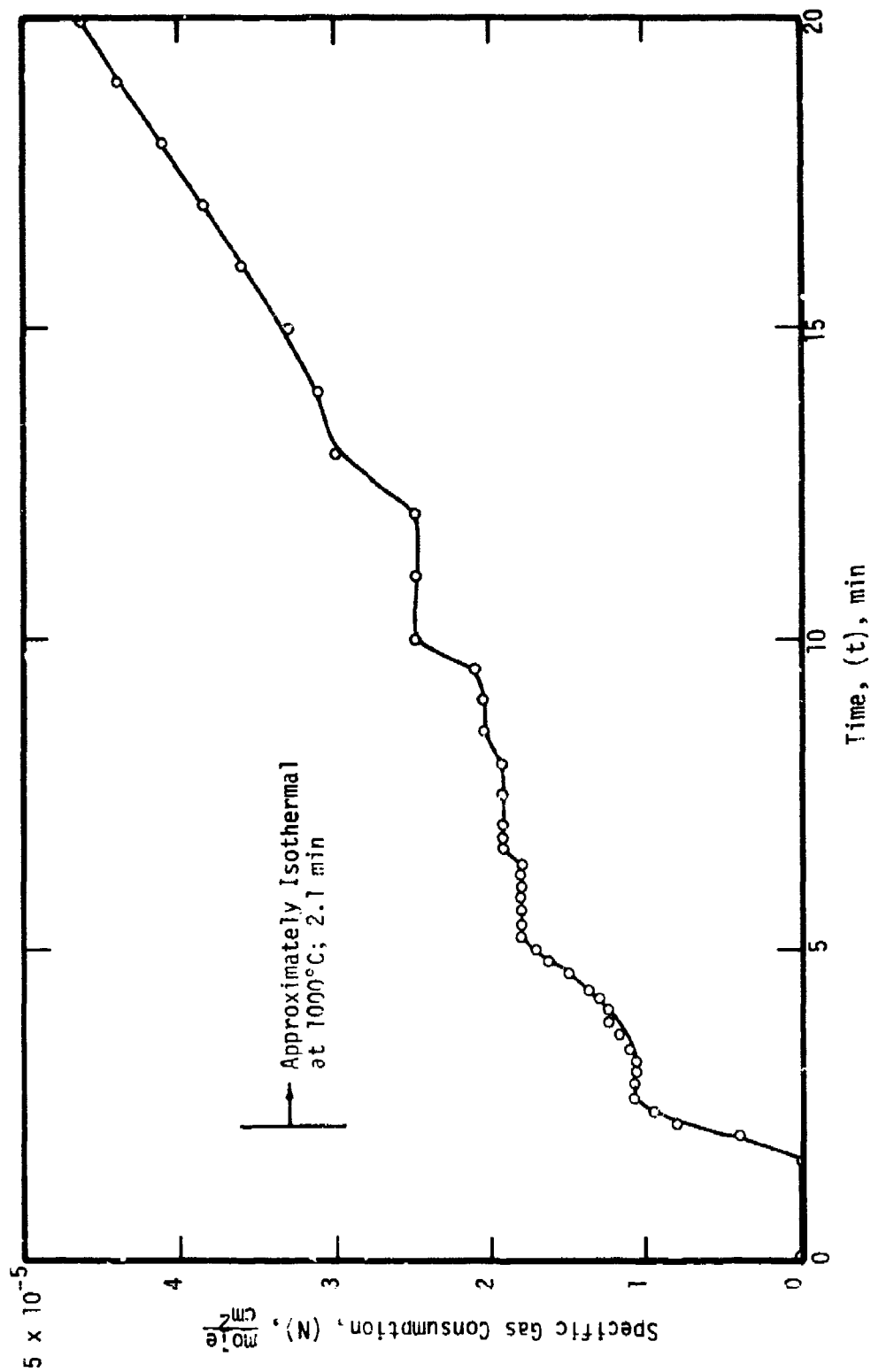


Figure 64. - Initial behavior of the specific gas consumption (N) for unalloyed titanium (Type 2) specimen no. 09191 heated in 200 torr O_2 at the rate of $8^\circ C/s$ to $1000^\circ C$.

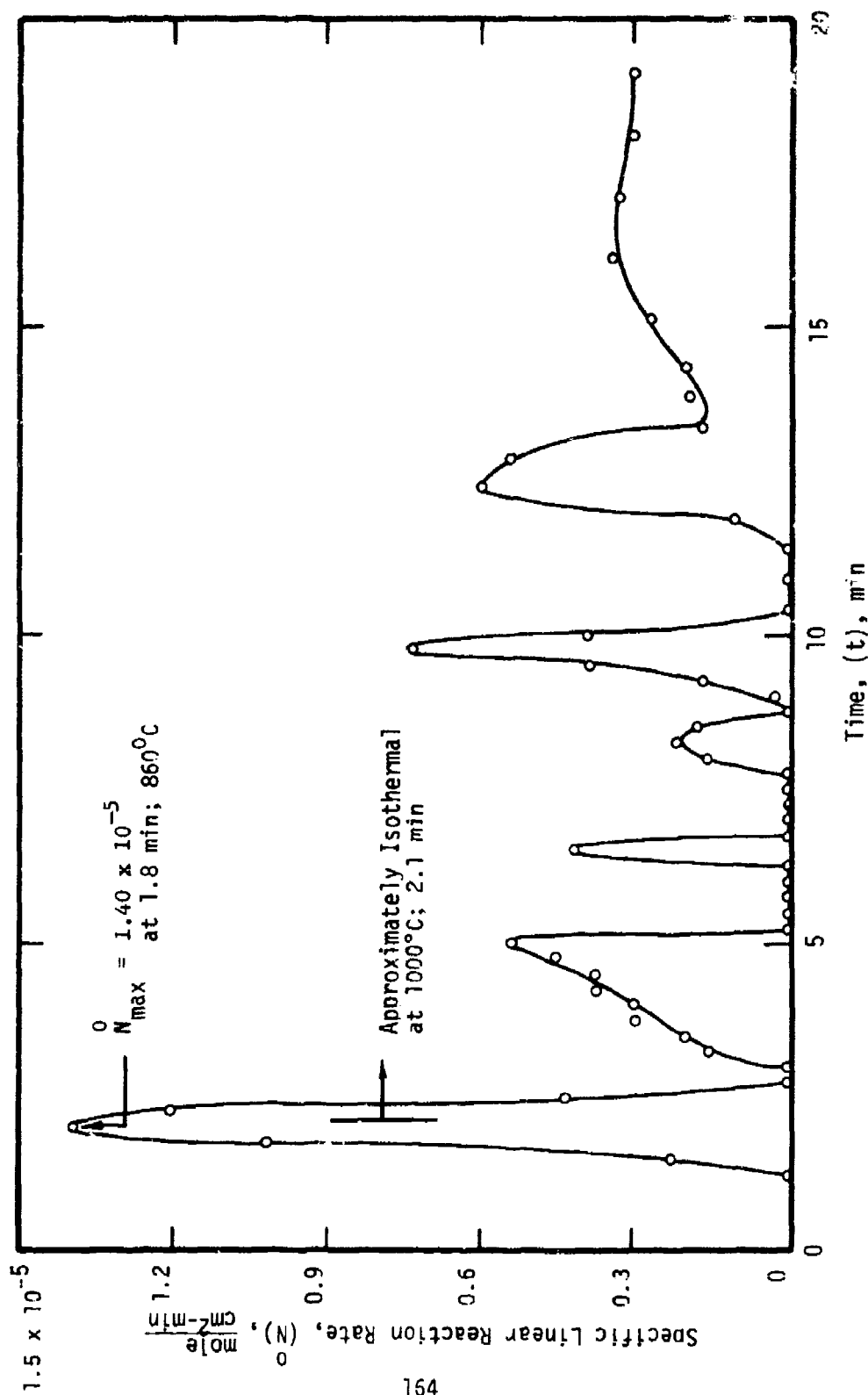


Figure 65. - Initial behavior of the specific linear reaction rate (\dot{N}) for unalloyed titanium (Type 2) specimen no. 09191 heated in 200 torr O_2 at the rate of 8°C/s to 1000°C.

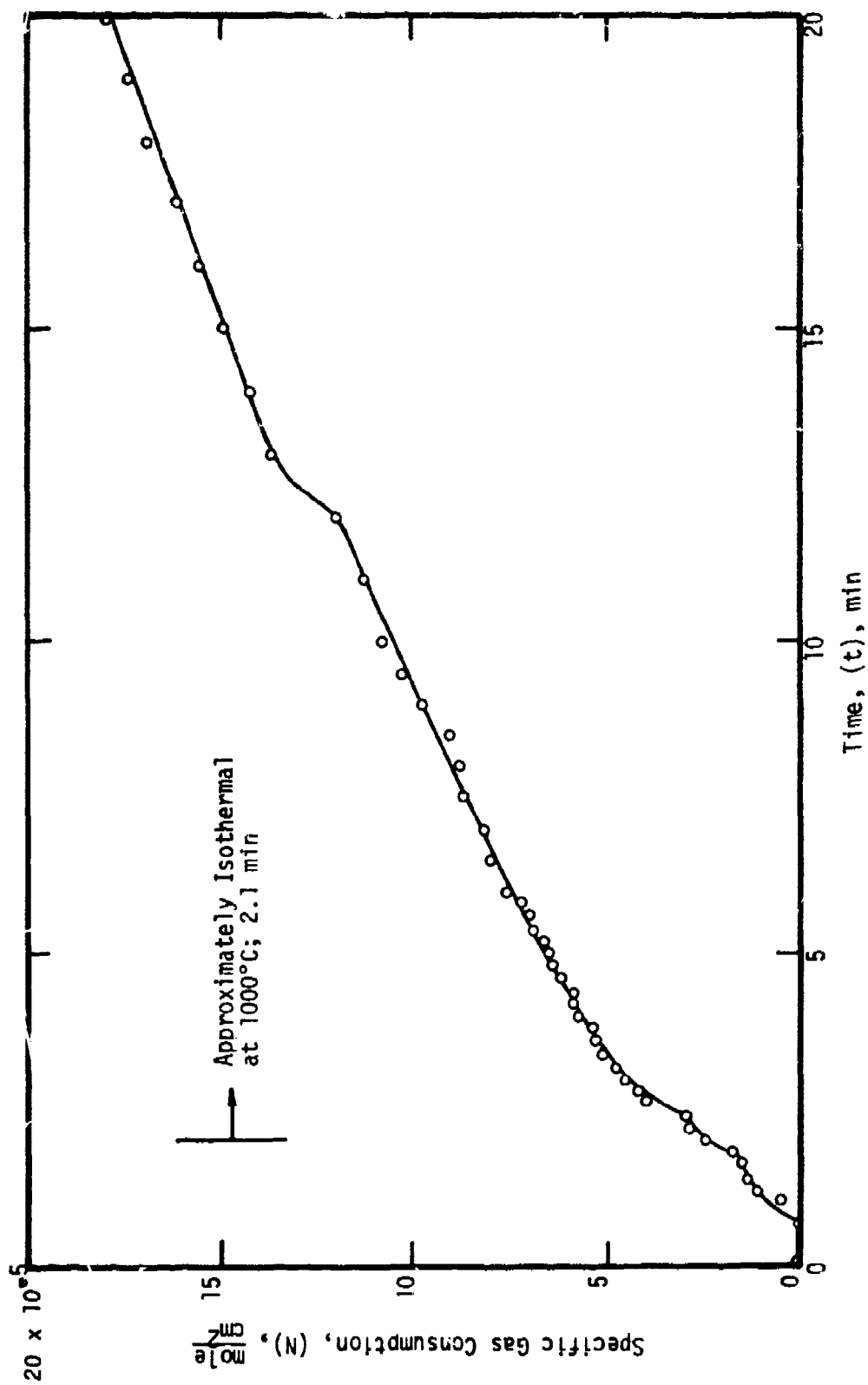


Figure 66. - Initial behavior of the specific gas consumption (N) for unalloyed titanium (Type 2) specimen no. 09192 heated in 400 torr O_2 at the rate of 8°C/s to 1000°C .

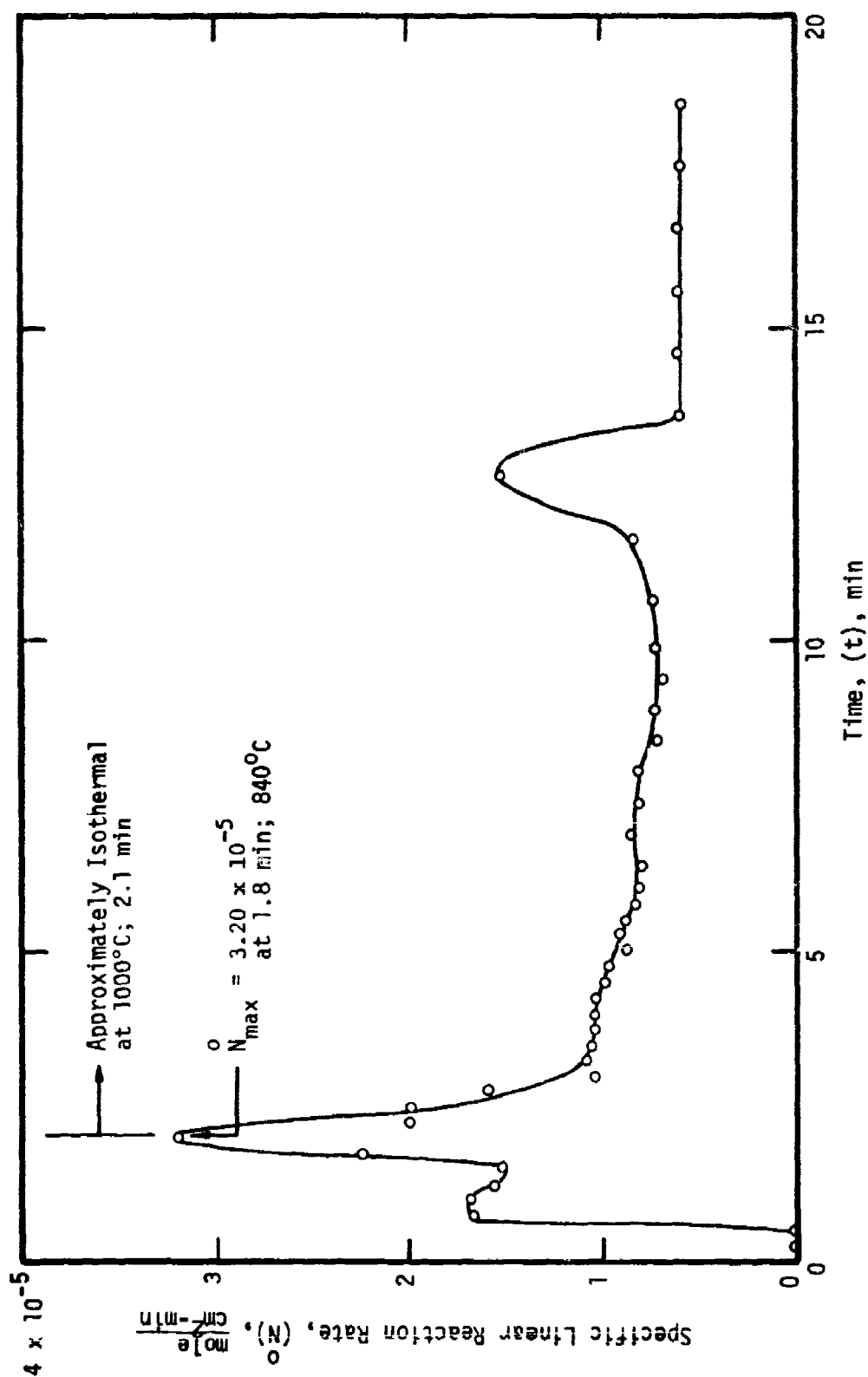


Figure 67. - Initial behavior of the specific linear reaction rate (N) for unalloyed titanium (Type 2) specimen no. 09192 heated in 400 torr O_2 at the rate of 8°C/s to 1000°C.

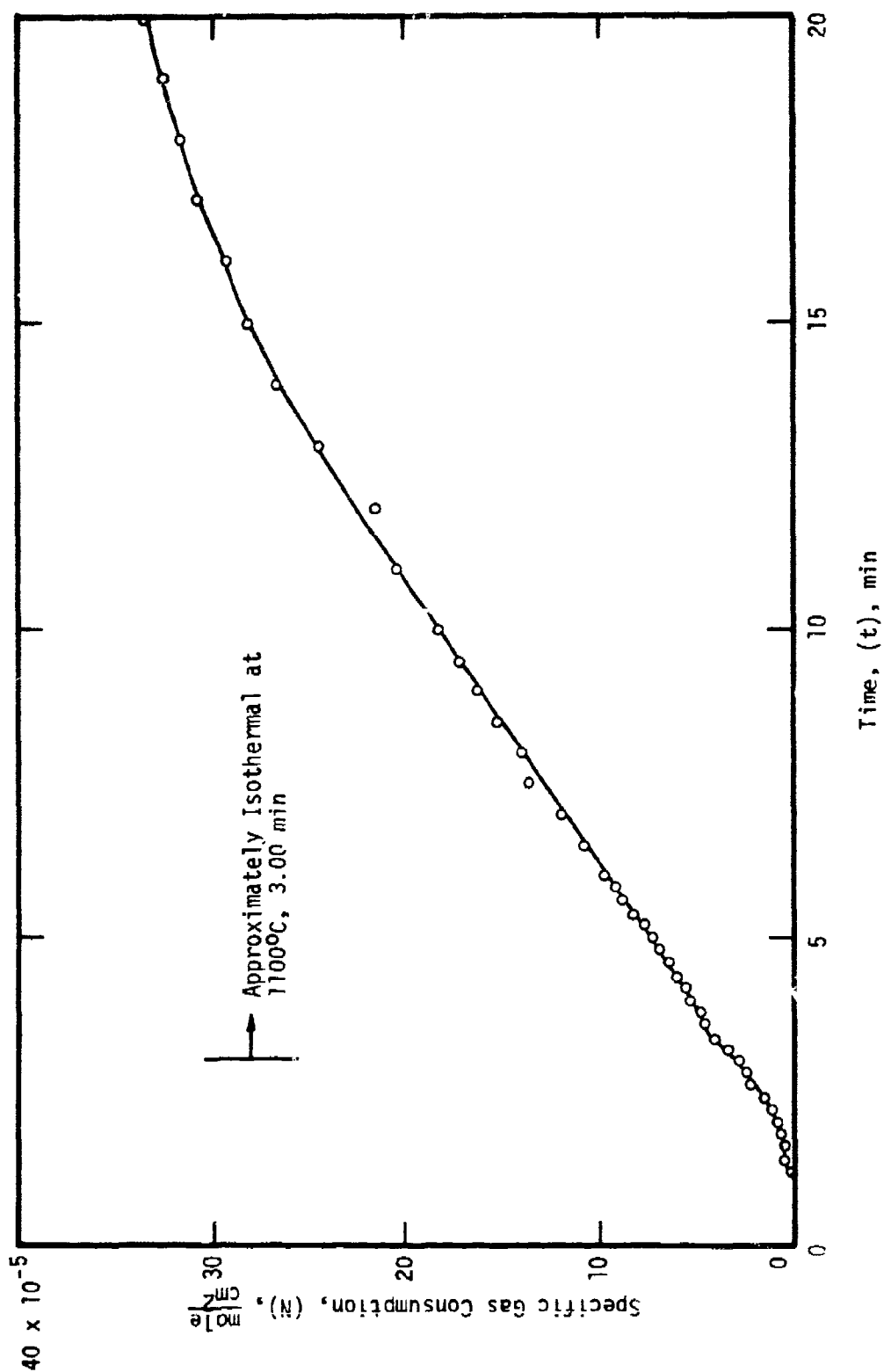


Figure 68. - Initial behavior of the specific gas consumption (N) for unalloyed titanium (Type 2) specimen no. 401151 heated in 200 torr O_2 at the rate of 8°C/s to 1100°C .

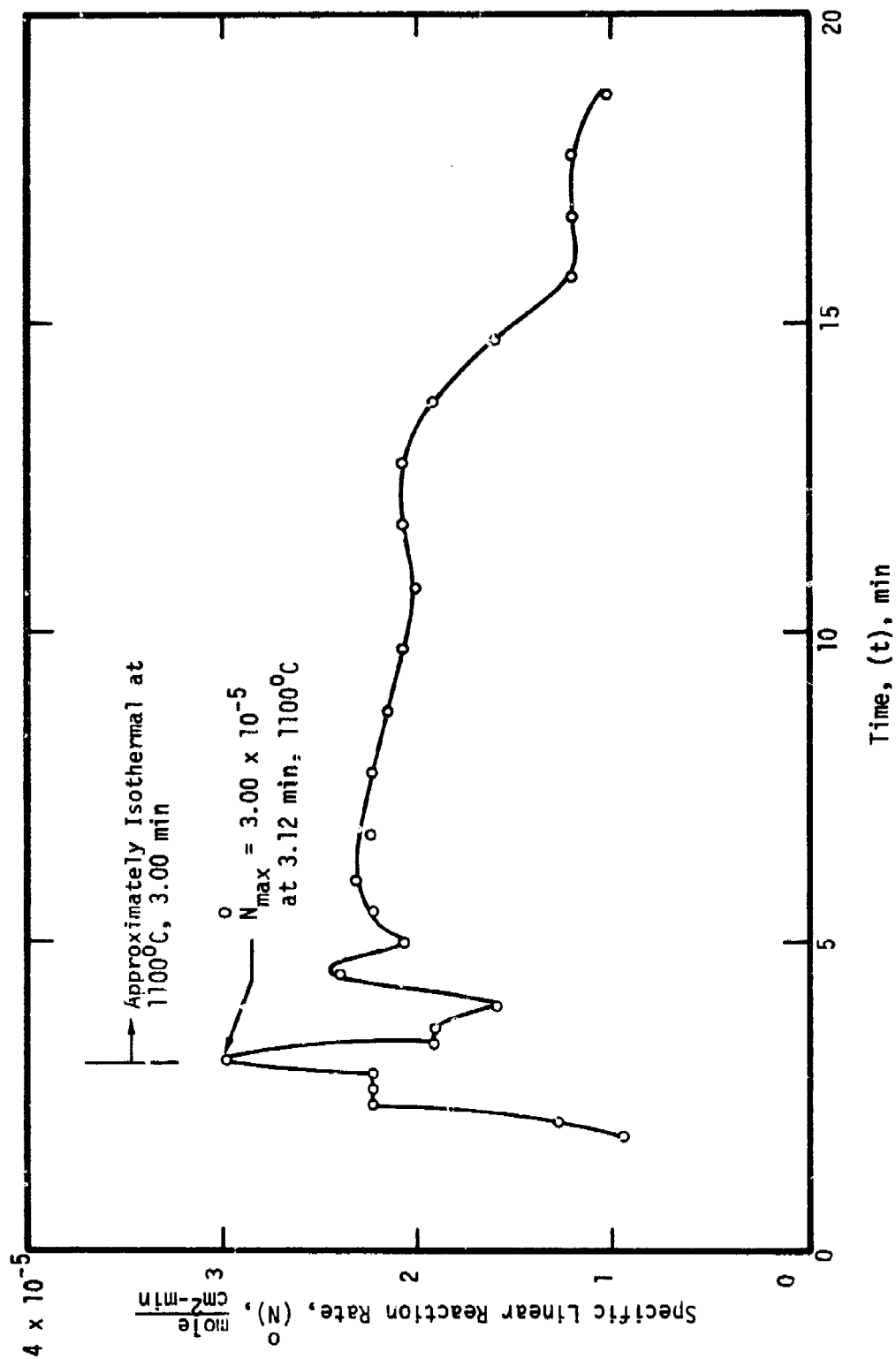


Figure 69. - Initial behavior of the specific linear reaction rate (\bar{N}) for unalloyed titanium (Type 2) specimen no. 401151 heated in 200 torr O_2 at the rate of 8°C/s to 1100°C.

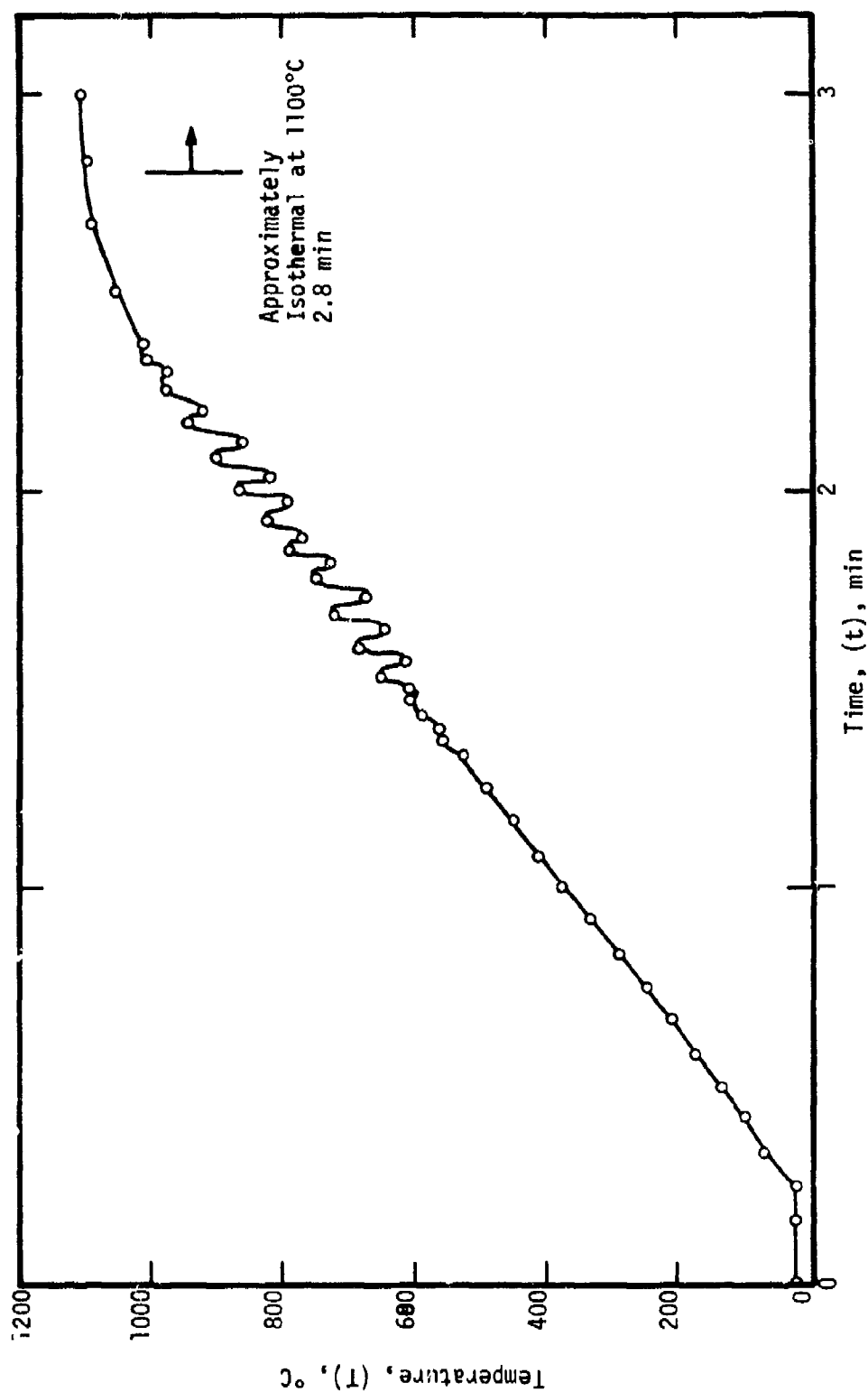


Figure 70. - Initial time-temperature profile for unalloyed titanium (Type 2) specimen no. 405151 heated in 200 torr O_2 at the rate of 8°C/s to 1100°C. Note temperature instability for material cold worked 87 percent.

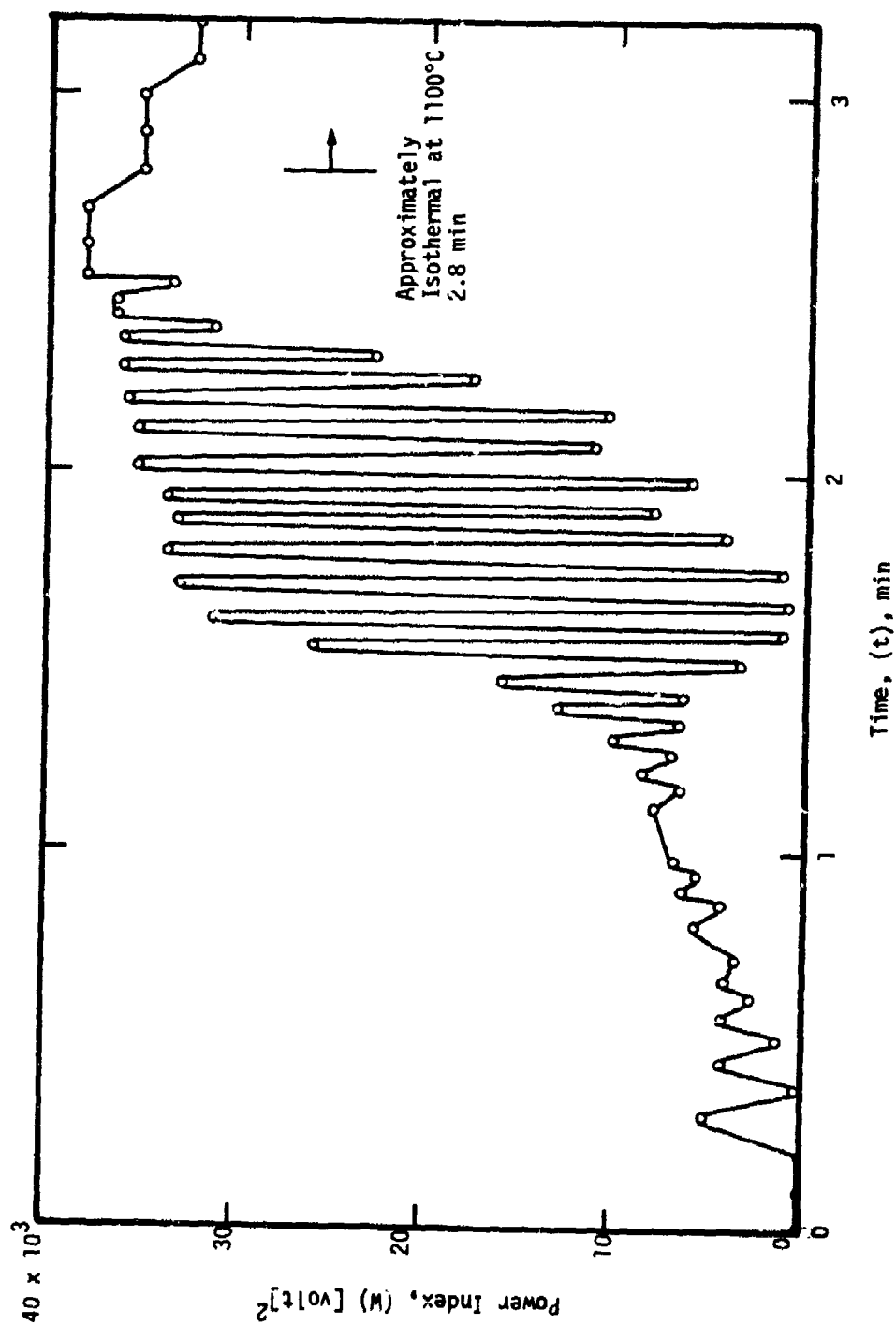


Figure 71. - Initial behavior of the power index (W) for unalloyed titanium (Type 2) specimen no. 405151 heated in 200 torr O₂ at the rate of 8°C/s to 1100°C. Note power instability for material cold worked 87 percent.

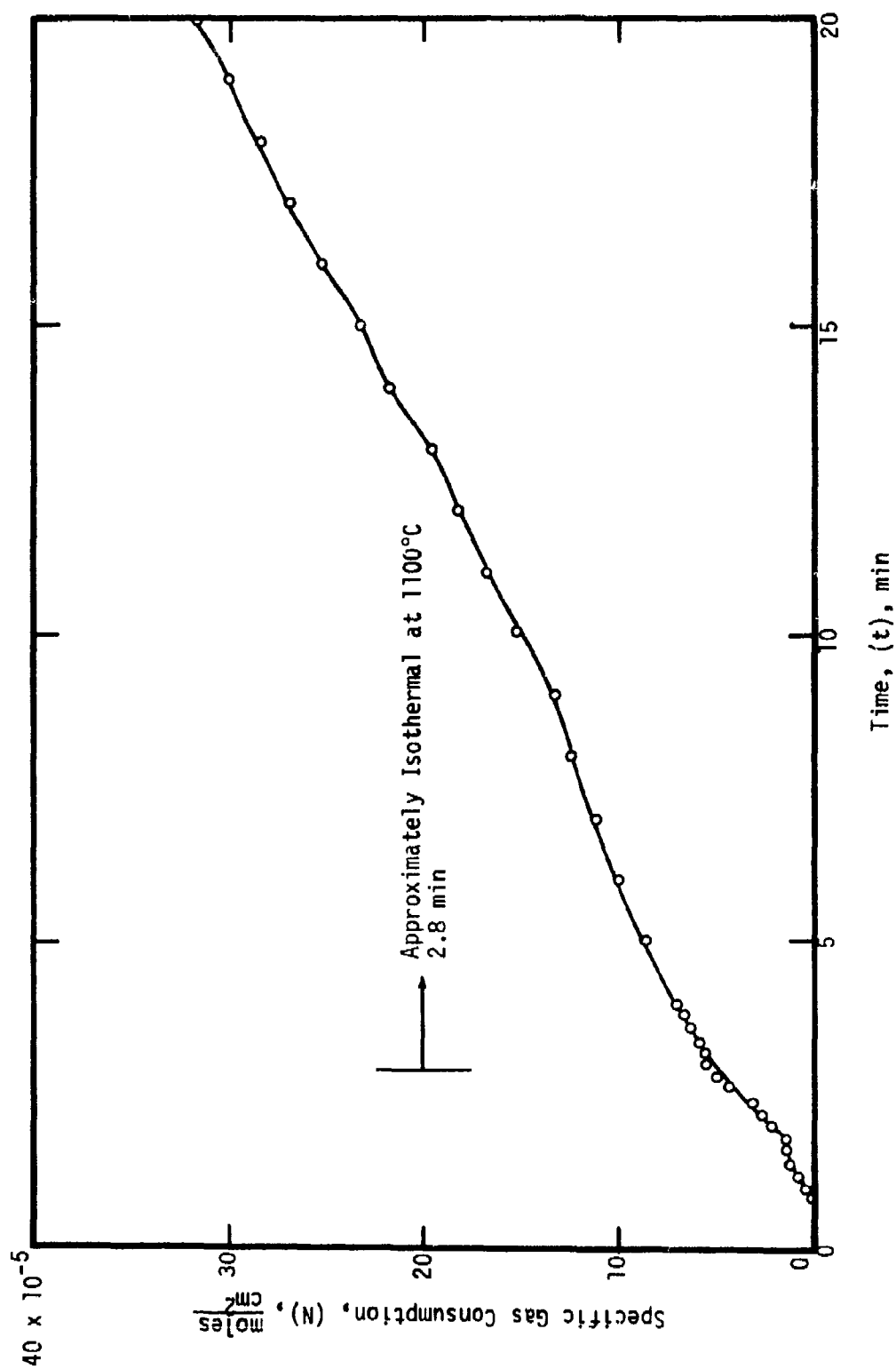


Figure 72. - Initial behavior of the specific gas consumption (N) for unalloyed titanium (Type 2) specimen no. 405151 heated in 200 torr O_2 at the rate of 8°C/s to 1100°C. Material cold worked 87 percent.

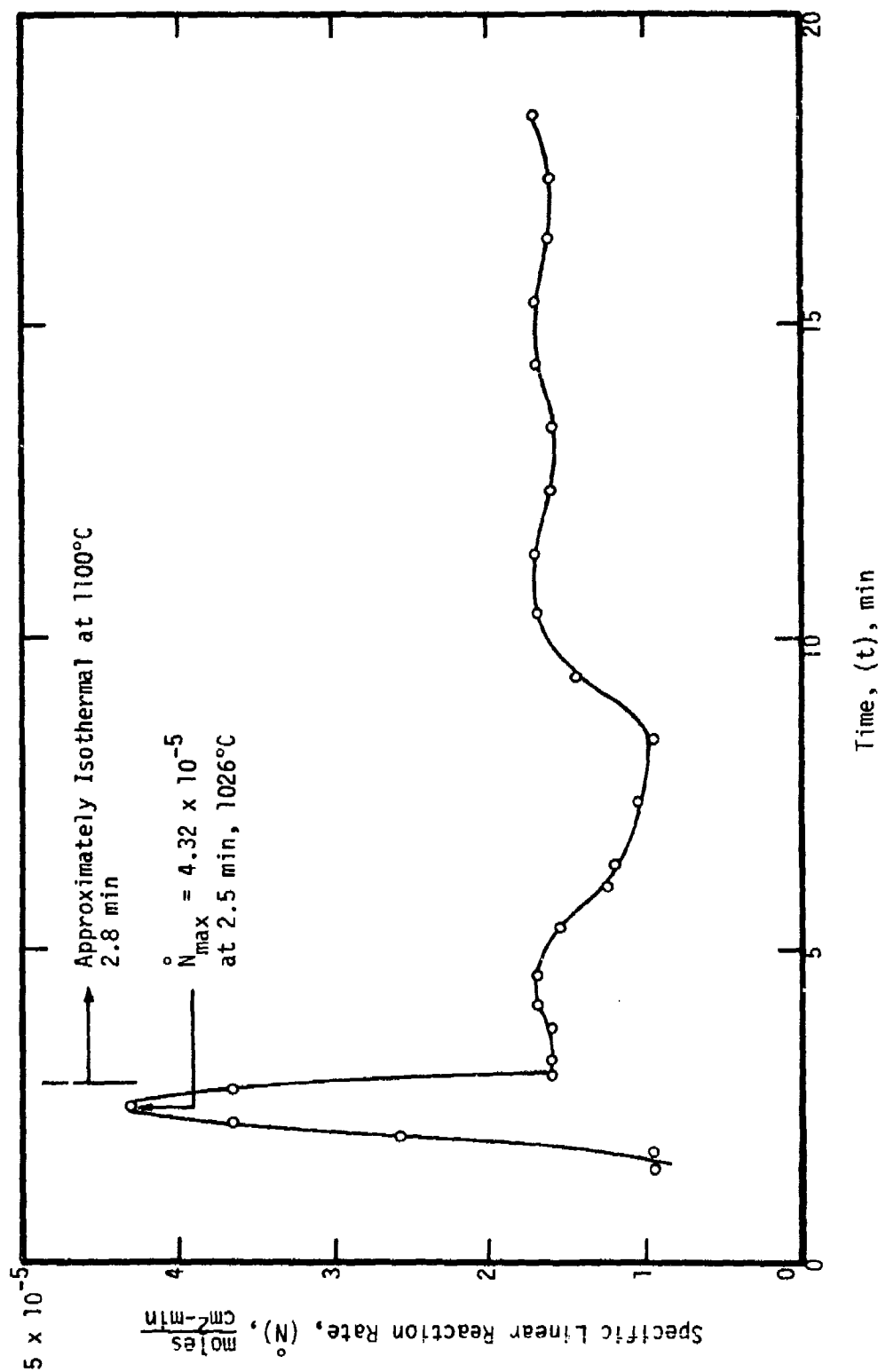


Figure 73. - Initial behavior of the specific linear reaction rate (\dot{N}) for unalloyed titanium (Type 2) specimen no. 405151 heated in 200 torr O_2 at the rate of 8°C/s to 1100°C. Material cold worked 87 percent.

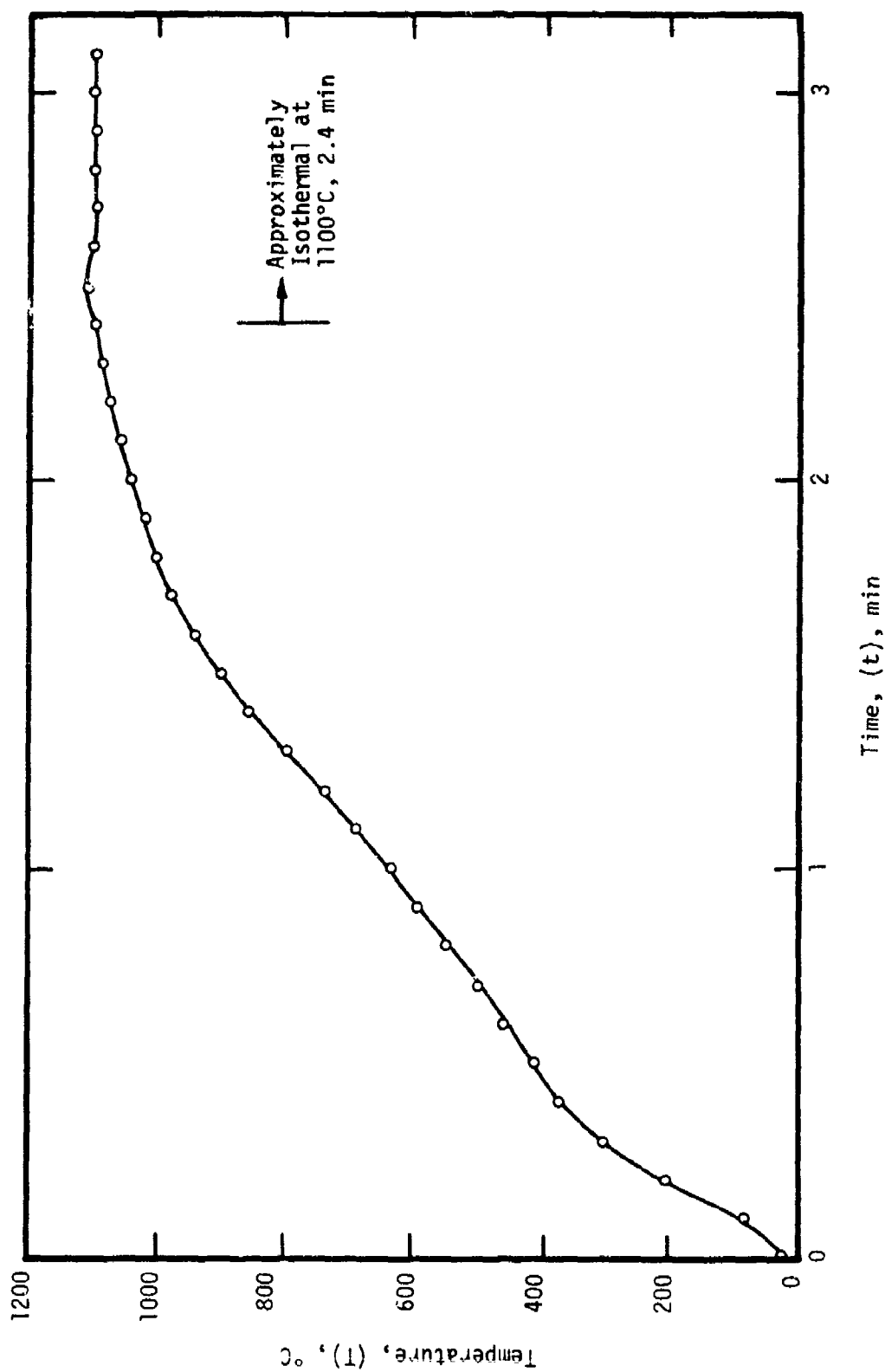


Figure 74. - Initial time-temperature profile for unalloyed titanium (Type 2) specimen no. 405221 heated in 200 torr O_2 at the rate of approximately 10°C/s to 1100°C . Material cold worked 87 percent.

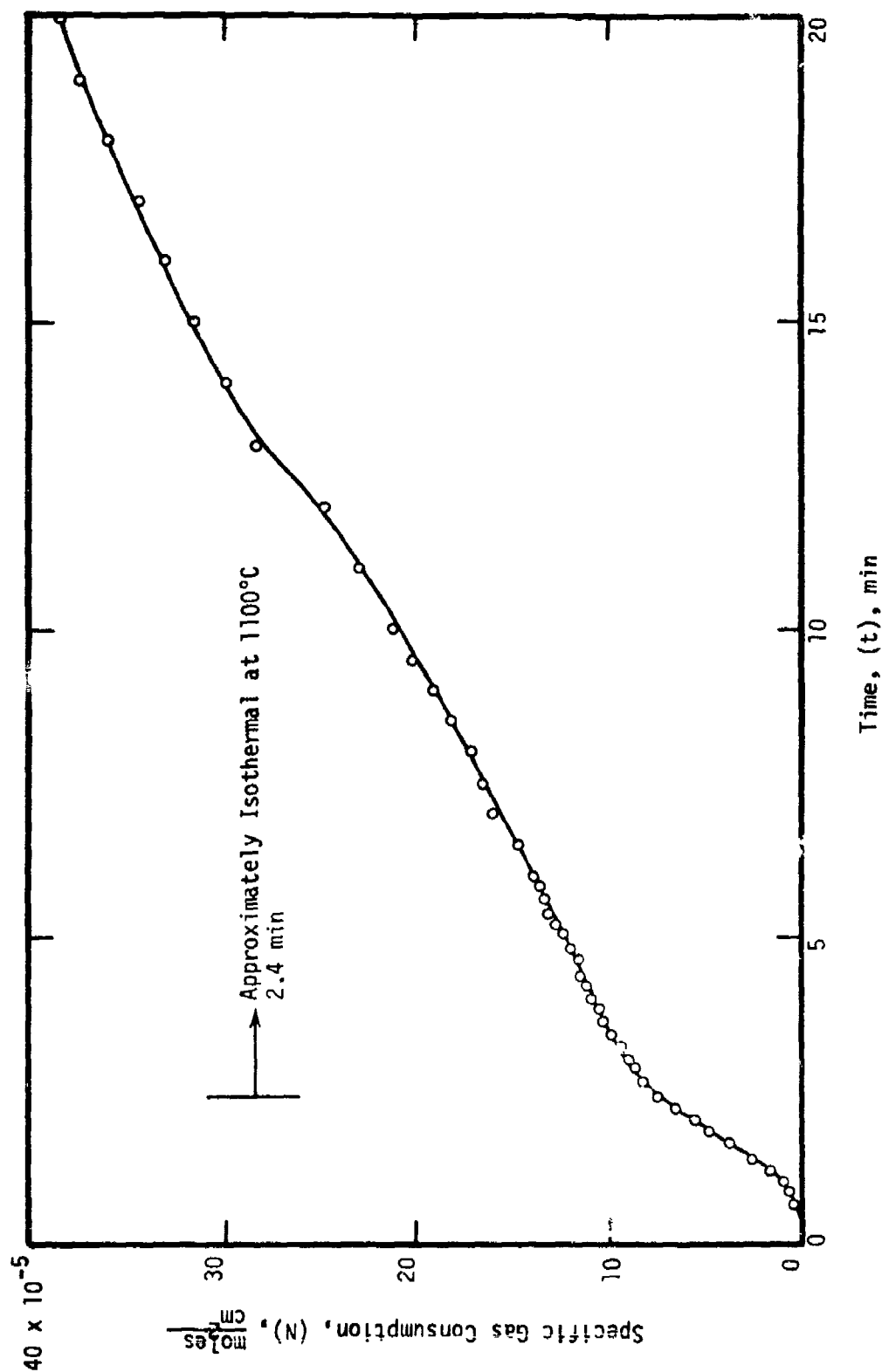


Figure 75. - Initial behavior of the specific gas consumption (N) for unalloyed titanium (Type 2) specimen no. 405221 heated in 200 torr O_2 at the rate of approximately 10°C/s to 1100°C. Material cold worked 87 percent.

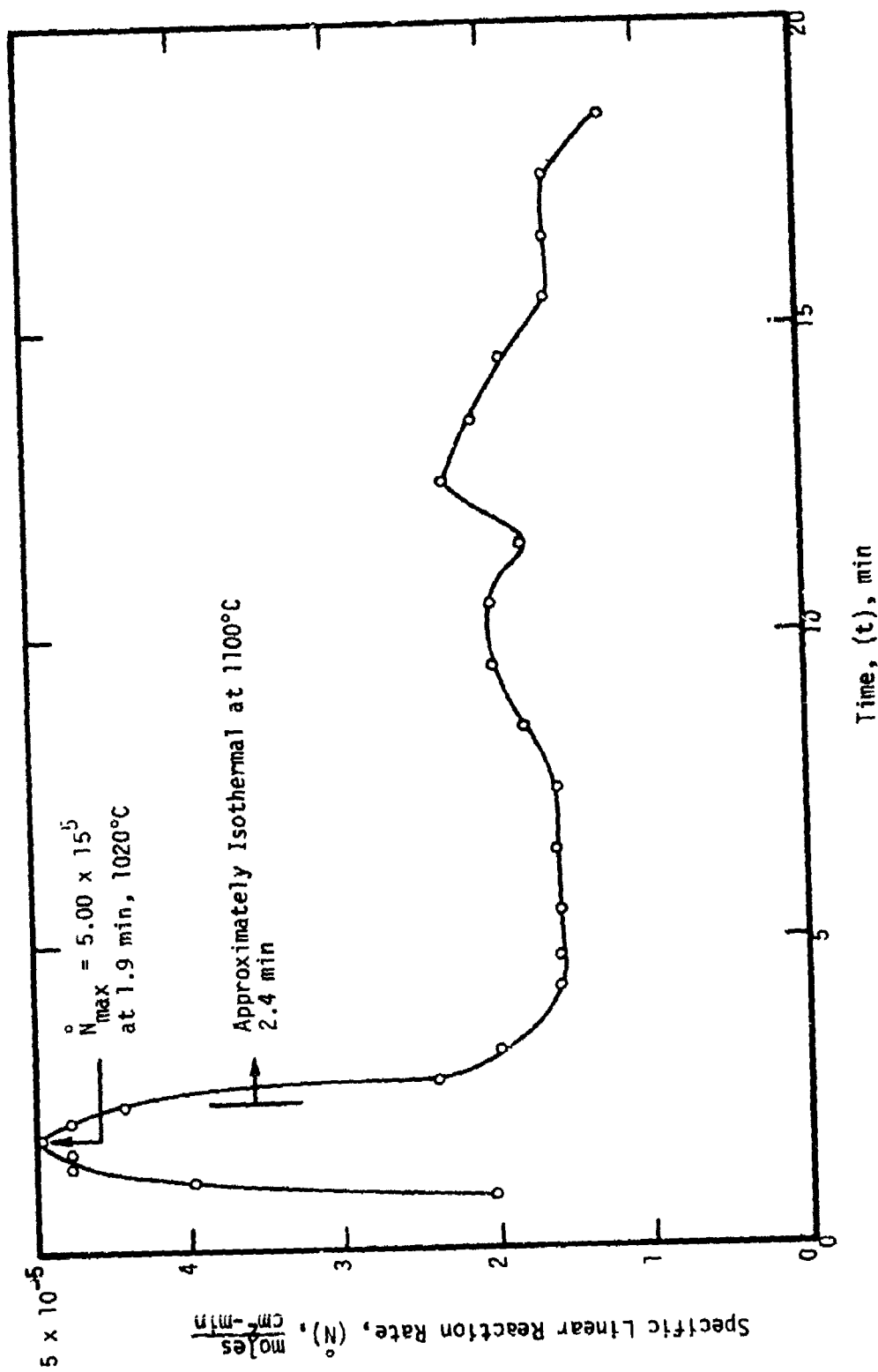


Figure 76. - Initial behavior of the specific linear reaction rate (\bar{N}) for unalloyed titanium (Type 2) specimen no. 405221 heated in 200 torr O_2 at the rate of approximately 10°C/s to 1100°C . Material cold worked 87 percent.

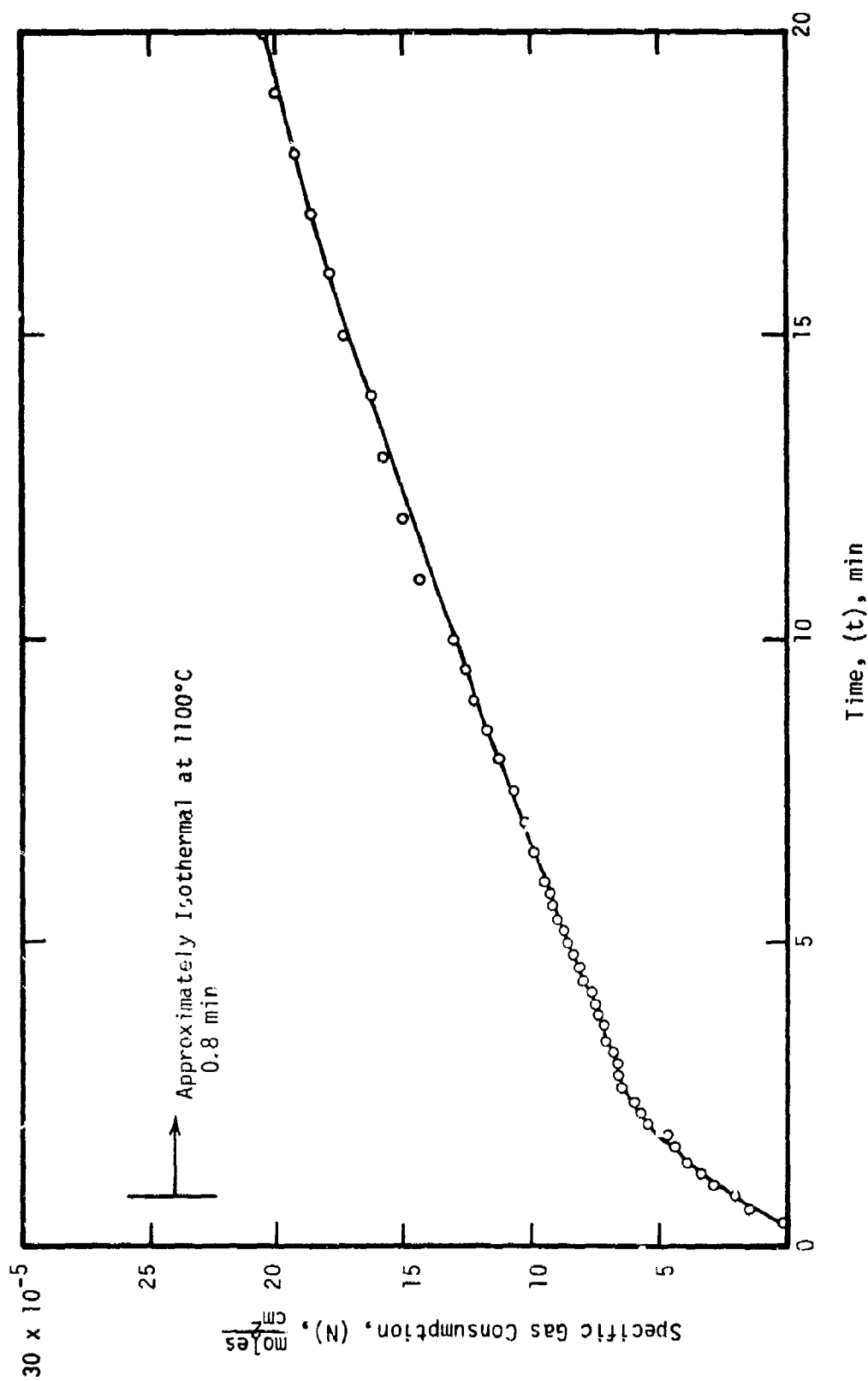


Figure 77. - Initial behavior of the specific gas consumption (N) for unalloyed titanium (Type 2) specimen no. 408191 heated in 200 torr O_2 at the rate of 22°C/s to 1100°C. Material cold worked 76 per cent.

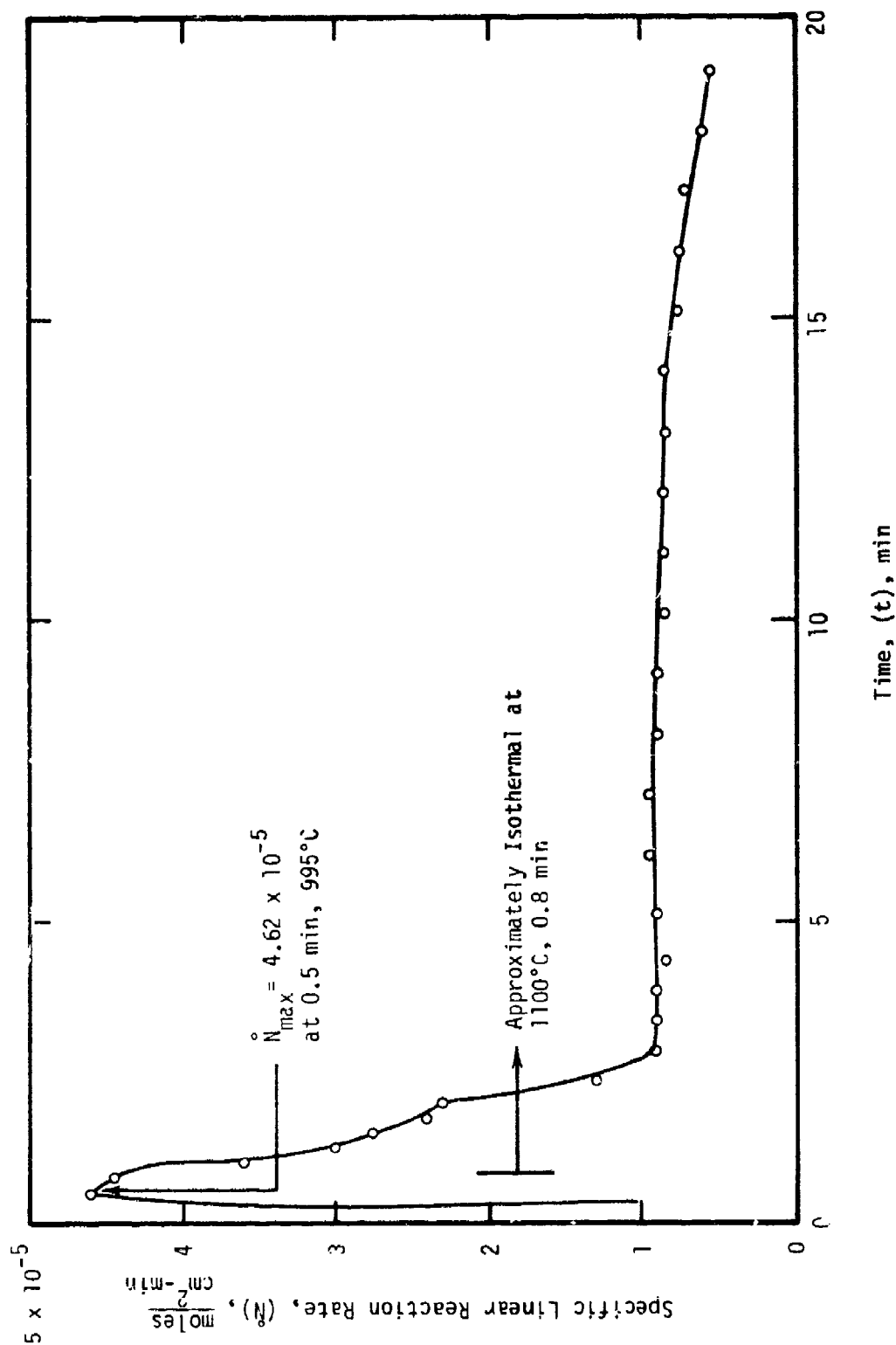


Figure 78. - Initial behavior of the specific linear reaction rate (\dot{N}) for unalloyed titanium (Type 2) specimen no. 408191 heated in 200 torr O_2 at the rate of 22°C/s to 1100°C. Material cold worked 76 percent.

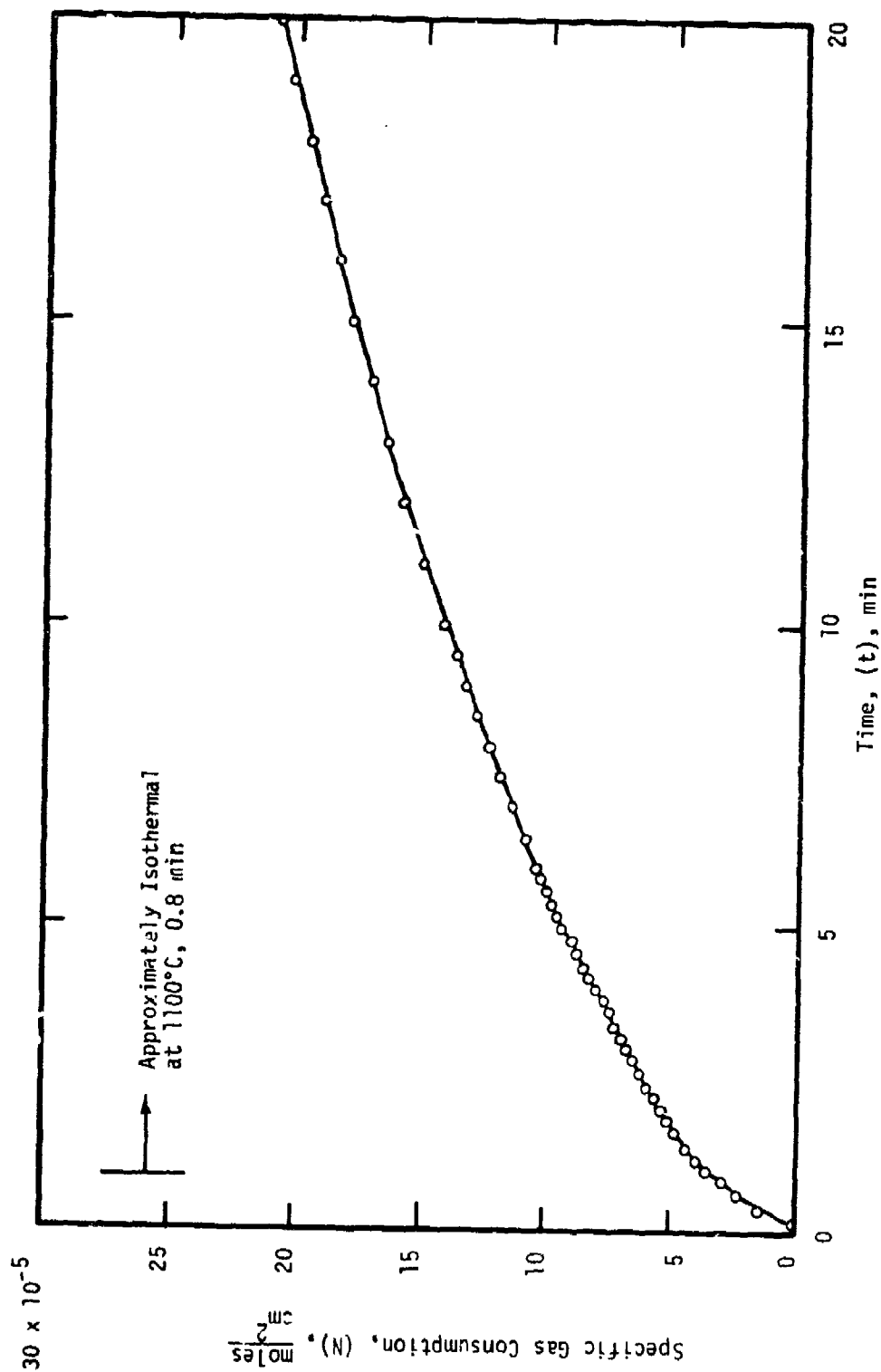


Figure 79. - Initial behavior of the specific gas consumption (N) for unalloyed titanium (Type 2) specimen no. 408741 heated in 200 torr O_2 at the rate of 22°C/s to 1100°C. Material cold worked 61 percent.

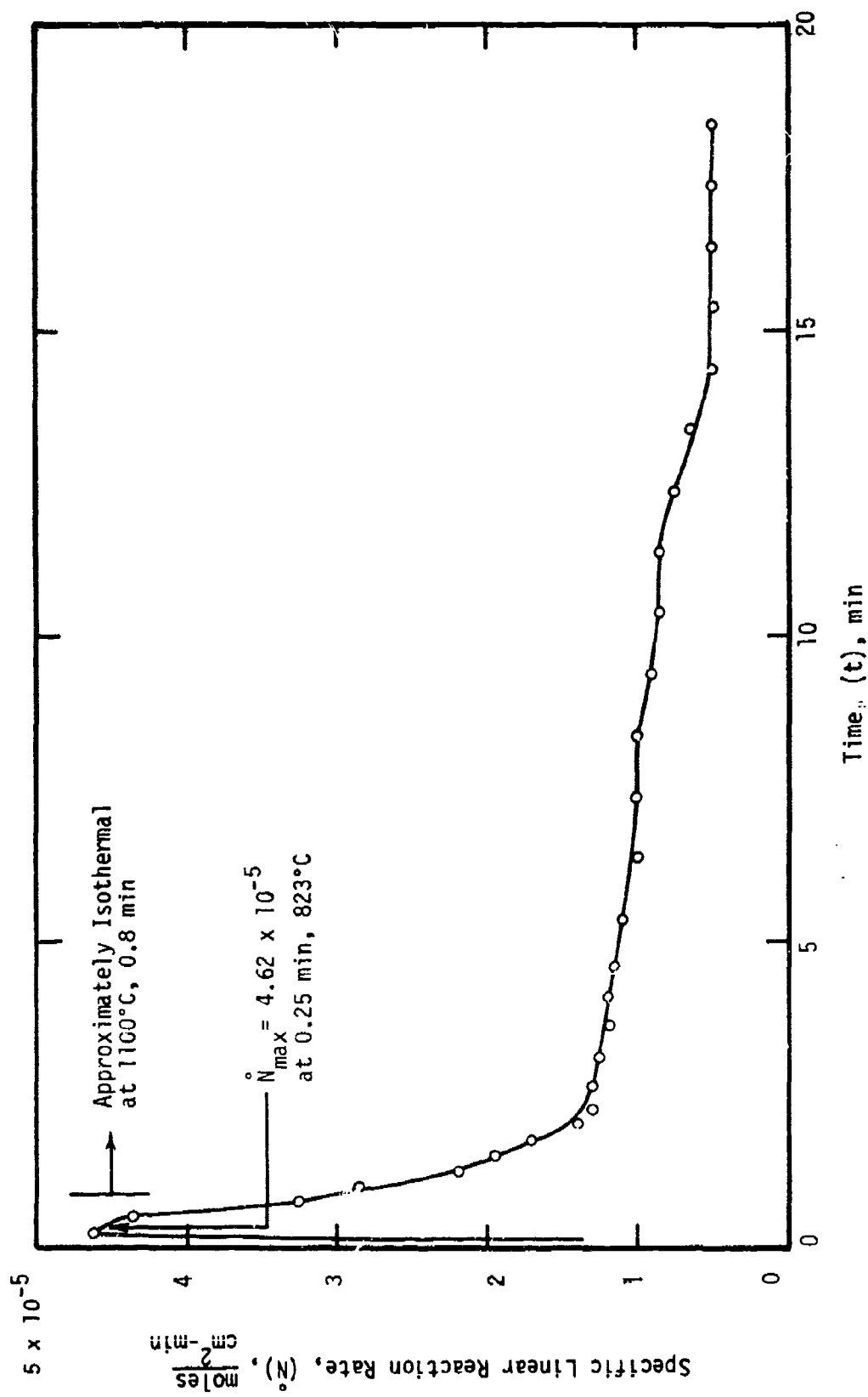


Figure 80. - Initial behavior of the specific linear reaction rate (\dot{N}) for unalloyed titanium (Type 2) specimen no. 408141 heated in 200 torr O_2 at the rate of 22°C/s to 1100°C. Material cold worked 61 percent.

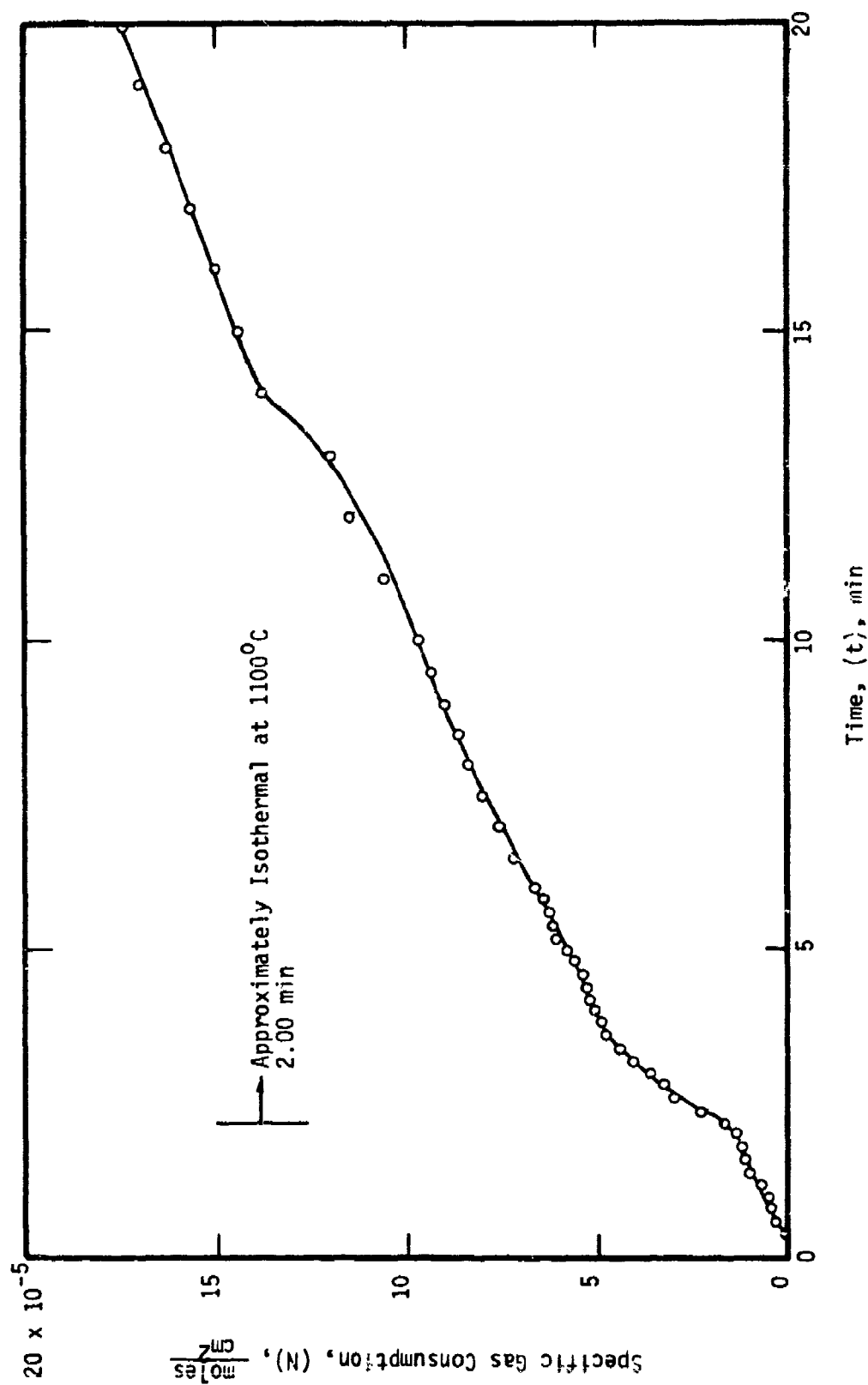


Figure 81. - Initial behavior of the specific gas consumption (N) for unalloyed titanium (Type 2) specimen no. 401021 heated in 200 torr O_2 at the rate of 8°C/s to 1100°C . Specimen descaled and re-oxidized.

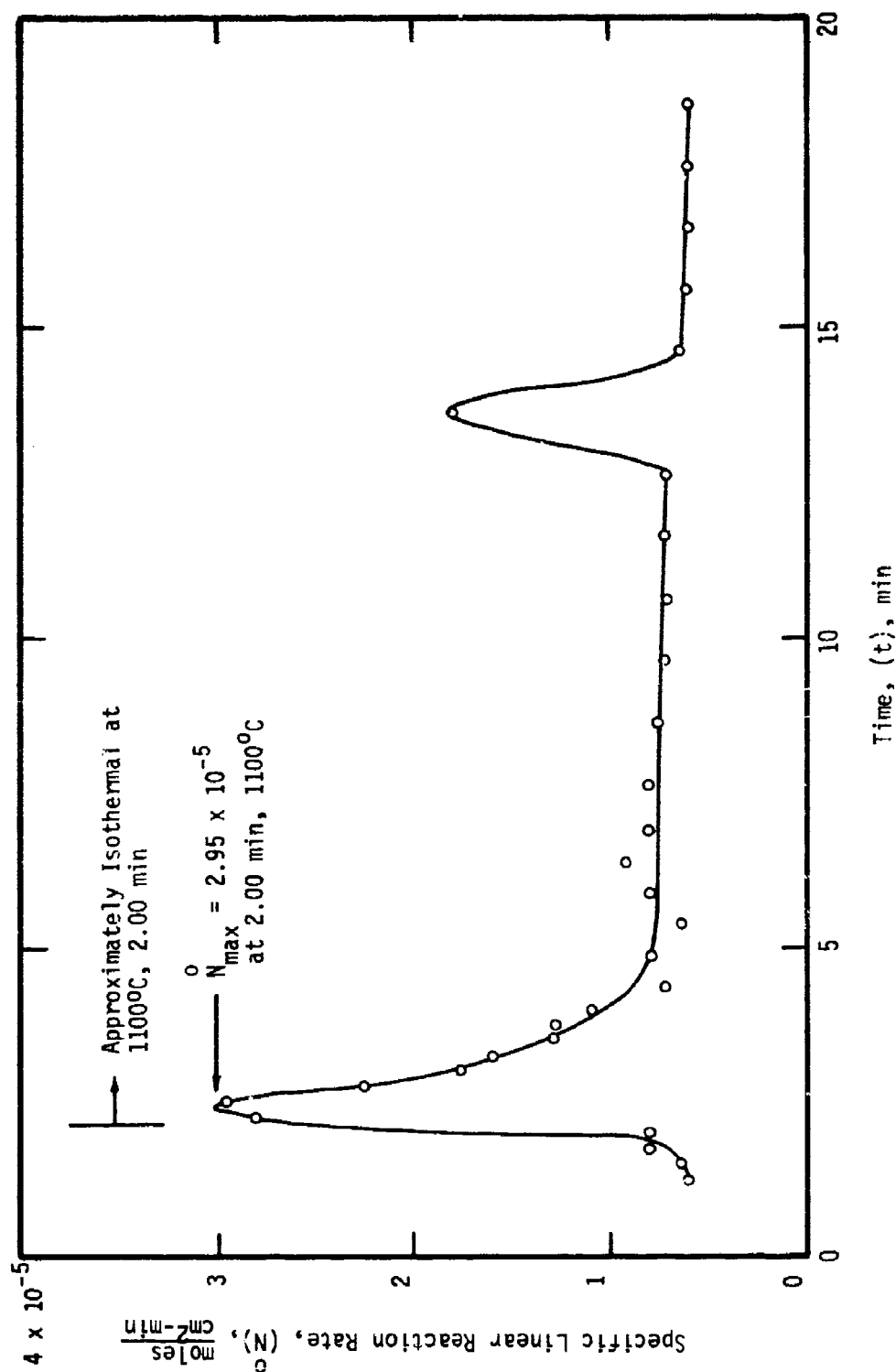


Figure 82. - Initial behavior of the specific linear reaction rate (N) for unalloyed titanium (Type 2) specimen no. 401021 heated in 200 torr O_2 at the rate of 8°C/s to 1100°C. Specimen descaled and reoxidized.

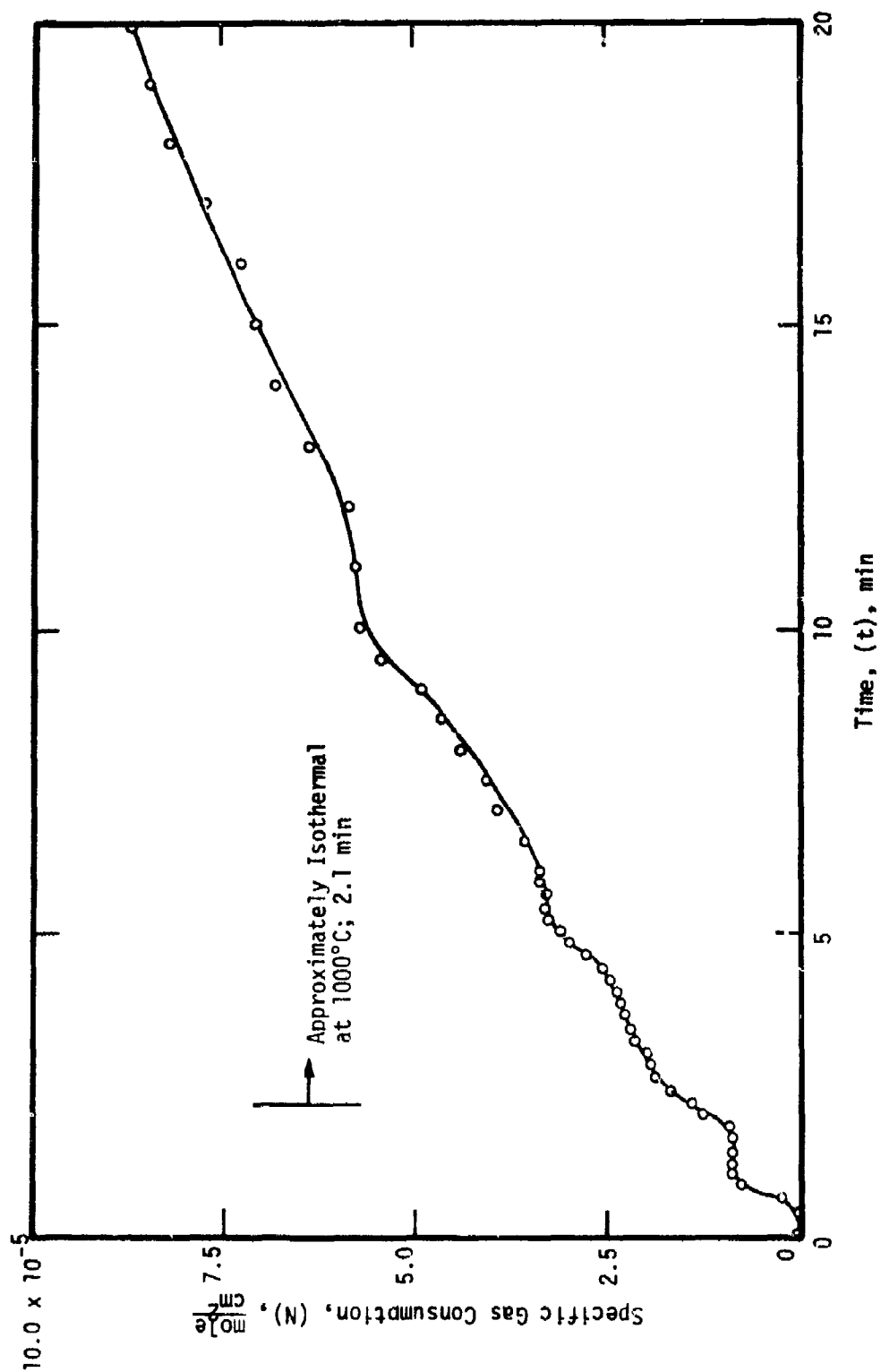


Figure 83. - Initial behavior of the specific gas consumption (N) for unalloyed titanium (Type 3) specimen no. 09194 heated in 200 torr O_2 at the rate of 8°C/s to 1000°C .

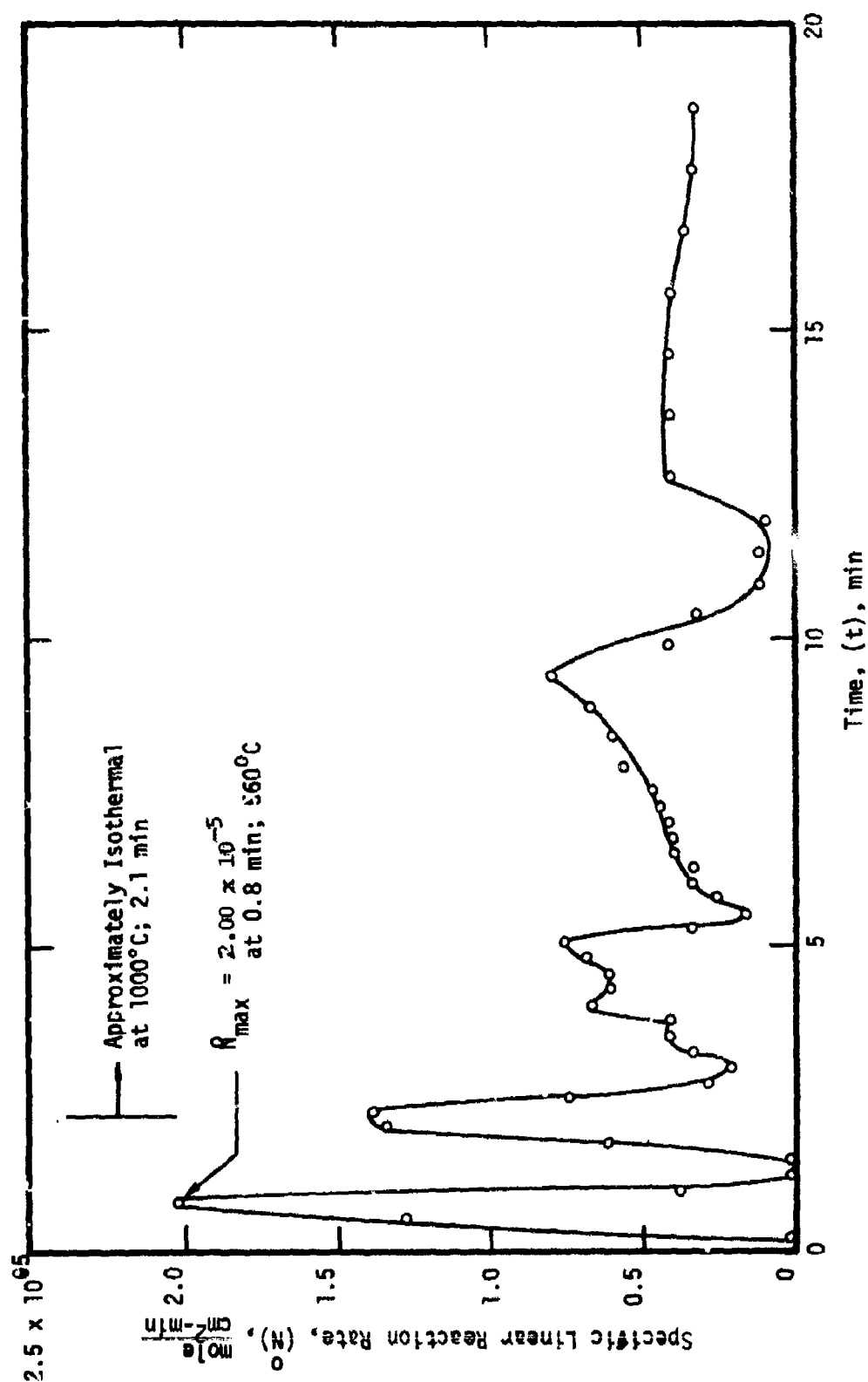


Figure 84. - Initial behavior of the specific linear reaction rate (\bar{R}) for unalloyed titanium (Type 3) specimen no. 09194 heated in 200 torr O_2 at the rate of 8°C/s to 1000°C.

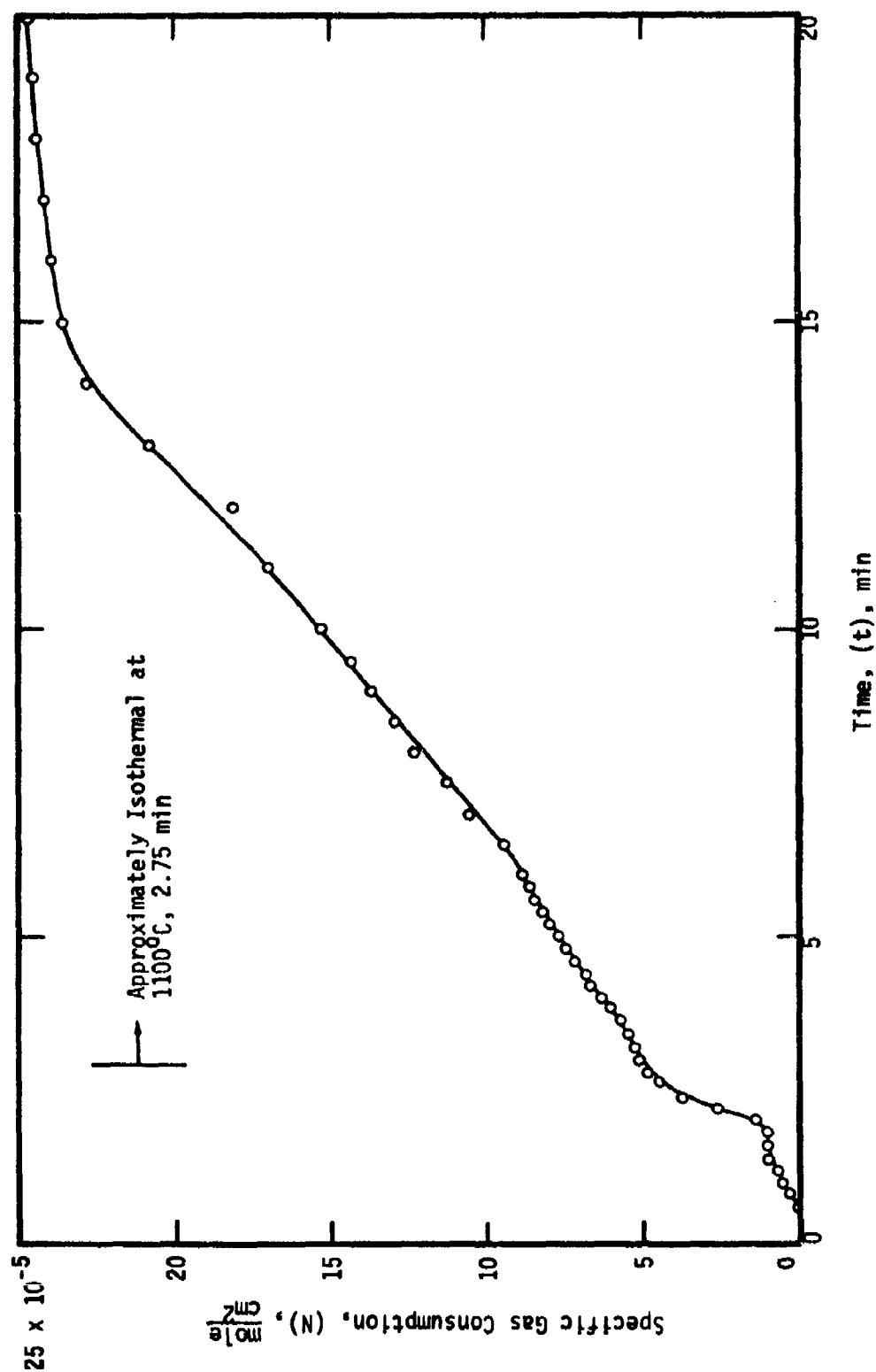


Figure 85. - Initial behavior of the specific gas consumption (N) for unalloyed titanium (Type 3) specimen no. 11201 heated in 200 torr O_2 at the rate of 8°C/s to 1100°C . Material cold worked 39 percent.

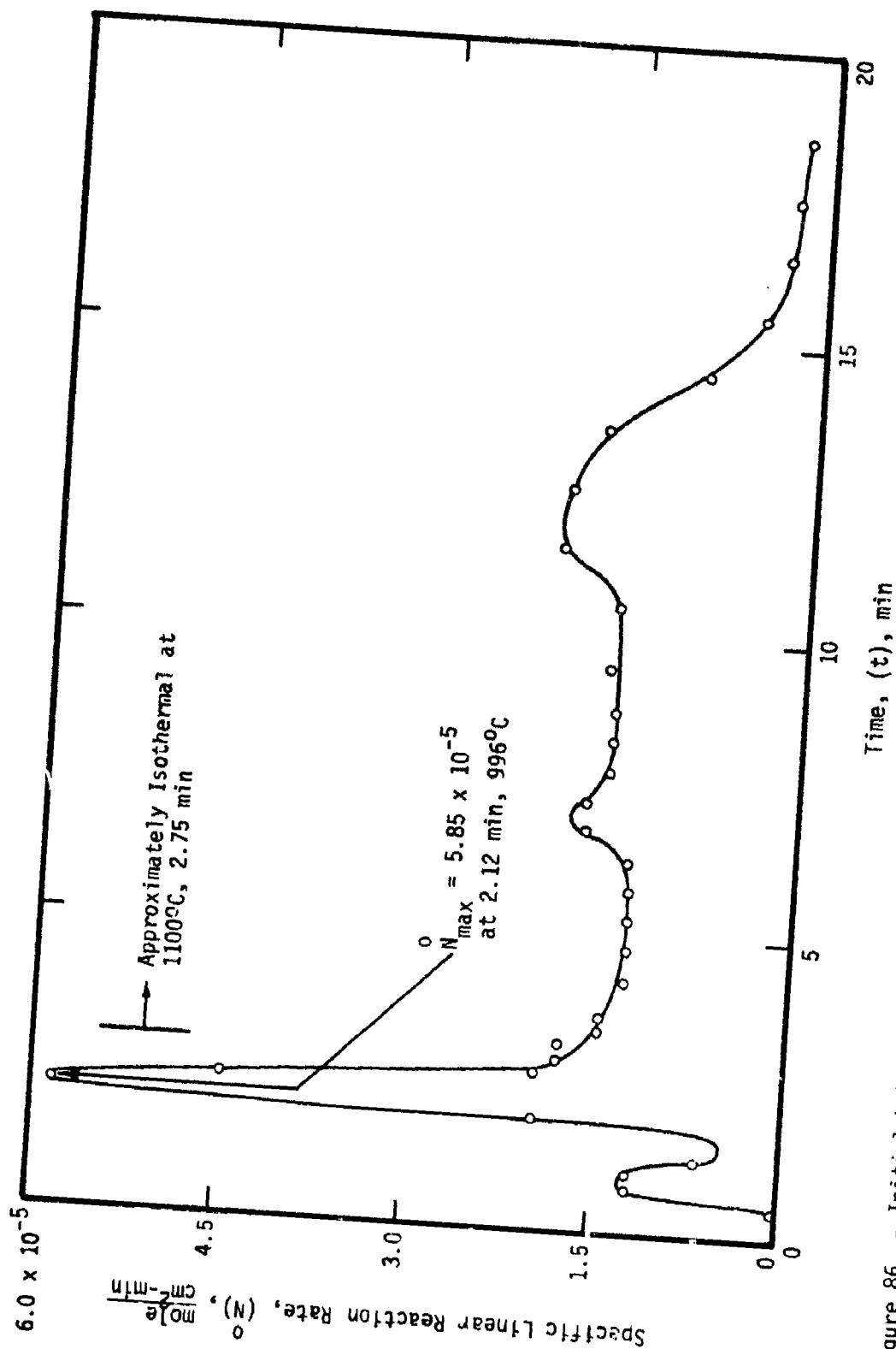


Figure 86. - Initial behavior of the specific linear reaction rate (\bar{N}) for unalloyed titanium (Type 3) specimen no. 11201 heated in 200 torr O_2 at the rate of 8°C/s to 1100°C. Material cold worked

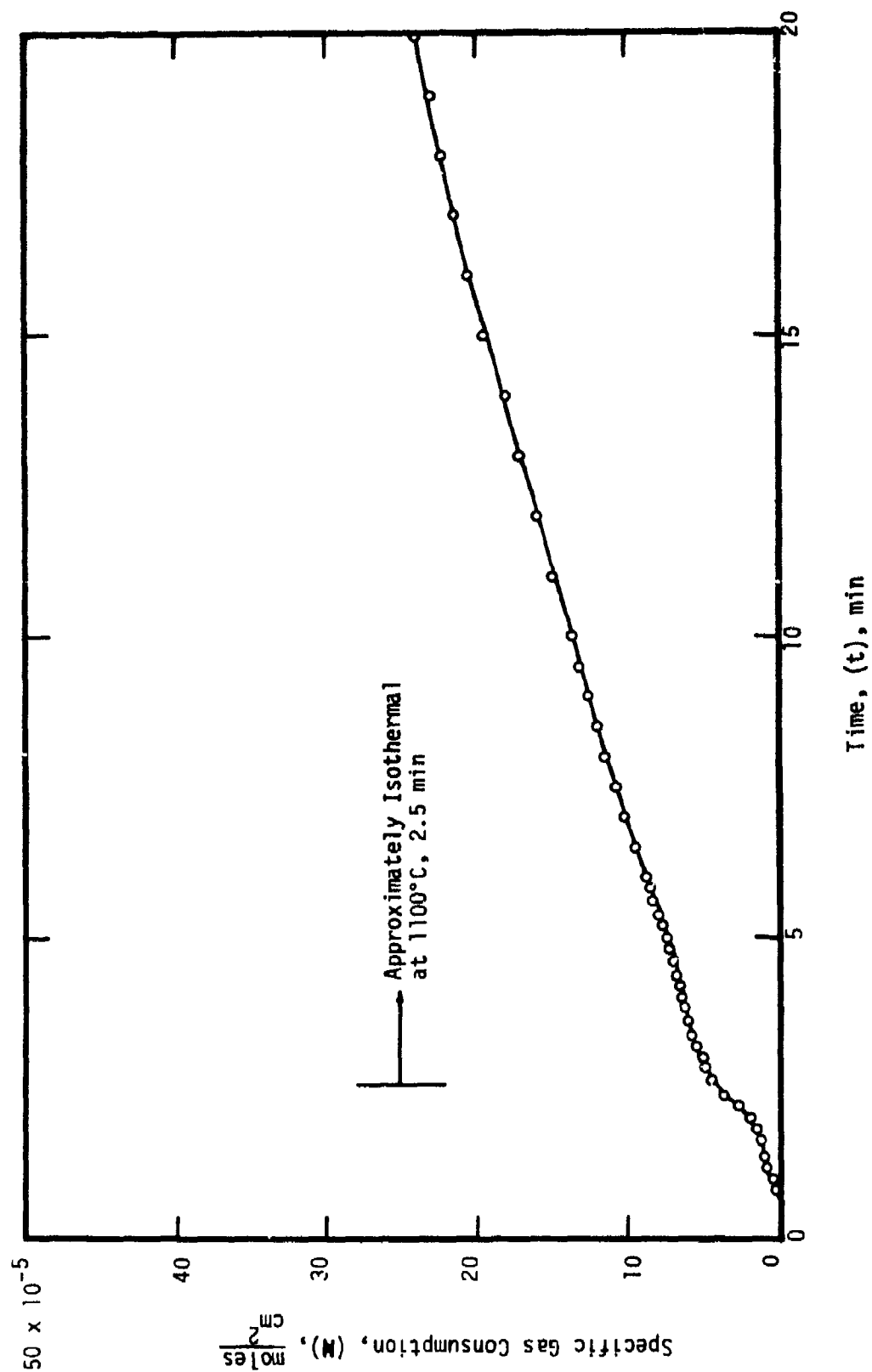


Figure 87. - Initial behavior of the specific gas consumption (M) for unalloyed titanium (Type 3) specimen no. 405021 heated in 200 torr O_2 at the rate of 8°C/s to 1100°C .

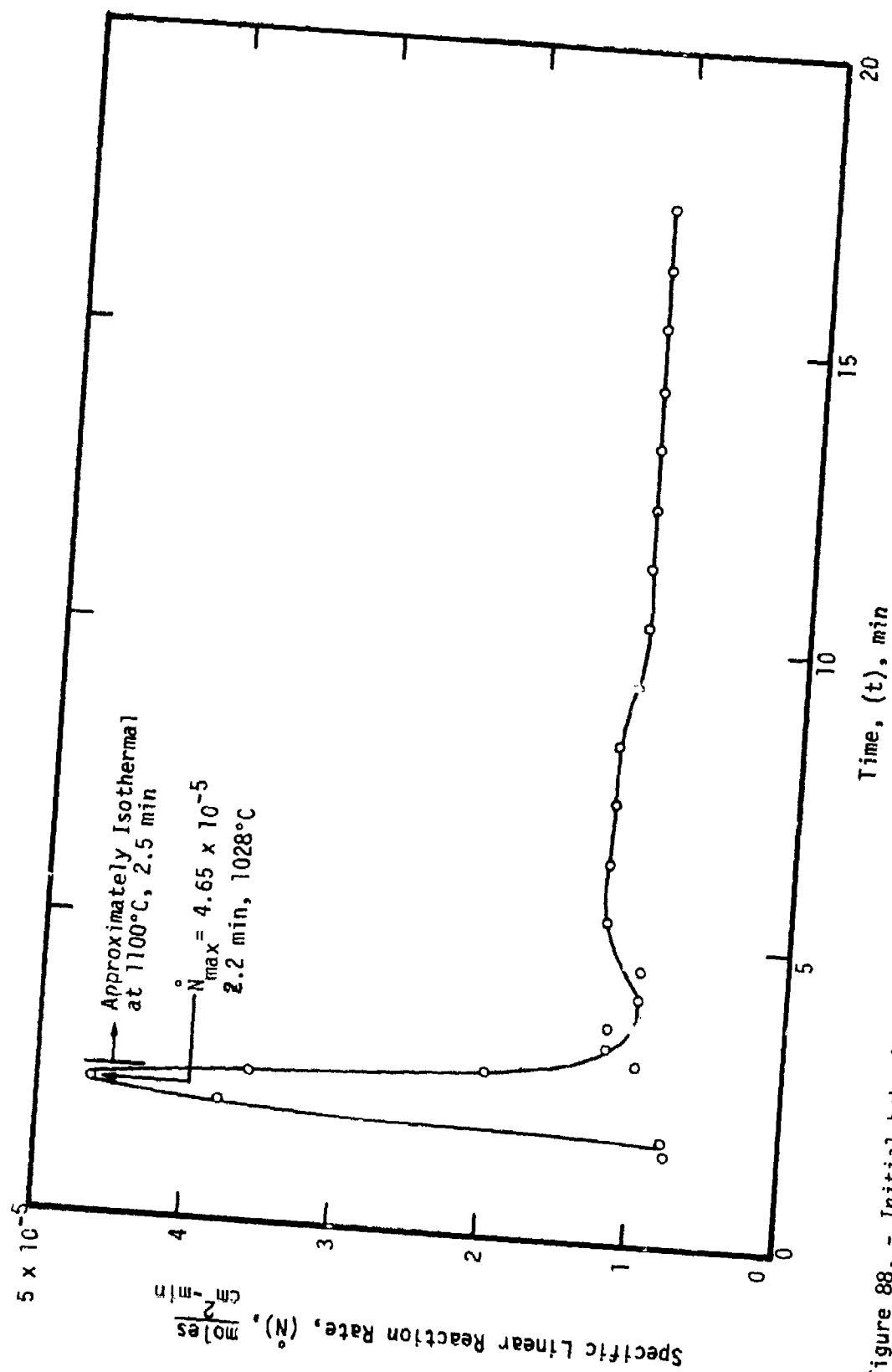


Figure 88. - Initial behavior of the specific linear reaction rate (\dot{N}) for unalloyed titanium (Type 3) specimen no. 405021 heated in 200 torr O_2 at the rate of 8°C/s to 1100°C.

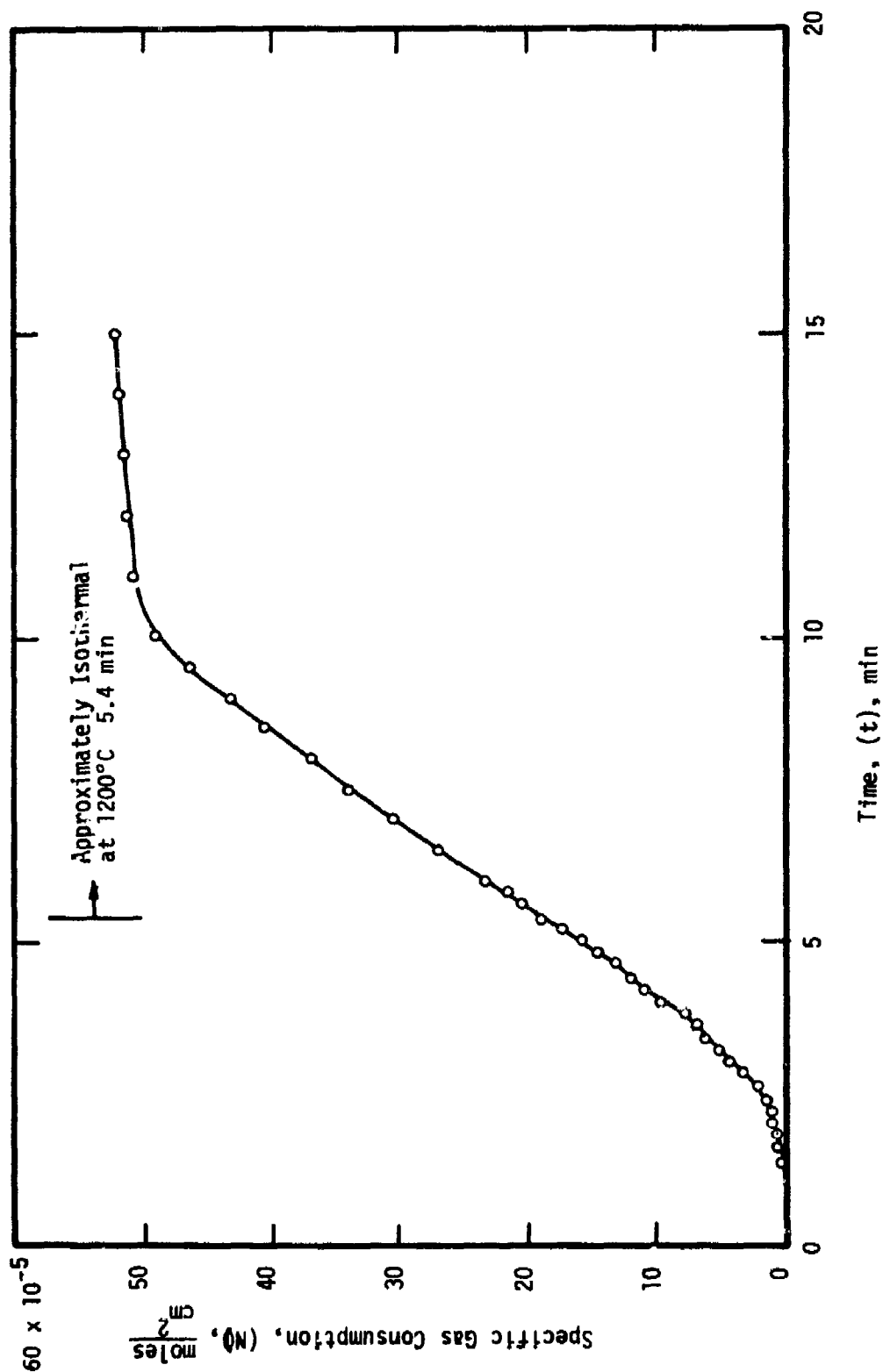


Figure 89. - Initial behavior of specific gas consumption (N) for unalloyed titanium (Type 3) specimen no. 405023 heated in 200 torr O_2 at the rate of 5.9°C/s to 1200°C.

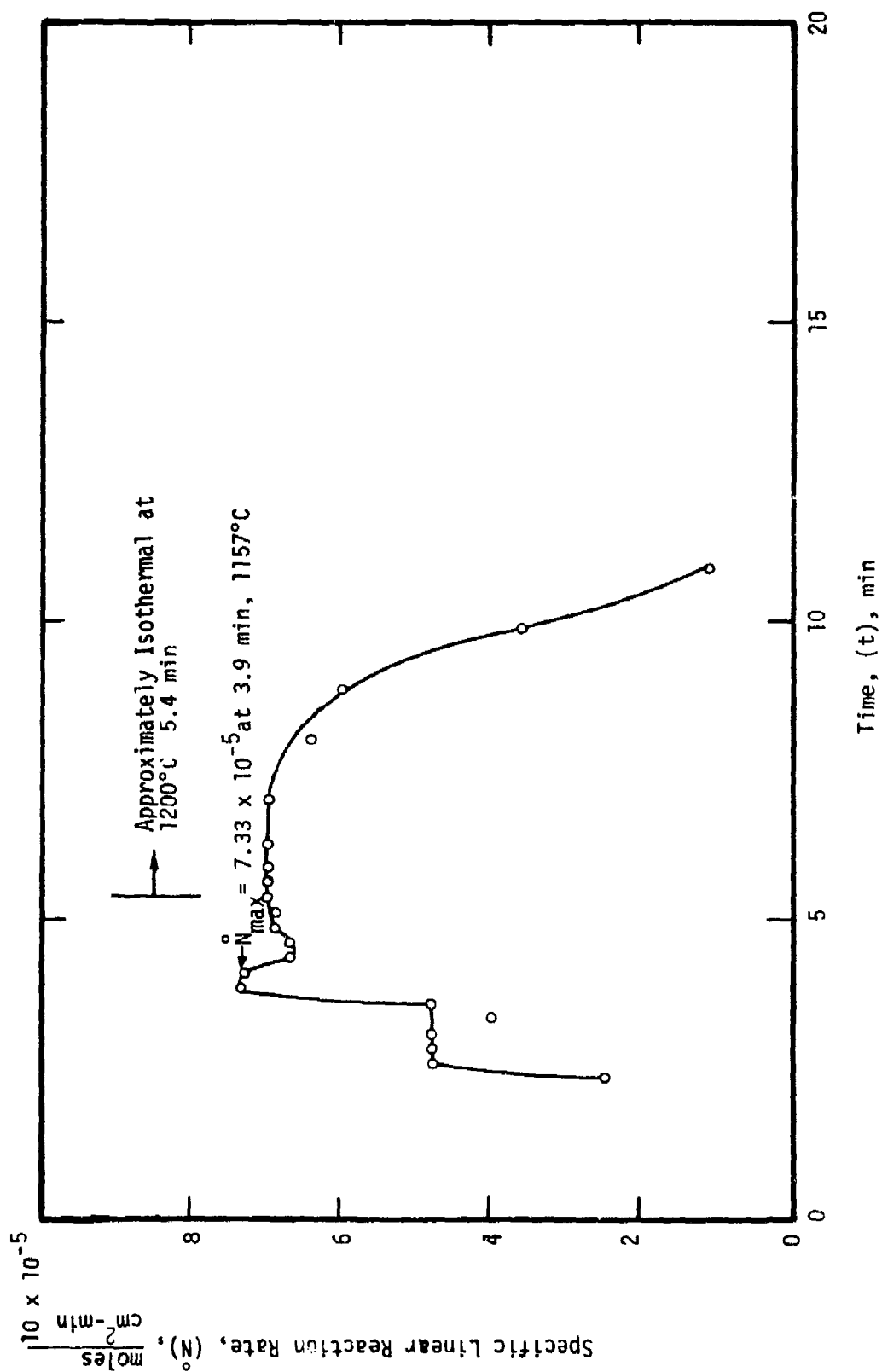


Figure 90. - Initial behavior of the specific linear reaction rate (\bar{N}) for unalloyed titanium (Type 3) specimen no. 405023 heated in 200 torr O_2 at the rate of 5.9°C/s to 1200°C .

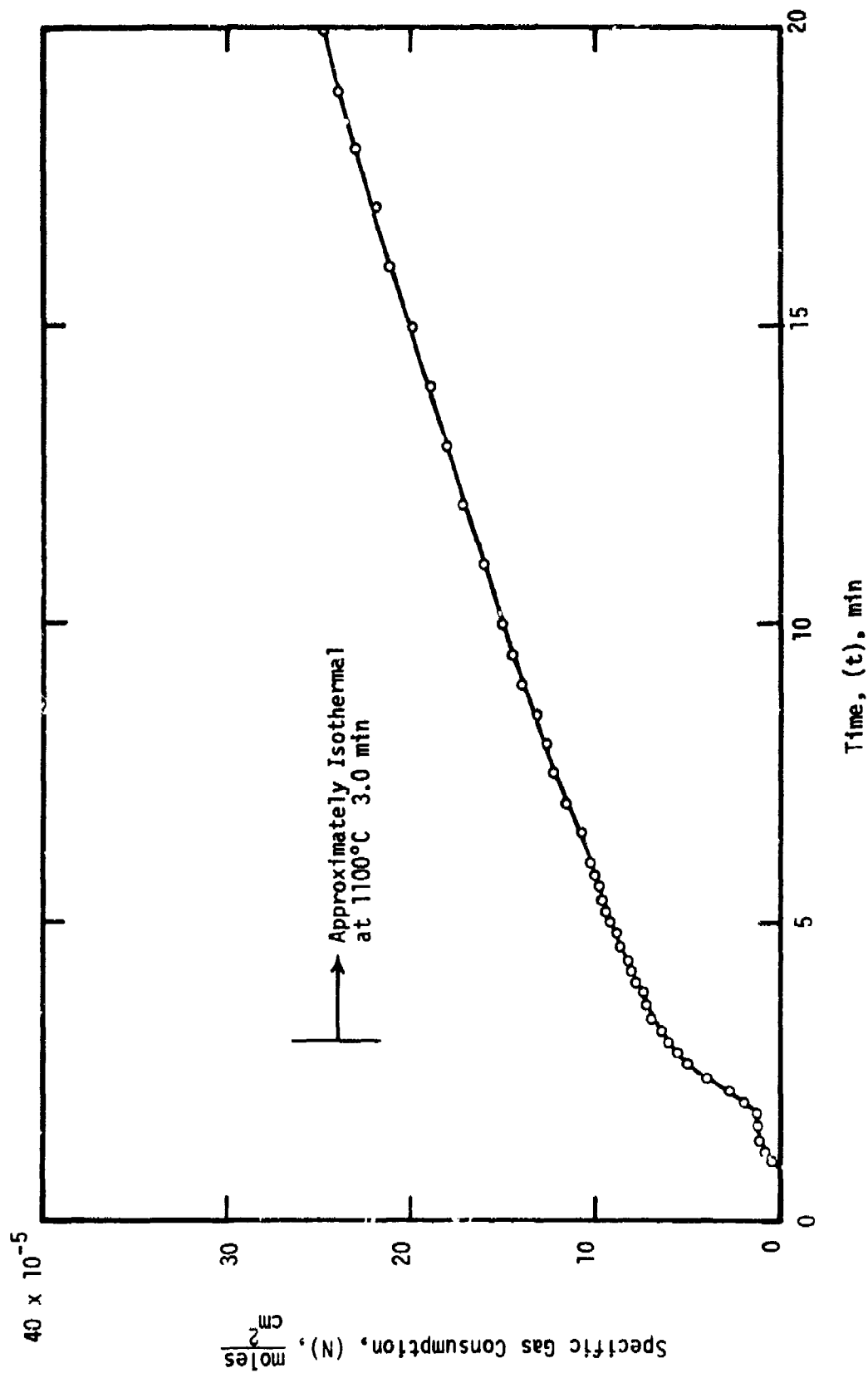


Figure 91. - Initial behavior of the specific gas consumption (N) for unalloyed titanium (Type 4) specimen no. 407162 heated in 200 torr O_2 at the rate of 8°C/s to 1100°C .

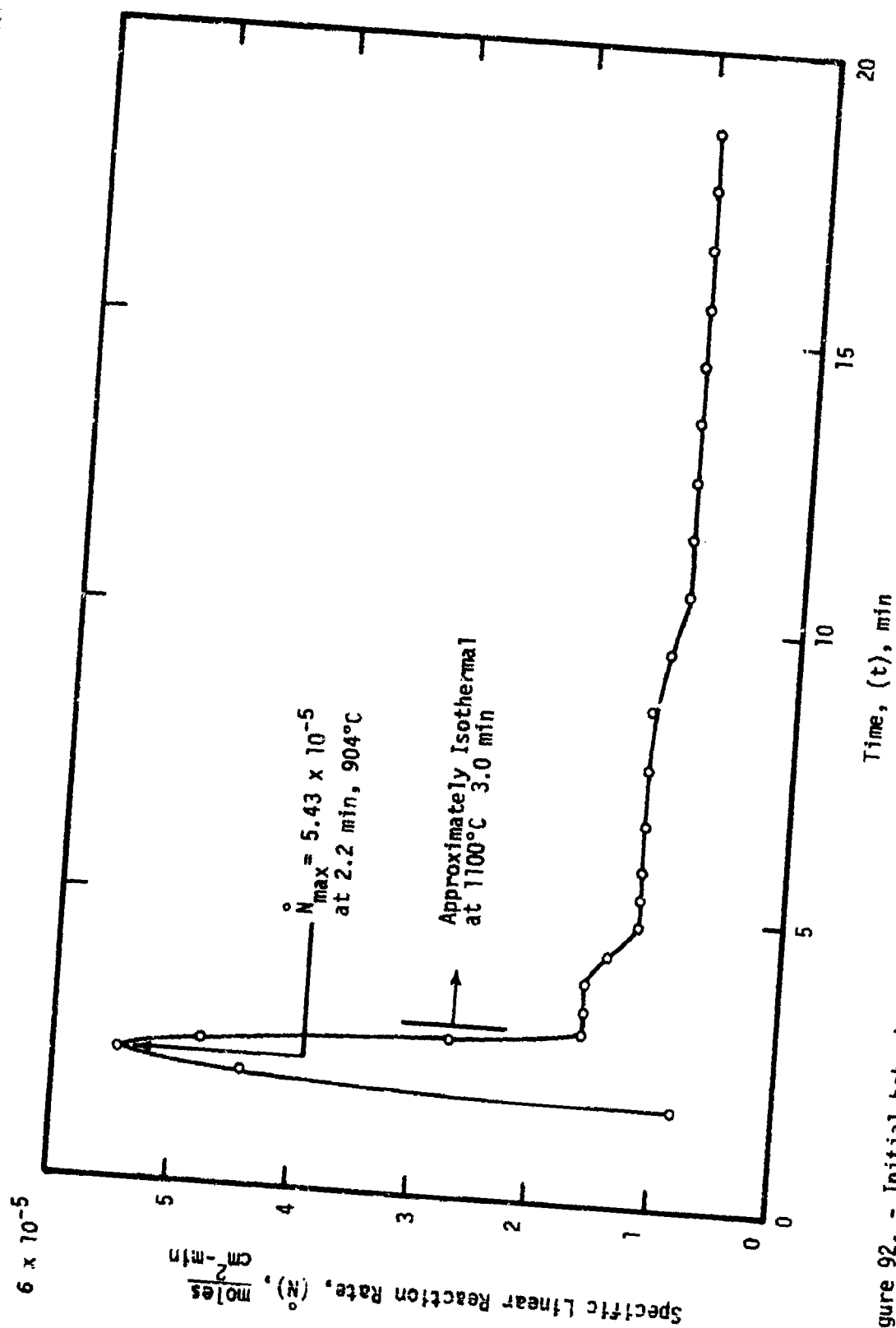


Figure 92. - Initial behavior of the specific linear reaction rate (\dot{N}) for unalloyed titanium (Type 4) specimen no. 407162 heated in 200 torr O_2 at the rate of 8°C/s to 1100°C.

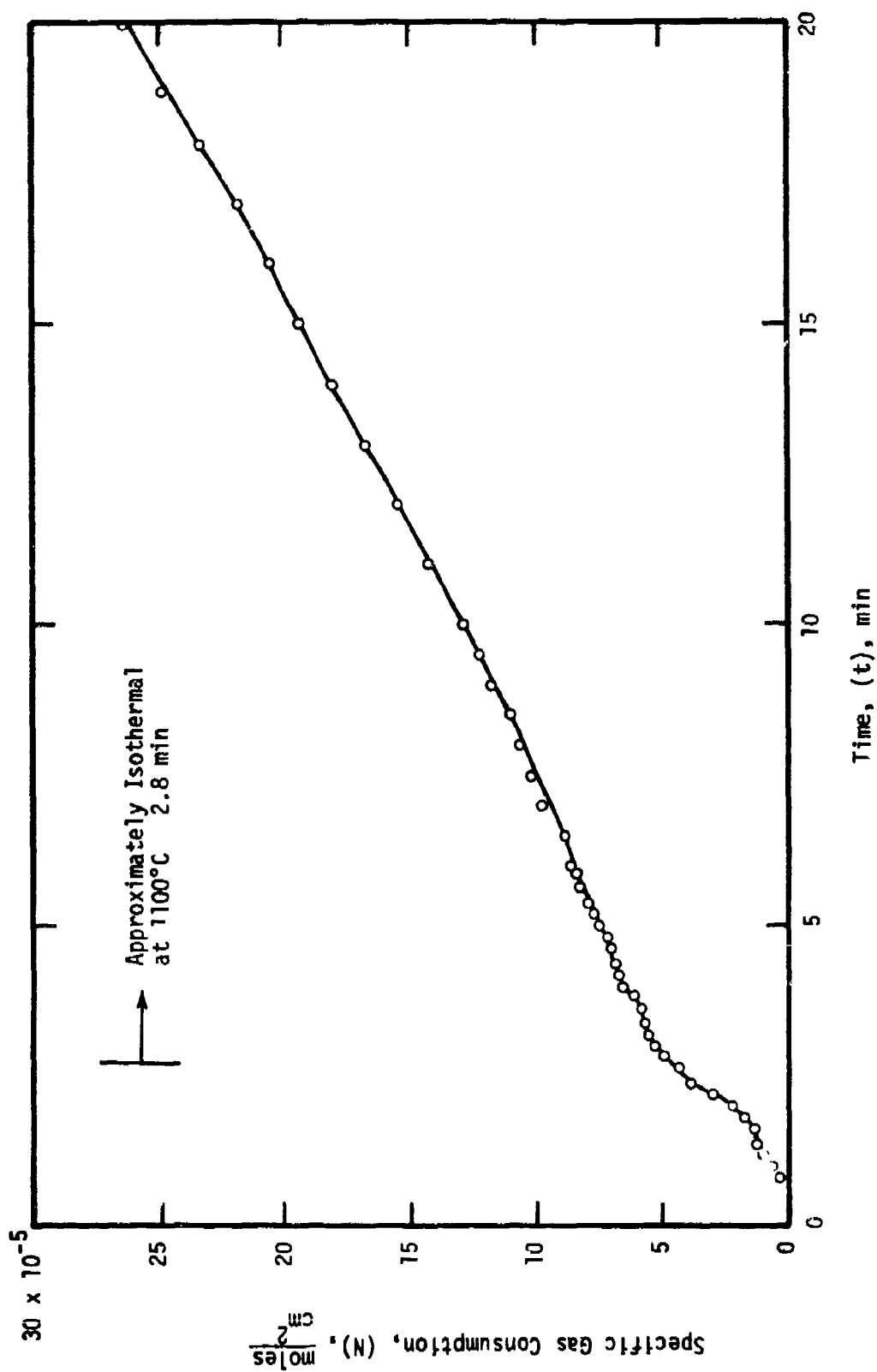


Figure 93. - Initial behavior of the specific gas consumption (N) for unalloyed titanium (Type 5) specimen no. 408143 heated in 200 torr O_2 at the rate of 8°C/s to 1100°C .

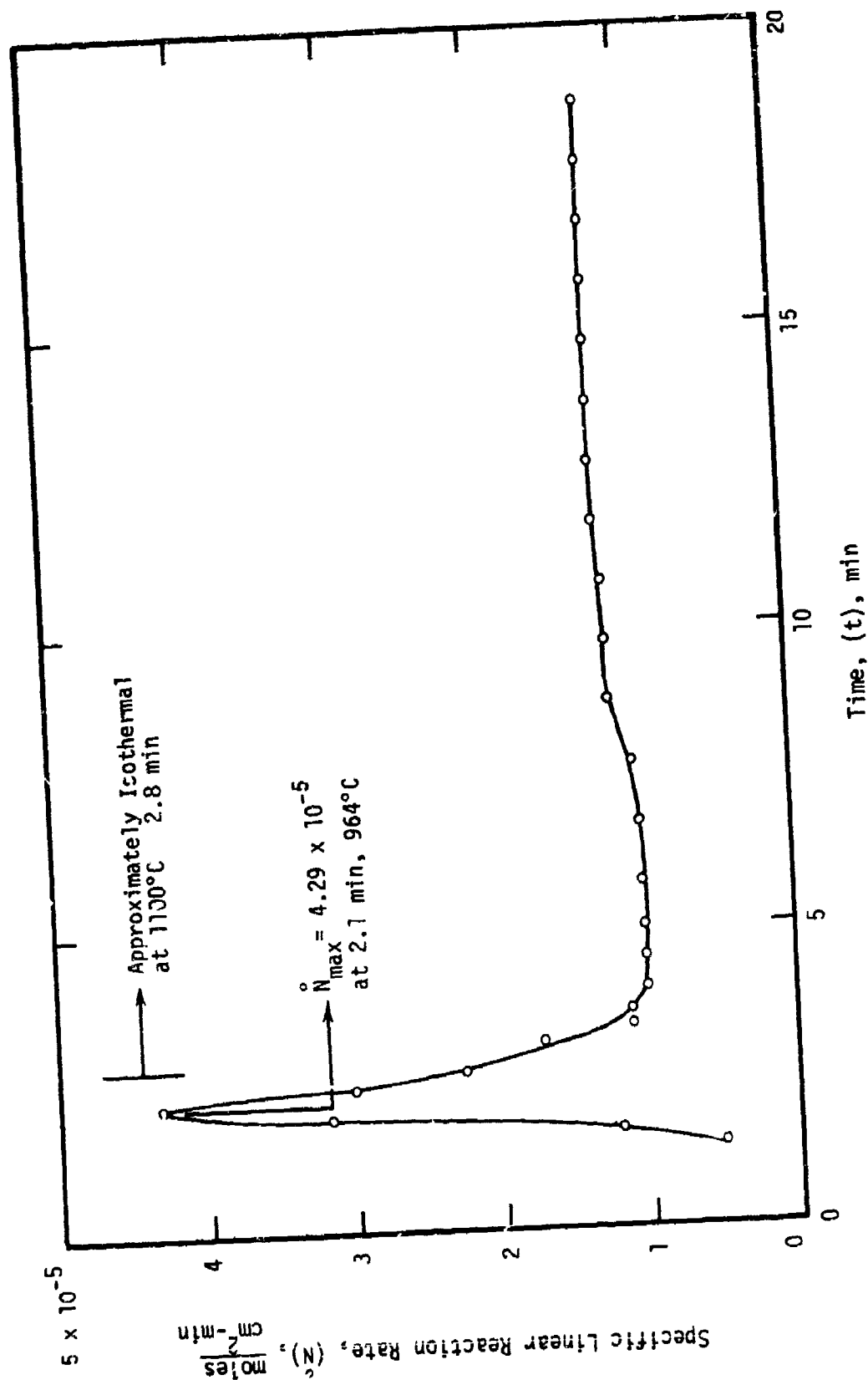


Figure 94. - Initial behavior of the specific linear reaction rate (\dot{N}) for unalloyed titanium (Type 5) specimen no. 408143 heated in 200 torr O_2 at the rate of 8°C/s to 1100°C .

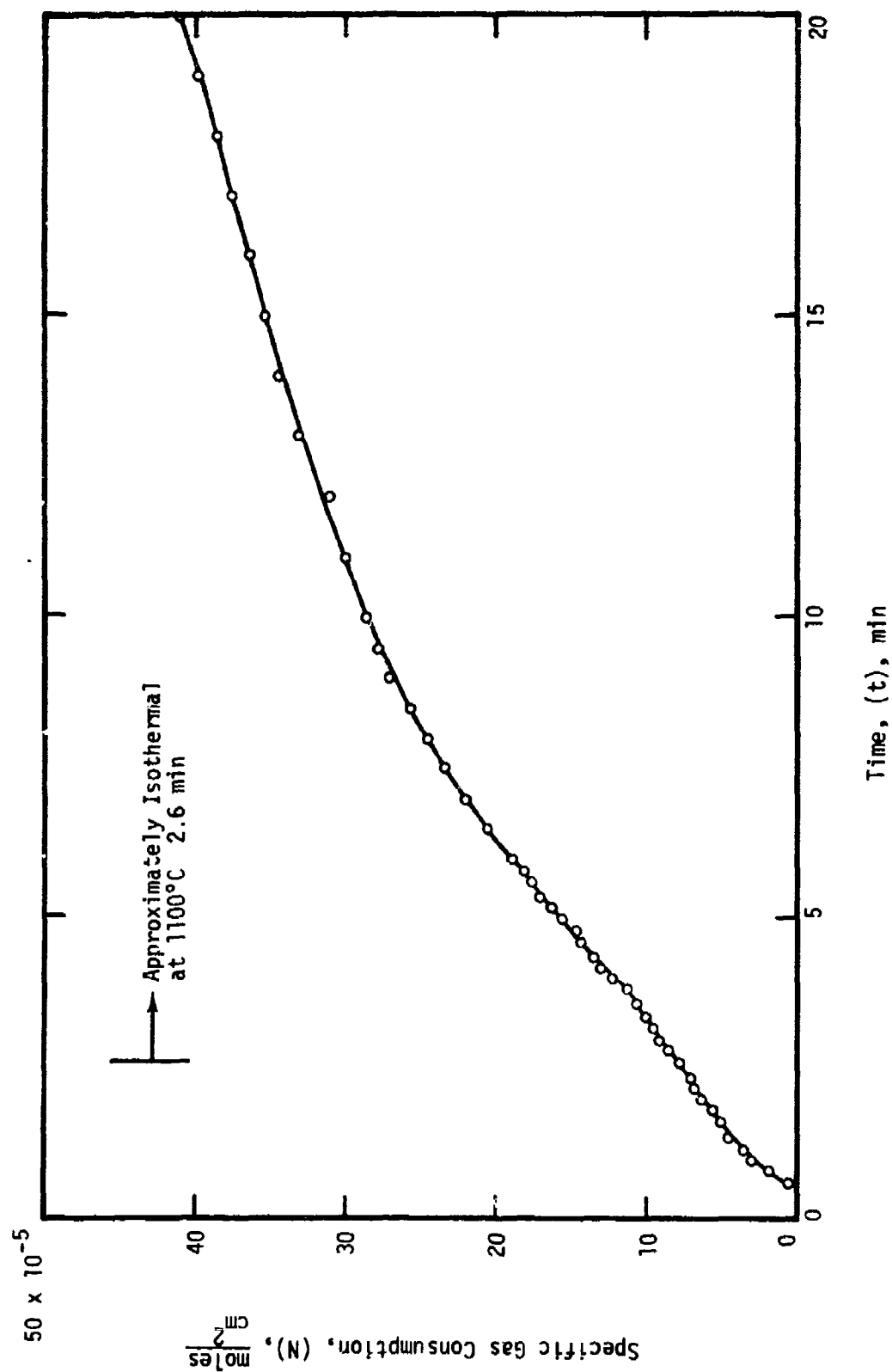


Figure 95. - Initial behavior of the specific gas consumption (N) for unalloyed titanium (Type 5) specimen no. 408282 heated in 200 torr O_2 at the rate of approximately 18°C/s to 1100°C .

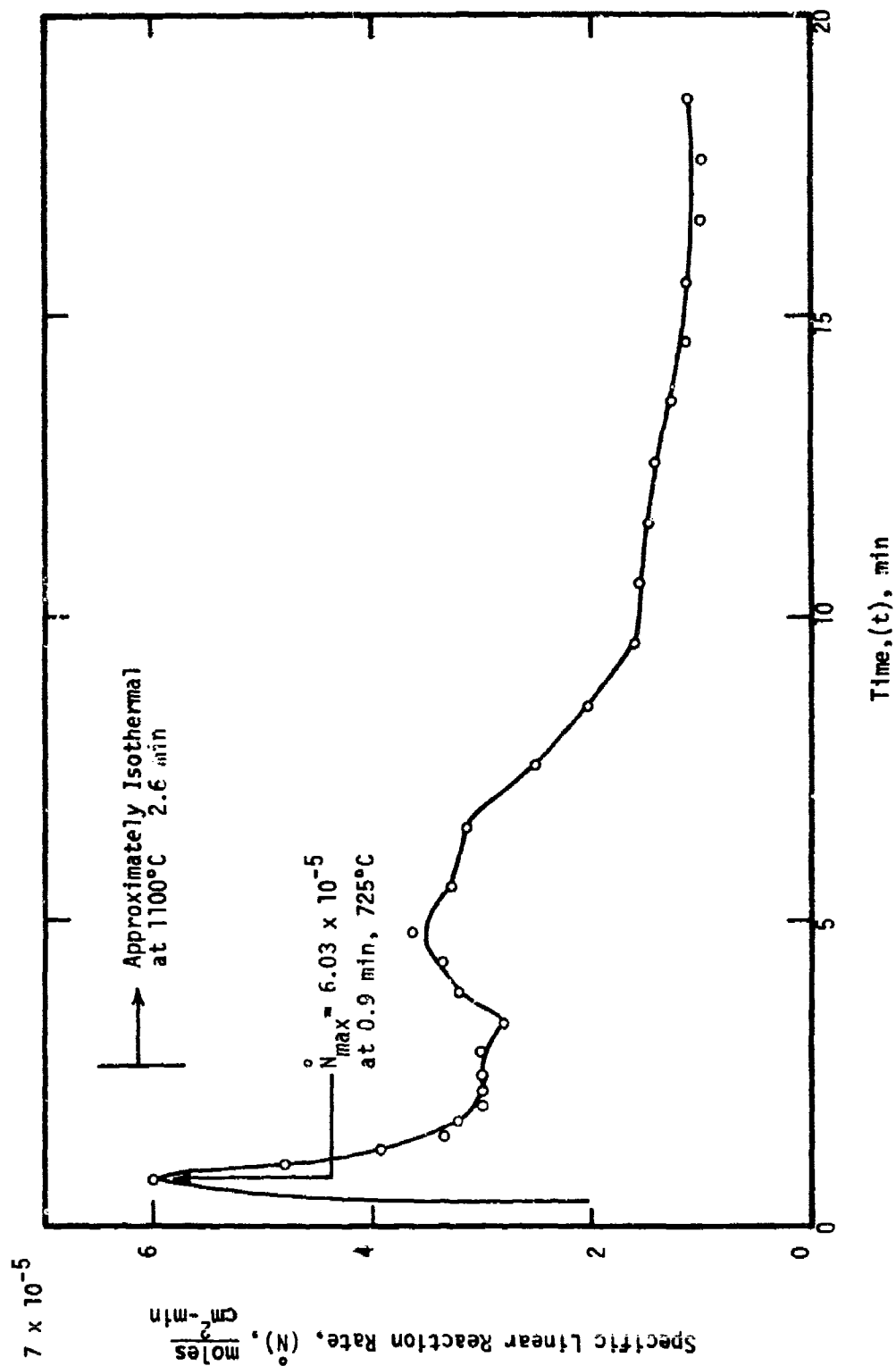


Figure 96. - Initial behavior of the specific linear reaction rate (\dot{N}) for unalloyed titanium (Type 5) specimen no. 408282 heated in 200 torr O_2 at the rate of approximately 18°C/s to 1100°C .

considered as being composed of multiple sigmoidal steps which, in turn, give rise to multiple separated maximum in the corresponding (\dot{N} vs. t) curves; e.g., see Figures 51, 65, 67, 81, and 83. This same type of phenomenon also occurs at the highest heating rate in other tests; however, it does not occur at the lowest heating rate (0.5°C/s) for any maximum temperature investigated. These observations suggest that this phenomenon may arise as result of limited plasticity of the oxide upon the metal substrate, especially during heating.

If this hypothesis is true, then more rapid heating should produce an increased amount of "damage" in the oxide resulting in an increased degree of reaction during heating.* Thus, "damage" such as the generation of fissures within the oxide, will increase the proximity of the reactants and, thereby, the rate of reaction. A test of this concept is illustrated in Figure 97 in which it is seen that (\dot{N}_{\max}) is directly related to the heating rate, (\dot{T}), for specimens of similar thickness.

Specimens of reduced thickness, and especially those which have been cold-worked, exhibit thermal instabilities which are not characteristic of thicker specimens. Such instabilities are illustrated in Figures 70 and 71 for the temperature and power index curves, respectively, of a specimen which had been cold-worked 87 percent. It is believed that the oscillations in temperature are due to local self-heating during oxidation; i.e., the generation of local "hot spots" produced by the heat of reaction. This phenomena, although believed to be a precursor to ignition did not lead to an abnormally large gas consumption or reaction rate, see Figures 72 and 73. It is also noted that such instabilities are associated with "closed-loop" programmer control. A similar specimen heated more rapidly, but under

*Note that the maximum value of the specific linear reaction rate (\dot{N}_{\max}) usually occurs during initial heating.

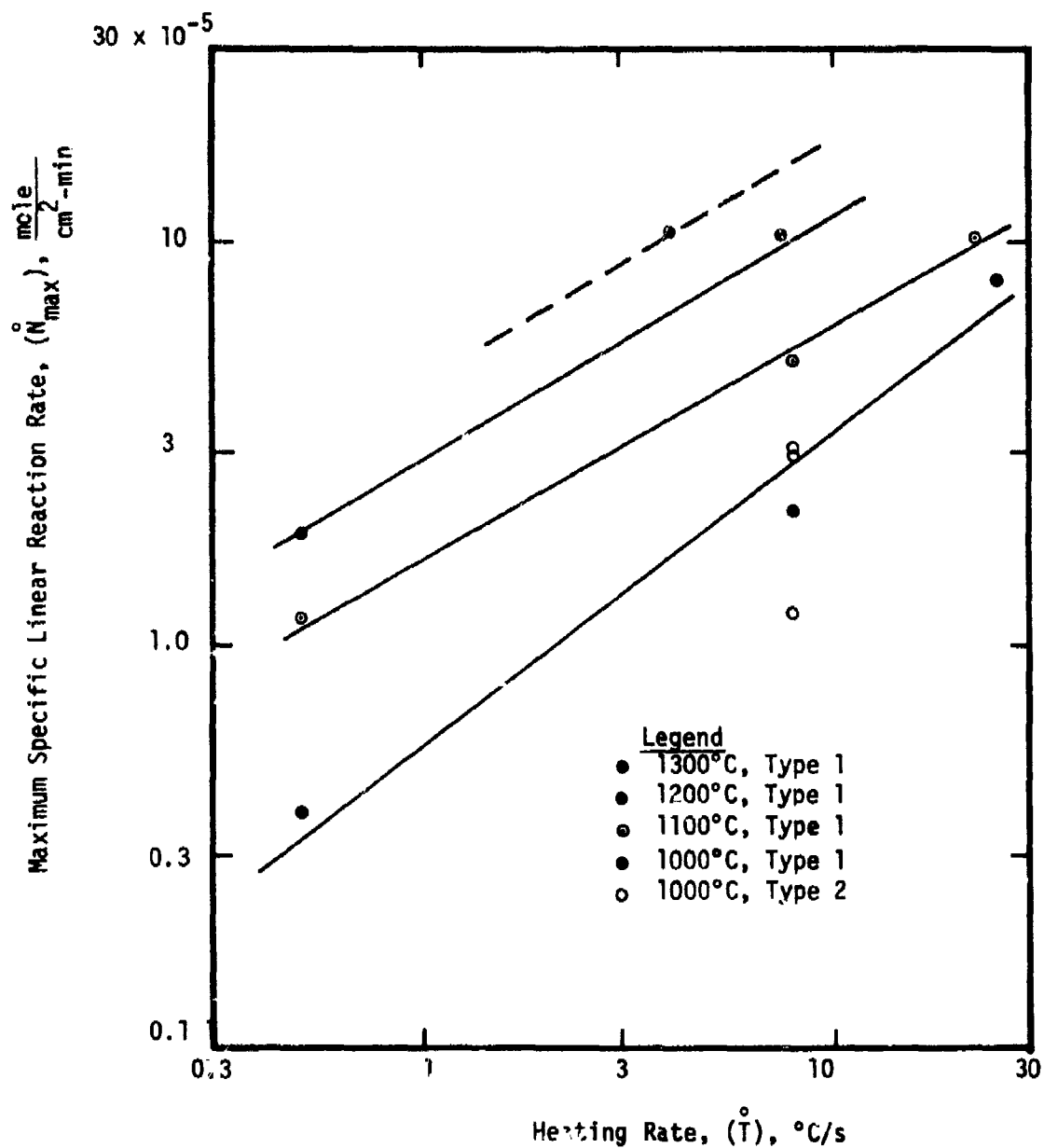


Figure 97. - Initial response of unalloyed titanium (Type 1 and 2) specimens in 200 torr oxygen for the temperature range 1000° to 1300°C.

"open-loop" conditions did not produce such oscillations (see Figure 74) but did provide larger values of gas consumption and reaction rate, as expected (see Figures 75 and 76).

The single test conducted at higher ambient oxygen pressure (400 torr vs. 200 torr) indicated that the reaction proceeded much more rapidly than would be expected on the basis of an oxide defect-controlled oxidation rate. Figures 66 and 67, when compared with Figures 64 and 65 indicate that both the total gas consumption and the rate of reaction in the early portions of these tests are roughly proportional to the total oxygen pressure. This observation parallels that of Stringer (ref. 16) who attributed this type of pressure sensitivity to stress-induced fissures in the rutile scale.

The longer-term (one hour) behavior of oxygen consumption by unalloyed titanium has also been investigated through the analysis of (N) vs (t) and (N^2) vs (t) curves (the latter not illustrated). Here, results are somewhat less certain in view of the fact that oxygen pressure monotonically decreases during the term of testing which, as has just been discussed, decreases the reactivity of titanium with oxygen. This difficulty notwithstanding, we observed that the reaction proceeds under a "mixed rate law" at 1000°C which is slower than linear, but faster than parabolic; probably indicating a true parilinear-to-linear rate behavior at long times. Further, the slowest heating rate (0.5°C/s) which produces most oxide during heating appears to favor a more nearly linear post-isothermal behavior than do the higher heating rates. This observation leads to the postulated concept of a critical oxide thickness which may be associated with the alteration of oxidation kinetics which, in turn, could rationalize the inverse dependencies upon heating rate exhibited by the long-term gravimetric and short-term linear reaction rate data alluded to earlier.

At higher temperatures (1100° and 1200°C), the one-hour reaction kinetics present a somewhat clearer picture. At 1100°C, and regardless of the applied heating rate, parabolic kinetics were favored while at 1200°C, sub-parabolic reaction kinetics were favored. These observations favor the viewpoint that plasticity in the oxide (perhaps including sinterability) has contributed to providing titanium with more protective scales at higher temperatures.

4c. REACTION OF UNALLOYED TITANIUM WITH NITROGEN AND MIXED GASES - (RHC) TESTS

Data derived from the volumetric apparatus for the reaction of unalloyed titanium in nitrogen and mixed gas (RHC)-type tests are presented in Figures 98 through 122. In all cases, only the initial gas consumption (N) and linear reaction rate (\dot{N}) curves are illustrated as other behaviors are similar to those schematically described in Figure 41 above.

Data derived from the volumetric apparatus for the reaction of unalloyed titanium in 200 torr nitrogen are presented in Figures 98 through 106. As titanium is heated in 200 torr nitrogen to the maximum temperature, both the initial and long-term gas consumption behaviors are complex. None of the individual behaviors are simple and the range in types of behavior is broad.

The simplest of the initial behaviors, observed only one time and for titanium (Type 2), involved a rapid initial reaction (as may occur during absorption of gas) followed by a slower linear rate of reaction (typical of non-protective scales), see Figure 102. The rapid step occurred during heating (at approximately 400°C) and the subsequent linear rate appeared to be independent of temperature over both the remainder of the heating period and the initial portion of the constant-temperature (1000°C) period. Even for this simplest case, there is a later discontinuity in the consumption curve,

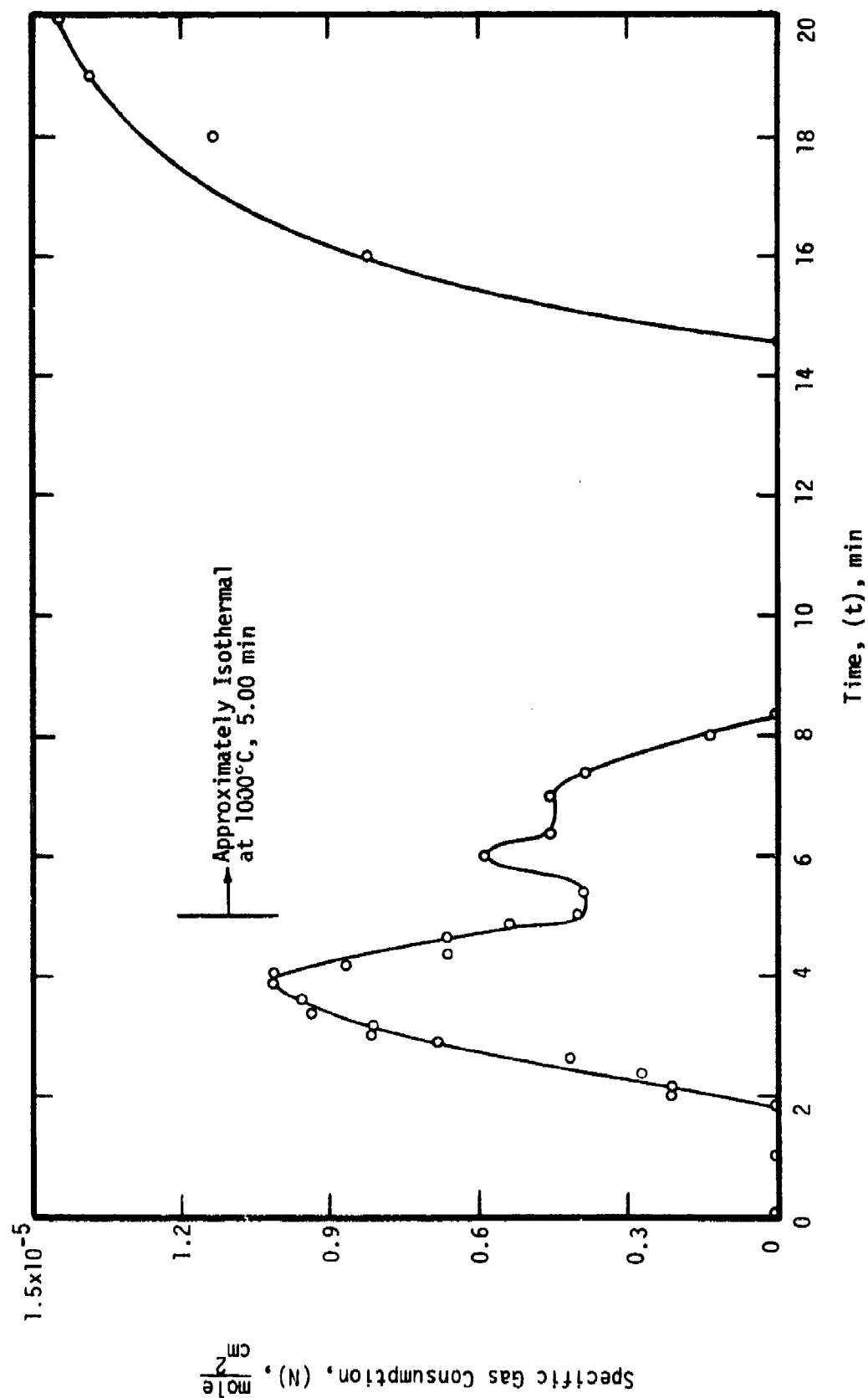


Figure 98. - Initial behavior of the specific gas consumption (N) for unalloyed titanium (Type 1) specimen no. 07311 heated in 200 torr H_2 at the rate of 8°C/s to 1000°C.

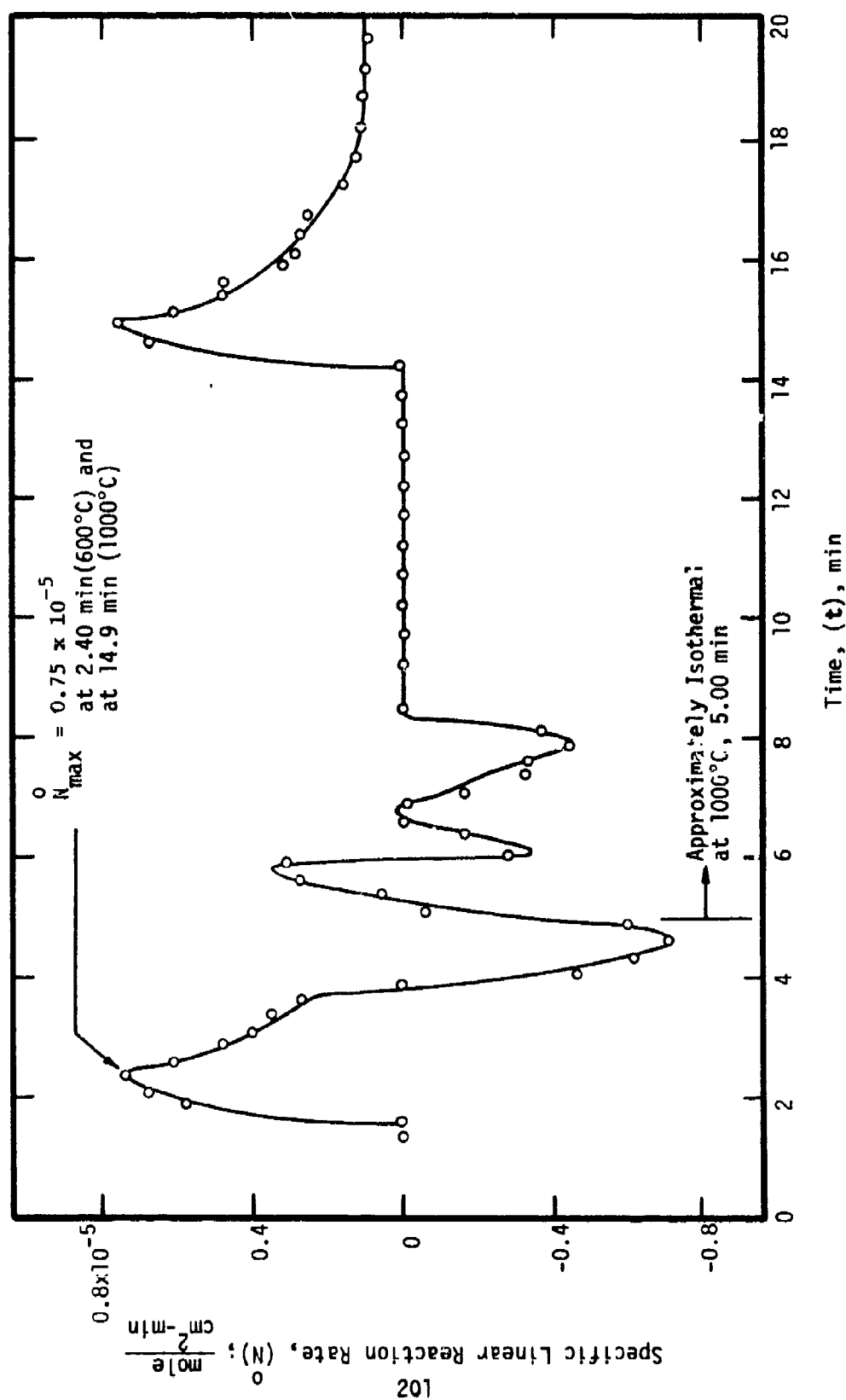


Figure 99. - Initial behavior of the specific linear reaction rate (\dot{N}) for unalloyed titanium (Type 1) specimen no. 07311 heated in 200 torr N_2 at the rate of 8°C/s to 1000°C.

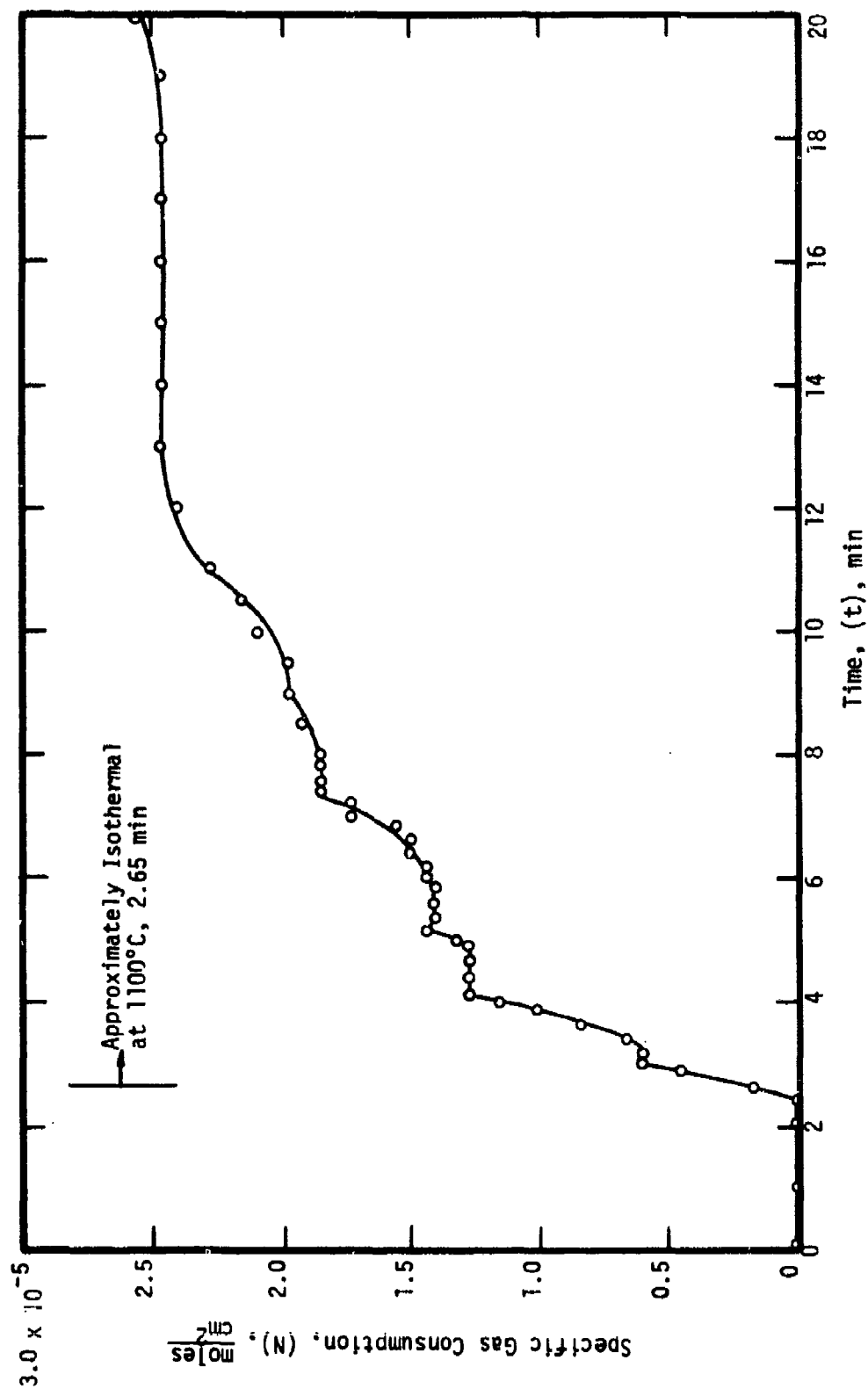


Figure 100. - Initial behavior of the specific gas consumption (N) for unalloyed titanium (Type 1) specimen no. 07312 heated in 200 iorr N_2 at the rate of 8°C/s to 1100°C .

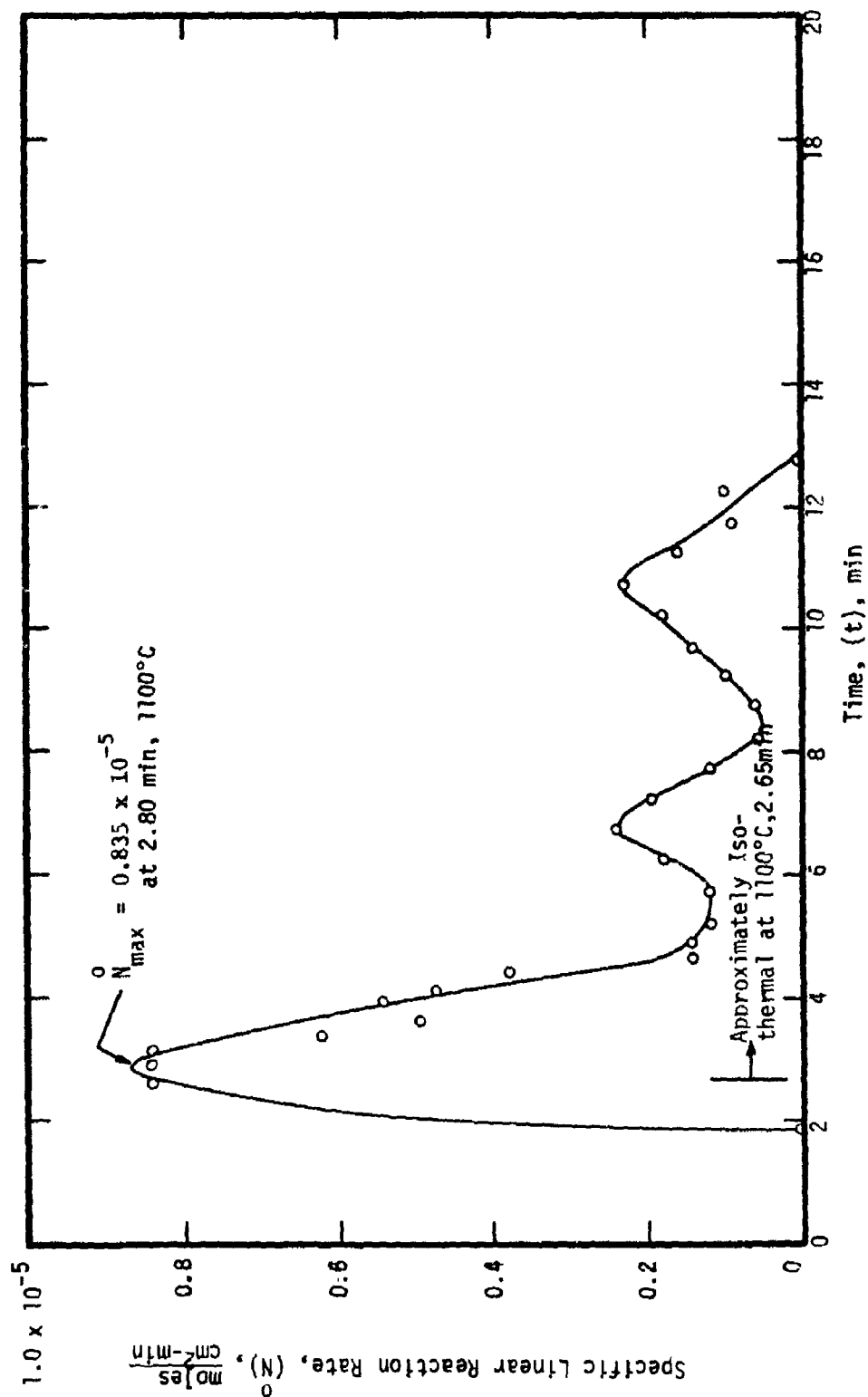


Figure 101. - Initial behavior of the specific linear reaction rate (\bar{N}) for unalloyed titanium (Type 1) specimen no. 07312 heated in 200 torr N_2 at the rate of 8°C/s to 1100°C.

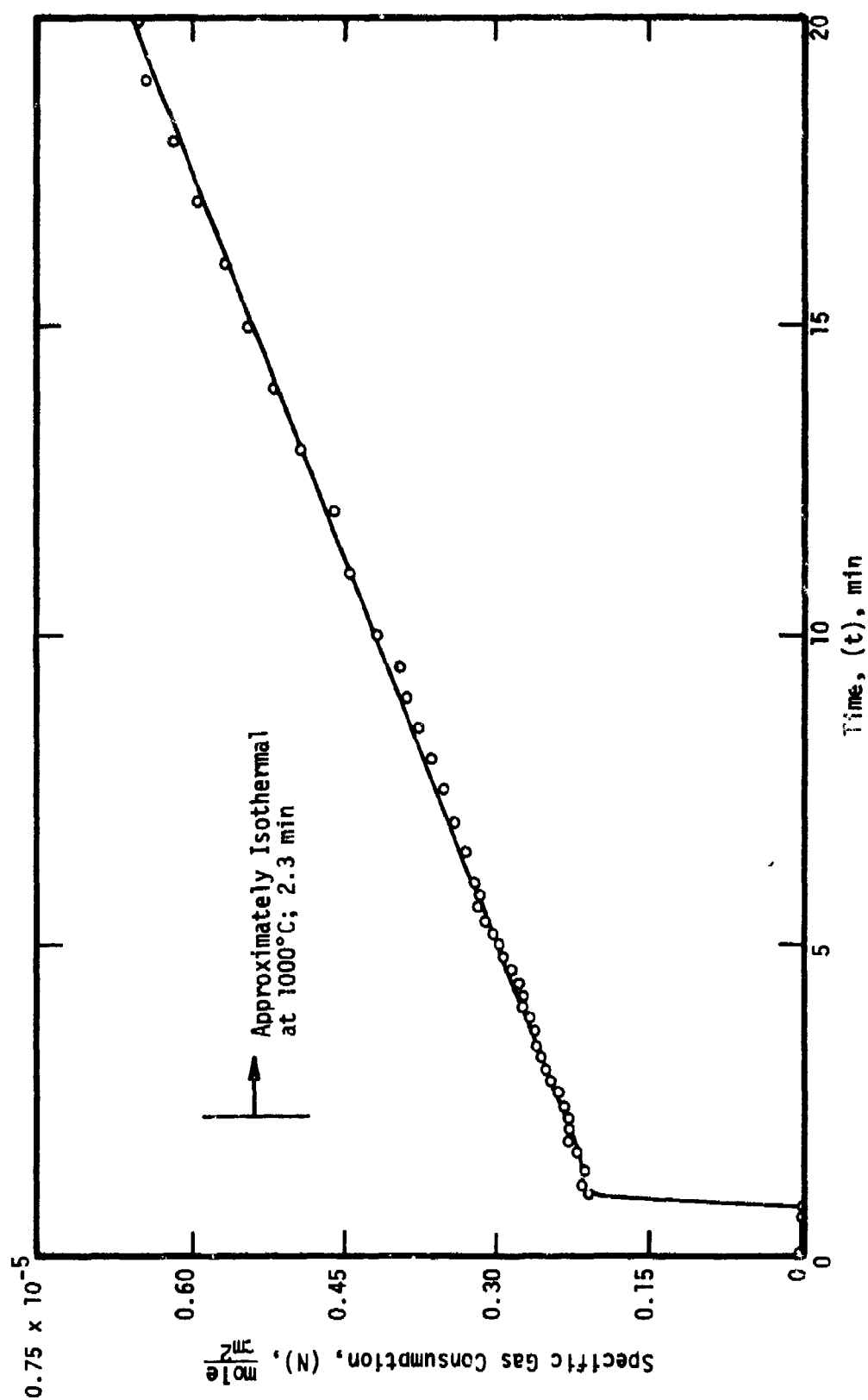


Figure 102. - Initial behavior of the specific gas consumption (N) for unalloyed titanium (Type 2) specimen no. 09193 heated in 200 torr N_2 at the rate of $8^\circ C/s$ to $1000^\circ C$. Data less certain; system leak noted.

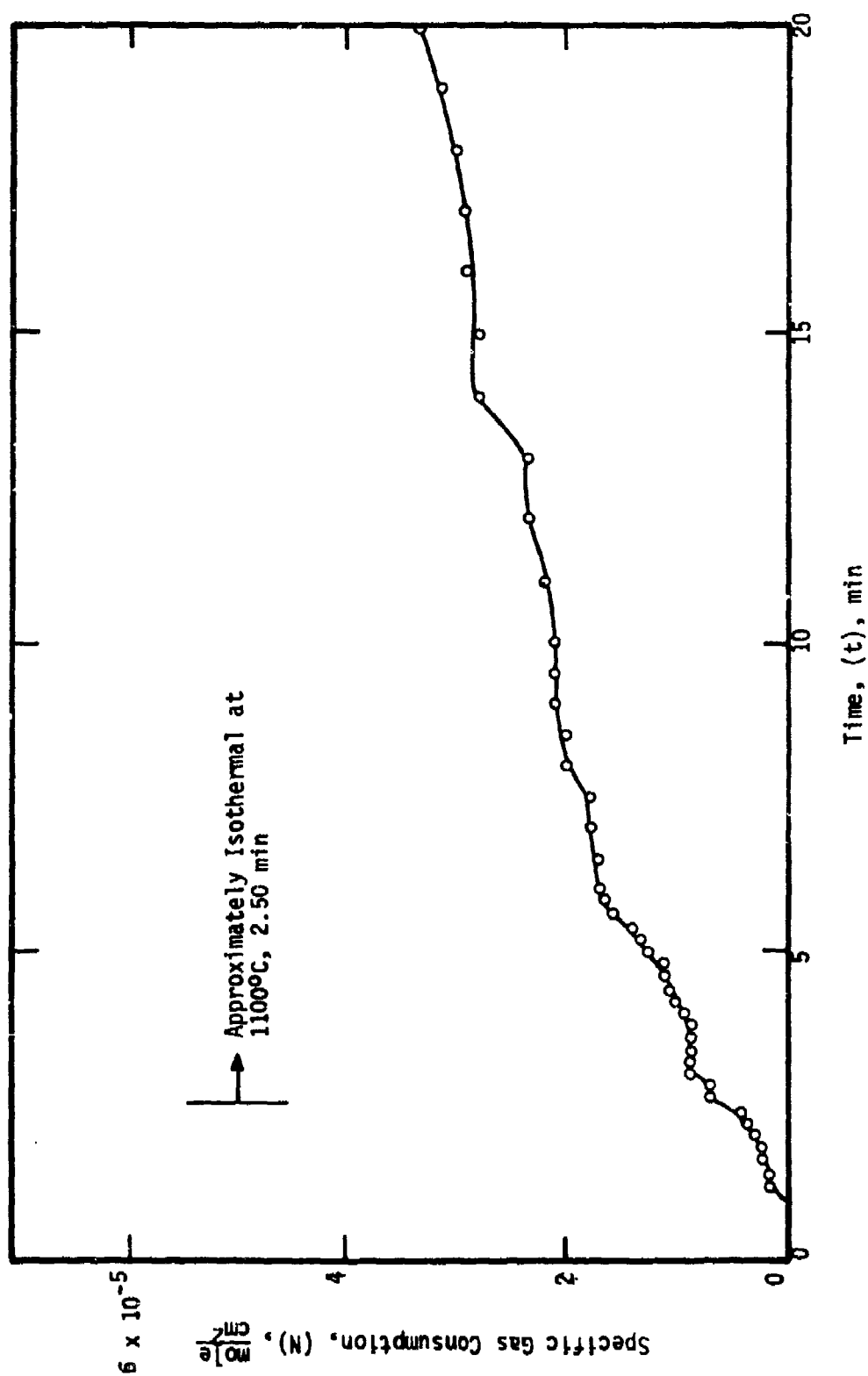


Figure 103. - Initial behavior of the specific gas consumption (N) for unalloyed titanium (Type 2) specimen no. 402192 heated in 200 torr N_2 at the rate of 8°C/s to 1100°C .

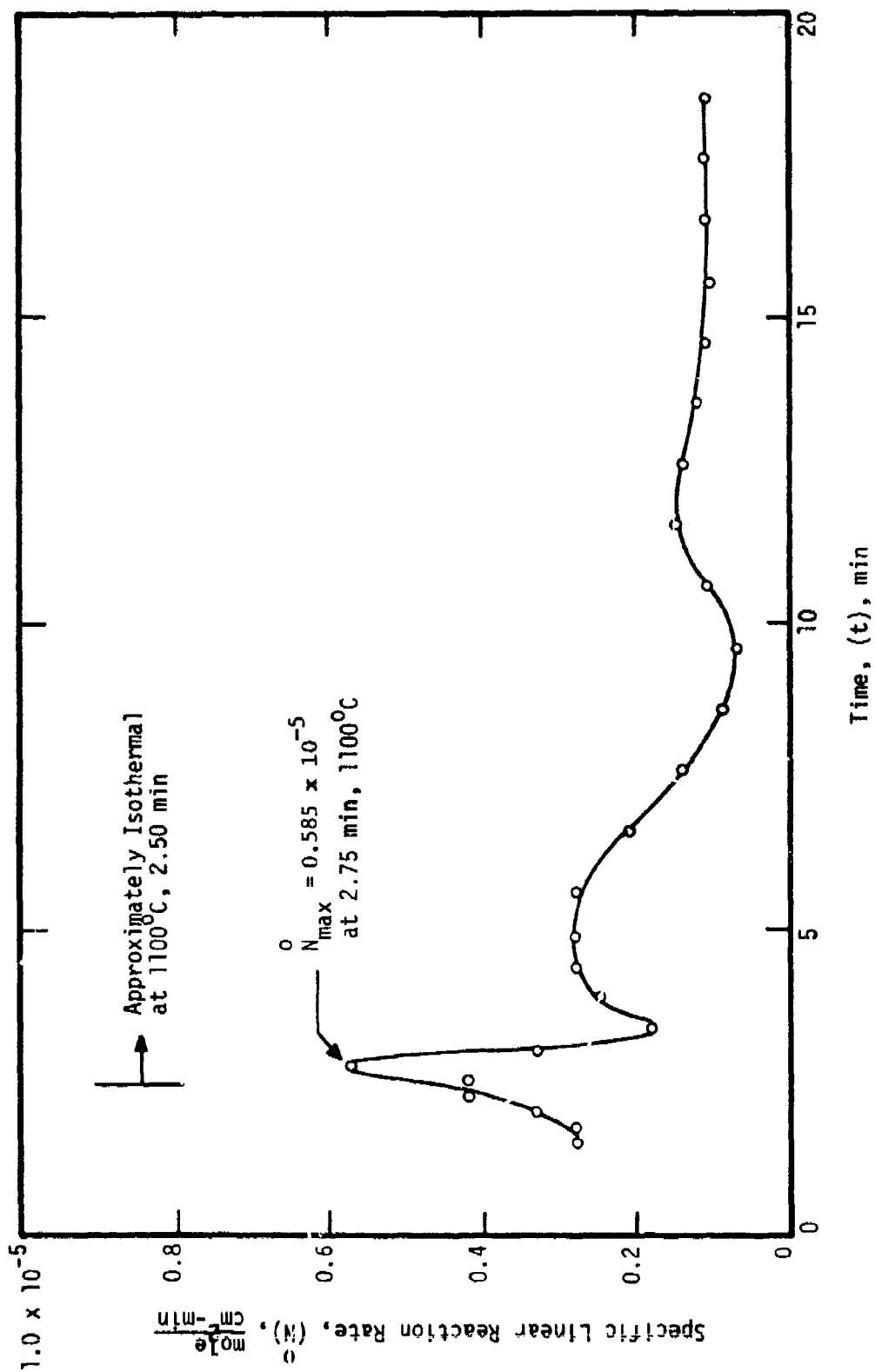


Figure 104. - Initial behavior of the specific linear reaction rate (\bar{N}) for unalloyed titanium (Type 2) specimen no. 402192 heated in 200 torr N_2 at the rate of 8°C/s to 1100°C.

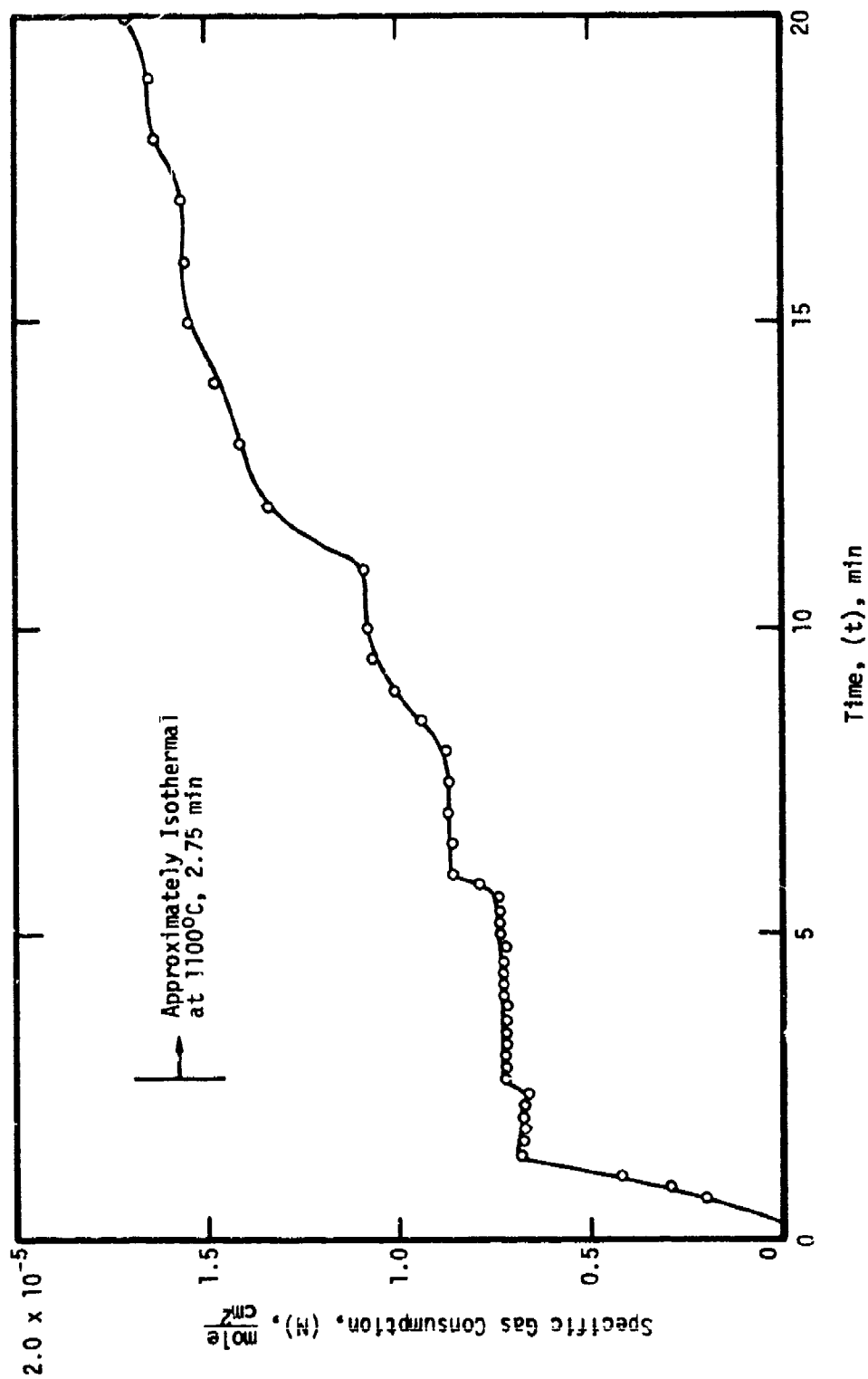


Figure 105. - Initial behavior of the specific gas consumption (N) for Ti-6Al-4V (Type 1) specimen no. 401162 heated in 200 torr N_2 at the rate of 8°C/s to 1100°C .

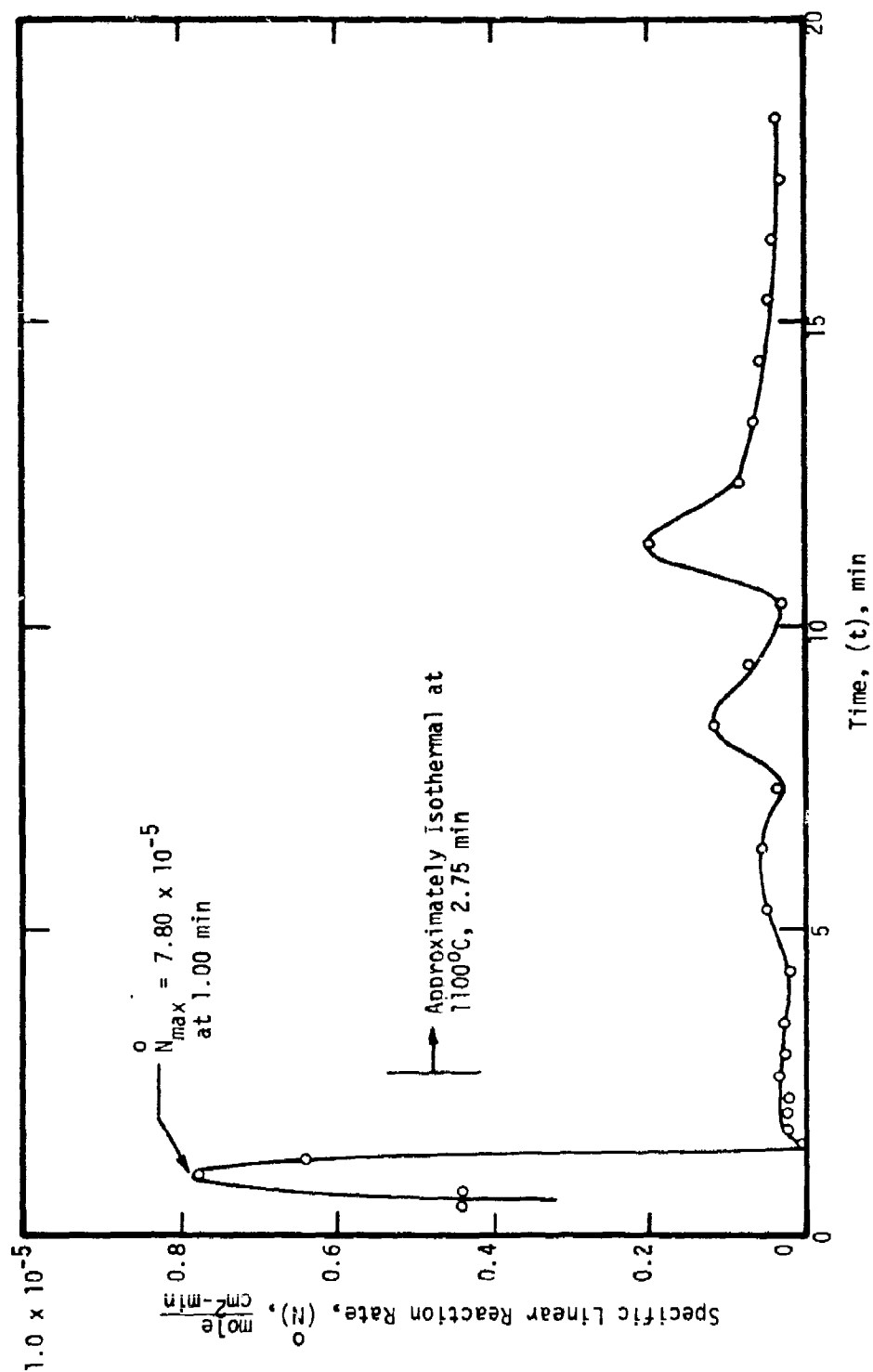


Figure 106. - Initial behavior of the specific linear reaction rate (\bar{N}) for Ti-6Al-4V alloy (Type 1) specimen no. 401162 heated in 200 torr H_2 at the rate of 8°C/s to 1100°C.

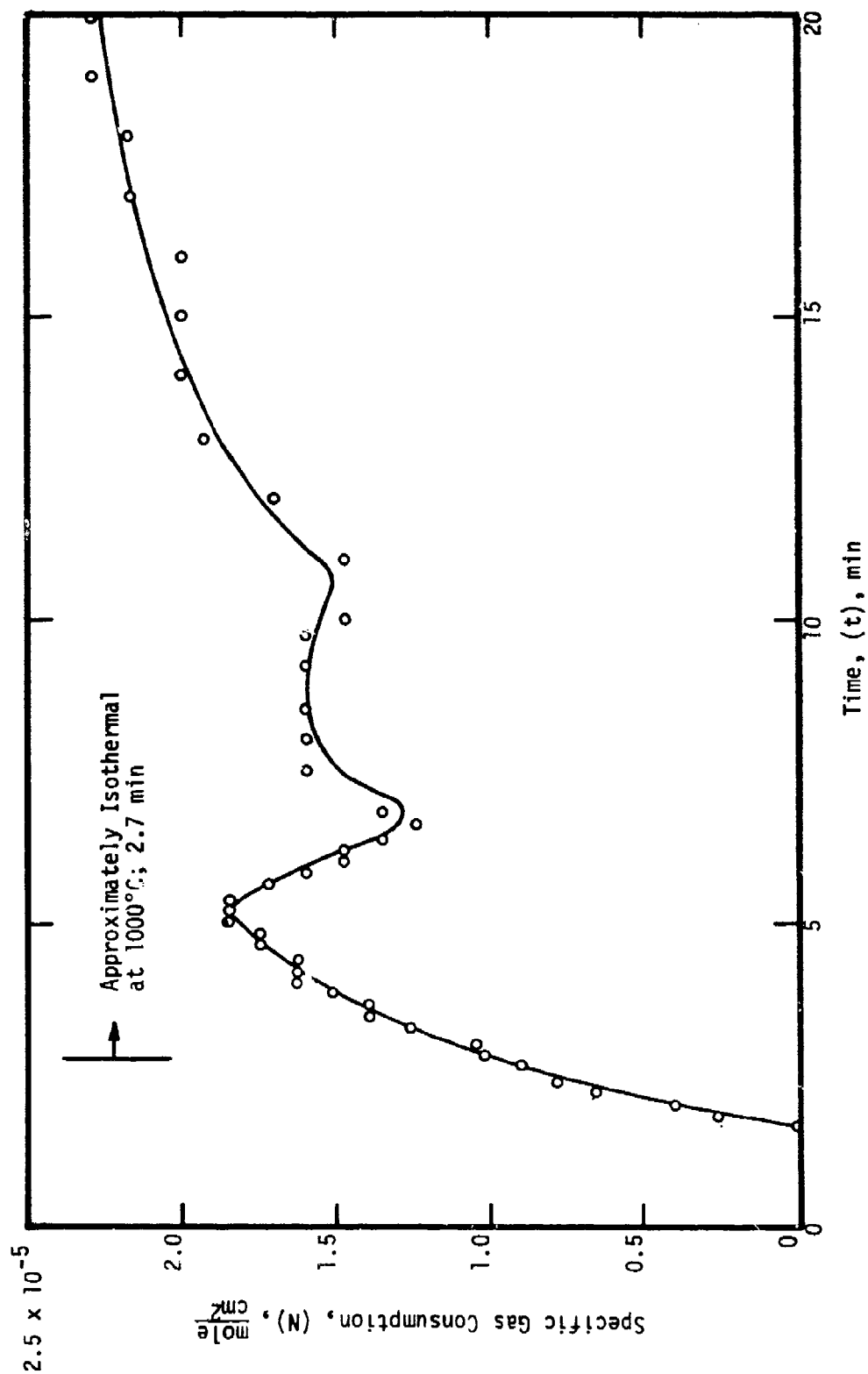


Figure 107. - Initial behavior of the specific gas consumption (N) for unalloyed titanium (Type 1) specimen no. 07313 heated in 200 torr O_2 plus 200 torr N_2 at the rate of $8^\circ C/s$ to $1000^\circ C$.

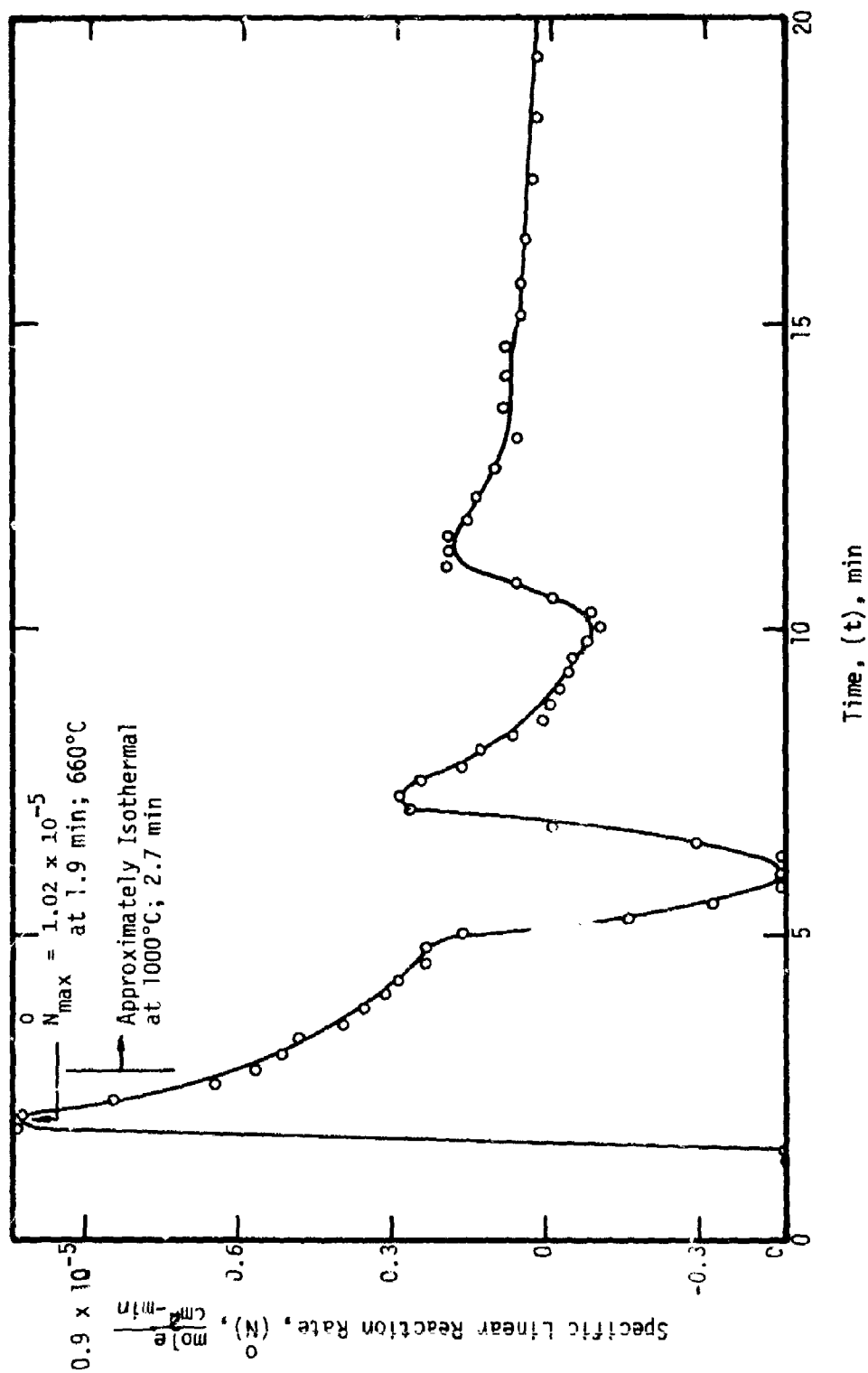


Figure 108. - Initial behavior of the specific linear reaction rate (\dot{N}) for unalloyed titanium (Type 1) specimen no. 07313 heated in 200 torr O_2 plus 200 torr N_2 at the rate of 8°C/s to 1000°C.

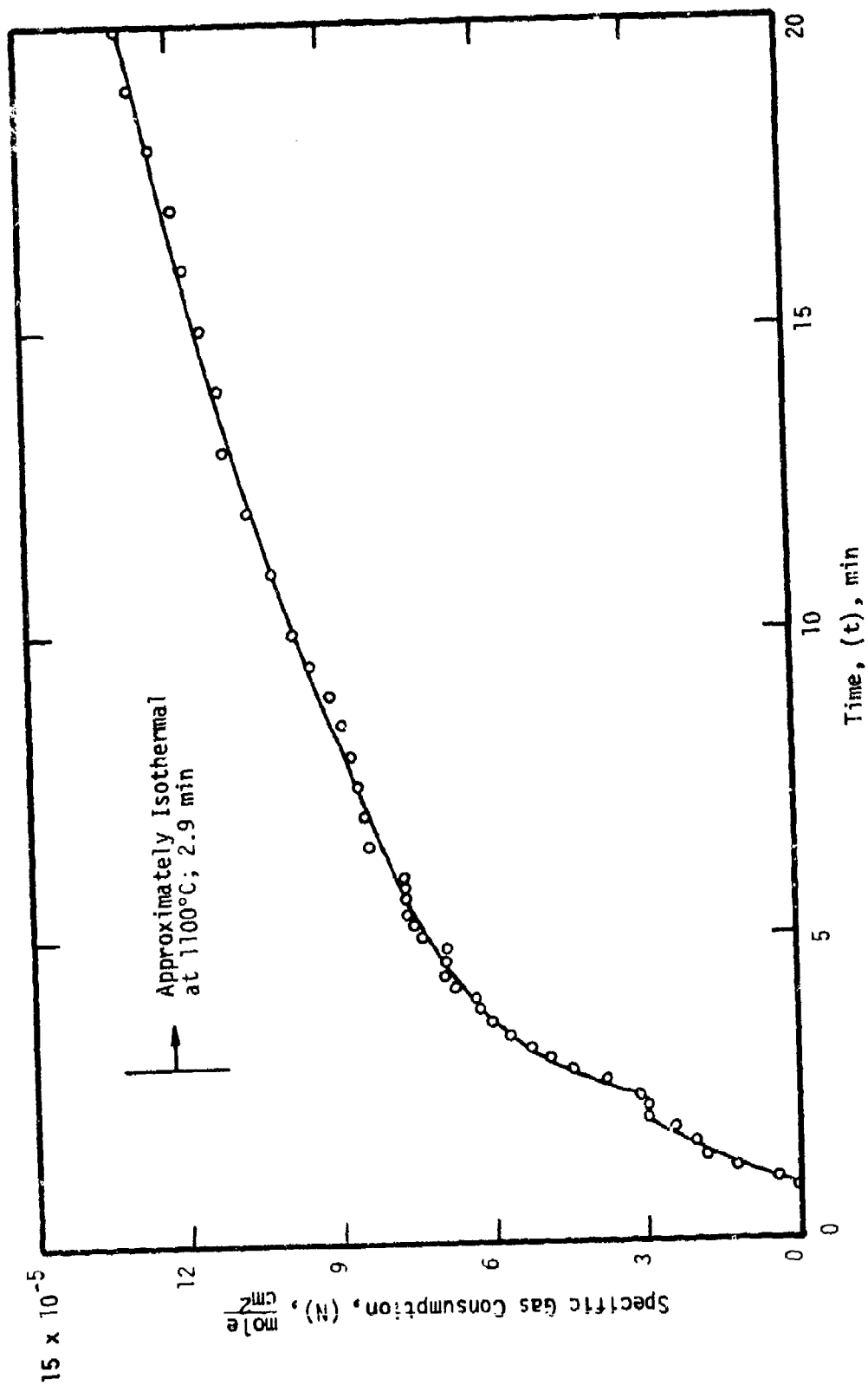


Figure 109. - Initial behavior of the specific gas consumption (N) for unalloyed titanium (Type 1) specimen no. 08011 heated in 200 torr O₂ plus 200 torr N₂ at the rate of 8°C/s to 1100°C.

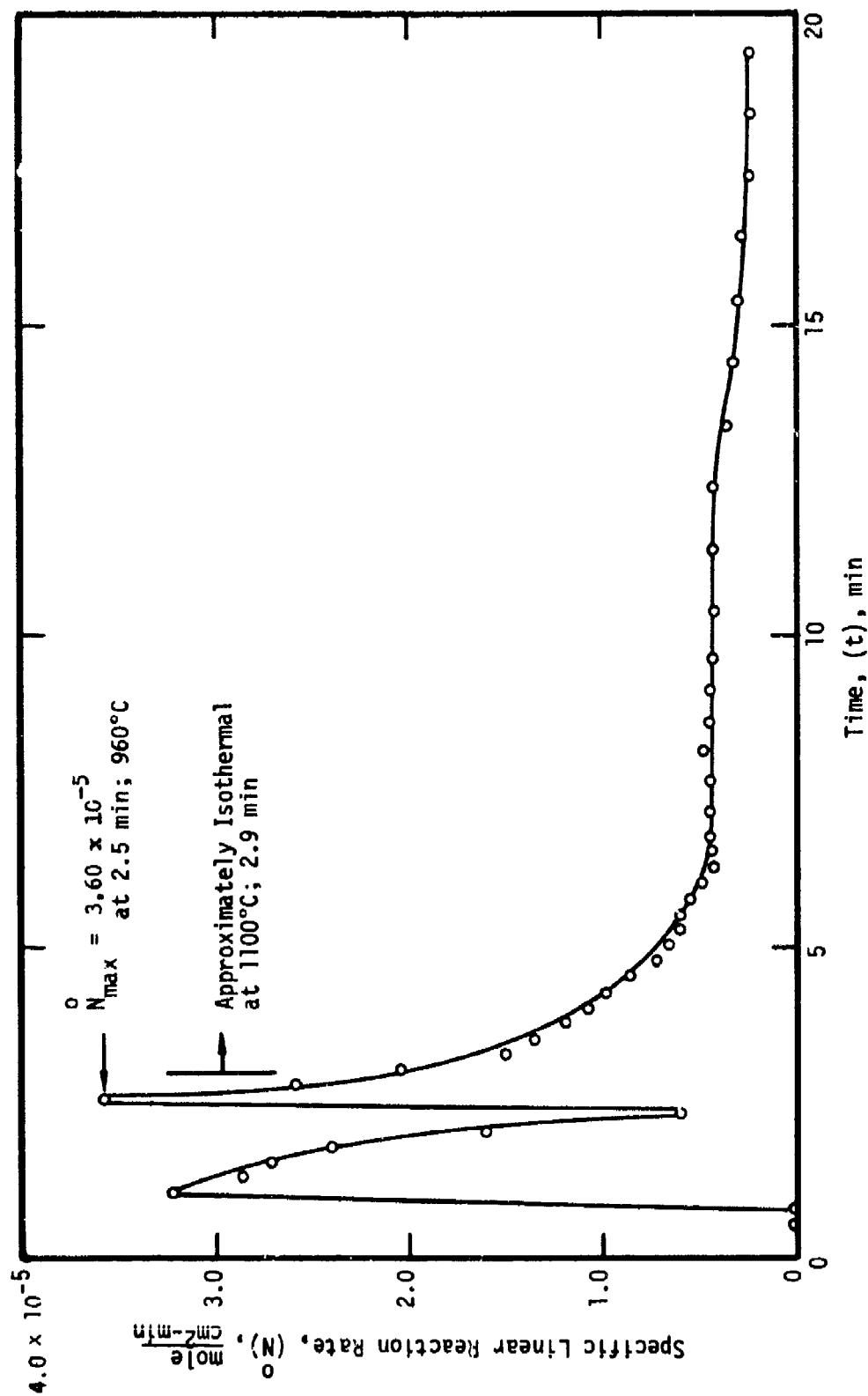


Figure 110. - Initial behavior of the specific linear reaction rate (\bar{N}) for unalloyed titanium (Type 1) specimen no. 08011 heated in 200 torr O_2 plus 200 torr N_2 at the rate of 8°C/s to 1100°C.

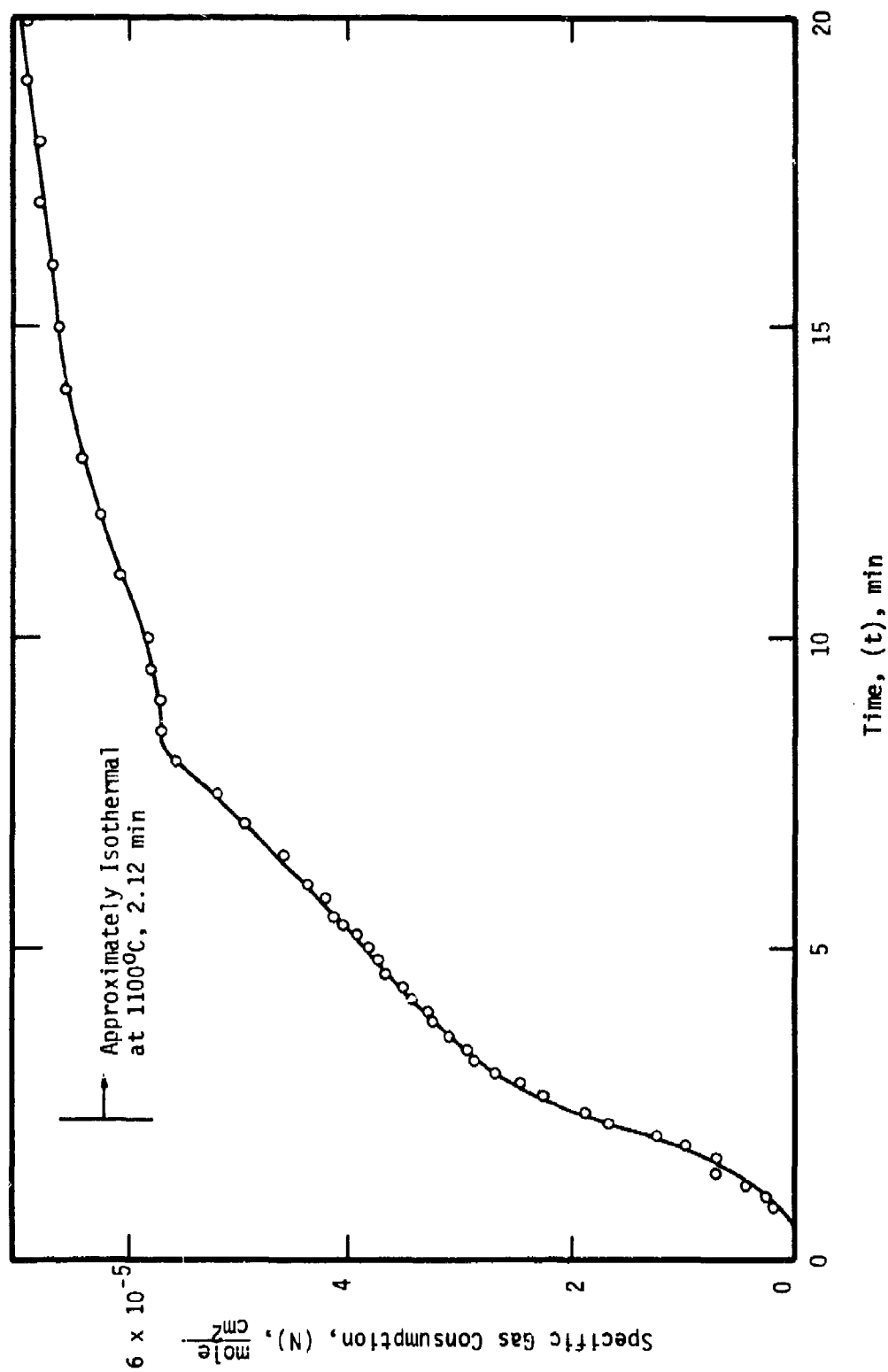


Figure 111. - Initial behavior of the specific gas consumption (N) for unalloyed titanium (Type 2) specimen no. 402193 heated in 100 torr O_2 plus 100 torr N_2 at the rate of 8°C/s to 1100°C .

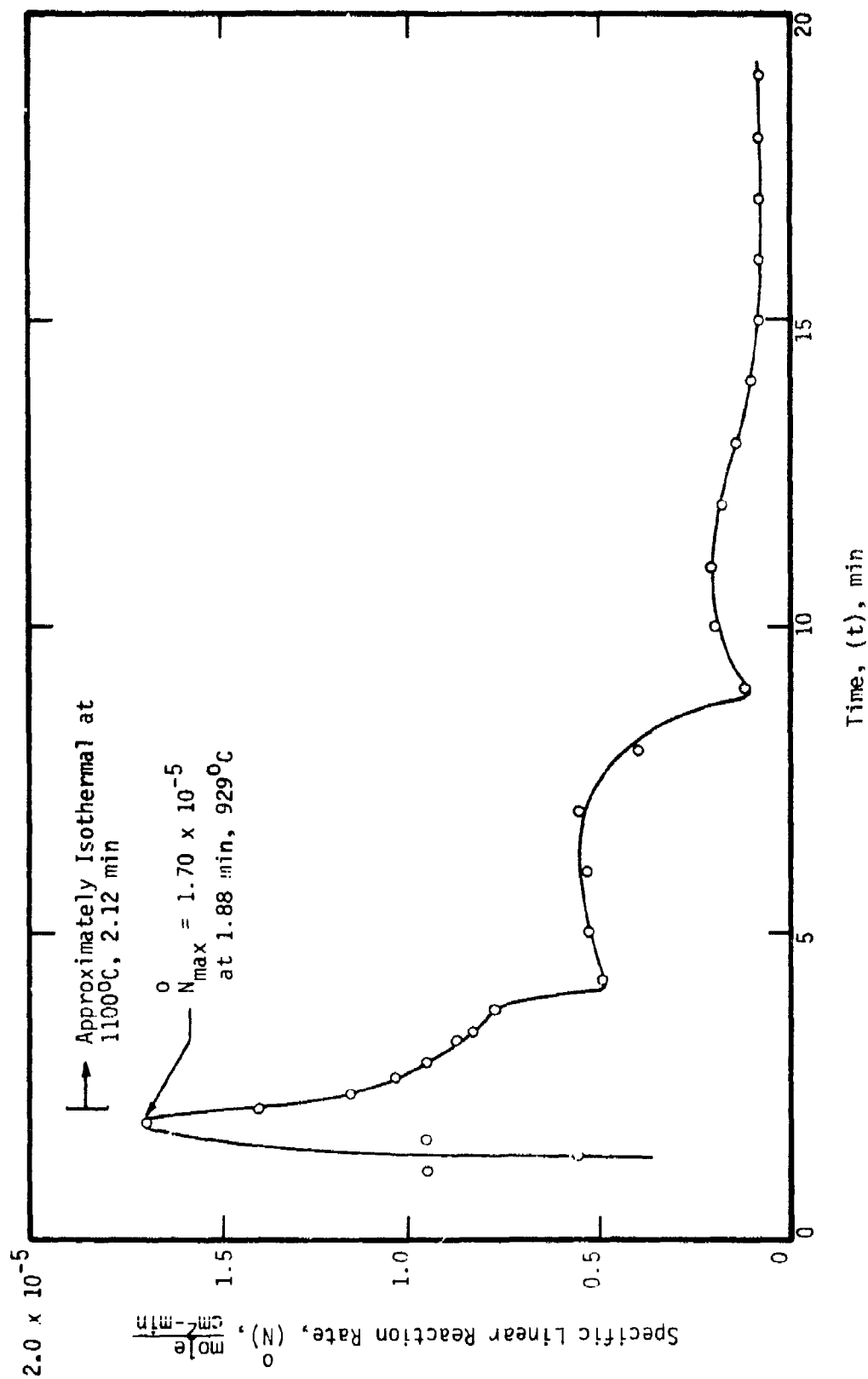


Figure 112. - Initial behavior of the specific linear reaction rate (\bar{N}) for unalloyed titanium (Type 2) specimen no. 402193 heated in 100 torr O_2 plus 100 torr N_2 at the rate of 8°C/s to 1100°C.

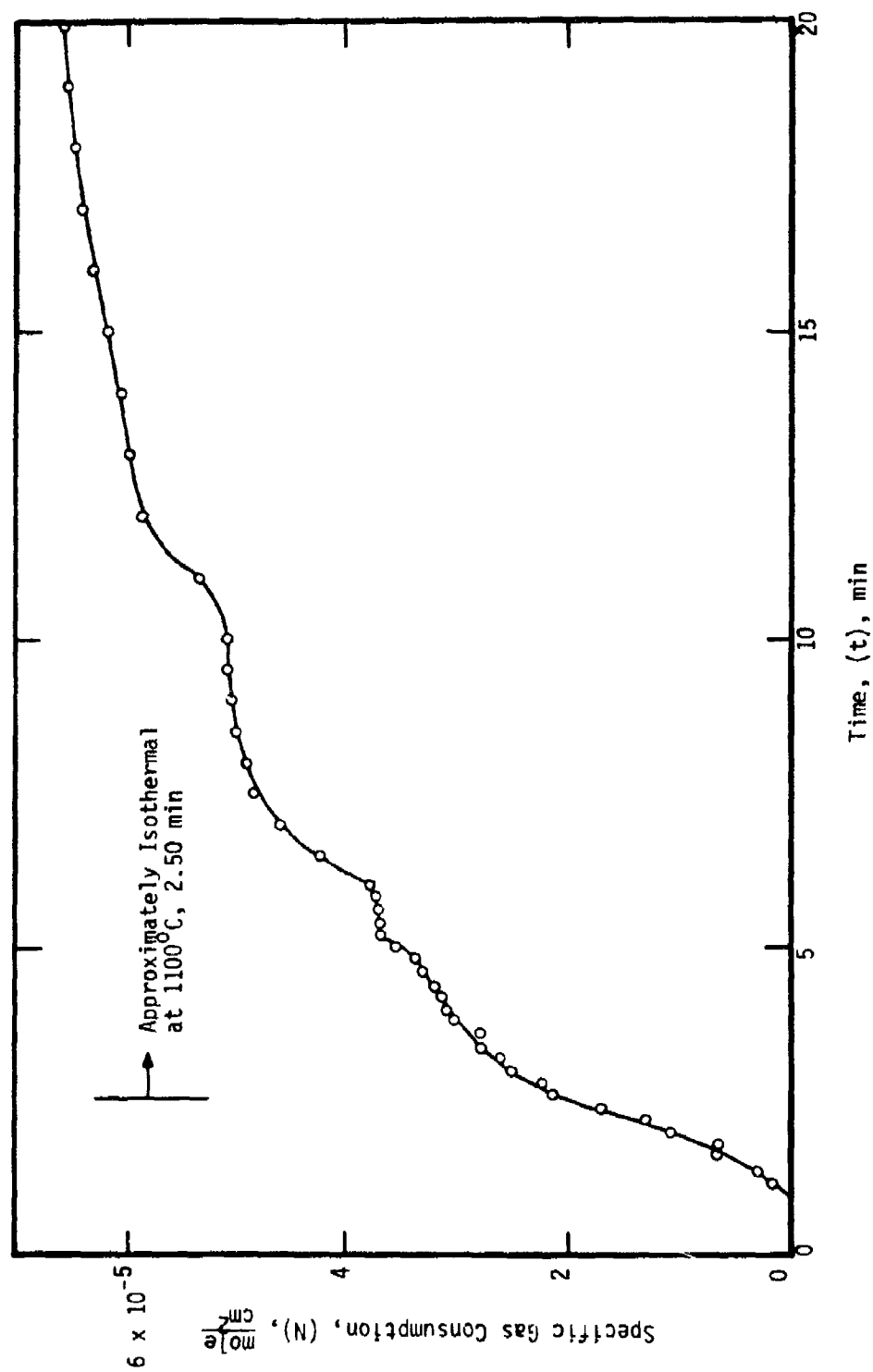


Figure 113. - Initial behavior of the specific gas consumption (N) for unalloyed titanium (Type 2) specimen no. 402194 heated in 50 torr O_2 plus 150 torr N_2 at the rate of 8°C/s to 1100°C .

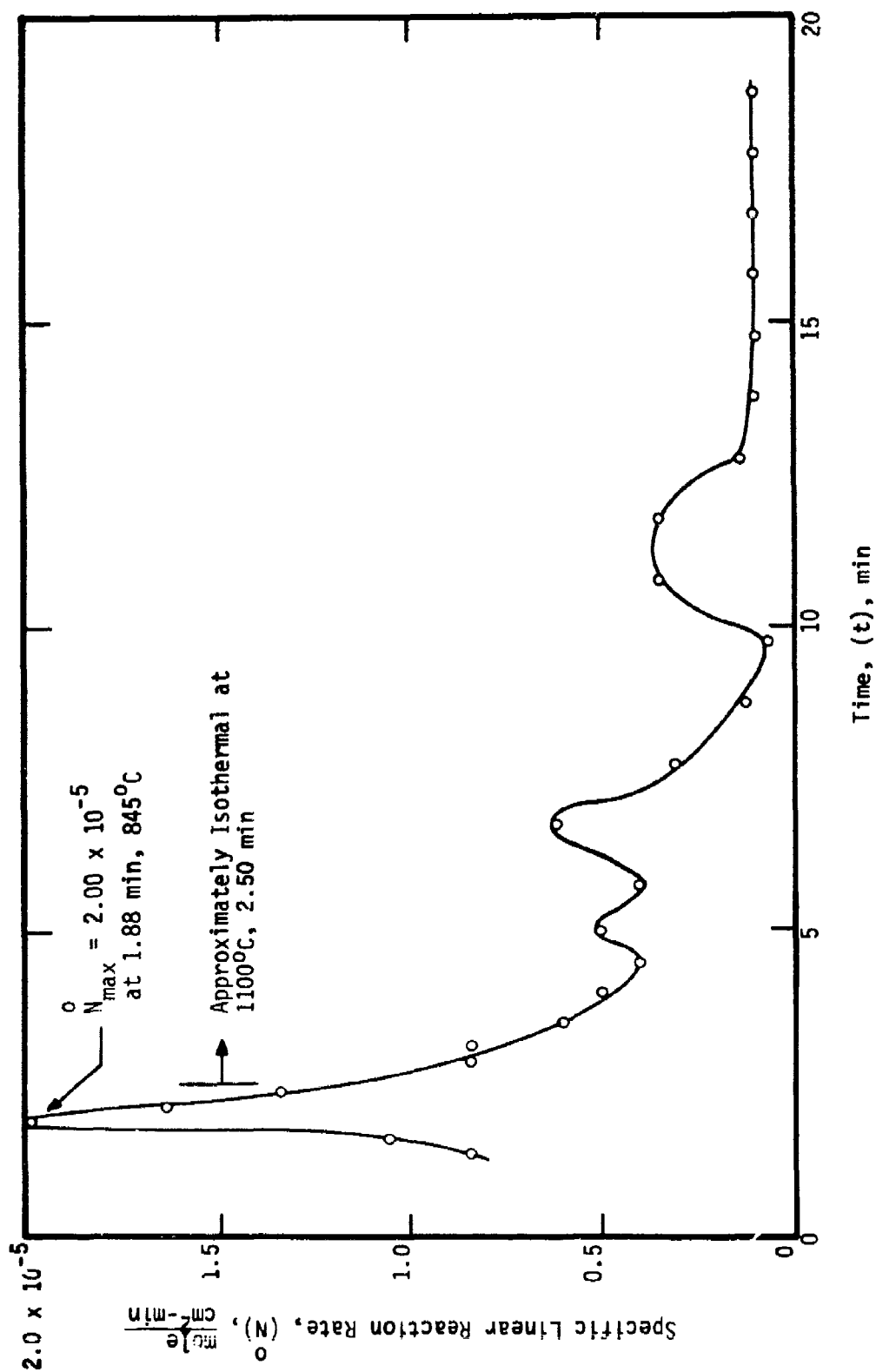


Figure 114. - Initial behavior of the specific linear reaction rate (\bar{N}) for unalloyed titanium (Type 2) specimen no. 402194 heated in 50 torr O_2 plus 150 torr N_2 at the rate of 8°C/s to 1100°C.

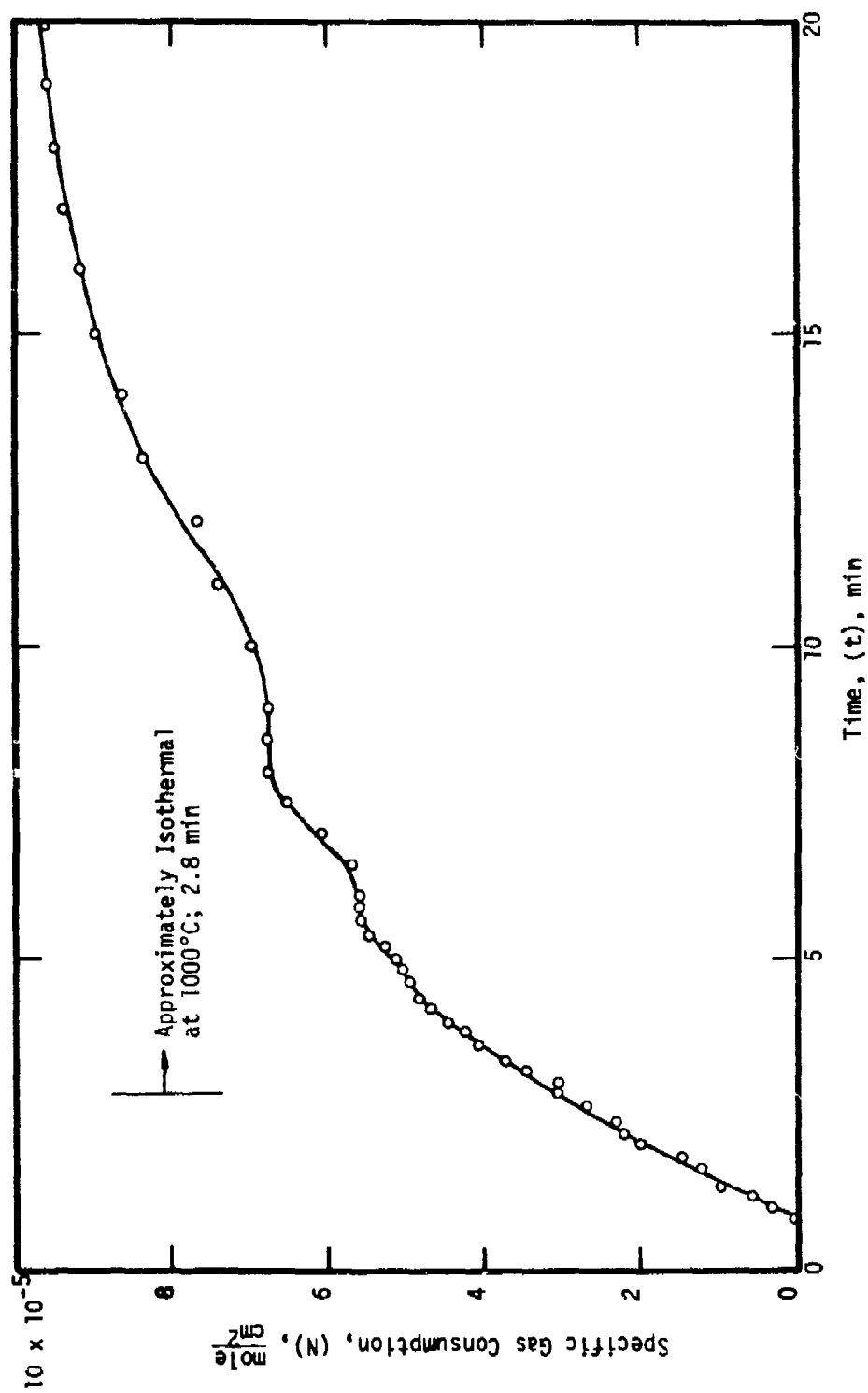


Figure 115. - Initial behavior of the specific gas consumption (N) for unalloyed titanium (Type 1) specimen no. 08021 heated in 200 torr O_2 plus 200 torr He at the rate of 8°C/s to 1000°C .

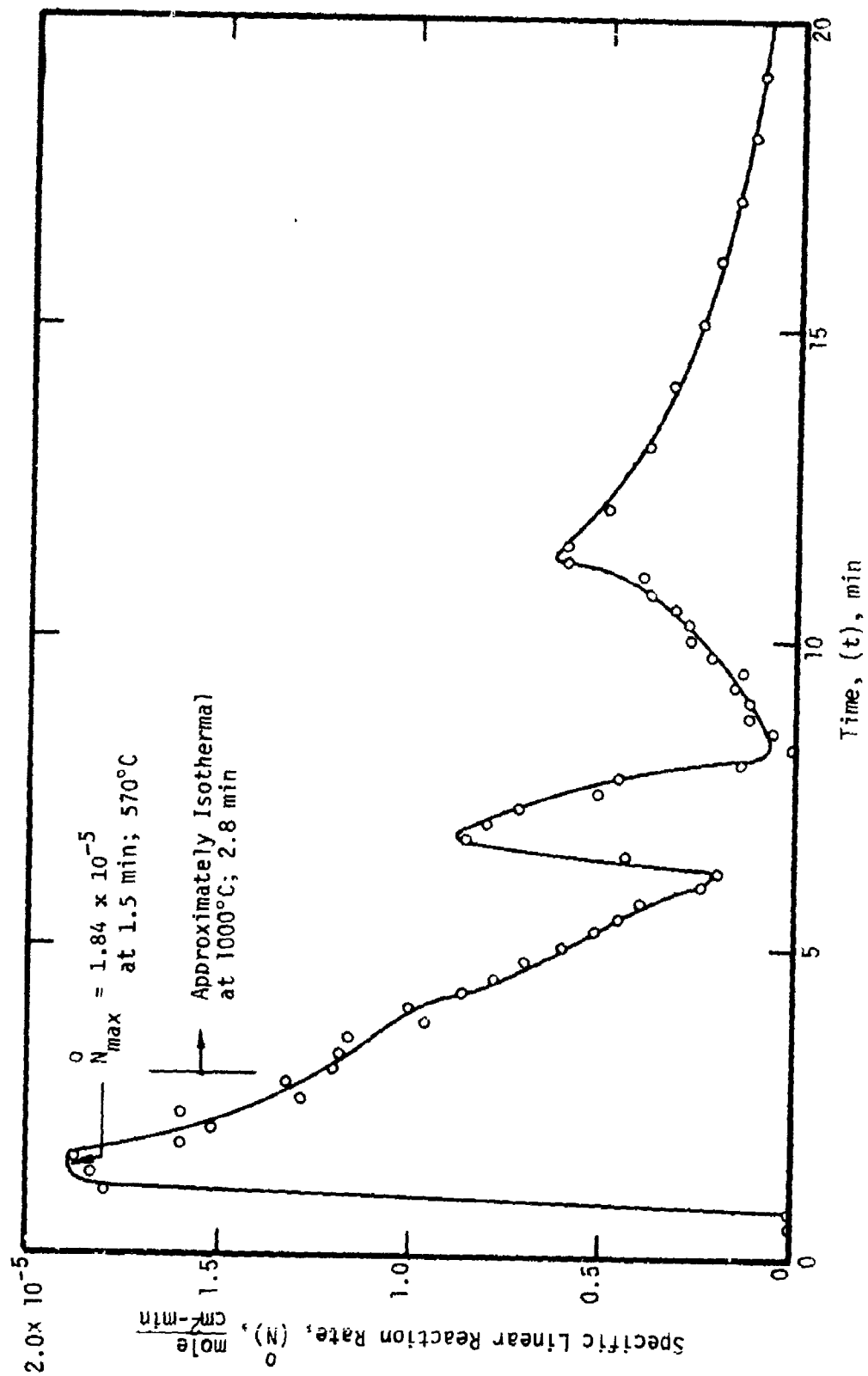


Figure 116. - Initial behavior of the specific linear reaction rate (\dot{N}) for unalloyed titanium (Type 1) specimen no. 08021 heated in 200 torr O_2 plus 200 torr He at the rate of 8°C/s to 1000°C.

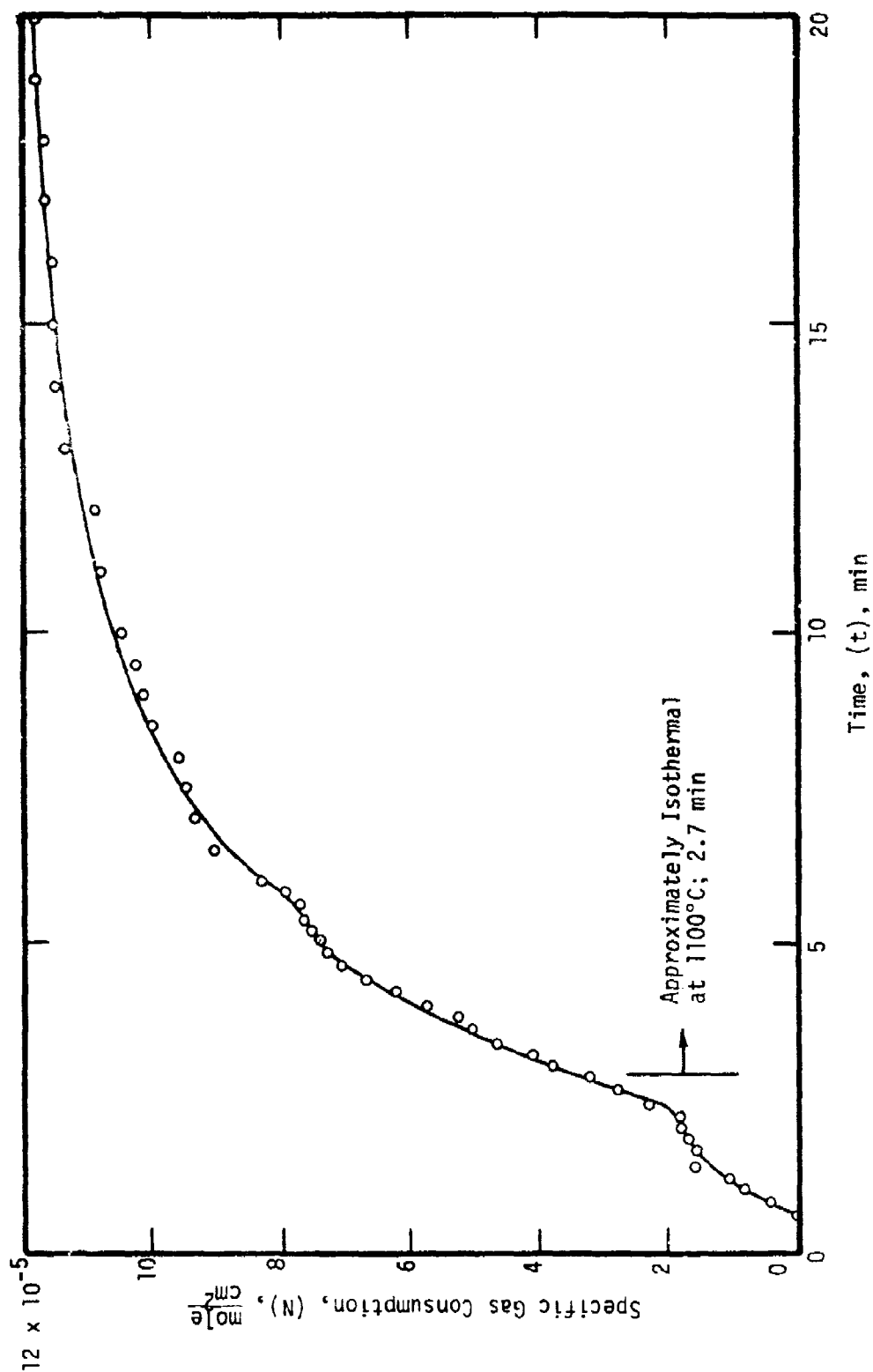


Figure 117. - Initial behavior of the specific gas consumption (N) for unalloyed titanium (Type 1) specimen no. 08171 heated in 200 torr O_2 plus 200 torr He at the rate of 8°C/s to 1100°C .

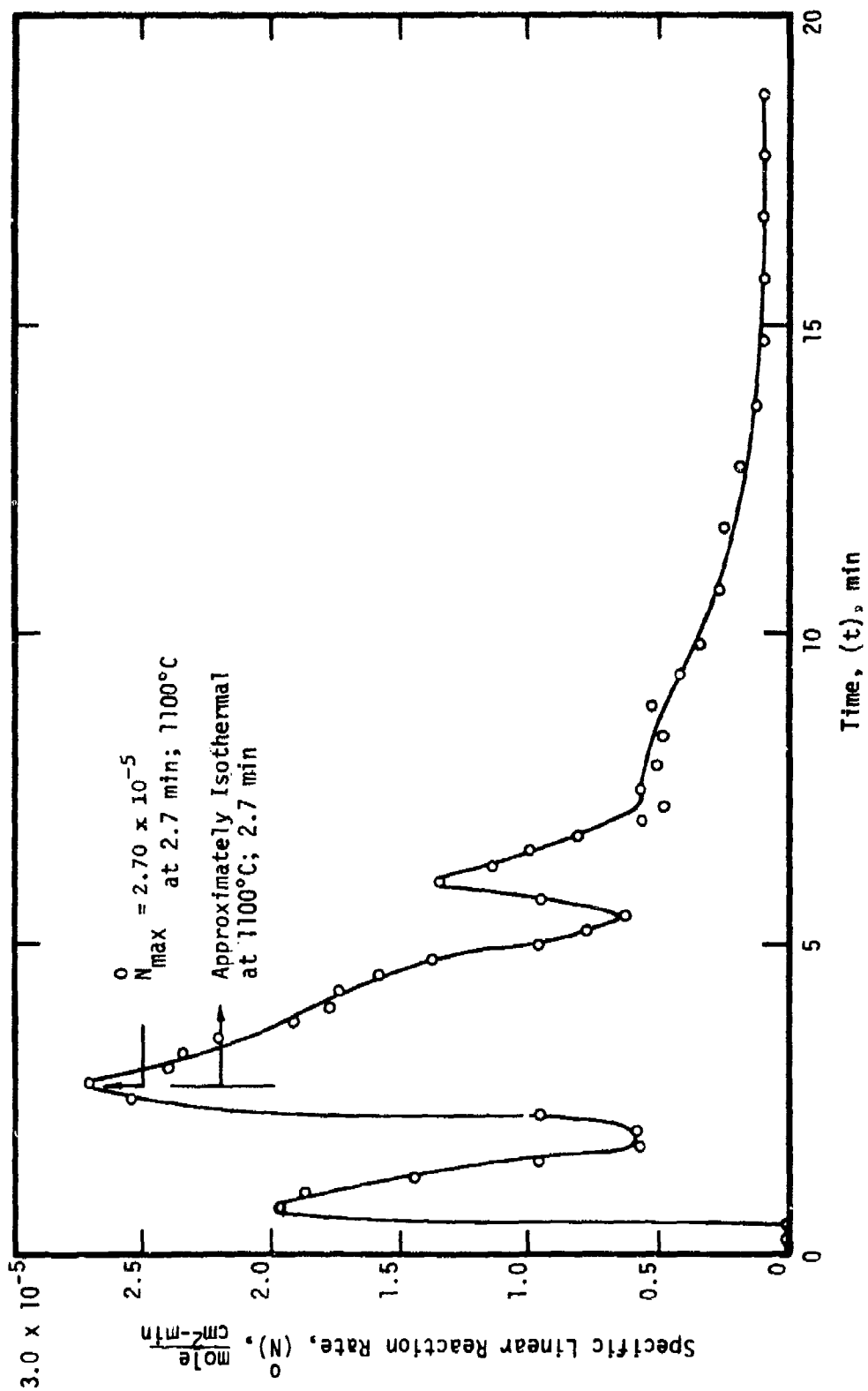


Figure 118. - Initial behavior of the specific linear reaction rate (\bar{N}) for unalloyed titanium (Type 1) specimen no. 08171 heated in 200 torr O_2 plus 200 torr He at the rate of 8°C/s to 1100°C.

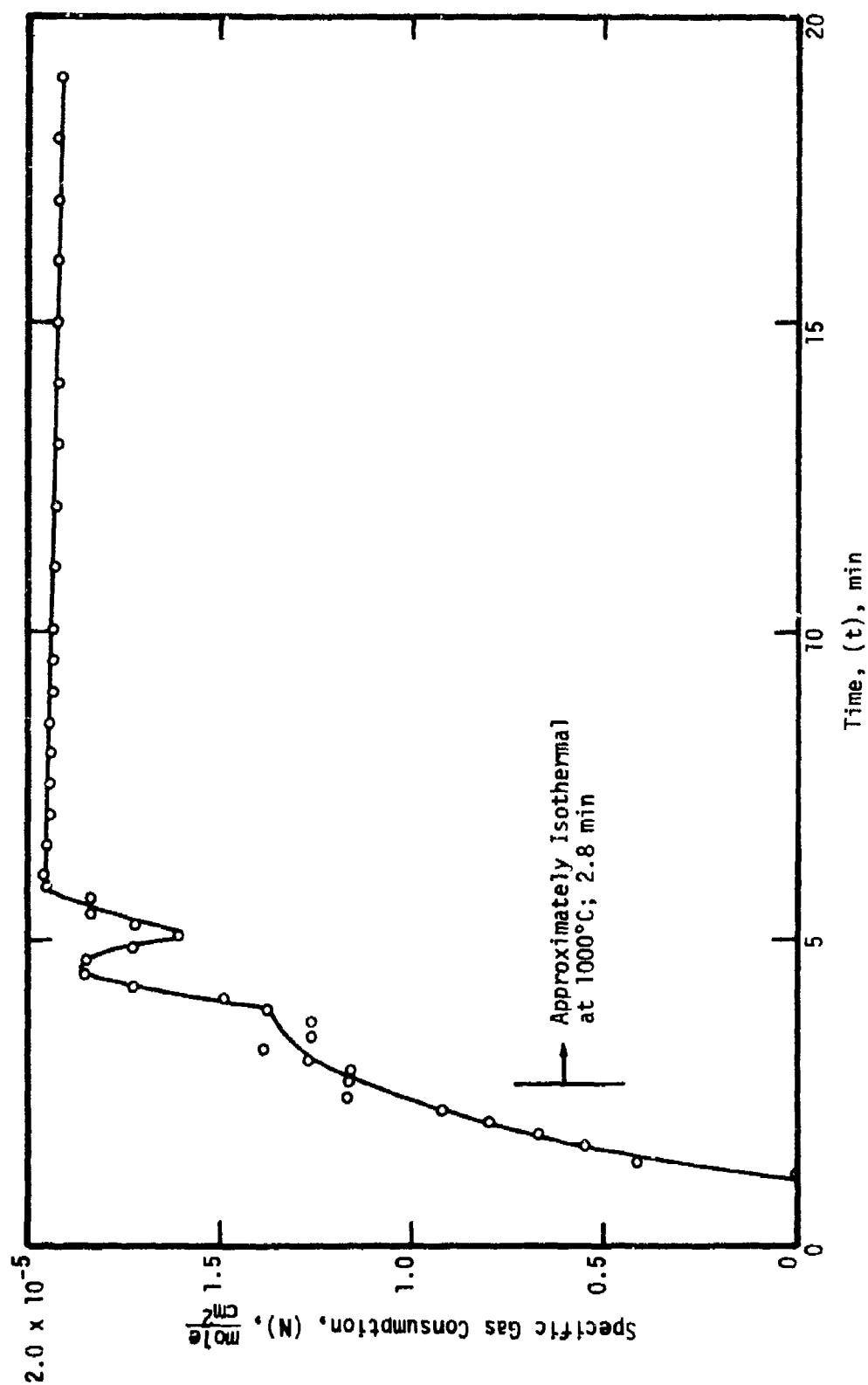


Figure 119. - Initial behavior of the specific gas consumption (N) for unalloyed titanium (Type 1) specimen no. 08023 heated in 200 torr N_2 plus 200 torr He at the rate of 8°C/s to 1000°C.

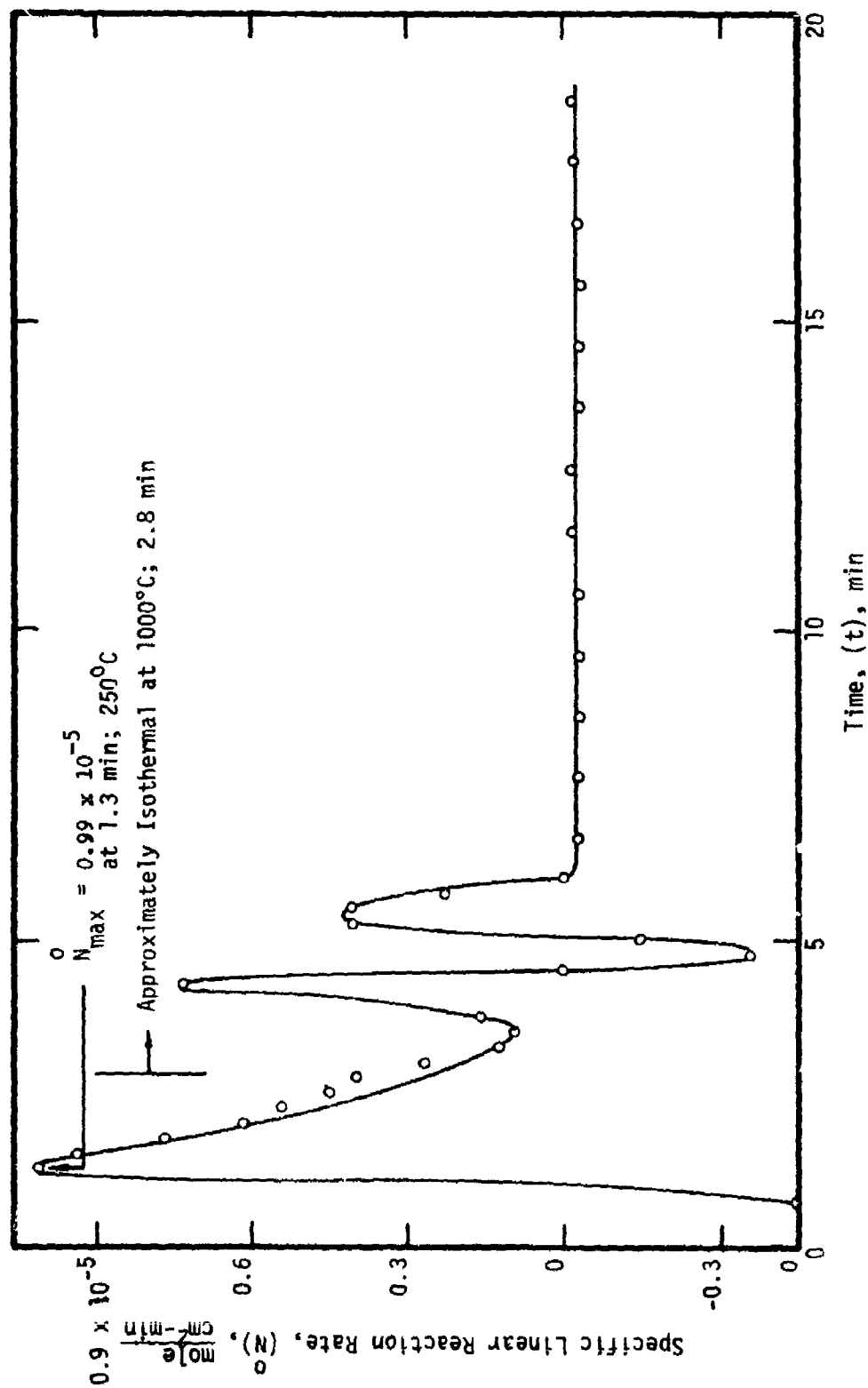


Figure 120. - Initial behavior of the specific linear reaction rate (\bar{N}) for unalloyed titanium (Type 1) specimen no. 08023 heated in 200 torr N_2 plus 200 torr He at the rate of 8°C/s to 1000°C.

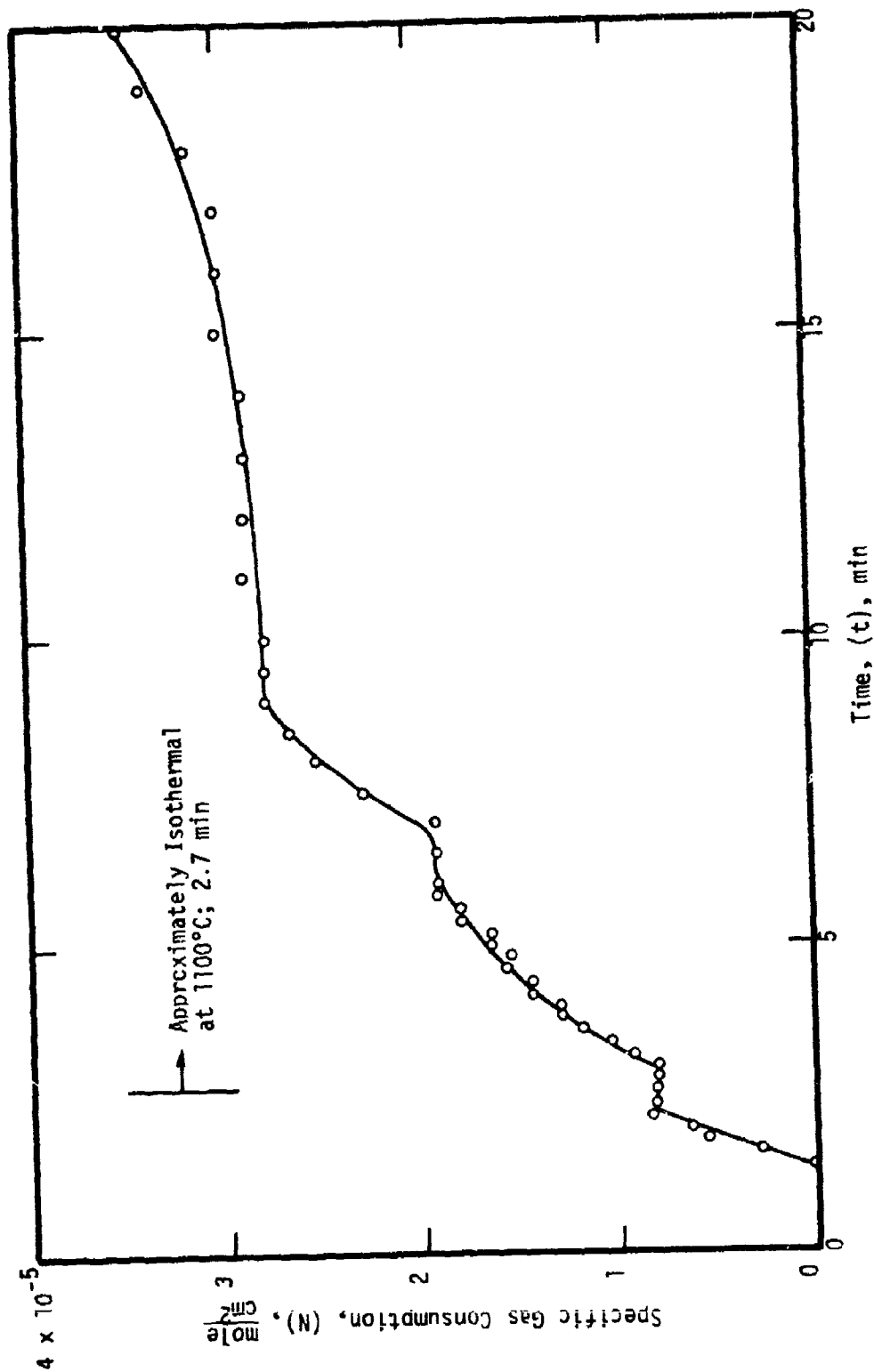


Figure 121. - Initial behavior of the specific gas consumption (N) for unalloyed titanium (Type 1) specimen no. 09051 heated in 200 torr N₂ plus 200 torr He at the rate of 8°C/s to 1100°C.

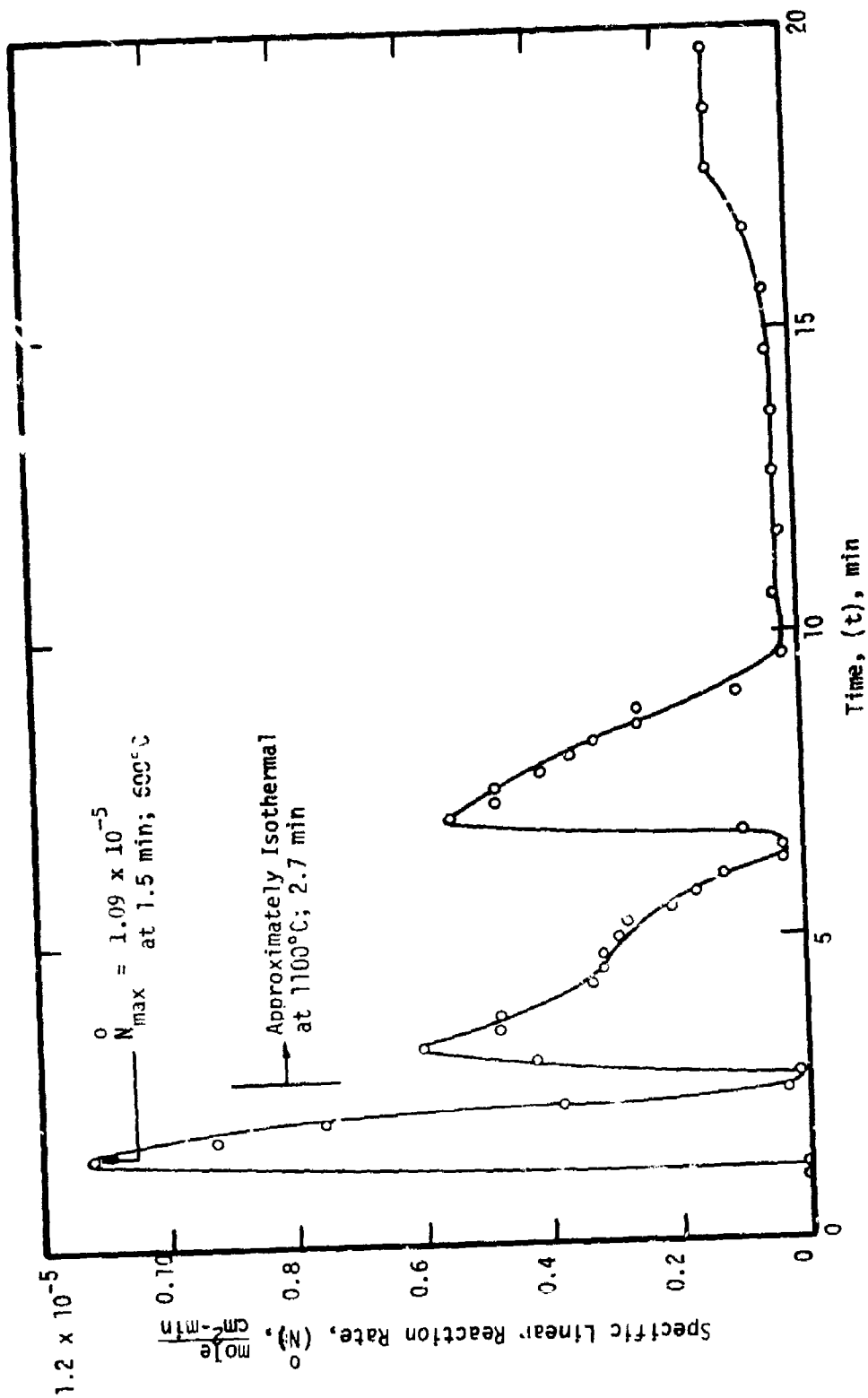


Figure 122. - Initial behavior of the specific linear reaction rate (\bar{N}) for unalloyed titanium (Type 1) specimen no. 09051 heated in 200 torr N_2 plus 200 torr He at the rate of 8°C/s to 1100°C.

not illustrated, as would be induced by a process involving scale "damage" and its subsequent "repair".

The next order of complexity in behavior type involves the specimen exposed at 1100°C. In this case, Figure 100, the nitrogen fixation appears to occur in a repeated discontinuous pattern of rapid consumption and low or zero consumption. The time derivative of this type of behavior, representing the specific linear reaction rate (\dot{N}), therefore exhibits multiple maxima, the first of which occurs at or prior to the time at which (T_{\max}) is reached, see Figure 101. As will become evident, the multiple-maxima pattern is typical of titanium exposure in the range of nitrogen-bearing atmospheres investigated.

The longer-term behavior indicates that after an initial quiescent period, lasting from approximately the tenth to the twenty-fifth minute of isothermal conditions, there is a relatively rapid fixation of nitrogen maintained during the remainder of the test. This behavior is also somewhat irregular in that it approximates an overall linear behavior but exhibits perturbations in the form of "scallop". The entire behavior is suggestive of alternate periods of: 1) reaction of titanium with nitrogen followed by 2) some type of "conditioning" of the fixed nitrogen or reaction product necessary to the continuance of reaction. Further research will be needed to clarify the causes of the observed behavior.

The most complex of the observed types of behavior was observed for the specimen of titanium (Type 1) exposed at 1000°C. The overall behavior (Figure 98) was similar to that just cited above; however, with the additional complication that nitrogen was initially apparently both first fixed and later liberated by the titanium specimen. This complication in the nitrogen consumption curve produced in the time derivative of this curve (\dot{N}), not only

multiple maxima, but also negative values for the specific linear reaction rate. This phenomena also extends to other cases of titanium exposure in nitrogen-bearing atmospheres.

For comparative purposes, a single test utilizing a Ti-6Al-4V alloy (Type 1) specimen was conducted in 200 torr nitrogen. As had been indicated earlier, the long-term nitrogen consumption was considerably less (by a factor of approximately 3) for the alloy than for the unalloyed titanium. A similar factor applies for the short-term isothermal data; compare Figures 100 and 105. However, during anisothermal heating at 8°C/s, the Ti-6Al-4V alloy reacts somewhat faster (and therefore at a much lower temperature) than does unalloyed titanium; compare Figures 101 and 106. Thus, it appears that the alloy forms a protective film rapidly at low temperature and in such manner that it subsequently acts as a relatively stable diffusion barrier against further reaction. It is implicit in this argument that the film must also be resistant to thermal stresses generated during heating and after its initial formation; a condition requiring considerable plasticity of the film.

Data derived from the volumetric apparatus for the reaction of unalloyed titanium in mixtures of oxygen and nitrogen, oxygen and helium, and nitrogen and helium at 1000° and 1100°C are presented in Figures 107 through 122. In each case, the general form of the initial portions of the gas consumption curves closely resemble those derived from exposure in nitrogen at 1100°C, Figure 100 and 101 for (N vs. t) and (\dot{N} vs. t), respectively. The specific gas consumption curves exhibit non-uniform behaviors which lead to multiple maxima in the (\dot{N} vs. t) curves. In addition, at 1000°C the nitrogen-bearing gas mixtures exhibit negative values (minima) in their reaction rate (\dot{N} vs. t) curves, Figure 108 and 120, qualitatively similar to that exhibited in nitrogen alone, Figure 99. In this sense, and as alluded to previously,

exposure in gas mixtures produces behaviors intermediate to those produced by the single gas species involved.

Two tests were conducted using unalloyed titanium (Type 2) specimens exposed to oxygen-nitrogen mixtures at 200 torr total pressure and containing approximately 50 and 75 percent nitrogen. In general, it was found that the behavior of the oxidation process changed in a smooth fashion from the behaviors evidenced in pure oxygen (200 torr) to those enhanced in pure nitrogen (200 torr). Thus, no documentation for a pronounced synergistic effect has been observed.

The maximum specific linear reaction rate data vary in a relatively smooth fashion from the higher values for pure oxygen to the intermediate values for gas mixtures and, finally, to the lowest values for pure nitrogen.* Similarly the early isothermal rates of oxidation decrease in a regular fashion from those observed for pure oxygen to those observed for pure nitrogen; see, for example, Figures 81, 103, 111, and 113. Finally, the character of these gas consumption curves changes in a smooth fashion from initial near-linear behavior in oxygen to the typical "stepped" behavior in nitrogen with the curves for the mixtures exhibiting a "weighted average" type of behavior.

In retrospect, the apparent change in activation energy associated with testing in different types of apparatus (an air-containing tube furnace vs. the volumetric apparatus), probably arises as a result of trace impurities generated either by the apparatus or contained in laboratory air.

The reaction of unalloyed titanium on mixtures of either 200 torr oxygen plus 200 torr helium or 200 torr nitrogen plus 200 torr helium was similar in degree to that observed with the respective unmixed gases. There did

*The earlier (lower temperature) associated with (N_{\max}^0) in the case of mixed gases is the only indication that the reaction may be accelerated at low temperatures by a synergistic effect.

exist a tendency for the data from these mixed gas tests to produce relatively strong multiple minima and maxima in the reaction rate curves, see Figures 116, 118, 120, and 122. This behavior strongly suggests that oxygen "starvation" in the region of the apparatus immediately adjacent to the specimen may have occurred. It is, of course, also possible that preferential starvation of the more reactive gas component in any gas mixture can similarly occur; however, this effect can not be used to reconcile similar behaviors in unmixed nitrogen.

As with the case of nitrogen, the long-term (one-hour) behaviors in mixed gases are somewhat complex, especially for those gas mixtures containing nitrogen whose behavior parallels that of nitrogen. Reaction of titanium with oxygen-helium gas mixture is nearly parabolic at 1000°C, but at 1100°C, it exhibits a period of quiescence not associated with tests conducted in oxygen alone. This behavior may also be rationalized on the basis of localized oxygen "starvation", although more complex processes may be involved.

4d. REACTION OF TITANIUM-BASE ALLOYS WITH OXYGEN-(RHC) TESTS

Data derived from the volumetric apparatus for the reaction of Ti-6Al-4V, Ti-8Mn, and β -III alloy specimens in 200 torr oxygen (RHC)-type tests are presented in Figures 123 through 168. In all cases, only the initial gas consumption (N) and linear reaction rate (\dot{N}) curves are illustrated as other behaviors are similar to those schematically described in Figures 41 above.

As with the case of unalloyed titanium, the alloy specimens react in a manner such that the specific oxygen consumption (N) is of sigmoidal character. It follows that the time derivatives of these curves, representing specific linear reaction rates (\dot{N}), similarly exhibit a single maximum which in many instances occurs prior to the time at which the "hold" portion of the

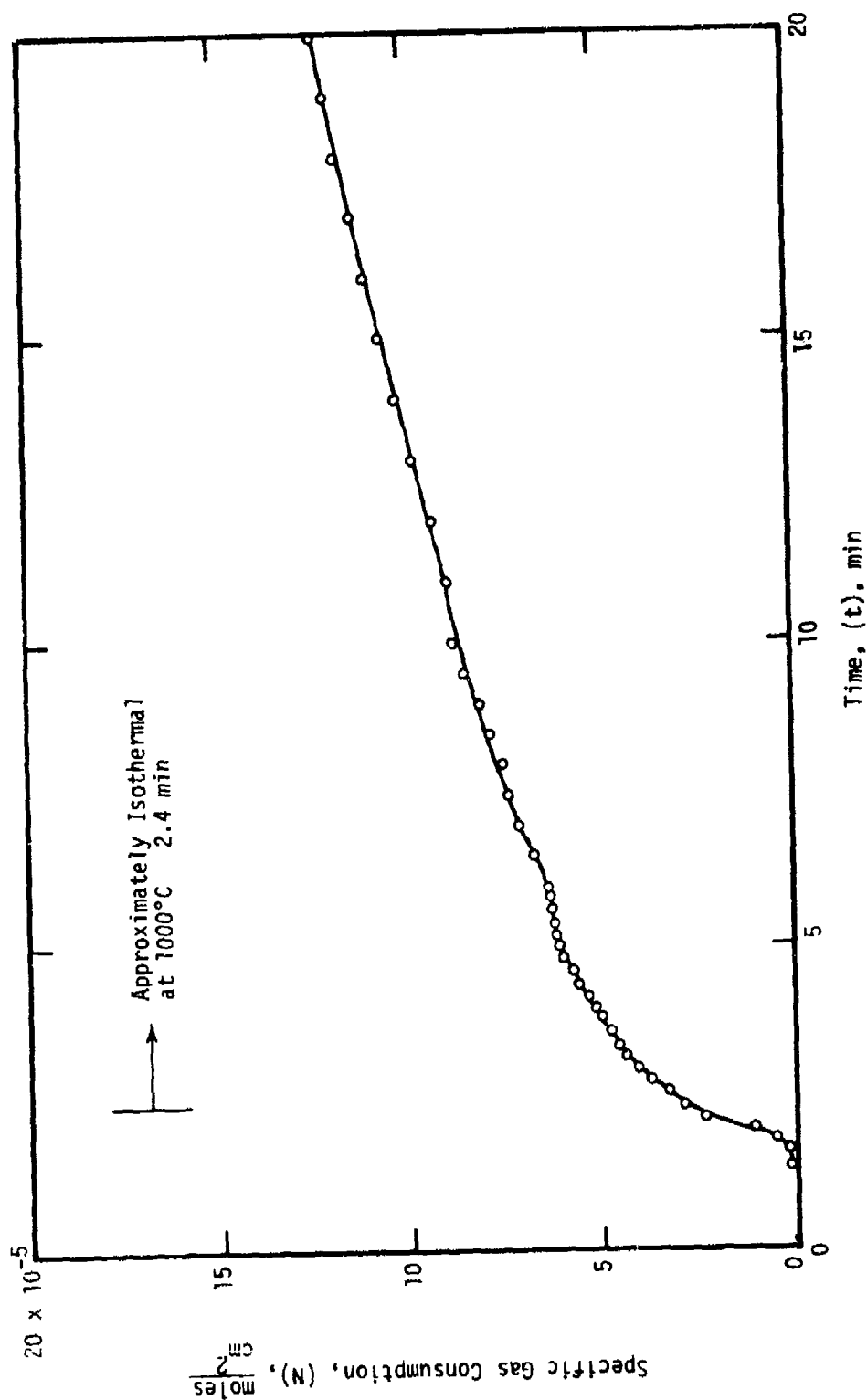


Figure 123.- Initial behavior of the specific gas consumption (N) for Ti-6Al-4V alloy (Type 1) specimen no. 407161 heated in 200 torr O_2 at the rate of 8°C/s to 1000°C. Material milled from .152 cm to .119 cm.

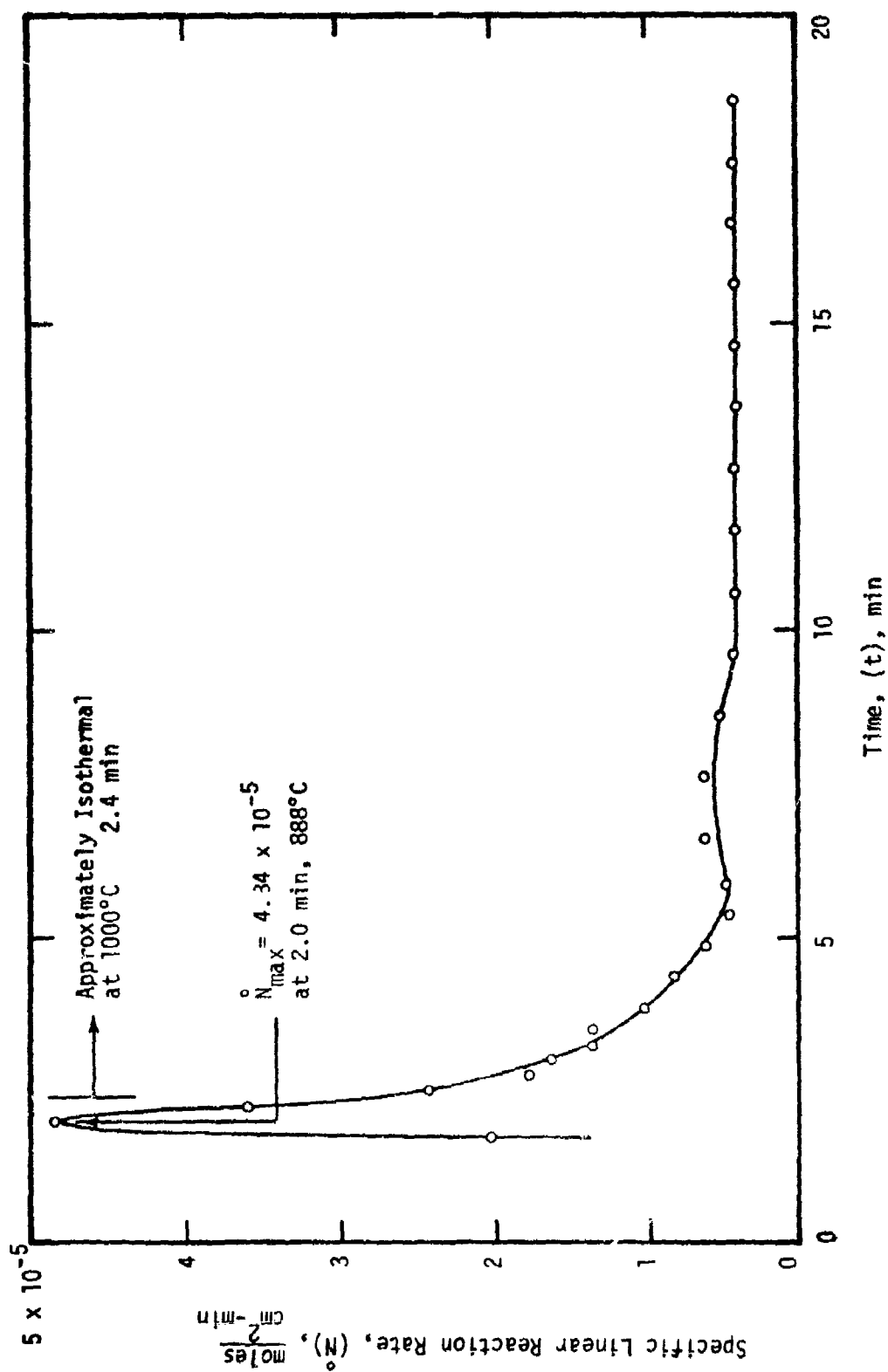


Figure 124.- Initial behavior of the specific linear reaction rate (\dot{N}) for Ti-6Al-4V alloy (Type 1) specimen no. 407161 heated in 200 torr O_2 at the rate of 8°C/s to 1000°C . Material milled from .152 cm to .119 cm.

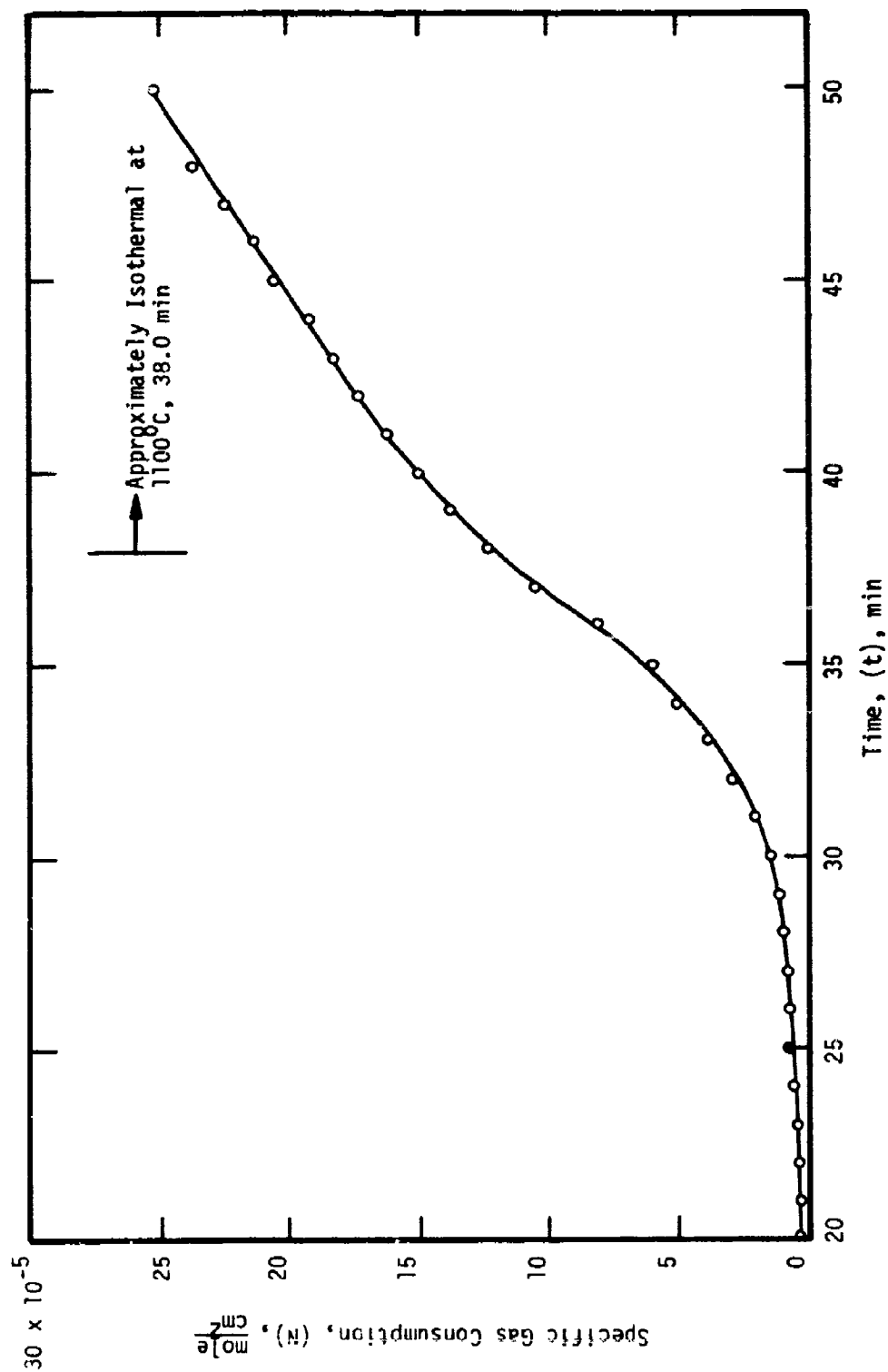


Figure 125.- Initial behavior of the specific gas consumption (N) for Ti-6Al-4V alloy (Type 1) specimen no. 401161 heated in 200 torr O_2 at the rate of $0.5^\circ\text{C}/\text{s}$ to 1100°C .

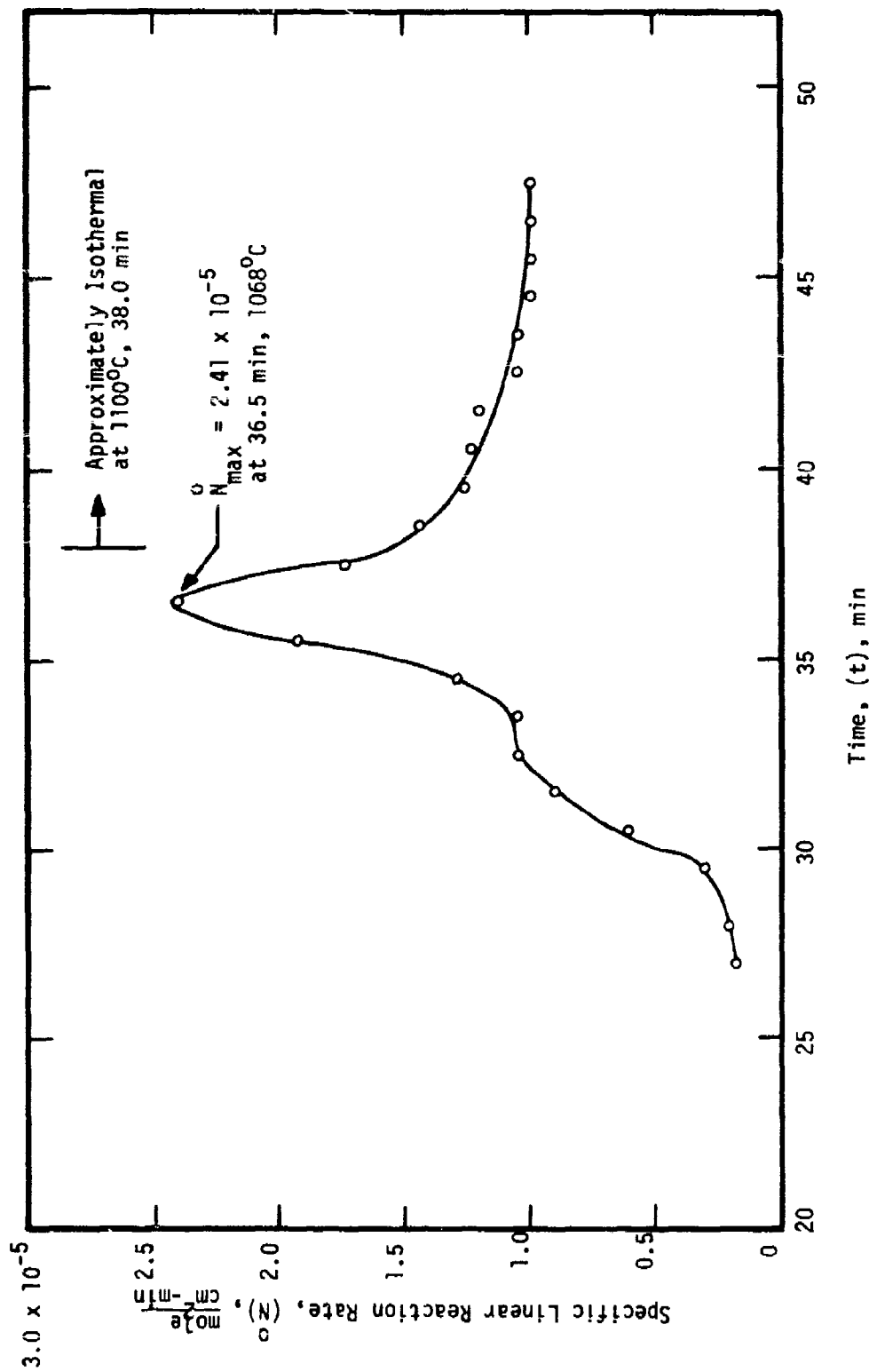


Figure 126.- Initial behavior of the specific linear reaction rate (\dot{N}) for Ti-6Al-4V alloy (Type 1) specimen no. 401161 heated in 200 torr O_2 at the rate of 0.5°C/s to 1100°C.

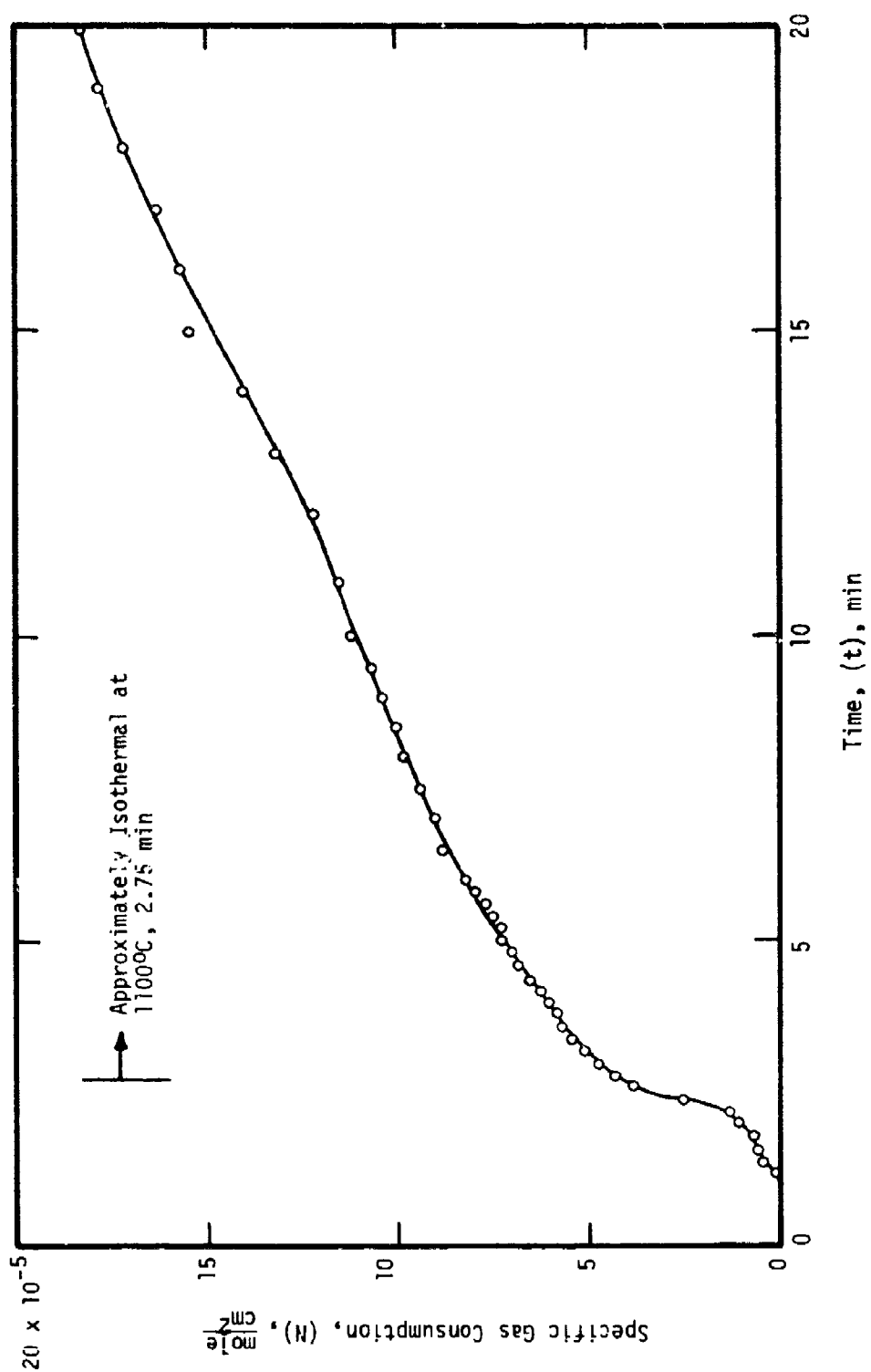


Figure 127.- Initial behavior of the specific gas consumption (N) for Ti-6Al-4V alloy (Type 1) specimen no. 11202 heated in 200 torr O_2 at the rate of $8^\circ C/s$ to $1100^\circ C$.

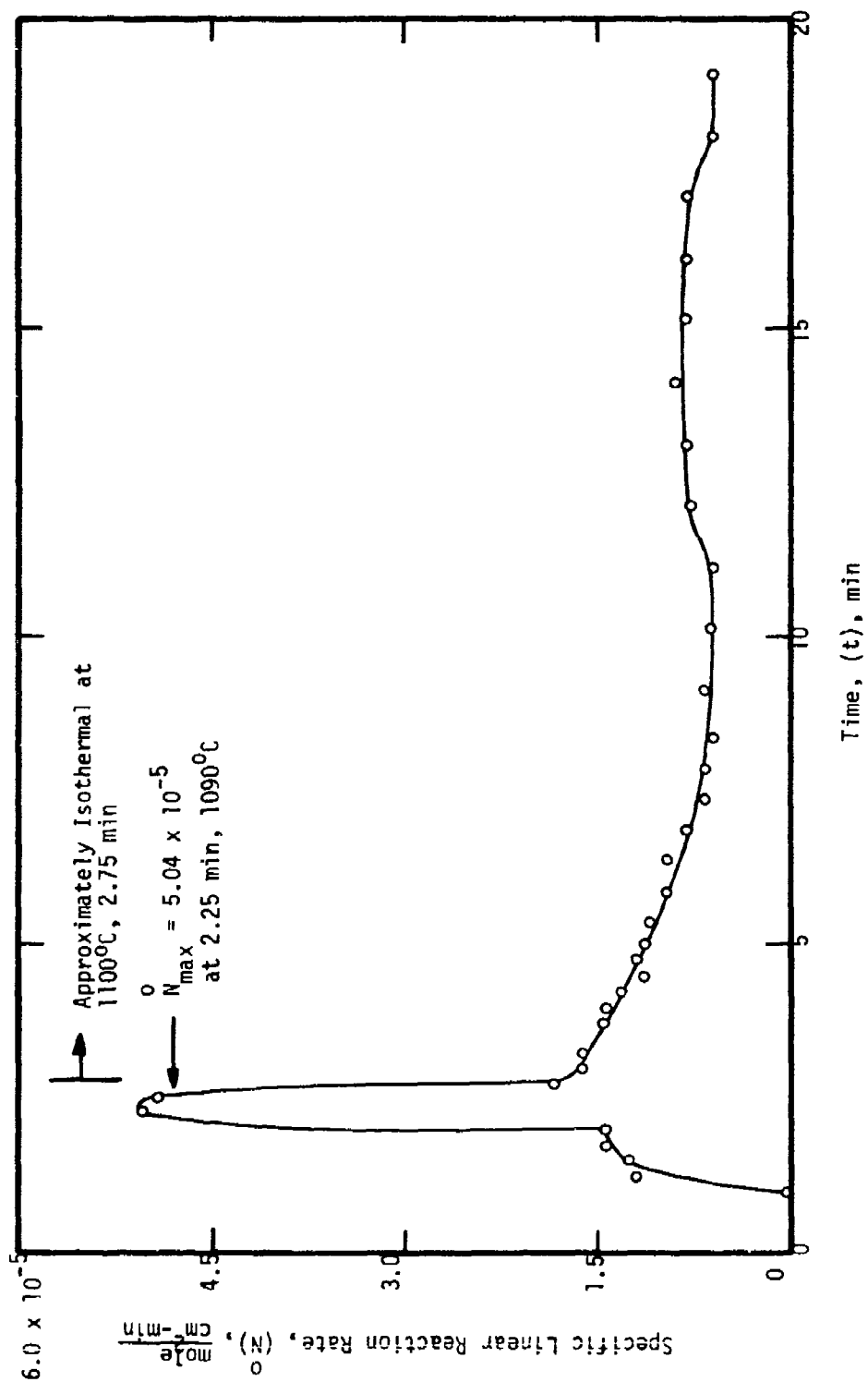


Figure 128.- Initial behavior of the specific linear reaction rate (\bar{N}) for Ti-6Al-4V alloy (Type 1) specimen no. 11202 heated in 200 torr O_2 at the rate of 8°C/s to 1100°C.

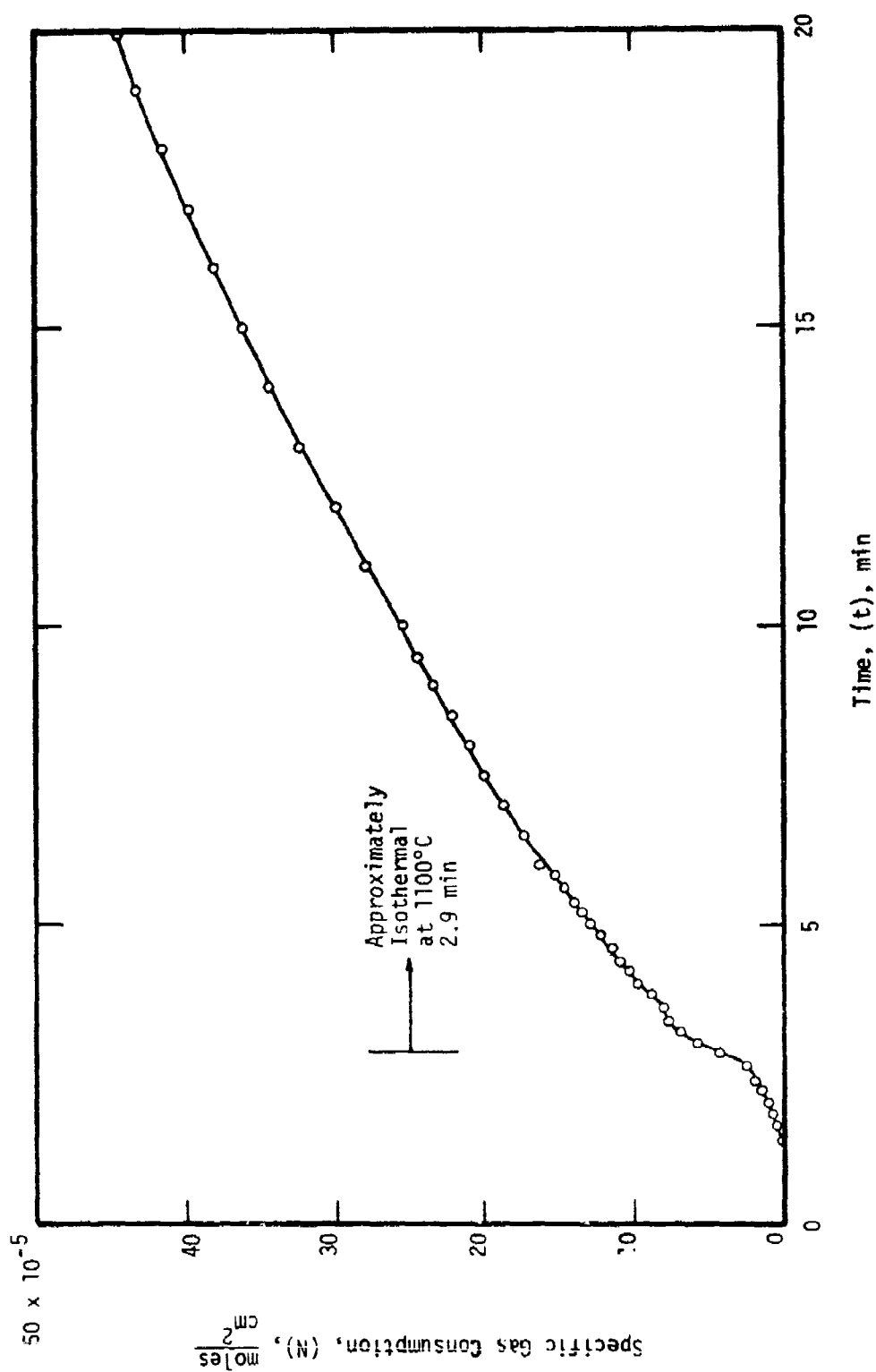


Figure 129.- Initial behavior of the specific gas consumption (N) for Ti-6Al-4V alloy (Type 1) specimen no. 405071 heated in 200 torr O_2 at the rate of 8°C/s to 1100°C. Material milled from .152 cm to .119 cm.

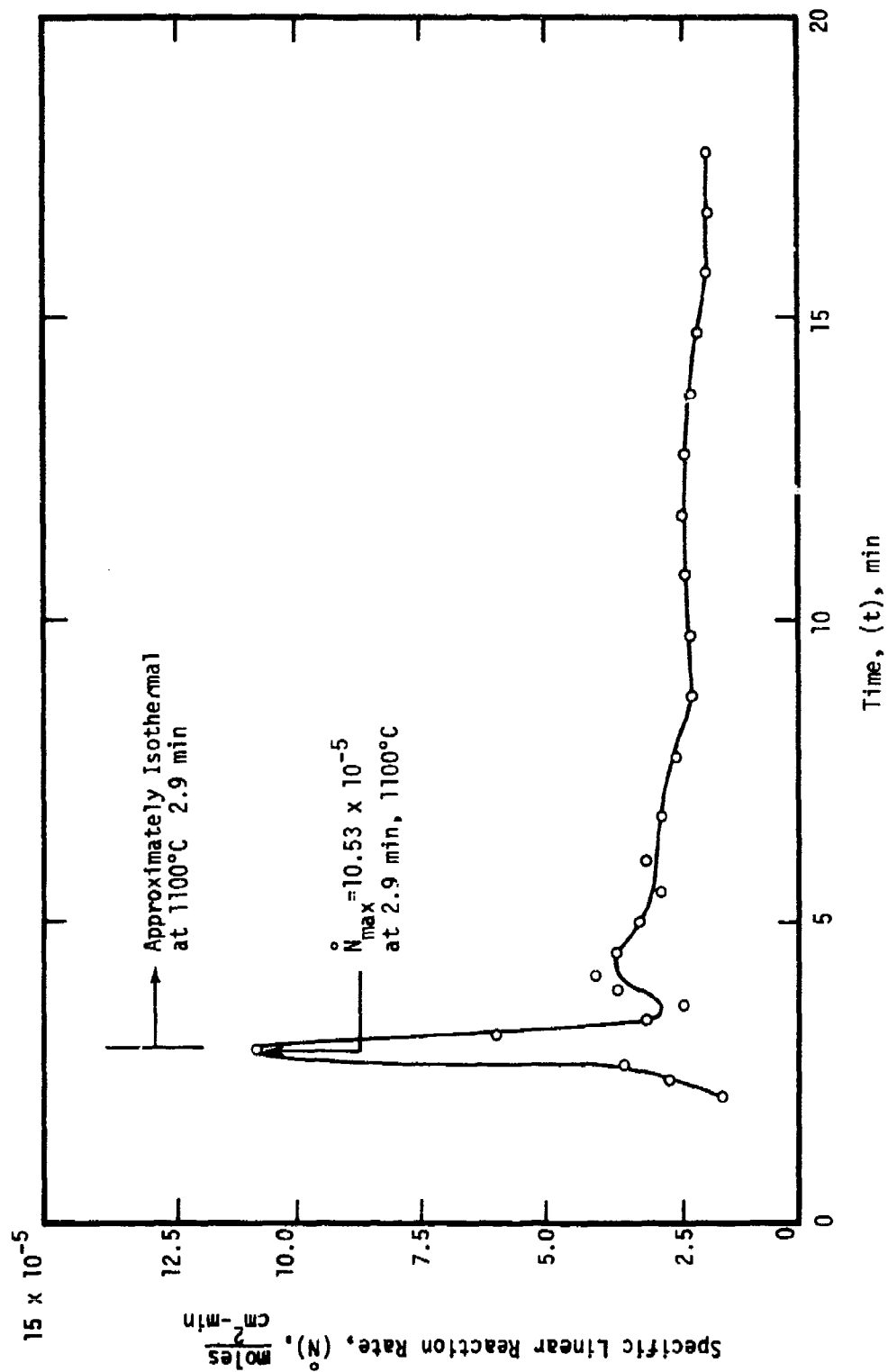


Figure 130.- Initial behavior of the specific linear reaction rate (\dot{N}) for Ti-6Al-4V alloy (Type 1) specimen no. 405071 heated in 200 torr O_2 at the rate of 8°C/s to 1100°C . Material milled from .152 cm to .119 cm.

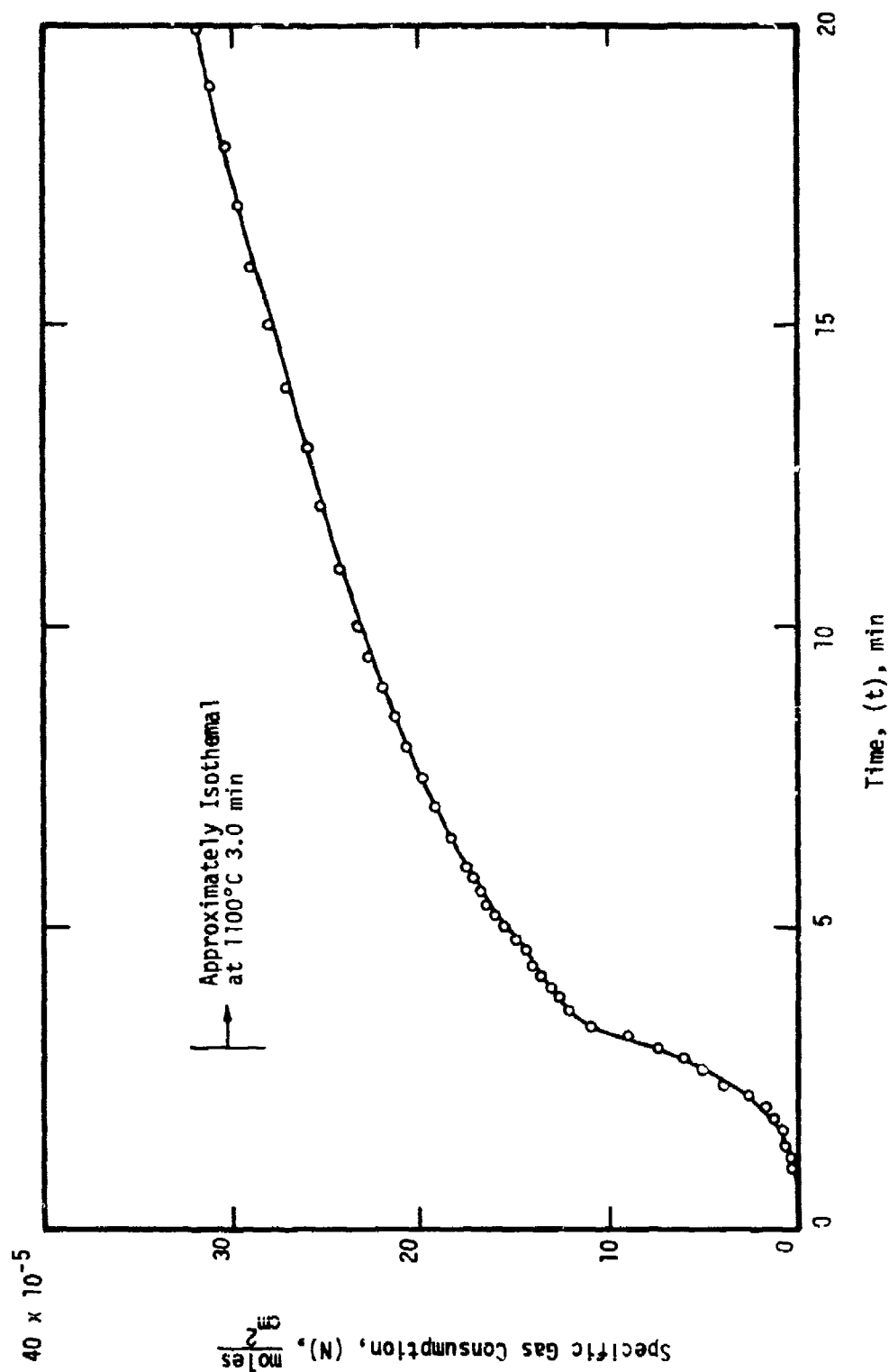


Figure 131.- Initial behavior of the specific gas consumption (N) for Ti-6Al-4V alloy (Type 1) specimen no. 405072 heated in 200 torr O_2 at the rate of $8^\circ C/s$ to $1100^\circ C$. Material milled from .152 cm to .119 cm.

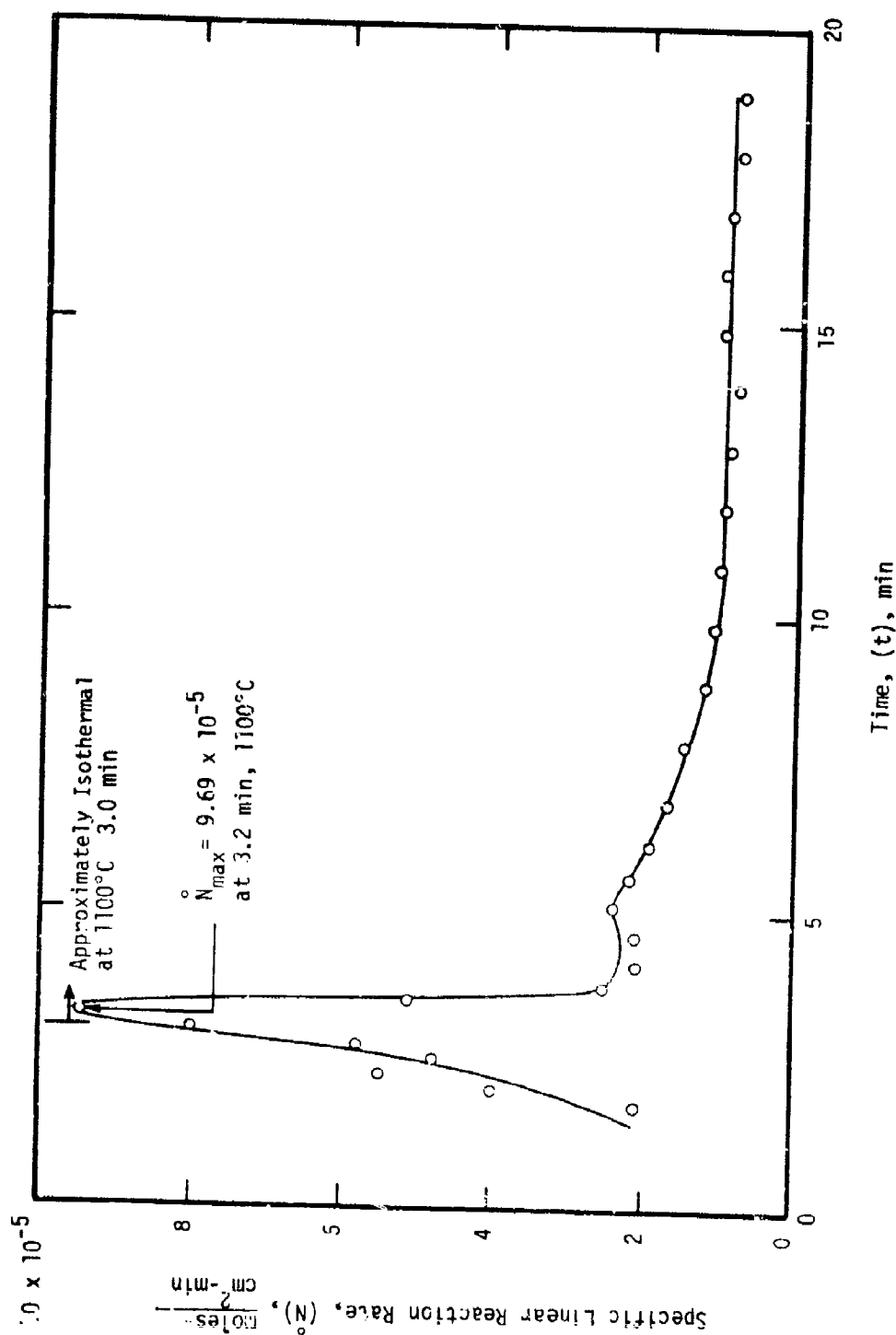


Figure 132.- Initial behavior of the specific linear reaction rate (\dot{N}) for Ti-6Al-4V alloy (Type 1) specimen no. 405072 heated in 200 torr O_2 at the rate of 8°C/s to 1100°C. Material milled from .152 cm to .119 cm.

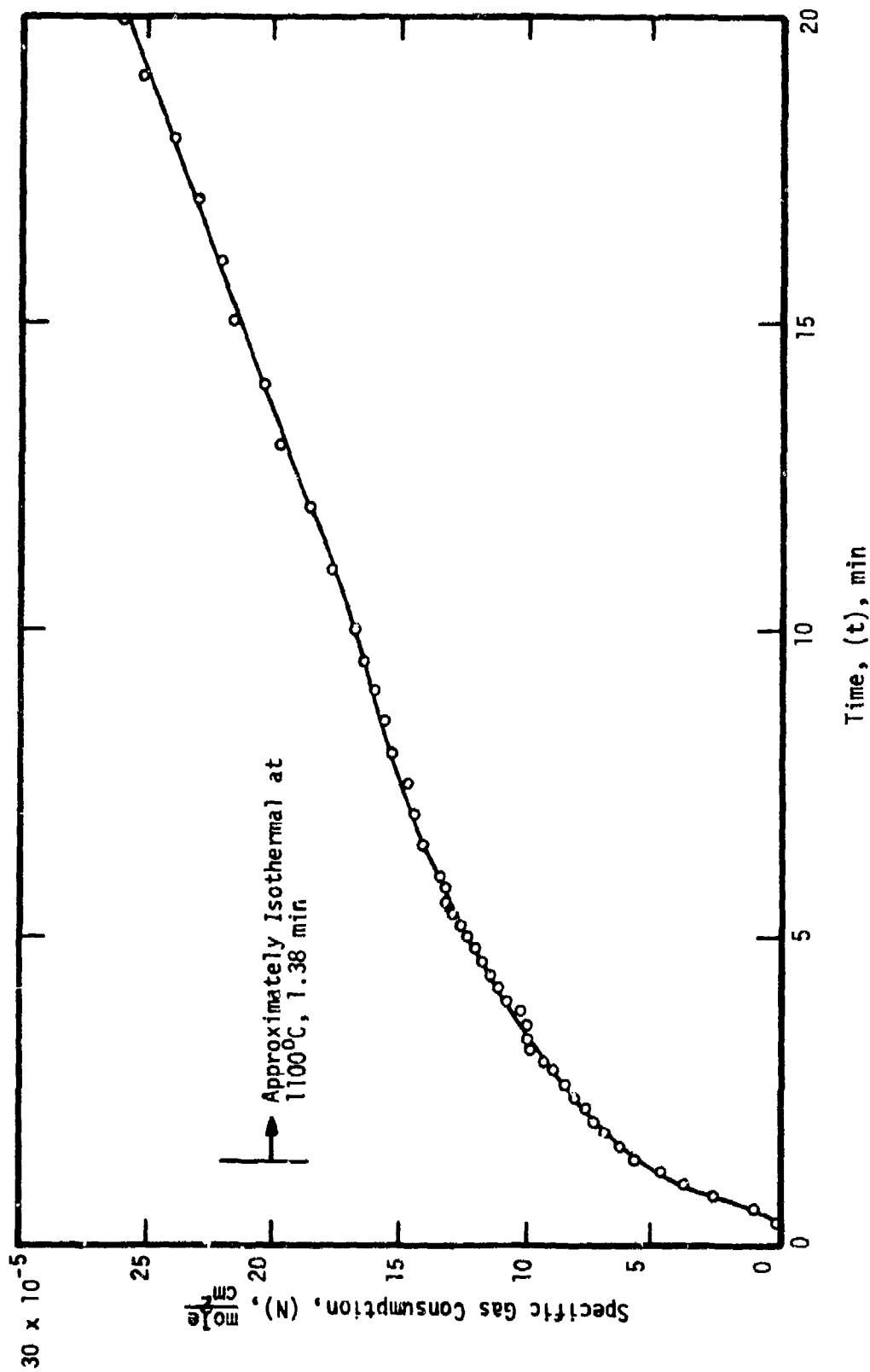


Figure 135.- Initial behavior of the specific gas consumption (N) for Ti-6Al-4V alloy (Type 1) specimen no. 401092 heated in 200 torr O_2 at the rate of 22°C/s to 1100°C.

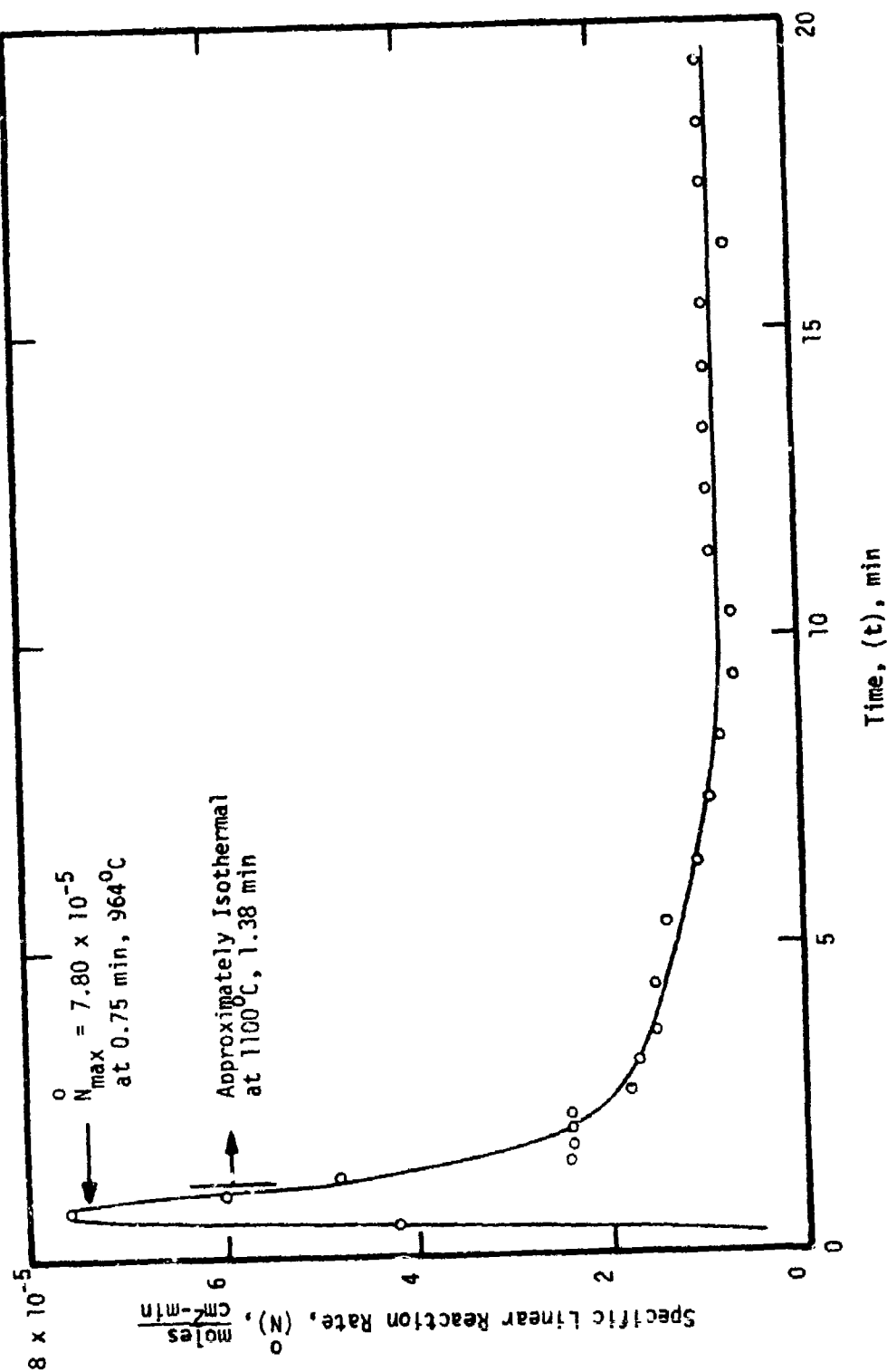


Figure 134.- Initial behavior of the specific linear reaction rate (\bar{N}) for Ti-6Al-4V alloy (Type 1) specimen no. 401092 heated in 200 torr O_2 at the rate of 22°C/s to 1100°C .

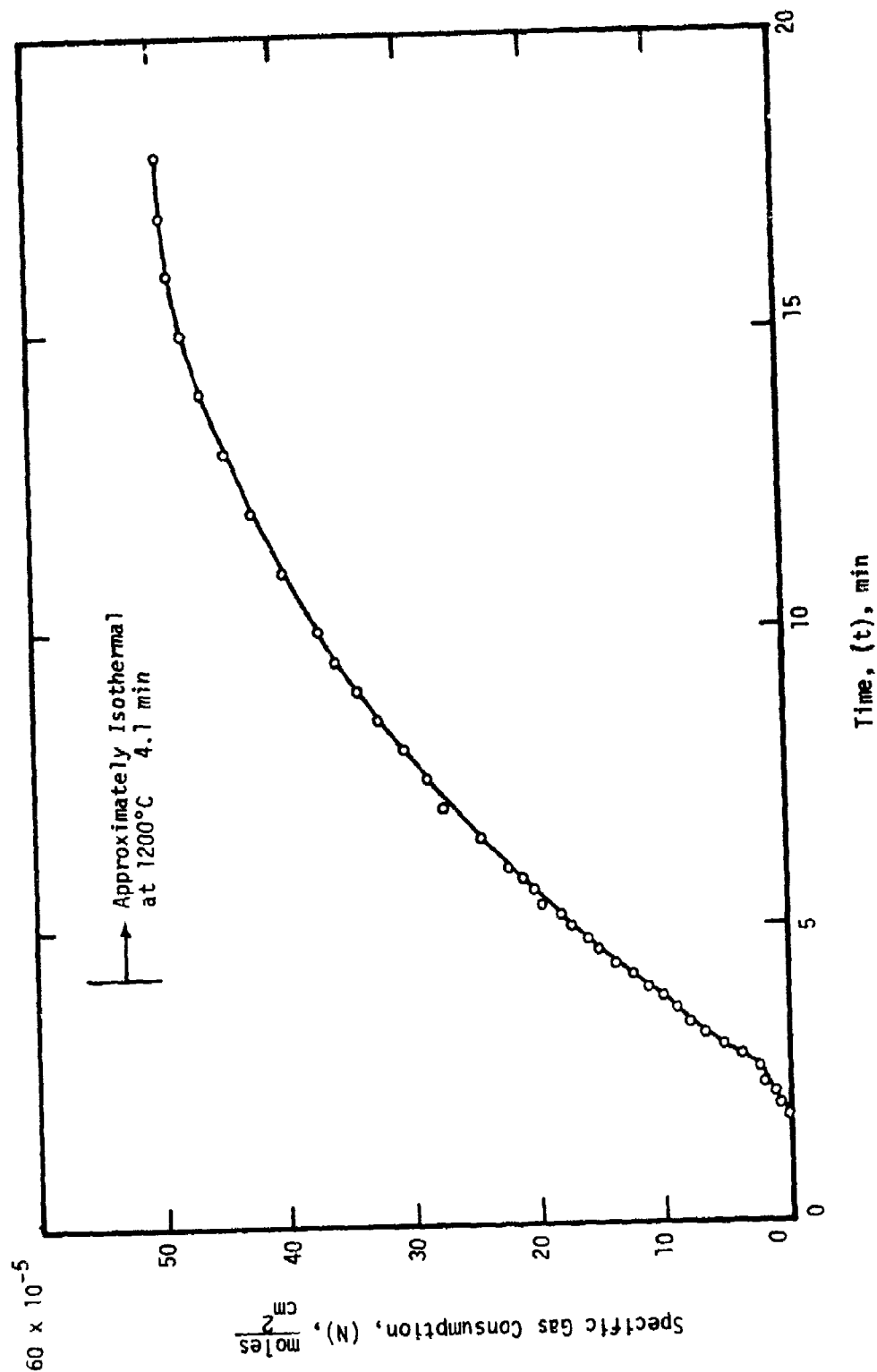


Figure 135.- Initial behavior of the specific gas consumption (N) for Ti-6Al-4V alloy (Type 1) specimen no. 407243 heated in 200 torr O_2 at the rate of 5.9°C/s to 1200°C. Material milled from .152 cm. to .119 cm.

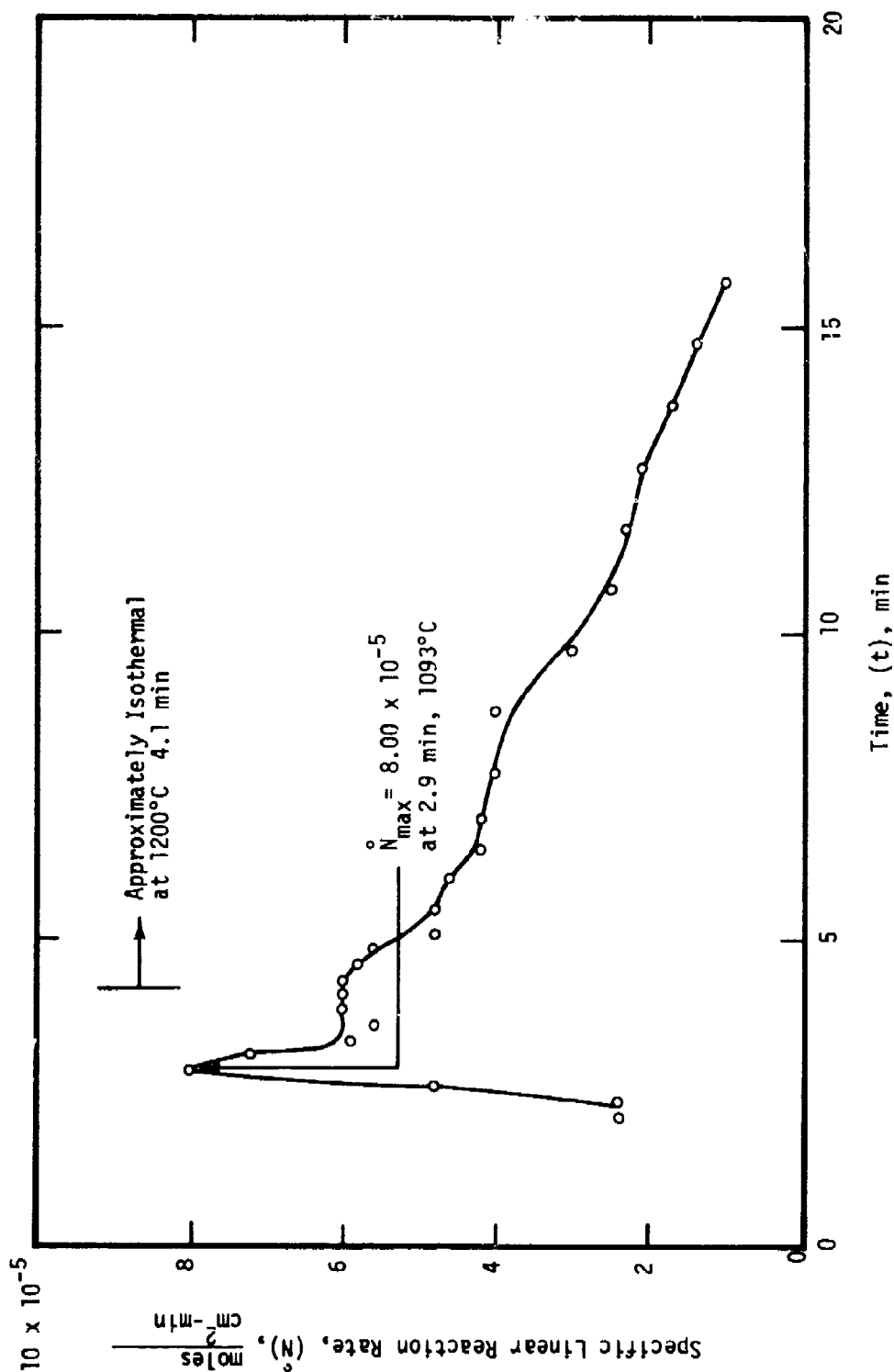


Figure 136.- Initial behavior of the specific linear reaction rate (\bar{N}) for Ti-6Al-4V alloy (Type 1) specimen no. 407243 heated in 200 torr O_2 at the rate of 5.9°C/s to 1200°C. Material milled from .152 cm to .119 cm.

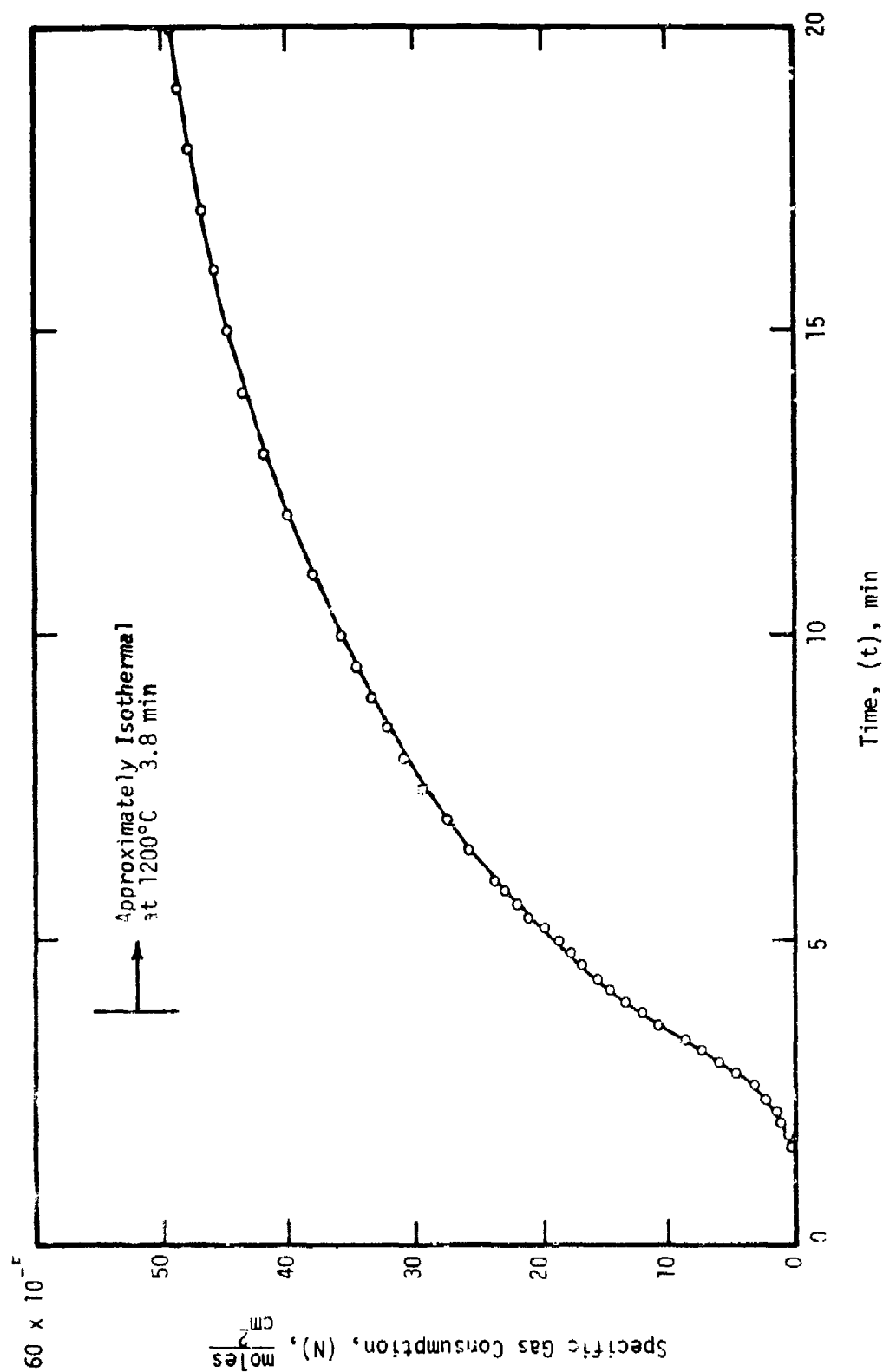


Figure 137.- Initial behavior of the specific gas consumption (N) for Ti-6Al-4V alloy (Type 1) specimen no. 408081 heated in 200 torr O_2 at the rate of 5.9°C/s to 1200°C . Material milled from .152 cm to .119 cm.

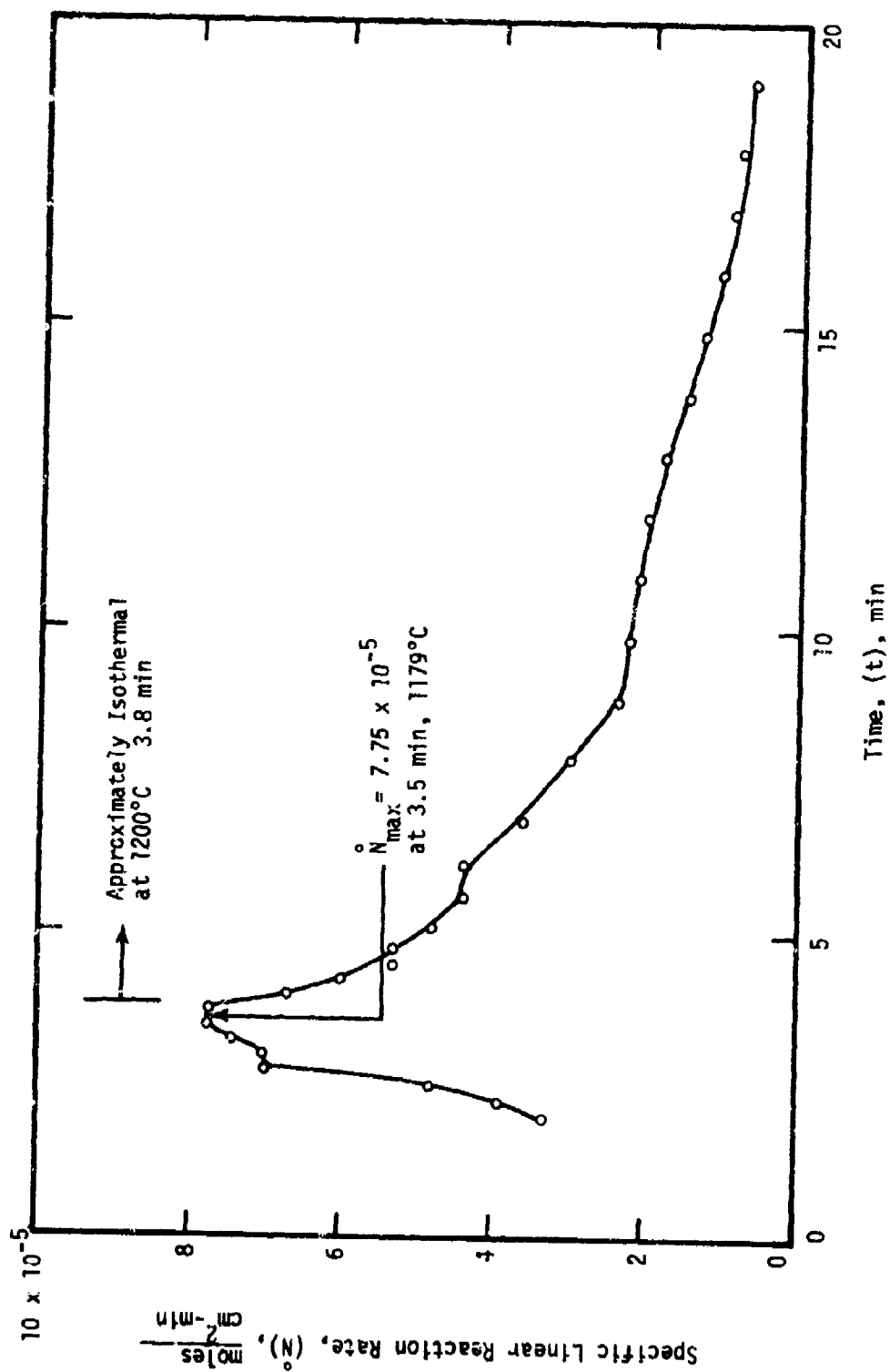


Figure 138.- Initial behavior of the specific linear reaction rate (\dot{N}) for Ti-6Al-4V alloy (Type 1) specimen no. 408081 heated in 200 torr O_2 at the rate of 5.9°C/s to 1200°C. Material milled from .152 cm to .119 cm.

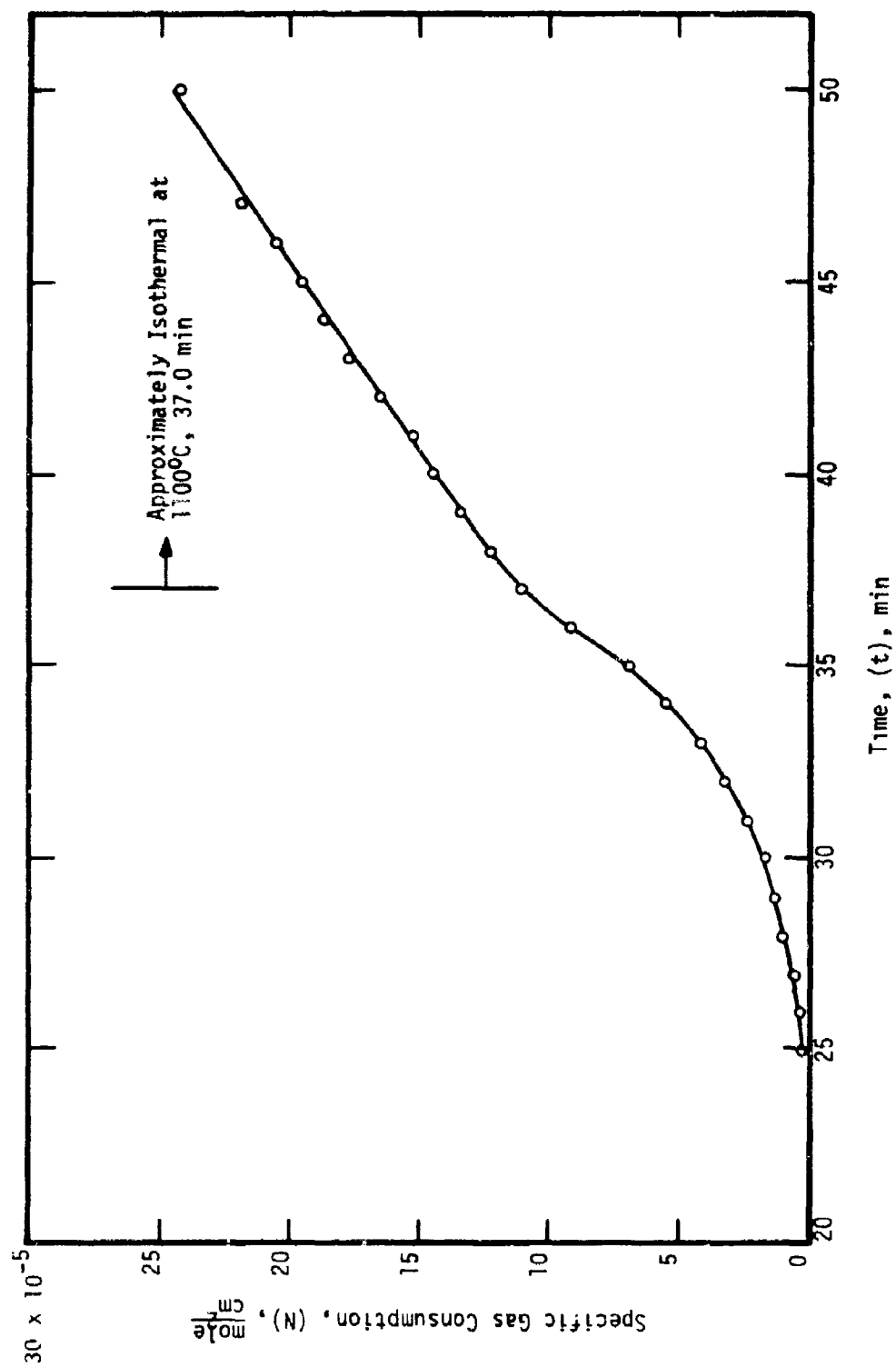


Figure 139.- Initial behavior of the specific gas consumption (N) for Ti-6Al-4V alloy (Type 2) specimen no. 402042 heated in 200 torr O_2 at the rate of $0.5^\circ\text{C}/\text{s}$ to 1100°C .

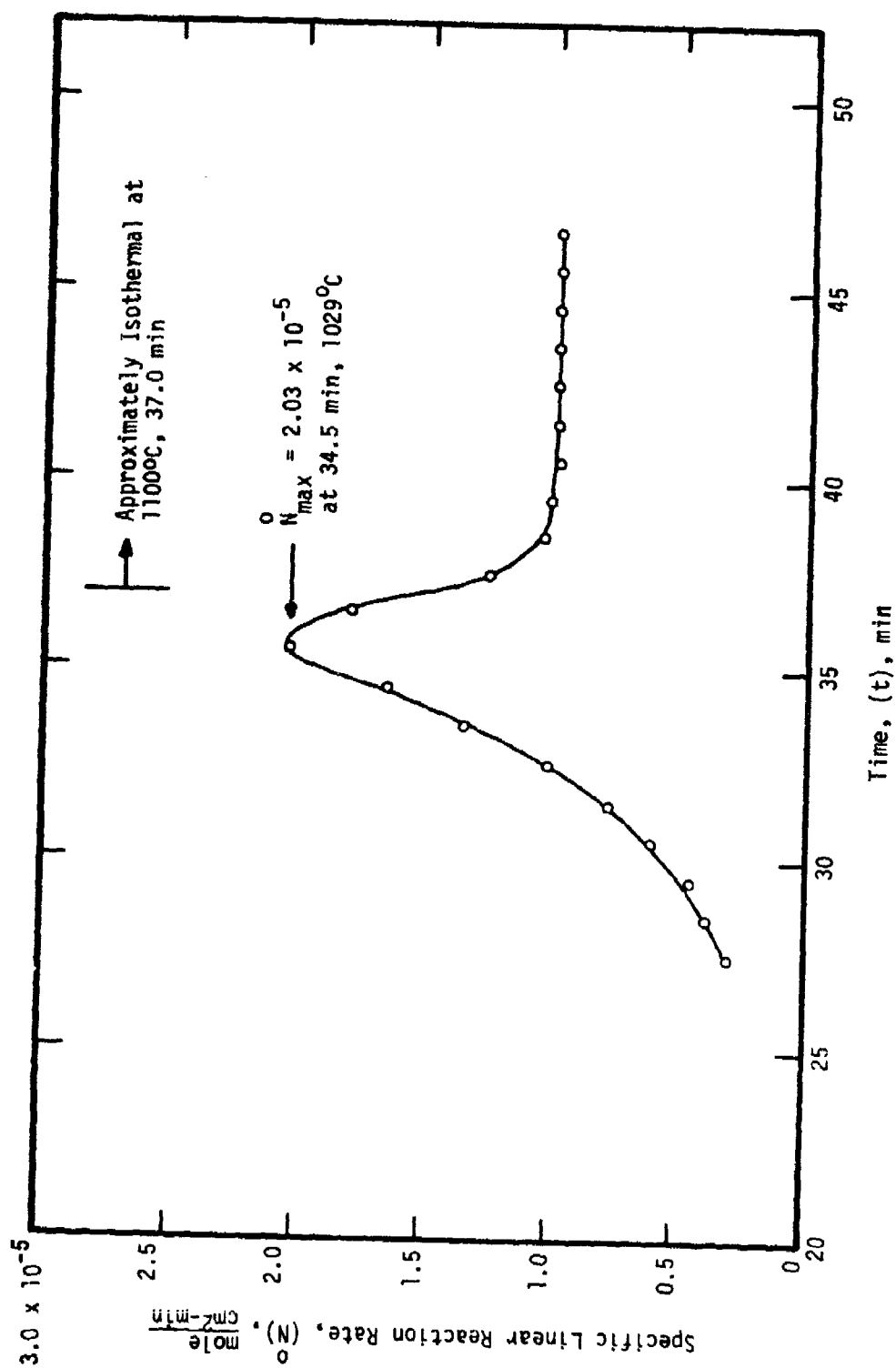


Figure 140.- Initial behavior of the specific linear reaction rate (\bar{N}) for Ti-6Al-4V alloy (Type 2) specimen no. 402042 heated in 200 torr O_2 at the rate of 0.5°C/s to 1100°C.

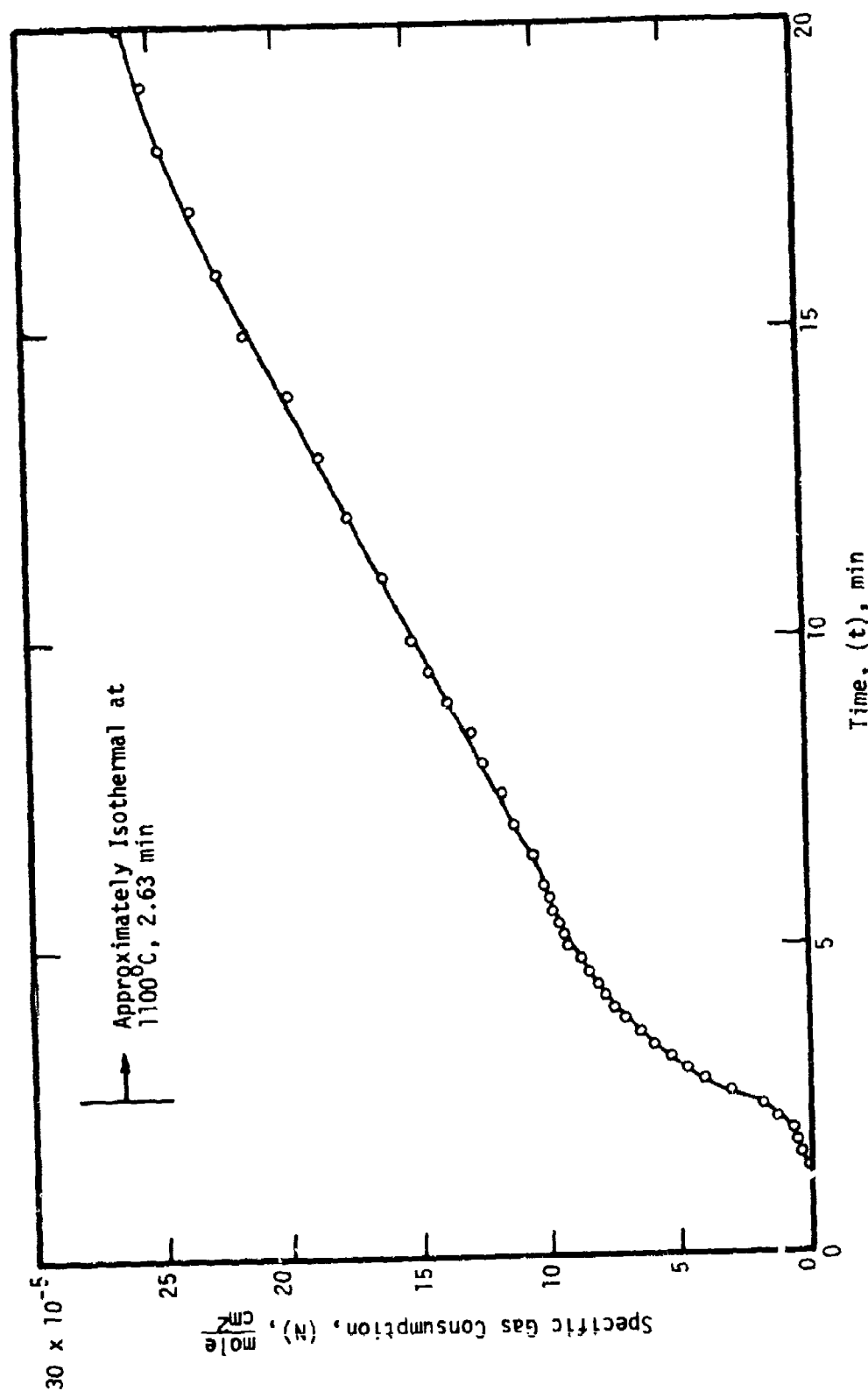


Figure 141.- Initial behavior of the specific gas consumption (N) for Ti-6Al-4V alloy (Type 2) specimen no. 401152 heated in 200 torr O_2 at the rate of 8°C/s to 1100°C.

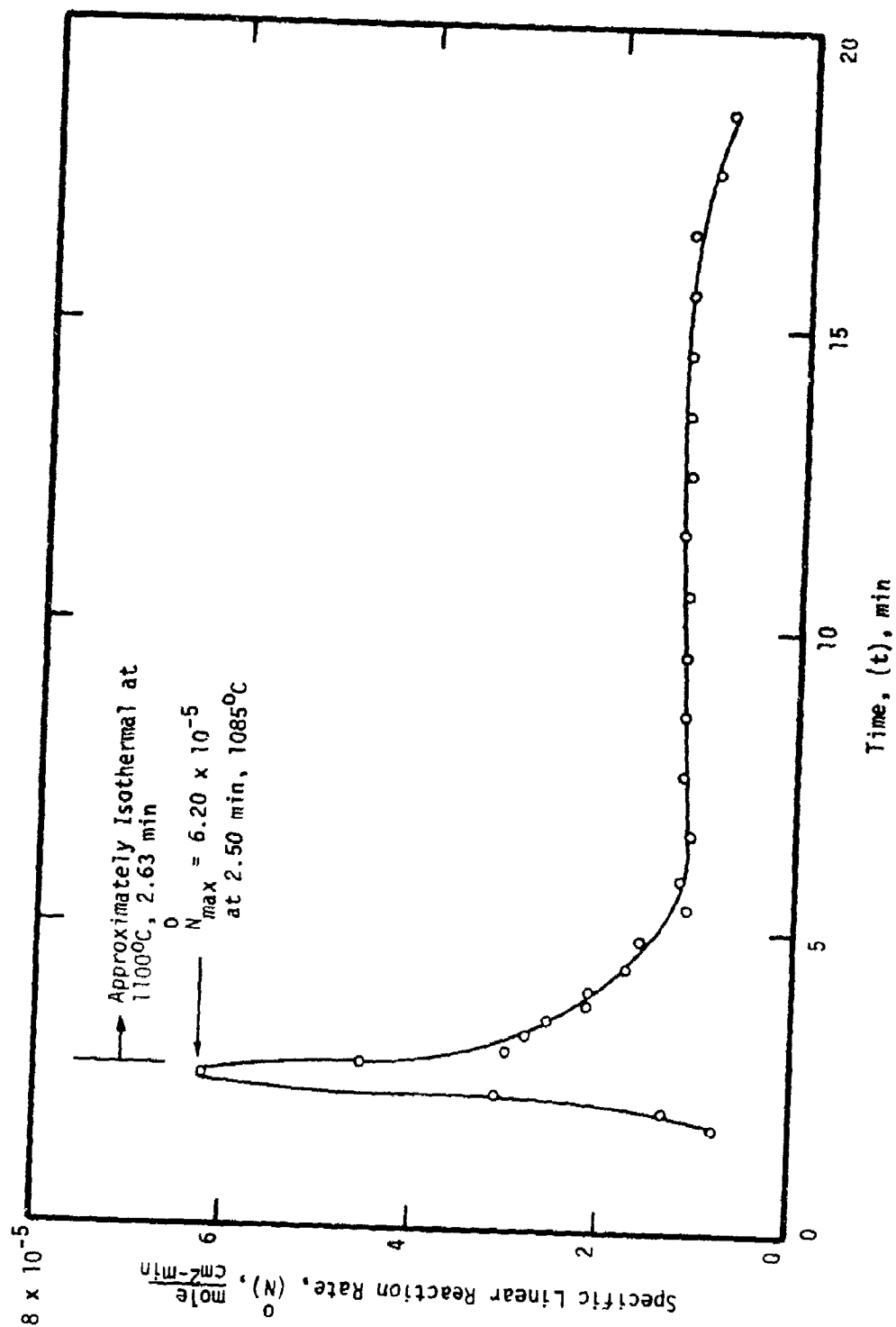


Figure 142.- Initial behavior of the specific linear reaction rate (\dot{N}) for Ti-6Al-4V alloy (Type 2) specimen no. 401152 heated in 200 torr O_2 at the rate of 8°C/s to 1100°C.

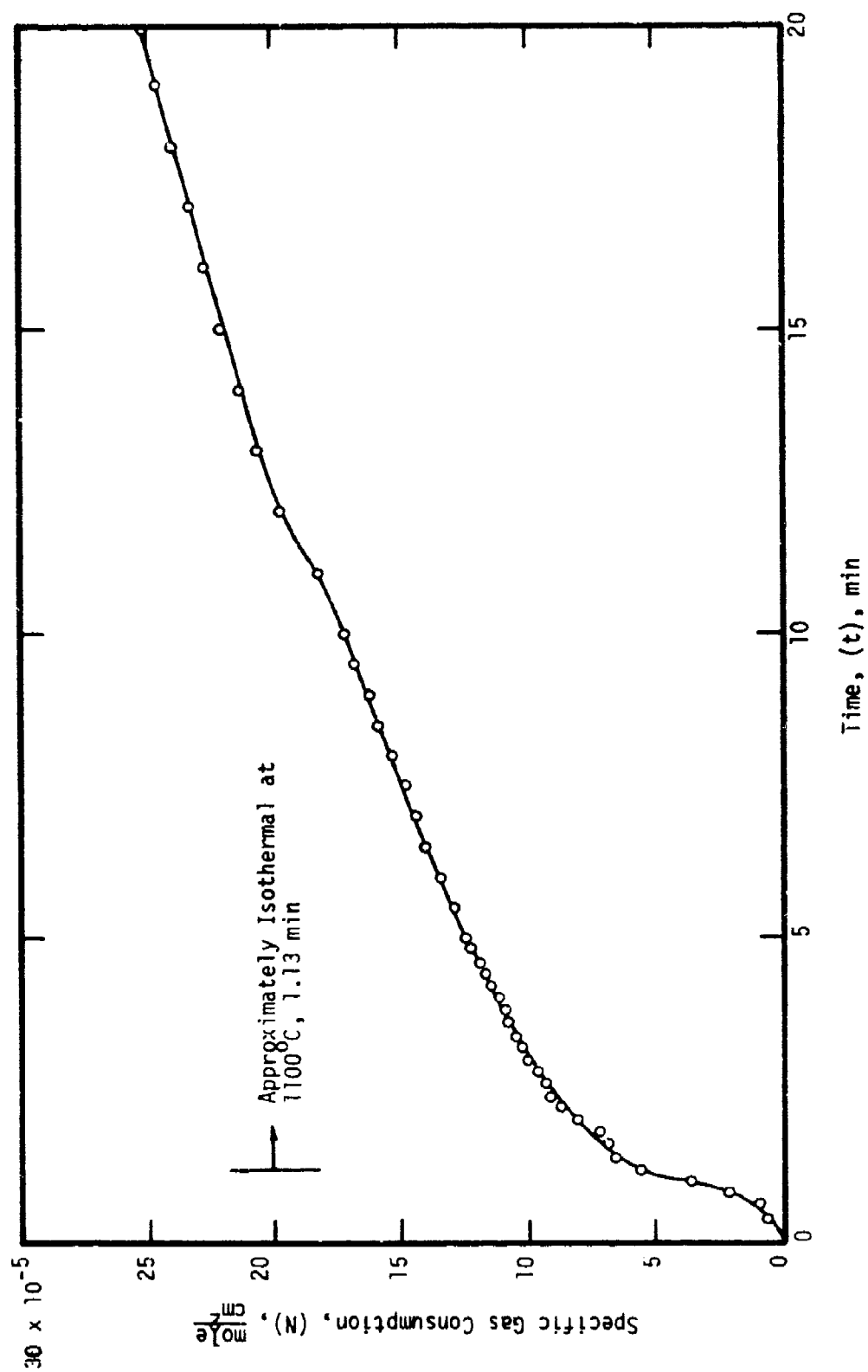


Figure 143.- Initial behavior of the specific gas consumption (N) for Ti-6Al-4V alloy (Type 2) specimen no. 402043 heated in 200 torr O_2 at the rate of 22°C/s to 1100°C .

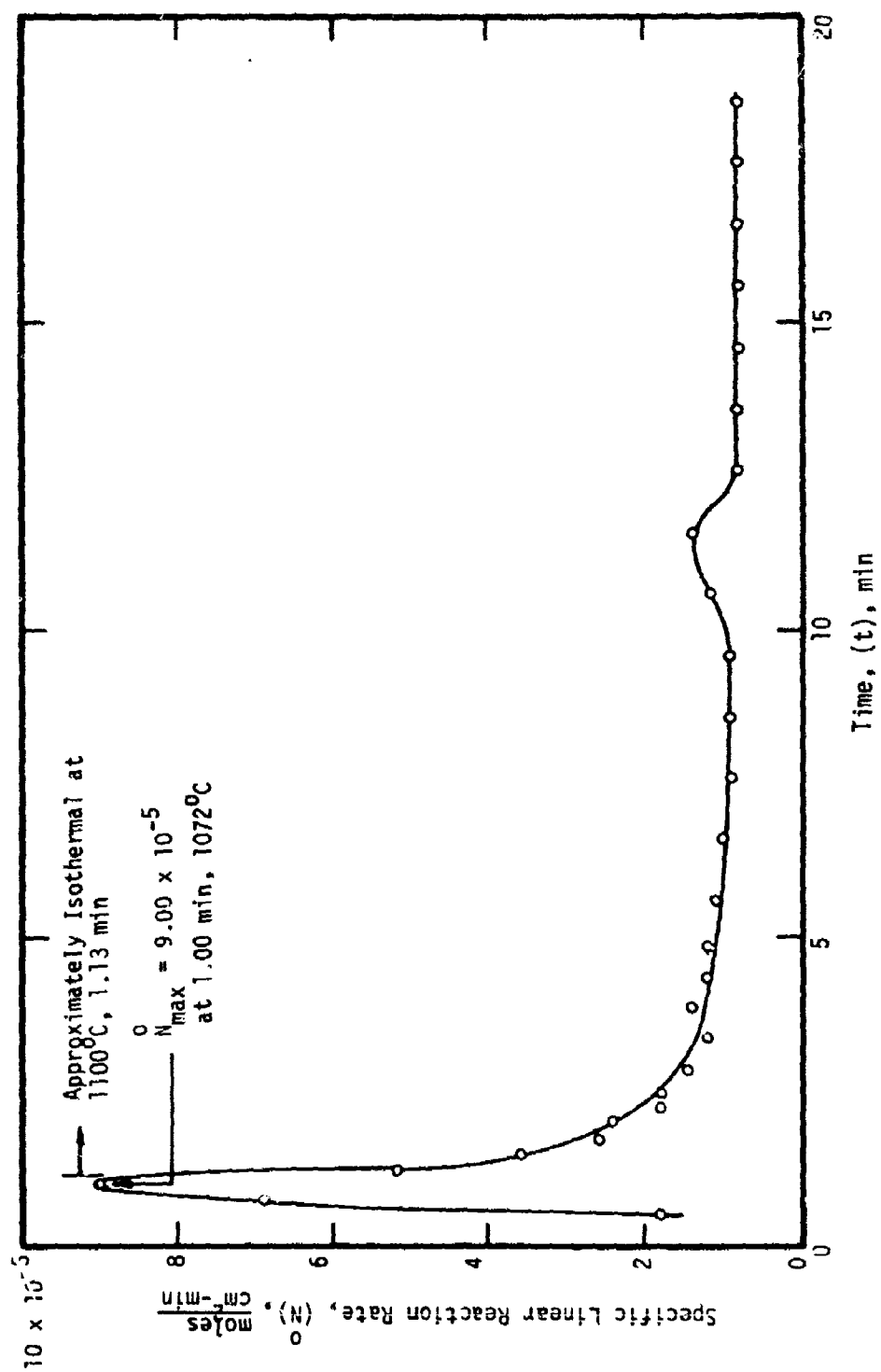


Figure 144.- Initial behavior of the specific linear reaction rate (\dot{N}) for T1-6Al-4V alloy (Type 2) specimen no. 402043 heated in 200 torr O_2 at the rate of 22°C/s to 1100°C.

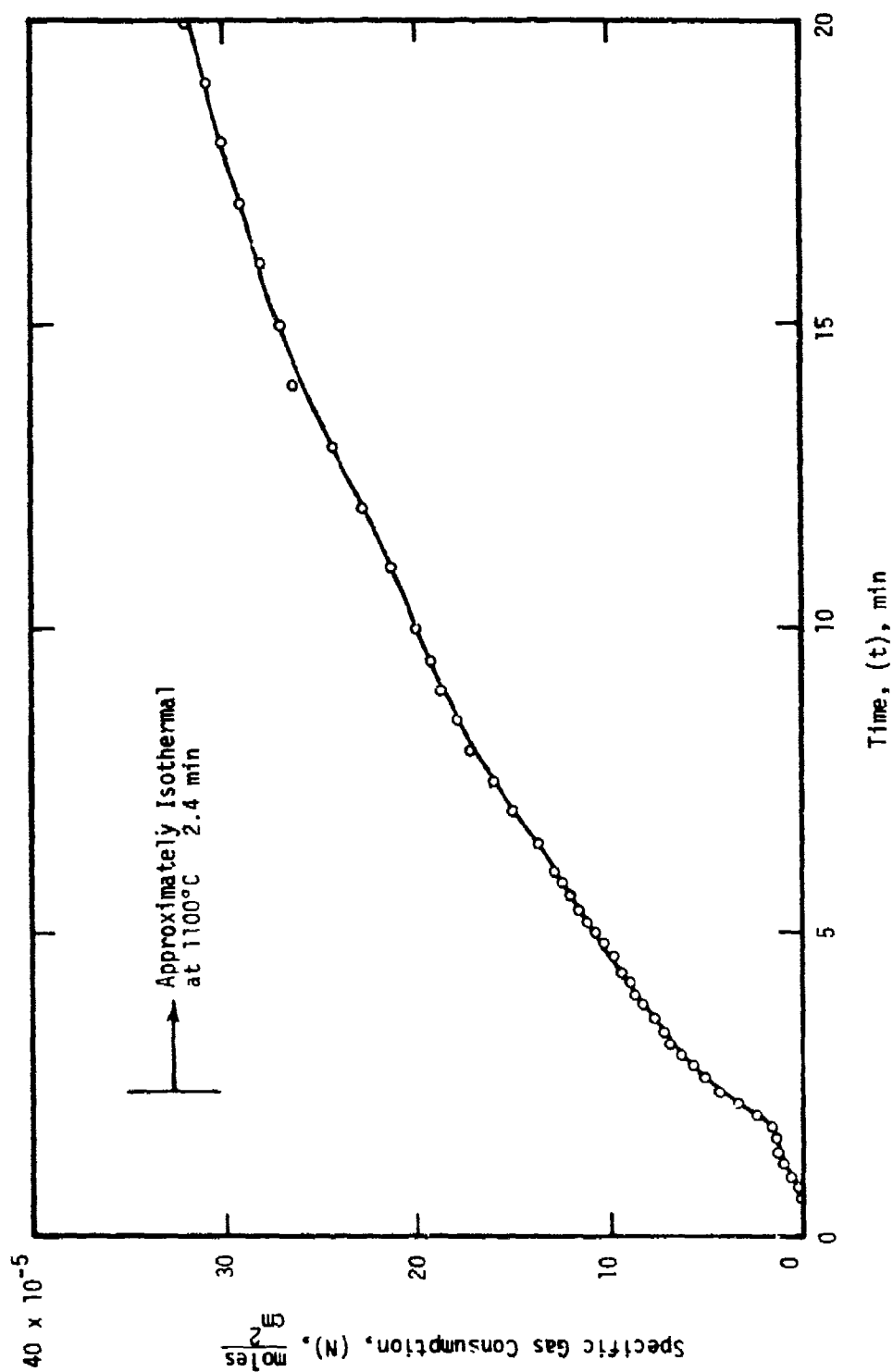


Figure 145.- Initial behavior of the specific gas consumption (N) for Ti-6Al-4V alloy (Type 3) specimen no. 406171 heated in 200 torr O_2 at the rate of 8°C/s to 1100°C.

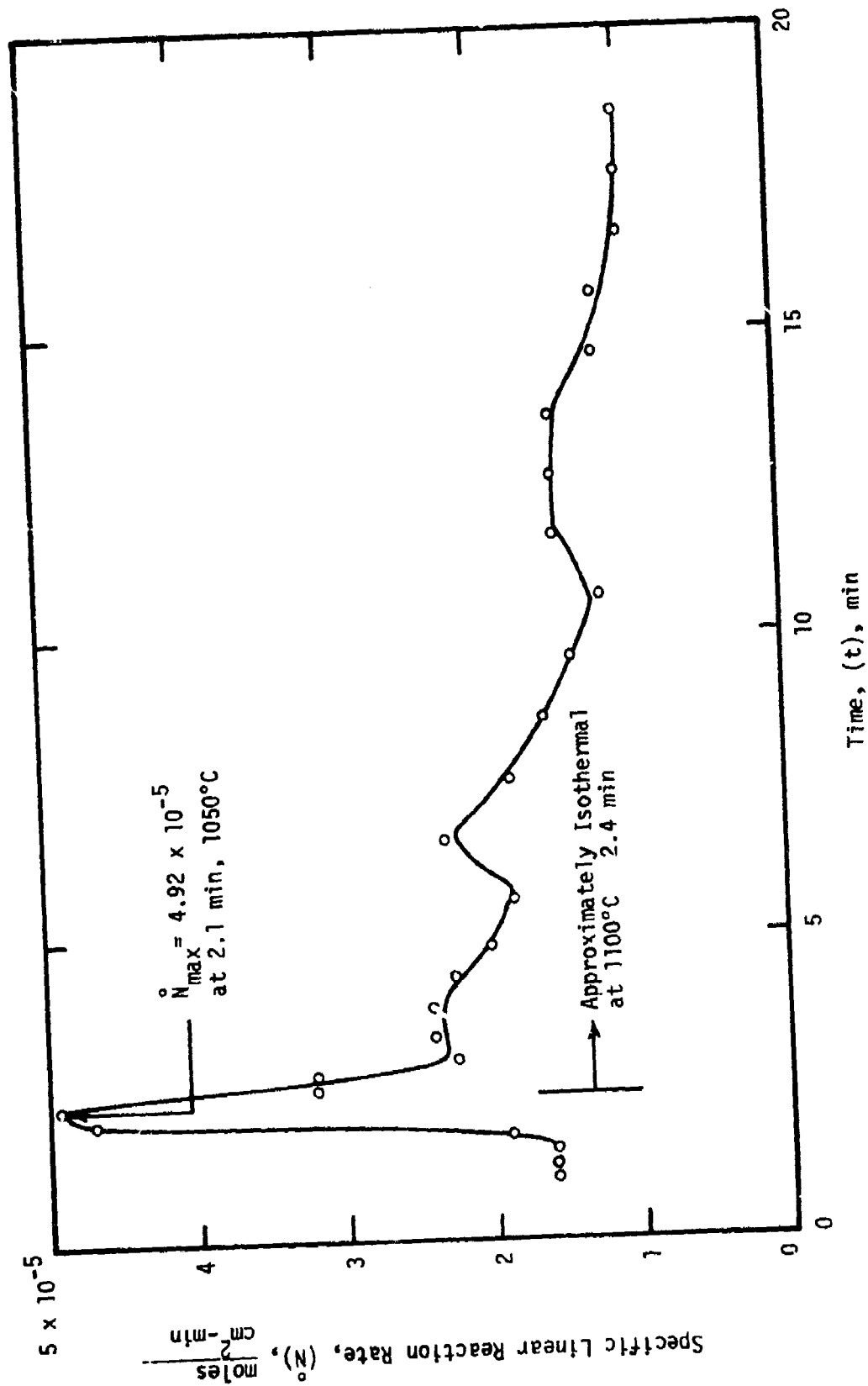


Figure 146.- Initial behavior of the specific linear reaction rate (\dot{N}) for Ti-6Al-4V alloy (Type 3) specimen no. 406171 heated in 200 torr O_2 at the rate of 8°C/s to 1100°C.

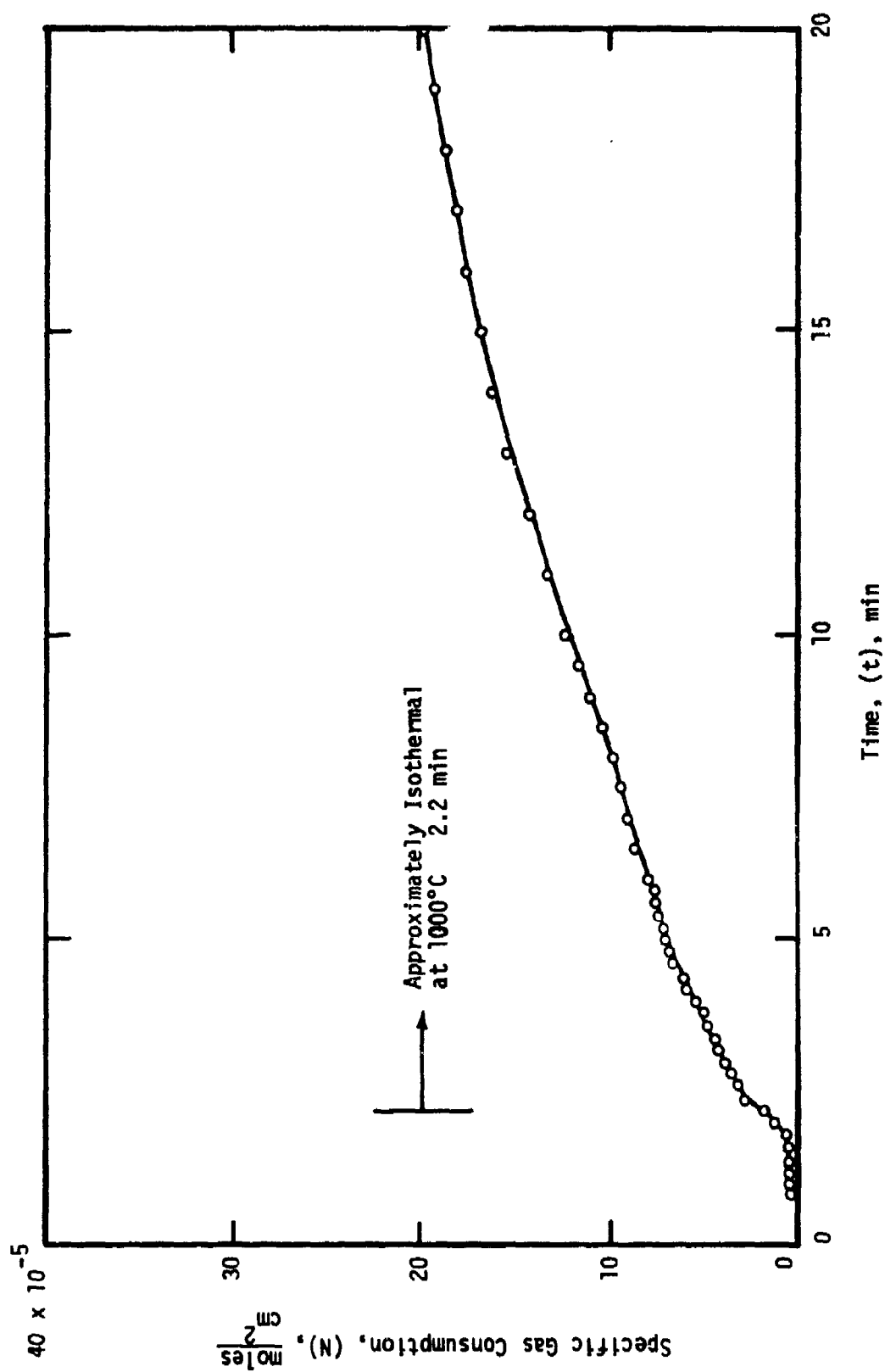


Figure 147.- Initial behavior of the specific gas consumption (N) for Ti-8Mn alloy specimen no. 406032 heated in 200 torr O_2 at the rate of 8°C/s to 1000°C .

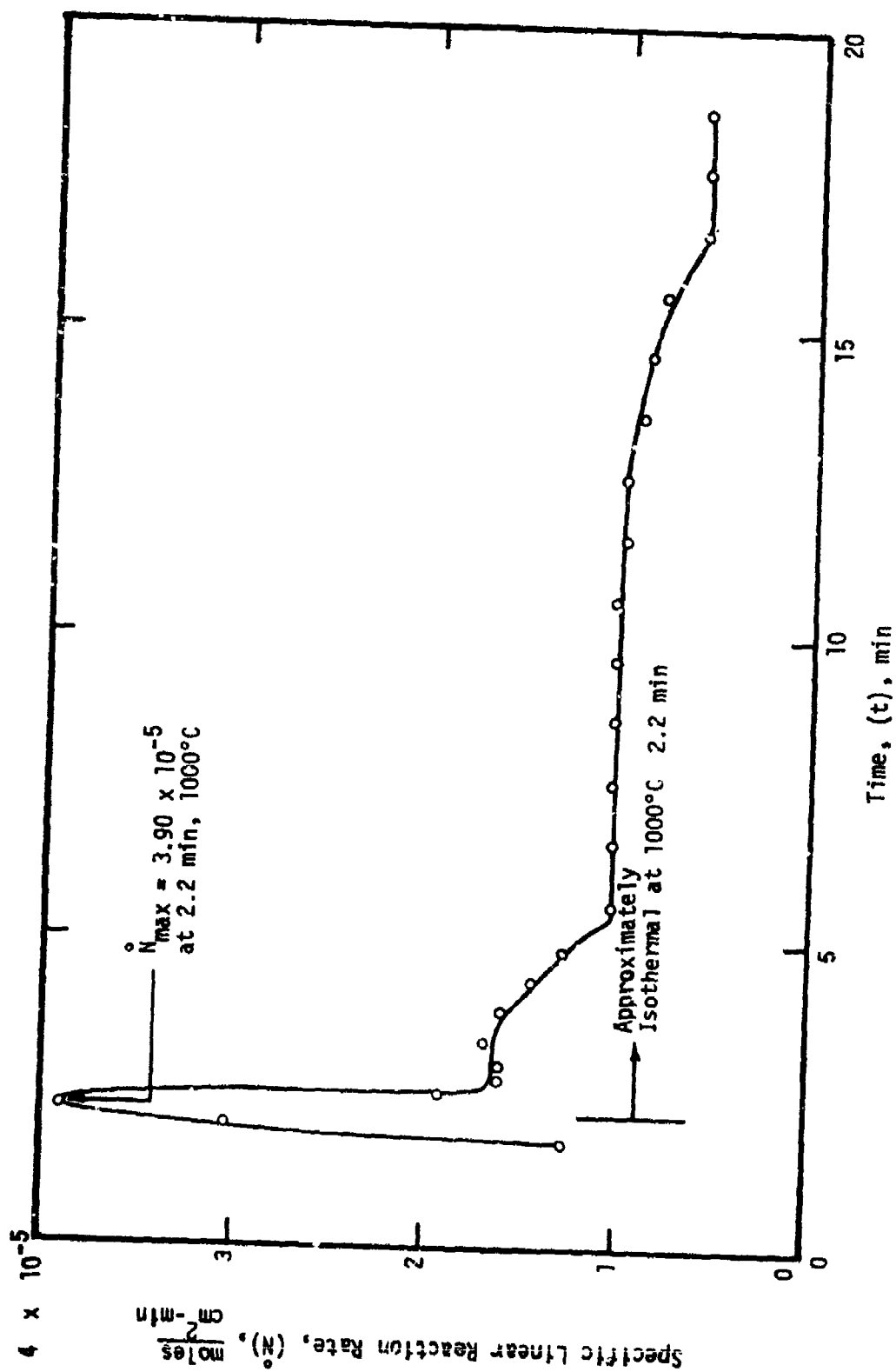


Figure 148.- Initial behavior of the specific linear reaction rate (\dot{N}) for Ti-8Mn alloy specimen no. 406032 heated in 200 torr O_2 at the rate of 8°C/s to 1000°C .

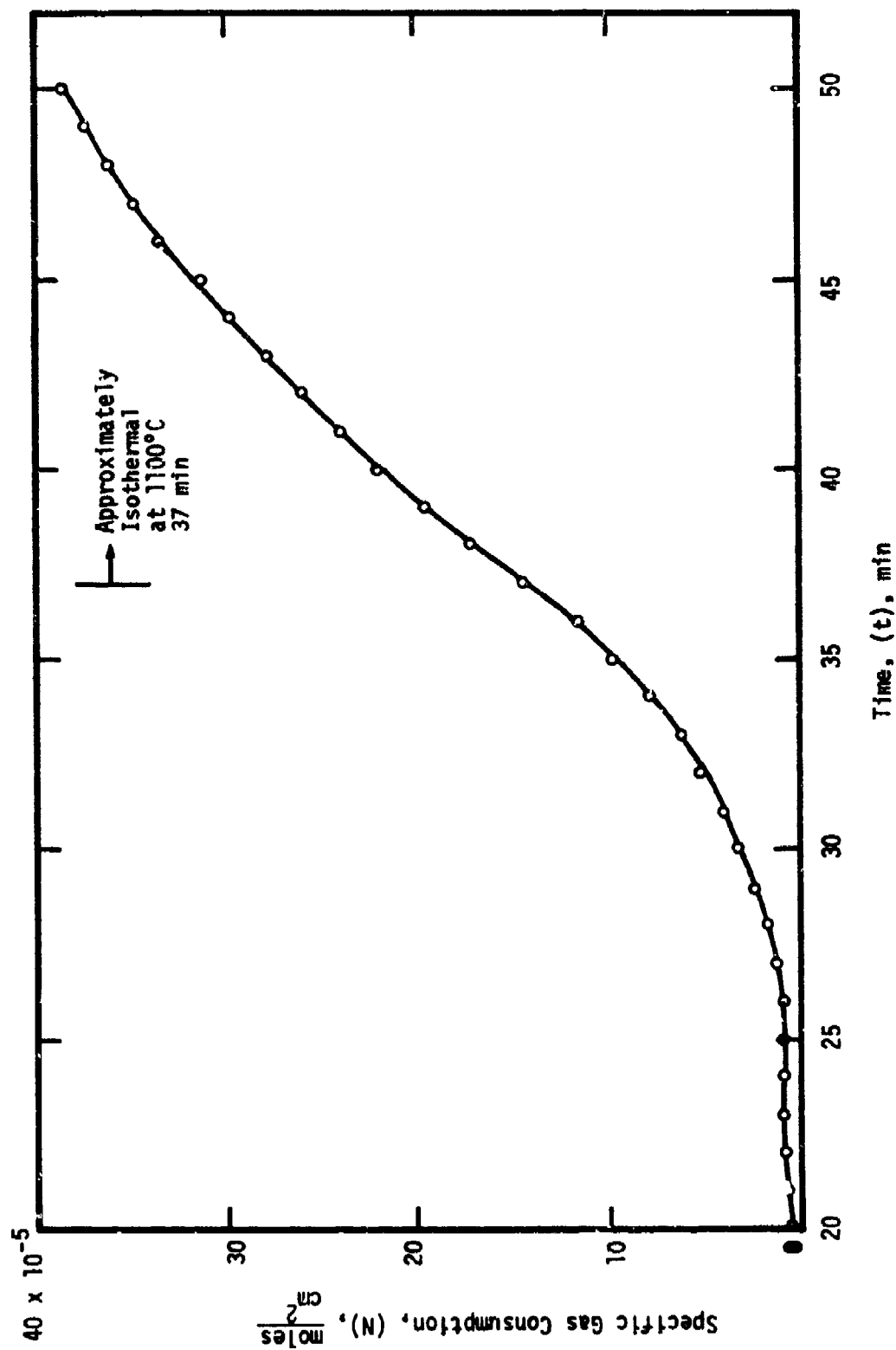


Figure 149.- Initial behavior of the specific gas consumption (N) for Ti-8Mn alloy specimen no. 405074 heated in 200 torr O_2 at the rate of 0.5°C/s to 1100°C .

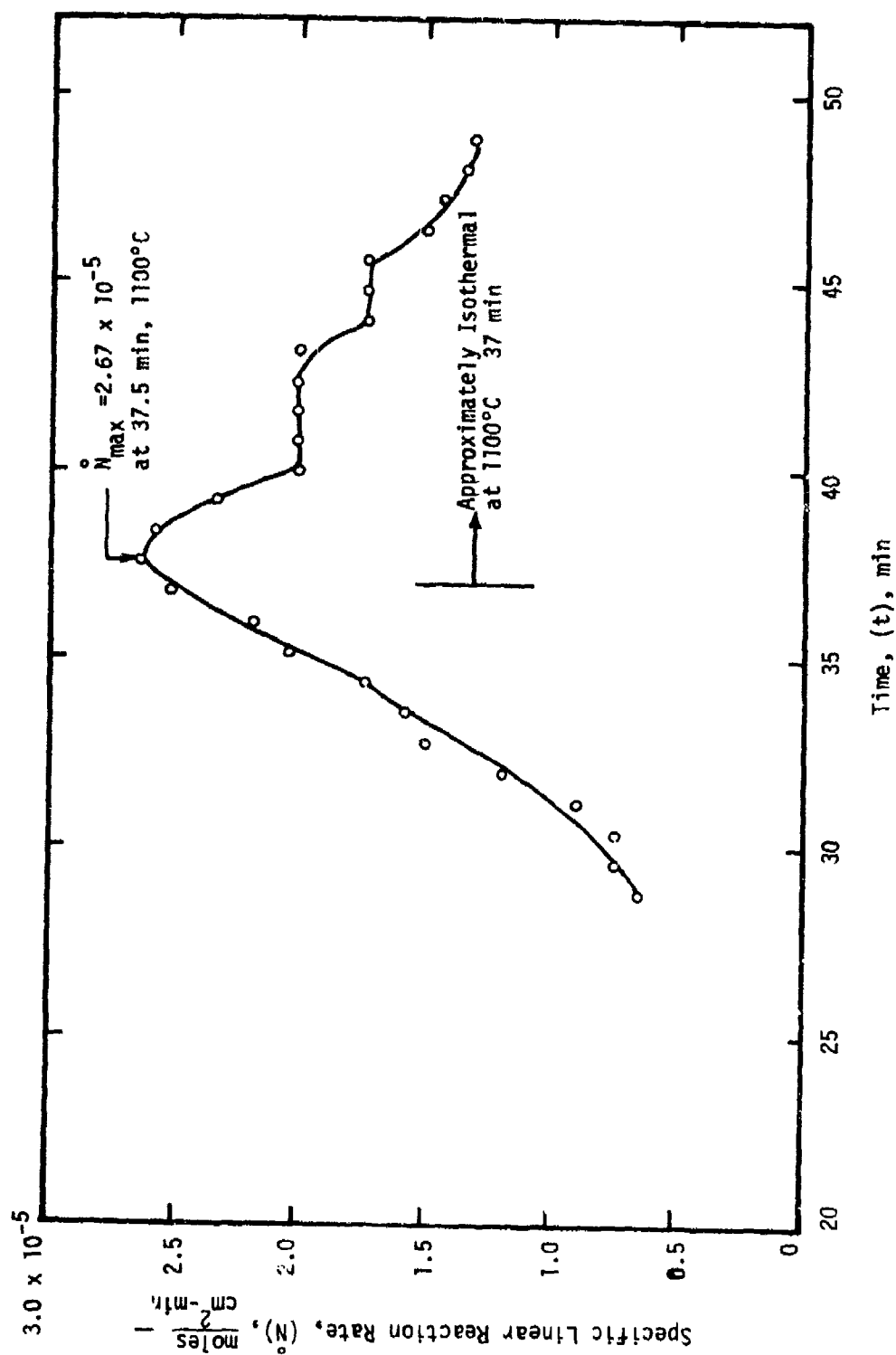


Figure 150.- Initial behavior of the specific linear reaction rate (\bar{N}) for Ti-8Mn alloy specimen no. 4C5074 heated in 200 torr O_2 at the rate of 0.5°C/s to 1100°C .

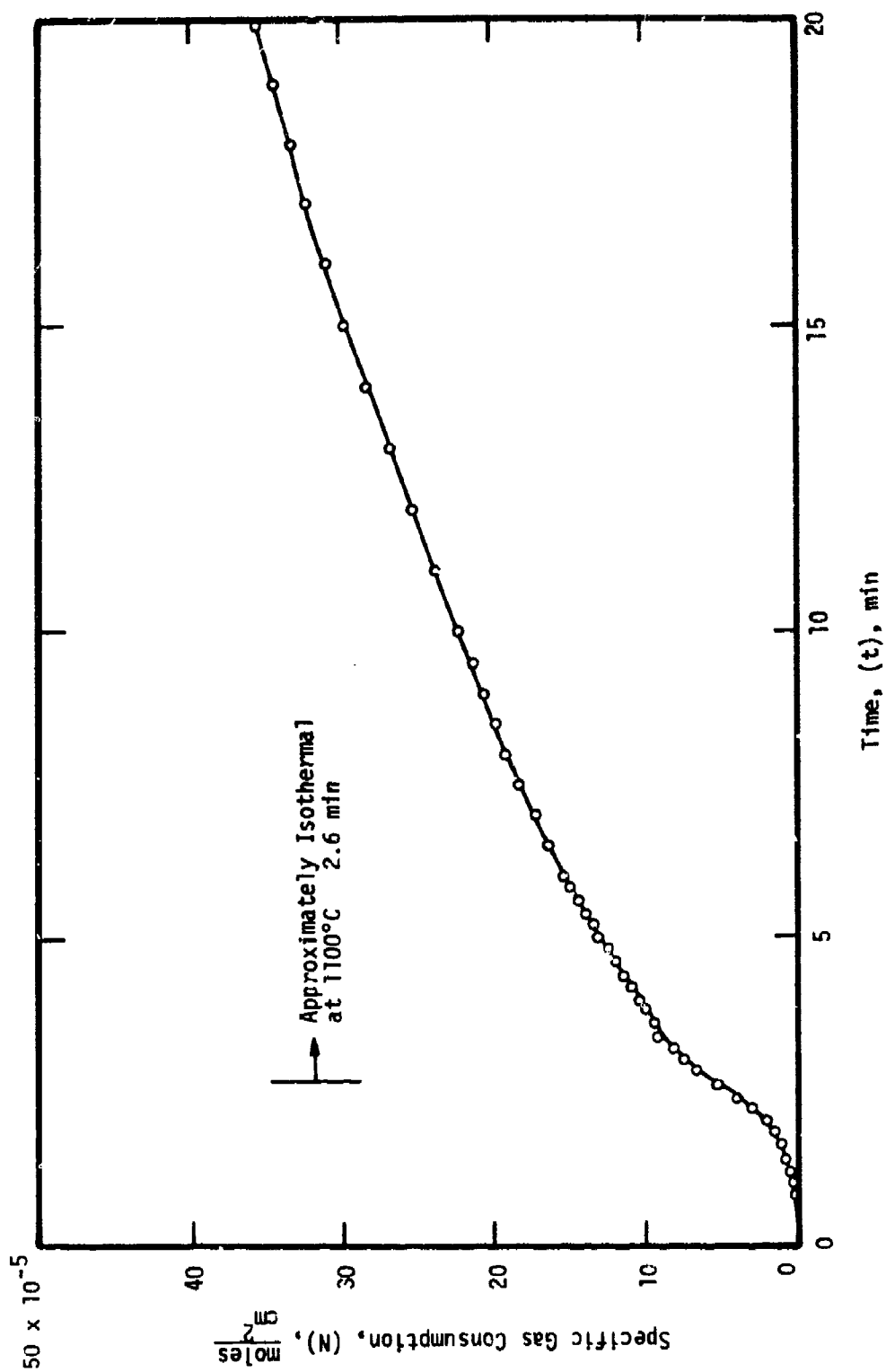


Figure 151.- Initial behavior of the specific gas consumption (N) for Ti-8Mn alloy specimen no. 405073 heated in 200 torr O_2 at the rate of 8°C/s to 1100°C.

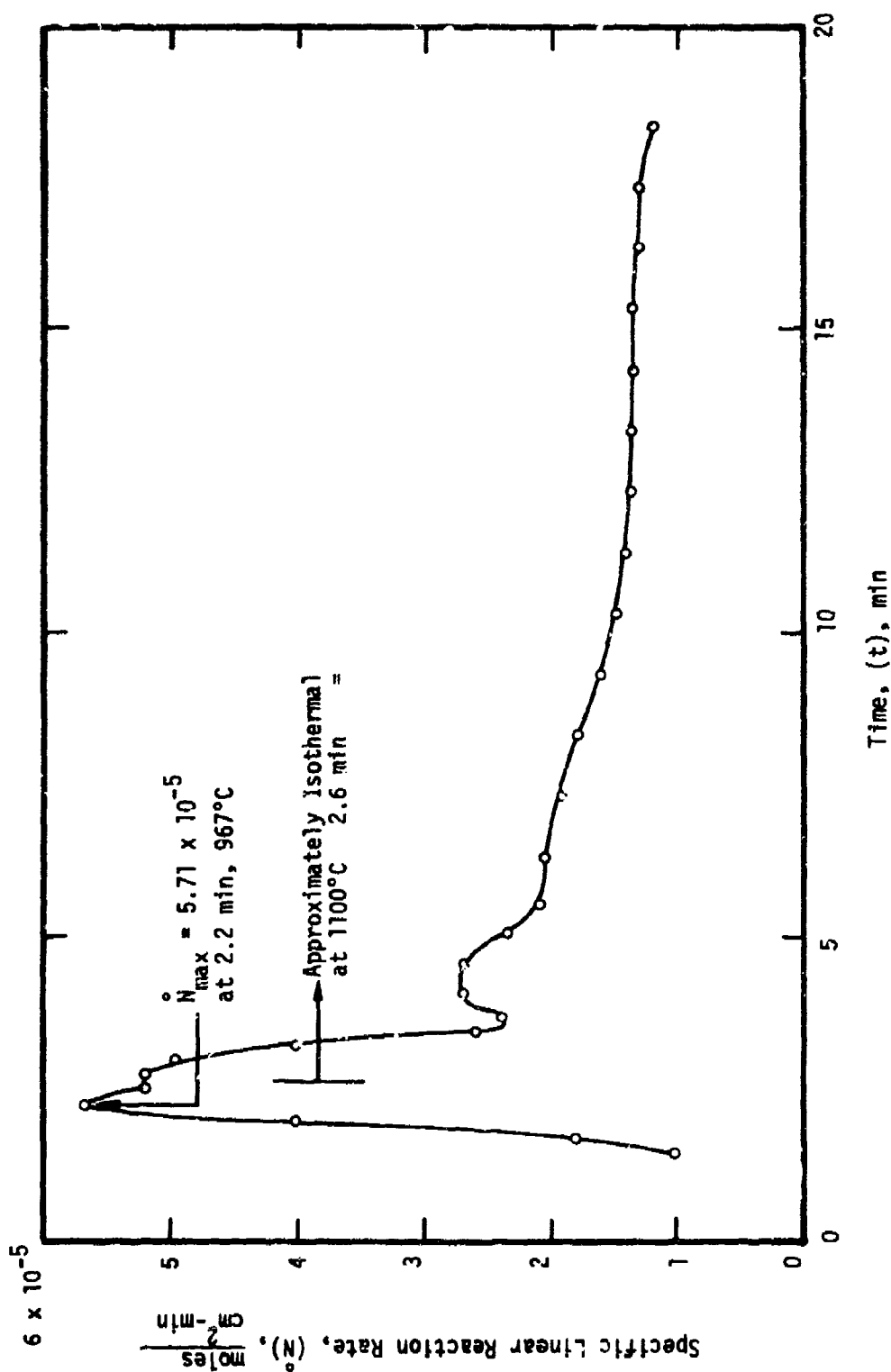


Figure 152.- Initial behavior of the specific linear reaction rate (\dot{N}) for Ti-8Mn alloy specimen no. 405073 heated in 200 torr O_2 at the rate of 8°C/s to 1100°C.

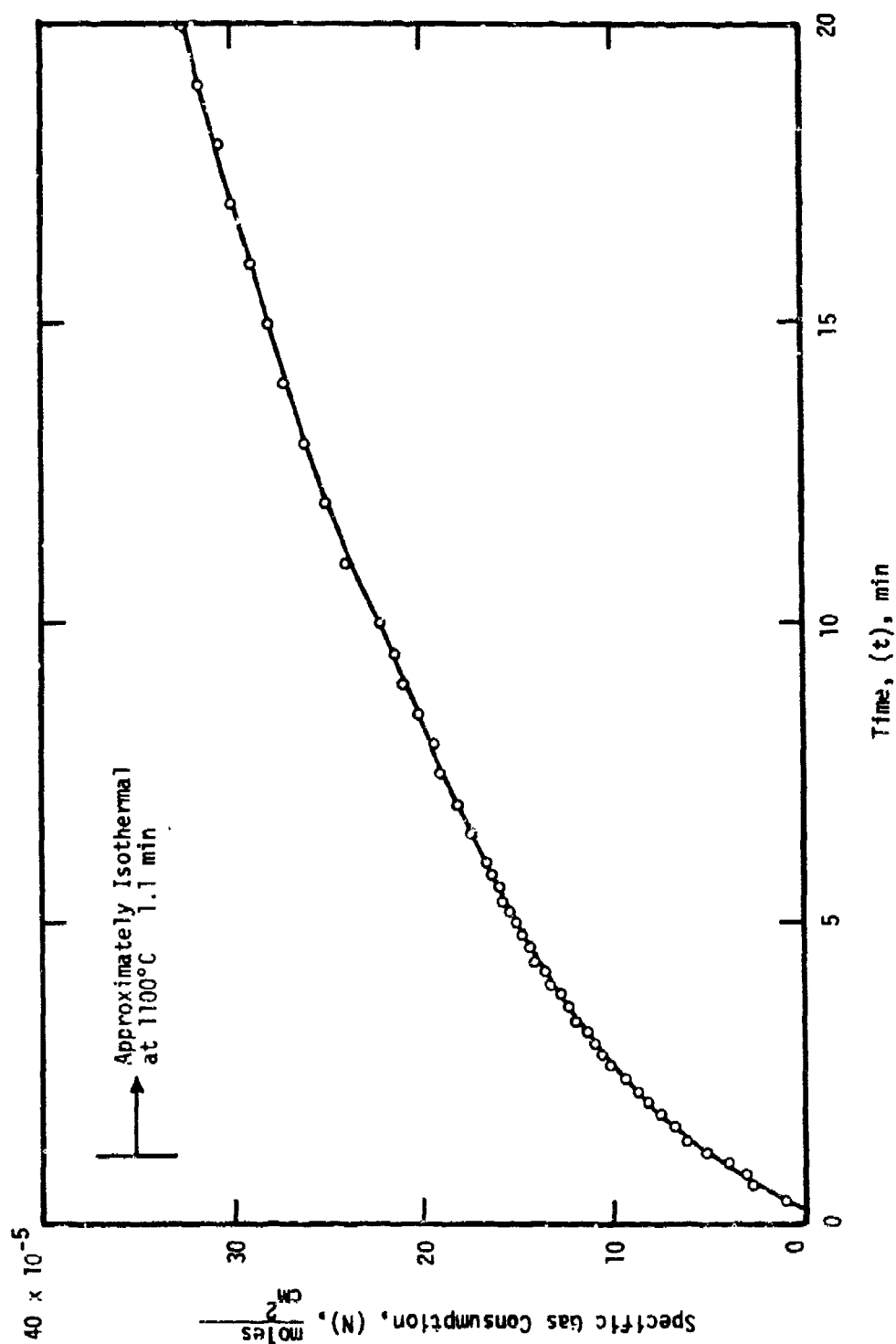


Figure 153.- Initial behavior of the specific gas consumption (N) for Ti-8Mn alloy specimen no. 406031 heated in 200 torr O_2 at the rate of $22^\circ C/s$ to $1100^\circ C$.

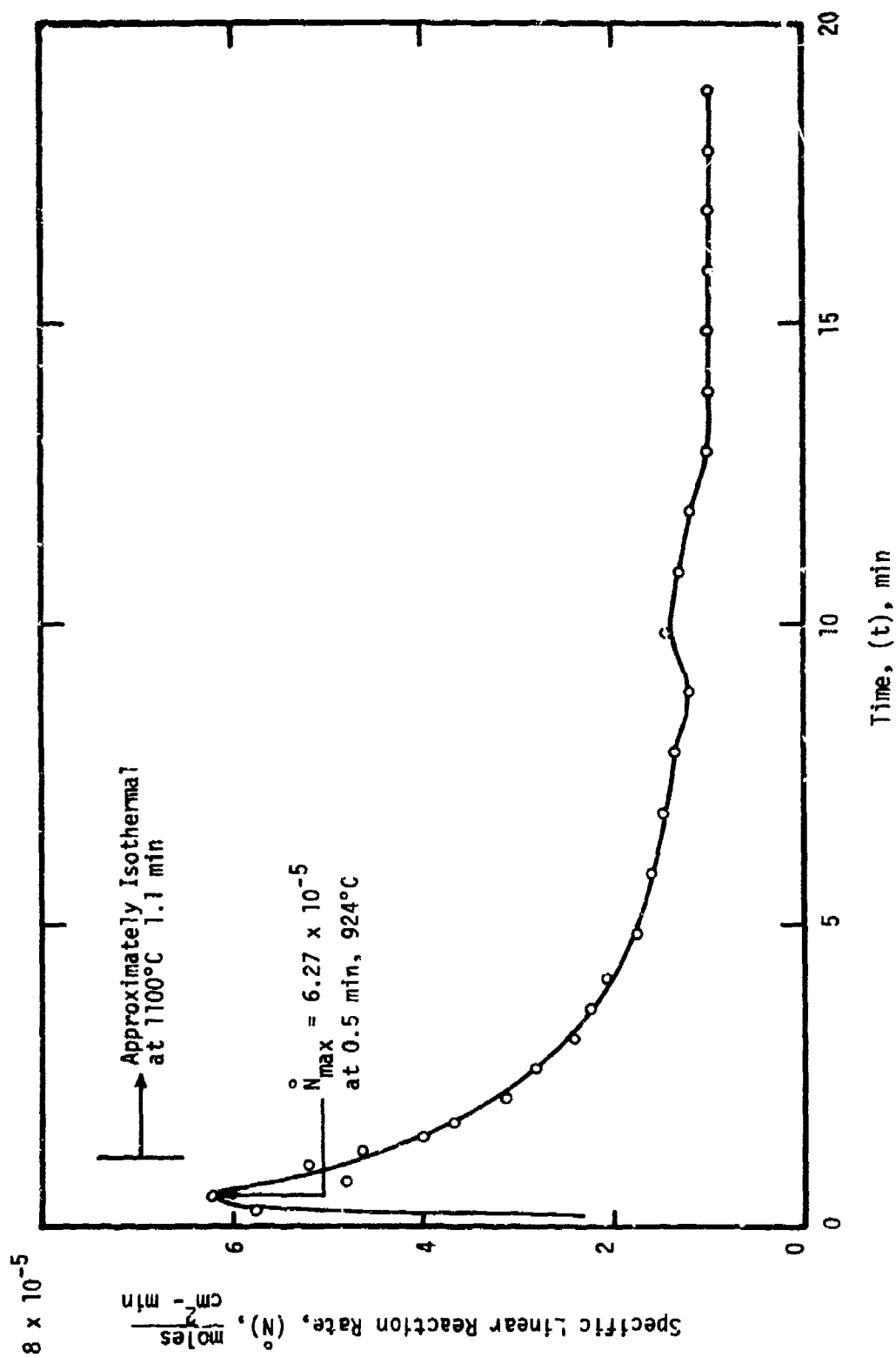


Figure 154.- Initial behavior of the specific linear reaction rate (\dot{N}) for Ti-8Mn alloy specimen no. 406031 heated in 200 torr U_2 at the rate of 22°C/s to 1100°C .

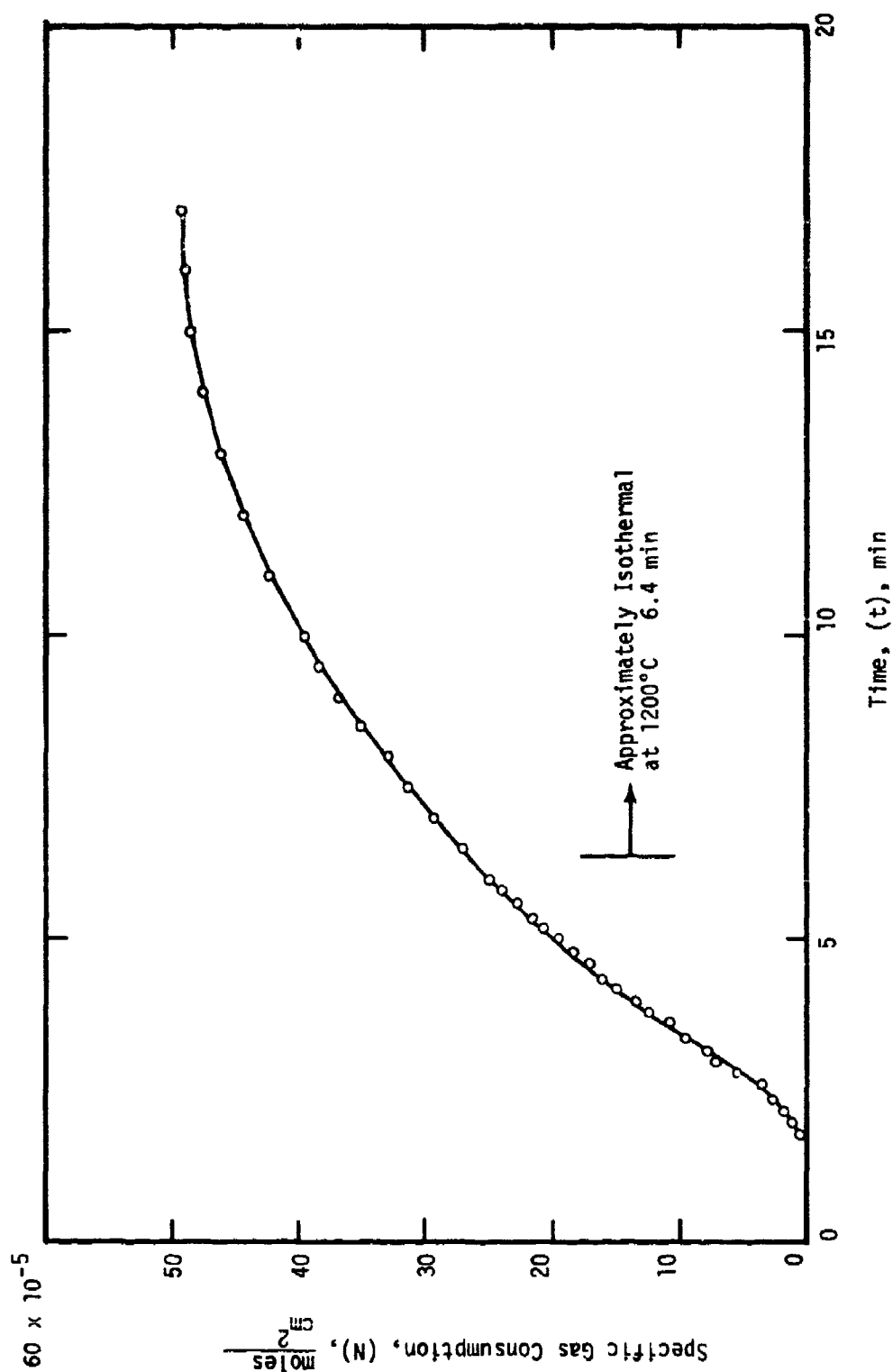


Figure 155.- Initial behavior of the specific gas consumption (N) for Ti-8Mn alloy specimen no. 407242 heated in 200 torr O_2 at the rate of 5.9°C/s to 1200°C.

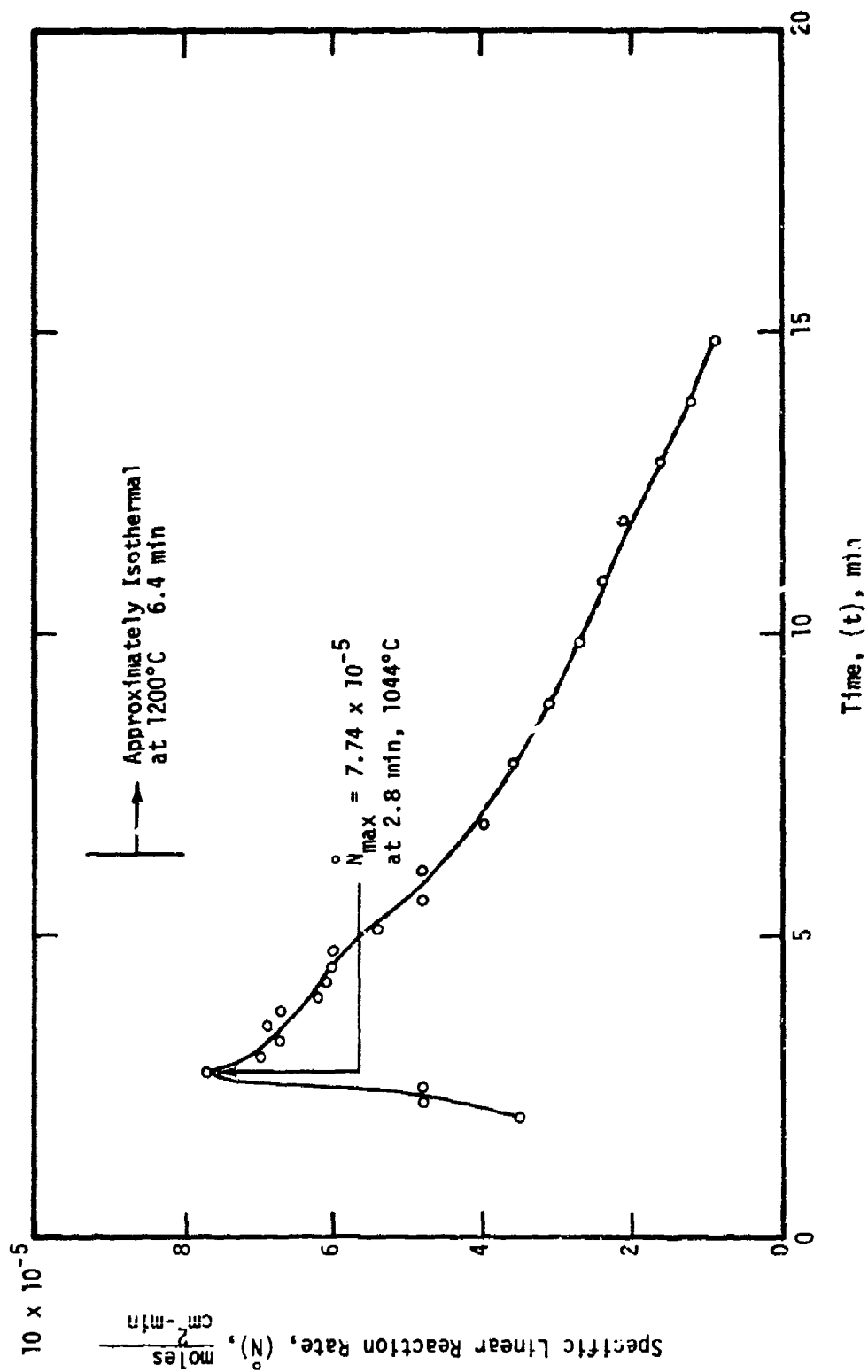


Figure 156.- Initial behavior of the specific linear reaction rate (\dot{N}) for Ti-8Mn alloy specimen no. 407242 heated in 200 torr O_2 at the rate of 5.9°C/s to 1200°C .

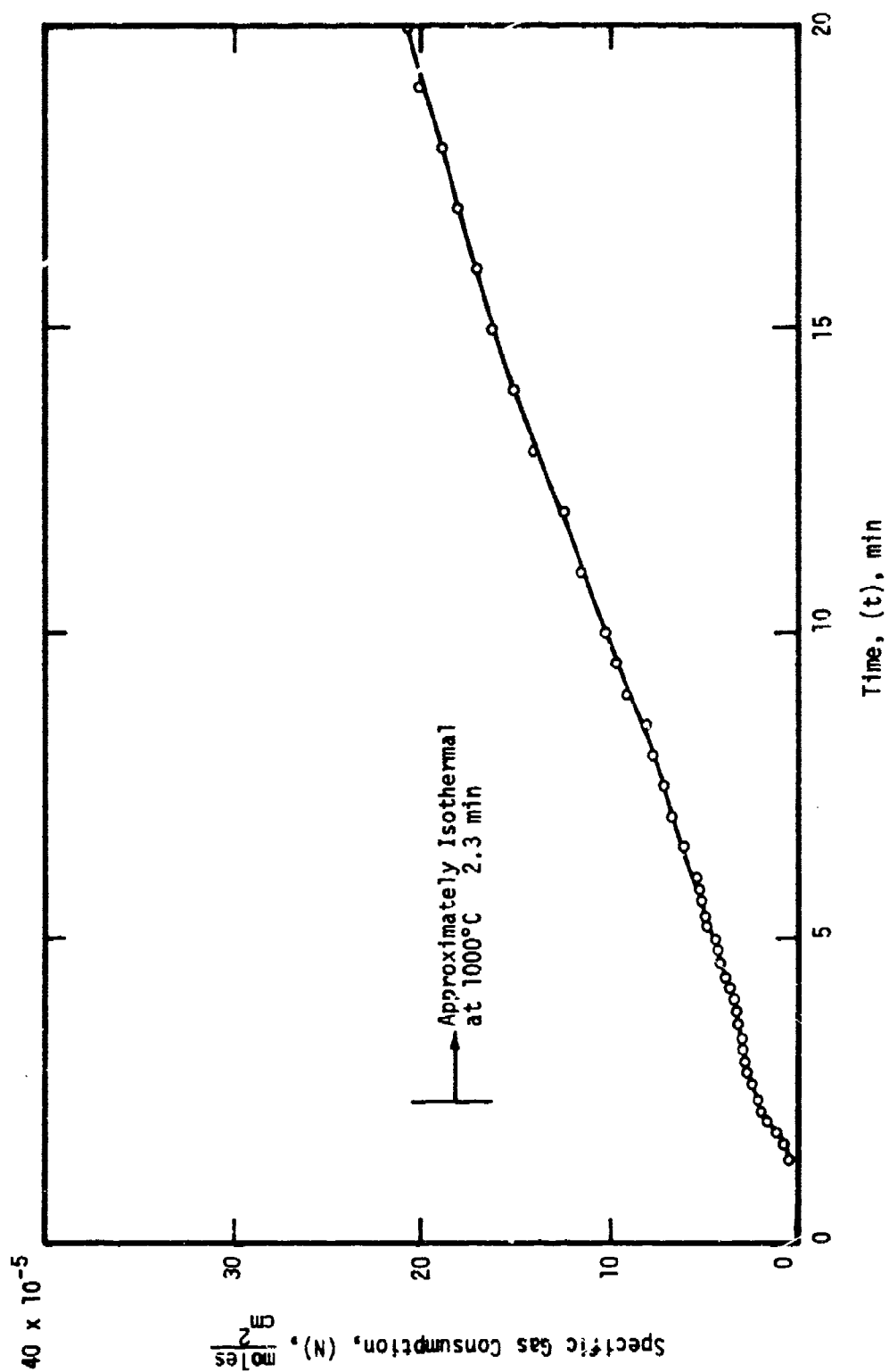


Figure 157.- Initial behavior of the specific gas consumption (N) for Ti-4-III alloy specimen no. 406191 heated in 200 torr O_2 at the rate of 8°C/s to 1000°C.

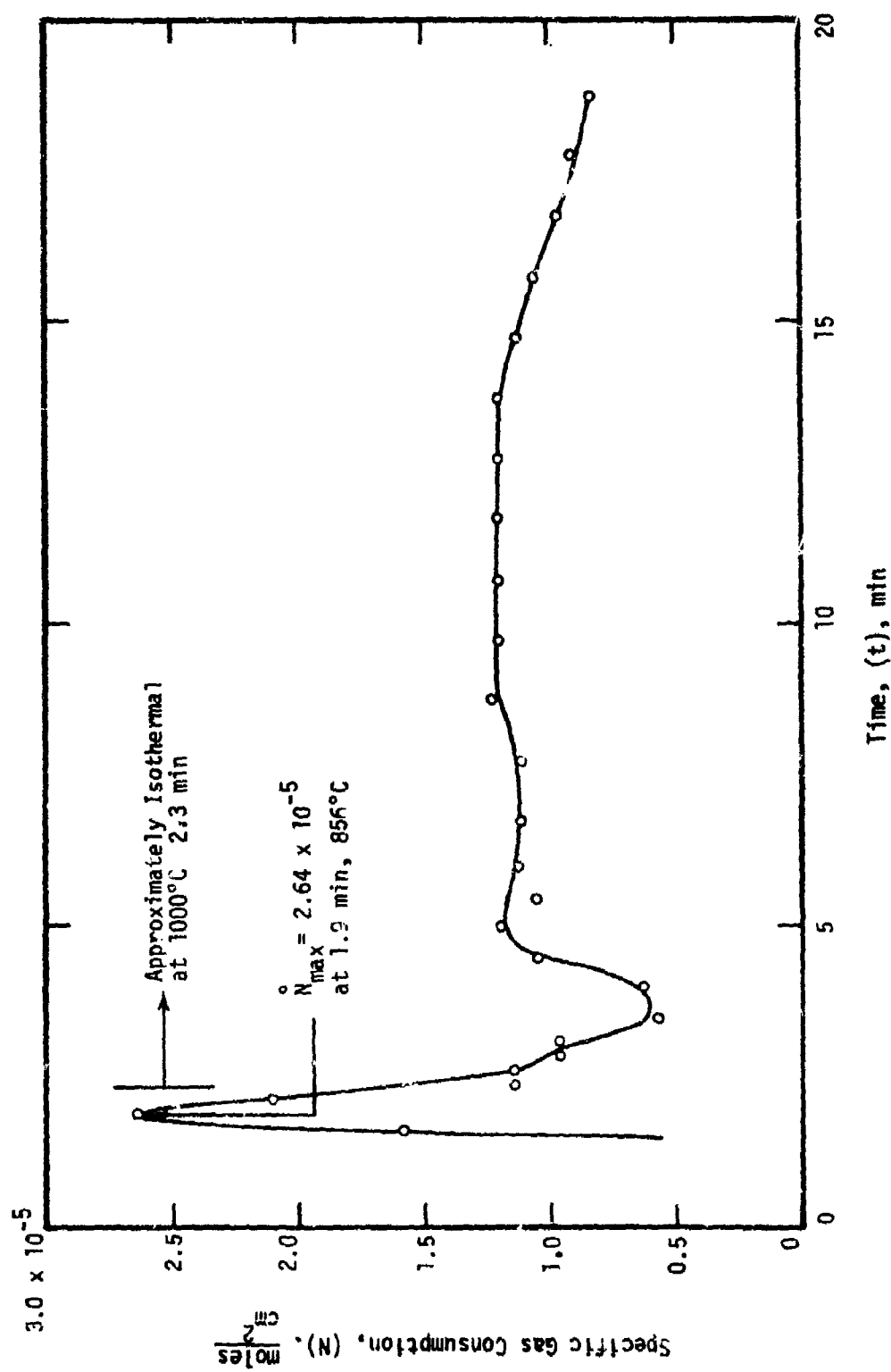


Figure 158.- Initial behavior of the specific linear reaction rate (\dot{N}) for Ti-8-III alloy specimen no. 406191 heated in 200 torr O_2 at the rate of 8°C/s to 1000°C.

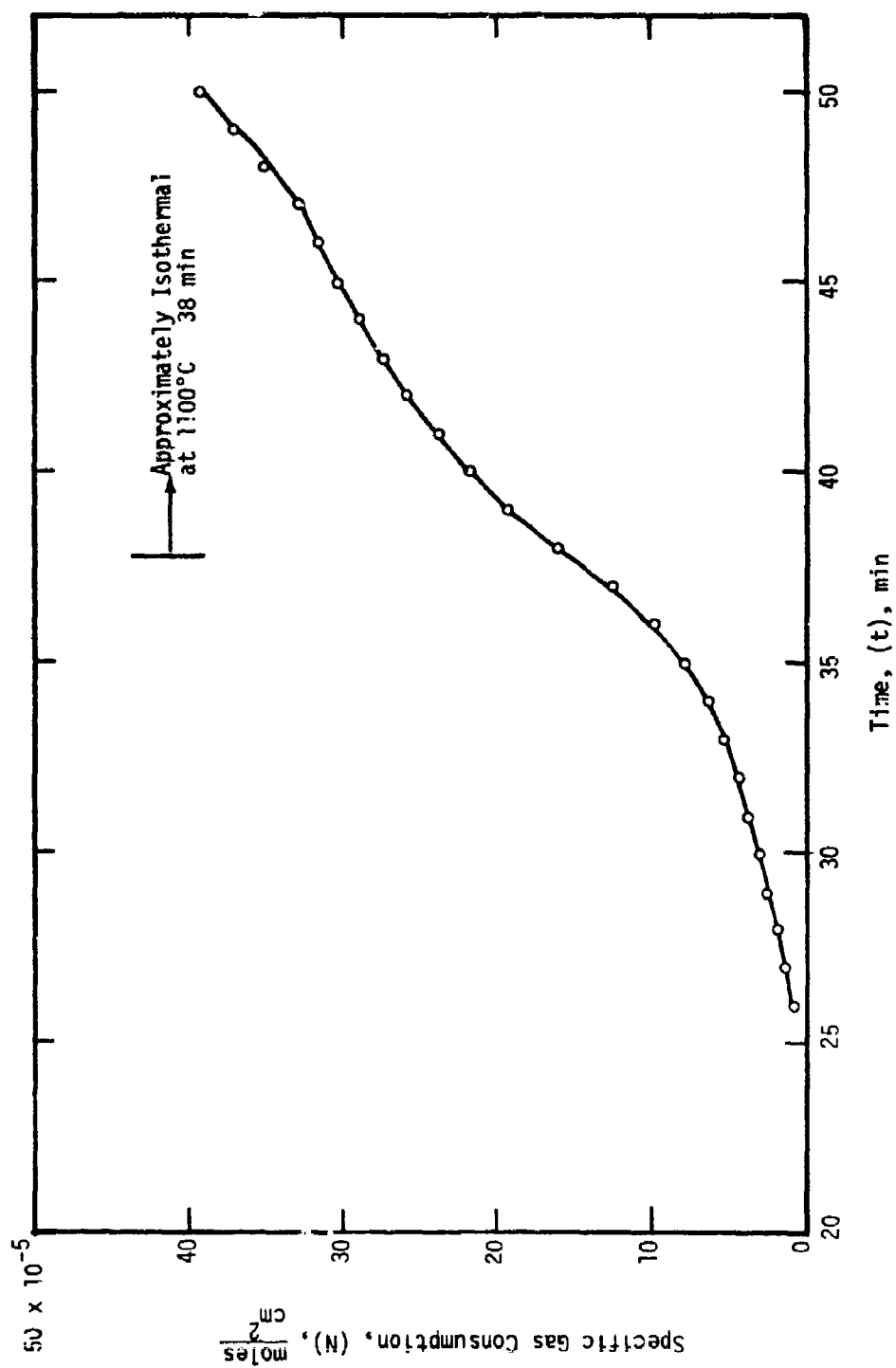


Figure 159.- Initial behavior of the specific gas consumption (H) for Ti-β-III alloy specimen no. 406174 heated in 200 torr O₂ at the rate of 0.5°C/s to 1100°C.

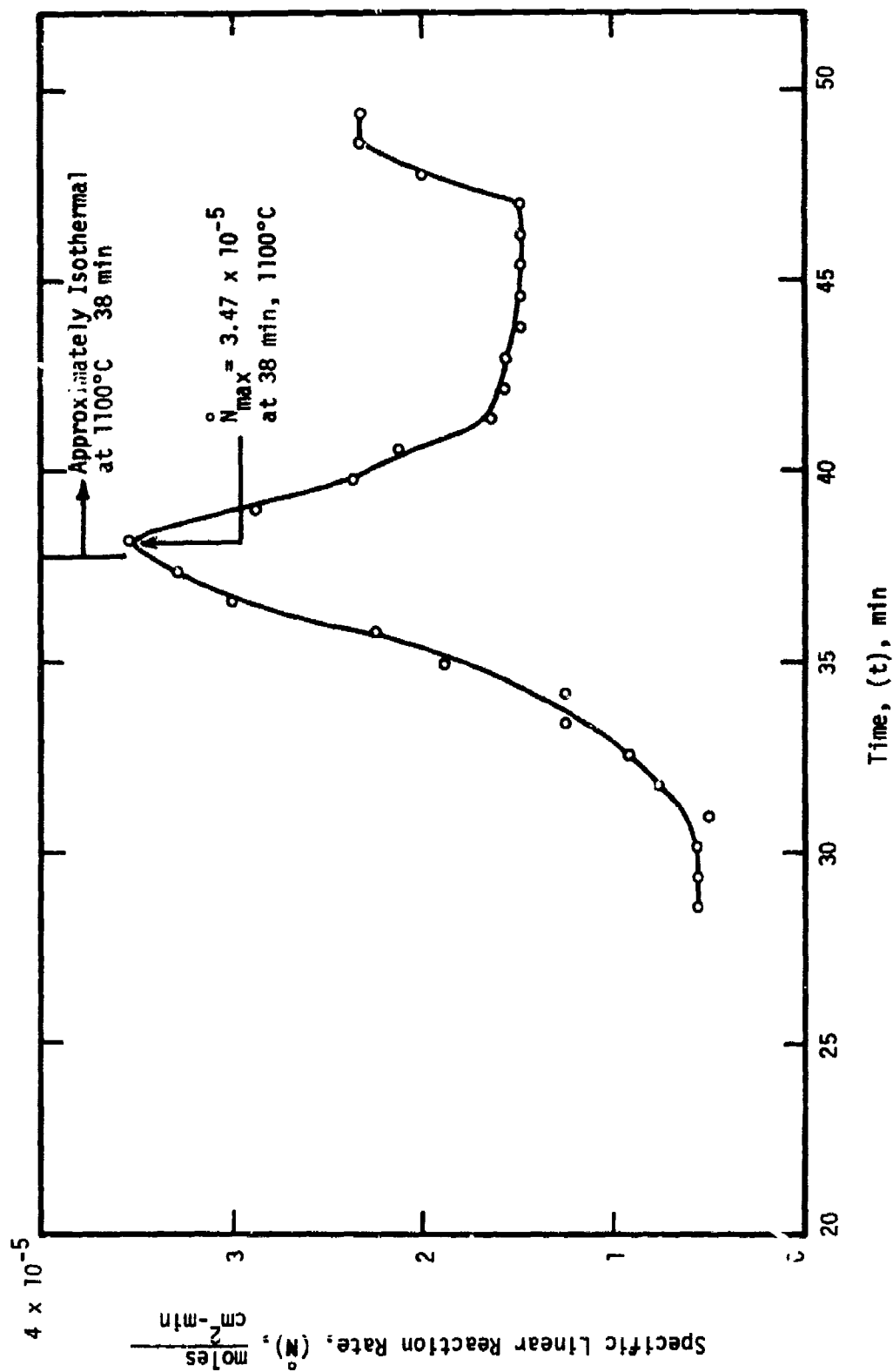


Figure 160.- Initial behavior of the specific linear reaction rate for Ti-6-III alloy specimen no. 406174 heated in 200 torr O_2 at the rate of 0.5°C/s to 1100°C .

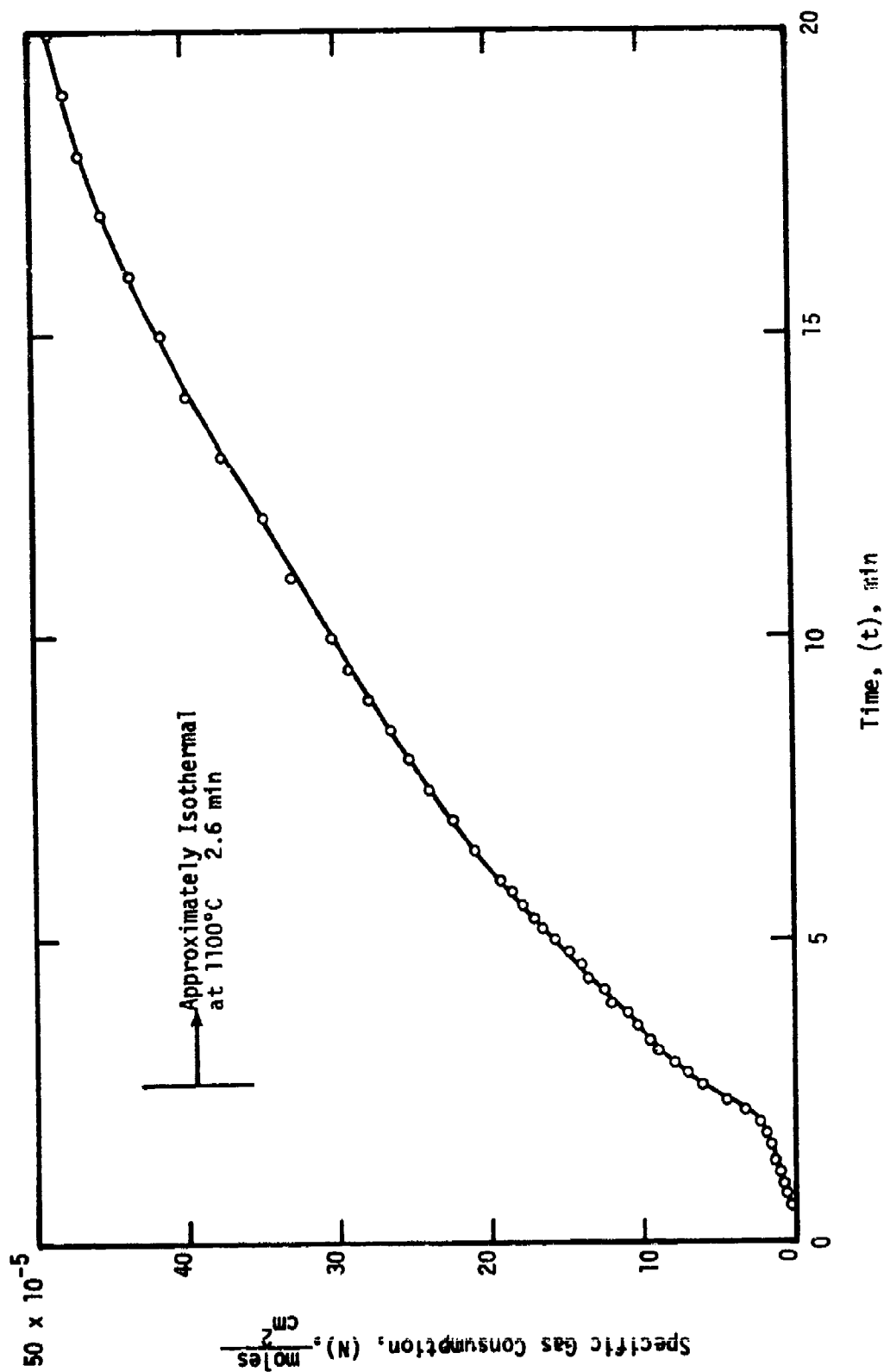


Figure 161.- Initial behavior of the specific gas consumption rate (N) for Ti-6-III alloy specimen no. 406173 heated in 200 torr O₂ at the rate of 8°C/s to 1100°C.

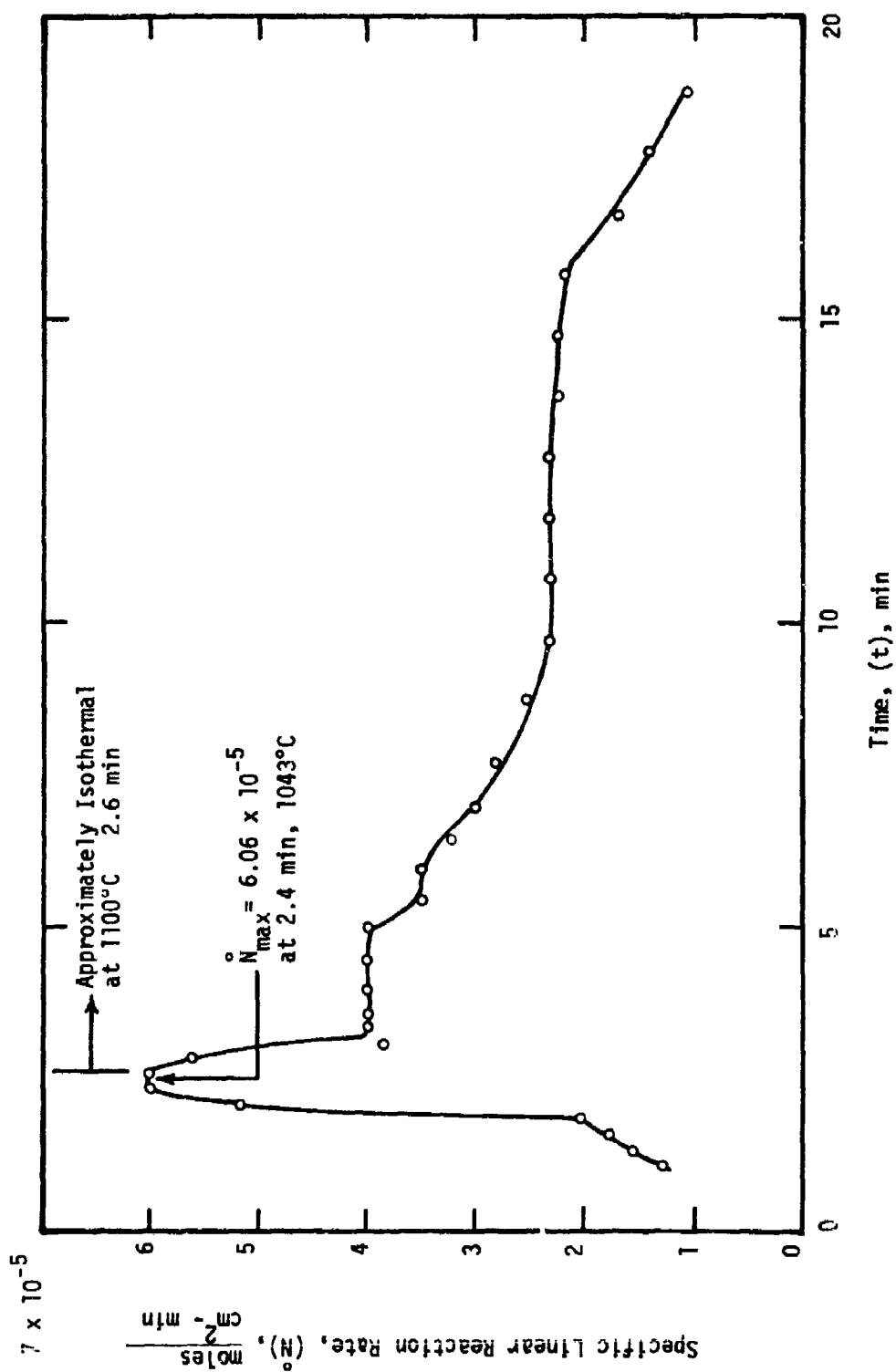


Figure 162.- Initial behavior of the specific linear reaction rate (\dot{N}) for Ti-6-III specimen no. 406173 heated in 200 torr O_2 at the rate of 8°C/s to 1100°C.

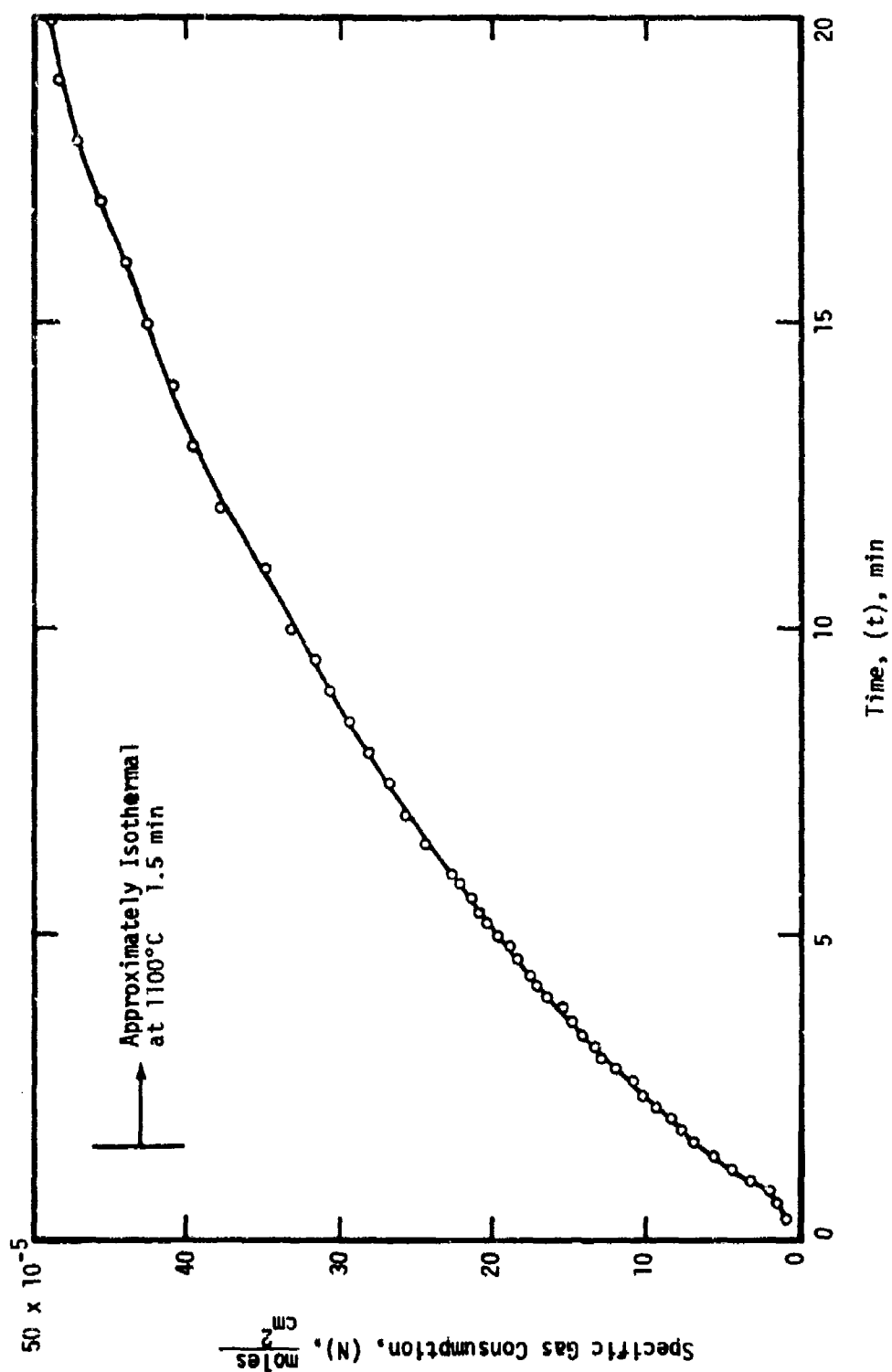


Figure 163.- Initial behavior of the specific gas consumption (N) for Ti-6-III alloy specimen no. 406175 heated in 200 torr O_2 at the rate of 22°C/s to 1100°C.

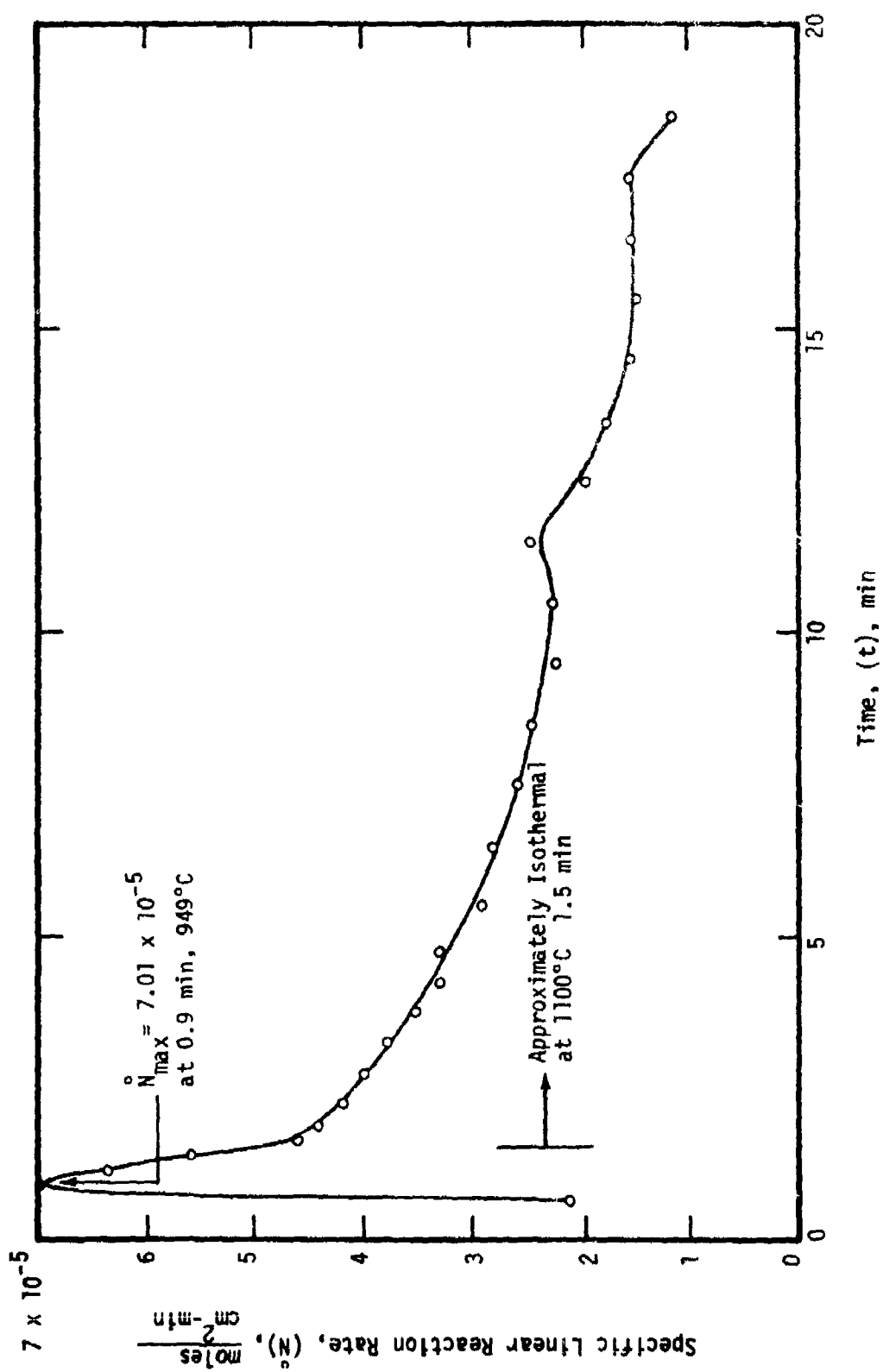


Figure 164.- Initial behavior of the specific linear reaction rate (\dot{N}) for Ti-0-III alloy specimen no. 406175 heated in 200 torr O_2 at the rate of 22°C/s to 1100°C.

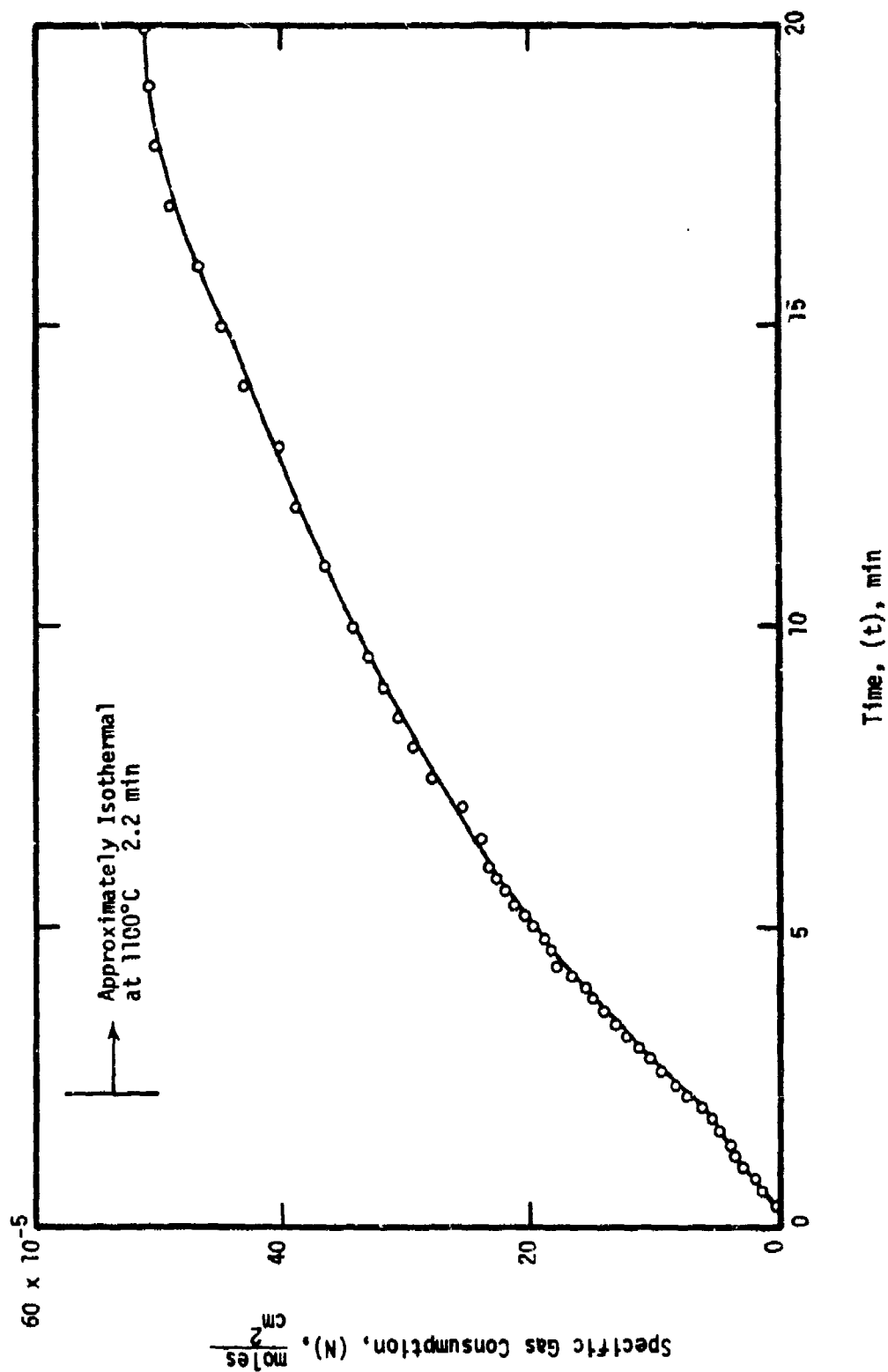


Figure 165.- Initial behavior of the specific gas consumption (N) for Ti-8-III alloy specimen no. 409231 heated in 200 torr O_2 at the rate of 2°C/s to 1100°C. Material milled and polished to .0330 cm.

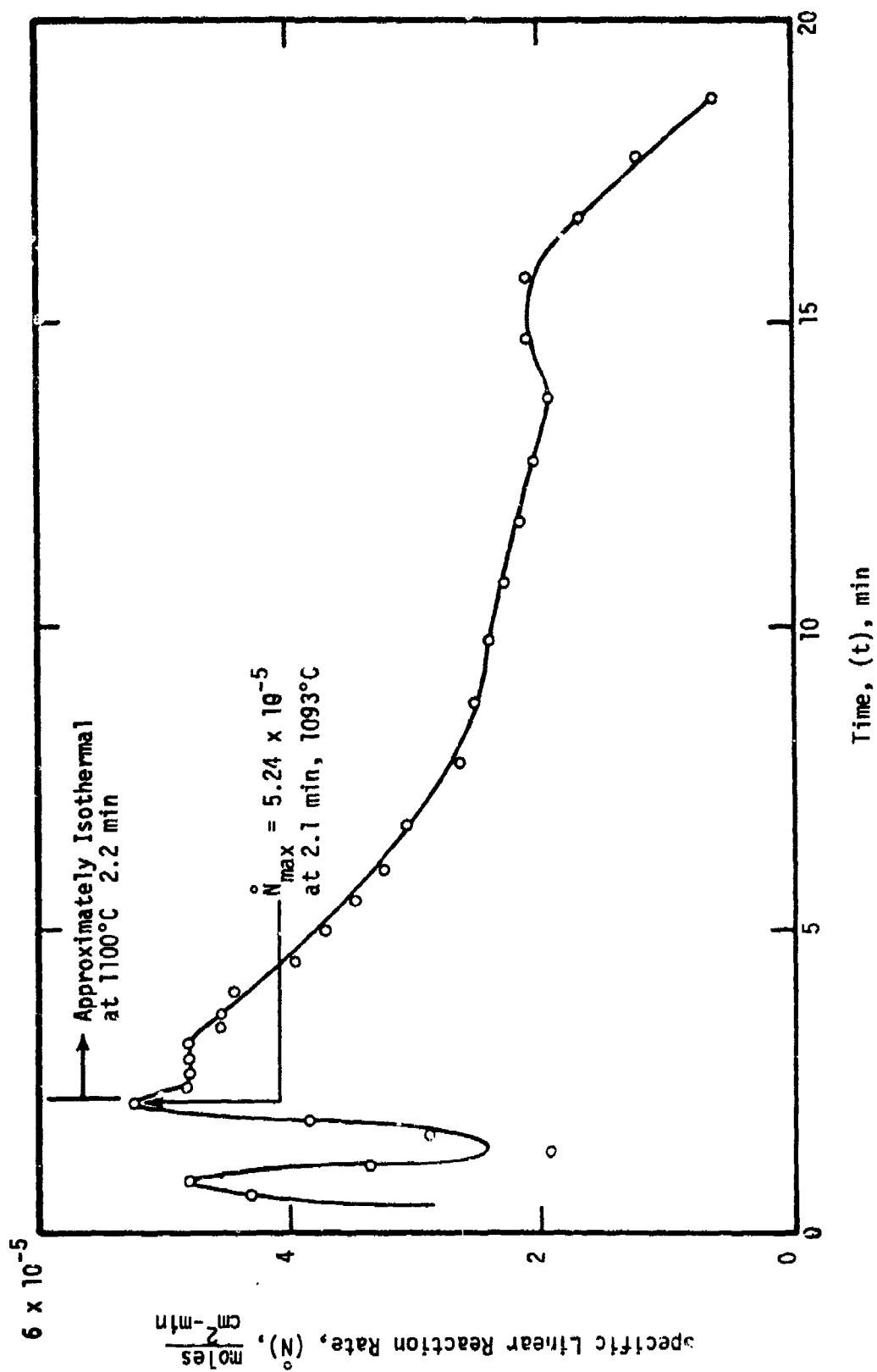


Figure 166.- Initial behavior of the specific linear reaction rate (\dot{N}) for Ti- β -III specimen no. 40923] heated in 200 torr O_2 at the rate of 22°C/s to 1100°C. Material milled and polished to .0330 cm.

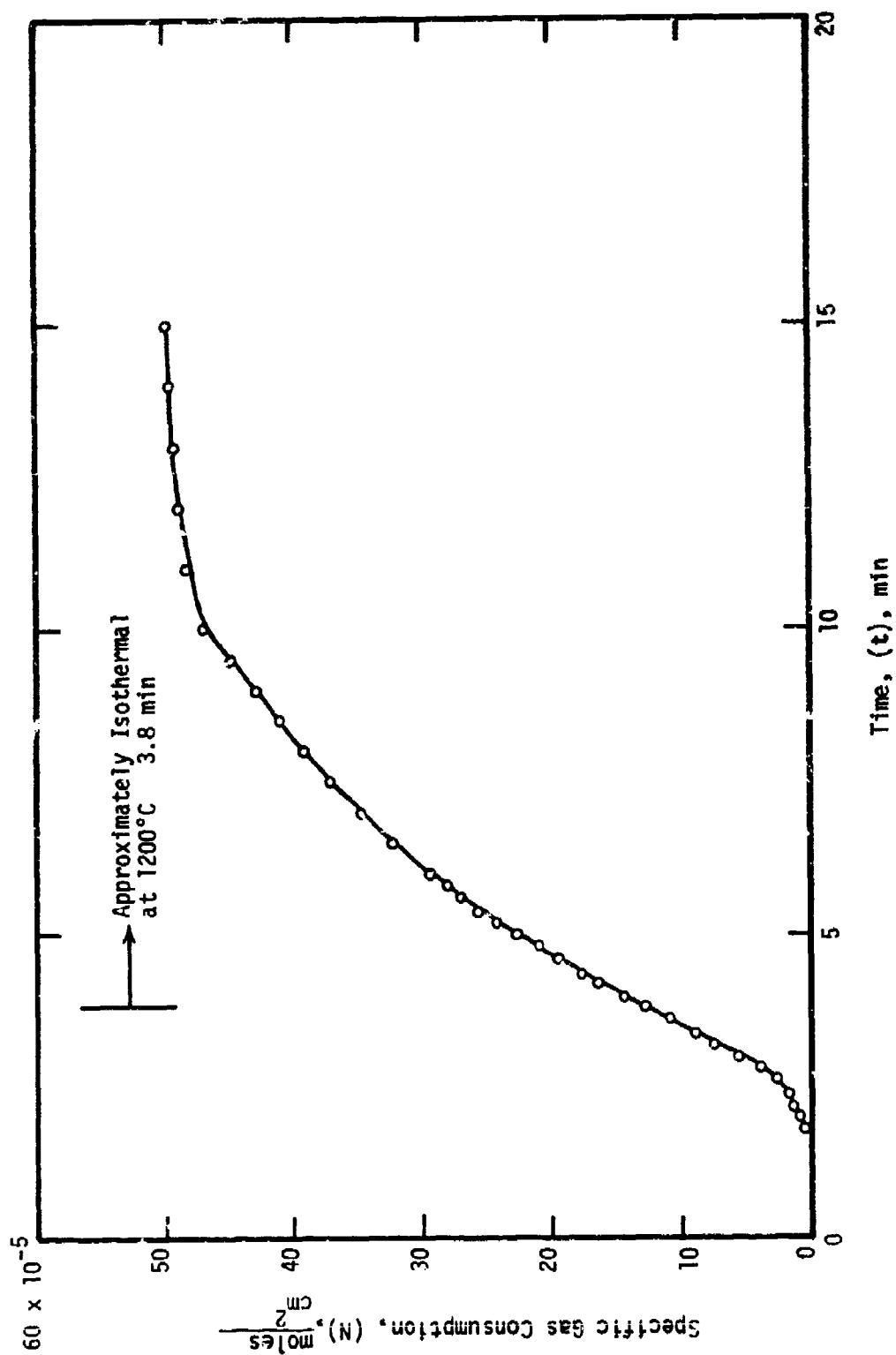


Figure 167.- Initial behavior of the specific gas consumption (N) for Ti-8-III alloy specimen no. 407241 heated in 200 torr O_2 at the rate of 5.9°C/s to 1200°C .

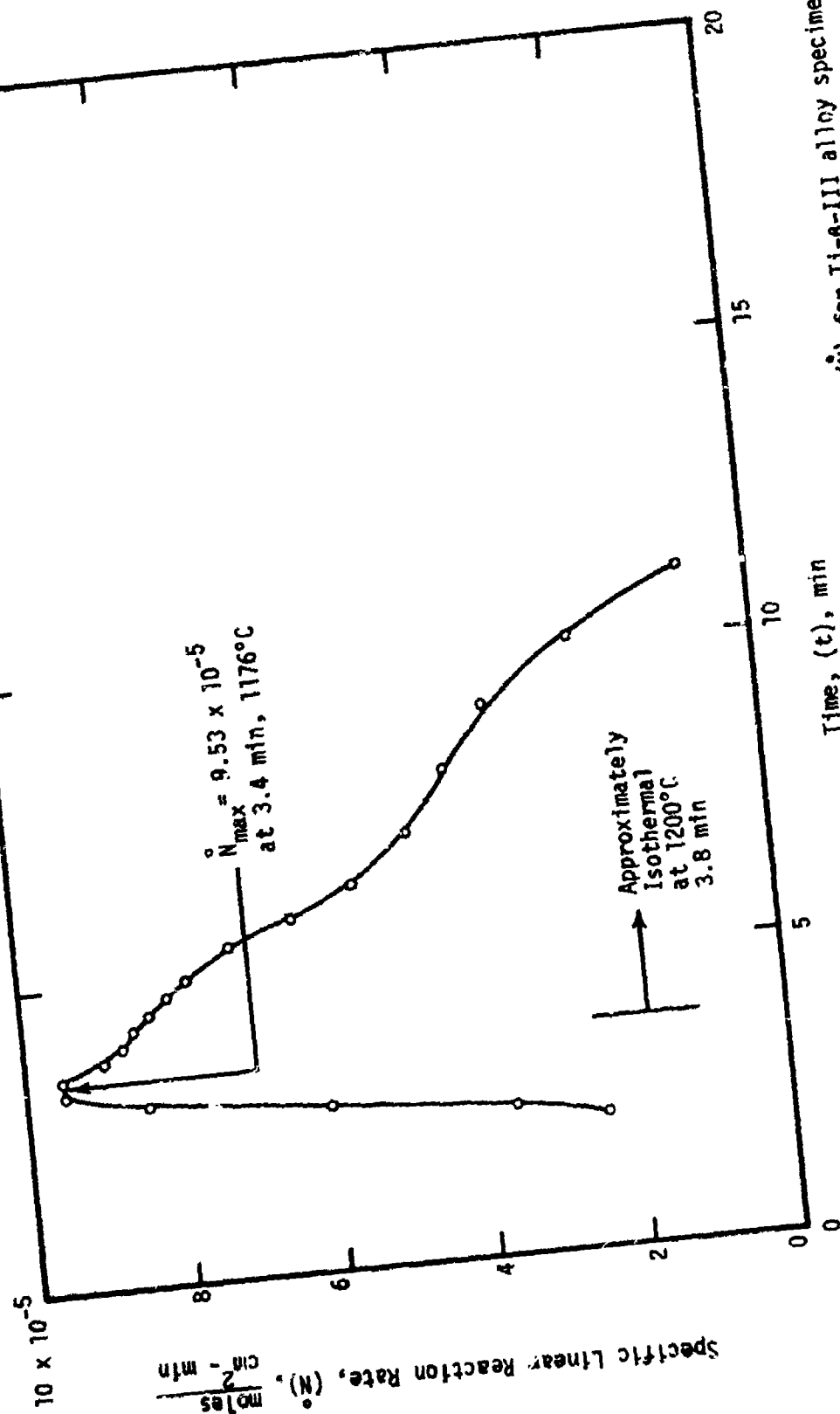


Figure 168.- Initial behavior of the specific linear reaction rate (\bar{N}) for Ti- β -III alloy specimen no. 407241 heated in 200 torr O_2 at the rate of 5.9°C/s to 1200°C.

test is in effect; i.e., (\dot{N}_{\max}) occurs prior to the instant at which (T_{\max}) does.

The Ti-6Al-4V alloy (Type 1, 2, and 3) specimens appear to react more strongly during the heating period per se than do their unalloyed counterparts for the range of temperatures (1000° to 1200°C) and heating rates (0.5° to 22°C/s) investigated. This effect is evidenced by the sharper sigmoidal behavior usually associated with the alloy specimen specific gas consumption curves; compare, for example, Figures 68 and 141. The trend for more rapid initial reaction is maintained throughout the initial portions of the isothermal exposure, thereby providing a larger gross consumption of oxygen by the alloyed than by the unalloyed specimens. As a result of this high early reactivity, especially during heating, the maximum specific linear reaction rate (\dot{N}_{\max}) for the alloy specimens occurs prior to the time at which the maximum temperature is attained, increases with increasing heating rate, and has an intensity which is usually larger than that associated with the unalloyed material.

Unlike the unalloyed titanium specimens, the Ti-6Al-4V alloy specimens only relatively rarely exhibit multiple separated maxima in their rate (\dot{N} vs. t) curve behavior. When this phenomena does occur, it is associated with either the higher (22°C/s) heating rate or with thin substrates; see Figures 144 and 146. These observations suggest that the scales formed upon the alloy specimens may be somewhat more plastic than those formed upon the unalloyed material.

For the Ti-6Al-4V alloy specimens, there is a general trend indicative of increasing reactivity with decreasing specimen thickness; compare, for example, Figures 127 and 128 with Figures 129 and 130, respectively. As cited above, this is expected on the basis that (α)-phase stabilization throughout

the bulk of thin specimens may occur by the inward diffusion of oxygen which, in turn, evidently provides relatively non-resistant (α - β) phase boundaries for subsequent attack by oxygen.

The isothermal (post-heating) oxidation of Ti-6Al-4V alloy specimens is essentially linear with time for a period of 10 to 20 minutes after the maximum temperature has been achieved. For those cases in which linear behavior was not observed, the deviations were always negative and probably occurred as a result of oxygen starvation (as opposed to any real mechanistic change). Such deviations were observed only for those specimens which were oxidized at the highest temperature; see for example, Figures 135 and 137.

The Ti-8Mn and β -III alloy specimens react with oxygen in a manner which is qualitatively similar to that exhibited by the Ti-6Al-4V alloy specimens. Specifically, this includes: early rapid reactivity relative to unalloyed titanium, absence of multiple maxima in the specific linear reaction rate behavior, and near-linear oxidation kinetics in the isothermal portions of the temperature program. In general, the reactivities of the materials investigated increase in the order: unalloyed titanium, Ti-6Al-4V, Ti-8Mn, and β -III alloy; see for example Figures 87, 131, 151, and 161 representing specimens of similar thickness which we subjected to the same thermal program.

4e. SUMMARY OF REACTION PARAMETERS FOR (RHC)-TYPE TESTS OF TITANIUM-BASE MATERIALS

In this section are discussed two parameters which deal with the initial stages of reaction between unalloyed titanium and oxidizing gas. The data presented are based upon analyses of: 1) the specific linear reaction rate curves, and 2) the power index curves; as illustrated schematically in Figure 41 above.

The first of these parameters, (\dot{N}_{\max}) , is derived from the specific reaction rate curves and represents the maximum value of the specific (linear) reaction rate observed during the course of reaction. It has been found that the event corresponding to this observation always occurs early in the course of reaction and usually occurs during the heating process. The behavior of this parameter for tests of unalloyed titanium conducted in 200 torr oxygen was discussed in part previously, see Figure 97. A summary of values of (\dot{N}_{\max}) for all alloys, gases, gas mixtures, and heating conditions is presented in Table XX.

As discussed previously, the values of (\dot{N}_{\max}) for unalloyed titanium in 200 torr oxygen tend to increase either: 1) with heating rate at a fixed maximum temperature, or 2) with maximum temperature at a fixed heating rate; see Figure 97. For these specimens, the data of Table XX also indicates a strong tendency for (\dot{N}_{\max}) to occur at temperatures below the maximum test temperature; i.e., during heating. This behavior is accentuated with the thinner titanium (Type 3, 4, and 5) specimens one of which experienced maximum reactivity at 560°C during heating at 8°C/s to 1000°C. There are also trends indicating that more rapid heating and prior cold work both produce a maximum in the reaction rate at lower temperatures.*

With regard to reaction in other unmixed gases for unalloyed titanium specimens heated at 8°C/s, the value of (\dot{N}_{\max}) is somewhat larger in 400 torr oxygen and much smaller in 200 torr nitrogen than in 200 torr oxygen, as expected. These observations are commensurate with other measures (longer term) of the reaction in these gases presented earlier. In mixed gases, the

*The assigned temperatures corresponding to the maximum value of the specific linear reaction rate may be somewhat in question as the recording thermocouple was not usually welded to the test specimen. This aspect will be discussed more fully below.

TABLE XX

VALUES OF THE MAXIMUM LINEAR REACTION RATE (N_{\max}°) AND THE TEMPERATURE AT WHICH IT OCCURRED
FOR TITANIUM AND TITANIUM-BASE ALLOY SPECIMENS

Specimen Number	Test Atmosphere	Heating Rate ($^{\circ}\text{C}/\text{s}$)	Maximum Temperature ($^{\circ}\text{C}$)	N_{\max}° (moles/ $\text{cm}^2\text{-min}$) $\times 10^{-5}$	$T(N_{\max}^{\circ})$ ($^{\circ}\text{C}$)
A. UNALLOYED TITANIUM (TYPE 1)					
06051	200 torr O_2	0.5	1000	0.39	965
06141	200 torr O_2	0.5	1000	0.70	947
06132	200 torr O_2	8	1000	2.36	885
06133	200 torr O_2	25	1000	8.11	850
06131	200 torr O_2	0.5	1100	1.34	1100
06071	200 torr O_2	8	1100	5.05	1030
06142	200 torr O_2	22	1100	10.3	1065
08012	200 torr O_2	0.5	1200	1.87	1110
08013	200 torr O_2	~7.5	1200	10.8	1200
07091	200 torr O_2	~4	1300	11.3	1160
07311	200 torr N_2	8	1000	0.75	1000
07312	200 torr N_2	8	1100	0.84	1100
07313	200 torr $\text{O}_2 +$ 200 torr N_2	8	1000	1.02	660
08011	200 torr $\text{O}_2 +$ 200 torr N_2	8	1100	3.60	960

TABLE XX - continued

Specimen Number	Test Atmosphere	Heating Rate (°C/s)	Maximum Temperature (°C)	$\frac{N_{\max}}{2} \text{ (moles/cm}^2\text{-min)} \times 10^{-5}$	$T(N_{\max})$ (°C)
08021	200 torr O ₂ + 200 torr He	8	1000	1.84	570
08071	200 torr O ₂ + 200 torr He	8	1100	2.70	1100
08023	200 torr N ₂ + 200 torr He	8	1000	0.99	1000
09051	200 torr N ₂ + 200 torr He	8	1100	1.09	1040
B. UNALLOYED TITANIUM (TYPE 2)					
09191	200 torr O ₂	8	1000	1.40	860
09192	400 torr O ₂	8	1000	3.20	840
401151	200 torr O ₂	8	1100	3.00	1100
401021	200 torr O ₂	8	1100	2.95	1100
405151 [1]	200 torr O ₂	8	1100	4.32	1025
405221 [1]	200 torr O ₂	~10	1100	5.00	1020
408191 [2]	200 torr O ₂	22	1100	4.62	995
408141 [3]	200 torr O ₂	22	1100	4.62	823
402192	200 torr N ₂	22	1100	0.59	1100
402281	200 torr N ₂	22	1100	0.60	1100
402193	100 torr O ₂ + 100 torr N ₂	22	1100	1.70	929
402194	50 torr O ₂ + 150 torr N ₂	8	1100	2.00	845

TABLE XX - continued

Specimen Number	Test Atmosphere	Heating Rate (°C/s)	Maximum Temperature (°C)	N_{\max} (moles/cm ² -min) $\times 10^{-5}$	$T(N_{\max})$ (°C)
C. UNALLOYED TITANIUM (TYPE 3)					
09194	200 torr O ₂	8	1000	2.00	560
11201 [4]	200 torr O ₂	8	1100	5.85	996
405021	200 torr O ₂	8	1100	4.65	1028
405023	200 torr O ₂	5.9	1200	7.33	1157
D. UNALLOYED TITANIUM (TYPE 4)					
407162	200 torr O ₂	8	1100	5.43	904
E. UNALLOYED TITANIUM (TYPE 5)					
408143	200 torr O ₂	8	1100	4.29	964
408282	200 torr O ₂	~18	1100	6.03	725
F. TITANIUM-6% ALUMINUM -4% VANADIUM (TYPE 1)					
407161 [5]	200 torr O ₂	8	1000	4.84	888
401161	200 torr O ₂	0.5	1100	2.41	1068
401091	200 torr O ₂	0.5	1100	2.70	1100
11202	200 torr O ₂	8	1100	5.04	1090
405071 [5]	200 torr O ₂	8	1100	10.53	1100
405072 [5]	200 torr O ₂	8	1100	9.69	1100
401092	200 torr O ₂	22	1100	7.80	964
407243 [5]	200 torr O ₂	5.9	1200	8.00	1093

TABLE XX - continued

Specimen Number	Test Atmosphere	Heating Rate ($^{\circ}\text{C/s}$)	Maximum Temperature ($^{\circ}\text{C}$)	N_{max} ($\text{moles/cm}^2\text{-min}$) $\times 10^{-5}$	$T(N_{\text{max}})$ ($^{\circ}\text{C}$)
408081 [5]	200 torr O_2	5.9	1200	7.75	1179
401162	200 torr N_2	8	1100	0.78	341
402042	200 torr O_2	G. TITANIUM-5% ALUMINUM -4% VANADIUM (TYPE 2)			
401152	200 torr O_2	0.5	1100	2.03	1029
402043	200 torr O_2	8	1100	6.20	1085
	200 torr O_2	22	1100	9.00	1072
406171	200 torr O_2	H. TITANIUM-5% ALUMINUM -4% VANADIUM (TYPE 3)			
	200 torr O_2	8	1100	4.92	1050
406032	200 torr O_2	I. TITANIUM-8% MANGANESE			
405074	200 torr O_2	8	1000	3.90	1000
405073	200 torr O_2	0.5	1100	2.67	1100
406031	200 torr O_2	8	1100	5.71	967
407242	200 torr O_2	22	1100	6.27	924
	200 torr O_2	5.9	1200	7.74	1044
406191	200 torr O_2	J. TITANIUM-8-III			
406174	200 torr O_2	8	1000	2.64	856
406173	200 torr O_2	0.5	1100	3.47	1100
	200 torr O_2	8	1100	6.06	1043

TABLE XX - continued

Specimen Number	Test Atmosphere	Heating Rate (°C/s)	Maximum Temperature (°C)	$\frac{N_{max}}{(moles/cm^2-min)} \times 10^{-5}$	$T(N_{max})$ (°C)
409231 [6]	200 torr O ₂	22	1100	5.24	1093
406175	200 torr O ₂	22	1100	7.01	949
407241	200 torr O ₂	5.9	1200	9.53	1176

Footnotes

- [1] Cold worked 87%
- [2] Cold worked 76%
- [3] Cold worked 61%
- [4] Cold worked 39%
- [5] Milled from .152 cm to .119 cm
- [6] Milled and polished to .0330 cm

behavior of (\dot{N}_{\max}) is less well defined on an intuitive basis. Oxygen-bearing gas mixtures produce lower values of (\dot{N}_{\max}) than does unmixed oxygen at 200 torr, regardless of whether the second gas is nitrogen or helium. These data are therefore compatible with the concept of "oxygen starvation" and indicate no synergistic role of nitrogen for those gas mixtures. Conversely, the dilution of nitrogen by helium slightly increases, rather than reduces, the observed values of (\dot{N}_{\max}) and therefore in no way supports the concept of "nitrogen starvation" in the immediate region of the specimen. It is noted that while nitrogen or nitrogen-bearing gas mixtures do not produce relatively large values of (\dot{N}_{\max}) , they do tend to induce maximum reactivity at temperatures much lower than those atmospheres which do not contain nitrogen. It is again suggested that this early rapid reaction provides a plastic diffusion-barrier film which attenuates subsequent reaction.

The values of (\dot{N}_{\max}) for the titanium-base alloy specimens investigated exhibited the same general behaviors with regard to maximum temperature, heating rate, specimen thickness, and prior cold work as did the unalloyed titanium specimens. As alluded to earlier, the reactivities of all alloy specimens were generally greater than those produced using the unalloyed materials when compared under conditions where alloy chemistry was the sole intentional variable. This observation is quantified for the 4 materials investigated in Figure 169 which involves data from specimens of nominally a single thickness subjected to various maximum temperatures at the same nominal heating rate.

Here, the maximum value of the specific linear reaction rate (\dot{N}_{\max}) is empirically treated as a rate constant and the graph is constructed in an Arrhenius format. Values of (\dot{N}_{\max}) are seen to increase with increasing maximum temperature for all materials except the Ti-6Al-4V alloy which exhibits a retrograde temperature behavior. At the lowest temperature investigated

(1000°C), the reactivities of the materials investigated increase in the order: unalloyed titanium, β -III, Ti-8Mn, and Ti-6Al-4V alloy; however, as the temperature is increased, the relative reactivity of the alloys interchange in the complex fashion illustrated in Figure 169. As will be discussed more fully below, it is this low-temperature reactivity which may be dominant in ignition-associated behavior.

The overall character of the power index (furnace voltage) curves for times involving heating and the first few minutes of isothermal condition are set by the two parameters external to the reaction chamber: the heating rate and the maximum temperature. Thus, for a given thermal program, differences in the power index curves reflect differences in specimen-associated properties. The second of the parameters which have been selected for summarization is the value of the power index at the fifth minute after "isothermal" conditions (maximum temperature) have been achieved; see Figure 41. This parameter, (W_5), is here designated as the energy coupling parameter and has previously been employed to differentiate the efficiency of infrared energy coupling for various specimen surface conditions (ref. 10). It is a measure of the power initially necessary to maintain a given maximum temperature and has the virtue that it is relatively free of transients generated by the heating process per se.

The data of Table XXI indicate that the observed values of (W_5) are strongly dependent upon maximum temperature and nearly independent of heating rate employed to raise the unalloyed titanium specimens to the maximum temperature. The first of these effects is to be expected as more power is necessary to maintain higher temperatures in the "isothermal" regions of the heating program. The near-independence of (W_5) upon heating rate would indicate that the surface oxides formed have the same properties in a radiation-coupling sense. However, close inspection of these data (and excepting only the singular

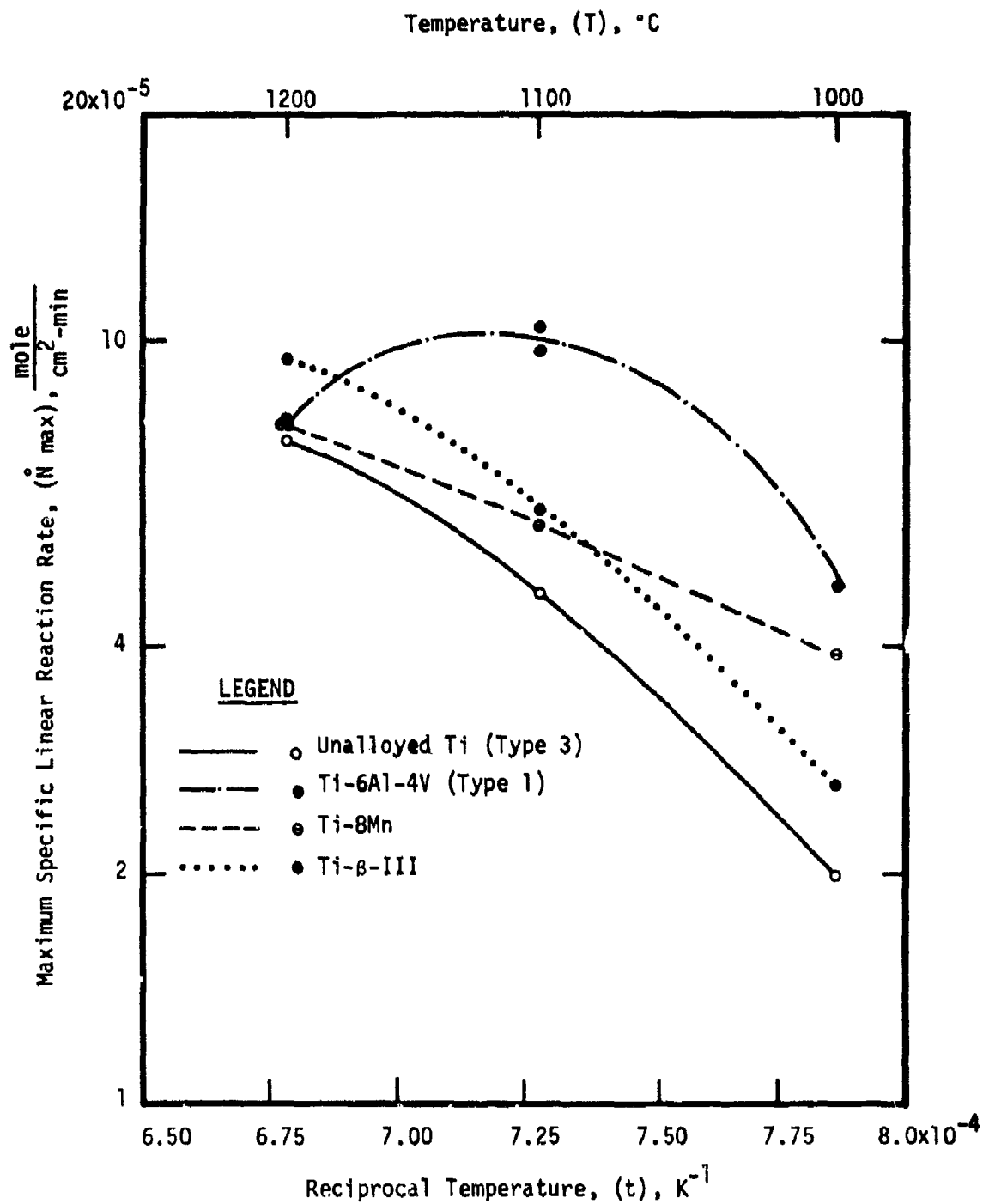


Figure 169.- Initial response of 0.102 cm thick titanium specimens in 200 torr oxygen for the temperature range 1000°C to 1200°C. Nominal heating rate 8°C/s.

TABLE XXI

VALUES OF THE ENERGY COUPLING PARAMETER (W_5)^{*} AS A FUNCTION OF THE HEATING RATE, MAXIMUM TEMPERATURE, AND GAS ATMOSPHERE FOR UNALLOYED TITANIUM

Maximum Temperature (°C)	Heating Rate (°C/S)	Atmosphere						
		200 Torr O ₂	200 Torr N ₂	400 Torr O ₂	200 Torr O ₂ ⁺ 200 Torr N ₂	200 Torr N ₂ ⁺ 200 Torr He	200 Torr O ₂ ⁺ 200 Torr He	
1000	0.5	11.1; 11.8	--	--	--	--	--	
	8	12.3; 13.0(2); 13.3(3)**	11.5; 12.7(2)	12.9(2)	11.6	13.2	14.8	
	25	11.9	--	--	--	--	--	
1100	0.5	16.2	--	--	--	--	--	
	8	16.4	17.9	--	18.2	20.7	21.5	
	22	16.6	--	--	--	--	--	
1200	0.5	25.4	--	--	--	--	--	
	7.5	27.7	--	--	--	--	--	
1300	4	38.4***	--	--	--	--	--	

*Tabular entries are for the Power index 5 minutes after the maximum temperature had been achieved and have units [volts]² x 10⁻³.

**Numbers in parentheses indicate unalloyed titanium type; no parentheses indicates type 1.

***Indicates maximum power condition.

datum for 25°C/s heating to 1000°C) do indicate a minor trend for increased power requirements with increased heating rates. The qualitative analysis of this effect on the basis of quantity of oxide present is difficult, as slower heating rates allow more time for initial oxide formation, whereas higher heating rates induce larger (initial) values of (\dot{N}_{\max}).

Another type of effect regarding (W_5) data is also noted here and involves the role of gas composition. The data of Table XXI clearly indicate a trend for higher values of (W_5) with gases of higher thermal conductivity; i.e., the lower the average molecular weight of the gas, the greater is the power necessary to maintain a selected maximum temperature.* One notable exception to this trend was the datum for the test conducted in 400 torr oxygen which apparently conducted heat away from the specimen with the same efficiency as oxygen at a pressure of 200 torr. This observation may be qualitatively rationalized on the basis that the self-heating effect is greater in 400 torr oxygen than in 200 torr oxygen as may be inferred from other evidence for larger degrees of reaction occurring with higher oxygen pressure.

The data of Table XXII gives further information concerning the coupling efficiency parameter (W_5) with special regard to the effects of prior cold work, specimen gage, and alloy type. The reader is cautioned that the data presented here has been perturbed by two factors: 1) the normal aging of the transmitting and reflecting surfaces of the furnace, and 2) coating of the reaction tube walls with reaction products especially in the case of alloy oxidation tests. Both of these factors will tend to increase the value of (W_5) and intercomparison with the data either between the subgroups of

*Also attendant with higher powers are shorter wavelengths of the intensity maxima for radiations issuing from the heating elements.

TABLE XXII
SELECTED VALUES OF THE ENERGY COUPLING PARAMETER (W_5) FOR TITANIUM AND TITANIUM-
BASE ALLOYS EXPOSED IN 200 TORR OXYGEN AT 1100°C

Specimen Number	Material (Type)	Heating Rate (°C/s)	Parameter (W_5) (volt) ² x 10 ⁻³	Remarks
401151	Unalloyed (2)	8	20.5	Annealed
401021	Unalloyed (2)	8	20.1	Annealed
405151	Unalloyed (2)	8	24.6	Cold worked 87%
405221	Unalloyed (2)	~10	25.1	Cold worked 87%
11201	Unalloyed (3)	8	19.0	Cold worked 39%
405021	Unalloyed (3)	8	22.0	Annealed
407162	Unalloyed (4)	8	24.8	Annealed
408143	Unalloyed (5)	8	24.3	Annealed
408282	Unalloyed (5)	~18	29.6	Annealed
401161	Ti-6Al-4V (1)	0.5	21.2	Annealed
11202	Ti-6Al-4V (1)	8	19.4	Annealed
405071	Ti-6Al-4V (1)	8	21.2	Milled to 0.119 cm
401092	Ti-6Al-4V (1)	22	19.3	Annealed
402042	Ti-6Al-4V (2)	0.5	21.0	Annealed
401152	Ti-6Al-4V (2)	8	19.5	Annealed
402043	Ti-6Al-4V (2)	22	21.0	Annealed

TABLE XXII - continued

Specimen Number	Material (Type)	Heating Rate ($^{\circ}\text{C/s}$)	Parameter (W_5) (volt) $^2 \times 10^{-3}$	Remarks
406171	Ti-6Al-4V (3)	8	24.1	Annealed
405074	Ti-8Mn	0.5	23.4	Annealed
405073	Ti-8Mn	8	22.5	Annealed
406031	Ti-8Mn	22	23.4	Annealed
406174	β -III	0.5	25.0	Annealed
406173	β -III	8	24.1	Annealed
406175	β -III	22	23.2	Annealed
409231	β -III	22	31.8	Milled and polished to 0.0330 cm

Table XXII or between Tables XXI and XXII may therefore be misleading.

Data presented for the unalloyed titaniums indicate that thinner annealed specimens require more power to maintain a given equilibrium temperature. Qualitatively, this effect is expected in light of radiation balance considerations provided the heat of chemical reaction does not enter into consideration. Cold working naturally reduces the specimen thickness and higher powers are therefore usually associated with the cold worked specimens. A single exception, specimen no. 11201 which reacted rapidly, exhibited a lower value of (W_5) than did the thicker annealed material. It is presumed that this behavior does represent one case where the heat of reaction did reduce the required power input.

The tests involving alloy specimens exhibited the same qualitative behavior patterns with regard to the energy coupling parameter (W_5) as did specimens of the unalloyed material. Specifically, higher powers were required to maintain higher temperatures, the parameter (W_5) was relatively insensitive to heating rate, and thinner gages required higher powers to maintain thermal equilibrium. The observed values of (W_5) were generally somewhat higher for alloys than for the unalloyed materials; however, this is probably not a real effect due to deposition of volatile species on the reaction tube walls.

4f. SPECIAL TESTS

During the course of this research, three types of special tests were conducted using unalloyed titanium (Type 2) as the specimen material. These tests involved: the certification of thermocouple mounting techniques, the exposure of specimens to cyclic thermal oxidation in order to gain insight into coupling processes, and a study of the reaction products formed in 200 torr oxygen by X-ray diffractometry.

In the first type of test, the Pt vs Pt-13% Rh recording thermocouple was welded to a titanium specimen. This procedure is atypical of our normal experimental procedure in which thermocouple beads are positioned in the immediate vicinity of specimen surfaces by carefully bending the bead toward the specimen but avoiding intimate contact of material and thermocouple. The results of this test, in terms of a time-temperature plot, are illustrated in Figure 170 for the case of heating in 200 torr oxygen at the rate of 8°C/s to 1100°C . Superimposed upon this graph is the time-temperature data for a similarly-shaped Ti-6Al-4V alloy specimen, (with near-surface thermocouple) similarly heated but otherwise chosen at random. It is seen that aside from a horizontal (time) displacement the two curves are nearly identical. This displacement is due in part to controller-programmer "backlash" and in no way influences any test parameter other than "clock time." The results are interpreted to mean that our testing technique is satisfactory with regard to temperature measurement by near-surface thermocouples.

In the second type of testing, the titanium specimens were provided with various types of pre-test treatments and then subjected to nominally identical thermal programs. The specimen preparations included: 1) a metallographic 600-grit silicon carbide finish on annealed stock, 2) a metallographic 1 μm diamond finish on annealed stock, and 3) a metallographic 600-grit silicon carbide finish on oxidized and descaled stock (specimen no. 401021). After mounting each of these specimens in the apparatus, 200 torr of oxygen was admitted and heating was induced at the rate of 8°C/s nominally to 1100°C (100% of program). The specimens were each then held isothermally for 5 minutes and subsequently cooled at the rate of 0.5°C/s to near ambient temperature. The heating, holding, and cooling cycles were then repeated two more times before the system was opened.* The results of these tests, in terms

*No oxygen gas was admitted between cycles.

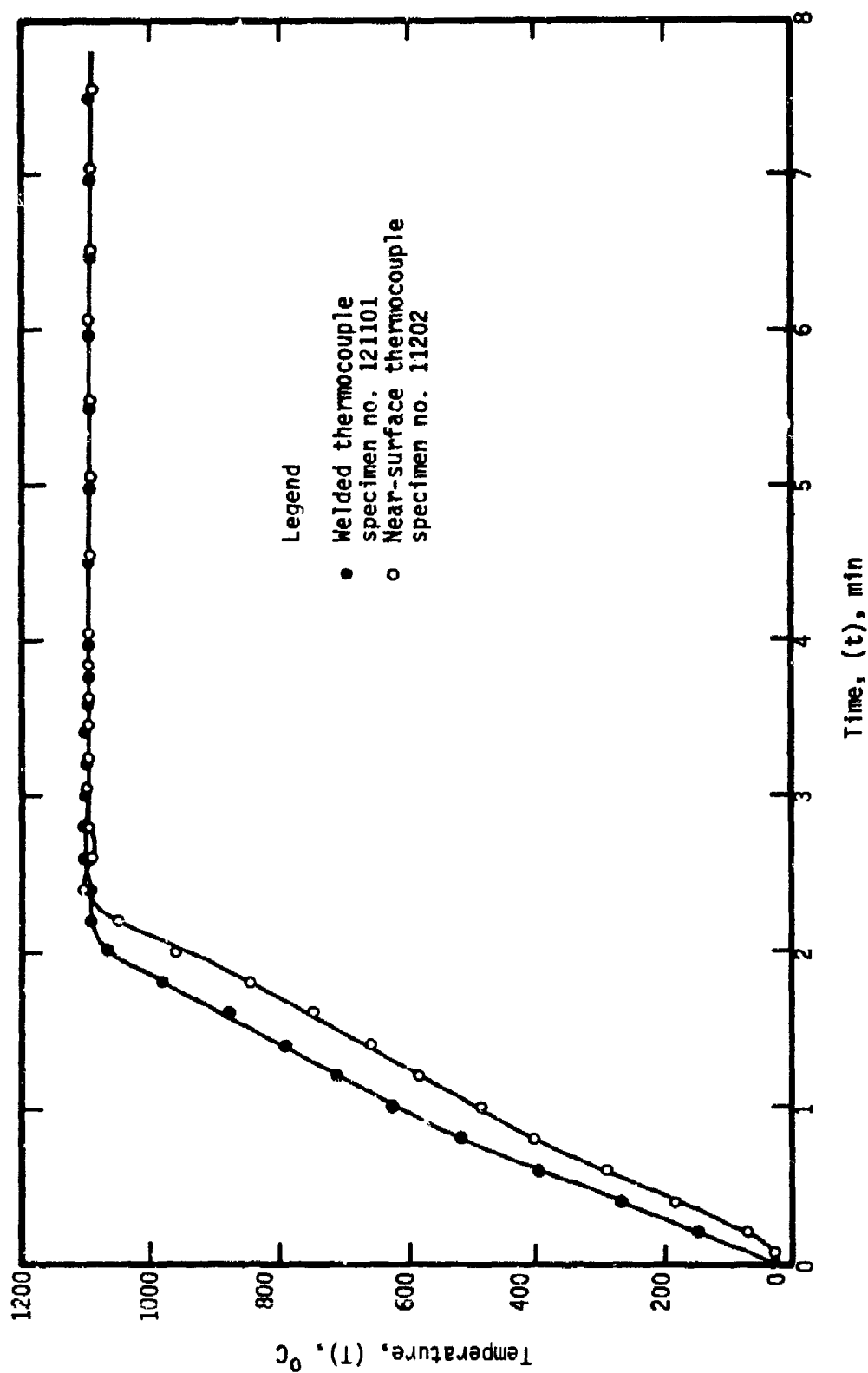


Figure 170. - Time-temperature histories for specimens with "welded" and "near-surface" thermocouple configurations, heated in 200 torr O_2 at $8^\circ C/s$ to $1100^\circ C$.

of (T vs. t), (W vs. t), and (P vs. t) plots are presented in Figures 171 through 179.

In each case, the temperature, power index, and pressure maxima are coincident in time within experimental error. The form and magnitude of the (T vs. t) curves and the (W vs. t) curves give qualitative indication of the efficiency of coupling infrared radiation to the specimens, while the (P vs. t) curves provide a qualitative index of the degree of reaction which has taken place. Cycle-to-cycle variations in these former curves further indicate the manner in which the coupling efficiency is modified by the formation of oxide scale during the previous cycle(s).

Figures 171 and 172 indicate that the radiation is initially strongly coupled to the annealed specimen prepared with 600-grit finish. The second and third cycle data of those figures indicate coupling becomes poorer as the oxide scale thickens. This is evidenced by lower temperatures and "softer" transitions from the heating to the isothermal segments of the curves illustrated in Figure 171, it is also apparent in the rising (W_{max}) and (W_5) values illustrated by the curves of Figure 172.

A similar behavior is exhibited by the specimen prepared with a 1 μ m surface finish. One noticeable difference is that the power index maximum (W_{max}) is extremely low for the first cycle of operation. It is inferred that this behavior arises as a result of the scratch wavelength of the surface being nearly equal to the peak intensity wavelength of the infrared furnace (1 μ m). Note that after some oxide formation (W_{max}) increases (coupling decreases) due to the presence of the surface compound and the specimen behaves the same as if it had been prepared to a 600-grit finish with regard to the power index.

The data of Figures 177 and 178 indicate that the coupling is initially,

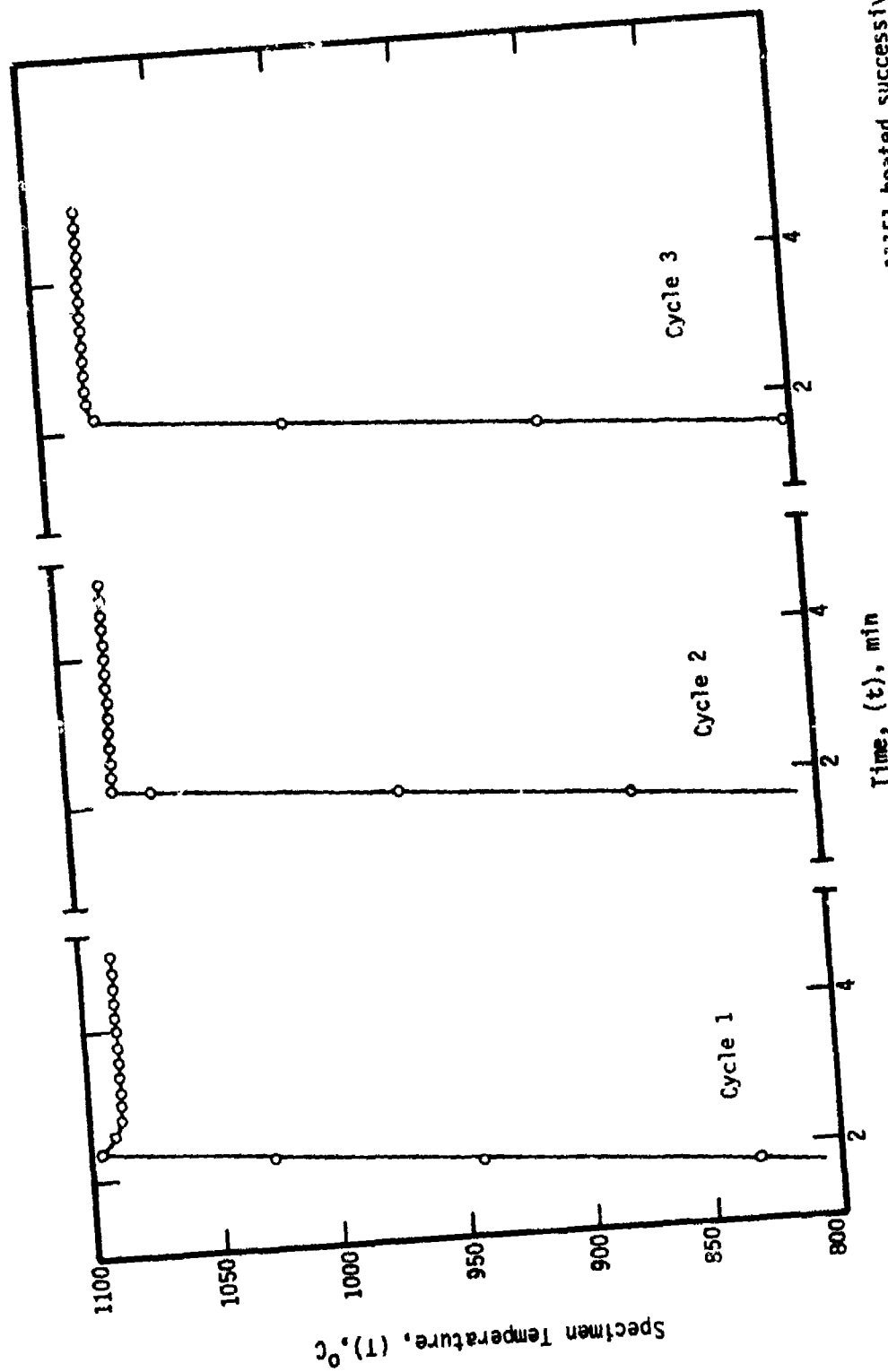


Figure 171. - Transient thermal behavior for unalloyed titanium (Type 2) specimen no. 11151 heated successively three times in 200 torr O_2 at the rate of $8^\circ C/s$ nominally to $1100^\circ C$; 600-grit finish.

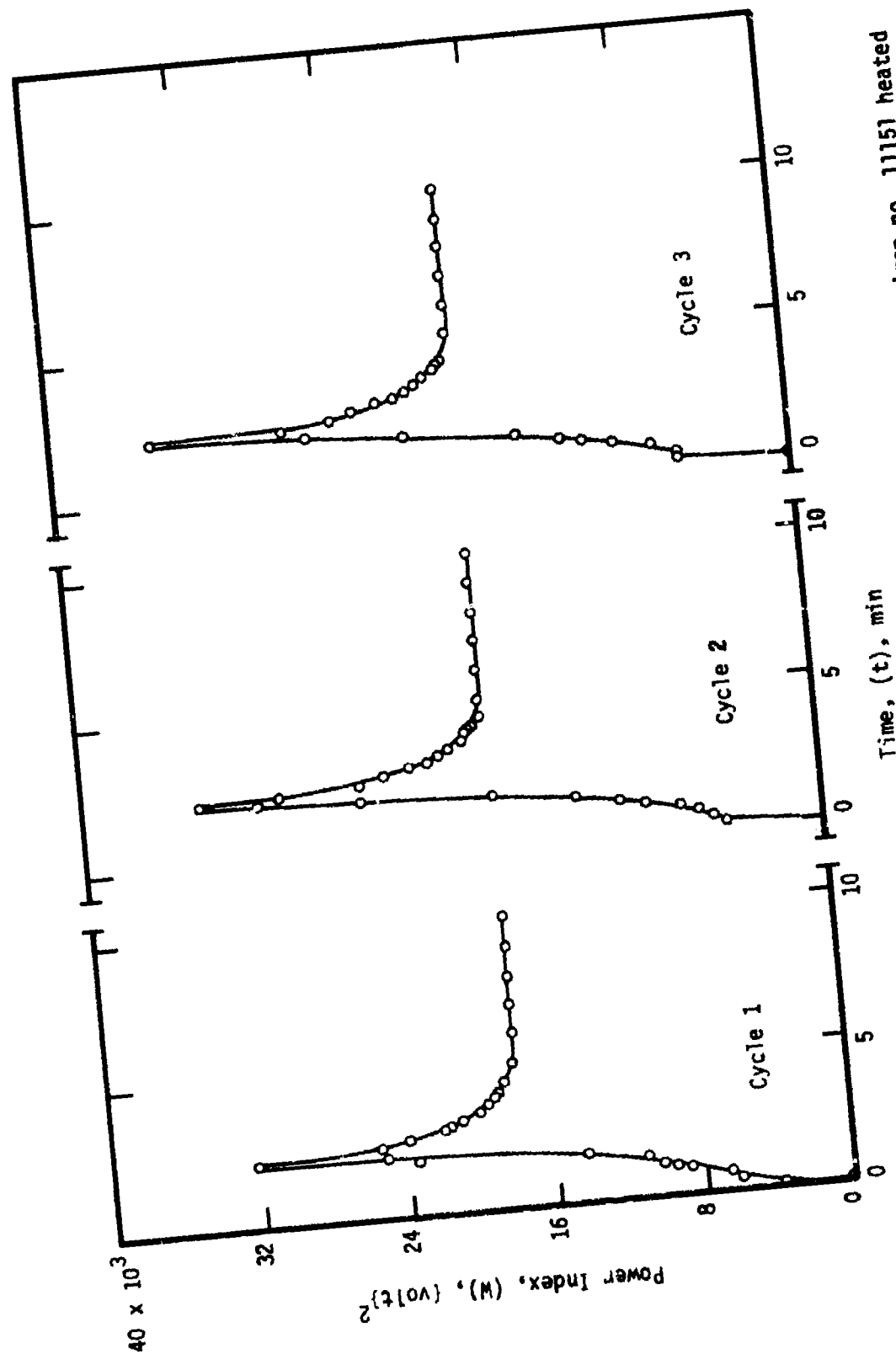


Figure 172. - Transient furnace power behavior for unalloyed titanium (Type 2) specimen no. 11151 heated successively three times in 200 torr O_2 at the rate of $8^\circ C/s$ nominally to $1100^\circ C$; 600-grit finish.

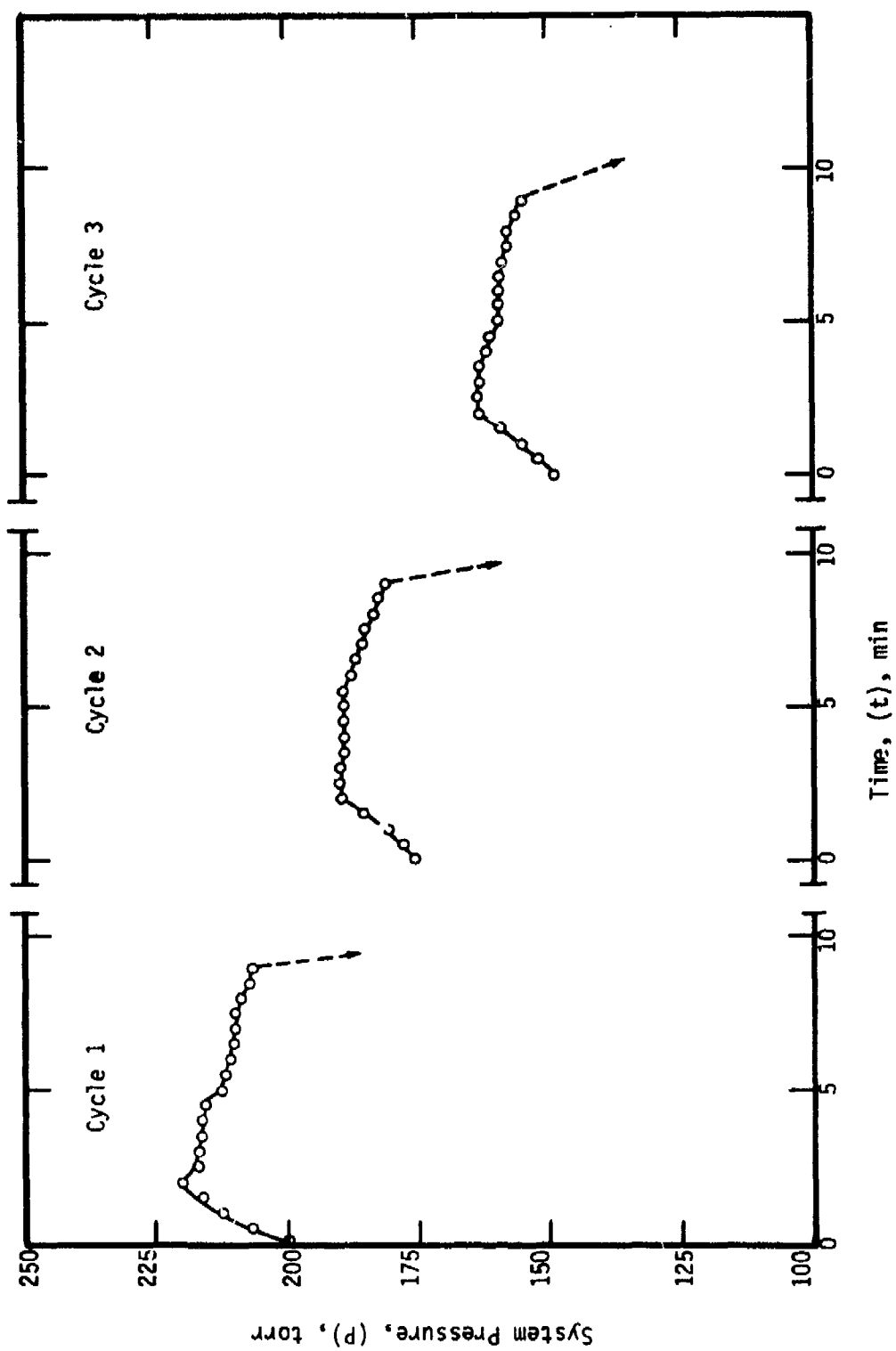


Figure 173. - Transient system pressure behavior for unalloyed titanium (Type 2) specimen no. 11151 heated successively three times in 200 torr O_2 at the rate of $8^\circ C/s$ nominally to $1100^\circ C$; 600-grit finish.

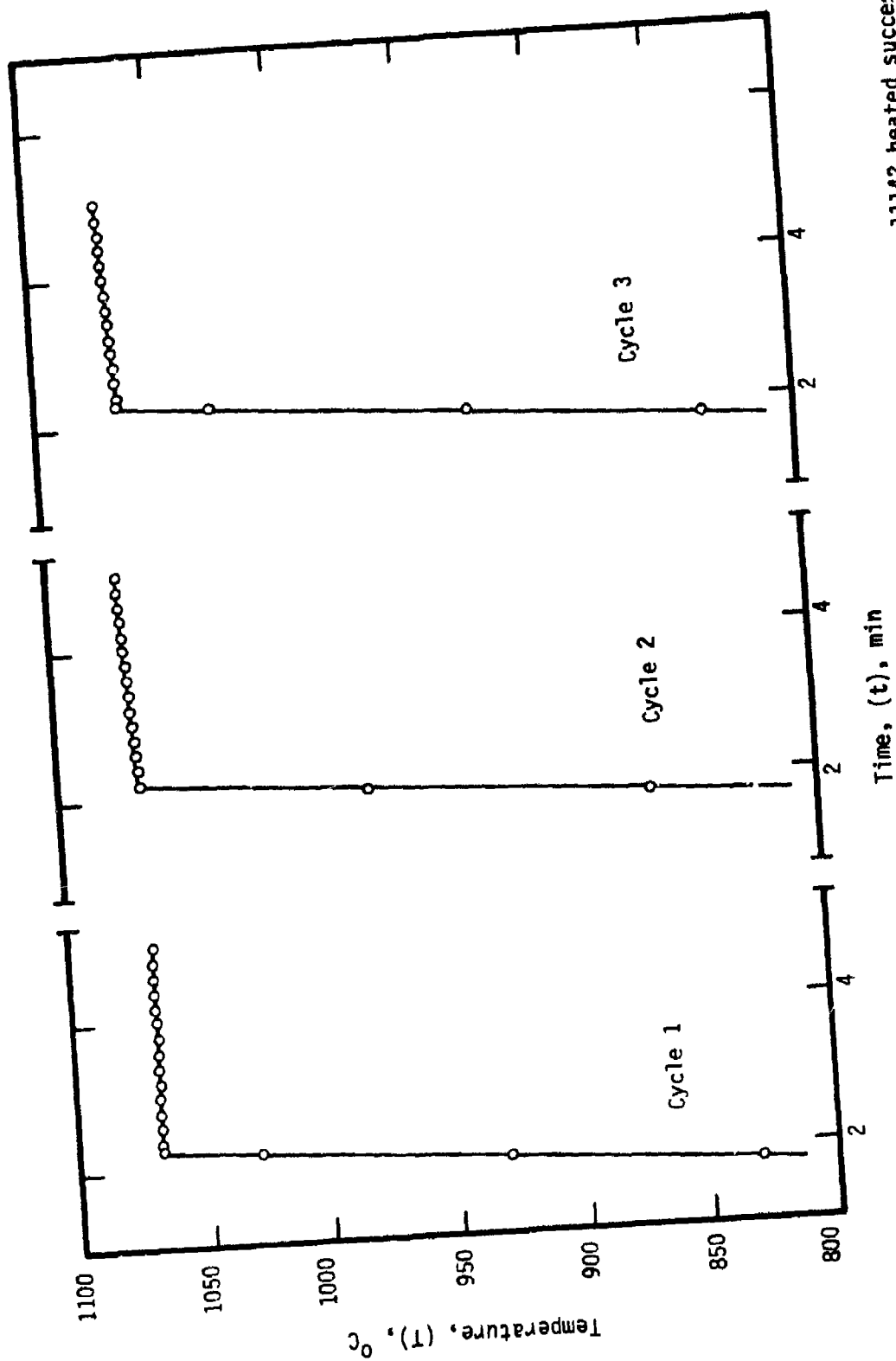


Figure 174. - Transient thermal behavior for unalloyed titanium (Type 2) specimen no. 11142 heated successively three times in 200 torr O_2 at the rate of $8^\circ C/s$ nominally to $1100^\circ C$; 1 μm finish.

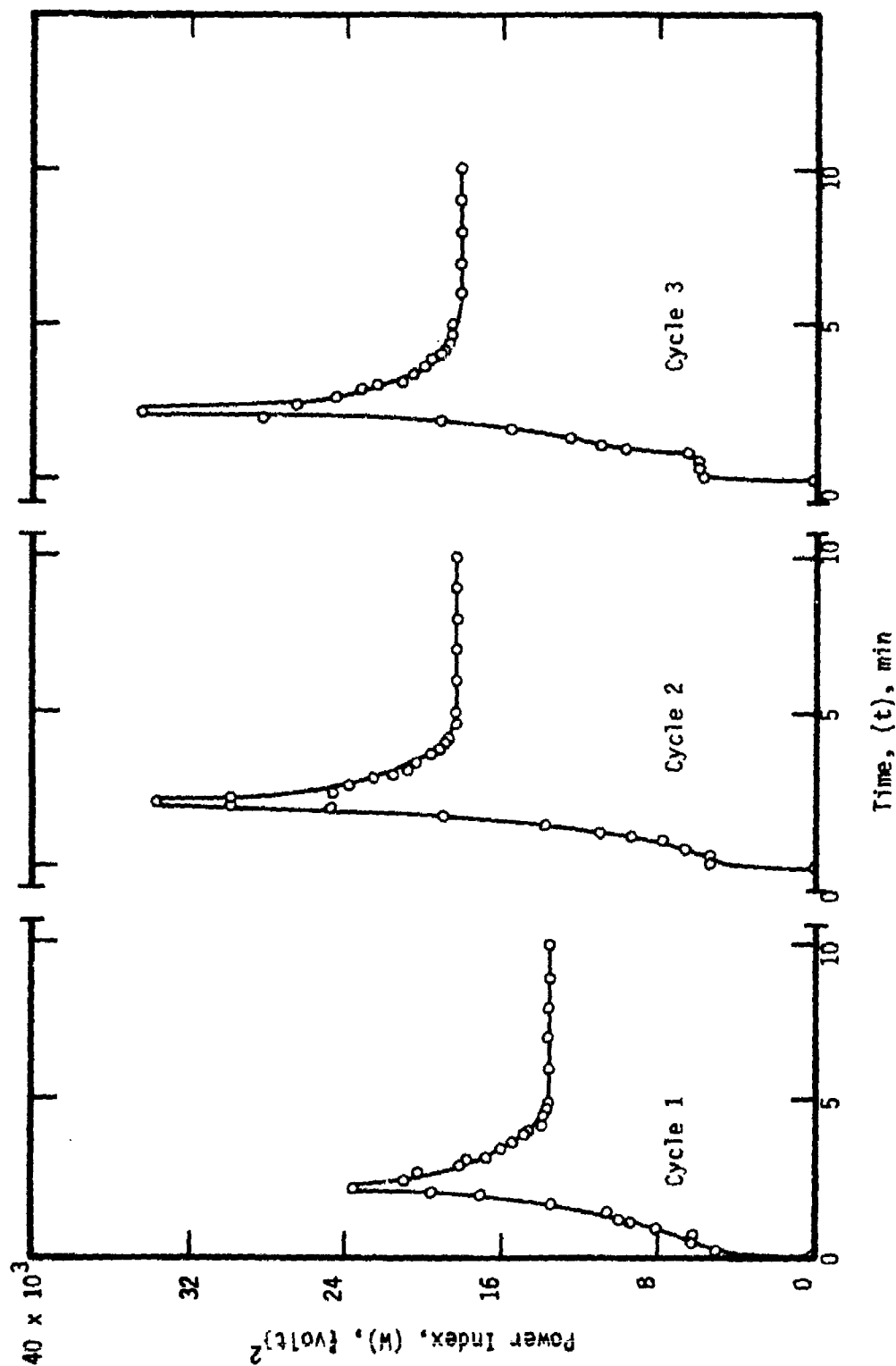


Figure 175. - Transient furnace power behavior for unalloyed titanium (Type 2) specimen no. 11142 heated successively three times in 200 torr O_2 at the rate of $8^\circ C/s$ nominally to $1100^\circ C$; $1\mu m$ finish.

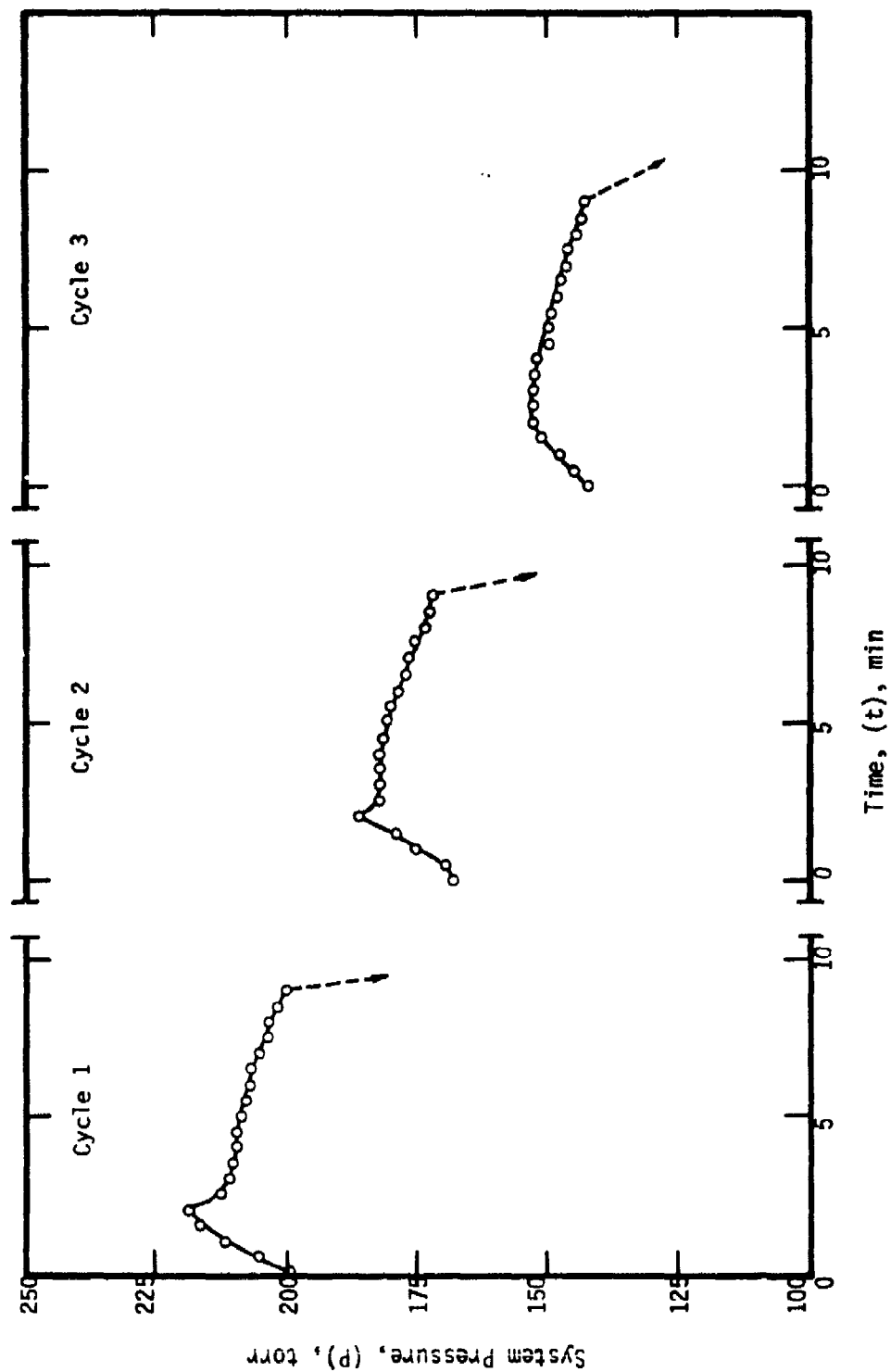


Figure 176. - Transient system pressure behavior for unalloyed titanium (Type 2) specimen no. 11142 heated successively three times in 200 torr O_2 at the rate of $8^\circ C/s$ nominally to $1100^\circ C$; $1\mu m$ finish.

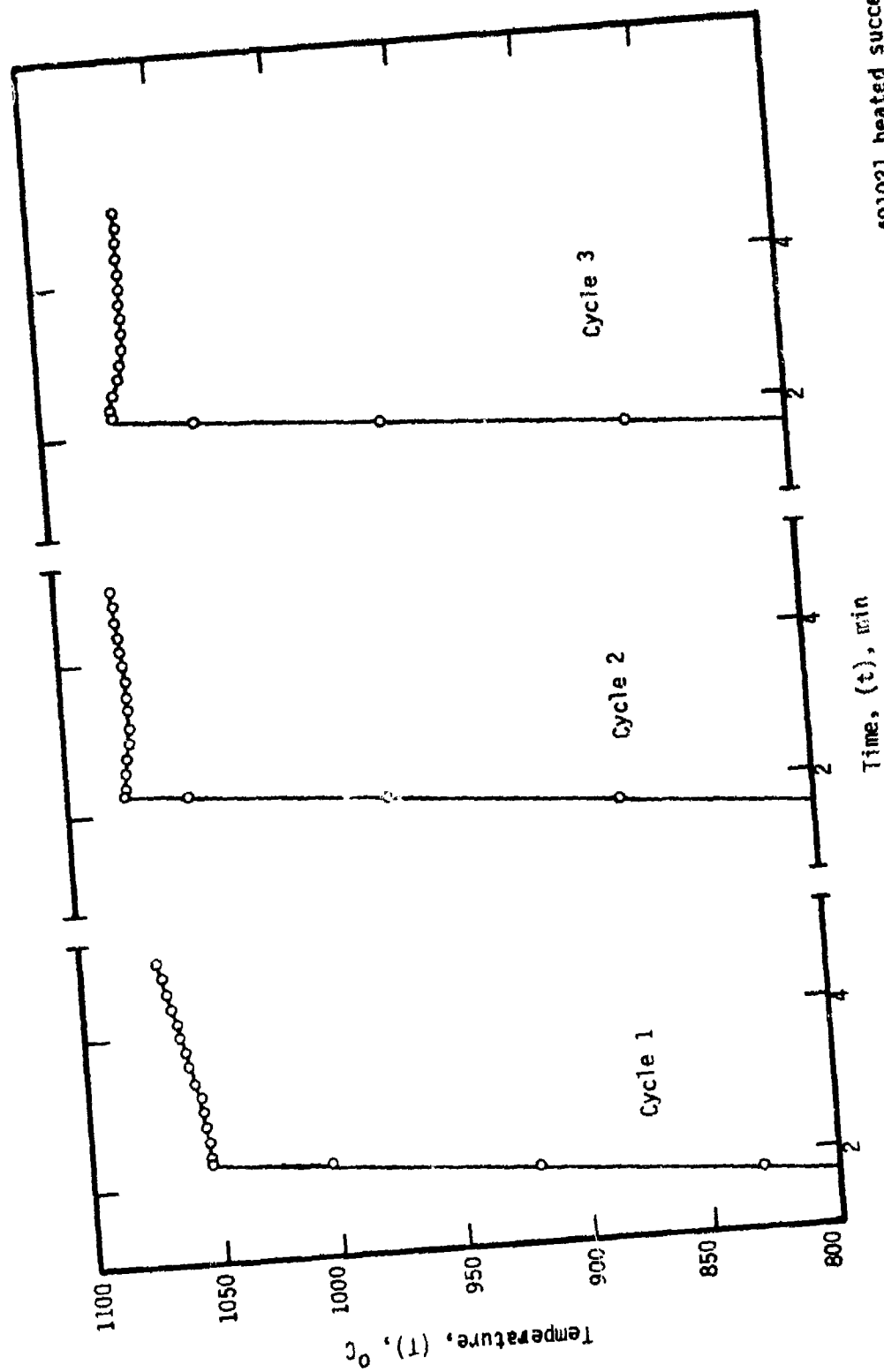


Figure 177. - Transient thermal behavior for unalloyed titanium (Type 2) specimen no. 401021 heated successively three times in 200 torr O_2 at the rate of $8^\circ C/s$ nominally to $1100^\circ C$; 600-grit finish after oxidation and descaling.

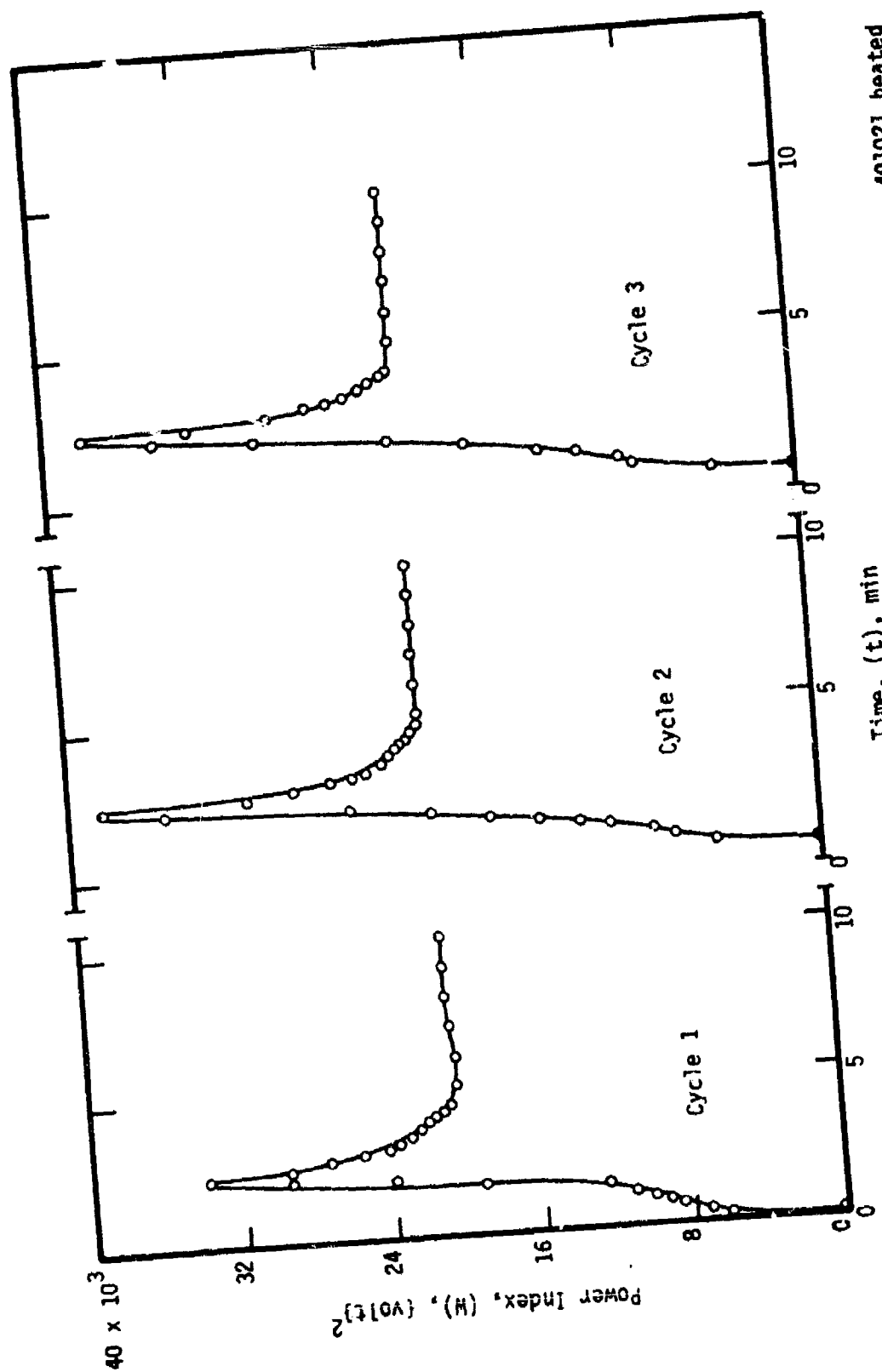


Figure 178. - Transient furnace power behavior for unalloyed titanium (Type 2) specimen no. 401021 heated successively three times in 200 torr O₂ at the rate of 8°C/s nominally to 1100°C; 600-grit finish after oxidation and descaling.

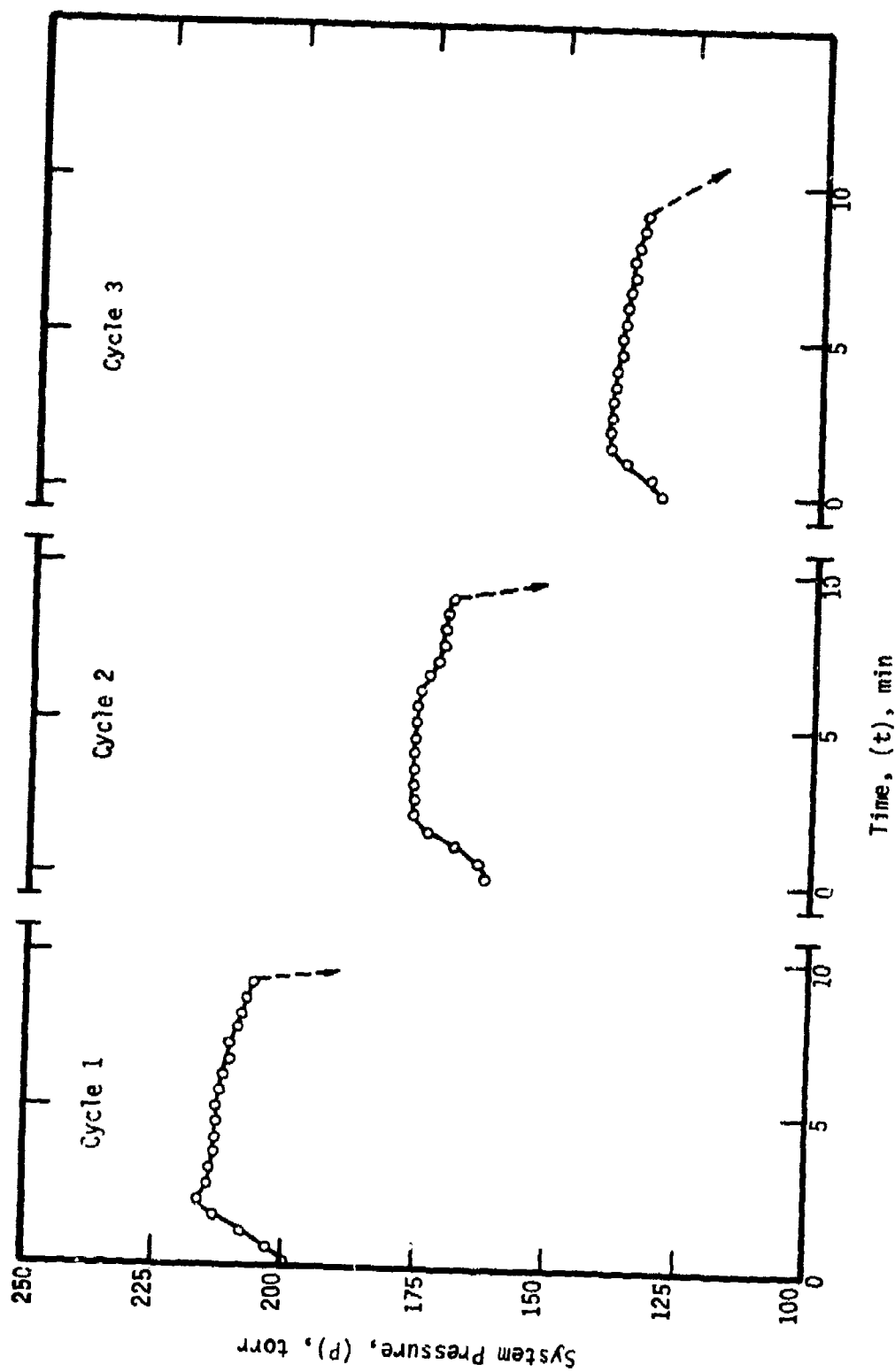


Figure 179. - Transient system pressure behavior for unalloyed titanium (Type 2) specimen no. 401021 heated successively three times in 200 torr oxygen at the rate of 8°C/s nominally to 1100°C; 600-grit finish after preoxidation and descaling.

and remains, somewhat poorer for the pre-oxidized material as higher values of power are required in both the short- and long-term. In addition, the "oxygen-doped" material appears to have consumed more oxygen (during the later stages of testing) than either of the other two specimens, compare Figures 173, 176, and 179.

In summary, it appears that the efficiency for energy coupling to unalloyed titanium is initially dependent upon the RMS surface roughness and that this dependence disappears with time as the scale builds and as the roughnesses of the metal-oxide interfaces are normalized. The outstanding exception to this occurs for the case of "oxygen-doped" titanium which remains less-strongly coupled than "undoped" materials. Thus, it may be that the radiation totally penetrates the scale layer and that coupling efficiency is fixed by the roughness of the substrate metal-oxide interface and the oxygen level of the substrate. Further investigation of this hypothesis is required for its certification.

In the third type of testing undertaken during this investigation, selected specimens of unalloyed titanium were subjected to inspection by x-ray diffractometry. Testing was carried out using the horizontal goniometer of a GE XRD-6D/F unit operating with a copper tube at 35KV and 16ma. The resulting CuK_α radiation was filtered with a nickel foil to enhance the $\text{K}_\alpha : \text{K}_\beta$ ratio. Specimens used in these tests were reacted at elevated temperatures with oxygen, nitrogen, and air; thus, oxides and nitrides are the expected reaction products. Standard x-ray diffraction data for α -titanium, TiO_2 (rutile), and TiN are presented in Table XXIII (see also refs. 22 and 23).

The most complex in this series of tests involved unalloyed specimen no. 40102'. The material from which this specimen was produced is characterized

TABLE XXIII

X-RAY DIFFRACTION DATA FOR UNALLOYED TITANIUM AND ITS COMPOUNDS
AS REPORTED IN THE POWDER DIFFRACTION FILE (REF. 15)

Diffracting Planes (hkl)	Interplaner Spacing _o (d_{hkl}), Å	Intensity Ratio (I/I_0)	Diffraction Angle* (2θ), degrees
UNALLOYED TITANIUM (CARD NO. 5-682)			
010	2.557	30	35.1
002	2.343	26	38.4
011	2.244	100	40.2
012	1.726	19	53.0
110	1.475	17	63.0
103	1.332	16	70.7
200	1.276	2	74.3
112	1.247	16	76.3
201	1.233	13	77.3
004	1.1708	2	82.3
202	1.1220	2	86.7
211	0.9458	11	109.1
TITANIUM DIOXIDE (RUTILE) - TiO_2 (CARD NO. 21-1276)			
110	3.25	100	27.4
101	2.487	50	36.1
200	2.297	8	39.2
111	2.188	25	41.2
210	2.054	10	44.1
211	1.6874	60	54.4
220	1.6237	20	56.6
002	1.4797	10	62.7

TABLE XXIII- concluded

X-RAY DIFFRACTION DATA FOR UNALLOYED TITANIUM AND ITS COMPOUNDS
AS REPORTED IN THE POWDER DIFFRACTION FILE (REF. 15)

Diffracting Planes (hkl)	Interplanar Spacing _o (d_{hkl}), Å	Intensity Ratio (I/I_0)	Diffraction Angle* (2θ), degrees
310	1.4528	10	64.0
301	1.3598	20	69.0
112	1.3465	12	69.8
330	1.0827	4	90.7
TITANIUM NITRIDE - TiN (CARD NO. 6-642)			
111	2.44	75	36.8
200	2.12	100	42.6
220	1.496	55	62.0
311	1.277	25	74.2
222	1.223	16	78.1
400	1.059	8	93.3
331	0.972	12	104.8
420	0.948	20	108.7
442	0.865	20	125.9

*Diffraction angles for nickel-filtered CuK_α radiation determined from tabular information of reference 16.

in the first columns of Table XXIV. Comparison of these data with those of Table XXIII indicates that the as-received material is probably textured as the basal plane { 0002 } reflection is extraordinarily strong indicating a preferred basal plan alignment with the rolling plane.*

After a one-hour exposure at 1100°C, the scale of this specimen was separated from its substrate and all three available interfaces were re-inspected by x-ray diffraction. The data from these tests is presented in the central portion of Table XXIV. Inspection of the scale sheet indicated: 1) that it was essentially rutile, 2) that it was strongly textured** at the gas interface with only the {110 } reflection and its higher orders { 220 } and { 330 } being recorded, and 3) that the strong texture at the gas-oxide interface was not maintained throughout the body of the scale, although it remains present to a degree.

Inspection of the substrate of this specimen immediately after removal of the scale indicated that traces of TiO_2 remained and that it probably was also oriented. After careful sanding of the surface with 600-grit silicon carbide paper, it was found that the substrate had little evidence of texture and produced a nearly-normal diffraction pattern, compare Tables XXIII and XXIV.

The same specimen was returned to the volumetric apparatus and subjected to three successive RC-type cycles to 1100°C in 200 torr oxygen. Subsequent to these tests, an x-ray analysis was again performed on the scale and substrate components of the specimens, see Table XXV. In this case, a slightly textured scale was produced upon the untextured substrate.

*The as-received specimen was prepared with a standard 600-grit silicon carbide finish procedure and such finish evidently does not interfere with texture determination.

**The scale may indeed, in this case, be an oriented overgrowth.

TABLE XXIV

X-RAY DIFFRACTION DATA FOR UNALLOYED TITANIUM (TYPE 2) BEFORE AND AFTER EXPOSURE TO 200 TORR OXYGEN AT 1100°C. FIRST TEST SERIES: SPECIMEN BLANK AND SPECIMEN NO. 401021.

As-Received Material I/I ₀	2θ	Scale Interfaces after RHC*				Base Metal after RHC*			
		Gas/oxide		Metal/oxide		As Removed		600-grit finish	
		I/I ₀	2θ Assignment	I/I ₀	2θ Assignment	I/I ₀	2θ Assignment	I/I ₀	2θ Assignment
-	-	100	28.0° TiO ₂	100	27.8° TiO ₂	45	27.9° TiO ₂	-	-
5	35.2°	-	-	-	-	40	35.2° Ti	29	35.1° Ti
-	-	(36.1° not obs.)		7	36.2° TiO ₂	(36.1° not obs.)		-	-
100	38.4°	-	-	-	-	28	38.0° Ti	26	38.2° Ti
-	-	(39.2° not obs.)		(39.2° not obs.)		-	-	-	-
34	40.2°	-	-	-	-	100	40.1° Ti	100	40.0° Ti
-	-	(41.2° not obs.)		25	41.4° TiO ₂	(41.2° not obs.)		-	-
-	-	(44.1° not obs.)		34	44.2° TiO ₂	(44.1° not obs.)		-	-
8	53.1°	-	-	-	-	(53.0° not obs.)		30	52.8° Ti
-	-	(54.4° not obs.)		30	54.5° TiO ₂	5	54.6° TiO ₂	-	-
-	-	51	56.4° TiO ₂	100	56.7° TiO ₂	9	56.8° TiO ₂	-	-
-	-	(62.7° not obs.)		(62.7 not obs.)		(62.7° not obs.)		-	-
2	63.1°	-	-	-	-	(63.0° not obs.)		7	62.7° Ti

TABLE XXIV - concluded

X-RAY DIFFRACTION DATA FOR UNALLOYED TITANIUM (TYPE 2) BEFORE AND AFTER EXPOSURE TO 200 TORR OXYGEN AT 1100°C. FIRST TEST SERIES: SPECIMEN BLANK AND SPECIMEN NO. 401021

As-Received Material I/I ₀ 2θ	Scale Interfaces after RHC*			Base Metal after RHC*		
	Gas/oxide		Metal/oxide I/I ₀ 2θ Assignment	As Removed		600-grit finish I/I ₀ 2θ Assignment
	I/I ₀	2θ Assignment		I/I ₀	2θ Assignment	
-	-	(64.0° not obs.)	24 63.8° 30 64.1° TiO ₂	(64.0° not obs.)	-	-
-	-	(69.0° not obs.)	25 69.0° TiO ₂	(69.0° not obs.)	-	-
-	-	(69.7° not obs.)	25 69.7° TiO ₂	(69.7° not obs.)	-	-
16 70.7°	-	-	-	(70.7° not obs.)	21 70.2°	Ti
(74.3° not obs.)	-	-	-	5 73.8°	Ti	(74.3° not obs.)
5 76.3°	-	-	-	18 75.4°	Ti	11 76.0°
(77.3° not obs.)	-	-	-	24 77.0°	Ti	30 77.2°
9 82.3°	-	-	-	(82.3° not obs.)	-	(82.3° not obs.)
(86.7° not obs.)	-	-	-	5 86.0°	Ti	(86.7° not obs.)
-	13 90.9°	Ti	49 90.9° TiO ₂	(90.7° not obs.)	-	-
(109.1° not obs.)	-	-	-	(109.1° not obs.)	12 109.6°	Ti

*Heated at 8°C/s to 1100°C in 200 torr O₂, held for one hour, then cooled at 0.5°C/s.

TABLE XXV

X-RAY DIFFRACTION DATA FOR UNALLOYED TITANIUM (TYPE 2) AFTER EXPOSURE TO
200 TORR OXYGEN AT 1100°C. SECOND TEST SERIES: SPECIMEN NO. 401021

Scale Interfaces after 3RC*					Base Metal after 3 RC*				
Gas/oxide		Metal/oxide			As Removed		600-grit finish		
I/I ₀	2 θ	Assignment	I/I ₀	2 θ	Assignment	I/I ₀	2 θ	Assignment	Assignment
-	-	-	-	-	7	24.2°	unknown	-	-
100	27.8°	TiO ₂	100	27.7°	TiO ₂	100	27.8°	TiO ₂	-
-	-	-	-	-	[27]	35.2°	Ti	26	35.1°
32	36.5°	TiO ₂	45	36.3°	TiO ₂	(36.1° not obs.)	-	-	-
-	-	-	-	-	-	(38.4° not obs.)	8	38.3°	Ti
(39.2° peak not obs.)			12	39.4°	TiO ₂	(39.2° not obs.)	-	-	-
-	-	-	-	-	[85]	40.1°	Ti	100	40.3°
38	41.6°	TiO ₂	33	41.5°	TiO ₂	15	41.5°	TiO ₂	-
32	44.4°	TiO ₂	12	44.2°	TiO ₂	5	44.4°	TiO ₂	-
					[65]	52.3°	Ti	7	52.9°
83	54.6°	TiO ₂	45	54.5°	TiO ₂	25	54.5°	TiO ₂	-
81	56.9°	TiO ₂	55	56.7°	TiO ₂	11	56.7°	TiO ₂	-
34	62.8°	TiO ₂	31	62.1°	TiO ₂	-	-	-	-
-	-	-	-	-	[20]	62.6°	Ti(?)	7	62.6°

TABLE XXV (concluded)

X-RAY DIFFRACTION DATA FOR UNALLOYED TITANIUM (TYPE 2) AFTER EXPOSURE TO
200 TORR OXYGEN AT 1100°C. SECOND TEST SERIES: SPECIMEN NO. 401021

Scale Interfaces after 3RC*					Base Metal after 3 RC*				
I/I ₀	Gas/oxide 2θ	Assignment	Metal/oxide		As Removed		600-grit finish		
			I/I ₀	2θ	Assignment	I/I ₀	2θ	Assignment	
35	64.1°	TiO ₂	18	64.1°	TiO ₂	(64.0° not obs.)	-	-	-
32	69.1°	TiO ₂	25	69.0°	TiO ₂	4	69.0	-	-
33	69.6°	TiO ₂	16	69.7°	TiO ₂	(69.8° not obs.)	-	-	-
-	-	-	-	-	-	-	-	4	70.0
-	-	-	-	-	-	(74.3° not obs.)	(74.3° not obs.)	-	Ti
-	-	-	-	-	-	[16]	75.3	Ti(?)	4
-	-	-	-	-	-	[100]	76.8°	Ti	13
36	91.0°	TiO ₂	(90.7° not obs.)	-	-	(90.7° not obs.)	-	-	-
-	-	-	-	-	-	(109.1° not obs.)	7	109.5°	Ti

*Heated at 8°C/s to 1100°C in 200 torr O₂, held for 5 minutes, then cooled at 0.5°C/s. Test repeated 3 times.

The metal-oxide interface of the substrate again contained traces of residual oxide; but no evidence for texture is cited for this material. The substrate metal did exhibit some anomalous intensity and positional relations (which may be due to oxygen solution); however, no systematic alterations were noted on cursory inspection. The resanded (600-grit) surface exhibited an essentially random, nearly-normal diffraction pattern as was the case prior to its exposure to cyclic oxidation.

Another specimen, exposed in air at 900°C for 4 hours in the conventional heating apparatus (spec. no. 05151), was inspected in a similar fashion to the above by x-ray diffraction techniques. As above, the oxide (rutile) spalled as a sheet and both interfaces were inspected. The results of these inspections are presented in Table XXVI. Contrary to the preceeding test, the oxide in this case was textured at the metal-oxide interface and essentially randomly oriented at the gas-oxide interface. The texture is apparently not simple and its existence at the metal-oxide interface (but not at the gas-oxide interface) is unusual in the experience of the principal investigator.

In the final series of x-ray examinations, two specimens which had been exposed in 200 torr nitrogen at 1100°C were examined. The specimens had been treated identically; however, the unalloyed one (spec. no. 402281) exhibited a relatively thick, black scale while the one which was alloyed (spec. no. 401162) exhibited a thinner, gold scale (or film). Results of these x-ray examinations are presented in Table XXVII.

Tentatively, the surface compound in both cases is identified as the nitride TiN; however, an unassignable reflection at approximately $24^{\circ} 2\theta$ was observed. The dark nitride (spec. no. 402281), appears to be essentially a thick (no Ti reflections noted), randomly-oriented product with a slightly

TABLE XXVI

X-RAY DIFFRACTION DATA FOR UNALLOYED TITANIUM (TYPE 1) AFTER EXPOSURE
IN AIR AT 900°C FOR 4 HOURS IN THE CONVENTIONAL HEATING
APPARATUS. SPECIMEN NO. 05151

Scale Interfaces - Air Test					
Gas/Oxide			Metal/oxide		
I/I_0	2θ	Assignment	I/I_0	2θ	Assignment
100	27.7°	TiO ₂	67	27.7°	TiO ₂
48	36.2	TiO ₂	100	36.2°	TiO ₂
7	49.4°	TiO ₂	9	39.4°	TiO ₂
25	41.4°	TiO ₂	48	41.4°	TiO ₂
10	44.2°	TiO ₂	8	44.3°	TiO ₂
77	54.3°	TiO ₂	91	54.4°	TiO ₂
21	56.6°	TiO ₂	16	56.8°	TiO ₂
13	62.7°	TiO ₂	33	62.8°	TiO ₂
10	64.1°	TiO ₂	9	64.2°	TiO ₂
23	68.9°	TiO ₂	29	69.0°	TiO ₂
13	69.7°	TiO ₂	29	69.8°	TiO ₂

TABLE XXVII

X-RAY DIFFRACTION DATA FOR UNALLOYED TITANIUM AND
 Ti-6Al-4V ALLOY AFTER EXPOSURE IN NITROGEN AT 1100°C

Unalloyed Titanium			Ti-6Al-4V		
Spec. No.	402281-black product		Spec. No.	401162-gold product	
I/I ₀	2θ	Assignment	I/I ₀	2θ	Assignment
65	24.0°	Unknown	62	23.8°	Unknown
-	-	-	28	35.4°	Ti
63	36.7	TiN	(100)	37.0°	TiN
-	-	-	26	40.3°	Ti
100	42.7°	TiN	(94)	42.8°	TiN
69	61.4°	TiN	(59)	61.9°	TiN
-	-	-	100	63.2°	Ti
32	73.5°	TiN	(35)	74.3°	TiN
-	-	-	13	76.0°	Ti
20	77.3°	TiN(?)	(20)	77.8°	TiN
12	92.5°	TiN	(93.3° peak not obs.)		
12	104.4°	TiN	(104.8° peak not obs.)		
20	108.3°	TiN	(108.7° peak not obs.)		
-	-	-	15	110.0°	Ti

dilated lattice. Conversely, the golden nitride is thin enough that the reflections of the substrate (somewhat textured) pass through the film and are more dominant than reflections from the film itself. Further, the film appears to be oriented upon the substrate with the octahedral planes preferentially parallel to the specimen surface. The degree of orientation here does not approach that of an oriented overgrowth.

In summary, it appears from these few x-ray studies that orientation effects both within the substrate and subsequently within the reaction products upon them must be considered in an overall description of the reaction mechanism. It is noted that there was found no evidence for oxides other than TiO_2 (rutile) or for nitrides other than TiN and that in air at 900°C there was no evidence for nitride formation.

5. REACTION OF TITANIUM-BASE MATERIALS IN OXYGEN LEADING TO IGNITION DURING HEATING

This section deals with the processes which are believed to occur during the initial stages of interaction between titanium-base materials and a reactive gas. Special emphasis is here placed upon the generation of mechanical forces and their effects upon reactivity which can ultimately lead to ignition under conditions of anisothermal oxidation.

In order to set the stage for interpreting the experimental results of this research, some brief comments regarding the nature of anisothermal oxidation are presented here. Titanium and its alloys have been observed to oxidize in a manner describable by the parabolic rate law, at least for the case of short-term high-temperature oxidation (ref. 2). We assume this and further assume that the parabolic rate constant for these materials is phenomenologically describable by an Arrhenius-type relationship. This being the case, the problem which next arises is how properly to account for the scaling behavior

under conditions of non-constant temperature (anisothermal) oxidation. At least two distinct approaches may be taken: 1) to maintain the activation energy (Q) a constant or 2) to allow (Q) to vary with the temperature (or time), and therefore the degree of completion of the reaction. We have chosen the former approach upon the basis of simplicity.

If one considers the regime of heating a clean specimen in an oxidizing atmosphere from room temperature at a linear rate (r) and to a maximum temperature (T_m), then the rate of reaction will increase exponentially with temperature but will decrease in inverse proportion to the average scale thickness. Thus, during heating, the rate of reaction increases; while after the maximum temperature is attained, and thereafter maintained, the rate of reaction decreases. For this idealized case, we may calculate the specific weight gain of a titanium specimen under anisothermal (continuous heating) conditions. This calculation is especially simple if the specimen experiences a linear heating rate. The method of this calculation for such conditions is outlined in Appendix V and a schematic graphical presentation resulting from it has been presented in Figure 41. This figure indicates that, given such heating conditions, the quantity of gas fixed exhibits a sigmoidal character which, in turn, gives rise to a maximum specific linear reaction rate (\dot{N}_{max}) occurring at the instant that the maximum temperature is achieved.

The behavior schematically illustrated in Figure 41 represents a "model" against which we shall compare our experimental results. As will be seen below, the experimental data are in qualitative agreement with the model but in some cases deviate quantitatively from it. These deviations, in turn, are discussed in terms of concepts intentionally omitted from the simplistic model; specifically: the effect of mechanical strain upon reaction kinetics and the effect of depositing the heat of reaction in the near-surface zone of the specimen.

In order to utilize the model described in Appendix V, it was necessary to determine experimentally the parabolic rate constants, (K_p) , as a function of temperature for titanium. Because it was suspected that any perturbations on the modeled scaling behavior due to heating would be least at longer times it was the long-term data which was analyzed to provide these determinations. In the scheme of these experiments, long-term isothermal exposure was 1 hour. The values of (K_p) , determined as the squared total weight gain divided by the isothermal exposure time, did not exhibit a systematic variation with heating rate. Analyses of these data, when plotted in Arrhenius format for unalloyed titanium, $Q=58.7$ K-cal/mole and $A=7.26 \times 10^{-4}$ mg²/cm⁴-sec.

The results of this calculation, applied during the period of dynamic heating and utilizing the above constants, indicated that the specific weight gain increases in a monotone fashion with increasing oxidation temperature. The time derivative of this curve is everywhere positive and monotone increasing and, thus, does not predict a maximum in (\dot{N}) prior to the onset of the isothermal portion of our (RHC) tests. After reaching the isothermal portion of a typical heating program, the rate of reaction must decrease as indicated by the time derivative of the parabolic rate law and, hence, a maximum in the reaction rate is predicted at the instant (T_{max}) is reached.

Conversely, our observations indicate that maxima in the specific reaction rate occur during heating which implies that the model presented in Appendix V must be modified in some manner so as to produce this effect.* It is believed that such modification may be most realistically achieved through considerations of the mechanical forces generated during the heating period.

*Evidence secured at Clemson University and independent of this research indicates that nickel also oxidizes in an accelerated manner during heating; however, this phenomena is associated with gross oxide plasticity.

Whatever the origin of these forces, they must result in an increase in the effective area of reaction in order to produce the observed maxima in (\dot{N}) during heating of titanium and its alloys.* In the initial stages of heating, titanium is to a good approximation a single material; however, as reaction proceeds the specimen becomes a composite material of very special mechanical properties and geometry. Three parallel zones develop within the specimen (external scale, gas solution, and unaffected "core" metal) and with each pair of these zones there is developed an interphase boundary which attempts to maintain coherency during subsequent heating. With this description of oxidizing titanium, we may now catalog some of the processes which could lead to the generation of mechanical forces in the composite, these include:

- 1) Strains arising from differential thermal expansion between any two phases,
- 2) Strains arising as a result of recrystallization and grain growth within any one phase,
- 3) Strains arising from phase changes within any one phase, and
- 4) Strains arising in the phase(s) of the diffusion zone as a result of gas solution.

Of these possible sources of mechanical force, and therefore of \dot{N} , multiplication, one must be selected which can account for the observation that the maximum specific reaction rate (\dot{N}_{\max}) increases with increasing heating rate, see for example, Figure 97. The first of the listed force sources appears to be the most likely candidate as the thermal strain is directly proportional to the temperature rise and the thermal strain rate,

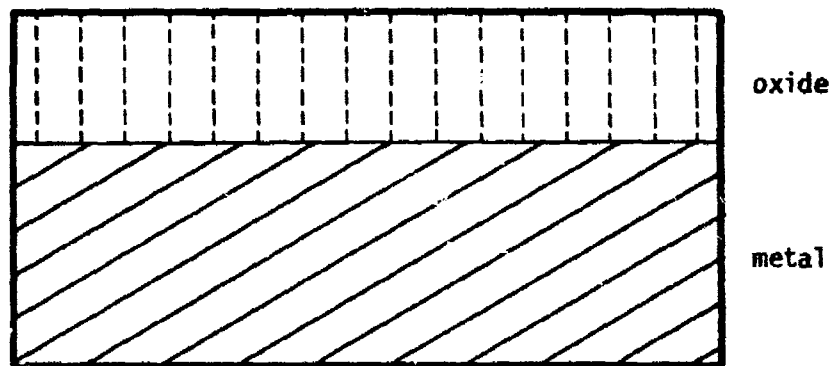
*As with many measurements made in the field of high-temperature oxidation this is an "integral" measurement in that its basis is a summation of incremental reactivities over the entire reaction surface (vs. projected surface).

which must be compensated for by phase plasticity*, is directly proportional to the heating rate.

A schematic illustration based on this idea for an oxidizing titanium specimen is presented in Figure 180 where the microstructural features of oxide and substrate have been grossly oversimplified. The upper sketch is meant to illustrate the condition of a small region of the surface of a specimen undergoing high-temperature oxidation during heating. The dashed lines within the oxide phase represent the diffusion flux paths involved with the scale-forming reaction. In the lower sketch is the same region of surface after the temperature has increased an amount (Δt) during some time interval (Δt). Because the metallic substrate will expand more than the scale layer over this temperature interval, it is here assumed that the relatively thin oxide will undergo a non-uniform plastic deformation. This deformation, in turn, will produce an increase in surface area and an increase in net reactivity as the diffusion flux density is increased. In addition, it is seen that the diffusion paths created as a result of the plastic deformation of the scale are shorter than they otherwise would be. These two effects, oxide area generation and diffusion length reduction, are postulated to reinforce one another to provide a maximization of (\dot{N}) during the heating period and a dependence of (\dot{N}) upon heating rate qualitatively similar to those required by observation.

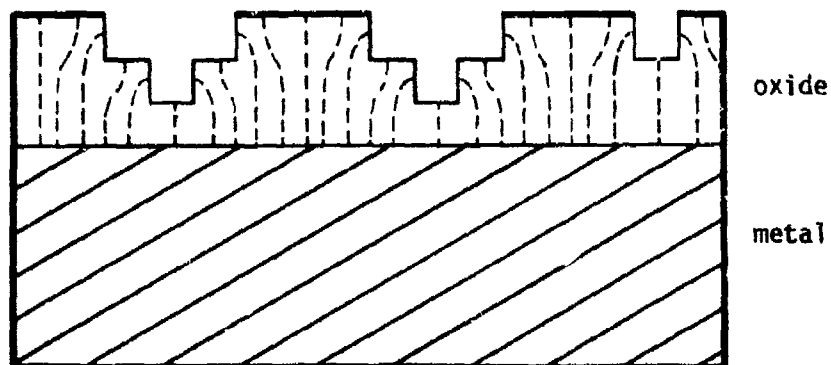
The above discussion has not at all encompassed the concepts of the thermal gradient generation or entrapment of the heat of reaction both of which are recognized: to exist, to develop strain fields, and to increase in importance as the rate of heating is increased. Effects of the deposited heat of reaction will be discussed below.

*At high temperatures, the plasticity may be evidenced as a creep strain in the oxide or metal or both; at lower temperatures, other types of "damage" may be incurred in the oxide and/or metal.



Temperature: T

Time: t



Temperature: T

Time: t

Figure 180. - Schematic illustration of the effect of oxide plasticity arising as a result of differential thermal expansion during concurrent heating and oxidation. Dashed lines indicate diffusion flux paths available to the reaction.

In order to test these concepts, selected oxidation data for unalloyed titanium specimens were analyzed by the method outlined in Appendix V. Only the results of those (RHC)-type tests having programmed maximum temperatures of 1100°C and heating rates of 0.5°, 8°, and 22°C/s will be discussed here as they are representative of similar tests conducted using other maximum temperatures. The values of (Q) and (A) derived above from long-term data were used to model the oxidation behavior and convergence of predicted and observed reactivities is therefore forced only at long times.

Typical comparisons of the short-term modeled and observed degrees of reaction, in terms of specific oxygen consumption, are presented in Figures 181 and 182 for heating rates of 0.5° and 22°C/s, respectively. The total number of moles fixed during heating bears an inverse relation to the heating rate, as expected. Additionally, at the higher heating rate the reaction occurs sooner and with more intensity than predicted, as might qualitatively be expected from the discussion involving Figure 180. Note that the observed and predicted values of gas consumption near the end of the heating period are almost equal for the slowest heating rate investigated, see Figure 181.

The dependence of the reactivity of titanium upon heating rate is more clearly demonstrated in Figure 183 where the specific linear reaction rates predicted by the model are compared with those observed.* Here it is seen that there is qualitative agreement in that larger values of the maximum, (\dot{N}_{\max}) , are in both cases associated with higher heating rates. However, Figure 183 also indicates that as the heating rate is increased: 1) the half-

*The time axis of this figure represents the time as counted from the initiation of heating and is compressed on a logarithmic scale only to facilitate delineation of (\dot{N}) for various heating rates.

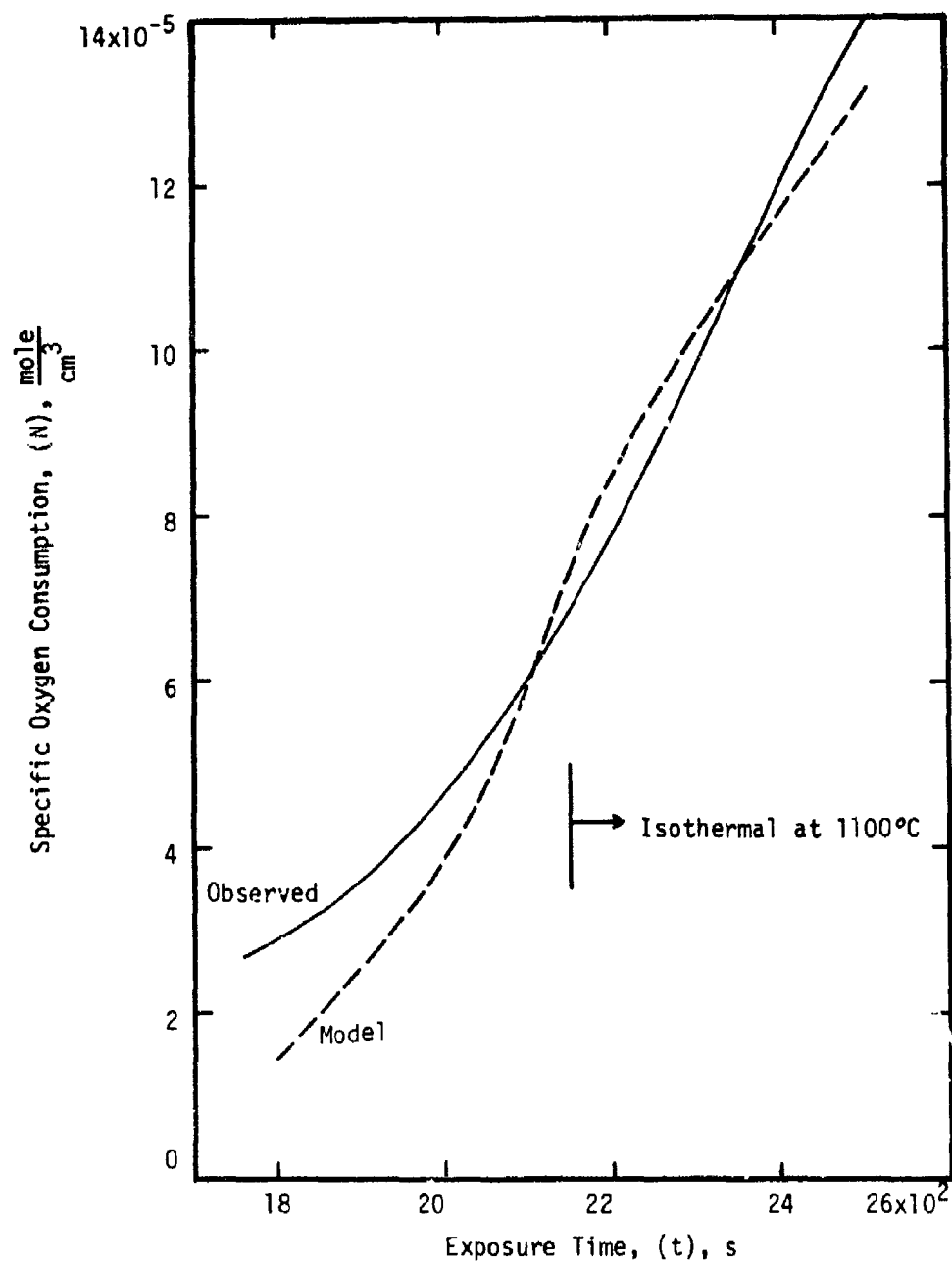


Figure 181.- Comparison of observed and predicted gas consumptions for unalloyed titanium (Type 1) specimen no. 06131 heated at the rate of 0.5°C/s to 1100°C.

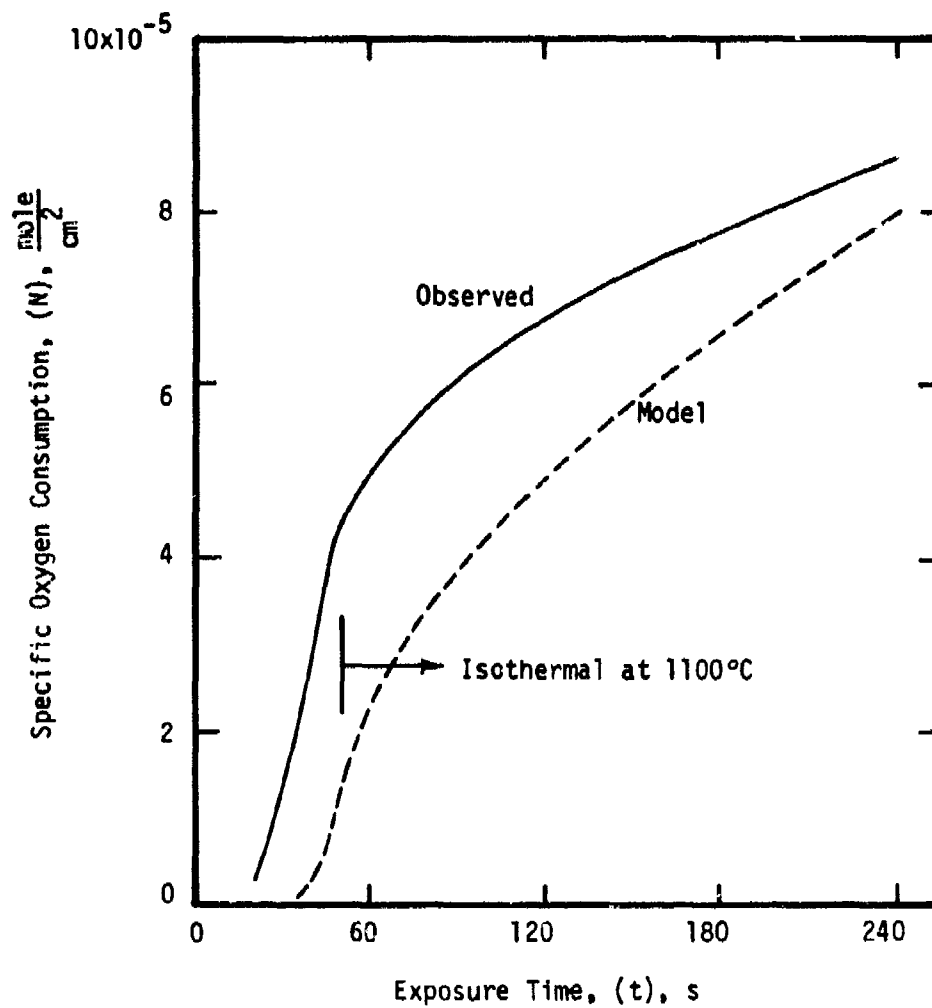


Figure 182.- Comparison of observed and predicted gas consumptions for unalloyed titanium (Type 1) specimen no. 06142 heated at the rate of 22°C/s to 1100°C.

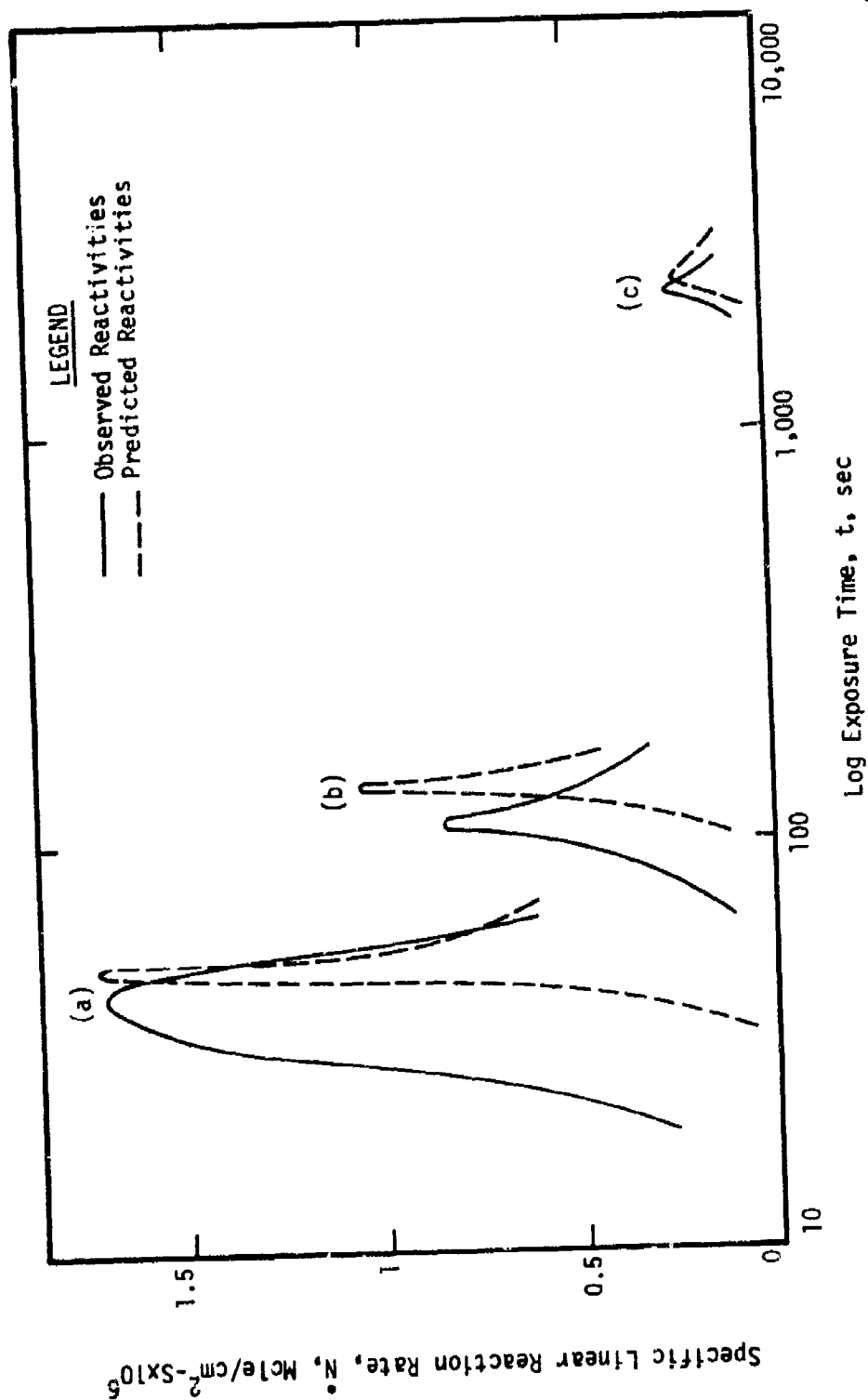


Figure 183.- Comparison of observed and predicted reactivities of unalloyed titanium (Type 1) specimens heated to 1100°C and subsequently held isothermally. (a) Specimen no. 06142 heated at 22°C/s; (b) specimen no. 06071 heated at 8°C/s; (c) specimen no. 06131 heated at 0.5°C/s.

width of the (\dot{N}) pulses broaden systematically with respect to prediction, 2) the time at which (\dot{N}_{\max}), is achieved becomes less than predicted, and 3) commensurately, the temperature at which (\dot{N}_{\max}) is achieved becomes systematically lower. Thus, while the predicted temperature corresponding to (\dot{N}_{\max}) is 1100°C independent of heating rate, the observed temperatures for the heating rates, investigated were: 1100°C for 0.5°C/s, 1050°C for 8°C/s and 1020°C for 22°C/s. Again, it is seen that only for the lowest heating rate are the observed and predicted behaviors quite similar with regard to all aspects of the (\dot{N}) pulses.

The peculiar heating rate sensitivity of the initial reactivity of titanium cited above must be considered in light of intrinsic and inter-related characteristics of the metal-oxide systems involved. First, it is the consensus that the major site of oxide formation for titanium is other than at the gas-oxide interface. It follows that any area multiplication per se at that interface will not drastically alter the reaction kinetics of titanium. Second, there is little if any evidence for oxide upheaval or other plastic deformation for cases in which titanium was heated in oxygen and immediately cooled (RC-type tests). Rather, the surfaces are composed of faceted oxide grains. This lack of plasticity of titanium oxide is in agreement with corresponding determinations of oxide plasticity made using bulk specimens (ref. 24). Finally, the coefficients of thermal expansion of titanium and its oxide are not "matched" over the temperature interval investigated (ref. 25). This factor alone can give rise to large strains in the scale during anisothermal oxidation (ref. 26).

The above considerations lead us to propose that at low heating rates an oxide of limited plasticity forms upon titanium in such manner as to provide an interfacial reaction area (beneath the microscopic gas-oxide interface) approximately equal to the geometric projected specimen area.

At high heating rates, we propose that this effective area is increased by a mechanism associated with the differential thermal expansion of titanium and its oxide scale, see Figure 180.

In addition to the strain-enhanced reactivity cited above, yet another factor enters the reaction scheme at high heating rates; namely, the deposition of the chemical heat of reaction at or near the metal surface. It is convenient to consider the chemical heat input in terms of an average heat flux delivered into the oxidizing substrate volume defined as follows:

$$\dot{q}_v = (\dot{N}) (\Delta H) (S_v) \beta \text{ [cal/cm}^3 \text{ - s]} \quad \text{Eq. (4)}$$

where (\dot{N}) , [mole O_2 /cm²-s] is the actual specific linear reaction rate based on the true area of the reaction interface; (ΔH) [cal/mole O_2] is the heat of oxide formation; (S_v) , [cm²/cm³], is the macroscopic surface-to-volume ratio; and (β) is a function governing the partition of heat into and out of the specimen.

In the case of titanium, the chemical heat is deposited at a site between the gas-oxide and metal-oxide interfaces where it may be considered to be effectively trapped ($\beta=1$) and can be utilized to produce very rapid ($>10^3$ °C/s) local superheating of the metal. So initiated, this effect induces a "bootstrap" reaction sequence of heat generation and oxidation acceleration which can ultimately lead to ignition of the metal. In support of this concept, we have experimentally induced ignition of unalloyed titanium, Ti-6Al-4V, Ti-8Mn, and β -III titanium alloy specimens, as indicated by the data of Table XXVIII. Here it is indicated that ignition may occur at temperatures as low as 388°C for specimens heated in stagnant 200 torr oxygen at heating rates between 28° and 100°C/s. Tests of this nature were reproducible when conducted using relatively thin (0.010 to 0.025 cm) specimens, for which the values of (S_v) and therefore (\dot{q}_v) , are large. The low macroscopic specimen

TABLE XXVIII
SUMMARY OF DATA FOR TESTS OF TITANIUM AND TITANIUM-BASE
ALLOYS LEADING TO IGNITION IN 200 TORR OXYGEN

Specimen Number	Heating Rate (°C/s)	Sensible Igni-Temperature (°C)	Reaction Rate[1] (\dot{N}_{max}), $\times 10^{-5}$	Remarks
A. UNALLOYED TITANIUM-(TYPE 2)				
405141	100	~539	~334	Cold worked 87%
405142	100	573	4810	Cold worked 87%
B. UNALLOYED TITANIUM-(TYPE 4)				
406103	100	822	121	Annealed
C. UNALLOYED TITANIUM-(TYPE 5)				
406101	100	~439	~138	Annealed
406102	100	388	284	Annealed
408271	58	412	285	Annealed
408272	~58	ND	233	Pt securing wire; no thermocouple
408273	~58	ND	398	Chromel securing wire; no thermocouple
408281	28	564	386	Annealed
D. TITANIUM-6% ALUMINUM-4% VANADIUM				
406104	100	647	262	Annealed
E. TITANIUM-8% MANGANESE				
409172	75	448	358	Milled and polished to .0251 cm
409192	48	469	305	Milled and pol- ished to .0279 cm
409232	53	682	780 [2]	Milled and pol- ished to .0343 cm
F. TITANIUM- β -III				
409171	82	410	459	Milled and pol- ished to .0239 cm
409191	72	452	203	Milled and pol- ished to .0287 cm

FOOTNOTES

[1] Values of \dot{N}_{max} may be somewhat low due to slow response time of pressure transducer.

[2] Prior contamination of tube possibly makes this value uncertain.

temperatures at which ignition was sensibly detected (400°C) further reinforces the concept of localized heating.

The observed ignition behavior of titanium-base materials is viewed as a natural extension of their high-temperature oxidation, but relegated to the regime of high heating rates for which values of (\dot{q}_v) are large. Thus, as the rate of heating is increased, it is expected that both the mechanical and chemical effects will act in concert to accelerate the rate of reaction and thereby lower the temperature at which ignition is sensibly detected (T_{ig}). A confirmation of this concept for the case of unalloyed titanium is illustrated by the graph of Figure 184. In this context, the graph of Figure 183 represents various precursor stages to the ignition phenomenon.

In a further attempt to demonstrate that oxidation and ignition are closely linked and represent differences in degree rather than kind, the curves of Figure 185 were constructed using calculations based upon equation 4. The data points entered upon these curves represent various specimens of unalloyed titanium subjected to a variety of heating rates in (RHC)-type tests to a maximum programmed temperature of 1100°C . In this semi-quantitative construction, only the maximum values of (\dot{q}_v) were used in defining the continuous curves and such values correspond to maximum values of (\dot{N}) calculated using the values of (Q) and (A) cited above and assuming (β) equals unity. From our somewhat limited data, it appears that there exists a critical value of the heat delivery parameter (\dot{q}_v^{max}) which, when exceeded, leads to ignition of specimens. Thus, this critical value appears to "separate" ignition from oxidation behaviors and a semi-quantitative "zone of ignition" is therefore superimposed upon the graph of Figure 185.

The calculation technique used here is obviously a gross oversimplification of the time state of affairs as it neglects the thermal properties

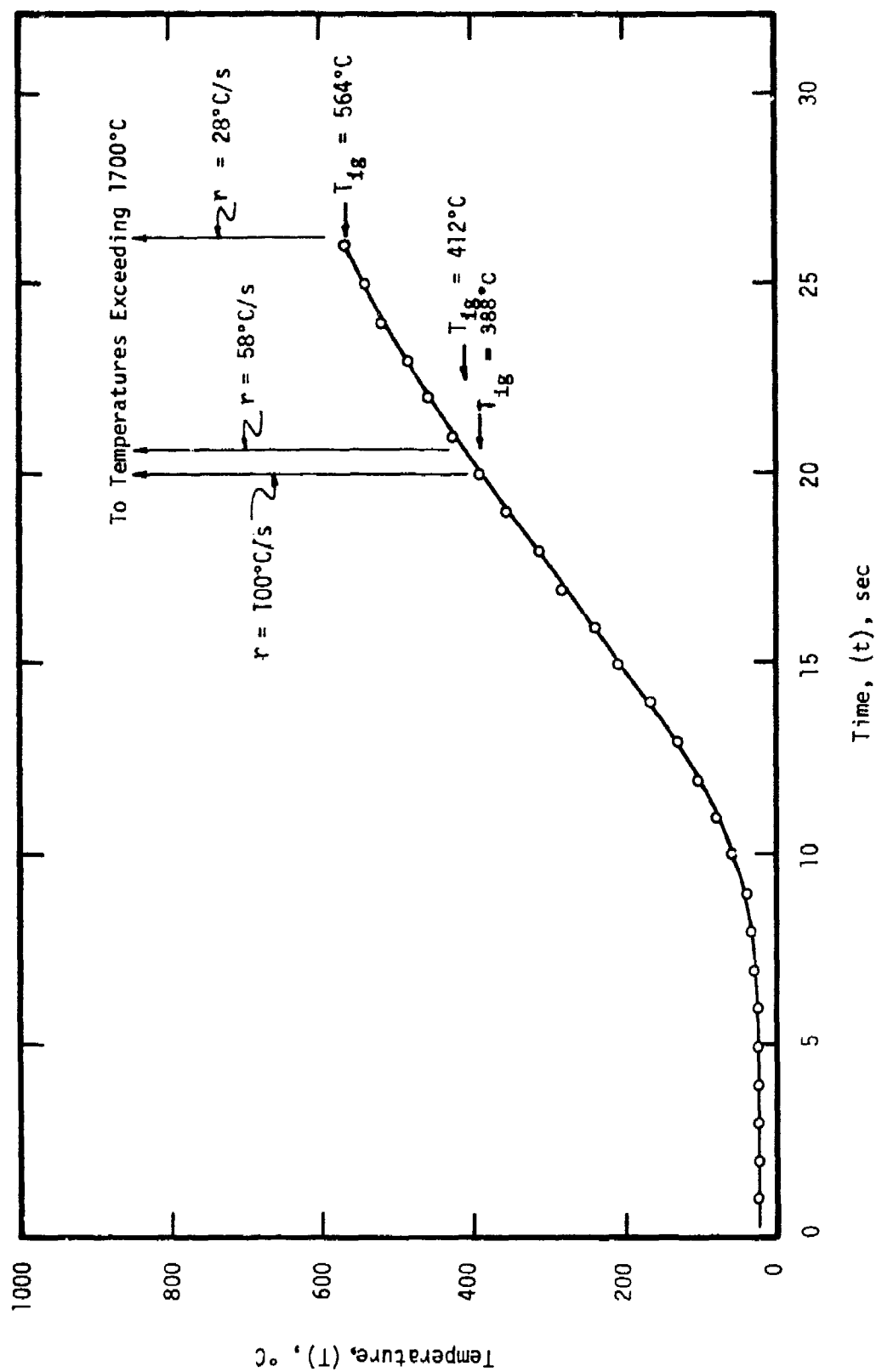


Figure 184.- Ignition behavior of three unalloyed titanium (Type 5) specimens in stagnant 200 torr oxygen illustrating the inverse relation between heating rate and sensible ignition temperature.

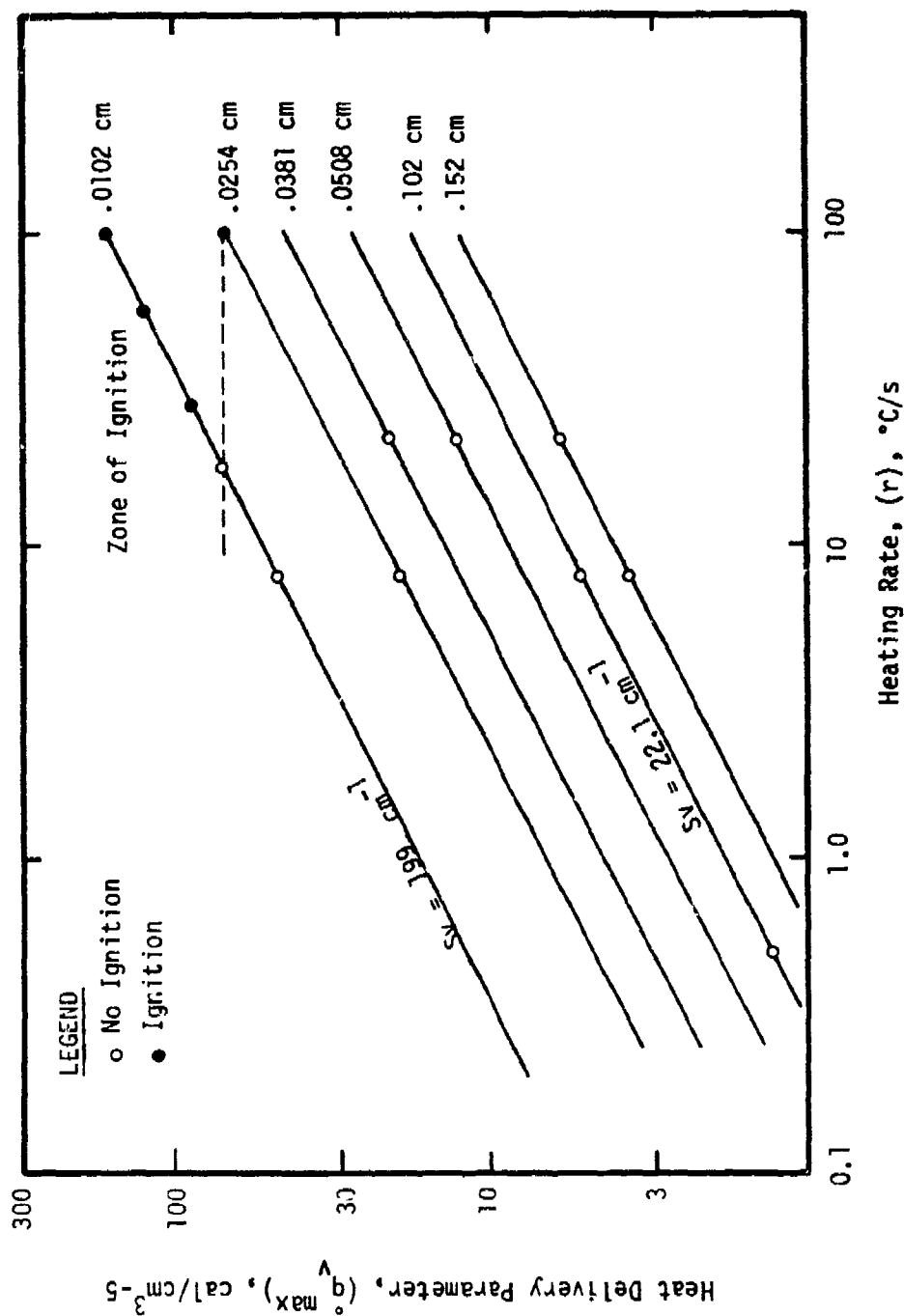


Figure 185.- Dependence of the heat delivery parameter upon heating rate and macroscopic surface-to-volume ratio for unalloyed titanium specimens which underwent oxidation and/or ignition.

of materials and heat transport considerations as well as area multiplication effects arising from mechanical strains. However, it is believed that this broad concept involving the application of heat delivery will be useful in first approximations of the ignition processes of titanium and other metals as well.

In our present investigation of titanium-base materials and in our previous studies concerning the oxidation of magnesium (ref. 10) it had been suspected that the platinum thermocouple elements may have catalyzed the gas-metal reactions. In order to test this hypothesis, especially with regard to the ignition of titanium, one specimen was subjected to an "open-loop" thermal program in the volumetric apparatus in the absence of platinum. As indicated in Table XXVIII, ignition ensued and it is therefore concluded that the presence of platinum in the vicinity of the specimen has little if any catalytic effect in the titanium-oxygen reaction.

The titanium-base alloys investigated exhibit oxidation-associated ignition during anisothermal oxidation in 200 torr oxygen much in the same manner as that described above for the unalloyed material. Figures 186, 187 and 188 represent the oxidation-ignition behaviors for Ti-6Al-4V, Ti-8Mn, and β -III titanium alloy specimens, respectively. These figures are plotted in a format identical to that used in Figure 184 for unalloyed titanium specimens and the assumptions involved are similarly identical. All alloys appear to have a larger zone of ignition than does the unalloyed material as the values of the critical heat delivery parameter is lower for them. This infers that the alloys are more prone to ignition than is unalloyed titanium; a conclusion which parallels the usually observed oxidation behavior of these materials. There is insufficient data available at this time to determine the relative susceptibilities to ignition for the

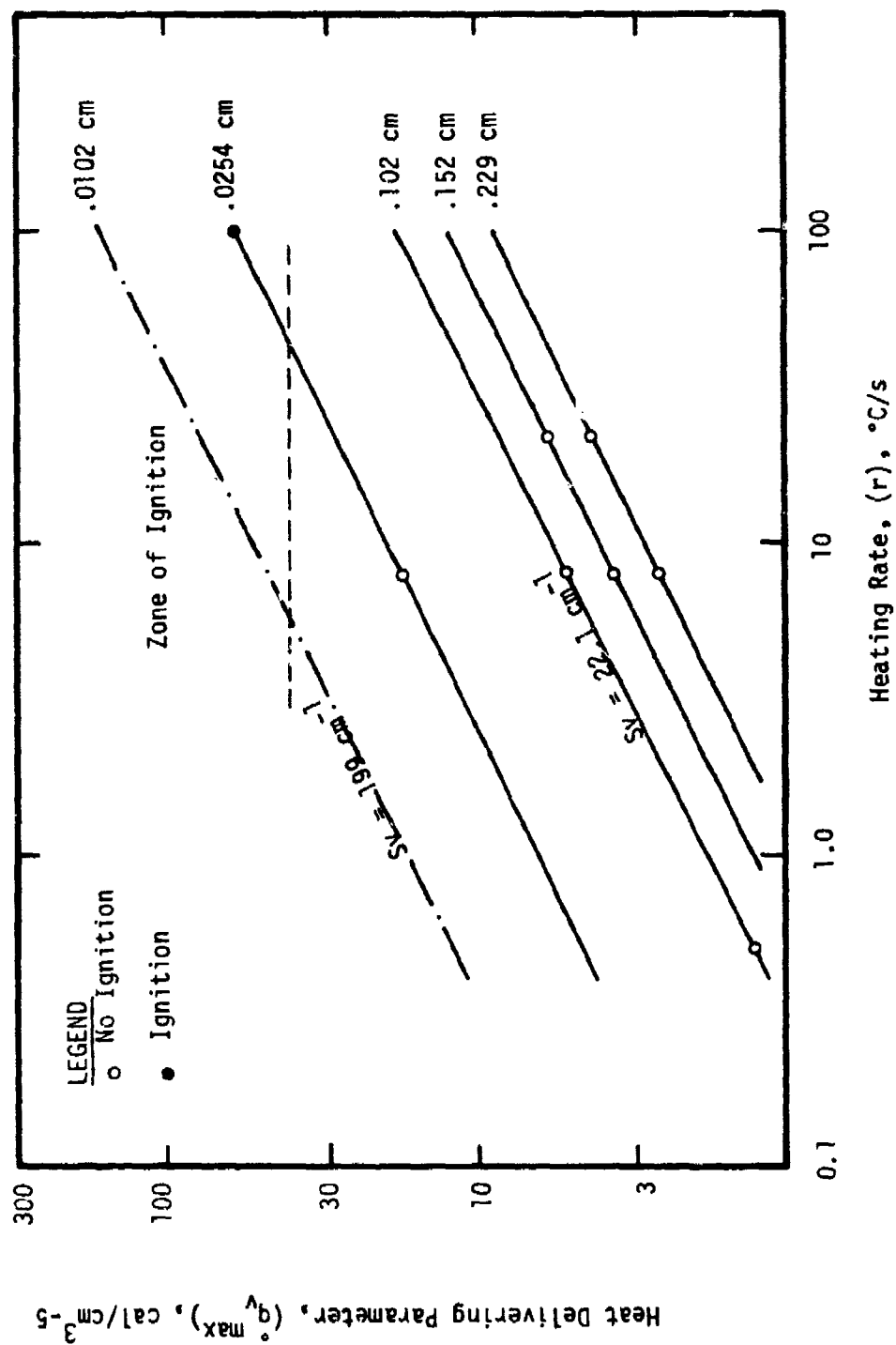


Figure 186.- Dependence of the heat delivering parameter upon heating rate and macroscopic surface-to-volume ratio for titanium-6% aluminum-4% vanadium specimens which underwent oxidation and/or ignition.

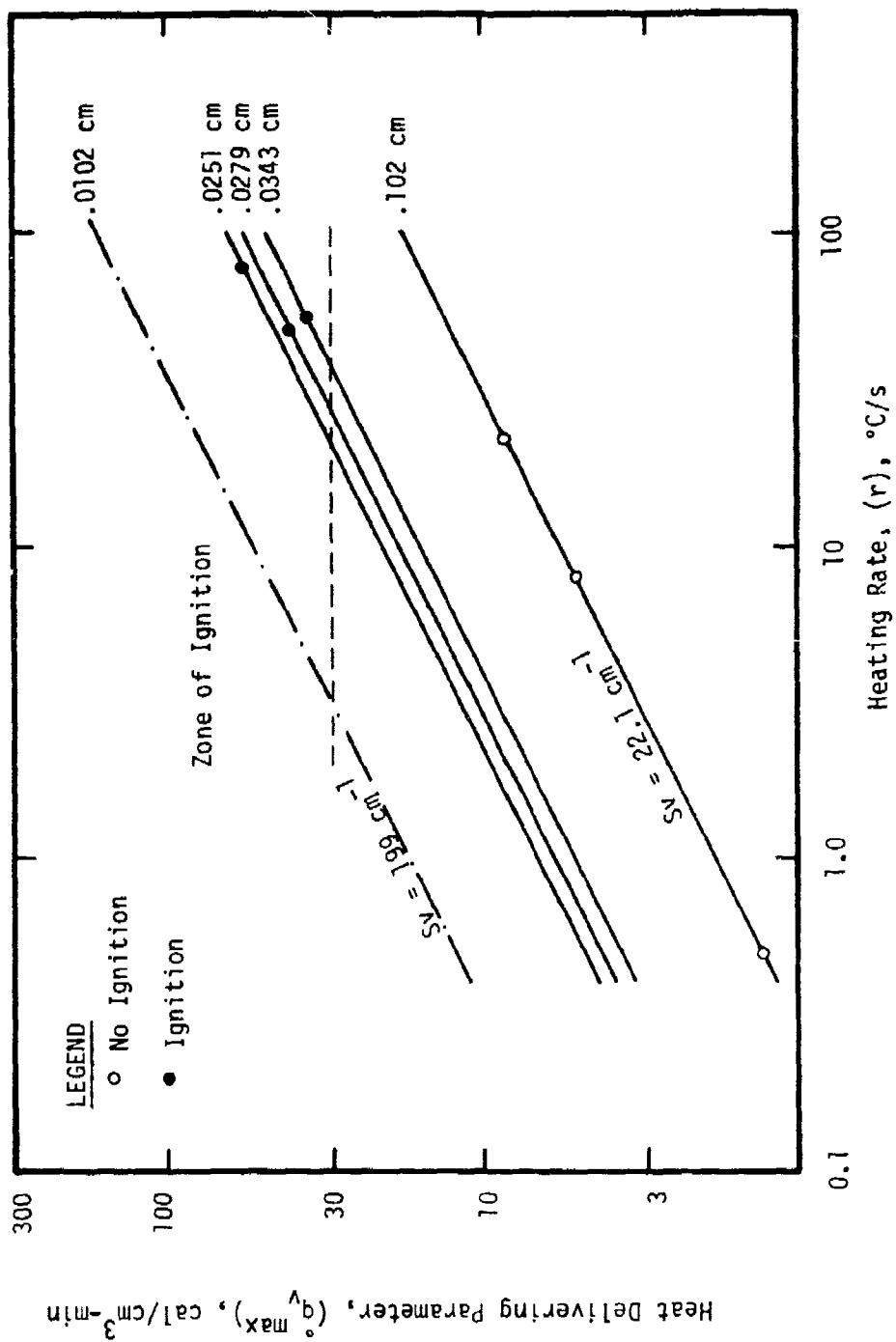


Figure 187.- Dependence of the heat delivering parameter upon heating rate and macroscopic surface-to-volume ratio for titanium-8% manganese specimens which underwent oxidation and/or ignition.

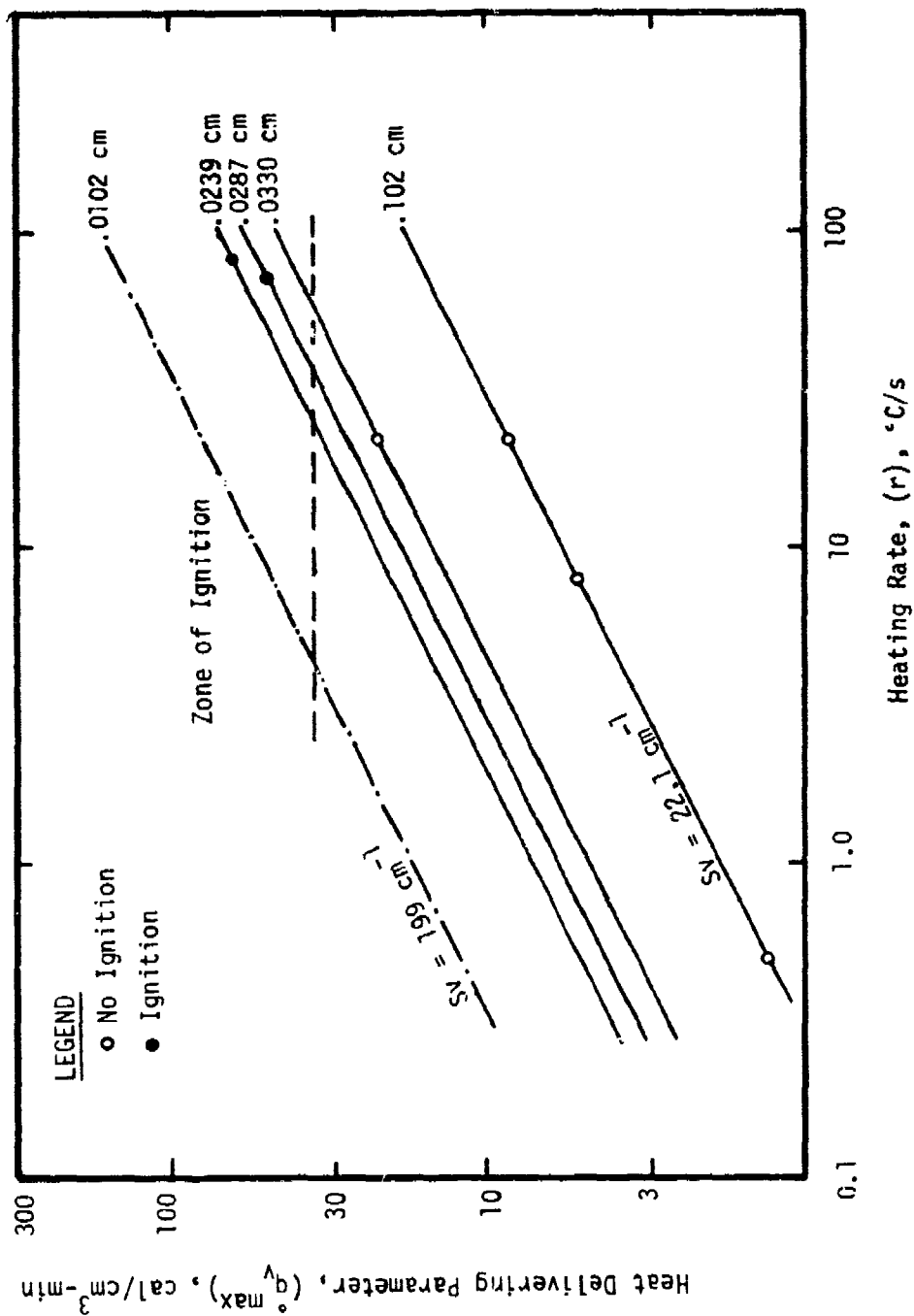


Figure 188.- Dependence of the heat delivering parameter upon heating rate and macroscopic surface-to-volume ratio for titanium- β -III specimens which underwent oxidation and/or ignition.

various alloys investigated. In retrospect, it appears that titanium-base materials of arbitrary dimension may be ignited in oxygen-bearing atmospheres by any radiative energy source which has the capability of inducing a sufficiently large rate of surface heating.

SECTION IV

CONCLUSIONS

During the course of this research, the anisothermal reaction of unalloyed titanium, Ti-6Al-4V, Ti-8Mn, and β -III titanium alloy specimens have been studied in oxygen, nitrogen, and gas mixtures bearing these gases over the temperature range from 800° to 1300°C. The conclusions drawn from this research, some of which must be considered as being tentative, are as follows:

1) The maximum value of the specific linear reaction rate of titanium-base materials in 200 torr oxygen increases as the heating rate is increased. In oxygen as well as in other gases this maximum usually occurs early in the thermal program during heating.

2) At heating rates of approximately 30° to 100°C/s, thin unalloyed titanium and titanium-base alloys specimens exhibit the phenomena of ignition and sustained burning in 200 torr stagnant oxygen. Under such conditions, sensible ignition temperatures as low as 400°C were observed and it is therefore inferred that local deposition of the chemical heat of reaction is causal to ignition.

3) The presence of stored energy of cold work in titanium-base materials exposed at elevated temperatures in 200 torr oxygen appears to: a) induce a higher specific linear reaction rate in the early stages of oxidation, b) induce intrusions and void formation in the oxygen-stabilized diffusion zones, c) enhance the thickness of the diffusion zones, and d) generally enhance the degree of advancement of the gas-metal reactions.

4) For all materials investigated, thin substrates are associated with higher degrees of reactivity. Very thin specimens (0.025 cm or less) of titanium-base materials were found to be (α)-stabilized throughout and evidence for internal cracking of the metal was cited. Some degree of self-heating is suggested by these observations. Anomalously rapid reactivity of very thick specimens was attributed to the generation of thermally-induced stresses.

5) For all materials investigated, those exposed specimens which were inspected exhibited (α)-stabilized diffusion zones at their surfaces. These diffusion zones were of the order of 100 μ m deep when developed at 1100°C in 200 torr oxygen and exhibited maximum hardnesses as large as 1400 KHN₁₀₀ (vs 200 to 400 KHN₁₀₀ for the core material). Hardening of unalloyed titanium by nitrogen was very much less marked than hardening by oxygen.

6) For all materials investigated, those exposed specimens which were investigated exhibited coarse (α + β) structures in their core regions. Evidence was cited that in some cases these structures existed during exposure and that the interphase boundaries may represent paths of easy diffusion for oxygen.

7) Volatile compounds are produced during the oxidation of titanium-base alloys which are most likely to be associated with the alloying elements present. While unalloyed titanium leaves no visually detectable deposit in the apparatus after exposure in 200 torr oxygen at temperatures between 1000° and 1200°C, the Ti-6Al-4V, Ti-8Mn and β -III titanium alloy specimens produced reddish-brown, brown, and black deposits, respectively, upon exposure.

8) In general, the reaction of unalloyed titanium specimens was found to be parabolic with an associated activation energy for parabolic kinetics of approximately 60 K-cal/mole in 200 torr oxygen over the temperature range 1000° to 1300°C. Conversely, the oxidation of alloy specimens was found to be essentially linear under these conditions and more rapid in the earliest stages of testing during heating. The reactivities of specimens of the materials investigated were found to increase in the following order: unalloyed titanium < Ti-6Al-4V < Ti-8Mn < β -III titanium alloy.

9) The reaction of unalloyed titanium in oxygen was found to increase with increasing oxygen pressure in an essentially linear fashion. Mixed gases react with titanium qualitatively as the average of the individual component reactivities; as judged on the basis of several data indices. In oxygen-nitrogen gas mixtures, there is no evidence for synergistic effects.

10) The reaction of nitrogen with titanium is complex and slower than its reaction with oxygen. Initial reactions of nitrogen and nitrogen-bearing gas mixtures are of an interrupted nature leading to multiple maxima "breathing" in the specific linear reaction rate curves. The reaction of a single Ti-6Al-4V alloy specimen with 200 torr nitrogen at 1100°C is at least an order of magnitude slower than the reaction of this material with oxygen and is 2 to 5 times slower than the reaction of unalloyed titanium with 200 torr nitrogen. Evidence was found for an early reaction between nitrogen and unalloyed titanium or Ti-6Al-4V alloy specimens at very low temperatures. For both materials, it was postulated that an adherent but ductile film was formed in nitrogen which acts as a diffusion barrier to further reaction.

11) The energy coupling parameter (W_5) as well as other characteristics of the power index are initially dependent upon the RMS surface roughness of unalloyed titanium. Material which has been "oxygen-doped" appears to be coupled less strongly to the infrared radiation than does virgin material. This index was found to be sensitive to the specimen thickness and the atmosphere composition; thinner specimens and higher heat conductivities of gases usually requiring higher energy inputs to the specimen. No definitive relationship was found relating energy coupling with heating rate as judged by the parameter (W_5).

12) The major compounds formed on unalloyed titanium were TiO_2 (rutile) in oxygen and the nitride TiN in nitrogen. Tests conducted after exposure in air indicated only TiO_2 present. Evidence for textures in both the substrates and oxides were cited as were texture gradients in the scale. An oriented overgrowth of TiO_2 was observed in one case.

13) A mathematical technique was devised for calculating the degree of oxygen uptake by unalloyed titanium under conditions of anisothermal oxidation. Calculations based upon this technique provided a model against which short-term experimental data could be compared. Predicted and observed behaviors agreed well for low heating rates whereas mechanical strains had their least effect. Deviations from the modeled behavior at high heating rates were presumed to be associated with strain-enhanced reactivity.

REFERENCES

1. E. L. White and J. J. Ward: "Ignition of Metals in Oxygen", DMIC Report 224, February 1, 1966, 34 pp.
2. P. Kofstad: "High Temperature Oxidation of Metals", John Wiley and Sons, Inc., 1966, pp. 169-178.
3. C. E. Shamblan and T. K. Redden: "Air Contamination and Embrittlement of Titanium Alloys", in *The Science Technology and Application of Titanium*, edited by R. I. Jaffee and N. E. Promisel, Pergamon Press, 1966, pp. 199-208.
4. D. I. Layner, A. S. Bay, and M. I. Tsypin: "Titanium Oxidation Kinetics and Structure of the Scale", *Fiz. Metal. Metalloved.*, Vol. 16, 1963, pp. 225-231. (Translation)
5. C. J. Rosa: "Oxygen Diffusion in Alpha and Beta Titanium in the Temperature Range of 932° to 1142°C," *Metallurgical Transactions*, Vol. 1, 1970, pp. 2517-2522.
6. H. Kellner and Al Wingert: "Deformation of Titanium by Surface Oxidation", *Metallurgical Transactions*, Vol. 2, pp. 113-115.
7. T. G. Wahibeck and P. W. Gilles: "Reinvestigation of the Phase Diagram for the System Titanium-Oxygen", *Journal American Ceramic Society*, Vol. 49, 1966, pp. 180-183.
8. W. C. Reynolds: "Investigation of Ignition Temperature of Solid Metals", NASA TN D-182, October 1959, 71 pp.
9. G. H. Markstein: "Combustion of Metals", *AIAA Journal*, Vol. 1, 1963, pp. 550-562.
10. J. S. Wolf: "Oxide Growth Rates on Magnesium", Technical Report No. AFWL-TR-73-2, April, 1973, 140 pp.
11. P. H. Morton and W. M. Baldwin, Jr.: "The Scaling of Titanium in Air", *Transactions A.S.M.*, Vol. 44, 1952, pp. 1004-1029.
12. P. K. McAlpine and E. A. Soule: Prescot and Johnson's Qualitative Chemical Analysis, D. Van Nostrand Co., Inc., New York, 1933, pp. 391-394.
13. L. S. Richardson and N. J. Grant: "Reaction of Oxygen and Nitrogen with Titanium from 750° to 1050°C," *Jnl. of Metals*, Jan. 1954, pp. 69-70.
14. C. D. Hodgman, et al.: *Handbook of Chemistry and Physics*, 39th ed., Chemical Rubber Publishing Co., Cleveland, 1957, pp. 626-7.
15. L. S. Darken and R. W. Gurry: Physical Chemistry of Metals, McGraw-Hill Book Co., Ind., 1953, pg. 305.

16. J. Stringer: "The Effect of Pressure on the Second Stage Parabolic Rate in the Oxidation of Titanium," *Acta Met.*, Vol. 8, 1960, pp. 810-811.
17. H. R. Ogden and F. C. Holden: "Metallography of Titanium Alloys", TML Report No. 103, 29 May 1958, pp. 1-11.
18. E. S. Bumps, H. D. Kessler, and M. Hansen: "The Titanium-Oxygen System," *Trans. ASM*, Vol. 45, 1953, pp. 1008-1025.
19. O. Kubaschewski and B. E. Hopkins: "Oxidation of Metals and Alloys", 2nd Ed., Butterworths, 1962, pp. 9, 40.
20. F. N. Rhines and J. S. Wolf: "The Role of Oxide Microstructure and Growth Stresses in the High-Temperature Scaling of Nickel," *Met. Trans.*, Vol. 1, 1970, pp. 1701-1710.
21. M. H. Zirin: "An Observation of the Kinetic Behavior of a Parabolic Type Metal-Gas Reaction with Induced Cracks in the Scale", *J. Oxidn. of Metals*, Vol. 3, 1971, pp. 539-544.
22. L. G. Berry, et al.: Inorganic Index to the Powder Diffraction File, Joint Committee on Powder Diffraction Standards, Swarthmore, 1971.
23. Anon.: Tables for Conversion of X-ray Diffraction Angles to Interplanar Spacings, USGPO, Washington, 1950.
24. W. M. Hirthe and J. O. Brittain.: "High-Temperature Steady-State Creep in Rutile," *Journal of the American Ceramic Society*, Vol. 46, 1963, pp. 411-417.
25. R. E. Bolz and G. L. Tuve.: Handbook of Tables for Applied Engineering Science, Chemical Rubber Company, Cleveland, Ohio, 1970.
26. D. L. Douglass.: "Exfoliation and the Mechanical Behavior of Scales," Oxidation of Metals and Alloys, American Society for Metals, Metals Park, Ohio, 1970, pp. 137-155.

APPENDIX I

METHOD FOR DETERMINATION OF EFFECTIVE SYSTEM VOLUME

In the experimental portion of this research it is required that the oxygen consumption be determinable through observed pressure changes in the system. This, in turn, requires that the effective volume of the system (V_s) be known.

The determination of (V_s) in the laboratory was carried out by attaching to the system a calibrated volume (V_c) as shown schematically in Figure 189. If the system in equilibrium at temperature (T) contains (n_s) moles of an ideal gas at pressure (P_s) and the calibration volume at the same temperature contains (n_c) moles of an ideal gas at pressure (P_c) with the valve in the closed position then:

$$P_s V_s = n_s RT \text{ or } n_s = \frac{P_s V_s}{RT} \quad \text{Eq. (I-1)}$$

and:

$$P_c V_c = n_c RT \text{ or } n_c = \frac{P_c V_c}{RT} \quad \text{Eq. (I-2)}$$

where (R) is the gas constant.

After the valve between the volumes (V_s) and (V_c) is opened, the gas equilibrates within the combined chambers to attain some final pressure (P_f), and such that:

$$n_f = n_s + n_c = \frac{P_f (V_s + V_c)}{RT} \quad \text{Eq. (I-3)}$$

Upon substituting equations (1) and (2) into equation (3), one obtains:

$$V_c (P_c - P_f) = V_s (P_f - P_s) \quad \text{Eq. (I-4)}$$

By using various values of (P_s) and/or (P_c) and by observing the resultant values of (P_f), one may determine (V_s) graphically so long as (V_c) is known. This is performed by plotting the quantity $\{V_c (P_c - P_f)\}$

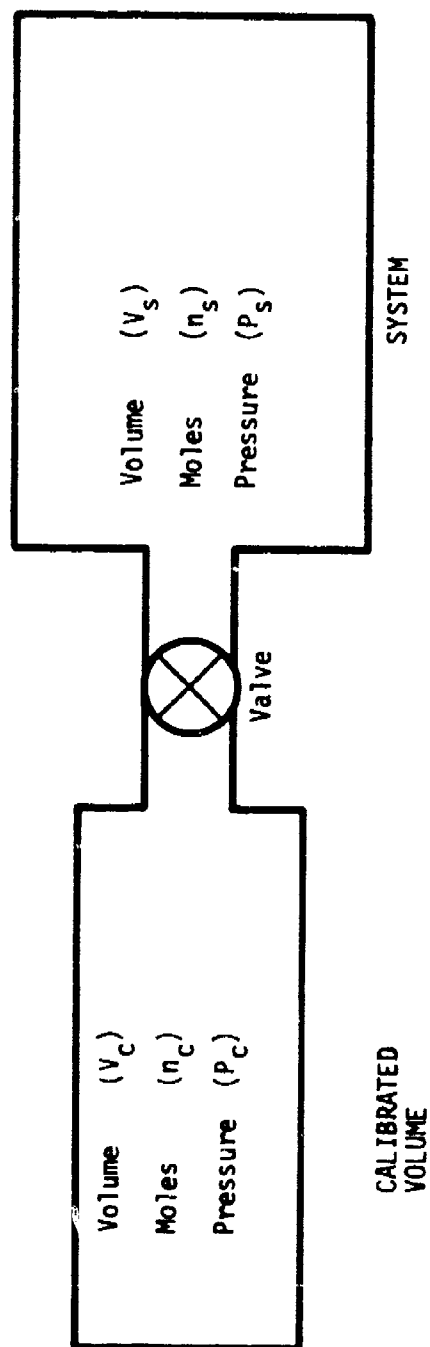


Figure 189. - Schematic diagram of the system with its attached calibrated volume used in considerations for calculating system volume.

versus the quantity $\{(P_f - P_s)\}$ and determining the slope of the resulting linear graph; this slope is identically (V_s) .

The data secured by this technique are presented in Table XXIX. These data, after manipulation in accordance with equation (4) above, are plotted in Figure 190 and the slope of the resultant curve yields 559 ml as the effective system volume.

TABLE XXIX
PRESSURE DATA USED IN DETERMINATION OF EFFECTIVE SYSTEM VOLUME [1]

Initial Pressure in System P_s (atm)	Initial Pressure in Calibrated Volume P_c (atm)	Final Pressure of System P_f (atm)	$V_c(P_c - P_f)$ (ml-atm)	$(P_f - P_s)$ (atm)
.900	1.00	.911	5.74	.011
.800	1.00	.824	17.4	.024
.700	1.00	.735	17.1	.035
.600	1.00	.645	22.9	.045
.500	1.00	.555	28.7	.055
.400	1.00	.469	34.2	.069
.300	1.00	.380	40.0	.080
.250	1.00	.332	43.1	.082
.200	1.00	.288	45.9	.088
.100	1.00	.199	51.7	.099
.050	1.00	.155	54.5	.105

[1] The calibrated volume (V_c) is 64.5 ± 0.25 ml.

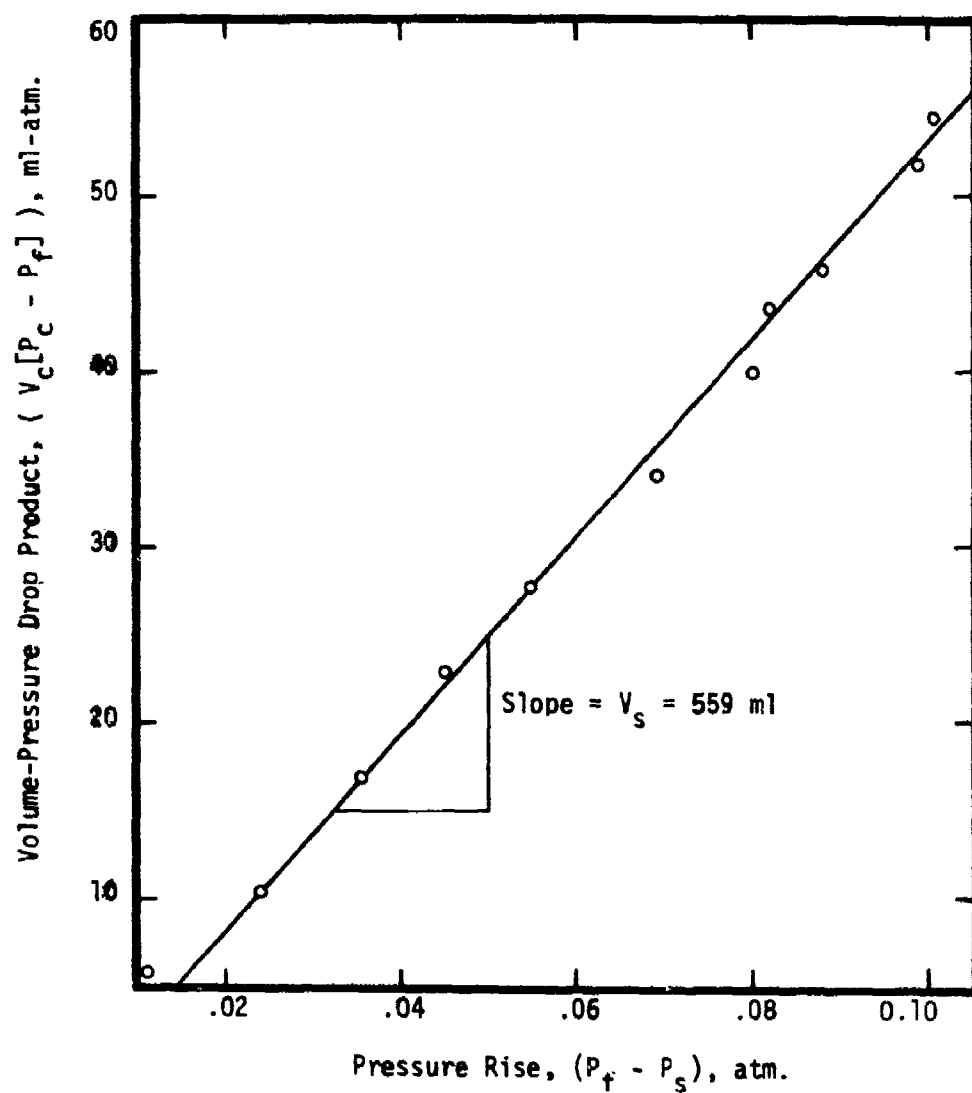


Figure 190. - Graph based on equation (4) of Appendix used in determination of effective system volume (V_s).

APPENDIX II
CONVERSION CONSTANTS USEFUL IN STUDYING THE
REACTION OF TITANIUM WITH OXYGEN

1. Specific weight gain.

The weight gain data will be used as a basis for further calculation.

Assume the specific weight gain:

$$W = 1 \text{ mg/cm}^2 \quad \text{Eq. (II-1)}$$

This quantity represents the mass of oxygen reacted and "fixed".

2. Volume of O_2 consumed.

If there is no vapor phase reaction between titanium and oxygen, and if the scale is completely adherent to the metal, then the volume of oxygen consumed by its reaction with titanium may be calculated.

Thus, for reactions in pure oxygen corresponding to a specific weight gain of 1 mg/cm^2 :

$$1 \text{ mg } (O_2)/\text{cm}^2 = 3.12 \times 10^{-5} \text{ mole } (O_2)/\text{cm}^2 \quad \text{Eq. (II-2)}$$

Assuming ideal behavior in the gas:

$$1 \text{ mg } (O_2)/\text{cm}^2 = 0.699 \text{ ml } (O_2) \text{ STP/cm}^2 \quad \text{Eq. (II-3)}$$

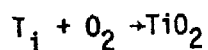
Thus, a weight gain of 1 mg/cm^2 is equivalent to a volume consumption (V_{O_2}) of $0.699 \text{ ml } O_2 \text{ STP/cm}^2$ under the above assumptions. This consideration holds for oxygen consumed by both solution processes and compound formation.

3. Oxide thickness.

If the scale formed is only TiO_2 , and is dense, adherent to the metal, and stress free; then, the scale thickness corresponding to a specific weight gain of 1 mg/cm^2 may be calculated provided the effects of oxygen solution are neglected.

Assuming that only TiO_2 forms, the specific mass of the scale may be

calculated on the basis of the reaction:



Eq. (II-4)

thus:

$$\text{TiO}_2 = M_{\text{O}_2} \times \frac{79.90 \text{ g/mole TiO}_2}{32.00 \text{ g/mole (O}_2)} = 2.497 \text{ mg (TiO}_2\text{)/cm}^2. \quad \text{Eq. (II-5)}$$

The volume of TiO_2 formed upon a unit area is given by:

$$V_{\text{TiO}_2} = \frac{M_{\text{TiO}_2}}{\rho_{\text{TiO}_2}} = \frac{2.397 \times 10^{-3} \text{ gm/cm}^2}{4.26 \text{ gm/cm}^3} = 5.86 \times 10^{-4} \frac{\text{cm}^3}{\text{cm}^2}, \quad \text{Eq. (II-6)}$$

which corresponds to a scale thickness of $5.86 \mu\text{m}$ being equivalent to a weight gain of 1 mg/cm^2 in the absence of oxygen solution in titanium.

APPENDIX III

PREPARATION OF SPECIMENS FOR METALLOGRAPHIC INSPECTION

Several specimens were prepared for metallographic inspection using the procedure outlined below:

- 1) Exposed titanium or titanium alloy specimens were first encapsulated in "Quick Mount" and then cut using a hand saw.

- 2) The cut specimens were remounted in "Quick Mount" using a one-inch diameter mold subsequent to the sawing operation.

- 3) Mounted specimens were then ground on silicon carbide papers successively through grits 180, 240, and 320 using paraffin-saturated kerosene as a cutting fluid. Care was taken to "cross" the polish directions and wash and rinse specimens between successive grits.

- 4) Beginning with 400-grit silicon carbide paper, the mounted specimens were polished by making "figure 8's" with the specimens on the paper. Paraffin-saturated kerosene was used as a cutting fluid, and each specimen was washed and rinsed following the 400-grit polish. The identical procedure was used to polish the specimen with 600-grit silicon carbide paper.

- 5) The mounted specimens were then polished using 6-micron diamond paste as the cutting agent and polishing oil as the lubricant in the following manner. An index card was placed on a polishing block and the diamond paste and oil were put on the back of the index card. The mounted specimen was polished by making "figure 8's" in the oil-paste mixture with light pressure. Each specimen is polished for approximately 2 minutes. Following the polishing, specimens were washed with liquid soap, rinsed in hot water, and then rinsed with ethanol.

- 6) Finally, the specimens were polished using 3-micron diamond paste as the cutting agent. The polishing procedure was identical to that used above with the 6-micron diamond paste.

7) Specimens were then etched in Kroll's reagent (30 sec.) and then subjected to a sequence of rinses including: Na_2CO_3 solution, hot tap water, and ethanol; followed by drying in a hot air stream.

APPENDIX IV

CALCULATION TECHNIQUE FOR OXYGEN CONSUMPTION^{*}

The quantity of oxygen consumed during the course of the reaction of titanium with undiluted oxygen may be calculated from the pressure-time traces generated by our apparatus. During the reaction, which takes place within a closed system of essentially constant volume, oxygen gas becomes fixed as a condensed phase and the system pressure subsequently decreases due to this effect. A complicating factor is involved in that during temperature changes, as in heating of the specimen, a pressure transient is generated; thus, upon heating of the specimen and its environment the pressure rises in a manner which is most easily determined empirically.

In order to obviate determination of the pressure transient, both a titanium specimen (test run) and the empty system^{**} (calibration run) are run independently for each combination of heating rate and maximum oxidation temperature investigated. A schematic representation of the superimposed pressure-time traces for one such "specimen pair" is illustrated in Figure 191, which also includes schematic conjugate temperature-time traces for these runs.

In the treatment below, the following assumptions are implicit: 1) that the oxygen gas is ideal, 2) that it is possible to define a mean effective system temperature, and 3) that there is no measurable reaction of oxygen with the normal system components. Reference to Figure 191 will prove convenient in following this treatment of the pressure-time traces.

^{*}A similar analysis applies when other reactive gases or gas mixtures are used.

^{**}The empty system is defined here as the complete test apparatus less only the titanium specimens.

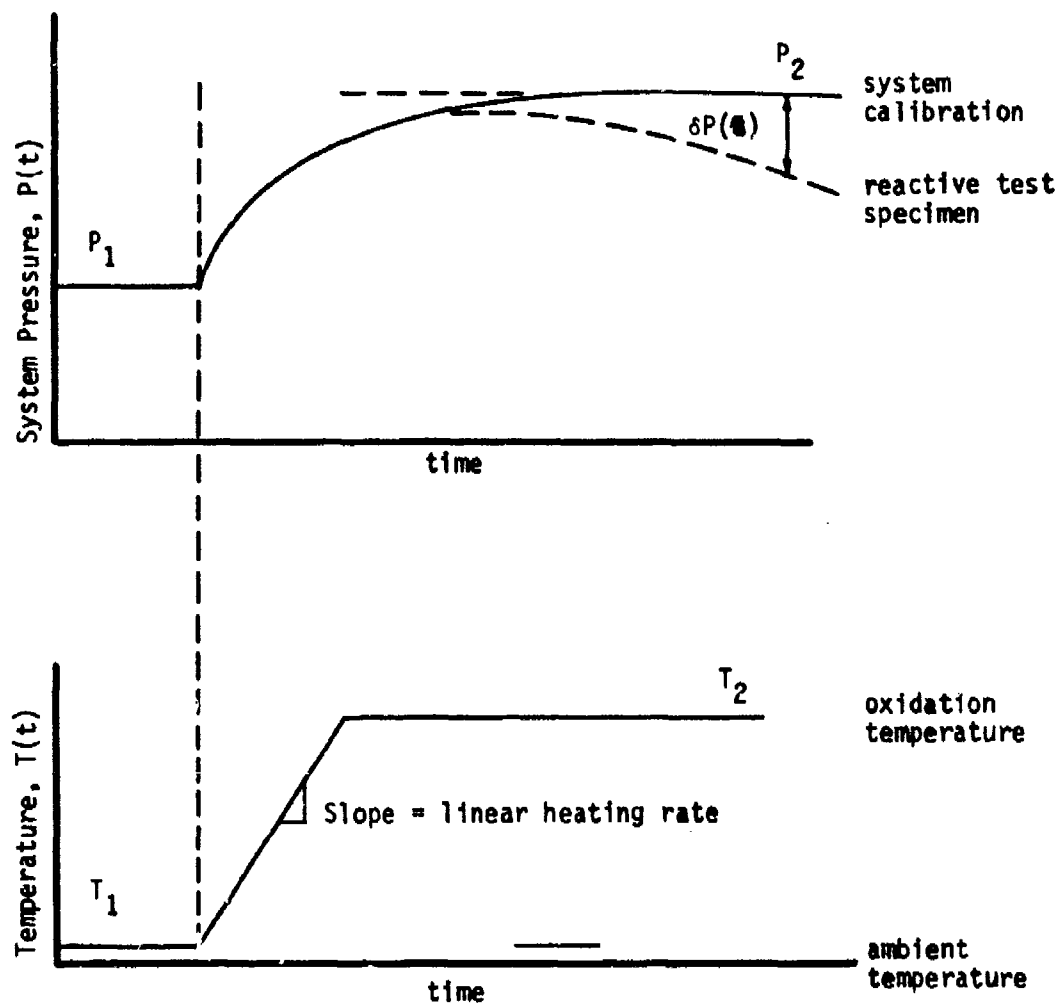


Figure 191-Schematic representations of pressure-time and temperature-time traces for the volumetric system.

Before heating is started, the system is filled with oxygen gas to pressure (P_1) and the mean effective system temperature (\bar{T}_1) is the ambient temperature of the laboratory (T_1). With a knowledge of the system volume (V_S), the number of moles of oxygen gas initially present (n_1) may be calculated by the ideal gas equation:

$$n_1 = \frac{V_S P_1}{R \bar{T}_1} \quad (\text{moles}) \quad \text{Eq. (IV-1)}$$

where pressure is given in atmospheres, volume in liters, temperature in degrees Kelvin, and the gas constant (R) has the value: $0.08205 \frac{\text{lit-atm}}{\text{mole-}^\circ\text{K}}$.

If we now consider heating of the empty system to some temperature of oxidation (eg., near 1000°C) for times long enough that the pressure equilibrates, then, at this steady-state condition, the mean effective system temperature (\bar{T}_2) is given by:

$$\bar{T}_2 = \frac{V_S P_2}{R n_2} \quad (^\circ\text{K}) \quad \text{Eq. (IV-2)}$$

However, since no gas is consumed, $n_1 = n_2$ and Eq. (1) may be substituted into Eq. (2):

$$\bar{T}_2 = \frac{P_2 \bar{T}_1}{P_1} \quad (^\circ\text{K}) \quad \text{Eq. (IV-3)}$$

It should be emphasized that whereas (\bar{T}_1) is equal to the initial specimen temperature, (\bar{T}_2) does not correspond with the specimen temperature in any simple fashion. Thus, for a specimen temperature of the order of 1000°C , the effective specimen temperature (\bar{T}_2) is of the order of a few hundred $^\circ\text{C}$. This difference arises from the fact that the effective system temperature is defined on a volume integral over heated and unheated segments of the system and that the vycor reaction tube represents a "cold wall" chamber.

It is also possible to define the effective system temperature for all transient pressures between (T_1) and (T_2) using the same approach as given above. Thus, from the observed pressure-time graph one can define the function:

$$P = P(t); P_1 \leq P(t) \leq P_2 \quad \text{Eq. (IV-4)}$$

where (t) is time. Then, through the use of Eq. (3):

$$T(t) = \frac{P(t)T_1}{P_1}; T_1 \leq T(t) \leq T_2 \quad \text{Eq. (IV-5)}$$

This concludes the gathering of essential information from the empty system pressure curve.

Let us now turn our attention to the reactive titanium specimen and its pressure behavior. The pressure decrement [$\delta P(t)$] of the reactive specimen with respect to the empty system is due to the consumption of oxygen by the specimen; i.e.:

$$\delta P(t) = \frac{RT(t)}{V_s} \delta n(t) \quad \text{Eq. (IV-6)}$$

Now [$T(t)$] is determinable as indicated by Eq. (5), and the pressure decrement [$\delta P(t)$] is determinable by a point-for-point graphical analysis of the pressure-time traces. Thus, the quantity of oxygen consumed may be determined uniquely as expressed by rearrangement of Eq. (6):

$$\delta n(t) = \frac{V_s \delta P(t)}{RT(t)} \quad (\text{mole}) \quad \text{Eq. (IV-7)}$$

The appropriate equation for data manipulation may now be had by eliminating the mean effective system temperature (T).

Substituting Eq. (5) into Eq. (7):

$$\delta n(t) = \frac{VP_1}{RT_1} \times \frac{\delta P(t)}{P(t)} \quad (\text{mole}) \quad \text{Eq. (IV-8)}$$

From this relationship, both the degree and rate of the reaction of titanium with oxygen may be determined graphically.

APPENDIX V

AN OXIDATION MODEL FOR TRANSIENT HEATING UNDER PARABOLIC REACTION KINETICS*

An oxidation model has been developed which predicts the specific weight change arising from oxygen fixation that occurs during the linear heating of metals in oxidizing atmospheres. Although this derivation is based upon metals which exhibit parabolic reaction kinetics, the model may be modified to apply to any metal which oxidizes with any known rate law and whose reactivity conforms to an Arrhenius-type temperature dependence.

The isothermal reaction of many metals with oxygen or other oxidizing gases at elevated temperature obeys the parabolic rate law:

$$W^2 = K_p t, \quad \text{Eq. (V-1)}$$

where (W) is the specific weight change and (t) is the duration of isothermal oxidation. Further, the parabolic rate constant (K_p) may often be described by the Arrhenius relation:

$$K_p = A \exp(-Q/RT), \quad \text{Eq. (V-2)}$$

where (A) is here assumed to be a temperature-independent constant, (Q) is the activation energy for oxidation, (R) is the gas constant, and (T) is the absolute temperature.

Under conditions of linear heating at rate (r) and from initial (usually ambient) temperature (T_I), the system temperature is given by:

$$T = T_I + rt. \quad \text{Eq. (V-3)}$$

Equation (V-1) may now be expressed in the form:

$$W^2 = At \exp(-Q/R(T_I + rt)), \quad \text{Eq. (V-4)}$$

and taking the derivative of this yields:

$$dW/dt = (A/2W) [\exp(-Q/R(T_I + rt))] [1 + Qrt/R(T_I + rt)^2] \quad \text{Eq. (V-5)}$$

In application, it is convenient to cast equation (V-5) in terms of temperature dependence, rather than time dependence and this is done through the use of equation (3) from which it follows that:

$$dW/dT = (A/2Wr)[\exp(-Q/RT)][1 + Q(T - T_I)/RT^2]. \quad \text{Eq. (V-6)}$$

to further simplify calculation, the dummy variable:

$$Z = Q/RT \quad \text{Eq. (V-7)}$$

is introduced and substituted into equation (V-6) to give:

$$2WdW = -(AQ/rR)[\exp(-Z)][1/Z^2 + 1/Z - 1/Z_I]dZ \quad \text{Eq. (V-8)}$$

where (Z_I) is the value of (Z) at $T = T_I$.

Under the assumption that the values of (A) and (Q) remain constant for the oxidation reaction during the process of heating, equation (V-8) may be integrated to yield the specific weight gain (W_m) associated with heating the specimen at constant rate (r) from (T_I) to some maximum temperature (T_m) :

$$W_m^2 = - (AQ/rR) \int_{Z_I}^{Z_m} [\exp(-Z)][1/Z^2 + 1/Z + 1/Z_I]dZ. \quad \text{Eq. (V-9)}$$

The integral of equation (V-9) is amenable to solution by graphical or computer techniques. Conversion from weight-based data to volume of gas consumed is made using the usual assumptions.